POLAR AND ALPINE MICROBIOLOGICAL AND BIOGEOCHEMICAL PROCESSES IN THE WARMING WORLD

EDITED BY: David Anthony Pearce and Alexandre Anesio
PUBLISHED IN: Frontiers in Microbiology

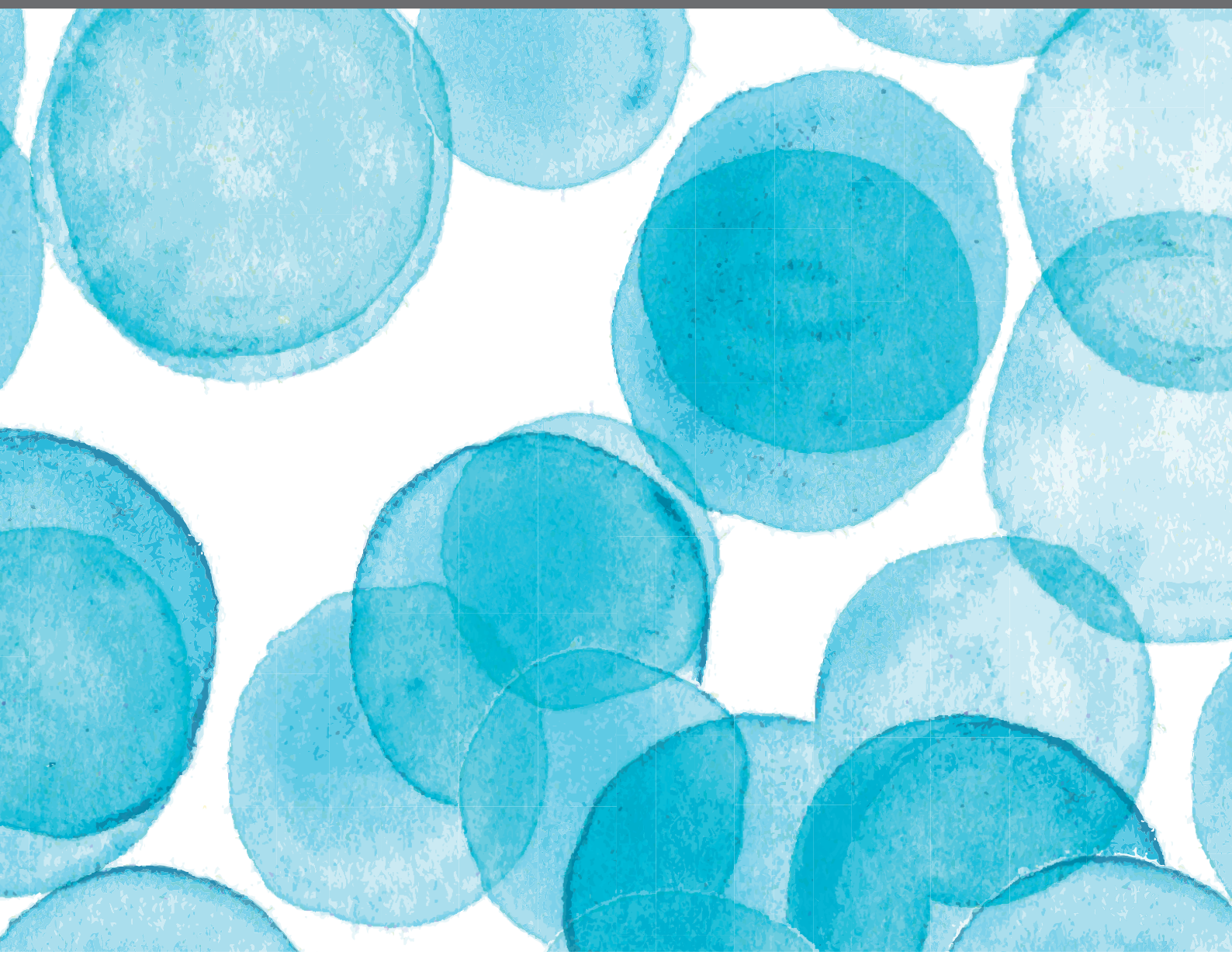

frontiers Research Topics

frontiers

ISSN 1664-8714
ISBN 978-2-88966-955-4
DOI 10.3389/978-2-88966-955-4

About Frontiers

Frontiers is more than just an open-access publisher of scholarly articles: it is a pioneering approach to the world of academia, radically improving the way scholarly research is managed. The grand vision of Frontiers is a world where all people have an equal opportunity to seek, share and generate knowledge. Frontiers provides immediate and permanent online open access to all its publications, but this alone is not enough to realize our grand goals.

Frontiers Journal Series

The Frontiers Journal Series is a multi-tier and interdisciplinary set of open-access, online journals, promising a paradigm shift from the current review, selection and dissemination processes in academic publishing. All Frontiers journals are driven by researchers for researchers; therefore, they constitute a service to the scholarly community. At the same time, the Frontiers Journal Series operates on a revolutionary invention, the tiered publishing system, initially addressing specific communities of scholars, and gradually climbing up to broader public understanding, thus serving the interests of the lay society, too.

Dedication to Quality

Each Frontiers article is a landmark of the highest quality, thanks to genuinely collaborative interactions between authors and review editors, who include some of the world's best academicians. Research must be certified by peers before entering a stream of knowledge that may eventually reach the public - and shape society; therefore, Frontiers only applies the most rigorous and unbiased reviews.
Frontiers revolutionizes research publishing by freely delivering the most outstanding research, evaluated with no bias from both the academic and social point of view. By applying the most advanced information technologies, Frontiers is catapulting scholarly publishing into a new generation.

What are Frontiers Research Topics?

Frontiers Research Topics are very popular trademarks of the Frontiers Journals Series: they are collections of at least ten articles, all centered on a particular subject. With their unique mix of varied contributions from Original Research to Review Articles, Frontiers Research Topics unify the most influential researchers, the latest key findings and historical advances in a hot research area! Find out more on how to host your own Frontiers Research Topic or contribute to one as an author by contacting the Frontiers Editorial Office: frontiersin.org/about/contact

POLAR AND ALPINE MICROBIOLOGICAL AND BIOGEOCHEMICAL PROCESSES IN THE WARMING WORLD

Topic Editors:
David Anthony Pearce, Northumbria University, United Kingdom
Alexandre Anesio, Aarhus University, Denmark

Citation: Pearce, D. A., Anesio, A., eds. (2021). Polar and Alpine Microbiological and Biogeochemical Processes in the Warming World. Lausanne: Frontiers Media SA. doi: 10.3389/978-2-88966-955-4

Table of Contents

frontiers in Microbiology

ORIGINAL RESEARCH
published: 03 April 2020
doi: 10.3389/fmicb.2020.00570

Prevalence of Antimicrobial Resistance and Hemolytic Phenotypes in Culturable Arctic Bacteria

Diana C. Mogrovejo[1†], Laura Perini[2†], Cene Gostinčar[2,3], Kristina Sepčić[2], Martina Turk[2], Jerneja Ambrožič-Avguštin[2], Florian H. H. Brill[1] and Nina Gunde-Cimerman[2]*

[1] Dr. Brill + Partner GmbH Institut für Hygiene und Mikrobiologie, Hamburg, Germany, [2] Department of Biology, Biotechnical Faculty, University of Ljubljana, Ljubljana, Slovenia, [3] Lars Bolund Institute of Regenerative Medicine, Qingdao, China

OPEN ACCESS

Edited by:
David Anthony Pearce, Northumbria University, United Kingdom

Reviewed by:
Rosa Del Campo, Ramón y Cajal Health Research Institute, Spain
William Hugo Gaze, University of Exeter, United Kingdom

***Correspondence:**
Laura Perini
lauraperini89@gmail.com;
laura.perini@bf.uni-lj.si

† These authors have contributed equally to this work and share first authorship

Specialty section:
This article was submitted to Extreme Microbiology, a section of the journal Frontiers in Microbiology

Received: *19 September 2019*
Accepted: *16 March 2020*
Published: *03 April 2020*

Citation:
Mogrovejo DC, Perini L, Gostinčar C, Sepčić K, Turk M, Ambrožič-Avguštin J, Brill FHH and Gunde-Cimerman N (2020) Prevalence of Antimicrobial Resistance and Hemolytic Phenotypes in Culturable Arctic Bacteria. Front. Microbiol. 11:570. doi: 10.3389/fmicb.2020.00570

Many Arctic biomes, which are populated with abundant and diverse microbial life, are under threat: climate change and warming temperatures have raised concerns about diversity loss and possible emergence of pathogenic microorganisms. At present, there is little information on the occurrence of Arctic virulence-associated phenotypes. In this study we worked with 118 strains of bacteria (from 10 sampling sites in the Arctic region, located in Greenland and the Svalbard Archipelago) isolated using R2A medium. These strains belong to 4 phyla and represent 36 different bacterial genera. Phenotypic resistance to 8 clinically important antimicrobials (ampicillin, chloramphenicol, ciprofloxacin, cefotaxime, erythromycin, imipenem, kanamycin, and tetracycline) and thermotolerance range were determined. In addition, a screening of all isolates on blood agar media and erythrocytes suspension of bovine and sheep erythrocytes for virulence-linked hemolytic activity was performed. Although antimicrobial resistance profiles varied among the isolates, they were consistent within bacterial families and genera. Interestingly, a high number of isolates (83/104) were resistant to the tested concentration of imipenem (4 mg/L). In addition, one third of the isolates showed hemolytic activity on blood agar, however, in only 5% of the isolates hemolytic activity was also observed in the cell extracts when added to erythrocyte suspensions for 60 min. The observed microbial phenotypes contribute to our understanding of the presence of virulence-associated factors in the Arctic environments, while highlighting the potential risks associated with changes in the polar areas in the light of climate change.

Keywords: Arctic, extremely cold environment, pathogens, hemolysis, antimicrobial resistance

INTRODUCTION

The Arctic region, once considered a "biological desert," is now regarded as a rich and dynamic ecosystem (Krajick, 2001; Post et al., 2009), characterized by diverse biomes that harbor species from all three domains of life (Anesio and Laybourn-Parry, 2012). Until the onset of global warming, the changes of extreme Arctic biomes progressed slowly, compared to temperate and

tropical regions, and served as proxies for unperturbed natural environments. In the last decades, researchers increasingly recognized the opportunities that the Arctic biomes represent for studying of diverse microbial communities and their interactions (Post et al., 2009).

Ongoing climate change is drastically altering our planet, increasing global air and ocean temperatures, causing widespread melting of snow and ice and rising global average sea levels (Intergovernmental Panel on Climate Change [IPCC], 2007). While every environment on Earth is influenced, Arctic environments are particularly affected and, in fact, their average temperatures have increased almost twice as fast as the global warming rate in the past 100 years (Intergovernmental Panel on Climate Change [IPCC], 2007).

Despite the fact that climate change directly affects microorganisms, microbial life is rarely studied in this context (Cavicchioli et al., 2019). When their interactions with other species are perturbed, the resulting pressures strongly influence microbial community composition and function and might play a role in the expression of bacterial virulence factors (Livermore, 2003). Additionally, altered climatic conditions might enable virulent and/or antimicrobial resistant microbes, originating from temperate regions, to reach previously pristine and unperturbed Arctic environments, spreading virulence factors and resistance genes (Altizer et al., 2013).

Antimicrobial resistance is the natural or acquired capacity of microorganisms to withstand the effects of an antimicrobial drug (Davies and Davies, 2010; World Health Organization [WHO], 2014). In fact, resistance to antimicrobials is widely considered to be one of the biggest health challenges of our time, leading to higher medical costs, prolonged hospital stays, and increased mortality rates (World Health Organization [WHO], 2014). Several studies have confirmed the presence of antimicrobial resistance genotypes and phenotypes in microorganisms from cold environments and suggested that the polar regions can be considered benchmarks for the study of antimicrobial resistance in pristine non-clinical environments (Yuan et al., 2014; Tam et al., 2015; Agnew et al., 2016; McCann et al., 2019).

Hemolysins, considered an important virulence factor, are compounds produced by a variety of bacterial species. These compounds are responsible for membrane damage, cell lysis and destruction of neighboring cells and tissues in order to provide nutrients, mainly iron, for the toxin-producing bacteria (Bullen et al., 2005). Iron is an essential element for living organisms as it plays catalytic, regulatory and structural roles in the cell and many authors have also pointed out its important role as a virulence regulator for commensal and pathogenic microorganisms (Messenger and Barclay, 1983; Litwin and Calderwood, 1993; Zughaier and Cornelis, 2018). Even though they are studied as major virulence factors in infection models of laboratory animals (Bhakdi et al., 1994; Bayley, 1997; Tomita and Kamio, 1997) and are commonly associated with pathogenic bacteria, the expression of hemolysins has rarely been assessed in bacterial isolates from environmental samples (Bevivino et al., 2002; González-Rodríguez et al., 2007) and, to the best of our knowledge, very few studies exist about the hemolytic activity of Arctic bacterial species, e.g., Mogrovejo-Arias et al. (2020).

Finally, an important bacterial trait is the microorganism's ability to grow at 37°C, the optimum temperature for most of human pathogens that allows microbial colonization, and is thus a prerequisite for pathogenic microbe-human interactions (Madigan et al., 2012). Research of Arctic microbes usually uses growth temperatures lower than 37°C, e.g., 4, 15, 20, or 27°C (Wiebe et al., 1992; Amato et al., 2007; Tam et al., 2015) and temperatures above 30°C are rarely used, as these are usually too high for the optimal growth of even the psychrotolerant species (Moyer and Morita, 2007).

Environmental or commensal microorganisms might become pathogenic under stressful conditions since bacterial species respond to environmental stress in a variety of ways, e.g., acceleration of horizontal gene transfer (Marshall et al., 2009). Accordingly, genes encoding traits that occur naturally in the environment, such as antimicrobial resistance and hemolytic activity, can be transferred between habitats by bacteria, bacteriophages or mobile genetic elements, resulting in a global-scale redistribution of resistance and virulence factors/genes (Marshall et al., 2009; Davies and Davies, 2010).

One of the main indirect effects of climate change could be the increase of infectious diseases (Kurane, 2010). The Arctic in this context represents an important source of microorganisms and mobile genetic elements that could transit into more human-associated environments (Edwards, 2015). Thus research on virulence-associated phenotypes in natural, non-clinical environments is necessary to understand the possible implications of the climate changes for public health (Martínez, 2008).

In the present study of bacterial isolates from the Arctic region, we investigated three phenotypes commonly associated with pathogenic bacteria, i.e., growth at 37°C, the hemolytic activity on blood agar plates at different temperatures as well as on erythrocyte suspensions and resistance to 8 different, commonly used and clinically relevant antimicrobials.

MATERIALS AND METHODS

Site and Samples Description

Samplings were performed during 2016 and 2017 summer/winter seasons in the south-western margin of Greenland, the Greenland Ice Sheet, and Svalbard, the areas of Ny-Ålesund and Longyearbyen (Perini et al., 2019a,b; Mogrovejo-Arias et al., 2020). The bacterial composition of these ecosystems has been studied extensively by culture-dependent as well as culture-independent methodologies (Perini et al., 2019a,b; Mogrovejo-Arias et al., 2020).

Glacial and subglacial ice, snow, lake ice, tap water, glacial meltwater, sediment, pond and sea water samples were collected from the locations shown in **Figure 1** and described in **Table 1**. Ice, snow, cryoconite, and sediment samples were collected using disposable sterile nitrile gloves and surface-sterilized tools and transferred into sterile Whirl-Pak® plastic bags. For snow and soil samples, 5 cm of the surface were discarded and a disinfected shovel or sterile spoon was used to store the sample in the sterile plastic bags. Tap water, glacial meltwater, pond

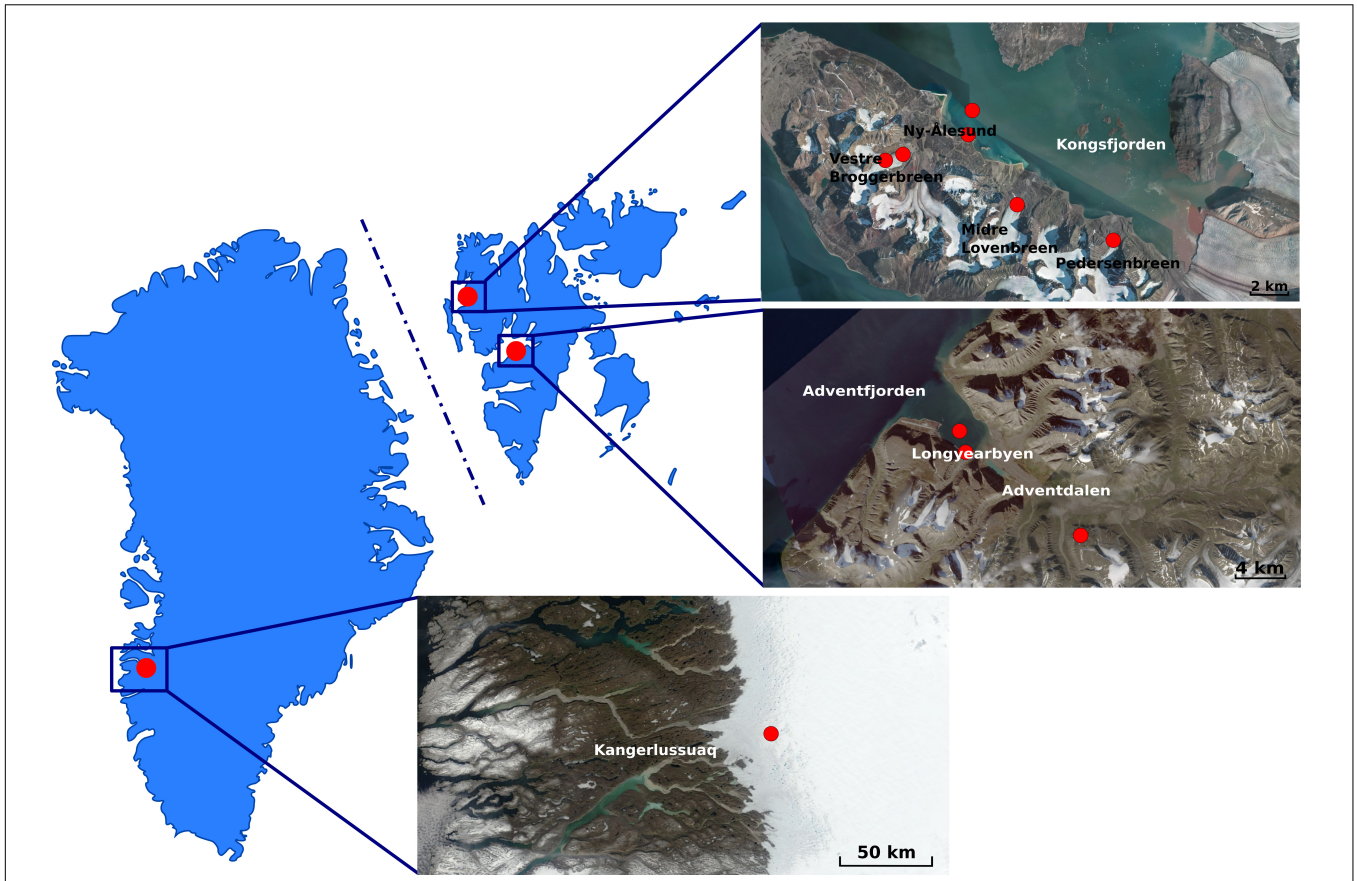

FIGURE 1 | Maps of Greenland **(Left)** and Svalbard **(Right)** Archipelago (Norway) indicating the areas where fieldwork was conducted. Red dots in the satellite images indicate the sampling sites. Greenland map was acquired as an image from Modis Satellite. Svalbard map was adapted as an image from TopoSvalbard credit NPI/USGS Landsat, courtesy of the Norwegian Polar Institute (available at: https://toposvalbard.npolar.no). Greenland and the Svalbard Archipelago are not drawn to scale.

and sea water were collected into plastic bottles previously washed with 15% hydrogen peroxide, followed by three washes with sterile water and three washes with the sample. Samples were processed as outlined by Mogrovejo-Arias et al. (2020) or processed within 24 h from their collection at the primary ice camp on the Greenland Ice Sheet, the NERC Arctic Research Station (Ny-Ålesund), or the University Centre in Svalbard (UNIS; Longyearbyen).

Cultivation and Isolation of Bacteria

Snow, supraglacial and subglacial ice were melted at+4°C in the dark prior filtration. After the outer surface layer of subglacial ice was melted, it was discarded, the remaining ice was washed with sterile water and only the second round of meltwater was used for analyses. Serial dilutions were used for soil and sediment samples. Water samples were filtered through Millipore membrane filters (0.45 μm pore size) in duplicates. Filters were placed onto R2A (BioLife), an oligotrophic medium for heterotrophic microorganisms.

Plates of all sample types were incubated at 5, 10, 15–17, and 37°C for up to 4 months in sterile plastic bags to preserve the humidity of the agar media. Negative control plates were prepared with sterile water frozen prior to culturing and processed as the samples. Two control agar plates were streaked for each testing temperature and incubated in the same conditions and for the same duration as the samples. Liquid and enrichment cultures were not used.

Bacterial Identification

Morphologically different colonies were selected and streaked onto fresh R2A plates in order to obtain pure cultures. The plates were incubated at the initial isolation temperature of each isolate and, in addition, at 37°C. DNA was extracted using PrepMan Ultra reagent (Applied Biosystems) according to the manufacturer instructions. 16S rRNA gene was amplified with 27f-lane, 1492R, 8F, and 1541R primers (Tam et al., 2015; Perini et al., 2019a; Mogrovejo-Arias et al., 2020). The 16S nucleotide amplicons were Sanger-sequenced by Microsynth AG (Switzerland). The resulting sequences were analyzed using MUSCLE software (Edgar, 2004) implemented in the MEGA7 package (Kumar et al., 2016) and compared against the GenBank database using the BLAST software.[1] The 16S rDNA sequences

[1]https://blast.ncbi.nlm.nih.gov/Blast.cgi

TABLE 1 | Sample types and GPS coordinates of the sampling locations for this study.

Sample type	Site description	Area, country	Season	Year	GPS coordinates
Dispersed cryoconite	Ice camp on GrIS	Kangerlussuaq, Greenland	Summer	2016	67°04′43″N 49°20′29″W
Supraglacial ice – clear ice				2016, 2017	
Supraglacial ice with high biomass inclusions of dark glacial algae – dark ice				2016, 2017	
Cryoconite				2016, 2017	
Supraglacial water				2017	
Snow	Ice camp on GrIS	Kangerlussuaq, Greenland	Summer	2017	67°04′43″N 49°20′29″W
	Seasonal pond, Adventdalen	Longyearbyen, Svalbard	Winter	2016	78°09′24″ N 16°01′59″ E
	Midtre Lovénbreen	Ny-Ålesund, Svalbard	Summer	2017	78°53′08″ N 12°02′44″ E
	Vestre Brøggerbreen	Ny-Ålesund, Svalbard	Summer	2017	78°54′42″ N 11°43′42″ E
Subglacial ice	Midtre Lovénbreen	Ny-Ålesund, Svalbard	Summer	2017	78°53′37″ N 12°04′13″ E
	Vestre Brøggerbreen	Ny-Ålesund, Svalbard	Summer	2017	78°54′55″ N 11°45′48″ E
	Pedersenbreen	Ny-Ålesund, Svalbard	Summer	2017	78°52′46″ N 12°17′57″ E
Tap water	UNIS	Longyearbyen, Svalbard	Winter	2016	78°13′21″ N 15°39′06″ E
Glacial melt water	Midtre Lovénbreen	Ny-Ålesund, Svalbard	Summer	2017	78°53′25″ N 12°03′15″ E
					78°53′36″ N 12°04′13″ E
Pond water	Ny-Ålesund area	Ny-Ålesund, Svalbard	Summer	2017	78°55′34″ N 11°56′21″ E
Sea water	Adventfjorden	Longyearbyen, Svalbard	Winter	2016	78°14′27″ N 15°36′59″ E
	Kongsfjorden	Ny-Ålesund, Svalbard	Summer	2017	78°55′33″ N 12°02′29″ E
Soil	Midtre Lovénbreen forefield	Ny-Ålesund, Svalbard	Summer	2017	78°53′54″ N 12°03′59″ E
	Vestre Brøggerbreen forefield	Ny-Ålesund, Svalbard	Summer	2017	78°55′20″ N 11°46′38″ E
Sediment	Marine sediment, Adventfjorden	Longyearbyen, Svalbard	Winter	2016	78°14′27″ N 15°36′59″ E
	Pond sediment, Ny-Ålesund area	Ny-Ålesund, Svalbard	Summer	2017	78°55′34″ N 11°56′21″ E

obtained in this study were deposited in the NCBI GenBank nucleotide database. All isolated strains used in this study have been deposited in the Ex Culture Collection of the Infrastructural Centre Mycosmo (MRIC UL) at the Department of Biology, Biotechnical Faculty, University of Ljubljana, Slovenia. Information on all isolates and accession numbers for their 16S rRNA sequences are listed in **Supplementary Table S1**.

Hemolytic Assay on Blood Agar

Bacterial isolates were cultured on Blood Agar Base (Fluka Analytical) containing 5% of sterile sheep or bovine blood and incubated at +15 and +37°C for up to 7 days. The use of human blood is generally discouraged (Buxton, 2005) and thus, it was not used in our experiments. The isolates were revived from stock cultures from the Ex Culture Collection of the Infrastructural Centre Mycosmo (MRIC UL), University of Ljubljana. Only actively growing cultures were tested. As controls, the following strains revived from the Ex Culture Collection of the Infrastructural Centre Mycosmo (MRIC UL), University of Ljubljana were used: EXB V-53 *Enterococcus faecalis* (no hemolysis, referred to as γ-hemolysis), EXB V-59 *Streptococcus pyogenes* (β-hemolysis), EXB V-62 *Streptococcus pneumoniae* (α-hemolysis).

Hemolytic Assay With Erythrocyte Suspension

Hemolytic activity of organic bacterial extracts was tested in real time using bovine and sheep erythrocyte suspensions rather than blood agar. Bacterial cultures (118 environmental and 3 control strains described in **Supplementary Table S2**) were grown in sterile Falcon tubes containing 20 mL of Nutrient Broth (BioLife). Tubes were shaken at 150 rpm and +15 or +25°C, based on their isolation temperature, for 3 days. Cultures were then centrifuged for 5 min at 12,000 × *g*, supernatant was discarded, and biomass was resuspended in 5 mL of non-denaturated 96% ethanol. Suspensions were vortexed for 5 sec, sonicated (40% amplitude, 20 s) to lyse the cells and shaken (150 rpm) at room temperature for 30 min. Suspensions were subsequently centrifuged (5 min at 12,000 × *g*), the supernatants were transferred into pre-weighted sterile Falcon tubes and the ethanol was evaporated under chemical fume hood in a flow of nitrogen gas. The dry weight of the crude extracts was determined gravimetrically, and the extracts were resuspended in an appropriate amount of non-denaturated 96% ethanol to a standard final concentration of 1 mg extract dry weight/mL.

Hemolytic activity was measured by a turbidimetric method using a microplate VIS absorption reader (Dynex Technologies, United States). Different volumes (0–25 μL) of ethanolic extracts, or of 96% ethanol alone, were pipetted into the wells on the 96-well microtiter plate, and combined with the appropriate volume of erythrocyte buffer (0.13 M NaCl, 0.02 M Tris, pH = 7.4) to obtain different final concentrations of the extract (0–250 μg/mL) in the 100 μL final volume. Right before measurement, 100 μL of bovine or sheep erythrocytes suspension in erythrocyte buffer (OD = 0.5 at 630 nm) was added into the wells. The decrease in apparent absorbance was measured for 60 min, in 30 s intervals, to determine the t_{50} (time necessary for

50% hemolysis). The hemolytic activity was expressed as $1/t_{50}$ (min^{-1}). When tested alone, ethanol did not induce any visible hemolysis during the 60 min.

Antimicrobial Susceptibility Test

Bacteria were cultured on Nutrient Agar (BioLife) plates containing 8 different commonly used antimicrobials and incubated at 15 or 25°C, based on the initial isolation temperature of each isolate. Results were observed as soon as the bacterial growth appeared (between 1 and 7 days). The following antimicrobials were used: ampicillin (AMP) 100 mg/L; chloramphenicol (CHL) 25 mg/L; cefotaxime (CTX) 2 mg/L; ciprofloxacin (CIP) 0.25 mg/L; erythromycin (ERY) 15 mg/L; imipenem (IPM) 4 mg/L; kanamycin (KAN) 50 mg/L; tetracycline (TET) 10 mg/L. As positive controls, wild type *Escherichia coli* strains EXB L-4239 A5 and EXB L-4240 A6 isolated from poultry and with known resistance profile were used [Ex Culture Collection of the Infrastructural Centre Mycosmo (MRIC UL), University of Ljubljana]. Imipenem-resistant strains were inoculated on nutrient agar plates with gradually increasing IPM concentrations (4, 6, 8, and 10 mg/L). Strains that showed resistance to higher concentrations were further inoculated in duplicate on CHROMID® CARBA SMART Agar (BioMérieux, France) and incubated at 15°C to screen for the production of specific carbapenemases: class A *Klebsiella pneumoniae* carbapenemases or KPC; Class B metallo-β-lactamases or MBL including New Delhi metallo-β-lactamases, NDM and Class D OXA-48-like carbapenemases (van Duin and Doi, 2017).

RESULTS

Bacterial Isolation and Identification

A total of 290 isolates were obtained from all the samples after incubation (**Supplementary Table S1**). Nutrient-rich samples, i.e., dark ice, cryoconite, sediment and soil, yielded the majority of isolates (159/290). The isolates belonged to four different phyla: Proteobacteria (104/290), Firmicutes (81/290), Actinobacteria (77/290), and Bacteroidetes (28/290). The most common genera in each phylum were: *Pseudomonas* (39/104), *Bacillus* (49/81), *Cryobacterium* (17/77), and *Flavobacterium* (21/28), respectively. Gram-positive isolates were slightly more frequent (158/290) than Gram-negative (132/290).

Based on 16S rDNA identification, abundance and morphological characteristics, 118 unique strains were selected for further tests (**Supplementary Table S2**). *Bacillus* sp. and *Pseudomonas* sp. were the most abundant genera in this study (38/118), accounting for more than 30% of the isolates selected for the tests. The majority of the chosen isolates (87/118) were psychrotolerant and were obtained at incubation temperatures of 15–17°C, followed by 17 mesophiles from incubation at 37°C and 14 psychrophiles obtained from incubation at 5–10°C.

Interestingly, 11 isolates obtained at low incubation temperatures (5–10°C) belonging to the genera *Pedobacter* (L-1969 and L-1973), *Sphingomonas* (L-1972), *Raoultella* (L-1980), *Flavobacterium* (L-1981), *Pseudomonas* (L-1983, N40, and N71), *Leifsonia* (An34), *Salinibacterium* (S58), and *Microbacterium* (S60) showed some degree of growth at 37°C on R2A. Out of the 87 psychrotolerant isolates, 74 were able to weakly grow at 37°C. Only 13 psychrotolerant isolates belonging to the genera *Rhodopseudomonas* (L-1894), *Cryobacterium* (L-2263 and L-2279), *Massilia* (L-2271, L-2283, and L-2653), *Flavobacterium* (L-2291 and L-2562), unidentified Oxalobacteraceae (L-2547), *Sphingomonas* (L-2552), *Pseudomonas* (L-2554), *Paenibacillus* (L-2661), and *Streptomyces* (N41) were not able to grow at 37°C.

Hemolysis on Blood Agar Plates

Two different experiments were performed to observe the hemolytic activity of the isolates. In the first one, the excretion of hemolytically active compounds resulted in either α- or β-hemolysis around the bacterial colonies on blood agar plates. A β-hemolytic reaction implies complete lysis of the red blood cells, causing a clear zone on the agar surrounding the colony and it is referred as true hemolysis. On the other hand, an α-hemolytic reaction occurs when the hemoglobin in the red blood cells is reduced to methemoglobin, causing a greenish discoloration on the agar surrounding the colonies. Finally, the absence of hemolysis or discoloration is referred to as γ-hemolysis (Buxton, 2005).

The tested bacterial strains displayed all three phenotypes (**Figure 2**). Our results showed that the hemolysis was influenced by the incubation temperature (**Table 2**). *Pseudomonas* spp. showed psychrotolerant behavior, that is, all of them grew at 15°C while only 50% grew at 37°C. Of these, 9/22 isolates were β-hemolytic on both types of blood at 15°C, whereas only 6/22 were hemolytic at 37°C. Isolate L-2644 was the only one that expressed β-hemolysis at both temperatures and on both blood types. No α-hemolytic phenotype was observed for this genus (**Table 2**).

Bacillus spp. exhibited greater temperature range tolerance, with all isolates growing at both 15 and 37°C. Although β-hemolytic phenotypes were common at 37°C (11/13 isolates),

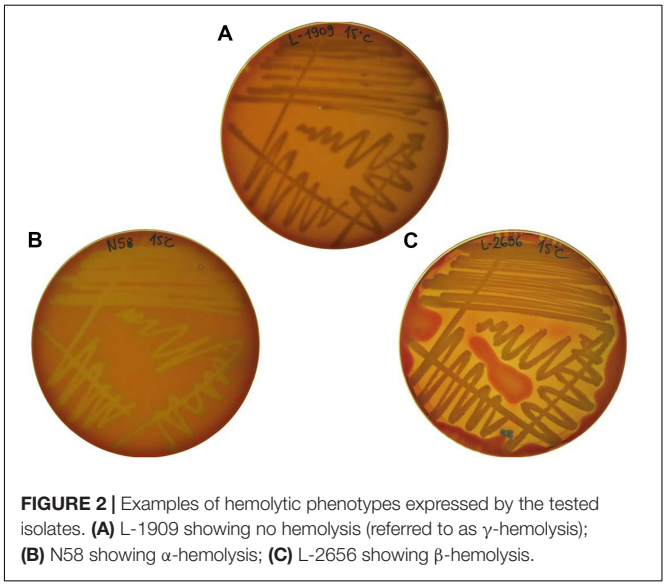

FIGURE 2 | Examples of hemolytic phenotypes expressed by the tested isolates. **(A)** L-1909 showing no hemolysis (referred to as γ-hemolysis); **(B)** N58 showing α-hemolysis; **(C)** L-2656 showing β-hemolysis.

TABLE 2 | List of the bacterial isolates tested for thermotolerance, hemolysis on blood agar at 15 and 37°C and resulting hemolytic phenotypes.

		Phenotype			
		Bovine blood		Sheep blood	
Isolate	Species	15°C	37°C	15°C	37°C
12396_bac	*Bacillus* sp.	γ	α, β−	γ	α, β−
12403-Bac	*Bacillus* sp.	γ	α, β−	γ	α, β−
L-1896	*Bacillus* sp.	γ	γ	γ	γ
L-1899	*Cryobacterium psychrotolerans*	γ	NG	γ	NG
L-1900	*Sphingomonas* sp.	γ	NG	γ	NG
L-1906	*Bacillus* sp.	γ	γ	γ	γ
L-1909	*Arthrobacter* sp.	γ	NG	γ	NG
L-1910	*Bacillus* sp.	γ	α	γ	α
L-1922	*Micrococcus* sp.	γ	β	γ	β
L-1964	*Pseudomonas* sp.	β+	NG	β+	NG
L-1969	*Pedobacter* sp.	β	β	β	β
L-1972	*Sphingomonas* sp.	γ	γ	γ	γ
L-1973	*Pedobacter* sp.	γ	β	γ	γ
L-1980	*Raoultella* sp.	γ	β	γ	β
L-1983	*Pseudomonas* sp.	γ	γ	γ	γ
L-1994	*Flavobacterium* sp.	β	γ	β	γ
L-1995	*Janthinobacterium* sp.	β	β	γ	β
L-2062	*Cryobacterium* sp.	γ	γ	γ	γ
L-2063	*Undibacterium* sp.	γ	NG	γ	γ
L-2137	*Pseudomonas* sp.	β−	β−	γ	γ
L-2142	*Pseudomonas* sp.	γ	β−	γ	γ
L-2145	*Pseudomonas* sp.	γ	β−	γ	γ
L-2265	*Pseudomonas* sp.	γ	β−	γ	γ
L-2266	*Janthinobacterium* sp.	γ	β−	γ	γ
L-2267	*Undibacterium* sp.	NG	NG	NG	NG
L-2270	Unidentified Oxalobacteraceae	NG	NG	NG	NG
L-2271	*Massilia* sp.	NG	NG	NG	NG
L-2273	*Sphingomonas* sp.	NG	NG	NG	NG
L-2275	*Massilia* sp.	NG	NG	NG	NG
L-2276	*Massilia* sp.	NG	NG	NG	NG
L-2279	*Cryobacterium* sp.	γ	α	γ	NG
L-2285	*Cryobacterium* sp.	β−	β−	γ	γ
L-2290	*Herminiimonas* sp.	NG	NG	NG	NG
L-2291	*Flavobacterium* sp.	NG	NG	NG	NG
L-2430	*Frigoribacterium* sp.	γ	β	γ	β
L-2433	*Curtobacterium* sp.	β+	NG	β	NG
L-2552	*Sphingomonas* sp.	γ	NG	γ	NG
L-2553	*Pseudomonas graminis*	γ	NG	γ	NG
L-2554	*Pseudomonas* sp.	γ	NG	γ	NG
L-2558	*Polaromonas* sp.	γ	NG	γ	NG
L-2560	*Flavobacterium* sp.	γ	NG	γ	NG
L-2571	*Cryobacterium* sp.	β−	β	γ	β
L-2573	*Flavobacterium* sp.	NG	NG	NG	NG
L-2575	*Pseudomonas* sp.	γ	NG	γ	NG
L-2577	*Massilia* sp.	NG	NG	NG	NG
L-2578	*Pseudomonas* sp.	γ	γ	γ	γ
L-2580	*Cryobacterium* sp.	γ	β	γ	β
L-2643	*Pseudomonas* sp.	β−	γ	γ	γ
L-2644	*Pseudomonas fluorescens*	β+	β−	β+	β−
L-2646	*Pseudomonas graminis*	γ	γ	γ	γ
L-2649	*Sphingomonas* sp. (*glacialis*)	γ	NG	γ	NG
L-2650	*Pseudomonas* sp.	β+	NG	β+	NG
L-2652	*Pseudomonas frederiksbergensis*	γ	γ	γ	β
L-2653	*Massilia* sp.	γ	NG	γ	NG
L-2656	*Pseudomonas fluorescens*	β+	β	β	γ
L-2657	*Pseudomonas* sp.	β+	NG	β	β
L-2658	*Pseudomonas fluorescens*	β+	NG	β	NG
L-2659	*Pseudomonas* sp.	β+	NG	β+	NG
L-2694	*Sphingomonas* sp.	γ	β	γ	α−
L-2696	*Pseudomonas* sp.	β−	γ	γ	β
An34	*Leifsonia* sp.	γ	α−	γ	α−
An58	*Enterococcus* sp.	γ	α−	α	γ
S3	*Micromonospora* sp.	γ	β	γ	β
S7	*Bacillus* sp.	β	β	β	β
S8	*Microbacterium* sp.	γ	α−	γ	α−
S10	*Oerskovia* sp.	α	α	α	β
S23b	*Microbacterium* sp.	γ	α	γ	β
S24	*Brevibacterium* sp.	γ	β−	γ	α
S26	*Microbacterium* sp.	γ	α	α	α
S27b	*Carnobacterium* sp.	α	α−	α	γ
S32	*Tessaracoccus* sp.	γ	α	α−	α
S44	*Bacillus* sp.	γ	β+	γ	β+
S58	*Salinibacterium* sp.	γ	α−	γ	α
S60	*Microbacterium* sp.	γ	α−	γ	α
S70	*Bacillus* sp.	γ	α	γ	α
S71	*Bacillus* sp.	γ	α−	γ	β
N2	*Exiguobacterium* sp.	γ	α−	γ	α−
N7	*Paenibacillus* sp.	γ	γ	γ	γ
N18	*Micromonospora* sp.	β	β+	β	β
N23	*Bacillus* sp.	γ	β+	γ	β+
N24	*Bacillus* sp.	γ	β+	γ	β+
N28	*Streptomyces* sp.	β−	γ	β+	β
N34	*Bacillus* sp.	β	β+	β−	β
N36a	*Pedobacter* sp.	α	α	β+	α
N39	*Carnobacterium* sp.	α	β	α	γ
N40	*Pseudomonas* sp.	β+	NG	β	NG
N41	*Streptomyces* sp.	γ	NG	γ	NG
N42	*Streptomyces* sp.	α	β	γ	β
N54	*Psychrobacillus* sp.	γ	γ	γ	γ
N58	*Carnobacterium* sp.	α+	NG	α+	NG
N61	*Psychrobacter* sp.	γ	NG	γ	NG
N71	*Pseudomonas* sp.	β+	NG	β+	NG
N83	*Bacillus* sp.	γ	β	γ	β
N106	*Salinibacterium* sp.	γ	α−	γ	α−

Hemolytic phenotypes: α, α-hemolytic; β, β-hemolytic; γ, non-hemolytic; +, signifies a stronger phenotype; −, signifies a weaker phenotype; NG, no growth.

at the lower temperature the phenotypes were mostly non-hemolytic. Two isolates, S7 and N34, expressed β-hemolysis at both temperatures and on both blood types. Of the *Micromonospora* spp., strain N18 presented β-hemolytic activity at both temperatures and blood types, while strain S3 was β-hemolytic only at 37°C in both blood types. Isolates of *Carnobacterium* spp. displayed the strongest α hemolysis of all the tested bacteria (**Figure 2B**). Interestingly, isolates L-1994 (*Flavobacterium* sp.) and L-1995, (*Janthinobacterium* sp.), obtained from tap water from Svalbard, that also showed β-hemolytic activity and the only isolate belonging to the Enterobacteriaceae family (L-1980, *Raoultella* sp.) displayed a β-hemolytic activity at 37°C, whereas they were non-hemolytic at 15°C.

In general, isolates that were non-hemolytic on bovine blood plates were also non-hemolytic on sheep blood plates (**Table 2**) except for *Pseudomonas* spp. L-2652 (β-hemolytic only on sheep blood at 37°C) and L-2696 (β-hemolytic at 15°C on bovine blood and at 37°C on sheep blood), *Enterococcus* sp. An58 (α-hemolytic at 37°C on bovine and at 15°C on sheep blood), and *Pedobacter* sp. N36a (β-hemolytic at 15°C on sheep blood but α-hemolytic at 37°C and at both temperatures on bovine blood). About 30% of the isolates showed non-hemolytic phenotypes on both blood types, e.g., *Sphingomonas* sp., *Psychrobacillus* sp. Species belonging to the genera *Herminiimonas* sp. and *Massilia* sp. did not grow at any temperature or blood type used in this experiment. The three control strains displayed their corresponding hemolytic phenotype on blood agar plates.

Hemolytic Assay With Erythrocyte Suspension

The second experiment involved the observation of hemolytic activity of the ethanolic extracts of bacterial lysates in a short assay (within a 60-min time frame) using erythrocyte suspensions. The objective of this experiment was to determine the potential presence of membrane-active secondary metabolites which could be present in the tested bacteria, and which could contribute to the pathogenicity of the producing organism.

In the assays with bovine and sheep erythrocytes in suspension, only 5 extracts in total were hemolytic within 60 min of the assay: *Pseudomonas* sp. L-2644, L-2656, and L-2657 together with *Micromonospora* sp. S3 and N18 (**Figure 3** and **Supplementary Figure S1**). *Pseudomonas* spp. showed faster hemolytic reactions on both blood types, compared to *Micromonospora* sp. In general, for the *Pseudomonas* sp. extracts higher values of $1/t_{50}$ were observed in bovine blood compared to sheep blood (**Figure 3**). Ethanolic extracts of the three control species displaying the hemolytic phenotype on blood agar plates were inactive on erythrocytes in suspension.

Antimicrobial Susceptibility Test

In total, 118 isolates were tested for antimicrobial resistance. The plates were read as soon as colonies were detected on them and the results are presented in **Table 3** (summary) and **Supplementary Table S3** (all results), except for 14 isolates that did not grow on the used media or in the presence of any of the antimicrobials tested. TET was the most effective antimicrobial, with most isolates (95/104) being susceptible, followed by KAN (84/104 susceptible isolates). At the other end of the spectrum, IPM was the least effective antimicrobial at the used concentration, with only 21/104 susceptible isolates. Resistant strains to higher concentrations of imipenem are mostly from the genera *Flavobacterium*, *Enterococcus*, *Janthinobacterium*, *Raoultella*, and, notably, *Pseudomonas*. Interestingly, not all *Pseudomonas* spp. behave alike. For instance, strains L-2652 (closely related to *P. frederiksbergensis*) and L-2553 and L-2646 (both closely related to *P. graminis*) were not resistant to >4 m/L of imipenem in the media. The following IPM-resistant strains were also carbapenemase producers (OXA-48 and other carbapenemases such as KPC, MBL, or NDM): *Flavobacterium* sp. (L-1994), *Janthinobacterium* sp. L-1995, *Pseudomonas* sp. N71 (L-5704), L-1983, L-2137, L-2142, L-2145, L-2554, L-2265, L-2575, L-2578, L2643, L-2644, L2650, L-2656, L-2658, and *Raoultella* sp. L-1980 (**Supplementary Table S4**).

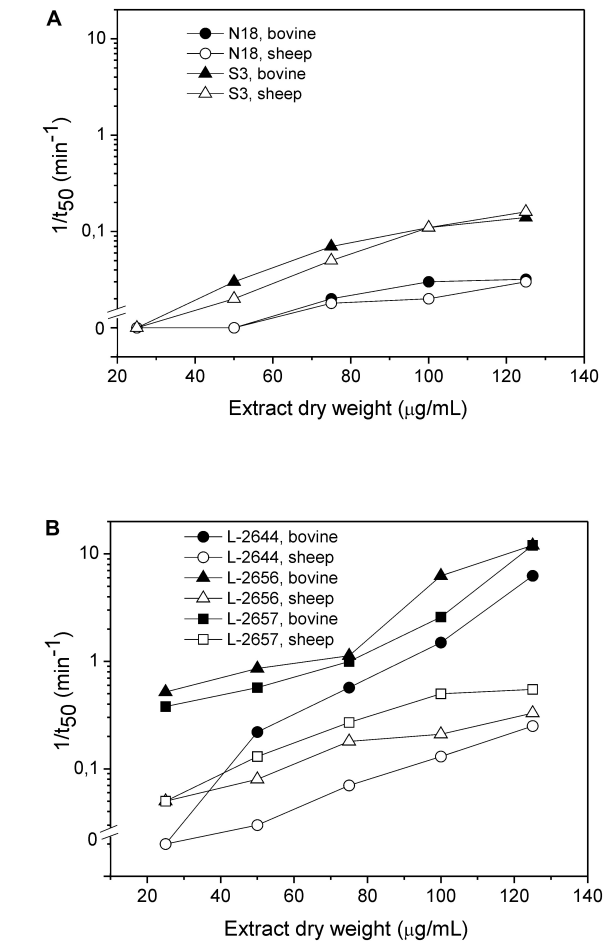

FIGURE 3 | Hemolytic activity of ethanolic extracts of *Micromonospora* sp. **(A)** and *Pseudomonas* sp. **(B)**. Dependence of the rate of hemolysis, $1/t_{50}$, on the dry extract concentration. The hemolytic activity was assayed against bovine (full symbols) and sheep (open symbols) erythrocytes.

TABLE 3 | Summary of results for antimicrobial susceptibility for the 104 isolates tested, showing number of isolates that are: − susceptible; (–) moderately susceptible; (+) moderately resistant; + resistant; M indicates the appearance of individual mutant colonies.

Summary	Growth	AMP	CHL	CIP	CTX	ERY	IPM	KAN	TET
−	17	74	77	47	41	64	21	84	95
(–)	9	2	4	11	9	6	13	9	7
(+)	11	1	1	5	5	7	9	4	0
+	67	27	22	17	49	27	61	6	2
M	0	0	0	24	0	0	0	1	0

After a week of incubation, resistant colonies (possible mutants) appeared only on plates containing CIP (24/104) and KAN (1/104). About 50% of the isolates (54/104) were resistant to CTX.

The species that were resistant to TET belonged to five genera only: *Pseudomonas* (L-1964, L-1983, L-2137, L-2142, and L-2643), *Janthinobacterium* (L-1995), *Oerskovia* (S10), *Flavobacterium* (L-1994), and *Rahnella* (L-2695). The isolates mentioned above (of which two were obtained from tap water), shared very similar antimicrobial resistance profiles, i.e., resistance to all antimicrobials tested except for KAN and individual mutant colonies for CIP.

All *Pseudomonas* sp. were resistant to multiple antimicrobials, including AMP, CHL, CTX, ERY, and IPM. However, the two isolates belonging to *Pseudomonas graminis* were susceptible to AMP, CHL, CIP, ERY, KAN, and TET. The majority (18/24) of individual mutant colonies were also observed among the *Pseudomonas* spp. isolates.

Generally, *Bacillus* spp. were susceptible to the majority of the antimicrobials tested (AMP, CHL, ERY, KAN, and TET), with a few exceptions in case of CIP, IPM, and CTX. *Micromonospora* spp. were predominantly susceptible to the antimicrobials tested, with resistance detected for CTX and ERY.

Isolates belonging to the Enterobacteriaceae family (i.e., *Rahnella* sp. L-2695 and *Raoultella* sp. L-1980) were resistant to AMP and IPM. Some isolates of the genera *Cryobacterium* (L-2062, L-2285, L-2571, and L-2580), *Massilia* (L-2271) and *Undibacterium* (L-2063 and L-2267), did not show growth on the control plates (nutrient agar without added antimicrobials) but generally showed better growth on the plates containing IPM.

DISCUSSION

Until recently, the Arctic represented a pristine environment, largely unaffected by anthropogenic influences. However, this geographic area is now experiencing the dramatic repercussions of climate change more than other regions on the planet (Intergovernmental Panel on Climate Change [IPCC], 2007). Due to its low adaptability, these consequences are amplified (Doney et al., 2012) and the stressful conditions they bring about might cause the release of environmental bacteria with potential virulence-associated phenotypes, e.g., compounds with hemolytic activity and antimicrobial resistance. Moreover, bacterial species in the short term are expected to come in contact more frequently with humans, animals, and plants outside of their current environments (Epstein, 2001; Cavicchioli et al., 2019; Hutchins et al., 2019).

Majority of Psychrotolerant Bacterial Isolates Are Able to Grow at 37°C

In this study, more than 70% of the culturable species obtained from the Arctic environmental samples were psychrotolerant, with an optimal growth temperature of about 15°C. Although a growth temperature range of 8–20°C (Moyer and Morita, 2007) should define psychrotolerant microorganisms, the majority of our psychrotolerant strains were able to grow at 37°C, indicating a broader range of temperature adaptation (Tindall, 2004). Interestingly, the 13 isolates obtained from incubation at 15–17°C that were not able to grow at 37°C might be considered as true psychrotolerants or true psychrophiles with slower growth rates at higher temperature, and a broader temperature growth range (Tindall, 2004; Moyer and Morita, 2007).

Environmental Strains Produce Compounds With Hemolytic Activity Expressed Differently at Low (15°C) and High (37°C) Temperatures

A considerable number of isolates in this study showed a hemolytic phenotype when cultured on blood agar plates, in accordance to recent reports (Mogrovejo-Arias et al., 2020). The type of blood used (bovine vs. sheep) did not affect hemolytic activity. Both α- and β-hemolytic phenotypes are considered as a virulence-associated determinant and of clinical relevance when assessing the significance of the hemolytic environmental species and/or strains (Bayley, 1997; Ramachandran, 2013).

While most of the bacterial isolates cultured on agar plates showed active growth, some genera (*Flavobacterium* sp., *Herminiimonas* sp., *Massilia* sp., *Sphingomonas* sp., and *Undibacterium* sp.) could not be assessed due to lack of growth, which was possibly inhibited by the high nutrient content of the culture medium used for this test (Tindall, 2004). In addition to an incubation temperature of 15°C, a suitable temperature for the growth of psychrotolerant bacteria, the blood agar plates were also incubated at 37°C in order to assess the hemolysis at a clinically relevant temperature and to investigate the influence of the temperature on the hemolysis activity. Several genera responded differently to the incubation temperature. For instance, *Pseudomonas* spp. had mostly hemolytic phenotypes at 15°C while *Bacillus* spp. expressed hemolytic activity mainly at 37°C. Differences in the hemolysins structures and modes

of action might explain that some of them have a lytic effect only above certain temperatures, at which the characteristics of erythrocyte membranes change due to increased membrane fluidity (Carr et al., 2001; Asam et al., 2015). Alternatively, the expression of hemolytic genes might be temperature-regulated (as described by Madrid et al., 2002) and could account for the differences observed in our experiments.

Pseudomonas sp. Organic Extracts Show Faster Hemolytic Response in Bovine Erythrocytes Suspension Than in Sheep Erythrocytes Within 60 min

Our study comprises a large and preliminary screening study of crude extracts where non-purified membrane-active compounds were present. To the best of our knowledge, it represents the first screening of this sort for hemolytic activity in Arctic environmental bacteria. The hemolytic activity of ethanolic extracts was tested in two types of erythrocyte suspensions: sheep and bovine. Sheep blood is commonly used as a standard for the determination of the hemolytic phenotype (Yeh et al., 2009; Atlas, 2010) and bovine erythrocytes have been previously used to determine the hemolytic capabilities of environmental extracts from different habitats and organisms (Sepčić et al., 2011).

The hemolytic potential of human-associated, pathogenic or opportunistic bacteria is regularly assessed using animal blood (Bevivino et al., 2002; González-Rodríguez et al., 2007) as it is suitable for carrying out microbiological tests used in routine identification and susceptibility profiling of known human pathogens (Yeh et al., 2009).

Anuclear, mature red blood cells are often used as a model to assess the membrane damage, either by monitoring the hemoglobin release or by measuring the turbidity of erythrocyte suspension. However, it should not be inferred that erythrocytes are the only target cells of the compounds observed in this study (Tomita and Kamio, 1997) given that hemolytic compounds can often also be cytolytic for cells of the immune system, e.g., macrophages and neutrophils (Asam et al., 2015), which, in the case of pathogenic organisms, greatly increases their potential virulence (Billington et al., 2000).

The discrepancies in membrane composition among different mammalian erythrocytes influence the hemolytic activity of hemolysins, which act by recognizing specific membrane lipids or membrane receptors (DuMont and Torres, 2014; Rojko and Anderluh, 2015). We observed that the lytic activity of the tested *Pseudomonas* sp. extracts was more pronounced on bovine erythrocytes than on the sheep ones (**Figure 3**). Red blood cell membranes from different mammals display different composition and physical characteristics (e.g., fluidity). Sheep erythrocytes contain a higher percentage of choline phospholipids (with sphingomyelin representing more than 50% of all the phospholipids) and acidic phospholipids, but a lower content of phosphatidylethanolamine compared to bovine erythrocytes (Bernheimer, 1974; Virtanen et al., 1998; Windberger et al., 2003). Cholesterol content, on the other hand, is higher in bovine red blood cells than in sheep ones (Nelson, 1967). Thus, the faster hemolytic reaction on bovine erythrocytes observed might be because the hemolytic compound(s) produced by the isolates in this study have greater affinity for cholesterol-enriched membrane domains.

Based on our results, the use of more than one type of blood is recommended as it widens the spectrum of observed hemolytic activities. Future research could benefit from the inclusion of assays with human blood, the results of which could be predicted to some extend based on similarities with the types of blood used in the present study.

Blood Agar and Turbidimetric Assays Highlight Different Compounds Responsible for Hemolysis

A greater number of isolates were found to have hemolytic activity on blood agar plates (around 30 isolates) vs. the activity of their ethanolic extracts on erythrocyte suspensions (5 isolates).

The culture conditions at which the isolates were grown in preparation for each test, i.e., solid media in agar plates vs. liquid media used for the suspension test, could account for the difference in the number of positive phenotypes as they directly affect gene expression (Favero et al., 2014).

Another possible explanation for such a remarkable difference between the tests is that each one assesses the presence of different compounds. Plates show the effects of a wider range of molecules produced by the bacteria in the course of their growth (e.g., proteinaceous endotoxins, exotoxins, pigments, and secondary metabolites). On the other hand, for the suspensions test, a limited selection of compounds was obtained in the extraction solvent (96% ethanol in this case). Ethanol allows the extraction of small, less polar molecules or secondary metabolites and likely excludes proteins (Sepčić et al., 2011). Crude extracts, moreover, might possess more than one hemolytically active and less polar compound, mainly acting as surfactants and whose function is independent of membrane lipid composition. This might explain the observed absence of hemolytic activity of the ethanolic extract of *S. pyogenes*, a bacterium commonly used as a positive β-hemolytic control in blood agar tests. In fact, the main hemolytic compounds characteristic of *S. pyogenes* are pore-forming proteinaceous cytotoxins streptolysin O and streptolysin S (Hynes and Sloan, 2016), which cannot be extracted with ethanol.

Finally, the growth phase of the culture at the moment of the test might vary, directly affecting the compounds produced by the bacteria. That is, compounds produced in actively growing cultures (for instance, liquid cultures) differ from those produced in cultures going through stationary phase (for instance, solid cultures).

Arctic Environmental Strains Show Widespread Resistance to Commercial Antimicrobials

Studying antimicrobial resistance profiles in Arctic isolates is gaining in importance since climate change is exerting a stronger pressure on this environment and higher temperatures are associated with increased antimicrobial resistance in common pathogens (Hutchins et al., 2019).

No breakpoint tables for Minimum Inhibitory Concentration or Zone Diameters have been established for Arctic species/strains (European Committee on Antimicrobial Susceptibility Testing [EUCAST], 2019). Therefore, the definition of resistance for these bacteria is difficult to ascertain. In this study, we performed screening for phenotypic resistance on media supplemented with antimicrobials as an indicator for the presence of resistance genes.

On one hand, we observed that a majority of the Arctic environmental isolates analyzed were resistant to at least one of the antimicrobials tested, suggesting a strong competitiveness in the habitat. Some isolates were resistant even toward broad-spectrum antimicrobials, such as ciprofloxacin and chloramphenicol. Similar results were found in other natural environments such as Antarctica (Tam et al., 2015), high-altitude wetlands in Argentina (Dib et al., 2008), and Siberia (Mindlin et al., 2008). On the other hand, almost all of the isolates were susceptible to tetracycline, contrary to what has been reported before for other cold environments (Perron et al., 2015). Since tetracycline could be naturally occurring in soils, such widespread susceptibility is surprising, but could be due to a lack of tetracycline producers in the Arctic. In accordance to our findings, Pal et al. (2016) reported that tetracycline resistance dominates human, human-impacted and animal microbiomes but not so far natural environments. The mutant phenotypes observed for ciprofloxacin are usually induced by low concentrations of this antimicrobial (Cirz and Romesberg, 2006).

Resistance to some antibiotics can occur quickly during selective enrichment, predominantly that which is triggered by point mutations in housekeeping genes, e.g., ribosomal proteins and efflux pumps. Accordingly, growth observed in plates containing ciprofloxacin, erythromycin, and kanamycin has been cautiously interpreted. The constant appearance of a low number of individual, presumably mutant, colonies is indicated in **Supplementary Table S3**.

Isolates belonging to the genus *Pseudomonas* were the ones with the strongest multidrug-resistant abilities, showing marked resistance tetracycline, and with frequent occurrence of individual mutant ciprofloxacin resistant colonies. Correspondingly, *Pseudomonas* spp. isolated from Antarctica showed a variety of antimicrobial resistant profiles (Tam et al., 2015). *Pseudomonas* sp. are known for its extended resistances to antimicrobials (European Committee on Antimicrobial Susceptibility Testing [EUCAST], 2019) and are known to possess capsules that might aid in lowering the concentration of antimicrobial that reaches the cells. In addition, *Pseudomonas* sp. possess efflux pumps which contribute to the multidrug resistance phenotype and might explain the mutant phenotypes observed (Okamoto et al., 2002; Aeschlimann, 2003). Even though efflux pumps can be also associated with other functions in the cell, the responsible genes can be transferred to other environments and into other species where the resistance phenotype becomes of clinical relevance (Graham et al., 2019).

Resistance to cefotaxime was observed in 50% of our isolates. Resistant phenotypes against this extended-spectrum β-lactam is considered of clinical relevance (Mir et al., 2016), especially among Gram-negative species and notoriously resistant *Pseudomonas* sp.

Finally, we observed that the concentration of imipenem used in this study favored, rather than inhibited, the growth of several isolates, notably *Massilia* sp. and *Cryobacterium* sp. As far as we can tell from searching the available literature, such observation hasn't been reported yet. Phenotypic resistance to imipenem is of high importance since carbapenemase-producing bacteria have become a major public health concern worldwide. In this study, we identified carbapenem resistant bacteria and predicted carbapenem resistance mechanisms (CRM) and the subsequent potential for horizontal spread. While the best known and currently most important CRM have been described in members of the Enterobacteriaceae family and for *Pseudomonas aeruginosa*, literature data about CRM in Gram-positive bacteria is scarce.

We have observed a variety of resistotypes for carbapenem resistance (CR) among several, but not all, *Bacillus* sp. isolates. Further, we retrieved CR isolates from the genera *Cryobacterium*, *Leifsonia*, and *Streptomyces*. This observation, in accordance with CR in Gram-positive bacteria, is likely the result of substitutions in amino acid sequences of penicillin-binding proteins (PBPs) or acquisition/production of new carbapenem-resistant PBPs (Papp-Wallace et al., 2011). Although chromosomally encoded, these alleles could spread horizontally by transformation or transduction.

Acquired carbapenem resistance in Gram-negative bacteria is a consequence of enzymatic inactivation of the drug, target site mutation and efflux pumps (Codjoe and Donkor, 2018). We hypothesize on putative resistance mechanisms on the basis of the most commonly described mechanism for strains of the same species/genus or other closely related bacteria, and our results of differential growth on nutrient agar plates supplemented with different concentrations of imipenem and commercial CHROMID® CARBA SMART agar plates. The majority of carbapenem resistant *Pseudomonas* isolates grew in plates containing 4–10 mg/L of imipenem and on both sections of the CARBA SMART plates. This indicates the presence of putative carbapenemase enzymes. *Pseudomonas* sp. L-2696, grew on nutrient agar plates with 10 mg/L of imipenem but not on CARBA SMART plates, indicating putative efflux pumps and/or target site mutation. Further studies, including cloning, would clarify the possibility and subsequent threat of horizontal transfer to clinically important *Pseudomonas* strains. *Flavobacterium* sp. L-1994 grew on both CARBA SMART sections, thus possibly encoding a carbapenemase. Naas et al. (2003) described the JOHN-1 β- metallo-β-lactamase from an *Flavobacterium johnsoniae*, an environmental plant pathogen which can also cause skin lesions in fish (Naas et al., 2003) and Kuai et al. (2011) described a KPC-2 enzyme from a *Flavobacterium odoratum* strain (Kuai et al., 2011). Carbapenemase genes have also been described from other members of the Flavobacteriaceae family, such as the chromosome-encoded metallo-β-lactamases MUS-1 and MUS-2 in *Myroides* and carbapenemases from *Chryseobacterium* strains (Al-Bayssari et al., 2015; Gudeta et al., 2016). *Janthinobacterium* sp. L-1995 grew on nutrient agar plates with imipenem at concentrations up to 4 mg/L and on both

media on CARBA SMART plates. Carbapenem resistance in member of this genus has been described by Rossolini et al. (2001) and also observed by Gudeta et al. (2016). The described carbapenemases were chromosomally encoded and not proven yet to be horizontally transferable. The most interesting isolates, given the relatedness to carbapenem resistant Enterobacteriaceae are *Rahnella* sp. L-2695 and *Raoultella ornithinolytica* L-1980. The former was negative for carbapenemase and positive for OXA-48-like hydrolytic activity and the later was positive for both. Besides the fact, that the presence of carbapenemases genes has been confirmed several times for *Raoultella* spp. a large plasmid carrying genes for NDM-1- and CTX-M-3 β-lactamases, has been detected in a carbapenemase-producing *R. ornithinolytica* strain from stool samples recently (Wang et al., 2019). Particularly interesting is the *Rahnella* sp. isolate L-2695, since it is, in addition to showing OXA-48-like carbapenemase activity, one of only two tetracycline resistant isolates. Integrons and chromosomal extended-spectrum class A β-lactamase have already been described in members of this genus (Ruimy et al., 2010; Koczura et al., 2016). To summarize; we predict chromosome encoded β-lactamases for the majority of the isolated imipenem resistant strains. According to literature data, the presence of plasmid or phage encoded resistance genes is less likely. Nevertheless, horizontal transfer events of resistance genes is a possible event, predominantly through transduction by phages.

CONCLUSION

To the best of our knowledge, this study is among the first screenings of Arctic environmental bacteria for hemolytic activity, a common bacterial virulence-associated phenotype, in extreme habitats. Hemolytic activity was temperature-dependent and observed in a third of the tested isolates on blood agar plates with both sheep and bovine blood types. In erythrocyte suspensions, the hemolysis occurred only in five isolates belonging to genera *Pseudomonas* and *Micromonospora*. The type of erythrocytes appears to influence the reaction time for the hemolytic compounds, as bovine blood was more readily lysed than sheep blood with *Pseudomonas* sp. extracts. In addition, the Arctic strains tested showed resistance to several commonly used and clinically relevant antimicrobials. However, the number of kanamycin and tetracycline resistant strains was rather low. Imipenem was the antimicrobial with most resistant isolates, possibly due to the low concentration tested or the widespread presence of chromosome encoded β-lactamases. In the context of our study, *Pseudomonas* was the genus with the highest potential clinical relevance: hemolytic on blood agar plates, hemolytic on erythrocyte suspensions and with a broad resistance profile to the antimicrobials tested. Studying potential pathogenic phenotypes of environmental strains provides insights into possible evolutionary adaptations and origins of clinically relevant bacteria and helps assessing the possible threats Arctic bacteria represent in other environments.

DATA AVAILABILITY STATEMENT

The datasets generated for this study can be found in GenBank with the following accession numbers: MK453054–MK453127, MK670504–MK670553, MN161207–MN161227, MH714605–MH714685, and MN450679–MN450730.

AUTHOR CONTRIBUTIONS

DM and LP collected the samples, performed the wet lab analyses, interpreted the data, and wrote the manuscript with input from all co-authors. CG, MT, JA-A, and KS designed and guided the execution of all experiments. MT and JA-A performed additional experiments with the imipenem-resistant strains. FB and NG-C supervised the project and contributed to the interpretation of the results and valuable discussion.

FUNDING

This project has received funding from the European Union's Horizon 2020 Research and Innovation Programme under the Marie Skłodowska-Curie grant agreement no. 675546. We acknowledge the financial support from the Slovenian Research Agency to the Infrastructural Centre Mycosmo (MRIC UL) and to the programs P1-0170 and P1-0207. We further acknowledge support from the United Kingdom Natural Environment Research Council Consortium Grant 'Black and Bloom' (NE/M021025/1).

SUPPLEMENTARY MATERIAL

The Supplementary Material for this article can be found online at: https://www.frontiersin.org/articles/10.3389/fmicb.2020.00570/full#supplementary-material

REFERENCES

Aeschlimann, J. R. (2003). The role of multidrug efflux pumps in the antibiotic resistance of *Pseudomonas aeruginosa* and other gram-negative bacteria. *Pharmacotherary* 23, 916–924. doi: 10.1592/phco.23.7.916.32722

Agnew, A., Wang, J., Fanning, S., Bearhop, S., and Mcmahon, B. J. (2016). Insights into antimicrobial resistance among long distance migratory East Canadian High Arctic light-bellied Brent geese (*Branta bernicla hrota*). *Ir. Vet. J.* 69:13. doi: 10.1186/s13620-016-0072-7

Al-Bayssari, C., Gupta, S. K., Dabboussi, F., Hamze, M., and Rolain, J. M. (2015). MUS-2, a novel variant of the chromosome-encoded β-lactamase MUS-1, from *Myroides odoratimimus*. *New Microbes New Infect.* 7, 67–71. doi: 10.1016/j.nmni.2015.06.007

Altizer, S., Ostfeld, R. S., Johnson, P. T. J., Kutz, S., and Harvell, C. D. (2013). Climate change and infectious diseases: from evidence to a predictive framework. *Science* 341, 514–519. doi: 10.1126/science.1239401

Amato, P., Hennebelle, R., Magand, O., Sancelme, M., Delort, A. M., Barbante, C., et al. (2007). Bacterial characterization of the snow cover at Spitzberg, Svalbard. *FEMS Microbiol. Ecol.* 59, 255–264. doi: 10.1111/j.1574-6941.2006.00198.x

Anesio, A. M., and Laybourn-Parry, J. (2012). Glaciers and ice sheets as a biome. *Trends Ecol. Evol.* 27, 219–225. doi: 10.1016/j.tree.2011.09.012

Asam, D., Mauerer, S., and Spellerberg, B. (2015). Streptolysin S of *Streptococcus anginosus* exhibits broad-range hemolytic activity. *Med. Microbiol. Immunol.* 204, 227–237. doi: 10.1007/s00430-014-0363-0

Atlas, R. (2010). *Handbook of Microbiological Media*, 4th Edn. Washington, D.C: ASM Press, doi: 10.1201/ebk1439804063

Bayley, H. (1997). Toxin structure: part of a hole? *Curr. Biol.* 7, R763–R767. doi: 10.1016/S0960-9822(06)00399-X

Bernheimer, A. (1974). Interactions between membranes and cytolytic bacterial toxins. *Biochim. Biophys. Acta* 344, 27–50. doi: 10.1016/0304-4157(74)90007-0

Bevivino, A., Dalmastri, C., Tabacchioni, S., Chiarini, L., Belli, M. L., Piana, S., et al. (2002). *Burkholderia cepacia* Complex Bacteria from Clinical and Environmental Sources in Italy: Genomovar Status and Distribution of Traits Related to Virulence and Transmissibility. *J. Clin. Microbiol.* 40, 846–851. doi: 10.1128/JCM.40.3.846-851.2002

Bhakdi, S., Grimminger, F., Suttorp, N., Walmrath, D., and Seeger, W. (1994). Proteinaceous bacterial toxins and pathogenesis of sepsis syndrome and septic shock: the unknown connection. *Med. Microbiol. Immunol.* 183, 343–344. doi: 10.1007/BF00196684

Billington, S. J., Jost, B. H., and Songer, J. G. (2000). Thiol-activated cytolysins: structure, function and role in pathogenesis. *FEMS Microbiol. Lett.* 182, 197–205. doi: 10.1016/S0378-1097(99)00536-4

Bullen, J. J., Rogers, H. J., Spalding, P. B., and Ward, C. G. (2005). Iron and infection: the heart of the matter. *FEMS Immunol. Med. Microbiol.* 43, 325–330. doi: 10.1016/j.femsim.2004.11.010

Buxton, R. (2005). *Blood Agar Plates and Hemolysis Protocols*. Available online at: https://www.asm.org/getattachment/7ec0de2b-bb16-4f6e-ba07-2aea25a43e76/protocol-2885.pdf (accessed December 19, 2018).

Carr, A., Sledjeski, D. D., Podbielski, A., Boyle, M. D. P., and Kreikemeyer, B. (2001). Similarities between Complement-mediated and Streptolysin S-mediated Hemolysis. *J. Biol. Chem.* 276, 41790–41796. doi: 10.1074/jbc.M107401200

Cavicchioli, R., Ripple, W. J., Timmis, K. N., Azam, F., Bakken, L. R., Baylis, M., et al. (2019). Scientists' warning to humanity: microorganisms and climate change. *Nat. Rev. Microbiol.* 17, 569–586. doi: 10.1038/s41579-019-0222-5

Cirz, R. T., and Romesberg, F. E. (2006). Induction and inhibition of ciprofloxacin resistance-conferring mutations in hypermutator bacteria. *Antimicrob. Agents Chemother.* 50, 220–225. doi: 10.1128/AAC.50.1.220-225.2006

Codjoe, F., and Donkor, E. (2018). Carbapenem resistance: a review. *Med. Sci.* 6:1. doi: 10.3390/medsci6010001

Davies, J., and Davies, D. (2010). Origins and evolution of antibiotic resistance. *Microbiol. Mol. Biol. Rev.* 74, 417–433. doi: 10.1128/MMBR.00016-10

Dib, J., Motok, J., Zenoff, V. F., Ordoñez, O., and Farías, M. E. (2008). Occurrence of resistance to antibiotics, UV-B, and arsenic in bacteria isolated from extreme environments in high-altitude (above 4400 m) Andean wetlands. *Curr. Microbiol.* 56, 510–517. doi: 10.1007/s00284-008-9103-2

Doney, S. C., Ruckelshaus, M., Emmett Duffy, J., Barry, J. P., Chan, F., English, C. A., et al. (2012). Climate change impacts on marine ecosystems. *Annu. Rev. Mar. Sci.* 4, 11–37. doi: 10.1146/annurev-marine-041911-111611

DuMont, A. L., and Torres, V. J. (2014). Cell targeting by the *Staphylococcus aureus* pore-forming toxins: It's not just about lipids. *Trends Microbiol.* 22, 21–27. doi: 10.1016/j.tim.2013.10.004

Edgar, R. C. (2004). MUSCLE: multiple sequence alignment with high accuracy and high throughput. *Nucleic Acids Res.* 32, 1792–1797. doi: 10.1093/nar/gkh340

Edwards, A. (2015). Coming in from the cold: potential microbial threats from the terrestrial cryosphere. *Front. Earth Sci.* 3:12. doi: 10.3389/feart.2015.00012

Epstein, P. R. (2001). Climate change and emerging infectious diseases. *Microbes Infect.* 3, 747–754. doi: 10.1016/S1286-4579(01)01429-0

European Committee on Antimicrobial Susceptibility Testing [EUCAST] (2019). *Breakpoint Tables for Interpretation of MICs and Zone Diameters - Version 9.0*. Available online at: http://www.eucast.org

Favero, D., Furlaneto-Maia, L., França, E. J. G., Góes, H. P., and Furlaneto, M. C. (2014). Hemolytic factor production by clinical isolates of *Candida* species. *Curr. Microbiol.* 68, 161–166. doi: 10.1007/s00284-013-0459-6

González-Rodríguez, N., Santos, J. A., Otero, A., and García-López, M.-L. (2007). Cell-associated hemolytic activity in environmental strains of *Plesiomonas shigelloides* expressing cell-free, iron-influenced extracellular hemolysin. *J. Food Prot.* 70, 885–890. doi: 10.4315/0362-028X-70.4.885

Graham, D. W., Bergeron, G., Bourassa, M. W., Dickson, J., Gomes, F., Howe, A., et al. (2019). Complexities in understanding antimicrobial resistance across domesticated animal, human, and environmental systems. *Ann. N. Y. Acad. Sci.* 1441, 17–30. doi: 10.1111/nyas.14036

Gudeta, D. D., Bortolaia, V., Amos, G., Wellington, E. M. H., Brandt, K. K., Poirel, L., et al. (2016). The soil microbiota harbors a diversity of carbapenem-hydrolyzing β-lactamases of potential clinical relevance. *Antimicrob. Agents Chemother.* 60, 151–161. doi: 10.1128/AAC.01424-15

Hutchins, D. A., Jansson, J. K., Remais, J. V., Rich, V. I., Singh, B. K., and Trivedi, P. (2019). Climate change microbiology — problems and perspectives. *Nat. Rev. Microbiol.* 17, 391–396. doi: 10.1038/s41579-019-0178-5

Hynes, W., and Sloan, M. (2016). "Secreted extracellular virulence factors," in *Streptococcus pyogenes: Basic Biology to Clinical Manifestations*, eds J. Ferretti, D. Stevens, and V. Fischetti (Oklahoma City: University of Oklahoma Health Sciences Center), 1–40.

Intergovernmental Panel on Climate Change [IPCC] (2007). "Climate change 2007: impacts, adaptation and vulnerability," in *Contribution of Working Group II to the Fourth Assessment Report of the Intergovernmental Panel on Climate Change*, eds M. L. Parry, O. F. Canziani, J. P. Palutikof, P. J. van der Linden, and C. E. Hanson (Cambridge: Cambridge University Press). doi: 10.1256/004316502320517344

Koczura, R., Mokracka, J., and Makowska, N. (2016). Environmental Isolate of *Rahnella aquatilis* Harbors Class 1 Integron. *Curr. Microbiol.* 72, 64–67. doi: 10.1007/s00284-015-0917-4

Krajick, K. (2001). Arctic life, on thin ice. *Science* 291, 424–425. doi: 10.1126/science.291.5503.424

Kuai, S., Huang, L., Pei, H., Chen, Y., and Liu, J. (2011). Imipenem resistance due to class a carbapenemase KPC-2 in a *Flavobacterium odoratum* isolate. *J. Med. Microbiol.* 60, 1408–1409. doi: 10.1099/jmm.0.029660-0

Kumar, S., Stecher, G., and Tamura, K. (2016). MEGA7: molecular evolutionary genetics analysis version 7.0 for bigger datasets. *Mol. Biol. Evol.* 33, 1870–1874. doi: 10.1093/molbev/msw054

Kurane, I. (2010). The effect of global warming on infectious diseases. *Public Health Res. Perspect.* 1, 4–9. doi: 10.1016/j.phrp.2010.12.004

Litwin, C. M., and Calderwood, S. B. (1993). Role of iron in regulation of virulence genes. *Clin. Microbiol. Rev.* 6, 137–149. doi: 10.1128/CMR.6.2.137

Livermore, D. M. (2003). Bacterial resistance: origins, epidemiology, and impact. *Clin. Infect. Dis.* 36, S11–S23. doi: 10.1086/344654

Madigan, M. T., Martinko, J., Stahl, D., and Clarck, D. (2012). *Brock Biology of Microorganisms*, 13th Edn. San Francisco, CA: Pearson Higher Education.

Madrid, C., Nieto, J. M., Paytubi, S., Falconi, M., Gualerzi, C. O., and Juárez, A. (2002). Temperature- and H-NS-dependent regulation of a plasmid-encoded virulence operon expressing *Escherichia coli* hemolysin. *J. Bacteriol.* 184, 5058–5066. doi: 10.1128/JB.184.18.5058-5066.2002

Marshall, B. M., Ochieng, D. J., and Levy, S. B. (2009). Commensals: underappreciated reservoir of antibiotic resistance. *Microbe* 4, 231–238. doi: 10.1128/microbe.4.231.1

Martínez, J. L. (2008). Antibiotics and antibiotic resistance genes in natural environments. *Science* 321, 365–367. doi: 10.1126/science.1159483

McCann, C. M., Christgen, B., Roberts, J. A., Su, J.-Q., Arnold, K., Gray, N. D., et al. (2019). Understanding drivers of antibiotic resistance genes in High Arctic soil ecosystems. *Environment* 125, 497–504. doi: 10.1016 j.envint.2019.01.034 doi: 10.1016/j.envint.2019.01.034

Messenger, A. J. M., and Barclay, R. (1983). Bacteria, iron and pathogenicity. *Biochem. Mol. Biol. Educ.* 11, 54–63. doi: 10.1016/0307-4412(83)90042-0

Mindlin, S. Z., Soina, V. S., Petrova, M. A., and Gorlenko, Z. M. (2008). Isolation of Antibiotic Resistance Bacterial Strains from Eastern Siberia Permafrost Sediments. *Russ. J. Genet.* 44, 27–34. doi: 10.1134/S1022795408010043

Mir, R. A., Weppelmann, T. A., Johnson, J. A., Archer, D., Morris, J. G., and Jeong, K. C. C. (2016). Identification and characterization of cefotaxime resistant bacteria in beef cattle. *PLoS One* 11:e0163279. doi: 10.1371/journal.pone.0163279

Mogrovejo-Arias, D. C., Brill, F. H. H., and Wagner, D. (2020). Potentially pathogenic bacteria isolated from diverse habitats in Spitsbergen, Svalbard. *Environ. Earth Sci.* 79:109. doi: 10.1007/s12665-020-8853-4

Moyer, C. L., and Morita, R. Y. (2007). *Psychrophiles and Psychrotrophs. Encyclopedia of Life Scienes*. New York, NY: John Wiley & Sons, Ltd, doi: 10.1002/9780470015902.a0000402.pub2

Naas, T., Bellais, S., and Nordmann, P. (2003). Molecular and biochemical characterization of a carbapenem-hydrolysing β-lactamase from *Flavobacterium johnsoniae*. *J. Antimicrob. Chemother.* 51, 267–273. doi: 10.1093/jac/dkg069

Nelson, G. J. (1967). Lipid composition of erythrocytes in various mammalian species. *Biochim. Biophys. Acta* 144, 221–232. doi: 10.1016/0005-2760(67)90152-X

Okamoto, K., Gotoh, N., and Nishino, T. (2002). Extrusion of penem antibiotics by multicomponent efflux systems MexAB-OprM, MexCD-OprJ, and MexXY-OprM of *Pseudomonas aeruginosa*. *Antimicrob. Agents Chemother.* 46, 2696–2699. doi: 10.1128/aac.46.8.2696-2699.2002

Pal, C., Bengtsson-Palme, J., Kristiansson, E., and Larsson, D. G. J. (2016). The structure and diversity of human, animal and environmental resistomes. *Microbiome* 4, 1–15. doi: 10.1186/s40168-016-0199-5

Papp-Wallace, K. M., Endimiani, A., Taracila, M. A., and Bonomo, R. A. (2011). Carbapenems: past, present, and future. *Antimicrob. Agents Chemother.* 55, 4943–4960. doi: 10.1128/AAC.00296-11

Perini, L., Gostinčar, C., Anesio, A. M., Williamson, C., Tranter, M., and Gunde-Cimerman, N. (2019a). Darkening of the Greenland ice sheet: Fungal abundance and diversity are associated with algal bloom. *Front. Microbiol.* 10:557. doi: 10.3389/fmicb.2019.00557

Perini, L., Gostinčar, C., and Gunde-Cimerman, N. (2019b). Fungal and bacterial diversity of Svalbard subglacial ice. *Sci. Rep.* 9:20230. doi: 10.1038/s41598-019-56290-5

Perron, G. G., Whyte, L., Turnbaugh, P. J., Goordial, J., Hanage, W. P., Dantas, G., et al. (2015). Functional characterization of bacteria isolated from ancient arctic soil exposes diverse resistance mechanisms to modern antibiotics. *PLoS One* 10:e0069533. doi: 10.1371/journal.pone.0069533

Post, E., Forchhammer, M. C., Bret-Harte, M. S., Callaghan, T. V., Christensen, T. R., Fox, A. D., et al. (2009). Ecological dynamics across the Arctic associated with recent climate change. *Science* 325, 1355–1358. doi: 10.1126/science.1173113

Ramachandran, G. (2013). Gram-positive and gram-negative bacterial toxins in sepsis: a brief review. *Virulence* 5, 213–218. doi: 10.4161/viru.27024

Rojko, N., and Anderluh, G. (2015). How lipid membranes affect pore forming toxin activity. *Acc. Chem. Res.* 48, 3073–3079. doi: 10.1021/acs.accounts.5b00403

Rossolini, G. M., Condemi, M. A., Pantanella, F., Docquier, J., Amicosante, G., Molecolare, B., et al. (2001). Metallo β-lactamase producers in environmental microbiota: new molecular class B enzyme in *Janthinobacterium lividum*. *Antimicrob. Agents Chemother.* 45, 837–844. doi: 10.1128/aac.45.3.837-844.2001

Ruimy, R., Meziane-cherif, D., Momcilovic, S., Arlet, G., Andremont, A., Courvalin, P., et al. (2010). RAHN-2, a chromosomal extended-spectrum class A b -lactamase from *Rahnella aquatilis*. *J. Antimicrob. Chemother.* 65, 1619–1623. doi: 10.1093/jac/dkq178

Sepčić, K., Zalar, P., and Gunde-Cimerman, N. (2011). Low water activity induces the production of bioactive metabolites in halophilic and halotolerant fungi. *Mar. Drugs* 9, 43–58. doi: 10.3390/md9010043

Tam, H. K., Wong, C. M. V. L., Yong, S. T., Blamey, J., and González, M. (2015). Multiple-antibiotic-resistant bacteria from the maritime Antarctic. *Polar Biol.* 38, 1129–1141. doi: 10.1007/s00300-015-1671-6

Tindall, B. J. (2004). Prokaryotic diversity in the Antarctic: the tip of the iceberg. *Microb. Ecol.* 47, 271–283. doi: 10.1007/s00248-003-1050-7

Tomita, T., and Kamio, Y. (1997). Molecular biology of the pore-forming cytolysins from *Staphylococcus aureus*, alpha- and gamma-hemolysins and leukocidin. *Biosci. Biotechnol. Biochem.* 61, 565–572. doi: 10.1271/bbb.61.565

van Duin, D., and Doi, Y. (2017). The global epidemiology of carbapenemase-producing Enterobacteriaceae. *Virulence* 8, 460–469. doi: 10.1080/21505594.2016.1222343

Virtanen, J. A., Cheng, K. H., and Somerharju, P. (1998). Phospholipid composition of the mammalian red cell membrane can be rationalized by a superlattice model. *Proc. Natl. Acad. Sci. U.S.A.* 95, 4964–4969. doi: 10.1073/pnas.95.9.4964

Wang, S., Xu, L., Chi, X., Li, Y., Kou, Z., Hou, P., et al. (2019). Emergence of NDM-1- and CTX-M-3- producing *Raoultella ornithinolytica* in human gut microbiota bacterial isolation and identification. *Front. Microbiol.* 10:2678. doi: 10.3389/fmicb.2019.02678

Wiebe, W. J., Sheldon, W. M., and Pomeroy, L. R. (1992). Bacterial growth in the cold: evidence for an enhanced substrate requirement. *Appl. Environ. Microbiol.* 58, 359–364. doi: 10.1128/aem.58.1.359-364.1992

Windberger, U., Bartholovitsch, A., Plasenzotti, R., Korak, K. J., and Heinze, G. (2003). Whole blood viscosity, plasma viscosity and erythrocyte aggregation in nine mammalian species: reference values and comparison of data. *Exp. Physiol.* 88, 431–440. doi: 10.1113/eph8802496

World Health Organization [WHO] (2014). *Antimicrobial Resistance Global Report on Surveillance*. Geneva: World Health Organization.

Yeh, E., Pinsky, B. A., Banaei, N., and Baron, E. J. (2009). Hair sheep blood, citrated or defibrinated, fulfills all requirements of blood agar for diagnostic microbiology laboratory tests. *PLoS One* 4:e6141. doi: 10.1371/journal.pone.0006141

Yuan, M., Yu, Y., Li, H. R., Dong, N., and Zhang, X. H. (2014). Phylogenetic diversity and biological activity of Actinobacteria isolated from the Chukchi Shelf marine sediments in the Arctic ocean. *Mar. Drugs* 12, 1281–1297. doi: 10.3390/md12031281

Zughaier, S. M., and Cornelis, P. (2018). Editorial: role of iron in bacterial pathogenesis. *Front. Cell. Infect. Microbiol.* 8:344. doi: 10.3389/fcimb.2018.00344

Conflict of Interest: DM was employed by Dr. Brill + Partner GmbH as part of a research network (European Union's Horizon 2020 Research and Innovation Programme, Marie Skłodowska-Curie grant agreement no. 675546). FB is Managing Director of Dr. Brill + Partner GmbH.

The remaining authors declare that the research was conducted in the absence of any commercial or financial relationships that could be construed as a potential conflict of interest.

frontiers in Microbiology

ORIGINAL RESEARCH
published: 15 April 2020
doi: 10.3389/fmicb.2020.00669

Patterns in Microbial Assemblages Exported From the Meltwater of Arctic and Sub-Arctic Glaciers

Tyler J. Kohler[1,2], Petra Vinšová[1], Lukáš Falteisek[1], Jakub D. Žárský[1], Jacob C. Yde[3], Jade E. Hatton[4], Jon R. Hawkings[5,6], Guillaume Lamarche-Gagnon[4], Eran Hood[7], Karen A. Cameron[8] and Marek Stibal[1]*

[1] Department of Ecology, Faculty of Science, Charles University, Prague, Czechia, [2] Stream Biofilm and Ecosystem Research Laboratory, School of Architecture, Civil and Environmental Engineering, École Polytechnique Fédérale de Lausanne, Lausanne, Switzerland, [3] Department of Environmental Sciences, Western Norway University of Applied Sciences, Sogndal, Norway, [4] School of Earth Sciences, University of Bristol, Bristol, United Kingdom, [5] National High Magnetic Field Laboratory, Department of Earth, Ocean & Atmospheric Science, Florida State University, Tallahassee, FL, United States, [6] GFZ German Research Centre for Geosciences, Potsdam, Germany, [7] Department of Natural Sciences, University of Alaska Southeast, Juneau, AK, United States, [8] Institute of Biological, Environmental and Rural Sciences, Faculty of Earth and Life Sciences, Aberystwyth University, Aberystwyth, United Kingdom

OPEN ACCESS

Edited by:
David Anthony Pearce, Northumbria University, United Kingdom

Reviewed by:
Trista J. Vick-Majors, Michigan Technological University, United States
Jon Telling, Newcastle University, United Kingdom

***Correspondence:**
Tyler J. Kohler
tyler.j.kohler@gmail.com

Specialty section:
This article was submitted to Extreme Microbiology, a section of the journal Frontiers in Microbiology

Received: *27 December 2019*
Accepted: *24 March 2020*
Published: *15 April 2020*

Citation:
Kohler TJ, Vinšová P, Falteisek L, Žárský JD, Yde JC, Hatton JE, Hawkings JR, Lamarche-Gagnon G, Hood E, Cameron KA and Stibal M (2020) Patterns in Microbial Assemblages Exported From the Meltwater of Arctic and Sub-Arctic Glaciers. Front. Microbiol. 11:669. doi: 10.3389/fmicb.2020.00669

Meltwater streams connect the glacial cryosphere with downstream ecosystems. Dissolved and particulate matter exported from glacial ecosystems originates from contrasting supraglacial and subglacial environments, and exported microbial cells have the potential to serve as ecological and hydrological indicators for glacial ecosystem processes. Here, we compare exported microbial assemblages from the meltwater of 24 glaciers from six (sub)Arctic regions – the southwestern Greenland Ice Sheet, Qeqertarsuaq (Disko Island) in west Greenland, Iceland, Svalbard, western Norway, and southeast Alaska – differing in their lithology, catchment size, and climatic characteristics, to investigate spatial and environmental factors structuring exported meltwater assemblages. We found that 16S rRNA gene sequences of all samples were dominated by the phyla Proteobacteria, Bacteroidetes, and Actinobacteria, with Verrucomicrobia also common in Greenland localities. Clustered OTUs were largely composed of aerobic and anaerobic heterotrophs capable of degrading a wide variety of carbon substrates. A small number of OTUs dominated all assemblages, with the most abundant being from the genera *Polaromonas*, *Methylophilus*, and *Nitrotoga.* However, 16–32% of a region's OTUs were unique to that region, and rare taxa revealed unique metabolic potentials and reflected differences between regions, such as the elevated relative abundances of sulfur oxidizers *Sulfuricurvum* sp. and *Thiobacillus* sp. at Svalbard sites. Meltwater alpha diversity showed a pronounced decrease with increasing latitude, and multivariate analyses of assemblages revealed significant regional clusters. Distance-based redundancy and correlation analyses further resolved associations between whole assemblages and individual OTUs with variables primarily corresponding with the sampled regions. Interestingly, some OTUs indicating specific metabolic processes were not strongly associated with corresponding meltwater characteristics (e.g., nitrification and inorganic nitrogen concentrations). Thus, while exported assemblage structure appears regionally specific, and probably reflects

differences in dominant hydrological flowpaths, OTUs can also serve as indicators for more localized microbially mediated processes not captured by the traditional characterization of bulk meltwater hydrochemistry. These results collectively promote a better understanding of microbial distributions across the Arctic, as well as linkages between the terrestrial cryosphere habitats and downstream ecosystems.

Keywords: glacial runoff, 16S rRNA gene, polar stream, biogeography, cryosphere, hydrology

INTRODUCTION

Glacier meltwater streams connect discrete cryosphere habitats with downstream freshwater and marine ecosystems across the Northern Hemisphere (e.g., Hood et al., 2009; O'Neel et al., 2015; Milner et al., 2017). In addition to exporting freshwater, glaciers and ice sheets also subsidize microbial productivity and respiration through the downstream delivery of particulate and dissolved material such as carbon (Bhatia et al., 2013a; Lawson et al., 2014; Kohler et al., 2017), macro- and micronutrients (Bhatia et al., 2013b; Hawkings et al., 2015; Dubnick et al., 2017a), and other weathering products (Hawkings et al., 2017; Hatton et al., 2019a; Stachnik et al., 2019). While recent progress has been made in determining factors that control the magnitude of these biogeochemical fluxes, important clues into solute generation and the operation of the subglacial drainage system may be uncovered through the investigation of more qualitative characteristics of these exports. For example, past work has successfully shown that chemical signatures of dissolved organic matter (Hood et al., 2009; Lawson et al., 2014; Dubnick et al., 2017b) and elemental isotopes (Kohler et al., 2017; Hatton et al., 2019b) are related to the hydrological and lithological characteristics of the glacial environment.

One potentially useful, yet under-utilized, tool for investigating hydrological and biogeochemical weathering processes are the diverse microbial cells collected and exported by meltwater from the glacial ecosystem. For example, subglacial microbes are found at the intersection of the glacier and the underlying bedrock, and are functionally diverse, having been shown to utilize a myriad of metabolic pathways operating over a spectrum of redox conditions (Boyd et al., 2010, 2011, 2014; Stibal et al., 2012a,c; Hamilton et al., 2013; Dieser et al., 2014), which may enable them to influence a host of weathering reactions and biogeochemical transformations (Sharp et al., 1999; Mitchell et al., 2013; Montross et al., 2013; Lamarche-Gagnon et al., 2019). Yet, due to their physical inaccessibility, these habitats are notoriously difficult to investigate, and much of our knowledge of these habitats at present comes from discrete samples taken from marginal areas (e.g., Boyd et al., 2011; Žárský et al., 2018). On the other hand, supraglacial (surface ice) microbial communities, which are comparatively straightforward to access, can include all three domains of life (Anesio et al., 2017), and include oxygenic, phototrophic and carbon-fixing taxa, with Cyanobacteria specifically playing an integral part in forming the matrix of cryoconite found in depressions on the glacier surface (Langford et al., 2010; Cook et al., 2016; Gokul et al., 2019).

Meltwater generated on glacier surfaces collects into supraglacial streams and lakes that eventually drain into moulins and crevasses to enter the subglacial hydrological system (Irvine-Fynn et al., 2011; Hotaling et al., 2017b). Within the subglacial environment, waters may be routed through lower residence time efficient/channelized drainage systems (analogous to subglacial 'stream channels'), or through a longer residence time distributed system, which may be more analogous to the saturated sediments of rivers (Tranter et al., 1996; Hubbard and Nienow, 1997; Irvine-Fynn et al., 2011). No matter the path, meltwater entrains debris and microbial cells *en route*, and is evacuated from the glacier terminus to form proglacial streams. Thus, a wealth of information on the physical/chemical characteristics and drainage pathways of a given drainage network can be obtained by analyzing the cells suspended in meltwater. Given recent advances in sequencing technologies and bioinformatics, these data have great potential to augment traditional physical and chemical clues for inferring hydrologic patterns and biogeochemical processes among diverse glacial habitats.

The physical characteristics (size and shape) and geographic location of glaciers (latitude, elevation, and aspect) promote differences in seasonal melt patterns and associated hydrological 'plumbing,' providing varying levels of meltwater exposure to subglacial habitats (Tranter et al., 1996; Wadham et al., 2010). Subglacial environments themselves are likely heterogeneous within systems (Graly et al., 2014) and across space and time because of differences in hydrologic regime (Tranter et al., 2005), underlying lithology (Mitchell et al., 2013), and organic matter reserves (Stibal et al., 2012c), all of which may dictate possible metabolic pathways and energy sources for microbes. Similarly, microbes inhabiting the supraglacial system can also differ spatially due to differences in dispersal, climate conditions, and allochthonous inputs (Stibal et al., 2012b; Cameron et al., 2016). Therefore, regionally specific assemblages may emanate from glacial rivers across the Arctic and sub-Arctic.

While temporal (Sheik et al., 2015; Dubnick et al., 2017a) and catchment-scale (Hauptmann et al., 2016; Cameron et al., 2017; Žárský et al., 2018) studies on cell export have been previously performed from a limited number of glacier streams, there are currently no studies that have made comparisons among major geographic regions. Thus, in this work, we ask two main questions: (1) How do exported meltwater assemblages compare among disparate, high latitude regions, and (2) can a combination of physical and chemical characteristics be used to explain the exported assemblage structure and provide clues into their origins? To test these questions, we collected and analyzed

meltwater samples from glaciers in six major (sub)Arctic regions differing in climate, glacier size, and bedrock lithology. We hypothesized that individual geographic regions should export unique microbial assemblages due to collective differences in latitude, climate, and geology. Furthermore, we predicted that physico-chemical variables commonly used to infer hydrological patterns would be useful in predicting likely sources of microbial cells from the supra- and subglacial environments.

MATERIALS AND METHODS

Study Sites

Meltwater samples were collected from 24 glaciers over six different Arctic and sub-Arctic regions over the 2015–2017 summers (**Figure 1**). A full list of their characteristics is given in **Table 1**. All sites were sampled as close to the glacier terminus as safely possible (most within ∼10 m), with exceptions noted below. Briefly, four streams were sampled from the Kuannersuit Valley, located in central Qeqertarsuaq (Disko Island), west Greenland, draining glaciers 6, 10, 11, and 13. Kuannersuit Valley is composed of a primarily basaltic landscape, and numerous glacier streams here originate from the island's largest ice cap, Sermersuaq, along with several valley and cirque glaciers (Žárský et al., 2018). Iceland was the second basaltic locality, and four sites were sampled: Sólheimajökull (outlet to Mýrdalsjökull), Skaftafellsjökull (south outlet to Vatnajökull), Eyjabakkajökull (north outlet to Vatnajökull), and Kaldalónsjökull (outlet to Drangajökull) (Björnsson et al., 2000; Tweed et al., 2005). Next, six localities were sampled on Svalbard. Two glaciers, Nansenbreen and Sefströmbreen, are located in Isfjorden, while Ebbabreen is located in Petuniabukta, and Midtre Lovénbreen near Ny-Ålesund, Kongsfjorden (Hagen et al., 1993). Lastly, cold-based glaciers Longyearbreen and Foxfonna were sampled near Longyearbyen. Three mainland Norway glaciers were sampled including Styggedalsbreen, Bøverbreen, and Austerdalsbreen, all of which are situated upon gneiss bedrock (Mateos-Rivera et al., 2016). Styggedalsbreen and Bøverbreen are located in the alpine Jotunheimen region, while Austerdalsbreen is an outlet glacier of Jostedalsbreen Ice Cap (Andreassen et al., 2012). Four outlet glaciers of the Juneau Icefield were sampled in coastal southeast Alaska; Herbert, Eagle, Lemon, and Mendenhall (Hood and Berner, 2009). Both Lemon Creek and Eagle River were sampled several km downstream due to inaccessibility, while Herbert and Mendenhall meltwater was sampled at the glacier snout. All four glaciers are underlain by felsic igneous intrusive bedrock. Finally, three outlet glaciers of the Greenland Ice Sheet (GrIS) were sampled, all of which drain Precambrian shield bedrock composed of Archaean gneiss and granite (Henriksen et al., 2009). Leverett Glacier was sampled several meters from its portal (Kohler et al., 2017), while Russell Glacier was sampled several hundred meters from its last glacial contact, upstream of the confluence with the Leverett River. Lastly, Qinnguata Kuussua, which drains the large Ørkendalen and Isorlersuup glaciers south of Leverett Glacier, was sampled immediately upstream of its confluence with the Akuliarusiarsuup Kuua to form the 'Watson River' near the town of Kangerlussuaq (Cameron et al., 2017).

Sampling

At each stream, three replicate microbiological samples were taken from the thalweg of the water column using a sterile syringe (except Foxfonna, where only one replicate was taken). Water was passed through Sterivex filters (0.22 μm; Millipore, Billerica, MA, United States) until they clogged, which was between 50 and 600 mL, with most having at least 300 mL (**Table 1**). Filters were flushed of water, filled with nucleic acid preservation buffer (LifeGuard, MO BIO, Carlsbad, CA, United States), and promptly frozen at −20°C. Given that time of day may have a strong influence on the hydrology of glacial systems (longer residence-time water may be disproportionately released at low flows), stream sampling was undertaken to roughly correspond with diurnal peaks in runoff if possible.

Chemical Analyses

Physical and hydrochemical characterization was conducted concurrently with microbial cell collection as described previously (Žárský et al., 2018). Briefly, conductivity and pH were measured *in situ* at each stream with either a Multi 3430 digital pH and conductivity meter (WTW, Weilheim, Germany) or a low range Hanna Combo (Hanna Instruments, United States) pH/conductivity meter. Latitude/longitude and elevation were measured by handheld GPS, and estimates of glacier areas were derived from the literature (**Table 1**). Meltwater samples for nutrient and dissolved organic carbon (DOC) analyses were collected directly from the stream via sterile syringe. Nutrient samples were filtered through 0.45 μm polyethersulfone GD/XP syringe filters (Whatman) into acid-washed 30 ml Nalgene HDPE bottles and immediately frozen at −20°C. Nutrient concentrations were determined by using a LaChat QuikChem 8500 flow injection analyser for nitrate (NO_3^-; QuikChem Methods 10−107−04−1−B; LOD = 1 μg L^{-1} = 71 nM), ammonium (NH_4^+; 10−107−06−1−Q; LOD = 8 μg L^{-1} = 571 nM) and soluble reactive phosphorus (SRP; 31-115-01-1-I; LOD = 1 μg L^{-1} = 32 nM). DOC samples were filtered through Whatman Puradisc AQUA syringe filters (cellulose acetate, 0.45 μm) into acid-washed 30 ml Nalgene HDPE bottles and frozen. DOC concentrations were determined using a Shimadzu TOC-L analyzer (Shimadzu, Kyoto, Japan) with high sensitivity catalyst (LOD for DOC = 20 μg L^{-1} = 1.7 μM).

Dissolved major ions (F^+, Na^+, K^+, Mg^{2+}, Ca^{2+}, Cl^-, SO_4^{2-}, and HCO_3^-) and dissolved silica (DSi) were sampled by taking meltwater from the thalweg with a clean, 1 l Nalgene bottle triple-rinsed with stream water. The water was filtered within 24 h through a 47 mm 0.45 μm cellulose nitrate filter membrane (Whatman) mounted on a clean Nalgene filter tower. Samples were stored in 30 ml HDPE Nalgene bottles, and kept refrigerated (∼4°C). Major ions were analyzed by ion chromatography on a Thermo Scientific Dionex ICS5000 + capillary system as described by Hawkings et al. (2015), with HCO_3^- estimated from charge deficit (Tranter et al., 2002), and DSi measured using a LaChat QuikChem 8500 flow injection analyzer (QuikChem Method 31-114-27-1-D) as described by Hawkings et al. (2017). Pre-weighed filters were used to determine total suspended solids (TSS) after drying the filters in an oven at 50°C overnight, re-weighing, subtracting the filter weight and normalizing by the

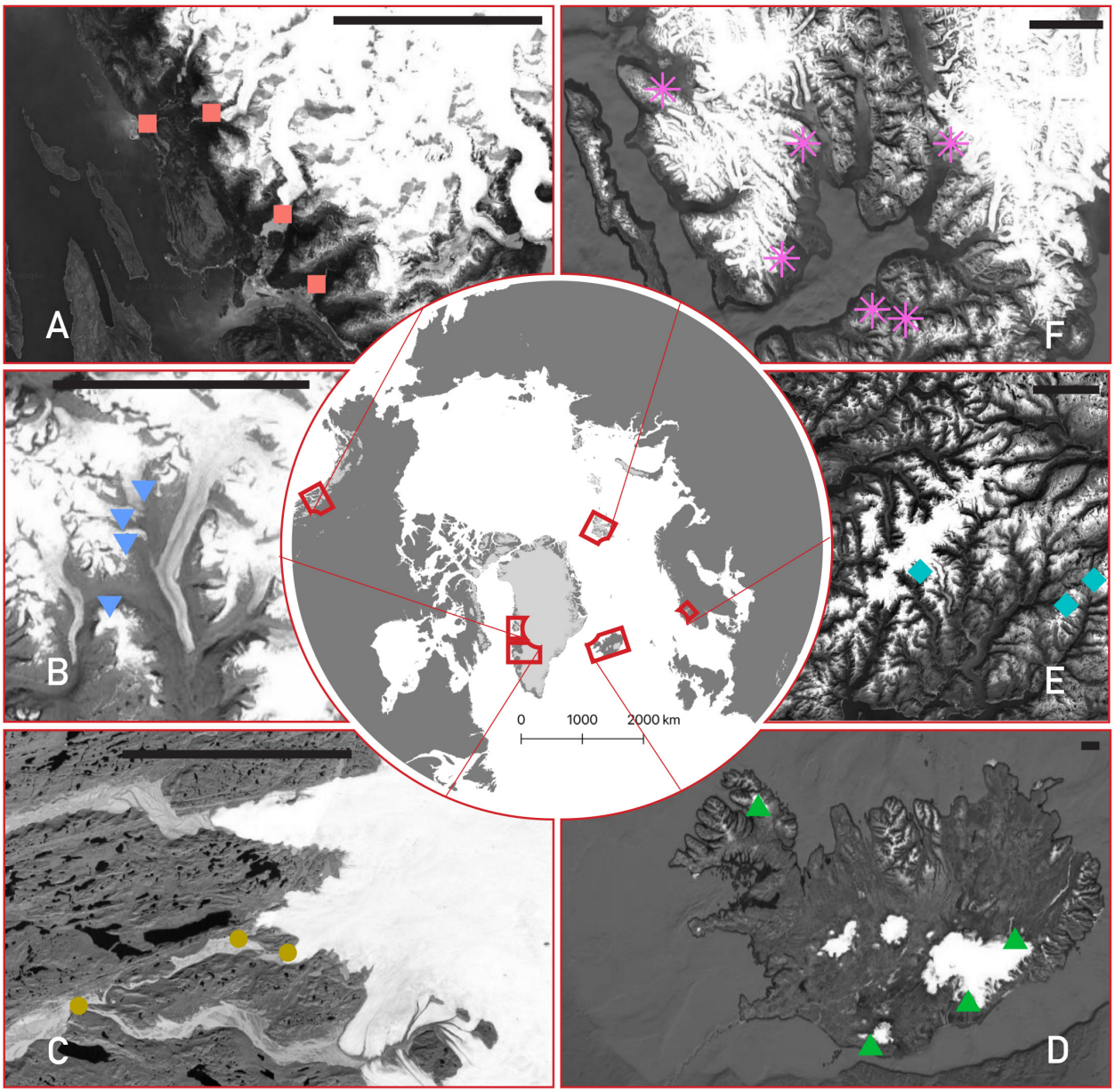

FIGURE 1 | Map of the six studied regions, with detailed insets for each showing the location of each glacier stream sampled. Counterclockwise from top-left: **(A)** southeast Alaska (red squares), **(B)** Qeqertarsuaq (Disko Island, blue upside-down triangles), **(C)** the Greenland Ice Sheet (gold circles), **(D)** Iceland (green triangles), **(E)** Norway (turquoise diamonds), and **(F)** Svalbard (purple asterisks). The scale bar in each panel represents 25 km. Background images are from Landsat/Copernicus and the United States Geological Survey, taken via Google and compiled with QGIS.

water volume that passed through (measured using a measuring cylinder and usually ∼300–500 mL). See Žárský et al. (2018) for further notes on analytical precision and accuracy.

Chemical Indices

From our geochemical data, we calculated two indices that have been used previously in interpreting patterns in weathering and hydrology (e.g., Dubnick et al., 2017b). The sulfate mass fraction (SMF) is defined as the concentration of sulfate (SO_4^{2-}), divided by the sum of sulfate and bicarbonate (HCO_3-; Brown et al., 1996; Tranter et al., 2002). High SMF (e.g., >0.5) values indicate that a larger proportion of protons are coming from sulfide oxidation compared to carbonation reactions, and is thus an indication of the influence of carbonation versus sulfide oxidation as proton/HCO_3^- sources (Wadham et al., 2004). Complementing this, we also calculated a divalent/monovalent (DiMo) ratio of major cations: $Ca^{2+} + Mg^{2+}/Na^+ + K^+$. This ratio is a crude approximation of the degree of carbonate dissolution versus silicate dissolution (Wadham et al., 2010). Higher DiMo values are likely to be more

TABLE 1 | Physical characteristics of meltwater streams.

Glacier	Region	Date sampled	Glacier area (km^2)	Latitude	Longitude	Elevation (m)	Vol. water filtered (mL)	Temperature (°C)	Conductivity (μS/cm)	pH	Total suspended solids (g/L)
Herbert	Alaska	27-Jun-17	60[a]	58.539120°	−134.684540°	280	3 × 300	0.30	21.00	7.70	0.339
Mendenhall	Alaska	28-Jun-17	127[a]	58.438010°	−134.544570°	113	3 × 300	0.20	18.00	8.61	0.219
Lemon	Alaska	29-Jun-17	15[a]	58.364320°	−134.478740°	20	3 × 360	5.30	38.00	7.81	0.025
Eagle	Alaska	29-Jun-17	53[a]	58.528640°	−134.805680°	6	3 × 480	3.70	18.00	8.07	0.050
Leverett	GrIS	5-Sep-17	1200[b]	67.064770°	−50.162940°	314	3 × 300	0.00	30.00	9.32	0.963*
Russell	GrIS	6-Sep-17	120[c]	67.076780°	−50.276820°	182	3 × 300	0.00	35.00	8.85	0.5*
Qinnguata Kuussua	GrIS	7-Sep-17	1800[d]	67.016170°	−50.653090°	42	3 × 300	0.00	33.00	8.75	NA
Sólheimajökull	Iceland	16-Aug-16	47[e]	63.534833°	−19.352194°	275	3 × 300	NA	48.00	8.78	0.500
Skaftafellsjökull	Iceland	17-Aug-16	100[f]	64.028667°	−16.932667°	153	3 × 250	NA	30.50	9.38	0.253
Eyjabakkajökull	Iceland	18-Aug-16	110[g]	64.666250°	−15.723694°	939	3 × 300	NA	5.60	8.24	0.283
Kaldalónsjökull	Iceland	20-Aug-16	37[g]	66.117611°	−22.287750°	318	3 × 500	NA	6.50	8.50	0.284
Styggedalsbreen	Norway	22-Sep-16	2.02[h]	61.488306°	7.880444°	1307	3 × 300	0.70	3.00	7.5**	0.009
Austerdalsbreen	Norway	24-Sep-16	19.85[h]	61.588500°	6.995333°	490	3 × 300	0.30	25.00	6.7**	0.026
Bøverbreen	Norway	25-Sep-16	6.75[h]	61.556694°	8.049500°	1432	3 × 300	0.70	2.00	6.1**	0.207
Glacier 6	Qeqertarsuaq	4-Aug-15	1.5[i]	69.715833°	−53.441617°	907	3 × 600	0.10	7.90	7.20	0.107
Glacier 10	Qeqertarsuaq	6-Aug-15	7[i]	69.766717°	−53.413400°	765	3 × 300	0.10	7.70	8.70	0.827
Glacier 11	Qeqertarsuaq	6-Aug-15	9.7[i]	69.784050°	−53.427200°	782	3 × 300	2.20	9.90	6.90	0.194
Glacier 13	Qeqertarsuaq	9-Aug-15	18[i]	69.801817°	−53.375900°	798	3 × 300	0.10	9.00	7.52	0.156
Midtre Lovénbreen***	Svalbard	19-Jul-16	6[j]	78.895567°	12.069350°	50	3 × 600	0.9	38.97	8.85	0.746
Nansenbreen	Svalbard	2-Aug-16	45.1[j]	78.353145°	14.075243°	154	2 × 150, 1 × 200	0.90	70.00	7.21	2.354
Sefströmbreen	Svalbard	4-Aug-16	155[j]	78.719740°	14.374894°	158	3 × 200	0.80	108.00	8.25	0.902
Ebbabreen	Svalbard	6-Aug-16	25[j]	78.726805°	16.794599°	288	3 × 300	0.60	112.00	7.60	0.363
Longyearbreen	Svalbard	10-Aug-16	4[j]	78.189720°	15.533134°	340	3 × 200	NA	210.00	8.37	0.599
Foxfonna	Svalbard	5-Aug-17	3.95[j]	78.15243°	16.10879°	425	1 × 100	0.10	25.00	8.10	NA

*Estimates of glacier area is given with relevant citations: [a]estimated from Hood and Berner (2009), [b]Palmer et al. (2011), [c]Van de Wal and Russell (1994), [d]Lindbäck et al. (2015), [e]Björnsson et al. (2000), [f]Tweed et al. (2005), [g]Björnsson et al. (2003), [h]Andreassen et al. (2012), [i]Žárský et al. (2018), [j]Hagen et al. (1993). *Averaged from samples taken over 2018 summer. **Measurements from August 2018. ***Data is averaged from 3 days around the sampling day (i.e., 16, 18, and 21 July 2016).*

associated with carbonate weathering and a channelized drainage system, whereas lower numbers may be proportionally high in contributions from the distributed drainage system (Wadham et al., 2010; Dubnick et al., 2017b). All values were converted to μeq L^{-1} before calculation.

Nucleic Acids Extraction, Quantification, and Sequencing

DNA from the suspended sediment samples was extracted, amplified, and sequenced identically as in Žárský et al. (2018). Briefly, DNA was extracted using the PowerWater Sterivex DNA Isolation Kit (MO BIO) following the manufacturer's protocol. Extracted DNA was quantified using a Qubit fluorometer and Qubit dsDNA HS Assay Kit (Invitrogen, Carlsbad, CA, United States). Template DNA samples were shipped to the Mr. DNA laboratory (Shallowater, TX, United States) where 16S rRNA gene V4 region primers 515f/806r (Caporaso et al., 2011) with barcode on the forward primer were used in a 28 cycle PCR using the HotStarTaq Plus Master Mix Kit (Qiagen, Hilden, Germany) with an initial melt step of 94°C for 3 min, followed by 28 cycles of 94°C for 30 s, 53°C for 40 s, and 72°C for 1 min. After amplification, PCR products were checked in 2% agarose gel and the samples were pooled in equimolar proportions. Pooled samples were purified using calibrated Ampure XP beads. Sequencing was performed on an Illumina MiSeq platform following the manufacturer's guidelines. The quality checked dataset is available in the MG-RAST database (Meyer et al., 2008) under the accession number MGP92375, and representative sequences of selected OTUs were given accession numbers MN880326-MN880375 in GenBank.

Bioinformatic Analysis

Sequence data were analyzed by the pipeline SEED v2.0.4 (Větrovský et al., 2018). Paired ends were joined by fastq-join (Aronesty, 2011), and all sequences with mismatches in tags were removed from the dataset. Chimeras were detected, and the non-chimeric sequences were clustered into operational taxonomic units (OTUs) using UPARSE implemented in USEARCH 8.1.1861 (Edgar, 2013), with a 97% similarity threshold. The consensus from each OTU was constructed from a MAFFT alignment (Katoh and Standley, 2013), based on the most abundant nucleotide at each position. Singletons, chloroplasts, and mitochondria were removed, and OTUs identified as obvious PCR contaminants (i.e., human pathogens and symbionts, organisms strikingly incompatible with the glacier environment, and known contaminants of DNA isolation kits) were deleted. The resulting reads ranged from 22,336 to 113,601 per sample (mean = 64,233), and the dataset was rarefied to the lowest number (22,336). The 50 most abundant OTUs were identified against the SILVA nr. 132 database in Mothur (Schloss et al., 2009), and their putative metabolisms and ecological roles were assessed by megaBLAST and BLASTn algorithms against the GenBank nt/nr database. The characteristics of described species were accepted for OTUs showing sequence similarity >97% with these species. Finally, to calculate un-weighted and weighted UniFrac distances, a phylogenetic tree was created with RAxML (Stamatakis, 2014) and included the top 1,371 OTUs by abundance. The resulting new dataset was rarefied to the minimum number of reads (21,518) and was used in all ordination analyses.

Statistical Analyses

To visualize differences in environmental variables between regions, we performed principle components analysis (PCA) with physical and hydrological variables hypothesized to have microbiological relevance using the *ggbiplot* package (Vu, 2011) in R. Variable distributions were investigated by plotting histograms, and were $\log_{10}$-transformed if necessary to create a normal distribution.

In order to ascertain differences in assemblage structure between regions, diversity indices (#OTUs, Chao1, and Shannon) were calculated for each sample using the full rarefied dataset and compared using Tukey's Honest Significant Differences test (TukeyHSD). We then created unconstrained ordinations (principle coordinates analysis; PCoA) to evaluate variability between samples and sites using both un-weighted (presence/absence based) and weighted (abundance based) UniFrac distances on the unfiltered, untransformed subsampled dataset. The significance of geographical region on assemblage structure was tested by using a permutational multivariate analysis of variance (PERMANOVA) using the *adonis()* function in the *vegan* package (Oksanen et al., 2018). This was followed by a homogeneity of dispersion test (i.e., to see if regional groupings have statistically similar/dissimilar dispersions) conducted with the *betadisper()* function in *vegan*. Lastly, to visualize differences in the distribution of particularly influential OTUs, the top 50 OTUs by abundance were plotted (averaged by site and $\log_{10} + 1$-transformed) in a heatmap. A dendrogram was produced with the *heatmap.2()* function in the *gplots* package (Warnes et al., 2019) using the 'average' clustering method and Euclidean distance. Significant clusters were identified using the *simprof()* function in the *clustsig* package (Whitaker and Christman, 2014), with identical clustering and distance methods described above, and with transformation = "identity" and alpha = 0.000001.

Distance-based redundancy analysis (dbRDA) models were then created for both the weighted and un-weighted UniFrac datasets to find the most parsimonious combination of environmental variables to explain variability in assemblage structure across all sites. Quinnguata Kuusua was assigned the same TSS value as for Leverett River given the similarity of the catchment size and close geographical proximity. Other sites/samples where environmental data were missing and could not be confidently substituted from other sources were removed from analysis (i.e., Foxfonna and Midtre Lovénbreen; **Table 2**). Instances where solute concentrations where below detection (e.g., DOC, **Table 2**) were replaced with half the detection limit value. Candidate models were constructed by including only environmental variables with variance inflation factors less than or equal to 5 to avoid including redundant, collinear parameters (SMF and DiMo were positively correlated with SO_4^{2-} and negatively correlated with SRP, and because of the presumed greater biological relevance of the latter variables, the former were excluded from analyses). These included $\log_{10}$-transformed

TABLE 2 | Hydrochemical characteristics of meltwater, including nutrient concentrations, major cations and anions, dissolved organic carbon (DOC), sulfate mass fraction (SMF), and the divalent: monovalent ratio (DiMo).

Site	SRP	NH_4^+	$NO_2^- + NO_3^-$	DIN	DSi	F^-	Cl^-	SO_4^{2-}	Na^+	K^+	Mg^{2+}	Ca^{2+}	HCO_3^-	DOC	SMF	DiMo
Herbert	2.5	0.0	12.1	12.1	378.4	80.4	234.1	2025.0	345.9	580.4	234.7	2138.3	6110.4	198.4	0.30	4.22
Mendenhall	2.4	3.0	14.4	17.4	288.2	77.5	283.3	1949.7	333.1	553.9	226.5	1911.2	5332.0	108.1	0.32	3.98
Lemon	1.3	0.0	33.8	33.8	690.7	85.1	272.8	2775.8	403.4	627.9	369.2	4481.6	13075.9	204.8	0.21	7.56
Eagle	0.6	0.0	16.1	16.1	516.7	75.5	370.3	667.7	463.7	493.6	249.3	1780.3	6807.8	227.9	0.11	3.33
Leverett	5.6	0.0	15.5	15.5	870.2	93.8	155.1	3333.4	1259.7	1008.9	357.3	2519.7	9424.1	218.1	0.31	1.92
Russell	2.3	34.1	23.7	57.8	986.7	85.7	148.5	3184.4	786.8	835.3	553.3	3379.1	11670.4	412.5	0.26	3.85
Qinnguata Kuussua	5.3	5.8	23.7	29.5	971.2	89.6	188.6	3308.3	1124.6	1007.1	462.9	2902.9	10739.3	233.0	0.28	2.45
Sólheimajökull	40.8	4.9	13.3	18.2	2661.7	540.3	2007.0	1928.3	5461.9	449.3	721.9	3217.0	20975.5	62.9	0.10	0.88
Skaftafellsjökull	25.7	8.9	27.1	36.0	1104.6	445.3	1785.3	739.2	3203.1	109.6	155.0	2166.3	10603.5	56.8	0.08	0.85
Eyjabakkajökull	8.8	5.0	5.7	10.7	464.5	420.0	94.5	140.0	400.8	29.2	101.3	529.6	1541.0	<LOD	0.10	1.91
Kaldalónsjökull	9.3	6.3	6.2	12.5	381.1	228.9	535.2	469.2	916.8	46.3	118.3	484.0	2320.5	<LOD	0.20	0.83
Styggedalsbreen	3.8	8.6	31.6	40.2	300.7	16.2	62.1	272.5	132.0	100.1	153.8	370.8	1902.6	105.4	0.15	3.75
Austerdalsbreen	2.2	5.5	56.4	61.9	747.3	174.4	234.0	6702.7	442.9	527.4	154.5	3212.0	3070.4	111.5	0.73	5.28
Bøverbreen	6.4	6.8	<LOD	6.8	139.1	21.1	77.7	433.0	119.2	248.1	54.3	167.7	735.0	84.0	0.43	1.11
Glacier 6	9.1	3.5	0.0	3.5	441.9	6.7	390.9	179.7	564.8	42.8	85.2	710.6	3233.7	192.3	0.07	1.66
Glacier 10	17.5	18.2	0.0	18.2	653.1	4.4	327.1	226.1	703.8	42.7	1335.3	751.5	10060.0	151.8	0.03	4.65
Glacier 11	17.7	25.9	0.0	25.9	221.7	5.2	157.9	102.1	253.9	41.2	91.1	185.2	1341.0	134.8	0.09	1.38
Glacier 13	29.8	9.5	29.5	39.0	974.1	5.9	226.3	206.0	1250.7	42.7	44.2	522.7	4498.9	155.5	0.05	0.54
Midtre Lovénbreen*	NA	NA	24.5	NA	NA	NA	205.0	6362.7	703.3	350.0	1068.0	6923.7	20421.3	269.6	0.72	11.01
Nansenbreen	2.1	13.0	4.2	17.2	128.1	143.8	83.4	14632.4	352.8	391.7	2027.8	13000.9	32105.9	169.7	0.37	32.16
Sefströmbreen	0.3	6.2	4.6	10.8	92.9	288.3	57.6	18922.1	108.8	104.9	998.1	19717.4	40419.1	84.4	0.37	143.75
Ebbabreen	0.0	12.5	15.2	27.6	85.2	50.8	1220.1	28347.7	1143.0	412.7	1576.7	19307.5	32080.8	80.9	0.53	18.14
Longyearbreen	1.2	31.7	309.6	341.3	372.2	53.9	1579.2	86419.4	15841.2	688.7	10156.4	13895.7	23665.5	187.7	0.82	2.16
Foxfonna	2.0	15.0	28.7	43.7	194.2	84.3	456.4	6119.5	1992.8	580.4	375.2	142.1	5733.1	640.2	0.58	0.37

*All concentrations are reported in parts per billion (ppb), and SMF and DiMo ratios were converted to μeq L^{-1} before calculation. *Data is averaged from 3 days around the sampling day (i.e., 16, 18, and 21 July 2016).*

glacier elevation, area, latitude, pH, DSi, DIN, Cl^-, DOC, TSS, SRP, and SO_4^{2-}. The best combination of variables for each of the un-weighted and weighted datasets was then isolated through backward selection using the *ordistep()* function in *vegan*. Significance of the full model, as well as individual terms, was assessed using the *anova()* function. In order to assess relationships between environmental variables and individual OTUs, Pearson correlation coefficients were calculated between the same environmental variables included in dbRDA candidate models and the top 50 OTUs using the *cor()* function in R. Heatmaps and dendrograms were subsequently generated using the *heatmap.2()* function, and significant clusters calculated as described above.

Unless otherwise stated, significance was designated at $\alpha = 0.05$, adjusted (Adj. R^2 values are reported, and all statistics and figures were generated using the R statistical environment (R Core Team, 2017), primarily using functions available within the phyloseq package (McMurdie and Holmes, 2013).

RESULTS

Differences in Glacier and Meltwater Characteristics

Regional differences were observed in the measured physical and chemical characteristics of glacial meltwater (**Figure 2**, see **Tables 1**, **2** for a full summary). Glaciers from Norway and Qeqertarsuaq were sampled at the highest elevations, and samples from the GrIS had the largest catchment areas and TSS concentrations. Iceland and Qeqertarsuaq, both being basaltic localities, clustered together in the PCA, while other regions did not show substantial overlap (**Figure 2**). These streams had among the greatest SRP and DSi concentrations, and lowest DiMo ratios (indicating the predominance of silicate over carbonate weathering). Meltwater streams from Svalbard displayed comparatively high conductivities, as well as the greatest DiMo values and SO_4^{2-} and DOC concentrations. SMF values were greatest in two of the Norway sites (Bøverbreen and Austerdalsbreen) and two of the Svalbard sites (Ebbabreen and Longyearbreen). Iceland, along with the GrIS outlet glaciers, also had the greatest pH values, while Alaskan and Norwegian glaciers had very low measured pH (6.1-7.5 for Norway; **Table 1**).

Meltwater Assemblage Structure

Stream assemblages were dominated by the domain Bacteria, and all streams exported substantially less than 1% of Archaea by relative abundance. In total, 404 orders from 58 unique phyla were identified from the full, rarefied dataset. All samples were dominated by the phylum Proteobacteria, which had a mean relative abundance of 50.4%, and ranged from 13.3 to 67.2% (**Supplementary Figure S1**). Proteobacteria was followed in abundance by Bacteroidetes (mean = 16.2, range = 2.38–26.5%), and Actinobacteria (mean = 9.86%, range = 3.38–45.4%). Several sites also had notable proportions of Acidobacteria (mean = 3.06%, range = 0.10–9.58%) and Verrucomicrobia (mean = 4.86%, range = 0.049–20.9%), which were highest in abundance at Greenland sites (Qeqertarsuaq and GrIS). Cyanobacteria averaged 1.10% across all samples, and ranged from 0 to 10.2%. In terms of orders, Betaproteobacteriales (i.e., Betaproteobacteria) was the most common (mean = 33.6%, range = 4.97–50.6%), followed by Sphingobacteriales (mean = 4.93%, range = 0.31–11.3%), Chitinophagales (mean = 4.54%, range = 0.09–24.9%), and Micrococcales (mean = 4.01%, range 0.40–10.9%). Cytophagales (mean = 3.93%, range = 0.27–15.3%) and Verrucomicrobiales (mean = 3.18%, range = 0.02–20.4%) furthermore made up a substantial proportion of a few samples.

In total, 16,986 OTUs were observed in the full rarefied dataset. Of these, 150 were observed at all sites, and 1,313 were observed within all six regions. In contrast, 6,637 OTUs were present at one site only, and 8,056 were observed from one region only. Alaska had the most unique OTUs with 3,239 (∼32% of its total diversity), followed by Norway with 1,116, Iceland with 1,076, Qeqertarsuaq with 994, Svalbard with 934, and the GrIS with 697 (∼16% of its total diversity). Calculated alpha diversity metrics showed strong variability among regions (**Figure 3**), and differences were significant among all of Observed OTU richness (ANOVA, $F = 13.63$, $p << 0.01$), Chao1 ($F = 17.33$, $p << 0.01$), and Shannon diversity ($F = 8.82$, $p << 0.01$). Specifically, Alaskan streams had significantly greater Observed OTU richness and Chao1 values than all other regions (TukeyHSD, $p < 0.01$ for all comparisons), with the exception of Norway in the case of Observed OTUs ($p = 0.11$). Similarly, Iceland, Norway, and Qeqertarsuaq regions had significantly greater Observed OTU richness and Chao1 values in comparison to Svalbard ($p < 0.03$ for all comparisons). On the other hand, Shannon diversity was more similar between regions with the exception of the Greenland Ice Sheet, which had substantially lower values, and all regions had significantly greater values in comparison ($p < 0.05$ for all). When compared with latitude, Observed OTU richness (Adj. $R^2 = 0.42$, $F = 51.89$, $p << 0.01$), Chao1 (Adj. $R^2 = 0.45$, $F = 57.38$, $p << 0.01$), and Shannon diversity (Adj. $R^2 = 0.06$, $F = 5.06$, $p = 0.03$) were all significantly and negatively correlated.

Principle coordinate analyses (PCoA) were conducted to assess relationships between assemblages across geographic regions. When un-weighted UniFrac distances were applied (i.e., OTUs receive equal weighting), 29.6% of the variability was explained by axis 1 and 2 combined (**Figure 4**). GrIS sites, and a subset of the Svalbard samples, clustered apart from other regions, while Norway, Iceland, Alaska, and Qeqertarsuaq samples formed an overlapping cluster. When tested with PERMANOVA, geographical regions were significant in explaining assemblage variability ($R^2 = 0.36$, pseudo$F = 7.18$, $p < 0.01$), although dispersions were significantly different by region (pseudo$F = 15.81$, $p < 0.01$). When weighted UniFrac distances were used (i.e., accounting for abundance), axis 1 and 2 together explained 50.0% of the variability (**Figure 4**). All regions clustered closely together, with Qeqertarsuaq, GrIS, and a subset of Alaskan sites oriented more toward the top of the figure, and with a subset of Svalbard sites oriented toward the bottom. Application of the PERMANOVA test suggested that these regional groupings were also significant different ($R^2 = 0.47$, pseudo$F = 11.51$, $p < 0.01$), although regions again significantly differed in their dispersions (pseudo$F = 7.55$, $p < 0.01$).

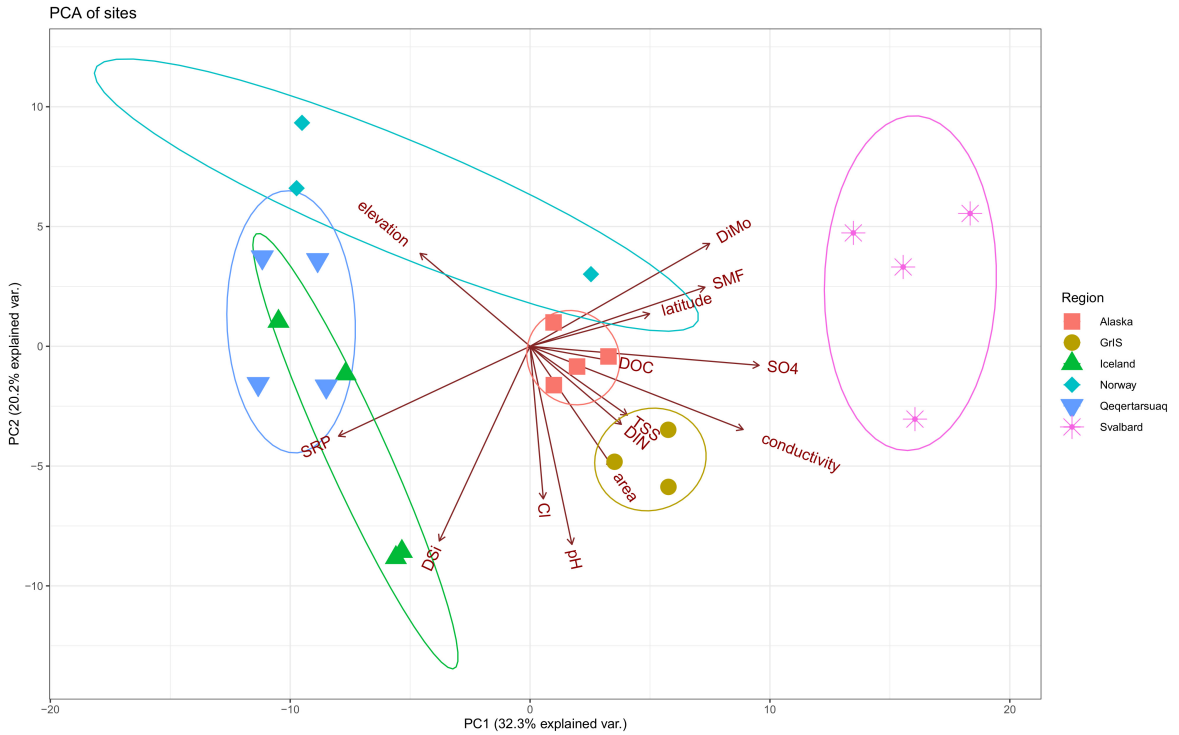

FIGURE 2 | Principle components analysis (PCA) showing differences in selected environmental variables by region. Alaska sites are shown in red squares, the Greenland Ice Sheet (GrIS) in gold circles, Iceland in green triangles, Norway in turquoise diamonds, Qeqertarsuaq in blue upside-down triangles, and Svalbard in purple asterisks. Sites with missing environmental data are excluded (i.e., Foxfonna and Midtre Lovénbreen, see **Tables 1**, **2**). Ellipse probabilities are set to 0.8.

In order to gain insight into influential taxa driving patterns in the PCoA analyses, the top 50 OTUs by abundance were identified and averaged by site (see **Supplementary Table S1** for full taxonomic and ecological information). Within sites, the top 50 OTUs collectively represented between 40 and 76% of the total number of reads in the full rarefied dataset (mean and median = 54%). When averages were plotted in a heatmap (**Figure 5**), multiple glaciers from the same region formed significant groups, but no glaciers from different regions significantly clustered together. In total, 13 significant clusters were formed, with Nansenbreen alone forming cluster a. Cluster b was formed by the Qeqertarsuaq sites (Glacier 6, 10, 11, and 13), and cluster c by the Norwegian sites (Austerdalsbreen, Bøverbreen, and Styggedalsbreen). Two of the Iceland sites, Kaldalónsjökull and Eyjabakkajökull, formed cluster d. Sefströmbreen and Russell glaciers both formed their own clusters, cluster e and f, respectively. Leverett and Qinnguata Kuusua from the GrIS formed cluster g, and Eagle and Lemon from Alaska formed cluster h. The remaining Iceland sites, Sólheimajökull and Skaftafellsjökull, clustered alone (clusters i and j, respectively). Alaskan glaciers Herbert and Mendenhall together formed cluster k, and Midtre Lovénbreen alone formed cluster l. Lastly, the remaining Svalbard sites, Foxfonna, Ebbabreen, and Longyearbreen, formed cluster m.

Three OTUs in particular were abundant at all sites, with the most common of these being *Polaromonas* sp. (**Figure 5** and **Supplementary Table S1**). On average, *Polaromonas* sp. accounted for 15% of all reads, ranging from 3 to 28% across samples. This was followed by *Methylophilus* sp. with an average relative abundance of 6% (ranging 1–15%) and *Nitrotoga* sp. with 4% (ranging <1–23%). However, at lower abundances, regional microbial assemblages became more distinct. For example, Greenland sites (GrIS and Qeqertarsuaq) had higher abundances of the Verrucomicrobium *Luteolibacter* sp., and GrIS and the larger Alaskan rivers (Eagle Glacier and Lemon Glacier) had high abundances of *Pseudarcicella* sp., which was at low abundances at all other sites. Svalbard sites (as well as Mendenhall Glacier, Herbert Glacier, and a few others) had high abundances of sulfur oxidizers *Sulfuricurvum* sp. from the phylum Epsilonbacteraeota (i.e., Epsilonproteobacteria), and *Thiobacillus* sp. from the phylum Proteobacteria (**Figure 5** and **Supplementary Table S1**). Finally, sites from the GrIS also had elevated abundances of *Planktophila* sp.

Correlations With Environmental Variables

We constructed dbRDA models to identify physical and chemical variables that best explain variability in exported microbial assemblage structure across sites (**Figure 6**). For the unweighed UniFrac dataset, the most parsimonious model included elevation ($F = 2.78$, $p = 0.01$), Cl^- ($F = 1.55$, $p = 0.06$), DOC ($F = 1.81$, $p = 0.03$), SO_4^{2-} ($F = 3.84$, $p < 0.01$), glacier area ($F = 3.04$, $p < 0.01$), and latitude ($F = 3.48$, $p < 0.01$). The *y*-axis explained 13.0% of the variability in the dataset, and was

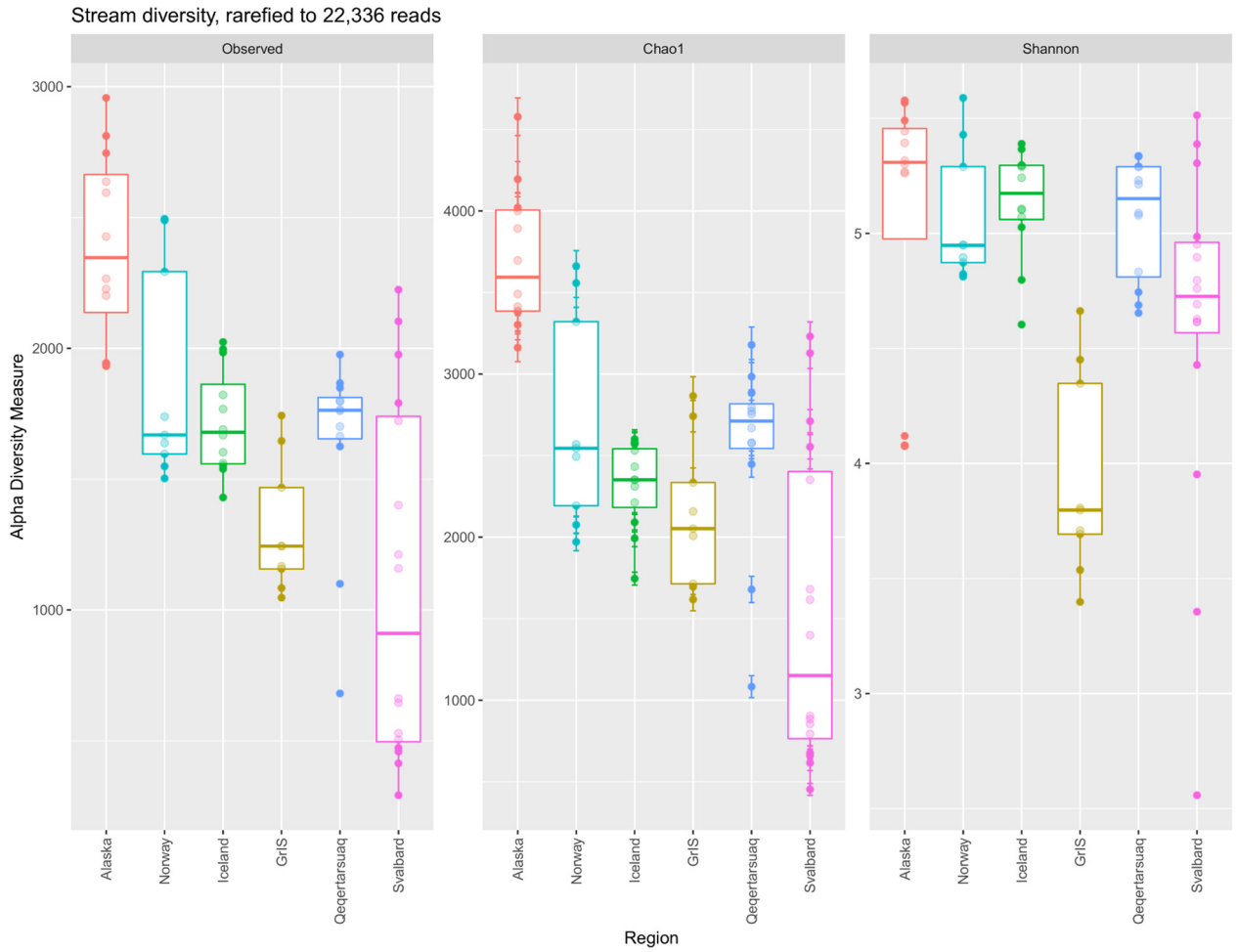

FIGURE 3 | Boxplots comparing the observed number of OTUs, Chao1, and Shannon diversity between major (sub)Arctic regions. The dataset was rarefied to 22,336 reads, and regions (*x*-axis) are ordered by increasing latitude.

driven primarily by elevation and latitude toward the bottom, and glacier area toward the top, being most strongly associated with GrIS samples. The *x*-axis explained 18.0% of the variability, and was primarily driven by SO_4^{2-} and latitude toward the right, corresponding mostly closely to Svalbard samples, and elevation and Cl^- concentrations toward the left, corresponding with Alaska, Norway, Iceland, and Qeqertarsuaq. The full model explained 31.0% of the variability, and was significant by ANOVA ($F = 2.75$, $p < 0.01$).

For the weighted UniFrac dataset (**Figure 6**), the most parsimonious model included DOC ($F = 3.46$, $p < 0.01$), glacier area ($F = 3.73$, $p < 0.01$), SO_4^{2-} ($F = 3.20$, $p = 0.01$), Cl^- ($F = 3.42$, $p < 0.01$), and latitude ($F = 6.20$, $p < 0.01$). The *y*-axis explained 11.2% of the variability, and was predominantly driven by DOC and glacier area toward the top, being most closely associated with GrIS samples. The *x*-axis explained 29.2% of the variability, and was driven primarily by latitude toward the right and Cl^-, SO_4^{2-}, and glacier area to the left. Svalbard and Qeqertarsuaq samples were most strongly oriented toward the right, while GrIS and Alaska were oriented toward the left. The full model explained 40.4% of the variability, and was significant by ANOVA ($F = 4.00$, $p < 0.01$).

The abundance of the top 50 OTUs was then compared with corresponding hydrochemical characteristics to determine possible drivers for common taxa (**Figure 7**). Based on these relationships, the row dendrogram split the top 50 OTU's into nine significant clusters. Cluster 1 included *Achromobacter* sp., *Caulobacter* sp., and *Pseudarcicella* sp., which were positively correlated with latitude, Cl^-, and SO_4^{2-} and negatively correlated with SRP and DSi. Cluster 2 was formed by *Sulfuricurvum* sp. alone, and cluster 3 included four OTUs (*Ferrunginibacter*, *Gemmatimonas* sp., *Acidimicrobinae*, and *Actinobacteria*). Both clusters 2 and 3 were positively correlated with DOC, but negatively correlated with TSS, latitude, elevation, and SRP. Cluster 4 included several of the most common OTUs, such as *Polaromonas* sp., *Rhodoferax* sp., and *Nitrotoga* sp., and was (mostly) positively correlated with pH, glacier area, TSS, and SRP. Cluster 5 hosted some of the remaining abundant OTUs, such as *Luteolibacter* sp., *Thiobacillus* sp., and *Glaciibacter* sp., and were negatively related to latitude, elevation, and SRP, but

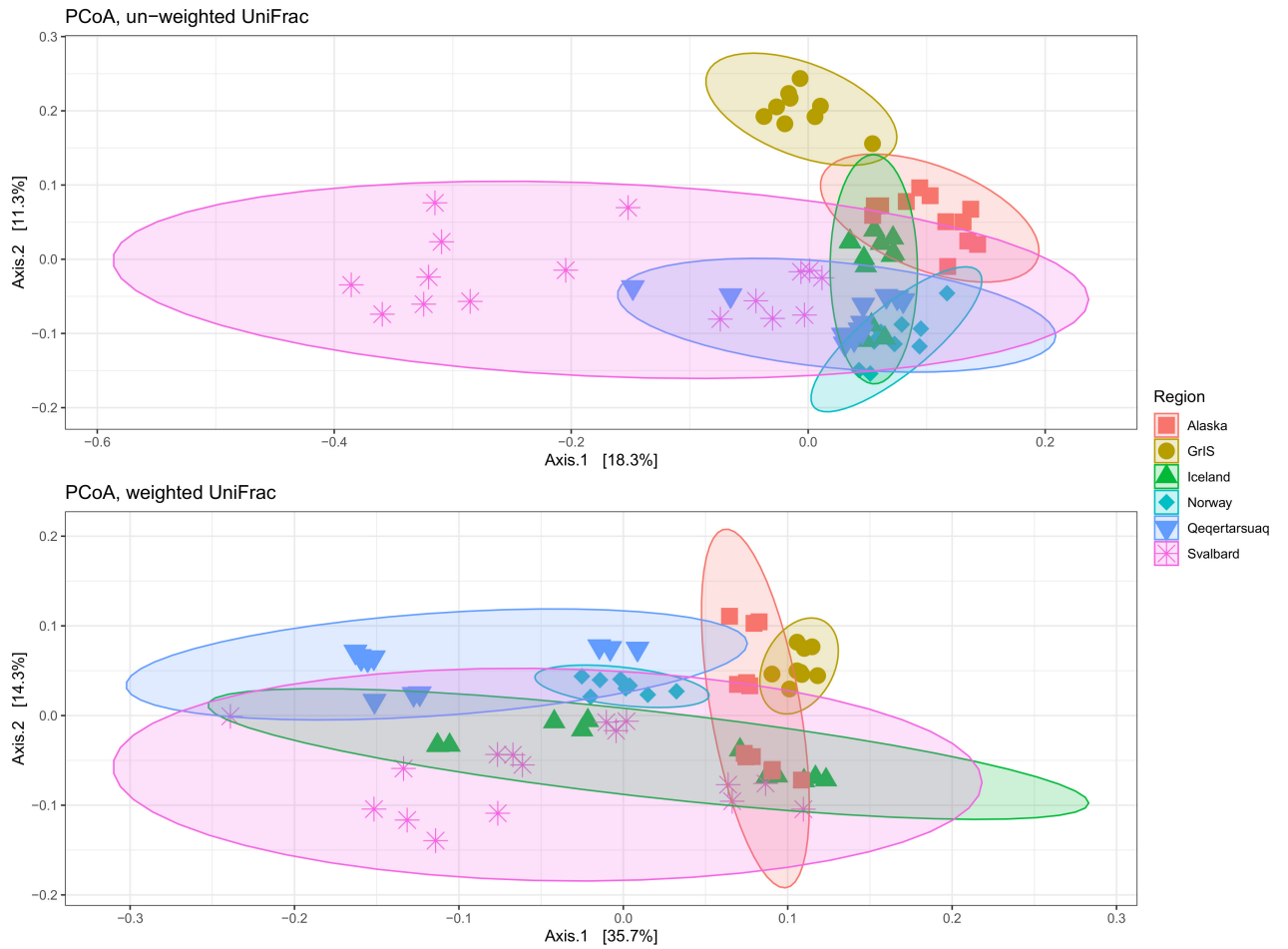

FIGURE 4 | Principle coordinates analysis (PCoA) showing differences between geographic regions on un-weighted **(top)** and weighted **(bottom)** UniFrac distances. Alaska sites are shown in red squares, the Greenland Ice Sheet (GrIS) in gold circles, Iceland in green triangles, Norway in turquoise diamonds, Qeqertarsuaq in blue upside-down triangles, and Svalbard in purple asterisks. Colored circles indicate 95% confidence intervals of regional categories.

positively correlated with DOC, pH, and glacier area. Cluster 6 was negatively correlated with DOC and SO_4^{2-} concentrations, but positively correlated with SRP and elevation. Clusters 7 and 9, the former of which hosted the common *Methylophilus* sp., were both negatively correlated with pH and Cl^- overall. However, cluster 9 was positively correlated with TSS, SO_4^{2-}, and latitude, while cluster 7 showed the opposite relationships. Lastly, cluster 8 showed positive relationships with SRP, latitude, and elevation, but showed mixed relationships with the remaining variables (**Figure 7**).

DISCUSSION

As glacial melt rates continue to increase across the northern hemisphere (Zemp et al., 2019), a fuller understanding of the consequences of deglaciation is warranted. One of the most conspicuous of the anticipated effects will be the altered production of meltwater (e.g., Milner et al., 2017; Huss and Hock, 2018), along with associated changes in hydrologic pathways (e.g., meltwater generated further inland and at greater elevations, intensifying connectivity between supra- and subglacial habitats), which ultimately have the greatest relevance for determining the quantity and character of solute and particulate fluxes. Yet, while the physical and chemical changes accompanying deglaciation may be comparatively straightforward to predict, the biological consequences for glacial ecosystems are far less intuitive (Fell et al., 2017; Hotaling et al., 2017a), and generalizations are inherently difficult to make due to differences in glacier size, elevation, bedrock, thermal regime, vegetation, and precipitation patterns (e.g., Carnahan et al., 2019). By studying microbial assemblages exported by glacier meltwater streams, it may be possible to investigate microbial processes taking place in the overall glacial system, and assess changes in structure and export over time.

Assemblage Structure

In this study, we performed a geographically broad survey of glacial streams from across the Arctic and sub-Arctic to investigate whether the composition of microbial assemblages is

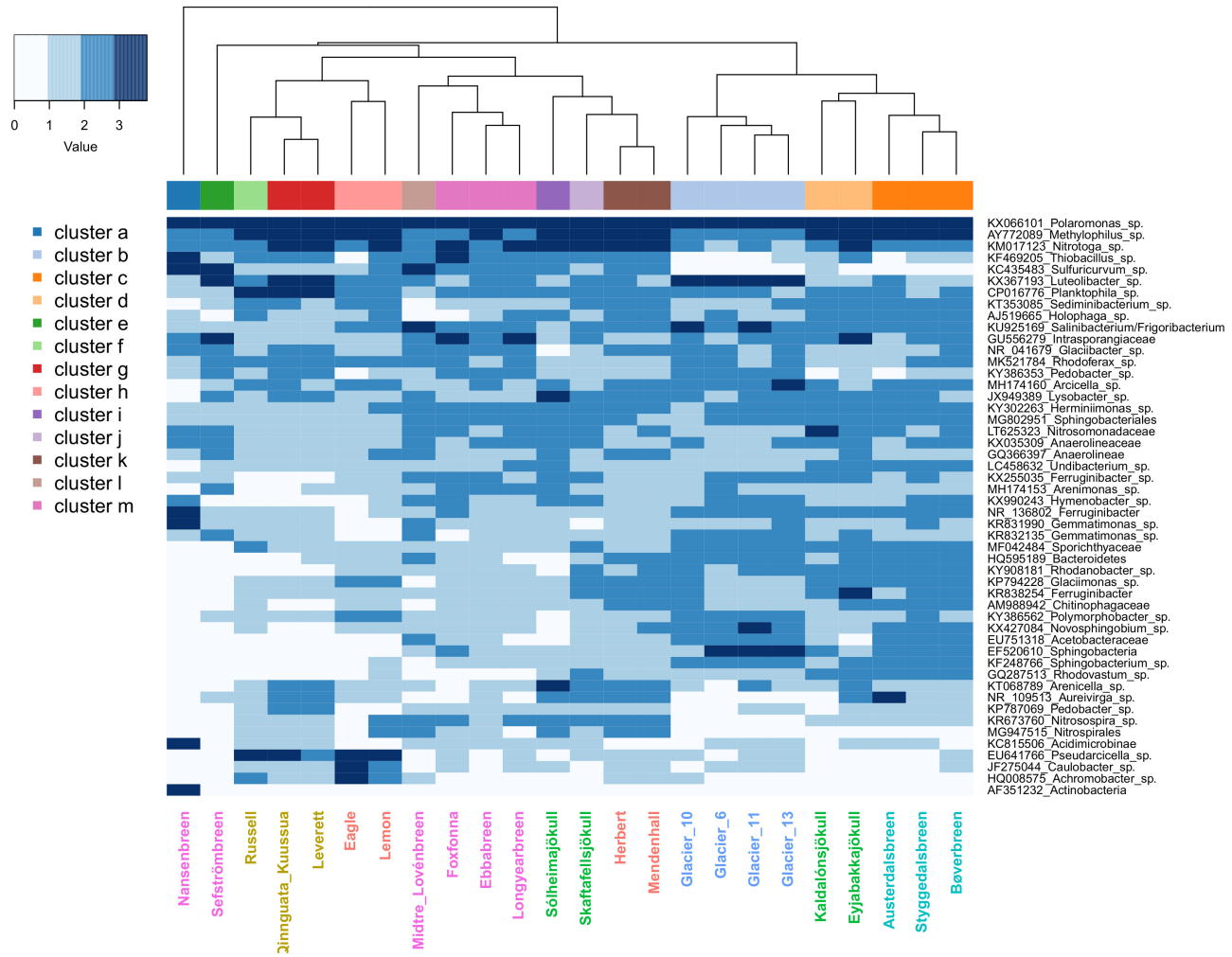

FIGURE 5 | Heatmap showing the $\log_{10}$ + 1-transformed abundance of the top 50 OTUs averaged by glacier stream site for the full rarefied dataset. Higher values are indicated by greater shade intensity. Site labels are colored by region, with Alaska sites indicated by red, the Greenland Ice Sheet (GrIS) by gold, Iceland by green, Norway by turquoise, Qeqertarsuaq by blue, and Svalbard by purple. The column side bar indicates the 13 significant site clusters.

linked to differences in geographic location and/or the physical and chemical characteristics of meltwater. We found meltwater assemblages to have the same coarse structure reported from other glacier streams (taking into consideration updates to the Silva database), being dominated by the phyla Proteobacteria and Bacteroidetes (Sheik et al., 2015; Cameron et al., 2017; Dubnick et al., 2017a). Interestingly, we found that all glacier meltwater streams export a small subset of the same OTUs at high relative abundances. A species of *Polaromonas* was the most abundant OTU recovered from all sites in this study, and belongs to a genus exhibiting a ubiquitous, global distribution throughout the cryosphere (Darcy et al., 2011). While the ecological role of *Polaromonas* spp. has not been decisively resolved, they are thought to be generalists, able to utilize a wide variety of carbon substrates and survive inhospitable periods (possibly including long-range dispersal) through dormancy (Darcy et al., 2011; Franzetti et al., 2013). The other abundant OTUs included the methylotrophic *Methylophilus* sp. and nitrogen oxidizing *Nitrotoga* sp., both of which are genera commonly recovered from cold environments globally (Achberger et al., 2016; Goordial et al., 2016; Boddicker and Mosier, 2018).

Yet, assemblages were also regionally unique, with up to a third of all OTUs from a given region being exclusive to that region. Most of these unique OTUs were found within the rare biosphere (exhibiting less than ∼0.1% relative abundance; Lynch and Neufeld, 2015), which helps to explain differences observed between the un-weighed and weighted UniFrac analyses. Interestingly, the three regions with the greatest number of unique OTUs (Alaska, Norway, and Iceland) clustered tightly together in the un-weighted UniFrac ordination (which is more sensitive to differences in low-abundance OTUs) while regions with fewer unique OTUs (specifically Svalbard and GrIS) presented less overlap with other regions and a greater dispersion between sites. However, when weighted UniFrac distances were plotted (taking into consideration OTU abundances), there was much greater overlap among regions, reflecting the high

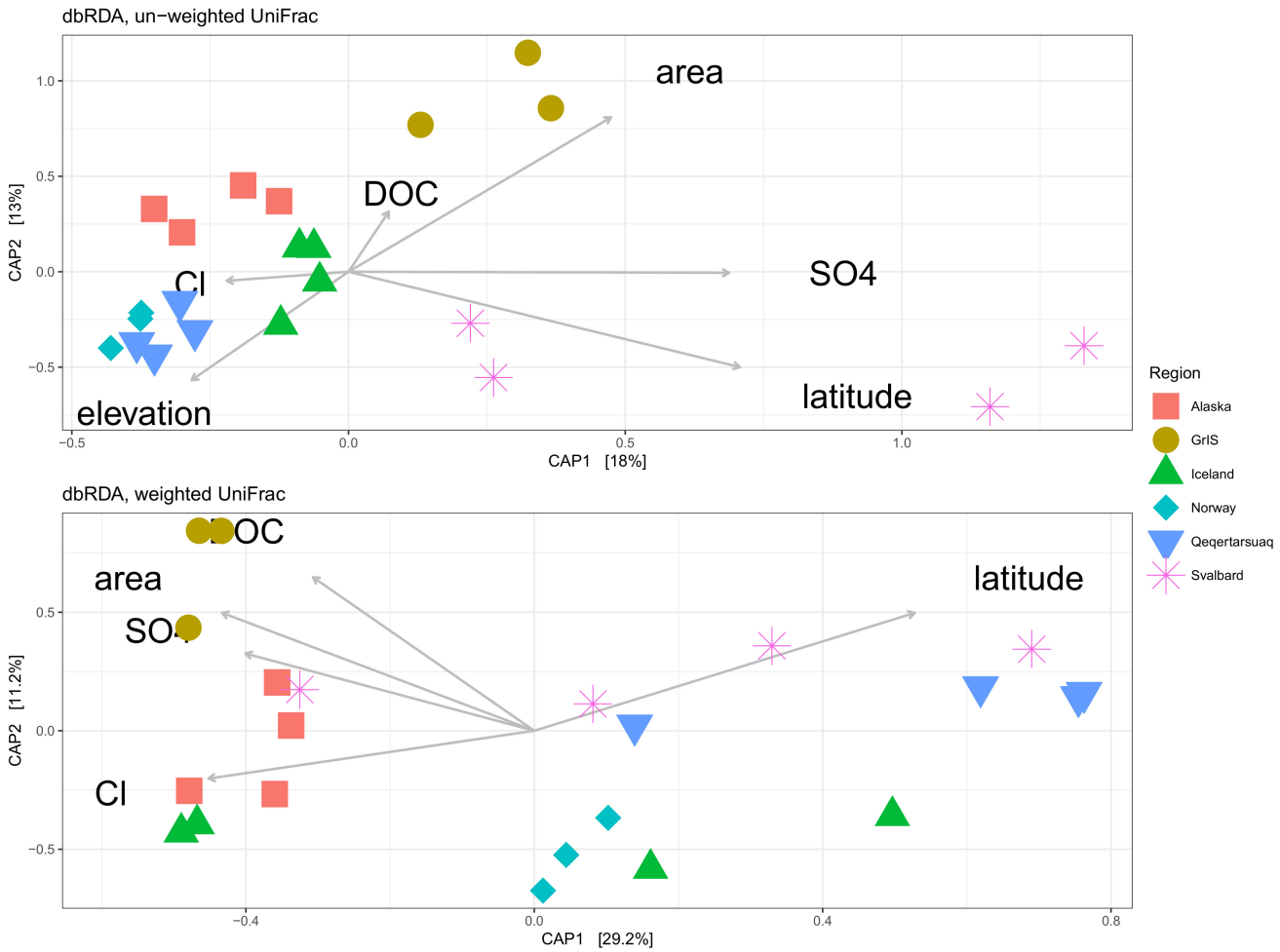

FIGURE 6 | Distance-based redundancy analysis (dbRDA) showing the most parsimonious combination of explanatory variables for explaining assemblage structure for both un-weighted **(top)** and weighted **(bottom)** UniFrac datasets. Sites with missing metadata were excluded (i.e., Foxfonna and Midtre Lovénbreen, see **Tables 1**, **2**). Alaska sites are shown in red squares, the Greenland Ice Sheet (GrIS) in gold circles, Iceland in green triangles, Norway in turquoise diamonds, Qeqertarsuaq in blue upside-down triangles, and Svalbard in purple asterisks.

relative abundances of the several aforementioned OTUs that were common to all sites. When a dendrogram was created to compare the relationships between sites and the top 50 OTUs, the 'high elevation' sites from Qeqertarsuaq, Iceland, and Norway were mostly oriented toward the right. These sites had relatively low relative abundances of sulfur oxidizers *Thiobacillus* and *Sulfuricurvum*, especially in comparison to the Svalbard sites, where SO_4^{2-} concentrations are commonly high (Yde et al., 2008). Meanwhile, the larger rivers sampled from Alaska (Lemon Glacier and Eagle Glacier) and the GrIS clustered to the left, set apart by relatively high abundances of *Pseudarcicella* sp. and *Planktophila* sp. As both *Pseudarcicella* (e.g., Cruaud et al., 2019) and *Planktophila* (Lee and Eom, 2016) are relatively common freshwater genera, their elevated relative abundances are potentially an indicator of lateral freshwater inputs between the source glacier and sampled sites.

Furthermore, regions differed in their magnitude of exported diversity, and alpha diversity decreased with increasing latitude. This pattern is a well-known phenomenon for macro-organisms (i.e., the Latitudinal Diversity Gradient, e.g., Pianka, 1966; Rohde, 1992; Hillebrand, 2004), and has more recently been observed for microorganisms in other biomes, such as the ocean (Fuhrman et al., 2008; Raes et al., 2018). As argued for other systems, this pattern may be a function of geological age, greater productivity (either from more calendar days with solar radiation, or potentially greater fluxes of allochthonous organic carbon transported to glacier surfaces), or a higher mean air temperature, which could enhance supraglacial metabolic activity. However, the Latitudinal Diversity Gradient has seen mixed support in terrestrial soil bacterial communities (Fierer and Jackson, 2006; Chu et al., 2010), and more work will be necessary to validate this pattern and identify its drivers within glacial environments. Importantly, most of the taxa identified in this study are not endemic (**Supplementary Table S1**), but bacteria with (putatively) cosmopolitan distributions. Thus, differences in among-site diversity are likely more attributable to

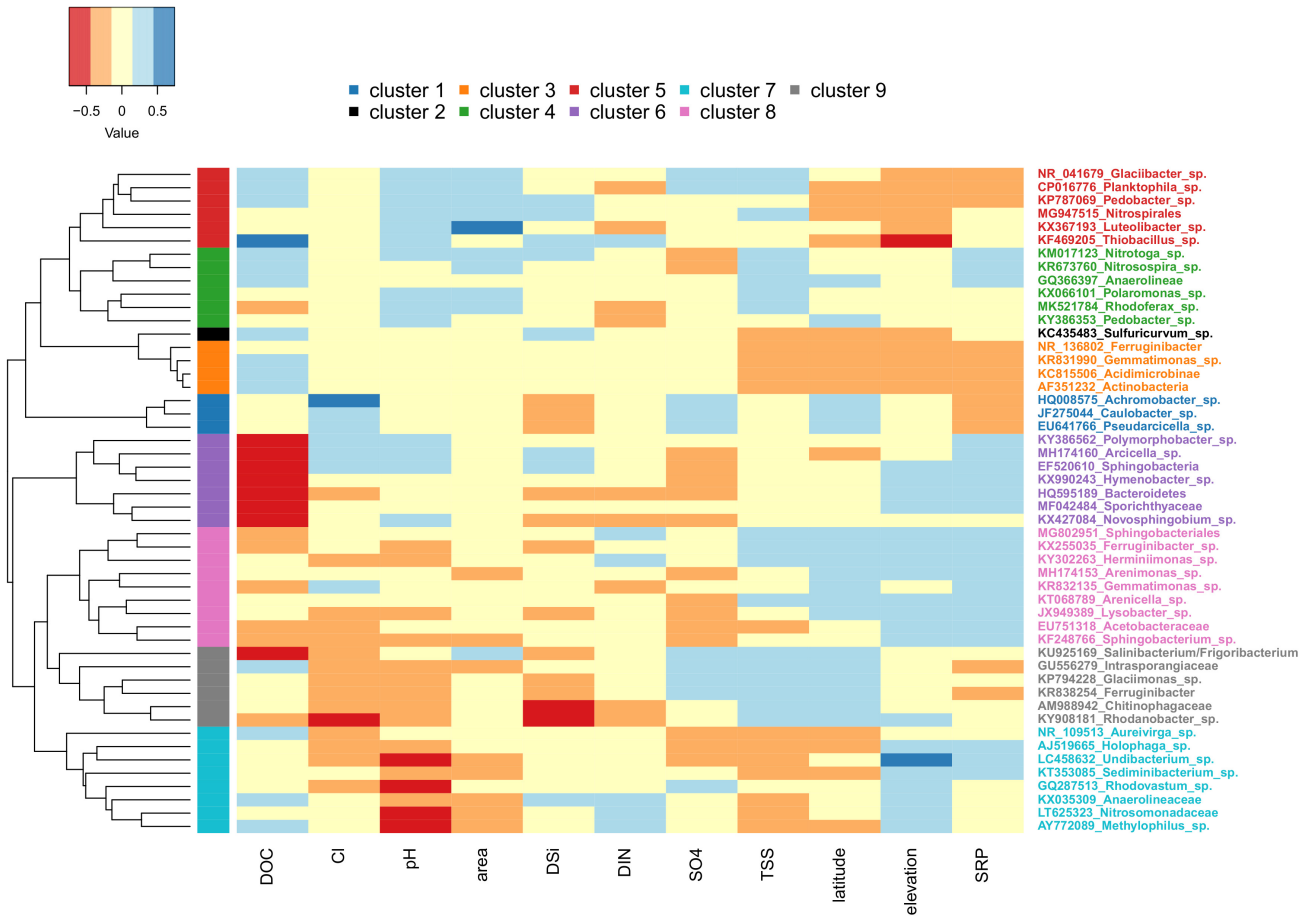

FIGURE 7 | Heatmap showing the relationship between environmental variables (only those with variance inflation factors less than or equal to 5 included) and the top 50 OTUs. Sites with missing metadata were excluded (i.e., Foxfonna and Midtre Lovénbreen, see **Tables 1**, **2**). Cool colors indicate high Pearson correlation coefficient values, and warm colors indicate low values. The row side bar indicates the nine significant OTU clusters.

the diversity of available niches rather than geographical isolation or dispersal limitation.

Relationships With Meltwater Characteristics

In addition to possible spatial patterns, we also hypothesized that assemblage structure would be related to the physical and chemical characteristics of the meltwater, reflecting dominant hydrologic processes as well as potential energy sources. We found that the most parsimonious models for both the un-weighted and weighted dbRDA analyses included DOC, SO_4^{2-}, latitude, glacier area, and Cl^-, indicating that similar factors are responsible for determining both the taxa present as well as their relative abundance in glacier meltwater. However, the magnitude of their importance differed between un-weighted and weighted analyses, and may therefore represent different mechanisms of influence. Specifically, physical variables such as latitude, glacier area, SO_4^{2-}, and elevation showed a high level of influence in the un-weighted analysis. These variables potentially represent a gradient of physical habitat types, which may in turn correspond to niche and taxonomic diversity. In contrast, Cl^-, SO_4^{2-}, and DOC exhibited a higher degree of influence in the weighted dbRDA analysis, and may reflect differences in the availability of necessary solutes/resources, which may allow a subset of taxa to proliferate.

Comparisons between the identity and inferred metabolisms of the top 50 OTUs (**Supplementary Table S1**) with environmental variables were made to help further disentangle factors structuring assemblages between sites and regions. Furthermore, we reasoned that clusters showing higher correlations with proxies generally associated with greater rates of subglacial weathering (e.g., TSS, SRP, pH, and DSi) may indicate a proportionately greater subglacial source of cells. A subset of the clusters indeed seemed reasonable from this perspective. For example, the OTUs composing clusters 4 and 5 were identified as aerobic autotrophs, and showed an overall positive correlation with pH, glacier area, and TSS, suggesting that these OTUs are disproportionately sourced from subglacial habitats (potentially utilizing basal melt as an oxygen source). Adding to this interpretation, *Thiobacillus* from cluster 5 is a commonly observed subglacial genus

(e.g., Achberger et al., 2016), and cluster 4 included *Rhodoferax* sp., which was previously found to dominate subglacial sediment samples from Qeqertarsuaq (Žárský et al., 2018). However, other clusters presented more ambiguous associations. For example, clusters 2 and 3 were disproportionately composed of OTUs inferred to be anaerobic, and while their positive relationship with DSi may collectively suggest a greater subglacial source, their negative relationships with TSS and SRP make this argument less strong. Similarly, members of clusters 6 and 8 are almost all inferred to be aerobic heterotrophs, yet showed mixed relationships with all of TSS, DSi, and pH. Thus, in the majority of cases, the origin of exported OTUs from the glacier environment was not possible to resolve with our cluster analysis.

Correlations between individual OTUs and the meltwater chemistry were also sometimes counterintuitive. For example, autotrophic sulfur oxidizers *Thiobacillus* sp. and *Sulfuricurvum* sp. correlated positively with DOC, but showed no relationship with SO_4^{2-}. Similarly, inferred nitrifiers (*Nitrotoga* sp. and *Nitrosospira* sp.) and nitrogen reducers (*Glaciimonas* sp., and *Intrasporangiaceae*) showed no relationship with DIN. Clusters 6 and 8, which were predominately composed of aerobic heterotrophs, were strongly negatively correlated with DOC (though they were positively correlated with SRP). A final example is from the Nansenbreen glacier, where sulfur oxidizers represent up to 25% of the top 50 OTUs, yet sulfate is only slightly elevated compared with other sites. While it is possible that comparisons with different chemical species might yield different results (e.g., H_2S instead of SO_4^{2-}), and we understand caution should be exercised in making conclusions from the inferred metabolisms of clustered OTUs, we still expected more robust relationships with some of these more specific taxa with solutes corresponding to their metabolisms.

One possible explanation for these results may be due to collinearity within sites. Sites strongly clustered within regions in the PCA analyses, suggesting strong site-related variability in environmental variables. Furthermore, it is likely that some samples play a disproportionate role in driving OTU responses given insufficient gradients for some variables. For example, Svalbard had the greatest values for many variables (including latitude, chemical indices, and conductivity), which set this region apart in the PCA, and thus generally represented the higher range of abiotic characteristics in individual comparisons. Therefore, it is difficult to say if correlations in general are an indicator of hydrologic processes, reflect biogeographic/regional patterns, or are entirely spurious. Furthermore, glaciers were sampled at different stages of hydrological development. As discussed previously by Hatton et al. (2019b), our 'spot sampling' approach may make potential signals difficult to identify and/or interpret due to their being taken out of the hydrological context of the site. Future efforts might find very different patterns and relationships with hydrochemical variables if samples are taken throughout different points in the year (Sheik et al., 2015; Dubnick et al., 2017a) or over a greater selection of sites.

Another confounding factor is the problem of scale and chemical mixing. In general, while glaciers host broad supra- and subglacial habitats, there are also 'microhabitats' within these heterogeneous domains with their own specific energy sources and chemical signatures, which is highlighted by our observation of a few taxa at relatively high abundances in a subset of sites. However, as solutes and particulates are collected by meltwater, they are diluted, and thus the unique physico-chemical characteristics of microhabitats (as well as supra- and subglacial chemical signals) can be 'averaged away', making them undetectable through bulk meltwater analyses. However, these microhabitats may be important hotspots of subglacial life given that any energy source is likely to have a large impact in an otherwise energy-limited environment. We argue that one considerable strength of analyzing the microbial assemblages of meltwater is that it may be possible to detect these microhabitats with the rationale that any spot with high microbial productivity is likely to have an elevated signature in the mixed community structure, though it may not necessarily be reflected by meltwater characteristics. Thus, OTUs that cannot be explained by bulk meltwater chemistry may actually be indicators of these otherwise undetectable microhabitats.

CONCLUSION

Our results suggest that glaciers export both shared cosmopolitan taxa that dominate assemblages, as well as microbes unique to particular regions and sites, and highlight the heterogeneous nature of glacial environments their associated microbiota. Greater exported diversity was uncovered at lower latitudes, which are also the most prone to physical reduction from climate change, and are thus the most likely to experience broad changes in the diversity of microbial export in the future. Furthermore, we found some assemblages contain individual OTUs with distinct metabolic signals, likely reflecting spatially confined energy sources that have small effects on overall water chemistry, but a great influence on meltwater assemblage structure. Thus, rather than reflecting biogeochemical characteristics of meltwater, we found microbial cells instead provide important information about glacier habitats that are essentially impossible to resolve by analyzing bulk meltwater chemistry alone. Given the contributions of glacier exports to stream microbial diversity, it follows that post deglaciation, a substantial source of this diversity may disappear, although the viability and potential functional roles performed by exported microbes (e.g., competition, nutrient cycling, genes for exchange, etc.) are poorly explored. Nonetheless, this work suggests that exported microbial cells show promise as biological tracers for investigating hydrological processes, exploring the heterogeneous nature of subglacial habitats, and monitoring changes in glaciated watersheds.

DATA AVAILABILITY STATEMENT

Sequence data are available through the MG-RAST database under the accession number MGP92375, and representative sequences of selected OTUs were given accession numbers MN880326-MN880375 in GenBank. All other data are available upon request to the corresponding author.

AUTHOR CONTRIBUTIONS

TK, JŽ, JY, and MS conceived of the project. TK, PV, JŽ, JY, LF, GL-G, EH, KC, and MS performed the fieldwork and collected samples. TK, PV, GL-G, JŽ, and LF performed molecular laboratory work. LF performed bioinformatics analyses. JRH and JEH performed all geochemical analyses. TK analyzed the data and wrote the manuscript with significant input and editing from all co-authors.

FUNDING

This research was supported by a Czech Science Foundation Grant to MS (GAČR 18-12630S). Field work was additionally supported by a Charles University Foundation Grant to JŽ (GAUK 279715) and a Research Council of Norway Arctic Field Grant to TK (RiS ID 10410) and PV (RiS ID 10645). TK was further supported by Charles University Research Centre Program No. 204069, JY by the Joint Programming Initiative (JPI-Climate) award #71126, and JRH by the European Union Horizon 2020 Research and Innovation Programme under the Marie Skłodowska-Curie Actions Fellowship ICICLES (Grant Agreement #793962).

ACKNOWLEDGMENTS

We thank Jasna Vukić, Maria Cavaco, Marie Bulínová, Torbjørn Dale, and Frej Yde for laboratory and field assistance. We also wish to thank the Czech Arctic Scientific Infrastructure of the University of South Bohemia in České Budějovice – the Josef Svoboda Station in Svalbard. Lastly, we thank the two reviewers whose comments greatly improved the manuscript.

SUPPLEMENTARY MATERIAL

The Supplementary Material for this article can be found online at: https://www.frontiersin.org/articles/10.3389/fmicb.2020.00669/full#supplementary-material

REFERENCES

Achberger, A. M., Christner, B. C., Michaud, A. B., Priscu, J. C., Skidmore, M. L., Vick-Majors, T. J., et al. (2016). Microbial community structure of subglacial Lake Whillans, West Antarctica. *Front. Microbiol.* 7:1457. doi: 10.3389/fmicb.2016.01457

Andreassen, L. M., Winsvold, S. H., Paul, F., and Hausberg, J. E. (2012). Inventory of norwegian glaciers. *Rapport* 38. 1–236.

Anesio, A. M., Lutz, S., Chrismas, N. A. M., and Benning, L. G. (2017). The microbiome of glaciers and ice sheets. *NPJ Biofilms Microbiomes* 3:10. doi: 10.1038/s41522-017-0019-0

Aronesty, E. (2011). *Command-Line Tools For Processing Biological Sequencing Data*. Available online at: http://code.google.com/p/ea-utils (accessed December 27, 2019).

Bhatia, M. P., Das, S. B., Xu, L., Charette, M. A., Wadham, J. L., and Kujawinski, E. B. (2013a). Organic carbon export from the Greenland ice sheet. *Geochim. Cosmochim. Acta* 109, 329–344. doi: 10.1016/j.gca.2013.02.006

Bhatia, M. P., Kujawinski, E. B., Das, S. B., Breier, C. F., Henderson, P. B., and Charette, M. A. (2013b). Greenland meltwater as a significant and potentially bioavailable source of iron to the ocean. *Nat. Geosci.* 6, 274–278. doi: 10.1038/ngeo1746

Björnsson, H., Pálsson, F., and Guðmundsson, M. T. (2000). Surface and bedrock topography of the Mýrdalsjökull ice cap. *Jökull* 49, 29–46.

Björnsson, H., Pálsson, F., Sigurðsson, O., and Flowers, G. E. (2003). Surges of glaciers in Iceland. *Ann. Glaciol.* 36, 82–90. doi: 10.3189/172756403781816365

Boddicker, A. M., and Mosier, A. C. (2018). Genomic profiling of four cultivated *Candidatus Nitrotoga* spp. predicts broad metabolic potential and environmental distribution. *ISME J.* 12, 2864–2882. doi: 10.1038/s41396-018-0240-8

Boyd, E. S., Hamilton, T. L., Havig, J. R., Skidmore, M. L., and Shock, E. L. (2014). Chemolithotrophic primary production in a subglacial ecosystem. *Appl. Environ. Microbiol.* 80, 6146–6153. doi: 10.1128/AEM.01956-14

Boyd, E. S., Lange, R. K., Mitchell, A. C., Havig, J. R., Hamilton, T. L., Lafrenière, M. J., et al. (2011). Diversity, abundance, and potential activity of nitrifying and nitrate-reducing microbial assemblages in a subglacial ecosystem. *Appl. Environ. Microbiol.* 77, 4778–4787. doi: 10.1128/AEM.00376-11

Boyd, E. S., Skidmore, M., Mitchell, A. C., Bakermans, C., and Peters, J. W. (2010). Methanogenesis in subglacial sediments. *Environ. Microbiol. Rep.* 2, 685–692. doi: 10.1111/j.1758-2229.2010.00162.x

Brown, G., Sharp, M., and Tranter, M. (1996). Subglacial chemical erosion: seasonal variations in solute provenance, Haut Glacier d'Arolla, Valais, Switzerland. *Ann. Glaciol.* 22, 25–31. doi: 10.3189/1996AoG22-1-25-31

Cameron, K. A., Stibal, M., Hawkings, J. R., Mikkelsen, A. B., Telling, J., Kohler, T. J., et al. (2017). Meltwater export of prokaryotic cells from the Greenland ice sheet. *Environ. Microbiol.* 19, 524–534. doi: 10.1111/1462-2920.13483

Cameron, K. A., Stibal, M., Zarsky, J. D., Gözdereliler, E., Schostag, M., and Jacobsen, C. S. (2016). Supraglacial bacterial community structures vary across the Greenland ice sheet. *FEMS Microbiol. Ecol.* 92:fiv164. doi: 10.1093/femsec/fiv164

Caporaso, J. G., Lauber, C. L., Walters, W. A., Berg-Lyons, D., Lozupone, C. A., Turnbaugh, P. J., et al. (2011). Global patterns of 16S rRNA diversity at a depth of millions of sequences per sample. *Proc. Natl. Acad. Sci.* 108, 4516–4522. doi: 10.1073/pnas.1000080107

Carnahan, E., Amundson, J. M., and Hood, E. (2019). Impact of glacier loss and vegetation succession on annual basin runoff. *Hydrol. Earth Syst. Sci.* 23, 1667–1681. doi: 10.5194/hess-23-1667-2019

Chu, H., Fierer, N., Lauber, C. L., Caporaso, J. G., Knight, R., and Grogan, P. (2010). Soil bacterial diversity in the Arctic is not fundamentally different from that found in other biomes. *Environ. Microbiol.* 12, 2998–3006. doi: 10.1111/j.1462-2920.2010.02277.x

Cook, J. M., Edwards, A., Bulling, M., Mur, L. A., Cook, S., Gokul, J. K., et al. (2016). Metabolome-mediated biocryomorphic evolution promotes carbon fixation in Greenlandic cryoconite holes. *Environ. Microbiol.* 18, 4674–4686. doi: 10.1111/1462-2920.13349

Cruaud, P., Vigneron, A., Fradette, M. S., Dorea, C. C., Culley, A. I., Rodriguez, M. J., et al. (2019). Annual bacterial community cycle in a seasonally ice-covered river reflects environmental and climatic conditions. *Limnol. Oceanogr.* 65, S21–S37. doi: 10.1002/lno.11130

Darcy, J. L., Lynch, R. C., King, A. J., Robeson, M. S., and Schmidt, S. K. (2011). Global distribution of polaromonas phylotypes-evidence for a highly successful dispersal capacity. *PLoS One* 6:e23742. doi: 10.1371/journal.pone.0023742

Dieser, M., Broemsen, E. L., Cameron, K. A., King, G. M., Achberger, A., Choquette, K., et al. (2014). Molecular and biogeochemical evidence for methane cycling beneath the western margin of the Greenland Ice Sheet. *ISME J.* 8, 2305–2316. doi: 10.1038/ismej.2014.59

Dubnick, A., Kazemi, S., Sharp, M., Wadham, J., Hawkings, J., Beaton, A., et al. (2017a). Hydrological controls on glacially exported microbial assemblages. *J. Geophys. Res. Biogeosci.* 122, 1049–1061. doi: 10.1002/2016JG003685

Dubnick, A., Wadham, J., Tranter, M., Sharp, M., Orwin, J., Barker, J., et al. (2017b). Trickle or treat: the dynamics of nutrient export from polar glaciers. *Hydrol. Process.* 31, 1776–1789. doi: 10.1002/hyp.11149

Edgar, R. C. (2013). UPARSE: highly accurate OTU sequences from microbial amplicon reads. *Nat. Methods* 10, 996–998. doi: 10.1038/nmeth.2604

Fell, S. C., Carrivick, J. L., and Brown, L. E. (2017). The multitrophic effects of climate change and glacier retreat in mountain rivers. *BioScience* 67, 897–911. doi: 10.1093/biosci/bix107

Fierer, N., and Jackson, R. B. (2006). The diversity and biogeography of soil bacterial communities. *Proc. Natl. Acad. Sci. U.S.A.* 103, 626–631. doi: 10.1073/pnas.0507535103

Franzetti, A., Tatangelo, V., Gandolfi, I., Bertolini, V., Bestetti, G., Diolaiuti, G., et al. (2013). Bacterial community structure on two alpine debris-covered glaciers and biogeography of *Polaromonas phylotypes*. *ISME J.* 7, 1483–1492. doi: 10.1038/ismej.2013.48

Fuhrman, J. A., Steele, J. A., Hewson, I., Schwalbach, M. S., Brown, M. V., Green, J. L., et al. (2008). A latitudinal diversity gradient in planktonic marine bacteria. *Proc. Natl. Acad. Sci. U.S.A.* 105, 7774–7778. doi: 10.1073/pnas.0803070105

Gokul, J. K., Cameron, K. A., Irvine-Fynn, T. D., Cook, J. M., Hubbard, A., Stibal, M., et al. (2019). Illuminating the dynamic rare biosphere of the Greenland Ice Sheet's Dark Zone. *FEMS Microbiol. Ecol.* 95:fiz177. doi: 10.1093/femsec/fiz177

Goordial, J., Davila, A., Lacelle, D., Pollard, W., Marinova, M. M., Greer, C. W., et al. (2016). Nearing the cold-arid limits of microbial life in permafrost of an upper dry valley. *Antarctica. ISME J.* 10, 1613–1624. doi: 10.1038/ismej.2015.239

Graly, J. A., Humphrey, N. F., Landowski, C. M., and Harper, J. T. (2014). Chemical weathering under the Greenland ice sheet. *Geology* 42, 551–554. doi: 10.1130/G35370.1

Hagen, J. O., Liestøl, O., Roland, E., and Jørgensen, T. (1993). Glacier atlas of Svalbard and jan mayen. *Nor. Polarinst. Medd.* 129:141.

Hamilton, T. L., Peters, J. W., Skidmore, M. L., and Boyd, E. S. (2013). Molecular evidence for an active endogenous microbiome beneath glacial ice. *ISME J.* 7, 1402–1412. doi: 10.1038/ismej.2013.31

Hatton, J. E., Hendry, K. R., Hawkings, J. R., Wadham, J. L., Kohler, T. J., Stibal, M., et al. (2019a). Investigation of subglacial weathering under the Greenland Ice Sheet using silicon isotopes. *Geochim. Cosmochim. Acta* 247, 191–206. doi: 10.1016/j.gca.2018.12.033

Hatton, J. E., Hendry, K. R., Hawkings, J. R., Wadham, J. L., Opfergelt, S., Kohler, T. J., et al. (2019b). Silicon isotopes in Arctic and sub-Arctic glacial meltwaters: the role of the subglacial environment in the silicon cycle. *Proc. Royal Soc. A* 475, 20190098. doi: 10.1098/rspa.2019.0098

Hauptmann, A. L., Markussen, T. N., Stibal, M., Olsen, N. S., Elberling, B., Balum, J., et al. (2016). Upstream freshwater and terrestrial sources are differentially reflected in the bacterial community structure along a small Arctic river and its estuary. *Front. Microbiol.* 7:1474. doi: 10.3389/fmicb.2016.01474

Hawkings, J. R., Wadham, J. L., Benning, L. G., Hendry, K. R., Tranter, M., Tedstone, A., et al. (2017). Ice sheets as a missing source of silica to the polar oceans. *Nat. Commun.* 8:14198. doi: 10.1038/ncomms14198

Hawkings, J. R., Wadham, J. L., Tranter, M., Lawson, E., Sole, A., Cowton, T., et al. (2015). The effect of warming climate on nutrient and solute export from the Greenland Ice Sheet. *Geochem. Perspect. Lett.* 1, 94–104. doi: 10.7185/geochemlet.1510

Henriksen, N., Higgins, A. K., Kalsbeek, F., Pulvertaft, T., and Christopher, R. (2009). "Greenland from Archaean to Quaternary: descriptive text to the 1995 Geological map of Greenland,' 1: 2 500 000," in *Geological Survey of Denmark and Greenland Bulletin 18*, 2nd Edn. (Copenhagen: Geological Survey of Denmark and Greenland).

Hillebrand, H. (2004). On the generality of the latitudinal diversity gradient. *Am. Nat.* 163, 192–211. doi: 10.1086/381004

Hood, E., and Berner, L. (2009). Effects of changing glacial coverage on the physical and biogeochemical properties of coastal streams in southeastern Alaska. *J. Geophys. Res. Biogeosci.* 114:G03001. doi: 10.1029/2009JG000971

Hood, E., Fellman, J., Spencer, R. G., Hernes, P. J., Edwards, R., D'Amore, D., et al. (2009). Glaciers as a source of ancient and labile organic matter to the marine environment. *Nature* 462, 1044–1047. doi: 10.1038/nature08580

Hotaling, S., Finn, D. S., Joseph Giersch, J., Weisrock, D. W., and Jacobsen, D. (2017a). Climate change and alpine stream biology: progress, challenges, and opportunities for the future. *Biol. Rev.* 92, 2024–2045. doi: 10.1111/brv.12319

Hotaling, S., Hood, E., and Hamilton, T. L. (2017b). Microbial ecology of mountain glacier ecosystems: biodiversity, ecological connections and implications of a warming climate. *Environ. Microbiol.* 19, 2935–2948. doi: 10.1111/1462-2920.13766

Hubbard, B., and Nienow, P. (1997). Alpine subglacial hydrology. *Quat. Sci. Rev.* 16, 939–955. doi: 10.1016/S0277-3791(97)00031-0

Huss, M., and Hock, R. (2018). Global-scale hydrological response to future glacier mass loss. *Nat. Clim. Change* 8, 135–140. doi: 10.1038/s41558-017-0049-x

Irvine-Fynn, T. D., Hodson, A. J., Moorman, B. J., Vatne, G., and Hubbard, A. L. (2011). Polythermal glacier hydrology: a review. *Rev. Geophys.* 49:RG4002. doi: 10.1029/2010RG000350

Katoh, K., and Standley, D. M. (2013). MAFFT multiple sequence alignment software version 7: improvements in performance and usability. *Mol. Biol. Evol.* 30, 772–780. doi: 10.1093/molbev/mst010

Kohler, T. J., Žárský, J. D., Yde, J. C., Lamarche-Gagnon, G., Hawkings, J. R., Tedstone, A. J., et al. (2017). Carbon dating reveals a seasonal progression in the source of particulate organic carbon exported from the Greenland Ice Sheet. *Geophys. Res. Lett.* 44, 6209–6217. doi: 10.1002/2017GL073219

Lamarche-Gagnon, G., Wadham, J. L., Lollar, B. S., Arndt, S., Fietzek, P., Beaton, A. D., et al. (2019). Greenland melt drives continuous export of methane from its bed. *Nature* 565, 73–77. doi: 10.1038/s41586-018-0800-0

Langford, H., Hodson, A., Banwart, S., and Bøggild, C. (2010). The microstructure and biogeochemistry of arctic cryoconite granules. *Ann. Glaciol.* 51, 87–94. doi: 10.3189/172756411795932083

Lawson, E. C., Wadham, J. L., Tranter, M., Stibal, M., Lis, G. P., Butler, C. E., et al. (2014). Greenland Ice sheet exports labile organic carbon to the Arctic oceans. *Biogeosciences* 11, 4015–4028. doi: 10.5194/bg-11-4015-2014

Lee, S. Y., and Eom, Y. B. (2016). Analysis of microbial composition associated with freshwater and seawater. *Biomed. Sci. Lett.* 22, 150–159. doi: 10.15616/BSL.2016.22.4.150

Lindbäck, K., Pettersson, R., Hubbard, A. L., Doyle, S. H., van As, D., Mikkelsen, A. B., et al. (2015). Subglacial water drainage, storage, and piracy beneath the Greenland ice sheet. *Geophys. Res. Lett.* 42, 7606–7614. doi: 10.1002/2015GL065393

Lynch, M. D. J., and Neufeld, J. D. (2015). Ecology and exploration of the rare biosphere. *Nat. Rev. Microbiol.* 13, 217–229. doi: 10.1038/nrmicro3400

Mateos-Rivera, A., Yde, J. C., Wilson, B., Finster, K. W., Reigstad, L. J., and Øvreås, L. (2016). The effect of temperature change on the microbial diversity and community structure along the chronosequence of the sub-arctic glacier forefield of Styggedalsbreen (Norway). *FEMS Microbiol. Ecol.* 92:fnw038. doi: 10.1093/femsec/fiw038

McMurdie, P. J., and Holmes, S. (2013). phyloseq: an r package for reproducible interactive analysis and graphics of microbiome census data. *PLoS One* 8:e61217. doi: 10.1371/journal.pone.0061217

Meyer, F., Paarmann, D., D'Souza, M., Olson, R., Glass, E. M., Kubal, M., et al. (2008). The metagenomics RAST server–a public resource for the automatic phylogenetic and functional analysis of metagenomes. *BMC Bioinformatics* 9:386. doi: 10.1186/1471-2105-9-386

Milner, A. M., Khamis, K., Battin, T. J., Brittain, J. E., Barrand, N. E., Füreder, L., et al. (2017). Glacier shrinkage driving global changes in downstream systems. *Proc. Natl. Acad. Sci. U.S.A.* 114, 9770–9778. doi: 10.1073/pnas.1619807114

Mitchell, A. C., Lafrenière, M. J., Skidmore, M. L., and Boyd, E. S. (2013). Influence of bedrock mineral composition on microbial diversity in a subglacial environment. *Geology* 41, 855–858. doi: 10.1130/G34194.1

Montross, S. N., Skidmore, M., Tranter, M., Kivimäki, A. L., and Parkes, R. J. (2013). A microbial driver of chemical weathering in glaciated systems. *Geology* 41, 215–218. doi: 10.1130/G33572.1

Oksanen, J., Blanchet, F. G., Friendly, M., Kindt, R., Legendre, P., McGlinn, D., et al. (2018). *vegan: Community Ecology Package. R Package Version 2.4-6*. Available online at: https://CRAN.R-project.org/package=vegan (accessed December 27, 2019).

O'Neel, S., Hood, E., Bidlack, A. L., Fleming, S. W., Arimitsu, M. L., Arendt, A., et al. (2015). Icefield-to-ocean linkages across the northern Pacific coastal temperate rainforest ecosystem. *BioScience* 65, 499–512. doi: 10.1093/biosci/biv027

Palmer, S., Shepherd, A., Nienow, P., and Joughin, I. (2011). Seasonal speedup of the Greenland Ice Sheet linked to routing of surface water. *Earth Planet. Sc. Lett.* 302, 423–428. doi: 10.1016/j.epsl.2010.12.037

Pianka, E. R. (1966). Latitudinal gradients in species diversity: a review of concepts. *Am. Nat.* 100, 33–46. doi: 10.1086/282398

R Core Team (2017). *R: A Language and Environment for Statistical Computing*. Vienna: R Foundation for Statistical Computing. Available online at: https://www.R-project.org/.

Raes, E. J., Bodrossy, L., van de Kamp, J., Bissett, A., and Waite, A. M. (2018). Marine bacterial richness increases towards higher latitudes in the eastern Indian Ocean. *Limnol. Oceanogr. Lett.* 3, 10–19. doi: 10.1002/lol2.10058

Rohde, K. (1992). Latitudinal gradients in species diversity: the search for the primary cause. *Oikos* 64, 514–527. doi: 10.2307/3545569

Schloss, P. D., Westcott, S. L., Ryabin, T., Hall, J. R., Hartmann, M., Hollister, E. B., et al. (2009). Introducing mothur: open-source, platform-independent, community-supported software for describing and comparing microbial communities. *Appl. Environ. Microbiol.* 75, 7537–7541. doi: 10.1128/AEM.01541-09

Sharp, M., Parkes, J., Cragg, B., Fairchild, I. J., Lamb, H., and Tranter, M. (1999). Widespread bacterial populations at glacier beds and their relationship to rock weathering and carbon cycling. *Geology* 27, 107–110. doi: 10.1130/0091-76131999027<0107:WBPAGB<2.3.CO;2

Sheik, C. S., Stevenson, E. I., Den Uyl, P. A., Arendt, C. A., Aciego, S. M., and Dick, G. J. (2015). Microbial communities of the Lemon Creek Glacier show subtle structural variation yet stable phylogenetic composition over space and time. *Front. Microbiol.* 6:495. doi: 10.3389/fmicb.2015.00495

Stachnik, L., Yde, J. C., Nawrot, A., Uzarowicz, L., Lepkowska, E., and Kozak, K. (2019). Aluminium in glacial meltwater demonstrates an association with nutrient export (Werenskiöldbreen, Svalbard). *Hydrol. Process.* 33, 1638–1657. doi: 10.1002/hyp.13426

Stamatakis, A. (2014). RAxML Version 8: a tool for phylogenetic analysis and post-analysis of large phylogenies. *Bioinformatics* 30, 1312–1313. doi: 10.1093/bioinformatics/btu033

Stibal, M., Hasan, F., Wadham, J. L., Sharp, M. J., and Anesio, A. M. (2012a). Prokaryotic diversity in sediments beneath two polar glaciers with contrasting organic carbon substrates. *Extremophiles* 16, 255–265. doi: 10.1007/s00792-011-0426-8

Stibal, M., Telling, J., Cook, J., Mak, K. M., Hodson, A., and Anesio, A. M. (2012b). Environmental controls on microbial abundance and activity on the Greenland ice sheet: a multivariate analysis approach. *Microb. Ecol.* 63, 74–84. doi: 10.1007/s00248-011-9935-3

Stibal, M., Wadham, J. L., Lis, G. P., Telling, J., Pancost, R. D., Dubnick, A., et al. (2012c). Methanogenic potential of Arctic and Antarctic subglacial environments with contrasting organic carbon sources. *Global Change Biol.* 18, 3332–3345. doi: 10.1111/j.1365-2486.2012.02763.x

Tranter, M., Brown, G. H., Hodson, A. J., and Gurnell, A. M. (1996). Hydrochemistry as an indicator of subglacial drainage system structure: a comparison of alpine and sub-polar environments. *Hydrol. Process.* 10, 541–556. doi: 10.1002/(sici)1099-1085(199604)10:4<541::aid-hyp391>3.0.co;2-9

Tranter, M., Sharp, M. J., Lamb, H. R., Brown, G. H., Hubbard, B. P., and Willis, I. C. (2002). Geochemical weathering at the bed of Haut Glacier d'Arolla, Switzerland—a new model. *Hydrol. Process.* 16, 959–993. doi: 10.1002/hyp.309

Tranter, M., Skidmore, M., and Wadham, J. (2005). Hydrological controls on microbial communities in subglacial environments. *Hydrol. Process.* 19, 995–998. doi: 10.1002/hyp.5854

Tweed, F. S., Roberts, M. J., and Russell, A. J. (2005). Hydrologic monitoring of supercooled meltwater from Icelandic glaciers. *Quat. Sci. Rev.* 24, 2308–2318. doi: 10.1016/j.quascirev.2004.11.020

Van de Wal, R. S. W., and Russell, A. J. (1994). A comparison of energy balance calculations, measured ablation and meltwater runoff near Søndre Strømfjord, West Greenland. *Glob. Planet. Change* 9, 29–38. doi: 10.1016/0921-8181(94)90005-1

Větrovský, T., Baldrian, P., and Morais, D. (2018). SEED 2: a user-friendly platform for amplicon high-throughput sequencing data analyses. *Bioinformatics* 34, 2292–2294. doi: 10.1093/bioinformatics/bty071

Vu, V. Q. (2011). *ggbiplot: A ggplot2 Based Biplot. R Package Version 0.55*. Available online at: http://github.com/vqv/ggbiplot (accessed December 27, 2019).

Wadham, J. L., Bottrell, S., Tranter, M., and Raiswell, R. (2004). Stable isotope evidence for microbial sulphate reduction at the bed of a polythermal high Arctic glacier. *Earth Planet. Sc. Lett.* 219, 341–355. doi: 10.1016/S0012-821X(03)00683-6

Wadham, J. L., Tranter, M., Skidmore, M., Hodson, A. J., Priscu, J., Lyons, W. B., et al. (2010). Biogeochemical weathering under ice: size matters. *Global Biogeochem. Cycles* 24:GB3025. doi: 10.1029/2009GB003688

Warnes, G. R., Bolker, B., Bonebakker, L., Gentleman, R., Huber, W., Liaw, A., et al. (2019). *gplots: Various R Programming Tools for Plotting Data. R Package Version 3.0.1.1*. Available online at: https://CRAN.R-project.org/package=gplots (accessed December 27, 2019).

Whitaker, D., and Christman, M. (2014). *Clustsig: Significant Cluster Analysis. R package Version 1.1*. Available online at: https://CRAN.R-project.org/package=clustsig (accessed December 27, 2019).

Yde, J. C., Riger-Kusk, M., Christiansen, H. H., Knudsen, N. T., and Humlum, O. (2008). Hydrochemical characteristics of bulk meltwater from an entire ablation season, Longyearbreen, Svalbard. *J. Glaciol.* 54, 259–272. doi: 10.3189/002214308784886234

Žárský, J. D., Kohler, T. J., Yde, J. C., Falteisek, L., Lamarche-Gagnon, G., Hawkings, J. R., et al. (2018). Prokaryotic assemblages in suspended and subglacial sediments within a glacierized catchment on Qeqertarsuaq (Disko Island), west Greenland. *FEMS Microbiol. Ecol.* 94:fiy100. doi: 10.1093/femsec/fiy100

Zemp, M., Huss, M., Thibert, E., Eckert, N., McNabb, R., Huber, J., et al. (2019). Global glacier mass changes and their contributions to sea-level rise from 1961 to 2016. *Nature* 568:382. doi: 10.1038/s41586-019-1071-0

Conflict of Interest: The authors declare that the research was conducted in the absence of any commercial or financial relationships that could be construed as a potential conflict of interest.

frontiers in Microbiology

ORIGINAL RESEARCH
published: 15 April 2020
doi: 10.3389/fmicb.2020.00569

Variation in Snow Algae Blooms in the Coast Range of British Columbia

*Casey B. Engstrom, Kurt M. Yakimovich and Lynne M. Quarmby**

Department of Molecular Biology and Biochemistry, Simon Fraser University, Burnaby, BC, Canada

Snow algae blooms cover vast areas of summer snowfields worldwide, reducing albedo and increasing snow melt. Despite their global prevalence, little is known about the algae species that comprise these blooms. We used 18S and *rbcL* metabarcoding and light microscopy to characterize algae species composition in 31 snow algae blooms in the Coast Range of British Columbia, Canada. This study is the first to thoroughly document regional variation between blooms. We found all blooms were dominated by the genera *Sanguina*, *Chloromonas*, and *Chlainomonas*. There was considerable variation between blooms, most notably species assemblages above treeline were distinct from forested sites. In contrast to previous studies, the snow algae genus *Chlainomonas* was abundant and widespread in snow algae blooms. We found few taxa using traditional 18S metabarcoding, but the high taxonomic resolution of *rbcL* revealed substantial diversity, including OTUs that likely represent unnamed species of snow algae. These three cross-referenced datasets (*rbcL*, 18S, and microscopy) reveal that alpine snow algae blooms are more diverse than previously thought, with different species of algae dominating different elevations.

Keywords: snow, algae, microbiome, amplicon, *rbcL*, 18S, alpine, metabarcoding

OPEN ACCESS

Edited by:
David Anthony Pearce, Northumbria University, United Kingdom

Reviewed by:
Stefanie Lutz, Agroscope, Switzerland
Hanzhi Lin, University of Maryland Center for Environmental Science (UMCES), United States

****Correspondence:***
Lynne M. Quarmby
quarmby@sfu.ca

Specialty section:
This article was submitted to Extreme Microbiology, a section of the journal Frontiers in Microbiology

Received: *21 January 2020*
Accepted: *15 March 2020*
Published: *15 April 2020*

Citation:
Engstrom CB, Yakimovich KM and Quarmby LM (2020) Variation in Snow Algae Blooms in the Coast Range of British Columbia. Front. Microbiol. 11:569. doi: 10.3389/fmicb.2020.00569

1. INTRODUCTION

Each summer, vast areas of snow surface are colored red by snow algae blooms in polar and alpine snowfields worldwide. Red snowfields have been found on every continent (Marchant, 1982; Yoshimura et al., 1997; Duval et al., 1999; Segawa et al., 2018; Vimercati et al., 2019) as well as overlying Arctic sea ice (Gradinger and Nurnberg, 1996). Snow algae blooms can be quite extensive: in Alaska, remote sensing suggests snow algae covered up to one third of a 1,900 km^2 icefield (Ganey et al., 2017). In recent years snow algae have received attention for their role in reducing snow surface albedo, which could substantially increase snow melt (Lutz et al., 2016; Ganey et al., 2017). Thus, snow algae could impact summer water supplies held in mountain snowpack, and reduce glacier mass balance. Snow algae blooms have been recorded throughout history since the time of the ancient Romans (Darwin, 1839; Elder, 1893), but we do not know whether the extent and duration of blooms are increasing with extended melt seasons due to global warming. Despite their potential impact on global albedo, we are only beginning to identify the algae species that comprise snow algae blooms.

Microscopy reveals a diversity of cell morphologies in snow algae blooms, but different species can look nearly identical, and the same species can look completely different depending on environmental conditions (Matsuzaki et al., 2019). The snow algae *Chloromonas krienitzii* are small green biflagellates in culture, but cells in field samples are nearly twice the diameter, with orange pigment, short spines, and thick cell walls (Matsuzaki et al., 2015). The environmental cues that

trigger this transformation are not well understood, but increased light intensity and nitrogen deprivation can trigger secondary pigment accumulation in snow algae (Leya et al., 2009), and also in the freshwater algae *Haematococcus pluvialis* (Shah et al., 2016). Green blooms of snow algae are less frequently described in the literature than red blooms, and some researchers have suggested that green snow develops into red snow (Mueller et al., 2001). Metabarcoding studies have found green and red snow with distinct community compositions (Lutz et al., 2015; Terashima et al., 2017), but there are some OTUs that are found in both green and red snow (Lutz et al., 2017), leaving open the possibility that red snow develops from green beginnings.

Green algae of class Chlorophyceae are predominant in many snow algae blooms, including the genera *Sanguina*, *Chloromonas*, and *Chlainomonas*. The genus *Sanguina* was only recently established and contains just two species; however, many sequences from red snow form a yet-unnamed sister clade to *Sanguina* (Procházková et al., 2019). *Sanguina* has been found in red and orange snow algae blooms worldwide (Procházková et al., 2019). Many species of snow algae have been assigned to *Chloromonas*, including at least twelve cultured representatives (Matsuzaki et al., 2019). Various *Chloromonas* species can form green, orange, or brown colored blooms on the snow surface, and are also found worldwide (Remias et al., 2013, 2018; Procházková et al., 2018b). Less is known about *Chlainomonas*, which has been found in central Europe, western USA, and New Zealand (Novis et al., 2008; Remias et al., 2016; Procházková et al., 2018a). The distinctive red-pigmented cells of this genus (nearly twice the diameter of *Sanguina nivaloides*) have only been reported from waterlogged snow overlying alpine lakes (Novis et al., 2008; Remias et al., 2016; Procházková et al., 2018b). 18S rDNA and *rbcL* sequences show that *Chlainomonas* is closely related to *Chloromonas* (Novis et al., 2008). While Chlorophyceae predominate in many snow algae blooms, other classes of snow algae have been reported: Chrysophyceae in yellow snow in Antarctica, the Alps, and Svalbard (Remias et al., 2019; Soto et al., 2020), and Trebouxiophyceae in green snow in Greenland (Lutz et al., 2015).

While many species of snow algae have been described on the basis of morphology and Sanger sequencing, metabarcoding studies have found red snow algae blooms are dominated by relatively few OTUs. Algae community composition was similar in 33 Arctic red snow samples, all of which were dominated by two OTUs of uncultured Chlamydomonadaceae, along with low relative abundance of *Raphidonema nivale* and *Chloromonas polyptera* (Lutz et al., 2016). Another study using ITS2 metabarcoding found 24 polar red snow sites contained similar algae assemblages, also dominated by two OTUs of uncultured Chlamydomonadaceae with secondary abundance of *Raphidonema* and *Chloromonadinia* (Segawa et al., 2018). Other studies using 18S metabarcoding were limited to class level taxonomic assignments of algae (Hamilton and Havig, 2017)—being highly conserved, short 18S reads cannot distinguish between closely related species or genera.

Based on how little is known about the regional variation in species composition of snow algae blooms, we set out to answer the following questions: what species of snow algae are found in our region? What patterns of co-occurrence exist between species? Which species are the most abundant? Are there distinct bloom types dominated by different species? To answer these questions, we assessed snow algae species composition in 33 samples from the Coast Range of British Columbia using light microscopy and 18S and *rbcL* (coding for Rubisco large subunit) metabarcoding. *rbcL* OTU richness was greater than 18S, revealing previously unknown diversity. By cross-referencing *rbcL*, 18S, and microscopy-based community composition we were able to account for some of the biases inherent in morphology-based identification and PCR-based metabarcoding. Our results show that snow algae species composition was highly variable from site to site, and blooms were dominated by different species at different elevations.

2. MATERIALS AND METHODS

2.1. Field Sampling and Microscopy

We collected 309 snow algae samples from alpine and subalpine sites in the Coast Range near Vancouver, British Columbia, Canada throughout the summer of 2018 (**Supplementary Figure S1**). We collected red, orange, and green snow samples from 13 different mountains from elevations ranging from 880 to 2,150 m above sea level (**Supplementary Table S2**). We collected samples from progressively higher elevations throughout the season as snow melted at lower elevations. We scooped samples from visibly colored snow into sterile 50 mL tubes, and kept samples cold during transport back to the lab by storing in snow. We melted each sample at room temperature on the lab bench, removed a 1 mL aliquot for light microscopy, and then stored the remaining sample at −20°C for up to eight months until DNA extraction.

We immediately fixed microscopy aliquots in 2% gluteraldehyde, which we stored at 4°C for up to 72 h. We quantified the relative abundance of morphospecies in 122 samples by identifying 100 cells on a haemocytometer under 400x light microscopy. We classified cell morphology based on similarity to published photographs of *Sanguina nivaloides* (Procházková et al., 2019), *Chloromonas* cf. *nivalis* (Procházková et al., 2018b), *Chloromonas* cf. *brevispina* (Matsuzaki et al., 2015), *Chlainomonas krienitzii* (Matsuzaki et al., 2015), *Chlainomonas rubra* (Novis et al., 2008). Cells that did not fall into one of these categories we classified as either "green cell" or "other." We did not attempt to identify green cells, as different taxa can look highly similar and are therefore prone to misidentification by light microscopy.

2.2. DNA Extraction and Amplicon Library Preparation

We selected 33 samples for *rbcL* and 18S metabarcoding. We chose this subset to include samples from different mountains, elevations, and dates, including samples containing distinct or unfamiliar cell morphologies. To lyse the cells we freeze-dried samples and mini-pestled 5–20 mg at room temperature before incubation in CTAB lysis buffer (CTAB extraction buffer, 2009). We extracted DNA in small batches of 5–6 samples at a time

using chloroform:isoamyl alcohol (Cubero et al., 1999), and purified DNA using ethanol and spin columns (Qiagen, Hilden) (**Supplementary Protocol S3**). As a negative control against cross-contamination we processed a tube of sterile distilled water alongside each batch, and tested this for DNA with a Qubit fluorometer (Thermo Fisher, Waltham, MA).

We designed custom primers to target a hypervariable region of snow algae *rbcL*. This gene is an established barcode for green algae, and is highly differentiated at the species level (Hall et al., 2010). We designed primers with the Eurofins primer design tool (https://eurofinsgenomics.eu/en/ecom/tools/pcr-primer-design/) based on the consensus of 20 GenBank snow algae sequences, targeting a 400 bp section of *rbcL* (**Supplementary Figure S5**). *Sanguina* sequences were not included because they were not available at the time. For 18S we used the universal primers Euk1181 and Euk1624 targeting the V7-V8 hypervariable regions (Wang et al., 2014) (**Supplementary Figure S4**). Primer sequences are available in **Supplementary Figure S6**.

We constructed our 18S and *rbcL* amplicon libraries using a standard two-step PCR protocol (**Supplementary Protocol S7**). The two-step PCR consists of an initial amplification of the region of interest, followed by a secondary amplification that attaches a barcode marker to each oligonucleotide, allowing samples to be pooled for high-throughput sequencing (Meyer and Kircher, 2010). We purified PCR product using Agencourt AMPure XP kit (Beckman Coulter, Brea, CA). We then standardized DNA concentration with Qubit, pooled samples, and sequenced our library on an Illumina MiSeq platform using the V3 kit (Illumina, San Diego, CA).

2.3. Bioinformatic Processing

We demultiplexed reads with CUTADAPT (Martin, 2011), and followed the default pipeline of DADA2 to filter, trim, denoise, dereplicate, merge paired-end reads, and remove chimeras (Callahan et al., 2016). We assigned taxonomy to amplicon sequence variants (ASVs) using IDTaxa, discarding assignments with a confidence score of 50% or lower. This is within IDTaxa's recommended settings of 40–60% (Murali et al., 2018). Because snow algae are not well represented on databases such as SILVA, we made custom databases for both 18S and *rbcL* using all available snow algae sequences on GenBank. Additionally, we classified 18S ASV taxonomy with SILVA, using the same 50% confidence cutoff as before (Quast et al., 2013).

We visualized *rbcL* ASV genetic distance using t-SNE (van der Maaten and Hinton, 2008), and then clustered ASVs by sequence similarity into OTUs using DBSCAN (Hahsler et al., 2019) with the epsilon parameter set equal to 4. The output of t-SNE depends on a user-specified parameter "perplexity," which determines whether the algorithm pays more attention to local or global clustering patterns (Wattenberg et al., 2016). To ensure that our results were not an artifact of this parameter selection, we ran the algorithm with a range of values from 10 to 50 and found no effect on the results. To validate this unconventional OTU clustering method (t-SNE and DBSCAN) we overlaid these OTU clusters on phylogenetic trees using IQTree (Nguyen et al., 2015) (**Supplementary Figures S8**, **S9**).

All scripts used in this analysis are freely available at https://github.com/cengstro/bc_snow_algae_amplicon.

3. RESULTS

We observed morphologically distinct snow algae blooms at different elevations (**Figure 1**; **Supplementary Figure S10**). We observed green, orange, and red snow as early as May 18 in forested areas, but did not observe snow algae above treeline (approximately 1,500 m in our study region) until June 20 (**Supplementary Table S2**). Red snow was prevalent in areas of high solar exposure above treeline, and most of these sites were dominated by cell morphologies we classified as *Sanguina cf. nivaloides*. Cells resembling *Chlainomonas rubra* were common at all elevations, often as the dominant cell type. Below treeline, the dominant cell morphologies were classified as *Chloromonas cf. brevispina*, *Chloromonas cf. nivalis*, and green cells that we did not attempt to classify.

Both 18S and *rbcL* amplicon libraries were dominated by reads assigned to Chlorophyta (**Figure 2**). We detected 68 algae amplicon sequence variants (ASVs) using 18S: 50 Chlorophyceae, 11 Trebouxiophyceae, and 7 Chrysophyceae. Our *rbcL* library detected 644 ASVs: 603 Chlorophyta and 41 Trebouxiophyceae. We found seven distinct *rbcL* ASV clusters (which we define here as OTUs) compared with just three 18S-defined algal OTUs (**Supplementary Figure S9**). In *rbcL*, the most abundant genera were *Chloromonas*, *Chlainomonas*, and *Sanguina*. Although the majority of ASVs were not assigned to genus level, our clustering showed that most ASVs were genetically similar to one of these three genera (**Figure 2**). OTUs "D" and "F" were closely related to *Chloromonas*, but they did not match any known species on GenBank. OTU "E" was not assigned to genus level, and the ten best BLAST matches included six different genera within Chlamydomonadaceae (86–87% sequence match), two of which were *Chloromonas* snow algae (LC012735).

18S and *rbcL* taxonomic composition varied with elevation. Low elevation samples were similar as shown by low *rbcL* UniFrac distances (Lozupone and Knight, 2005), while generally high elevation samples were more compositionally distinct (**Figure 3**). Samples collected latest in the season had the highest diversity (**Supplementary Figure S11**). Although there was no statistically significant trend between Shannon diversity and date, there was a weak correlation between Faith's phylogenetic diversity and date (Pearson's $r = 0.36$, $p = 0.04$). *Sanguina* predominated above 1,500 m, but was absent below this elevation (**Figure 4**). High-elevation samples contained one OTU of *Chloromonas* that was absent from low-elevation sites (**Figure 3** OTU "F"). *Raphidonema* was restricted to three samples from high-elevation snow overlying glaciers (best BLAST match to *Raphidonema longiseta*, KM462868.1). Most snow algae blooms above treeline were red, but we did collect two green snow samples from above treeline (N1.5, G1.4), both of which were dominated by *Chloromonas*. *Chlainomonas* was highly abundant at all elevations, in both high and low relative abundance. *Chloromonas krienitzii* was predominant around 1,200 m in clearings or sparse trees.

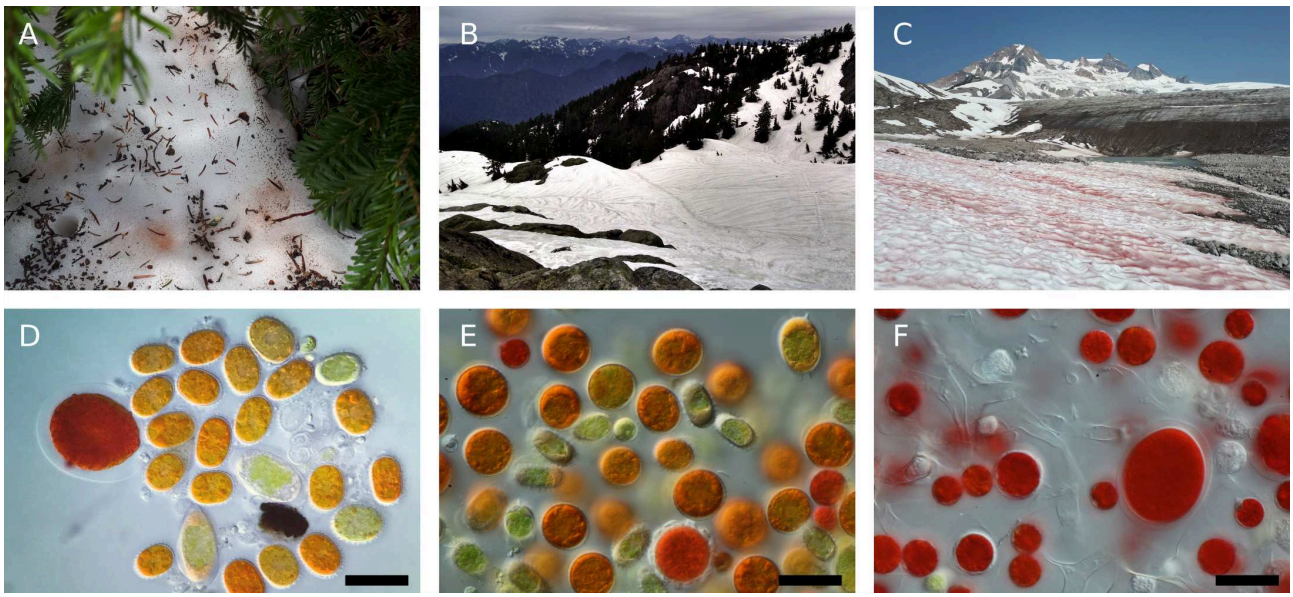

FIGURE 1 | Representative photographs of snow algae in the Coast Mountains of British Columbia. **(A)** Bronze colored snow algae blooms below conifer canopy. **(B)** Dark snow runnels containing snow algae (samples S2.2 and S9.2, **Supplementary Table S2**). **(C)** Red snow bloom above treeline at sample site G1.1. **(D)** Photomicrograph of bronze snow containing *Chloromonas cf. brevispina* and *Chloromonas cf. nivalis*. All photomicrographs taken with DIC light microscopy at 630x magnification, all scale bars 30 μm. **(E)** Photomicrograph of orange snow from the surface of a runnel containing *Chloromonas krienitzii* and *Chloromonas cf. nivalis*. **(F)** Photomicrograph of red snow containing *Sanguina nivaloides* and *Chlainomonas rubra* cell morphologies.

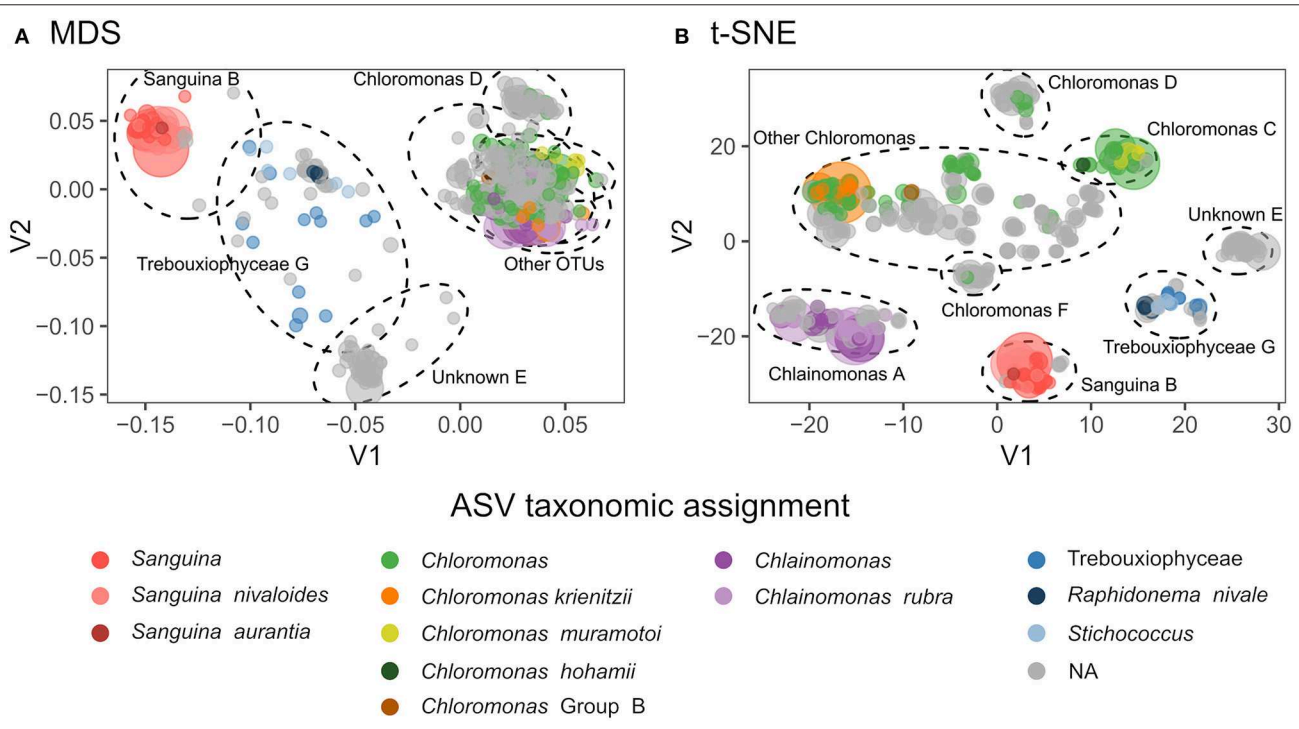

FIGURE 2 | (A) Multidimensional scaling (MDS) plot showing genetic distances between *rbcL* ASVs. Taxonomic assignments are indicated by color, and point size is proportional to total relative abundance. Dotted ellipses indicate OTU clusters. Stress = 0.13. **(B)** t-Distributed Stochastic Neighbor Embedding (t-SNE) dimensionality reduction of snow algae *rbcL* ASVs, with perplexity = 30. Dotted lines indicate OTU clustering by DBSCAN with eps=4.

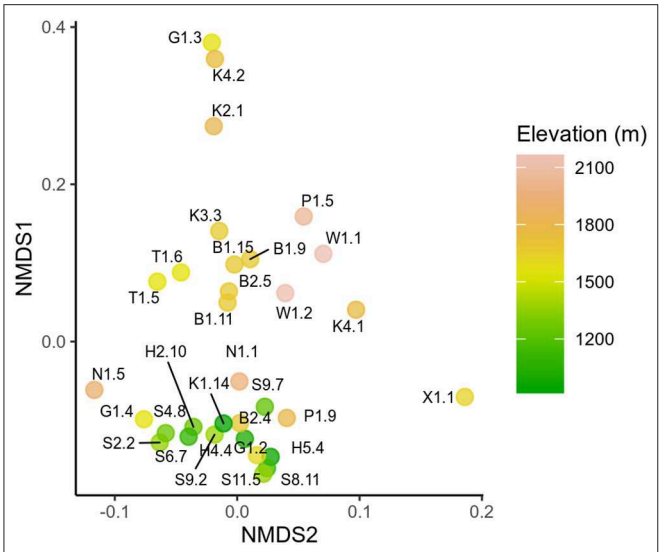

FIGURE 3 | Non-metric multidimensional scaling (NMDS) showing *rbcL* UniFrac distances between samples. Each sample is labeled by sample ID and colored by elevation.

At one site, we observed the snow transition from green to orange (**Supplementary Figure S12**). In May, the surface snow was white, with green snow 2–5 cm below the surface of a runnel (sample S2.2). On subsequent visits in June, the same runnel was orange on the surface with the green snow remaining below the surface (samples S4.6, S6.1, S9.2, S11.2). The green snow contained predominantly green cells, including cells with 2 or 4 flagella, while the orange snow contained predominantly orange spherical cells resembling *Chloromonas krienitzii* (Matsuzaki et al., 2015). Both green and orange snow were dominated by *rbcL* reads assigned to *C. krienitzii*, although the orange surface snow contained slightly higher abundance of *Chlainomonas* (**Supplementary Figure S12**).

4. DISCUSSION

Snow algae blooms are a widespread and globally important phenomenon, yet until now the distribution of distinct blooms within a region has not been well-documented. We present multiple data sets demonstrating elevational patterns in alpine snow algae bloom species composition. Most dramatically, *Sanguina* was dominant in red snow above treeline, while green and orange blooms of *C. krienitzii* were dominant in runnels at lower elevations. We found unexpected diversity within *rbcL* that we did not detect using 18S, including yet-unnamed species.

Community composition was consistent between 18S and *rbcL* libraries. However, in some cases we were able to distinguish taxa by *rbcL* that were not distinguished with 18S. For example, *Chlainomonas* was absent from our 18S dataset (**Figure 4**), likely because 18S of this genus is nearly identical to that of the closely-related *Chloromonas*. Because of this similarity, previous metabarcoding studies using 18S may have missed this genus. Indeed, our *rbcL* data suggest *Chlainomonas* may be more widely distributed than previously thought. Although previous work suggested that *Chlainomonas* is restricted to waterlogged snow overlying lakes (Novis et al., 2008; Procházková et al., 2018a), we did not find this to be the case. Only one *Chlainomonas*-dominant sample was located in waterlogged snow at the edge of a melt pool (sample S8.11), while the other *Chlainomonas*-dominant sample sites were not notably wetter than the surrounding snow, nor were they located over frozen lakes.

We noted that *Chlainomonas* was found in consistently higher relative abundance in our *rbcL* dataset than in cell counts (**Figure 3**). One possible explanation is that *rbcL* could have overestimated *Chlainomonas* due to higher *rbcL* copy number. *rbcL* is located in the plastid genome, and *Chlainomonas rubra* has multiple parietal chloroplasts per cell (Procházková et al., 2018b). Thus, *Chlainomonas* could have more copies of the plastid genome than genera with only one chloroplast such as *Sanguina* (Procházková et al., 2019). However, *Chlamydomonas reinhardtii* plastid genome copy number can vary depending on growth conditions (Eberhard et al., 2002). Accounting for the discrepancy between cell counts and rbcL relative abundance could prove challenging.

Our findings highlight the remaining unexplored diversity in the snow algae microbiome. Many ASVs were closely related to *Chloromonas*. Two *Chloromonas* OTUs "D" and "F" did not match any known species in GenBank (**Figure 2**). The majority of *Chloromonas rbcL* ASVs did not form distinct clusters. There were at least three species present in this group, however there could be more. One possibility is the 18S of OTU "E" is identical to other algae 18S. Indeed, *rbcL* diversity could be higher within *Chloromonas* than other genera because most *Chloromonas* species lack a pyrenoid (Nozaki et al., 2002), an organelle involved in the carbon-concentrating mechanism which contains high concentrations of cross-linked Rubisco. Perhaps due to the absence of a pyrenoid, many species of *Chloromonas* have high concentrations of non-synonymous mutations in the region of *rbcL* that codes for binding Rubisco together (Nozaki et al., 2002). While *rbcL* is a poor indicator of *Chloromonas* phylogeny (Nozaki et al., 2002), it nonetheless is highly differentiated between species and therefore is an effective barcode (Hall et al., 2010). Future studies could use ITS2, because compensatory base changes (CBCs) in this region correlate with species boundaries (Wolf et al., 2013).

The variation in species composition we observed could be due to differences in environmental conditions. Notably, *Sanguina* and *Chloromonas* "C" were only found in late summer samples from high alpine sites above 1,500 m (**Figure 3**). The lack of canopy cover at high elevations could select for light-tolerant species, but many low-elevation blooms were found in clearings that also received full sunlight (**Figure 4**). Nutrients could also impact snow algae species composition: garden fertilizer applied to experimental plots in Alaska stimulated snow algae growth (Ganey et al., 2017), and conifer litter was found to enhance the growth of the cultures of *Chloromonas pichinchae*, but not *Raphidonema nivale* (Hoham, 1976). Intriguingly, *Chloromonas* was dominant in low elevation sites with canopy cover, while we only found *Raphidonema* at high-elevation glacier sites. In Svalbard, *R. nivale* abundance increased on glacier surface

FIGURE 4 | Stacked barplots showing snow algae relative abundance, as measured by: **(top)** *rbcL* OTUs, **(middle)** 18S taxonomic assignment with custom snow algae database, and **(bottom)** cell morphology. Samples are arranged from low to high elevation left to right. Green triangles **(bottom)** indicate samples collected from sites below conifer canopy, and blue squares indicate samples collected from snow overlying glacier.

snow following wind storms, and the authors concluded that *Raphidonema* is a soil algae that can opportunistically colonize snow via wind (Stibal and Elster, 2005). Given the aerial dispersal capabilities of microalgae (Tesson et al., 2016) and genetic overlap between Arctic and Antarctic snow algae populations (Segawa et al., 2018) it seems unlikely that geographic distance would pose a barrier to snow algae distribution on a regional scale. Day length could also explain some of the seasonal variation we observed: peak snowmelt would coincide with longer day length at our high elevation sites, whereas

snowmelt coincides with shorter days at lower elevations. Site topography could also potentially influence species distribution: two sites dominated by *C. krienitzii* were in runnels overlying ephemeral streams, which could influence snow moisture and nutrient availability. However, measuring these environmental parameters is more challenging than it might initially appear. For example, depending on the time of day and weather we could visit the same bloom and get completely different measurements of temperature, irradiance, or snow moisture. The need for environmental data preceding the blooms is one of several issues that will be addressed in future work.

Previous work has shown that *Chloromonas krienitzii* undergoes distinct green and orange morphologies (Matsuzaki et al., 2015), but our study is the first to document this transition in the field. The transition occurred from May to June, suggesting that this process is mediated by seasonal changes. Although *Chlainomonas rbcL* was abundant in orange surface samples, our microscopic observations suggest that this was not the species responsible for the orange coloration, as orange *C. krienitzii* far outnumbered the red *Chlainomonas*. Secondary pigments likely protect snow algae from the damaging effects of intense solar irradiation at the snow surface (Bidigare et al., 1993), which could be why green cells were concentrated a few centimeters below the snow surface.

In conclusion, snow algae blooms contain diverse species assemblages, with different species occurring at different elevations. Blooms were dominated by three genera, *Chloromonas*, *Chlainomonas*, and *Sanguina*. We report substantially more species-level diversity than previous studies based on morphology or 18S sequence. Our work provides insight into the diversity and distribution of snow algae, the primary producers in a poorly understood yet globally important microbiome.

DATA AVAILABILITY STATEMENT

All raw sequence data are available under European Nucleotide Archive accession PRJEB34539. All scripts used in this study are available at https://github.com/cengstro/bc_snow_algae_amplicon.

AUTHOR CONTRIBUTIONS

CE, LQ, and KY designed this study. Samples collected by CE with assistance from KY and LQ. KY and CE prepared sequence libraries. CE and KY completed the bioinformatic analysis. CE wrote the manuscript with major input from LQ and KY. All authors discussed the results and contributed to the final manuscript.

FUNDING

This project was funded with a Sector Innovation Grant from Genome BC (SIP016), and a NSERC Individual Discovery Grant, both awarded to LQ.

ACKNOWLEDGMENTS

We thank Leah Tooman (Simon Fraser University) for assistance with sequencing, and Chris Rushton (Simon Fraser University) for assistance with bioinformatics.

SUPPLEMENTARY MATERIAL

The Supplementary Material for this article can be found online at: https://www.frontiersin.org/articles/10.3389/fmicb.2020.00569/full#supplementary-material

REFERENCES

Bidigare, R. R., Ondrusek, M. E., Kennicutt, M. C., Iturriaga, R., Harvey, H. R., Hoham, R. W., et al. (1993). Evidence a photoprotective for secondary carotenoids of snow algae. *J. Phycol.* 29, 427–434. doi: 10.1111/j.1529-8817.1993.tb00143.x

Callahan, B. J., McMurdie, P. J., Rosen, M. J., Han, A. W., Johnson, A. J. A., and Holmes, S. P. (2016). DADA2: High-resolution sample inference from Illumina amplicon data. *Nat. Methods* 13, 581–583. doi: 10.1038/nmeth.3869

CTAB extraction buffer (2009). *Cold Spring Harbor Protocols* 2009. doi: 10.1101/pdb.rec11984

Cubero, O. F., Crespo, A., Fatehi, J., and Bridge, P. D. (1999). DNA extraction and PCR amplification method suitable for fresh, herbarium-stored, lichenized, and other fungi. *Plant Syst. Evol.* 216, 243–249. doi: 10.1007/BF01084401

Darwin, C. (1839). *The Voyage of the Beagle*. London; New York, NY: Dent; Dutton. Available online at: https://search.library.wisc.edu/catalog/999467080402121

Duval, B., Duval, E., and Hoham, R. W. (1999). Snow algae of the Sierra Nevada, Spain, and High Atlas mountains of Morocco. *Int. Microbiol.* 2, 39–42.

Eberhard, S., Drapier, D., and Wollman, F.-A. (2002). Searching limiting steps in the expression of chloroplast-encoded proteins: relations between gene copy number, transcription, transcript abundance and translation rate in the chloroplast of *Chlamydomonas reinhardtii*. *Plant J.* 31, 149–160. doi: 10.1046/j.1365-313X.2002.01340.x

Elder, P. (1893). "Chap. 57 (56.) Showers of milk, blood, flesh, iron, wool, and baked tiles" in *The Natural History of Pliny*, Vol. 1 (London: George Bell & Sons). Available online at: https://books.google.ca/books?id=MZYVAAAAYAAJ&printsec=frontcover&dq=Showers+of+milk,+blood,+flesh,+iron,+wool,+and+baked+tiles%27%27+in+The+Natural+History+of+Pliny,+Volume+1.+Bohn%27s+Classical+Library&hl=en&sa=X&ved=0ahUKEwiB_sqO1cXoAhUkJDQIHR7KA8QQ6AEIKDAA#v=onepage&q&f=false

Ganey, G. Q., Loso, M. G., Burgess, A. B., and Dial, R. J. (2017). The role of microbes in snowmelt and radiative forcing on an Alaskan icefield. *Nat. Geosci.* 10, 754–759. doi: 10.1038/ngeo3027

Gradinger, R., and Nurnberg, D. (1996). Snow algal communities on arctic pack ice floes dominated by *Chlamydomonas nivalis* (Bauer) Wille. *Proc. NIPR Symp. Polar Biol.* 9, 35–43.

Hahsler, M., Piekenbrock, M., and Doran, D. (2019). Dbscan: fast density-based clustering with R. *J. Stat. Softw.* 91, 1–29. doi: 10.18637/jss.v091.i01

Hall, J. D., Fu, K., Lo, C., Lewis, L. A., and Karol, K. G. (2010). An assessment of proposed DNA barcodes in freshwater green algae. *Cryptog. Algol.* 31, 529–555.

Hamilton, T. L., and Havig, J. (2017). Primary productivity of snow algae communities on stratovolcanoes of the Pacific Northwest. *Geobiology* 15, 280–295. doi: 10.1111/gbi.12219

Hoham, R. W. (1976). The effect of coniferous litter and different snow meltwaters upon the growth of two species of snow algae in axenic culture. *Arct. Alpine Res.* 8, 377–386. doi: 10.1080/00040851.1976.12003886

Leya, T., Rahn, A., Lütz, C., and Remias, D. (2009). Response of arctic snow and permafrost algae to high light and nitrogen stress by changes in pigment composition and applied aspects for biotechnology: pigment change in snow algae. *FEMS Microbiol. Ecol.* 67, 432–443. doi: 10.1111/j.1574-6941.2008.00641.x

Lozupone, C., and Knight, R. (2005). UniFrac: a new phylogenetic method for comparing microbial communities. *Appl. Environ. Microbiol.* 71, 8228–8235. doi: 10.1128/AEM.71.12.8228-8235.2005

Lutz, S., Anesio, A. M., Edwards, A., and Benning, L. G. (2017). Linking microbial diversity and functionality of arctic glacial surface habitats. *Environ. Microbiol.* 19, 551–565. doi: 10.1111/1462-2920.13494

Lutz, S., Anesio, A. M., Field, K., and Benning, L. G. (2015). Integrated "Omics", targeted metabolite and single-cell analyses of arctic snow algae functionality and adaptability. *Front. Microbiol.* 6:1323. doi: 10.3389/fmicb.2015.01323

Lutz, S., Anesio, A. M., Raiswell, R., Edwards, A., Newton, R. J., Gill, F., et al. (2016). The biogeography of red snow microbiomes and their role in melting arctic glaciers. *Nat. Commun.* 7:11968. doi: 10.1038/ncomms11968

Marchant, H. J. (1982). Snow algae from the Australian snowy mountains. *Phycologia* 21, 178–184. doi: 10.2216/i0031-8884-21-2-178.1

Martin, M. (2011). Cutadapt removes adapter sequences from high-throughput sequencing reads. *EMBnet J.* 17, 10–12. doi: 10.14806/ej.17.1.200

Matsuzaki, R., Kawai-Toyooka, H., Hara, Y., and Nozaki, H. (2015). Revisiting the taxonomic significance of aplanozygote morphologies of two cosmopolitan snow species of the genus Chloromonas (Volvocales, Chlorophyceae). *Phycologia* 54, 491–502. doi: 10.2216/15-33.1

Matsuzaki, R., Nozaki, H., Takeuchi, N., Hara, Y., and Kawachi, M. (2019). Taxonomic re-examination of "Chloromonas nivalis (Volvocales, Chlorophyceae) zygotes" from Japan and description of *C. muramotoi* sp. nov. *PLoS ONE* 14:e0210986. doi: 10.1371/journal.pone.0210986

Meyer, M., and Kircher, M. (2010). Illumina sequencing library preparation for highly multiplexed target capture and sequencing. *Cold Spring Harb. Protoc.* 2010:pdb.prot5448. doi: 10.1101/pdb.prot5448

Mueller, T., Leya, T., and Fuhr, G. (2001). Persistent snow algal fields in spitsbergen: field observations and a hypothesis about the annual cell circulation. *Arctic Antarct. Alpine Res.* 33, 42–51. doi: 10.2307/1552276

Murali, A., Bhargava, A., and Wright, E. S. (2018). IDTAXA: A novel approach for accurate taxonomic classification of microbiome sequences. *Microbiome* 6:140. doi: 10.1186/s40168-018-0521-5

Nguyen, L.-T., Schmidt, H. A., Haeseler, A. von, and Minh, B. Q. (2015). IQ-TREE: a fast and effective stochastic algorithm for estimating maximum-likelihood phylogenies. *Mol. Biol. Evol.* 32, 268–274. doi: 10.1093/molbev/msu300

Novis, P. M., Hoham, R. W., Beer, T., and Dawson, M. (2008). Two snow species of the quadriflagellate green alga Chlainomonas (Chlorophyta, Volvocales): ultrastructure and phylogenetic position within the Chloromonas clade. *J. Phycol.* 44, 1001–1012. doi: 10.1111/j.1529-8817.2008.00545.x

Nozaki, H., Onishi, K., and Morita, E. (2002). Differences in pyrenoid morphology are correlated with differences in the rbcL genes of members of the chloromonas lineage (Volvocales, Chlorophyceae). *J. Mol. Evol.* 55, 414–430. doi: 10.1007/s00239-002-2338-9

Procházková, L., Leya, T., Křížková, H., and Nedbalová, L. (2019). *Sanguina nivaloides* and *Sanguina aurantia* gen. Et spp. Nov. (Chlorophyta): the taxonomy, phylogeny, biogeography and ecology of two newly recognised algae causing red and orange snow. *FEMS Microbiol. Ecol.* 95:fiz064. doi: 10.1093/femsec/fiz064

Procházková, L., Remias, D., Holzinger, A., Řezanka, T., and Nedbalová, L. (2018a). Ecophysiological and morphological comparison of two populations of *Chlainomonas* sp. (Chlorophyta) causing red snow on ice-covered lakes in the High Tatras and Austrian Alps. *Eur. J. Phycol.* 53, 230–243. doi: 10.1080/09670262.2018.1426789

Procházková, L., Remias, D., Rezanka, T., and Nedbalova, L. (2018b). *Chloromonas nivalis* subsp. *Tatrae*, subsp. Nov. (Chlamydomonadales, Chlorophyta): re-examination of a snow alga from the High Tatra Mountains (Slovakia). *Fottea* 18, 1–18. doi: 10.5507/fot.2017.010

Quast, C., Pruesse, E., Yilmaz, P., Gerken, J., Schweer, T., Yarza, P., et al. (2013). The SILVA ribosomal RNA gene database project: improved data processing and web-based tools. *Nucleic Acids Res.* 41, D590–D596. doi: 10.1093/nar/gks1219

Remias, D., Pichrtová, M., Pangratz, M., Lütz, C., and Holzinger, A. (2016). Ecophysiology, secondary pigments and ultrastructure of *Chlainomonas* sp. (Chlorophyta) from the European Alps compared with *Chlamydomonas nivalis* forming red snow. *FEMS Microbiol. Ecol.* 92:fiw030. doi: 10.1093/femsec/fiw030

Remias, D., Procházková, L., Holzinger, A., and Nedbalová, L. (2018). Ecology, cytology and phylogeny of the snow alga *Scotiella cryophila* K-1 (Chlamydomonadales, Chlorophyta) from the Austrian Alps. *Phycologia* 57, 581–592. doi: 10.2216/18-45.1

Remias, D., Procházková, L., Nedbalová, L., Andersen, R. A., and Valentin, K. (2019). Two new Kremastochrysopsis species, *K. austriaca* sp. Nov. And *K. americana* sp. Nov. (Chrysophyceae). *J. Phycol.* jpy.12937. doi: 10.1111/jpy.12937

Remias, D., Wastian, H., Lütz, C., and Leya, T. (2013). Insights into the biology and phylogeny of *Chloromonas polyptera* (Chlorophyta), an alga causing orange snow in Maritime Antarctica. *Antarct. Sci.* 25, 648–656. doi: 10.1017/S0954102013000060

Segawa, T., Matsuzaki, R., Takeuchi, N., Akiyoshi, A., Navarro, F., Sugiyama, S., et al. (2018). Bipolar dispersal of red-snow algae. *Nat. Commun.* 9:3094. doi: 10.1038/s41467-018-05521-w

Shah, M. M. R., Liang, Y., Cheng, J. J., and Daroch, M. (2016). Astaxanthin-producing green microalga *Haematococcus pluvialis*: from single cell to high value commercial products. *Front. Plant Sci.* 7:531. doi: 10.3389/fpls.2016.00531

Soto, D. F., Fuentes, R., Huovinen, P., and Gómez, I. (2020). Microbial composition and photosynthesis in Antarctic snow algae communities: integrating metabarcoding and pulse amplitude modulation fluorometry. *Algal Res.* 45:101738. doi: 10.1016/j.algal.2019.101738

Stibal, M., and Elster, J. (2005). Growth and morphology variation as a response to changing environmental factors in two Arctic species of Raphidonema (Trebouxiophyceae) from snow and soil. *Polar Biol.* 28, 558–567. doi: 10.1007/s00300-004-0709-y

Terashima, M., Umezawa, K., Mori, S., Kojima, H., and Fukui, M. (2017). Microbial community analysis of colored snow from an alpine snowfield in Northern Japan reveals the prevalence of betaproteobacteria with snow algae. *Front. Microbiol.* 8:1481. doi: 10.3389/fmicb.2017.01481

Tesson, S. V. M., Skjøth, C. A., Šantl-Temkiv, T., and Löndahl, J. (2016). Airborne microalgae: insights, opportunities, and challenges. *Appl. Environ. Microbiol.* 82, 1978–1991. doi: 10.1128/AEM.03333-15

van der Maaten, L., and Hinton, G. (2008). Visualizing data using t-SNE. *J. Mach. Learn. Res.* 9, 2579–2605.

Vimercati, L., Solon, A. J., Krinsky, A., Arán, P., Porazinska, D. L., Darcy, J. L., et al. (2019). Nieves penitentes are a new habitat for snow algae in one of the most extreme high-elevation environments on Earth. *Arctic Antarct. Alpine Res.* 51, 190–200. doi: 10.1080/15230430.2019.1618115

Wang, Y., Tian, R. M., Gao, Z. M., Bougouffa, S., and Qian, P.-Y. (2014). Optimal eukaryotic 18S and universal 16S/18S ribosomal RNA primers and their application in a study of symbiosis. *PLoS ONE* 9:e90053. doi: 10.1371/journal.pone.0090053

Wattenberg, M., Viégas, F., and Johnson, I. (2016). How to use t-SNE effectively. *Distill* 1:e2. doi: 10.23915/distill.00002

Wolf, M., Chen, S., Song, J., Ankenbrand, M., and Müller, T. (2013). Compensatory base changes in ITS2 secondary structures correlate with the biological species concept despite intragenomic variability in ITS2 sequences – a proof of concept. *PLoS ONE* 8:e66726. doi: 10.1371/journal.pone.0066726

Yoshimura, Y., Kohshima, S., and Ohtani, S. (1997). A community of snow algae on a Himalayan glacier: change of algal biomass and community structure with altitude. *Arctic Alpine Res.* 29:126. doi: 10.2307/1551843

Conflict of Interest: The authors declare that the research was conducted in the absence of any commercial or financial relationships that could be construed as a potential conflict of interest.

frontiers in Microbiology

ORIGINAL RESEARCH
published: 14 May 2020
doi: 10.3389/fmicb.2020.00824

Temperature Driven Membrane Lipid Adaptation in Glacial Psychrophilic Bacteria

*Noor Hassan[1,2], Alexandre M. Anesio[3], Muhammad Rafiq[1,2,4], Jens Holtvoeth[5], Ian Bull[5], Abdul Haleem[1], Aamer Ali Shah[1] and Fariha Hasan[1]**

[1] Applied Environmental and Geomicrobiology Laboratory, Department of Microbiology, Quaid-i-Azam University, Islamabad, Pakistan, [2] Bristol Glaciology Centre, School of Geographical Sciences, Faculty of Science, University of Bristol, Bristol, United Kingdom, [3] Department of Environmental Science, Aarhus University, Roskilde, Denmark, [4] Department of Microbiology, Balochistan University of Information Technology, Engineering and Management Sciences, Quetta, Pakistan, [5] Organic Geochemistry Unit, School of Chemistry, Cantock's Close, University of Bristol, Bristol, United Kingdom

Bacteria inhabiting non-polar glaciers are exposed to large variations in temperature, which significantly affects the fluidity of bacterial cell membranes. In order to maintain normal functions of the cell membranes, psychrophilic bacteria adapt by changing the composition of cell membrane fatty acids. However, information on the exact pattern of cell membrane adaptability in non-polar low-temperature habitats is scarce. In the present study, 42 bacterial strains were isolated from the Ghulmet, Ghulkin, and Hopar glaciers of the Hunza Valley in the Karakoram Mountain Range, Pakistan and their cell membrane fatty acid distributions studied, using gas chromatography/mass spectrometry (GC-MS) for the analysis of fatty acid methyl esters (FAMEs) liberated by acid-catalyzed methanolysis. Furthermore, Gram-negative and Gram-positive groups were grown under different temperature settings (5, 15, 25, and 35°C) in order to determine the effect of temperature on cell membrane (CM) fatty acid distribution. The analyses identified the major groups of cell membrane fatty acids (FA) as straight-chain monounsaturated fatty acids (*n*-MUFAs) and branched fatty acids (*br*-FAs), accounting for more than 70% of the fatty acids analyzed. The distribution of br-FAs and *n*-FAs in bacterial cell membranes was significantly affected by temperature, with the level of br-FAs decreasing relative to *n*-FAs with increasing temperature. Notably, the production of polyunsaturated fatty acids (PUFAs) was only seen at lower temperatures. This study contributes to understanding, for the first time, the role of br-FAs in the maintenance of cell membrane fluidity of bacteria inhabiting non-polar habitats.

Keywords: cell membrane, cold adaptation, fatty acids, non-polar glaciers, psychrophilic bacteria

OPEN ACCESS

Edited by:
Pierre Amato,
UMR 6296 Institut de Chimie de Clermont-Ferrand (ICCF), France

Reviewed by:
B. J. Wilkinson,
Illinois State University, United States
Craig Gatto,
Illinois State University, United States

***Correspondence:**
Fariha Hasan
farihahasan@yahoo.com

Specialty section:
This article was submitted to Extreme Microbiology, a section of the journal Frontiers in Microbiology

Received: *06 February 2020*
Accepted: *07 April 2020*
Published: *14 May 2020*

Citation:
Hassan N, Anesio AM, Rafiq M, Holtvoeth J, Bull I, Haleem A, Shah AA and Hasan F (2020) Temperature Driven Membrane Lipid Adaptation in Glacial Psychrophilic Bacteria. Front. Microbiol. 11:824. doi: 10.3389/fmicb.2020.00824

INTRODUCTION

By far, the largest part of the biosphere on Earth, which includes the oceans, is exposed to temperatures below 5°C either perennially or seasonally (Margesin et al., 2007; Margesin and Miteva, 2011; Hoshino and Matsumoto, 2012). Arctic and Antarctic habitats, ranging from high mountains to the deep ocean, experience subzero temperatures as they are deprived of direct sunlight. Among these cold habitats the deep sea represents the major component (almost 71% of the Earth is covered by ocean), with 90% of the volume of the ocean having a temperature of ∼5°C. Other large cold habitats include snow, permafrost, sea ice and glacial habitats (35, 24, 13,

and 10% coverage of the Earth surface, respectively) in addition to various other cold habitats such as lakes, cold soils (especially surface soils), cold deserts, and caves (Singh et al., 2006; Margesin and Miteva, 2011).

Bacteria inhabiting cold environments face prolonged frigid temperatures and daily freeze-thaw cycles (Montiel, 2000). They have to cope with special challenges to thrive under subzero temperatures, such as slow chemical reaction rates and limited enzyme activity, denaturation of proteins, increased water viscosity, decreased cell membrane fluidity (Russell, 1990; Crowe et al., 1992; Hassan et al., 2016) and limited water availability as a solvent for biochemical reactions (Wynn-Williams, 1990). However, bacteria have remarkable adaptive abilities that enable them to survive harsh and highly variable environmental conditions, including changes in pH and temperature (Ganzert et al., 2011; Bajerski and Wagner, 2013). These adaptation mechanisms include the expression of heat/cold shock proteins, production of protective compatible solutes or an altered metabolism (Georlette et al., 2004). Another strategy employed by bacteria is the modification of the cell membrane structure as it is involved in important metabolic processes and is a vital interface in the electron transport chain (Denich et al., 2003).

Homeoviscous adaptation, i.e., the alteration of cell membrane composition to maintain cell membrane fluidity in response to environmental changes, has long been observed in bacterial communities (Sinensky, 1974) and in bacteria involved in the direct synthesis of fatty acids, with diverse melting points, to maintain the required physical properties needed of membrane lipids (Mansilla et al., 2004). An increase in the amount of low-melting-point fatty acids (such as monounsaturated fatty acids, polyunsaturated fatty acids and branched-chain fatty acids relative to their saturated straight analogs) provides adequate membrane fluidity in almost all organisms (Fulco, 1983; Hazel and Williams, 1990; Suutari and Laakso, 1994). Low temperature and high pressure play a significant role in probing the integrity of membranes, with evidence even for irreversible change, i.e., from a fluid to a rigid state (Cossins and MacDonald, 1984; Hazel and Williams, 1990). Bacterial adaptation to low temperature and high pressure typically involves an increased proportion of branched chain fatty acids (BCFA) and unsaturated fatty acids (UFA) into membrane phospholipids (DeLong and Yayanos, 1986; Wirsen et al., 1986; Nichols et al., 1997). However, to the best of our knowledge, these results have only been obtained by studying Gram-negative bacteria residing in deep sea or a very few Antarctic habitats. The current study aims to characterize the cell membrane fatty acid profiles of Gram-positive and Gram-negative psychrotolerant bacteria isolated from non-polar glaciers and determine the role of saturated and unsaturated, straight and BCFAs in bacterial adaptation to low temperatures.

MATERIALS AND METHODS

Sampling, Isolation and Identification of Bacterial Strains

Samples (ice, melted water, and sediment) were collected from three different glaciers, Ghulkin (36.42791 N, 74.80659 E), Ghulmet (36°12.474 N, 74°29.035 E) and Hopar (36.2108228 N, 74.7724664 E) of the Hunza Valley, Karakoram Mountains Range, Pakistan using Nasco Whirl–Pak bags and bottles (Fisher Scientific). A total of 42 different bacterial strains were isolated using R2A and Nutrient agar at 5, 15, and 35°C as incubation temperatures. Culture of each bacteria isolate was then preserved in 35% glycerol and stored at −20°C prior to further analysis.

The genomic DNA of all the bacteria isolates was extracted using the Invitrogen PureLink Microbiome DNA Kit (Invitrogen) following instructions given by manufacturer. After that 16S rRNA gene for all of the bacterial isolates was amplified using primers 27F and 1492R. PCR conditions used for 16S rRNA amplification were adjusted as preliminary denaturation at 94°C for 5 min, then 40 cycles of 94, 56, and 72°C each for 30 s and a final step of extension at 72°C for 8 min. PCR products were then purified using QIAquick PCR Purification Kit (QIAGEN) and sequenced from MRC PPU DNA sequencing and services, University of Dundee, United Kingdom. Subsequently, obtained sequences were trimmed via BioEdit software and submitted to GenBank for getting accession numbers (**Tables 1**, **2**).

Production Media for Bacterial Growth

The experiments for the analysis of cell membrane fatty acids of all bacteria isolates were performed in Nutrient Agar (NA) [g L^{-1}; D(+)-glucose 1, peptone 15, sodium chloride 6, yeast extract 3] and Reasoner's 2A (R2A) (gL^{-1}; casein acid hydrolysate 0.5, dextrose 0.5, dipotassium phosphate 0.3, magnesium sulfate 0.024, protease peptone 0.5, sodium pyruvate 0.3, starch soluble 0.5, yeast extract 0.5). The growth of isolates was conducted in 250 mL Erlenmeyer flasks with 50 mL production media at 15°C for 7 days. The biomass collection of bacteria isolates was achieved by centrifuging the cultures in 50 mL falcon tubes at 4,500 *g* at 10°C for 30 min. The resulting cell pellets were stored in 2 mL microcentrifuge tubes and freeze-dried prior to subsequent use.

Preparation of Fatty Acid Methyl Esters (FAMEs)

Fatty acid methyl ester from all bacterial cell cultures were extracted using the protocol described by El Razak et al. (2014). Two mL of 5% methanolic HCl was mixed with 0.1 g of each dried bacterial cell culture and heated at 70°C in a water bath for 120 min in sealed glass tubes. The sealed glass tubes were allowed to cool at 23°C for 30 min. Then, 1 mL Milli-Q® water was added to the tubes and vortexed, followed by 2 mL hexane and robust vortexing of the vial in order to extract the liberated fatty acid methyl esters (FAMEs). After phase separation, the solvent layer was transferred into a clean vial and the hexane removed under a gentle stream of nitrogen.

Analysis of Cell Membrane Fatty Acid Distributions From Different Temperature Regimes

A total of 10 bacterial species, representing 10 different bacterial genera belonging to both Gram-negative and Gram-positive

TABLE 1 | List of bacteria species produced straight chain monounsaturated fatty acids (*n-MUFAs) as major group of cell membrane (CM) fatty acids (FA).

Bacterial species	Accession No	% of *n*-MUFAs/CM FA	Major fatty acids (%/cell membrane FA)	
Deinococcus aquaticus GW7	MK456560	78.3	*n*-$C_{15:1(cis-10)}$	32.9
Massilia aurea HI1	MK456563	84.3	*n*-$C_{15:1(cis-10)}$	37.1
Massilia oculi GI1	MK456529	58.5	*n*-$C_{16:1(cis-9)}$	50.8
Pseudomonas brassicacearum GS2	MK606638	69.4	*n*-$C_{16:1(cis-9)}$	35.8
Pseudomonas migulae GS3	MK606639	49.0	*n*-$C_{16:1(cis-9)}$	23.2
Pseudomonas mandelii GS12	MK606643	72.0	*n*-$C_{16:1(cis-9)}$	32.0
Arthrobacter nitroguajacolicus GS13	MK456545	89.6	*n*-$C_{16:1(cis-9)}$	42.0
Paenisporosarcina macmurdoensis GS17	MK456549	42.0	*n*-$C_{16:1(cis-9)}$	15.8
Janthinobacterium lividum GW1	MK456554	67.1	*n*-$C_{16:1(cis-9)}$	52.9
Pseudomonas extremaustralis HS8	MK456576	60.1	*n*-$C_{16:1(cis-9)}$	35.1
Pseudomonas veronii HS9	MK456577	72.2	*n*-$C_{16:1(cis-9)}$	25.8
Pseudomonas fluorescens HS10	MK456578	71.7	*n*-$C_{16:1(cis-9)}$	29.3
Pseudarthrobacter sulfonivorans HS14	MK456582	70.6	*n*-$C_{16:1(cis-9)}$	34.1
Massilia timonae HI7	MK456568	66.0	*n*-$C_{16:1(cis-9)}$	65.7
Flavobacterium sinopsychrotolerans GS7	MK456539	89.0	*n*-$C_{18:1(*tr-9)}$	50.8
Paracoccus hibiscisoli GS9	MK456541	94.4	*n*-$C_{18:1(tr-9)}$	93.2
Brevundimonas vesicularis GS11	MK456543	72.0	*n*-$C_{18:1(tr-9)}$	35.9
Brevundimonas mediterranea GS18	MK456550	77.2	*n*-$C_{18:1(tr-9)}$	58.6
Brevundimonas intermedia GS21	MK456553	83.7	*n*-$C_{18:1(tr-9)}$	57.5
Sphingobium xenophagum GhS4	MK456509	75.1	*n*-$C_{18:1(tr-9)}$	60.0
Acinetobacter radioresistens GhS8	MK456513	78.0	*n*-$C_{18:1(tr-9)}$	41.0
Brevundimonas nasdae GhW6	MK456525	77.5	*n*-$C_{18:1(tr-9)}$	58.2
Sanguibacter antarcticus GhW7	MK456526	53.6	*n*-$C_{18:1(tr-9)}$	45.5
Rhizobium giardinii HI5	MK456567	72.8	*n*-$C_{18:1(tr-9)}$	61.7

*Keys: *tr, trans; *n, straight chain.*

TABLE 2 | List of bacteria species produced branched chain fatty acids (*br-FAs) as major group of cell membrane (CM) fatty acids (FA).

Bacterial species	Accession No	% of br-FA /CM FA	Major fatty acids (%/cell membrane FA)	
Enterobacter cloacae GhS11	MK456516	73.4	*i-$C_{15:0}$	34.4
Stenotrophomonas maltophilia GhS14	MK456519	73.3	i-$C_{15:0}$	32.3
Arthrobacter agilis GS1	MK456533	97.9	*a-$C_{15:0}$	58.2
Rhizobium herbae GS14	MK606644	96.6	a-$C_{15:0}$	42.3
Sporosarcina psychrophila GS15	MK456547	82.2	a-$C_{15:0}$	59.6
Deinococcus depolymerans GhS1	MK456506	50.6	a-$C_{15:0}$	28.5
Staphylococcus equorum GhS5	MK456510	90.2	a-$C_{15:0}$	55.4
Arthrobacter sulfureus GhS9	MK456514	98.5	a-$C_{15:0}$	56.4
Enterobacter mori GhS12	MK456517	95.2	a-$C_{15:0}$	58.9
Plantibacter auratus HI4	MK456566	89.0	a-$C_{15:0}$	51.9
Arthrobacter psychrolactophilus HS1	MK456569	93.8	a-$C_{15:0}$	60.3
Pseudarthrobacter scleromae HS2	MK456570	91.1	a-$C_{15:0}$	47.7
Bacillus butanolivorans HS4	MK456572	84.0	a-$C_{15:0}$	40.1
Bacillus simplex HS7	MK456575	93.8	a-$C_{15:0}$	49.4
Delftia acidovorans HS13	MK456581	89.0	a-$C_{15:0}$	59.3
Pseudomonas frederiksbergensis HW2	MK456589	88.4	a-$C_{15:0}$	44.0
Sphingomonas faeni GW8	MK456561	96.6	a-$C_{17:0}$	38.5
Acidovorax radices GW9	MK456562	98.3	a-$C_{17:0}$	43.6

*Keys: *br, branched chain; *i, iso; *a, anteiso.*

groups, were selected in order to determine the variation or similarity in composition of bacterial cell membrane fatty acids growing under different temperature regimes. The selection criteria of bacteria isolates was based on their ability to grow over a wide range of temperatures and their first time study on selected temperatures. Briefly, bacteria isolates were grown at 5, 15, 25,

and 35°C using NB medium for 7 days. The bacterial biomass was obtained by centrifuging 40 mL falcon tubes containing bacterial cultures at 4,500 *g* at 10°C for 30 min. The pelleted bacterial cells were then subjected to FAME extraction as above.

Gas Chromatography-Mass Spectrometry (GC-MS) Analysis

Fatty acid methyl esters derived from the bacteria isolates were analyzed by GC-MS. The GC-MS comprised a Thermo Scientific Trace 1300 gas chromatograph coupled via a heated transfer line to a Thermo Scientific ISQ LT single quadrupole mass spectrometer. The GC was fitted with a programmable temperature vaporising (PTV) injector and an Agilent-HP 1 capillary column coated with a 100% dimethylpolysiloxane stationary phase (50 m × 0.32 mm internal diameter × 0.17 mm film thickness). The carrier gas was helium at a flow rate of 2 mL min^{-1}. The PTV was programmed to heat up to 300°C at 14°C sec^{-1}, transferring the analytes onto the column. The GC temperature program started with an initial temperature of 50°C, held for 1 min, then heated to 100°C at 10°C min^{-1}, then to 250°C at 4°C min^{-1} and finally to 300°C at 20°C min^{-1}. The final temperature was maintained for 5 min. Compounds were identified by their mass spectra, retention times and elution order in comparison to a commercial reference standard (Sigma Aldrich C_4-C_{24} FAME mix, inclusive of unsaturated compounds). Individual FAMEs were quantified by their peak areas relative to the peak area of an internal standard (methyl tetracosanoate, Sigma-Aldrich) and corrected for variable levels of ionization by a response factor that was calculated from analyses of the reference standard mix at the start of each analytical sequence. In addition, correlations between different temperature and fatty acids were also assessed in this study using GraphPad Prism 5.00.

RESULTS

In the current study, 42 different bacterial isolates representing 23 different genera were identified by 16S rRNA sequencing (**Tables 1**, **2**). *Pseudomonas* was the most dominant genus followed by *Arthrobacter*, *Brevundimonas,* and *Massilia*. In addition, cell membrane fatty acids analyses revealed that in 24 out of 42 bacterial strains straight-chain monounsaturated fatty acids (MUFAs) were the major group of cell membrane (CM) fatty acid (FA), whereas 18 species were found to have branched fatty acids, both saturated and monounsaturated, as the dominant FAs in their cell membranes. The most important membrane fatty acids found in the 42 cold-tolerant bacterial species are listed in **Tables 1**, **2**. The main individual *n*-MUFAs detected were *n*-$C_{15:1(cis-10)}$, *n*-$C_{16:1(cis-9)}$, and *n*-$C_{18:1(tr-9)}$, whilst the dominant br-FAs are *i*-$C_{15:0}$, *a*-$C_{15:0}$, and *a*-$C_{17:0}$. Most of the bacteria isolates were found to possess *a*-$C_{15:0}$ (15 bacteria isolates) followed by *n*-$C_{16:1(cis-9)}$ (12 bacteria isolates) and *n*-$C_{18:1(tr-9)}$ (10 bacteria isolates) in their cell membranes. Only 1 species was found to produce *i*-$C_{15:0}$, whereas 2 of each isolate produced *ai*-$C_{17:0}$ and *n*-$C_{15:1(cis-10)}$ as the primary cell membrane fatty acid moieties. Very few of the bacterial species studied produce polyunsaturated fatty acids (**Table 3**).

In 32 out of 42 bacterial species, either br-FAs or *n*-MUFAs accounted for more than 70% of all quantified cell membrane FAs. In *Paracoccus hibiscisoli* GS9, *n*-MUFAs account for 94% of the determined FAs, followed by *Arthrobacter nitroguajacolicus* GS13 (89.6%), *Flavobacterium sinopsychrotolerans* GS7 (89.0%), *Massilia aurea* HI1 (84.3%) and *Brevundimonas intermedia* GS21 (83.7%), with 11 species showing relative amounts of *n*-MUFAs of more than 70%. The proportion of br-FAs reaches 98.5% in *Arthrobacter sulfureus* GhS9 followed by *Acidovorax radices* GW9 (98.3%), *Arthrobacter agilis* GS1 (97.9%), *Sphingomonas faeni* GW8 (96.7%), *Rhizobium herbae* GS14 (96.6%), *Enterobacter mori* GhS12 (95.2%), *Bacillus simplex* HS7 (93.8%), *Arthrobacter psychrolactophilus* HS1 (93.7%), *Pseudarthrobacter scleromae* HS2 (91.1%) and *Staphylococcus equorum* GhS5 (90.2%). The remaining 7 strains contain 70% br-FA in their cell membranes. Some strains show a dominance of a single compound such as *n*-$C_{18:1(tr-9)}$ in *Paracoccus hibiscisoli* GS9 and *Rhizobium giardinii* HI5, with 93.3 and 61.7% of the quantified FAs, respectively.

In the current study, the effect of different temperatures on the distribution of fatty acids in the cell membranes of 10 bacterial species have been comprehensively determined (**Table 4**). The selected bacteria belong to Gram-negative (e.g., *Flavobacterium sinopsychrotolerans* GS7, *Paracoccus hibiscisoli* GS9, *Janthinobacterium lividum* GW1, *Sphingomonas faeni* GW8, *Brevundimonas nasdae*-GhW6, *Rhizobium giardinii* HI5 and *Pseudomonas extremaustralis*-HS8) and Gram-positive groups (e.g., *Sporosarcina psychrophila* GS15, *Staphylococcus equorum* GhS5 and *Arthrobacter psychrolactophilus* HS1). Correlations were used to represent association of temperatures with cell

TABLE 3 | Distribution of polyunsaturated fatty acids (PUFAs) in bacteria cell membranes at different temperatures.

Bacterial species	PUFAs	μg g^{-1} (temperatures °C)			
		5	15	25	35
Flavobacterium sinopsychrotolerans GS7	$C_{18:3(cis-6)}$	0.28	5.41	ND*	ND
	$C_{18:3(cis-9)}$	0.15	0.27	ND	ND
	$C_{18:3isomer}$	0.11	ND	ND	ND
Janthinobacterium lividum GW1	$C_{17:3}$	75.7	ND	ND	ND
	$C_{18:2(cis-9)}$	1.99	ND	ND	ND
	$C_{18:2(tr-9)}$	0.97	ND	ND	ND
	$C_{18:3(cis-6)}$	0.22	ND	ND	ND
	$C_{18:3}$ isomer	0.40	ND	ND	ND
Brevundimonas nasdae GhW6	$C_{18:2(cis-9)}$	54.3	0.32	ND	ND
	$C_{18:2(tr-9)}$	49.2	0.16	ND	ND
	$C_{20:3(cis-8)}$	0.84	ND	ND	ND
	$C_{20:3(cis-11)}$	1.05	ND	ND	ND
Sphingomonas faeni GW8	$C_{15:2(cis)}$	21.7	ND	ND	ND
	$C_{15:2(tr)}$	30.9	ND	ND	ND
	$C_{18:2(cis-9)}$	0.09	0.14	ND	ND
	$C_{18:2(tr-9)}$	0.04	0.34	ND	ND

*Keys: *not detected.*

TABLE 4 | Temperature derived distributions of the major groups of fatty acids in cell membranes of bacteria species.

Bacteria	Temp (°C)	Percentage (%) of major groups of fatty acids				
		a. br-SFAs	*b. n*-SFAs	*c. br*-MUFAs	*d. n*-MUFAs	*e.* PUFAs
1. Flavobacterium sinopsychrotolerans GS7	5	0.4	10	0.6	89	–
	15	0.4	18.1	0.5	81	–
	25	0.2	35.6	0.2	64	–
	35	0.2	24.5	0.3	75	–
2. Paracoccus hibiscisoli GS9	5	4	5	1	89	1
	15	0.3	4	0.3	93.5	2
	25	0.1	6	0.1	93	–
	35	0.2	9.8	-	90	–
3. Janthinobacterium lividum GW1	5	–	27	0.2	68.8	4
	15	1.2	30	1.1	67	0.07
	25	5	40	–	55	–
	35	–	58	–	36	–
4. Brevundimonas nasdae GhW6	5	0.1	10	1.9	88	–
	15	0.3	20	1.7	78	–
	25	0.4	27	2.6	70	–
	35	0.5	33	2.5	64	–
5. Rhizobium giardinii HI5	5	–	1.9	10	88	–
	15	–	5.9	21	73	–
	25	0.1	15.9	20	64	–
	35	0.4	22.6	13	63	–
6. Pseudomonas extremaustralis HS8	5	26	8	7	59	–
	15	24	14	2	60	–
	25	11	30	1	58	–
	35	–	46.9	0.1	53	–
7. Sphingomonas faeni GW8	5	65	1	30	1	3
	15	80	1.9	16	2	0.1
	25	72	23	0.2	4.8	–
	35	7	51	–	42	–
8. Sporosarcina psychrophile GS15	5	85.3	1	13.2	1.5	–
	15	86.2	1	10.1	2.7	–
	25	90.6	2.4	3.4	3.6	–
	35	90	4	–	–	–
9. Staphylococcus equorum GhS5	5	71	2	19	8	–
	15	77	2	13	8	–
	25	86	5	7	2	–
	35	94	4	1	1	–
10. Arthrobacter psychrolactophilus HS1	5	85	0.4	14.5	0.1	–
	15	94	1.4	4.5	0.1	–
	25	98	1.5	0.5	–	–
	35	98	1.8	–	0.2	–

membrane fatty acids (**Tables 5**, **6**). The Gram-negative strains accumulated straight-chain monounsaturated fatty acids (*n*-MUFAs) as the major group of cell membrane fatty acids except *Sphingomonas faeni* GW8 (**Table 4**). The highest quantity of *n*-MUFAs were produced at lower temperature, i.e., 5 and 15°C, and lower levels at higher temperature, i.e., 25 and 35°C, but *n*-MUFAs still formed the major group of cell membrane fatty acids at all temperatures, except for *Janthinobacterium lividum* GW1, which generated relative levels of straight-chain saturated fatty acids (*n*-SFA) of up to 58% at 35°C as compared to 36% of *n*-MUFAs. In addition, Gram-positive bacteria revealed predominantly branched-chain fatty acids, both saturated and monounsaturated, as the major groups among the analyzed cell membrane FAs (**Table 4**). However, at all temperatures, bacterial strains tend to incorporate higher levels of saturated branched-chain fatty acids into their cell membranes compared to branched-chain monounsaturated fatty acids (br-MUFAs). Saturated fatty acids occur only at very low levels (between 1.8 and 4%) in Gram-positive bacteria at all temperatures. In addition, Gram-positive bacteria exhibit the

TABLE 5 | Correlations of cell membrane fatty acids produced by Gram-negative bacteria species at different temperature.

Correlations					
Fatty acids (mg/g)	**Temperature (°C)**				**Correlation (R^2)**
	5	**15**	**25**	**35**	
***Rhizobium giardinii* HI5**					
n-$C_{16:0}$	0.034	0.135	0.253	0.404	*0.991***
n-$C_{18:0}$	0.085	0.163	0.252	0.369	*0.991***
ai-$C_{19:1}$	0.315	0.606	0.803	0.961	*0.980**
n-$C_{16:1(cis-9)}$	1.313	0.872	0.531	0.122	*0.997***
n-$C_{18:1(tr-9)}$	1.116	1.248	1.501	1.694	*0.987***
***Brevundimonas nasdae* GhW6**					
n-$C_{15:0}$	0.072	0.149	0.174	0.212	*0.943**
n-$C_{16:0}$	0.195	0.423	0.520	0.724	*0.979**
n-$C_{17:1(tr-10)}$	0.328	0.189	0.153	0.071	*0.944**
n-$C_{16:1(cis-9)}$	0.643	0.371	0.114	0.070	*0.928*
n-$C_{18:1(tr-9)}$	1.716	1.765	1.923	2.045	*0.964**
***Flavobacterium sinopsychrotolerans* GS7**					
n-$C_{16:0}$	0.215	0.378	0.542	0.923	*0.948**
n-$C_{17:0}$	0.036	0.046	0.150	0.233	*0.923*
n-$C_{16:1(cis-9)}$	1.073	0.930	0.422	0.291	*0.936*
n-$C_{17:1(tr-10)}$	0.757	0.536	0.145	0.115	*0.920*
n-$C_{18:1(tr-9)}$	1.247	1.762	1.82	2.032	*0.874*
***Paracoccus hibiscisoli* GS9**					
n-$C_{16:0}$	0.0003	0.001	0.004	0.010	*0.879*
n-$C_{18:0}$	0.046	0.051	0.092	0.140	*0.911*
ai-$C_{15:0}$	0.012	0.015	0.022	0.028	*0.977**
i-$C_{17:1}$	1.200	0.946	0.03	0.014	*0.880*
n-$C_{18:1(tr-9)}$	0.043	0.720	1.201	1.576	*0.982***
***Janthinobacterium lividum* GW1**					
n-$C_{16:0}$	0.491	0.521	0.739	0.845	*0.932*
n-$C_{18:0}$	0.003	0.005	0.04	0.059	*0.914*
n-$C_{16:1(cis-9)}$	0.831	0.636	0.015	0.007	*0.884*
n-$C_{16:1(tr-9)}$	0.015	0.058	0.268	0.404	*0.949**
i-$C_{17:0}$	0.0006	0.001	0.023	0.017	*0.665*
***Sphingomonas faeni* GW8**					
n-$C_{16:0}$	0.059	0.251	0.478	0.580	*0.979**
n-$C_{18:0}$	0.015	0.401	0.540	0.613	*0.876*
ai-$C_{15:0}$	0.573	0.279	0.124	0.063	*0.911*
i-$C_{16:0}$	0.290	0.177	0.091	0.043	*0.969**
ai-$C_{17:0}$	0.477	0.225	0.076	0.056	*0.880*
***Pseudomonas extremaustralis* HS8**					
n-$C_{16:0}$	0.154	0.329	0.551	0.888	*0.977**
i-$C_{15:0}$	0.228	0.161	0.129	0.004	*0.937*
ai-$C_{15:0}$	0.432	0.231	0.094	0.0002	*0.972**
ai-$C_{17:1}$	0.084	0.057	0.004	0.000	*0.918*
n-$C_{16:1(cis-9)}$	0.961	0.751	0.676	0.618	*0.904*

*Keys: *Correlation is significant at the 0.05 level (two-tailed). **Correlation is significant at the 0.01 level (two-tailed).*

TABLE 6 | Correlations of cell membrane fatty acids produced by Gram-positive bacteria species at different temperature.

Correlations					
Fatty acids (mg/g)	**Temperature (°C)**				**Correlation (R^2)**
	5	**15**	**25**	**35**	
***Staphylococcus equorum* GhS5**					
n-$C_{16:0}$	0.005	0.009	0.034	0.062	*0.923*
i-$C_{15:0}$	0.132	0.251	0.323	0.438	*0.991***
ai-$C_{15:0}$	0.742	0.920	1.130	1.390	*0.992***
i-$C_{19:1}$	0.165	0.094	0.032	0.009	*0.957**
ai-$C_{19:1}$	0.255	0.177	0.061	0.002	*0.986***
***Sporosarcina psychrophila* GS15**					
i-$C_{15:0}$	0.037	0.103	0.254	0.305	*0.962**
ai-$C_{15:0}$	1.055	1.145	1.438	1.605	*0.964**
ai-$C_{17:0}$	0.144	0.265	0.339	0.597	*0.933*
i-$C_{15:1}$	0.342	0.279	0.102	0.0001	*0.970**
ai-$C_{15:1}$	0.867	0.771	0.214	0.0004	*0.932*
***Arthrobacter psychrochitiniphilus* HS1**					
n-$C_{16:0}$	0.002	0.011	0.02	0.041	*0.948**
ai-$C_{15:0}$	0.805	0.994	1.101	1.186	*0.964**
ai-$C_{17:0}$	0.635	0.635	0.794	0.874	*0.997***
ai-$C_{15:1}$	0.350	0.165	0.013	0.004	*0.894*
ai-$C_{16:1}$	0.014	0.008	0.004	0.0006	*0.982**

*Keys: *Correlation is significant at the 0.05 level (two-tailed). **Correlation is significant at the 0.01 level (two-tailed).*

highest levels of saturated branched-chain fatty acids (br-SFAs) in their cell membranes at higher temperature, e.g., 25 and 35°C, and gradually decreasing levels of br-SFAs with decreased temperature, i.e., 5 and 15°C. Similarly, the highest levels of branched chain monounsaturated fatty acids were seen at low temperature (5 and 15°C) as compared to high temperature (25 and 35°C).

Temperature greatly influences the distribution of individual fatty acids in cell membranes of all bacterial strains (**Table 5**). The straight-chain fatty acids such as $C_{15:0}$, $C_{16:0}$, $C_{17:0}$, and $C_{18:0}$ occur at higher levels at higher temperatures such as 25 and 35°C but at lower levels under lower temperatures, i.e., 5 and 15°C. Similarly, Gram-negative bacteria were observed to contain high levels of *n*-$C_{16:1(cis-9)}$ and *n*-$C_{18:1(tr-9)}$ with increasing temperature, although their production was also high at lower temperatures as well. Monounsaturated fatty acids such as *n*-$C_{16:1(tr-9)}$ and *n*-$C_{17:1(tr-10)}$ were also among those fatty acids whose production was enhanced at higher temperatures but decreased at low temperatures. Likewise, high levels of the branched saturated fatty acid, *i*-$C_{17:0}$, were observed at 35°C but with lower levels at 5°C. *Sphingomonas faeni* GW8 produces *i*-$C_{16:0}$ at higher levels at lower temperatures but at lower levels at 25 and 35°C. In addition, Gram positive bacterial strains were observed to generate the branched chain saturated component, *a*-$C_{15:0}$, at high levels in their cell membranes. The levels of br-SFAs such as *i*-$C_{15:0}$ and *a*-$C_{15:0}$ gradually elevated with increasing temperature but with no sufficient difference. On the other hand, branched chain monounsaturated fatty acids such as *i*-$C_{15:1}$, *a*-$C_{15:1}$, *i*-$C_{19:1}$ and *a*-$C_{19:1}$ were produced by bacteria at lower levels at 25 and 35°C but found at higher levels at 5 and 15°C. Moreover, the straight chain fatty acids such as $C_{16:0}$ and $C_{18:0}$ were observed at high levels at increased temperature such

as 25 and 35°C but in at low levels at lower temperature, i.e., at 5 and 15°C.

DISCUSSION

The present work aimed to study the distribution of saturated and unsaturated, normal and branched phospholipid fatty acids (PLFAs) in cell membranes of cold-tolerant bacterial strains belonging to both Gram-negative and Gram-positive groups. The comprehensive PLFA profiles of bacteria from Pakistan glaciers obtained in this study could be used to identify and quantify bacteria in cold habitats as each bacterial species displays a unique cell membrane fatty acid profile. Most importantly, the saturated $C_{16:0}$ fatty acid is the most common FA, observed at high levels in all types of bacteria. Using PLFAs as bio-markers for bacterial identification and quantification continues to increase in popularity in the scientific community (Willers et al., 2015). PLFAs are the primary component of bacterial cell membranes; they degrade very rapidly upon cell death (White et al., 2009). Therefore, they are considered to be more representative of living bacterial biomass and more accurate than DNA-based approaches as PLFAs are more readily transformed following cell−death compared to DNA (Feinstein et al., 2009). Several researchers have used PLFA profiles for the quantification of bacteria in a given environment in order to understand function of genes involved in metabolic activities, for the screening of pathogenic bacteria, or the determination of community structures and bacterial diversity (Kellogg et al., 2001; Jungblut et al., 2009; Frostegard et al., 2011; Buhring et al., 2012; Naeher et al., 2012). Here we suggest that the comparison of PLFA distributions of bacteria isolated from cold environments with bacteria inhabiting warmer habitats, for identification purposes, would be misguided as fatty acid composition and quantity alter greatly alongside changes in the surrounding environment (Willers et al., 2015). However, PLFAs may be useful in association with the study of physiological changes in bacteria.

Most of the Gram-negative bacteria exhibit *n*-MUFAs as the major group of cell membrane FAs while those of Gram-positive species are dominated by br-SFAs, a characteristic pattern previously reported by Frostegard and Baath (1996). The *a*-$C_{15:0}$, *n*-$C_{16:0}$ and *n*-$C_{18:1}$ as the dominant cell membrane FAs in Gram-positive species in the current study corroborates with the literature (Gillan et al., 1983; Breulmann et al., 2014; Dong et al., 2014; Fichtner et al., 2014; Reinsch et al., 2014). More specifically, *n*-$C_{16:1}$ and the monounsaturated fatty acid *n*-$C_{18:1}$ were the major types of fatty acid in cell membranes of the studied bacterial species summarized **Table 1**. Previous research has shown *n*-$C_{16:1}$ and *n*-$C_{18:1}$ as the most predominant PLFA and signature biomarkers of Gram-negative bacteria (Buckeridge et al., 2013; Djukic et al., 2013; Tavi et al., 2013; Zheng et al., 2013; Banks et al., 2014; Lange et al., 2014; Reinsch et al., 2014; Zhang et al., 2014).

Apart from general interspecies PLFA distributions we evaluated the effect of growth temperature on the relative distributions and levels of major FAs in cell membranes of Gram-negative and Gram-positive bacteria. Notably, increasing temperature caused a substantial decline in the relative amount of br-SFAs and br-MUFAs, in particular, in Gram-positive species (*Sporosarcina psychrophila* GS15, *Sphingomonas faeni* GW8, *Staphylococcus equorum* GhS5, *Arthrobacter psychrolactophilus* HS1) from about 90% at 5 and 15°C to less than 1% at 35°C while the amount of saturated normal FAs increased from an initial range of 0.4–2% to 1.8–51%. These observations corroborate the role of br-FAs in the adaptability of these bacteria toward changes in temperature. It has been reported that br-FAs maintain the normal liquid-crystalline (fluid) state of bacterial PLFA by lowering the melting point and, thus, enabling membranes to perform normal cellular function at low temperature (Suutari and Laakso, 1994; Bowles et al., 1996; Sun et al., 2012). An increased production of br-FAs by psychrophilic bacteria in response to lower temperatures has been observed previously, e.g., for the food pathogen *Listeria monocytogenes* (Annous et al., 1997). However, to the best of our knowledge, this is the first time that such temperature adaption is reported for bacteria species *Sporosarcina psychrophila*, *Sphingomonas faeni*, *Staphylococcus equorum,* and *Arthrobacter psychrolactophilus*. Other Gram-positive bacteria for which equivalent changes in PLFA composition at lower temperature has been observed include *Staphylococci*, incorporating increasing amounts of br-MUFAs into their cell membranes (Onyango and Alreshidi, 2018). Suutari and Laakso (1992) reported increased production of lower-melting point *a*-FAs at low temperature for *Bacillus subtilis* and *Bacillus megaterium* but decreased *i*-FA production. Similarly, Annous et al. (1997) reported an increase in levels of short-chain and *a*-branched-chain FAs in the cell membrane of *Listeria monocytogenes* with the temperature decreasing from 45 to 5°C.

Changes in FA distributions from different growth temperatures were similarly pronounced for the Gram-negative bacteria investigated, *Flavobacterium sinopsychrotolerans* GS7, *Paracoccus hibiscisoli* GS9, *Janthinobacterium lividum* GW1, *Brevundimonas nasdae* GhW6, *Rhizobium giardinii* HI5 and *Pseudomonas extremaustralis* HS8. In particular, the relative levels of saturated fatty acids such as $C_{15:0}$, $C_{16:0}$, $C_{17:0}$, and $C_{18:0}$ vary significantly. High levels of saturated FAs lower the membrane fluidity, thus, helping bacteria to survive at higher temperatures (Knothe and Dunn, 2009). Although *n*-MUFAs were the main group of membrane FAs of the investigated Gram-negative bacterial strains at all temperatures, the relative level of *n*-$C_{16:1(cis-9)}$ decreased considerably with increasing temperature. The accumulation of MUFAs especially with *cis*-conformation has been reported as a means of lowering the FA melting point and improving cell membrane fluidity at low temperatures (Russell, 1989; Mangelsdorf et al., 2009). For example, saturated *n*-$C_{16:0}$ has a melting point of 63°C whereas the introduction of one double bond, i.e., converting *n*-$C_{16:0}$ to *n*-$C_{16:1}$, lowers the melting point significantly to −1°C (Knothe and Dunn, 2009).

As far as we know, membrane FA adaption to growth temperature has not yet been reported for the above-mentioned Gram-negative species. Similar patterns were observed by Theberge et al. (1996) for the FA composition of *Rhizobium leguminosarum* at temperatures of 10, 15, 22, and 30°C, with

higher levels of MUFAs and $C_{18:1}$, in particular, at lower temperatures. Bajerski et al. (2017) evaluated the FA profile of *Chryseobacterium frigidisoli* and found monounsaturated *i*-$C_{17:1}$ at high levels at lower temperature (10°C), confirming the role of unsaturated membrane FAs with a lower melting point in cold adaptation (Russell, 1984, 1989). In contrast, *Pseudomonas syringae*, which was isolated from ice samples of Antarctica, contains high levels of saturated and *trans*-monounsaturated FAs although fatty acids with the *cis*-isomers were also detected (Kiran et al., 2005).

Overall, the observed shifts in the distributions of saturated and unsaturated, normal and branched FAs with growth temperature appear consistent across the investigated 10 strains of Gram-positive and Gram-negative bacteria. This points toward the potential for the development of temperature-sensitive molecular ratios for (non-polar) glacial settings with high proportions of bacterial biomass such as glacial ice, melted water and sediments. Such approaches remain to be tested *in situ*.

CONCLUSION

The analysis of cell membrane fatty acids of 42 cold-tolerant bacteria isolated from various glaciers of the Karakoram Mountain Range has revealed straight-chain monounsaturated fatty acids and branched-chain fatty acids as the dominant compounds among cell membrane fatty acids in Gram-positive and Gram-negative species, respectively. In addition, fatty acid distributions in bacterial cell membranes are significantly affected by growth temperature. In particular, a pronounced shift from enhanced proportions of monounsaturated to saturated branched and normal fatty acids with increasing temperature has been observed in Gram-negative bacteria species, whereas a notable increase in branched and normal saturated fatty acids with increased temperatures has witnessed in Gram-positive bacteria. Our study demonstrates the role of fatty acids for the maintenance of cell membrane fluidity in bacteria living in non-polar glacial habitats. The observed temperature-dependent shifts in fatty acid distributions may furthermore contribute to the development of temperature-sensitive molecular proxies in order to track temperature changes in (sub-) glacial environmental archives with high proportions of bacterial biomass. Finally, the capability of psychrophilic bacteria to produce biodesirable fatty acids, e.g., polyunsaturated fatty acids, represents an alternative source of such fatty acids for heterotrophic organisms in glacial environments.

DATA AVAILABILITY STATEMENT

All datasets generated for this study are included in the article.

AUTHOR CONTRIBUTIONS

NH, FH, and AA designed the research work. NH, MR, AH, and FH collected the samples from glaciers. AS, NH, and MR isolated and identified bacteria species. IB, JH, and NH carried out the GS/MS and afterward data analysis. FH and AA supervised the whole research work. FH and NH wrote the manuscript. All authors read and approved the final manuscript.

FUNDING

Funds for the research work were provided by Commonwealth Scholarship Commission, United Kingdom. In addition, NERC Life Sciences Mass Spectrometry Facility, School of Chemistry, University of Bristol, also supported this study.

ACKNOWLEDGMENTS

We are thankful to Dr. Simmon Cobb, Senior Teaching Laboratory Technician and Mr. James Williams, the Analytical Research Technician in LOWTEX for providing technical help during research work.

REFERENCES

Annous, B. A., Becker, L. A., Bayles, D. O., Labeda, D. P., and Wilkinson, B. J. (1997). Critical role of anteiso-C15: 0 fatty acid in the growth of *Listeria monocytogenes* at low temperatures. *Appl. Environ. Microbiol.* 63, 3887–3894.

Bajerski, F., and Wagner, D. (2013). Bacterial succession in Antarctic soils of two glacier forefields on Larsemann Hills, East Antarctica. *FEMS. Microbiol. Ecol.* 85, 128–142. doi: 10.1111/1574-6941.12105

Bajerski, F., Wagner, D., and Mangelsdorf, K. (2017). Cell membrane fatty acid composition of *Chryseobacterium frigidisoli* PB4T, isolated from Antarctic glacier forefield soils, in response to changing temperature and pH conditions. *Front. Microbiol.* 8:677. doi: 10.3389/fmicb.2017.00677

Banks, M. L., Kennedy, A. C., Kremer, R. J., and Eivazi, F. (2014). Soil microbial community response to surfactants and herbicides in two soils. *Appl. Soil Ecol.* 74, 12–20.

Bowles, B. L., Foglia, T. A., and Juneja, V. K. (1996). Temperature induced shifts in the fatty acid profile of *Staphylococcus aureus* WRRC B124 1. *J. Rap. Methods Aut. Microbiol.* 4, 235–245.

Breulmann, M., Masyutenko, N. P., Kogut, B. M., Schroll, R., Dörfler, U., Buscot, F., et al. (2014). Short-term bioavailability of carbon in soil organic matter fractions of different particle sizes and densities in grassland ecosystems. *Sci. Total Environ.* 497, 29–37. doi: 10.1016/j.scitotenv.2014.07.080

Buckeridge, K. M., Banerjee, S., Siciliano, S. D., and Grogan, P. (2013). The seasonal pattern of soil microbial community structure in mesic low arctic tundra. *Soil Biol. Biochem.* 65, 338–347.

Buhring, S. I., Schubotz, F., Harms, C., Lipp, J. S., Amils, R., and Hinrichs, K. U. (2012). Lipid signatures of acidophilic microbial communities in an extreme acidic environment–Río Tinto, Spain. *Org. Geochem.* 47, 66–77.

Cossins, A. R., and MacDonald, A. G. (1984). Homeoviscous theory under pressure: II. The molecular order of membranes from deep-sea fish. *BBA Biomembranes* 776, 144–150.

Crowe, J. H., Hoekstra, F. A., and Crowe, L. M. (1992). Anhydrobiosis. *Annu. Rev. Physiol.* 54, 579–599.

DeLong, E. F., and Yayanos, A. A. (1986). Biochemical function and ecological significance of novel bacterial lipids in deep-sea procaryotes. *Appl. Environ. Microbiol.* 51, 730–737.

Denich, T. J., Beaudette, L. A., Lee, H., and Trevors, J. T. (2003). Effect of selected environmental and physico-chemical factors on bacterial cytoplasmic membranes. *J. Microbiol. Methods* 52, 149–182.

Djukic, I., Zehetner, F., Watzinger, A., Horacek, M., and Gerzabek, M. H. (2013). In situ carbon turnover dynamics and the role of soil microorganisms therein: a climate warming study in an Alpine ecosystem. *FEMS Microbiol. Ecol.* 83, 112–124. doi: 10.1111/j.1574-6941.2012.01449.x

Dong, H. Y., Kong, C. H., Wang, P., and Huang, Q. L. (2014). Temporal variation of soil friedelin and microbial community under different land uses in a long-term agroecosystem. *Soil Biol. Biochem.* 69, 275–281.

El Razak, A. A., Ward, A. C., and Glassey, J. (2014). Screening of marine bacterial producers of polyunsaturated fatty acids and optimisation of production. *Microbial. Ecol.* 67, 454–464. doi: 10.1007/s00248-013-0332-y

Feinstein, L. M., Sul, W. J., and Blackwood, C. B. (2009). Assessment of bias associated with incomplete extraction of microbial DNA from soil. *Appl. Environ. Microbiol.* 75, 5428–5433. doi: 10.1128/AEM.00120-09

Fichtner, A., Von Oheimb, G., Härdtle, W., Wilken, C., and Gutknecht, J. L. M. (2014). Effects of anthropogenic disturbances on soil microbial communities in oak forests persist for more than 100 years. *Soil Biol. Biochem.* 70, 79–87.

Frostegard, A., and Baath, E. (1996). The use of phospholipid fatty acid analysis to estimate bacterial and fungal biomass in soil. *Biol. Fert. Soils* 22, 59–65.

Frostegard, A., Tunlid, A., and Baah, E. (2011). Use and misuse of PLFA measurements in soils. *Soil Biol. Biochem.* 43, 1621–1625.

Fulco, A. J. (1983). Fatty acid metabolism in bacteria. *Prog. Lipid Res.* 22, 133–160.

Ganzert, L., Lipski, A., Hubberten, H. W., and Wagner, D. (2011). The impact of different soil parameters on the community structure of dominant bacteria from nine different soils located on Livingston Island, South Shetland Archipelago, Antarctica. *FEMS Microbiol. Ecol.* 76, 476–491. doi: 10.1111/j.1574-6941.2011.01068.x

Georlette, D., Blaise, V., Collins, T., D'Amico, S., Gratia, E., Hoyoux, A., et al. (2004). Some like it cold: biocatalysis at low temperatures. *FEMS Microbiol. Rev.* 28, 25–42.

Gillan, F. T., Johns, R. B., Verheyen, T. V., Nichols, P. D., Esdaile, R. J., and Bavor, H. J. (1983). Monounsaturated fatty acids as specific bacterial markers in marine sediments. *Adv. Org. Geochem.* 1, 198–206. doi: 10.1016/j.scitotenv.2011.10.015

Hassan, N., Rafiq, M., Hayat, M., Shah, A. A., and Hasan, F. (2016). Psychrophilic and psychrotrophic fungi: a comprehensive review. *Rev. Environ. Sci. Biotechnol.* 15, 147–172.

Hazel, J. R., and Williams, E. E. (1990). The role of alterations in membrane lipid composition in enabling physiological adaptation of organisms to their physical environment. *Prog. Lipid Res.* 29, 167–227.

Hoshino, T., and Matsumoto, N. (2012). Cryophilic fungi to denote fungi in the cryosphere. *Fungal Biol. Rev.* 26, 102–105.

Jungblut, A. D., Allen, M. A., Burns, B. P., and Neilan, B. A. (2009). Lipid biomarker analysis of cyanobacteria-dominated microbial mats in meltwater ponds on the McMurdo Ice Shelf, Antarctica. *Org. Geochem.* 40, 258–269.

Kellogg, J. A., Bankert, D. A., Withers, G. S., Sweimler, W., Kiehn, T. E., and Pfyffer, G. E. (2001). Application of the Sherlock Mycobacteria Identification System using high-performance liquid chromatography in a clinical laboratory. *J. Clin. Microbiol.* 39, 964–970.

Kiran, M. D., Annapoorni, S., Suzuki, I., Murata, N., and Shivaji, S. (2005). Cis–trans isomerase gene in psychrophilic *Pseudomonas syringae* is constitutively expressed during growth and under conditions of temperature and solvent stress. *Extremophiles* 9, 117–125.

Knothe, G., and Dunn, R. O. (2009). A comprehensive evaluation of the melting points of fatty acids and esters determined by differential scanning calorimetry. *J. Am. Oil Chem. Soc.* 86, 843–856.

Lange, M., Habekost, M., Eisenhauer, N., Roscher, C., Bessler, H., Engels, C., et al. (2014). Biotic and abiotic properties mediating plant diversity effects on soil microbial communities in an experimental grassland. *PLoS One* 9:e96182. doi: 10.1371/journal.pone.0096182

Mangelsdorf, K., Finsel, E., Liebner, S., and Wagner, D. (2009). Temperature adaptation of microbial communities in different horizons of Siberian permafrost-affected soils from the Lena Delta. *Chem. D Erde Geochem.* 69, 169–182.

Mansilla, M. C., Cybulski, L. E., Albanesi, D., and de Mendoza, D. (2004). Control of membrane lipid fluidity by molecular thermosensors. *J. Bacteriol.* 186, 6681–6688.

Margesin, R., Fonteyne, P. A., Schinner, F., and Sampaio, J. P. (2007). *Rhodotorula psychrophila* sp. nov., *Rhodotorula psychrophenolica* sp. nov. and *Rhodotorula glacialis* sp. nov., novel psychrophilic basidiomycetous yeast species isolated from alpine environments. *Int. J. Syst. Evol. Microbiol.* 57, 2179–2184.

Margesin, R., and Miteva, V. (2011). Diversity and ecology of psychrophilic microorganisms. *Res. Microbiol.* 162, 346–361. doi: 10.1016/j.resmic.2010.12.004

Montiel, P. O. (2000). Soluble carbohydrates (trehalose in particular) and cryoprotection in polar biota. *Cryo Lett.* 21, 83–90.

Naeher, S., Smittenberg, R. H., Gilli, A., Kirilova, E. P., Lotter, A. F., and Schubert, C. J. (2012). Impact of recent lake eutrophication on microbial community changes as revealed by high resolution lipid biomarkers in Rotsee (Switzerland). *Org. Geochem.* 49, 86–95.

Nichols, D. S., Brown, J. L., Nichols, P. D., and McMeekin, T. A. (1997). Production of eicosapentaenoic and arachidonic acids by an Antarctic bacterium: response to growth temperature. *FEMS Microbiol. Lett.* 152, 349–354.

Onyango, L. A., and Alreshidi, M. M. (2018). Adaptive metabolism in staphylococci: survival and persistence in environmental and clinical settings. *J. Pathog.* 2018:1092632. doi: 10.1155/2018/1092632

Reinsch, S., Michelsen, A., Sárossy, Z., Egsgaard, H., Schmidt, I. K., Jakobsen, I., et al. (2014). Short-term utilization of carbon by the soil microbial community under future climatic conditions in a temperate heathland. *Soil Biol. Biochem.* 68, 9–19.

Russell, N. J. (1984). Mechanisms of thermal adaptation in bacteria: blueprints for survival. *Trends Biochem. Sci.* 9, 108–112.

Russell, N. J. (1989). Functions of lipids: structural roles and membrane functions. *Microbial. Lipid* 2, 279–365.

Russell, N. J. (1990). Cold adaptation of microorganisms. *Philos. Trans. R. Soc. Lond. B. Biol. Sci.* 326, 595–611.

Sinensky, M. (1974). Homeoviscous adaptation—a homeostatic process that regulates the viscosity of membrane lipids in *Escherichia coli*. *Proc. Natl. Acad. Sci.U.S.A.* 71, 522–525.

Singh, S. M., Puja, G., and Bhat, D. J. (2006). Psychrophilic fungi from *Schirmacher oasis*, East Antarctica. *Curr. Sci.* 90, 1388–1392.

Sun, Y., Wilkinson, B. J., Standiford, T. J., Akinbi, H. T., and O'Riordan, M. X. (2012). Fatty acids regulate stress resistance and virulence factor production for *Listeria monocytogenes*. *J. Bacteriol.* 194, 5274–5284. doi: 10.1128/JB.00045-12

Suutari, M., and Laakso, S. (1992). Unsaturated and branched chain-fatty acids in temperature adaptation of *Bacillus subtilis* and *Bacillus megaterium*. *BBA Lipids Lipid Metab.* 1126, 119–124.

Suutari, M., and Laakso, S. (1994). Microbial fatty acids and thermal adaptation. *Crit. Rev. Microbiol.* 20, 285–328.

Tavi, N. M., Martikainen, P. J., Lokko, K., Kontro, M., Wild, B., Richter, A., et al. (2013). Linking microbial community structure and allocation of plant-derived carbon in an organic agricultural soil using 13CO2 pulse-chase labelling combined with 13C-PLFA profiling. *Soil Biol. Biochem.* 58, 207–215.

Theberge, M. C., Prevost, D., and Chalifour, F. P. (1996). The effect of different temperatures on the fatty acid composition of *Rhizobium leguminosarum* bv. *viciae* in the faba bean symbiosis. *New Phytol.* 134, 657–664.

White, P. M., Potter, T. L., and Strickland, T. C. (2009). Pressurized liquid extraction of soil microbial phospholipid and neutral lipid fatty acids. *J. Agric. Food Chem.* 57, 7171–7177. doi: 10.1021/jf901257n

Willers, C., Jansen van Rensburg, P. J., and Claassens, S. (2015). Microbial signature lipid biomarker analysis–an approach that is still preferred, even amid various method modifications. *J. Appl. Microbiol.* 118, 1251–1263.

Wirsen, C. O., Jannasch, H. W., Wakeham, S. G., and Canuel, E. A. (1986). Membrane lipids of a psychrophilic and barophilic deep-sea bacterium. *Curr. Microbiol.* 14, 319–322.

Wynn-Williams, D. D. (1990). "Ecological aspects of Antarctic microbiology," in *Advances in Microbial Ecology*, ed. K. C. Marshall, (Boston, MA: Springer), 71–146.

Zhang, H., Ding, W., He, X., Yu, H., Fan, J., and Liu, D. (2014). Influence of 20–year organic and inorganic fertilization on organic carbon accumulation and microbial community structure of aggregates in an intensively cultivated sandy loam soil. *PLoS One* 9:e92733. doi: 10.1371/journal.pone.0092733

Zheng, J., Liang, R., Zhang, L., Wu, C., Zhou, R., and Liao, X. (2013). Characterization of microbial communities in strong aromatic liquor fermentation pit muds of different ages assessed by combined DGGE and PLFA analyses. *Food Res. Int.* 54, 660–666.

Conflict of Interest: The authors declare that the research was conducted in the absence of any commercial or financial relationships that could be construed as a potential conflict of interest.

frontiers in Microbiology

ORIGINAL RESEARCH
published: 20 May 2020
doi: 10.3389/fmicb.2020.00980

Comparison of Bacterial and Fungal Composition and Their Chemical Interaction in Free Tropospheric Air and Snow Over an Entire Winter Season at Mount Sonnblick, Austria

Nora Els[1], Marion Greilinger[2,3], Michael Reisecker[4], Romie Tignat-Perrier[5], Kathrin Baumann-Stanzer[3], Anne Kasper-Giebl[2], Birgit Sattler[1] and Catherine Larose[5]*

[1] Institute of Ecology, University of Innsbruck, Innsbruck, Austria, [2] Institute of Chemical Technologies and Analytics, Vienna University of Technology, Vienna, Austria, [3] Zentralanstalt für Meteorologie und Geodynamik (ZAMG), Vienna, Austria, [4] Avalanche Warning Service Tyrol, Department of Civil Protection, Federal State Government of Tyrol, Innsbruck, Austria, [5] Environmental Microbial Genomics Group, Laboratoire Ampère, École Centrale de Lyon, Écully, France

We investigated the interactions of air and snow over one entire winter accumulation period as well as the importance of chemical markers in a pristine free-tropospheric environment to explain variation in a microbiological dataset. To overcome the limitations of short term bioaerosol sampling, we sampled the atmosphere continuously onto quartzfiber air filters using a DIGITEL high volume PM10 sampler. The bacterial and fungal communities, sequenced using Illumina MiSeq, as well as the chemical components of the atmosphere were compared to those of a late season snow profile. Results reveal strong dynamics in the composition of bacterial and fungal communities in air and snow. In fall the two compartments were similar, suggesting a strong interaction between them. The overlap diminished as the season progressed due to an evolution within the snowpack throughout winter and spring. Certain bacterial and fungal genera were only detected in air samples, which implies that a distinct air microbiome might exist. These organisms are likely not incorporated in clouds and thus not precipitated or scavenged in snow. Although snow appears to be seeded by the atmosphere, both air and snow showed differing bacterial and fungal communities and chemical composition. Season and alpha diversity were major drivers for microbial variability in snow and air, and only a few chemical markers were identified as important in explaining microbial diversity. Air microbial community variation was more related to chemical markers than snow microbial composition. For air microbial communities Cl^-, TC/OC, SO_4^{2-}, Mg^{2+}, and Fe/Al, all compounds related to dust or anthropogenic activities, were identified as related to bacterial variability while dust related Ca^{2+} was significant in snow. The only common driver for snow and air was SO_4^{2-}, a tracer for anthropogenic sources. The occurrence of chemical compounds was coupled with boundary layer injections in the free troposphere (FT). Boundary layer injections also caused the observed variations in community composition and chemistry between the two compartments. Long-term monitoring is required for a more valid insight in post-depositional selection in snow.

Keywords: Sonnblick Observatory, air-snow comparison, seeding effect, PM10, microbial communities, 16S ribosomal RNA, ITS, 18S

OPEN ACCESS

Edited by:
Thulani Peter Makhalanyane, University of Pretoria, South Africa

Reviewed by:
Mircea Podar, Oak Ridge National Laboratory (DOE), United States
Atsushi Matsuki, Kanazawa University, Japan

****Correspondence:***
Nora Els
nora.els@uibk.ac.at

Specialty section:
This article was submitted to Extreme Microbiology, a section of the journal Frontiers in Microbiology

Received: *26 January 2020*
Accepted: *23 April 2020*
Published: *20 May 2020*

Citation:
Els N, Greilinger M, Reisecker M, Tignat-Perrier R, Baumann-Stanzer K, Kasper-Giebl A, Sattler B and Larose C (2020) Comparison of Bacterial and Fungal Composition and Their Chemical Interaction in Free Tropospheric Air and Snow Over an Entire Winter Season at Mount Sonnblick, Austria. Front. Microbiol. 11:980. doi: 10.3389/fmicb.2020.00980

INTRODUCTION

A major driver of aerobiological research is the assumption that airborne aerosols may act as a seeding source of surface microbes. This is especially presumed for snow and ice covered surfaces in remote areas (Pedgley, 1991; Cowan et al., 2011; Harding et al., 2011; Polymenakou, 2012; Hauptmann et al., 2014), since other sources, such as anthropogenic impacts, are considered minor.

Atmospheric processes of aerosolization, the properties of surrounding landscapes, the lifting of air beyond the boundary-layer to enable long-range transport of microbes from their source regions, the survival of microorganisms in changing temperature regimes of clouds or the ability to survive temperature extremes, as well as desiccation or nutrient limitation, are all factors impacting the composition and dispersion of aerosolized microbes (Möhler et al., 2007; Burrows et al., 2009; Bowers et al., 2011; Xia et al., 2013; Bianco et al., 2016; Carotenuto et al., 2017; Alsved et al., 2018; Evans et al., 2019; Tignat-Perrier et al., 2019). Bertolini et al. (2013) suggested meteorological factors together with the chemical composition of the airborne particulate matter as well as the air mass sources as driving factors for airborne microbial variability at ground level.

It is well known that the origin of the air mass impacts physico-chemical and microbial composition (Amato et al., 2007; Monteil et al., 2014) and that clouds, e.g., air or precipitation including Saharan dust, carry a specific microbial and chemical signature (Chuvochina et al., 2011; Peter et al., 2014; Meola et al., 2015; Weil et al., 2017; Greilinger et al., 2018).

Airborne microbes are known to act as ice nuclei (Christner et al., 2008), essential for precipitation formation, especially the formation of snow. The atmosphere has been suggested as a seeding source for snowpacks (Maccario et al., 2019). During winter deposition and snow cover formation interstitial air containing microbes might be included in the snow cover. The air movement within the snow cover allows an interaction of the entrapped air with the atmosphere over several meters depth (Domine and Shepson, 2002). With more compaction and the formation of ice lamellae within the snow cover, less air movement is possible, thus a direct interaction of the trapped air microbiota with the snow microbiota may occur. Once deposited, post-depositional selection processes occur in the snowpack to form a snow-specific microbial community (Segawa et al., 2005; Maccario et al., 2014).

The snow cover has been considered as a proxy for atmospheric and environmental conditions as well as for bioaerosol microbial composition in previous investigations (Cáliz et al., 2018; Spear et al., 2018; Triadó-Margarit et al., 2019). However, we recently showed that this is not the case for air microbial composition (Els et al., 2019). One of the limitations of aerobiological studies aiming to compare with stationary environmental systems like snow cover is that the air composition changes constantly. Biological air samples are usually only snapshots due to the nature of their limited sampling time. While snow is stationary, though also dynamic and exposed to snow drift and snow blowing (Gallée et al., 2001), it constantly interacts with the atmosphere. Besides the challenge of retrieving representative biological samples of air and snow, the bacterial abundance of one m^3 air equals one mL of molten snow. Thus, considerable air volumes are needed to reach comparable numbers of bacteria or fungi in snow.

Several studies revealed variability of PM10 aerosol ion composition on a seasonal basis (Perrone et al., 2010; Squizzato et al., 2013). The influence of the season was shown to be more significant than the short term variability of the meteorological parameters on air microbial community within the atmospheric boundary layer (ABL) and the free troposphere (FT) (Brodie et al., 2007; Fierer et al., 2008; Franzetti et al., 2011; Bowers et al., 2012, 2013; Bertolini et al., 2013). The term FT describes air masses well above the planetary boundary layer, where surface friction on the air motion is negligible and laminar air flow dominates. Measurements of atmospheric pollutants within the free-tropospheric air are representative for atmospheric background conditions, in contrast, within the planetary boundary layer, air movement is often turbulent including vertical mixing, thus measurements of atmospheric constituents predominately represent regional or local influences.

In this study we account for the typical weaknesses of air-snow comparisons and compare continuous PM10 aerosol filter samples with snow samples representative of the whole winter accumulation snow cover, all sampled at the remote high alpine site Hoher Sonnblick in the Austrian Alps. We investigated whether air and snow microbial and chemical composition were connected over the winter accumulation period in a pristine free-tropospheric environment. Being aware of seasonality in air microbial and chemical composition, we examined (I) if the air-snow interaction was the same over the winter accumulation period, (II) the significance of the air as a seeding source for bacteria and fungi to the high alpine snow cover, and (III) if the air and snow microbial variability is correlated with chemical composition.

MATERIALS AND METHODS

Study Site

Samples were collected at the top of Mount Sonnblick (3106 m asl., **Figure 1A**), Austria (47°3′14″ N, 12°57′27″ E), where a Global Atmosphere Watch meteorological observatory of the World Meteorological Organization (WMO) is operated. The site is exhaust neutral, supplied by electricity from the valley and equipped with an elevated air outlet to enable undisturbed aerosol measurements. The closest settlement is the village Rauris, 15 km away. Rauris village is located at 950 m asl., thus 2156 m below the sampling location on Mount Sonnblick. The area within a 100 km perimeter around the Sonnblick Observatory is sparsely populated.

Sampling

Snow Pit Sampling

A snow pit at the glacier field Goldbergkees (3043 m asl.) on top of Mount Sonnblick was sampled on the 3rd of May 2017 at the end of the winter accumulation period before significant snowmelt began (**Figures 1B,C**). Snow samples were representative for the whole winter accumulation period and sampling was performed

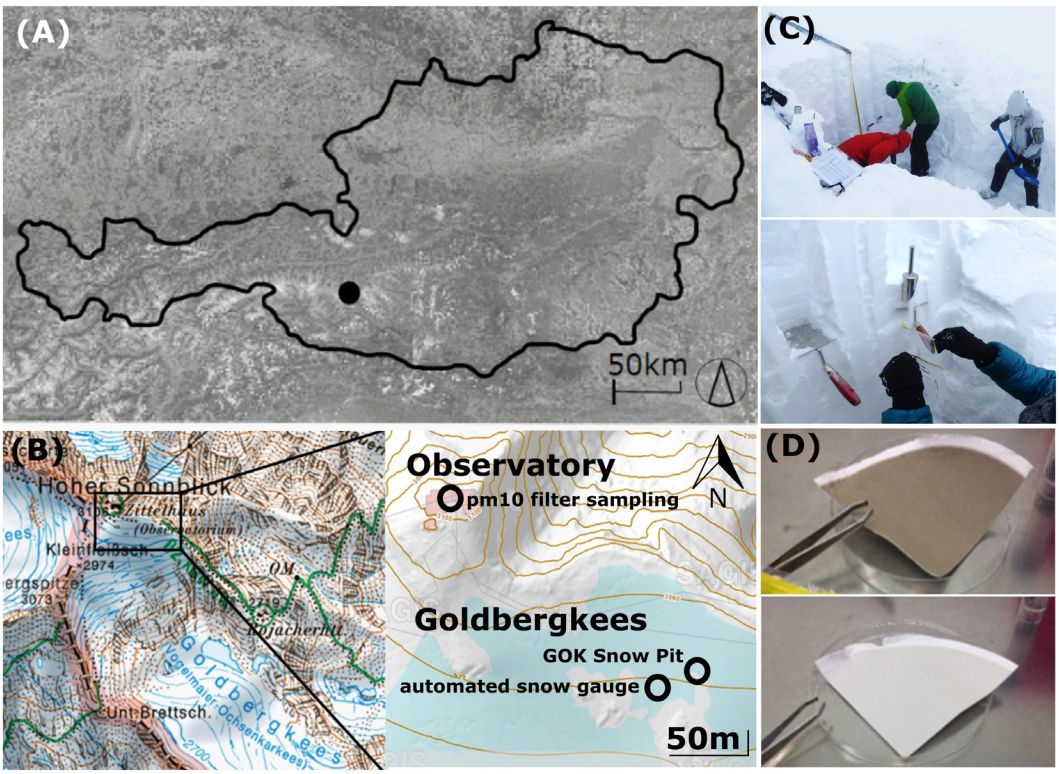

FIGURE 1 | (A) Location of the Sonnblick Observatory in Austria, **(B)** location of the PM10 filter sampling (ZAMG Sonnblick Observatory), the snow pit sampling and the automated snow gauge, source: www.salzburg.gv.at/sagisonline, **(C)** snow pit sampling, **(D)** exemplary PM10 quartz air filters for microbial analyses.

in 10 cm increments (n = 31, maximum snow depth of 310 cm). Microbial snow sampling was performed using a stainless steel shovel (ROTH) and sterile nasco whirl-paks (ROTH). A layer of approx. 2 cm above ground was not sampled due to suspected ground contamination and diffusion. Chemical snow sampling was performed in parallel to the microbial sampling within the same pit according to the methods described in Greilinger et al. (2016). Snow stratigraphy and snow density were measured on site (**Supplementary Figures S1, S2**). Gloves and masks were used to avoid contamination of all samples and the front of the profile was cleared off several times during the sampling. Meltwater percolation or updraft from underlying soil microbes is unlikely since outside temperatures were below 0°C during the snow cover period (**Supplementary Figures S3, S4**) and the base of the snow profile was solid rock. Microbial and chemical snow samples were kept frozen until their analysis and are named in all further graphs with the snow depth [cm] as increment name.

PM10 Quartz Fiber Filter Aerosol Sampling

Aerosols were sampled on quartz filters (Pallflex Tissuequartz, 2500 QAT-UP, size 150 mm, PALL Life Science Membrane, **Figure 1D**) using a high-volume sampler (Digitel DHA-80) with a PM10 cut off air inlet according to the European standard reference method EN12341:2014 for PM 10 sampling. The inlet is not heated to avoid losses of semi volatile compounds but single filters which might have been affected by a moisture entry during severe weather conditions were removed. Daily maintenance of the inlet is provided by the staff members continuously present at the site. Additionally, the inlet is surrounded by a wind shield with about 1 m in diameter and about 50 cm height to avoid sampling artifacts during extremely windy and harsh weather conditions, still ensuring a representative inflow into the sampler. Filters were sampled over the course of 1 week with some exceptions (see **Table 1**). Filters were placed directly from the manufacturers packaging into filter holders which were washed with milli-Q water and stored in a sealed stainless steel cylinder during transport and storage. Once back in the lab, PM10 filters were stored at −20°C until chemical and microbiological analysis. Seasons were allocated to the filter samples according to Greilinger et al. (2016), the snow increments were then allocated to the respective seasons by SNOWPACK modeling (see section "Snowpack Time Allocation Modeling") and validated with PCoA (**Figure 2** and **Supplementary Figure S5**).

DNA Extraction and Sequencing

Snow was molten at 4°C, filtered through a 0.2 μm polycarbonate filter (47 mm, Isopore) and then stored frozen at −20°C until DNA extraction, performed with the DNeasy Power Water extraction kit (QIAGEN) following the protocol provided with the kit.

From the filters DNA was also extracted using a DNeasy Power Water extraction kit (QIAGEN) using an adapted

TABLE 1 | Overview of air filter sampling times and volumes analyzed, if a notable precipitation event took place (indicated by x) or if Sahara event was detected during the sampling period (deduced from the aerosol measurements at the Sonnblick observatory and air mass back trajectories) and the allocated season according to Greilinger et al. (2016).

Filter name	Start [Date, Time]	End [Date, Time]	m^3 air on Filter	Precipitation	Sahara event	Season
F01	01.09.2016 15:26:18	08.09.2016 12:28:19	1361.29	x	x	Fall
F02	08.09.2016 12:30:40	15:09.2016 12:30:41	1394.24	–		Fall
F03	15.09.2016 12:31:46	22.09.2016 12:31:47	1385.12	x		Fall
F04	22.09.2016 12:40:53	29.09.2016 12:40:57	1383.97	–		Fall
F05	29.09.2016 13:56:14	06.10.2016 13:56:14	1373.93	x		Fall
F06	06.10.2016 14:52:22	13.10.2016 11:52:29	1373.19	x		Fall
F07	20.10.2016 13:12:15	27.10.2016 13:12:15	1368.28	x	x	Fall
F08	27.10.2016 14:32:41	03.11.2016 14:32:41	1369.97	–		Fall
F09	03.11.2016 15:34:30	10.11.2016 12:34:30	1348.28	x		Fall
F10	10.11.2016 12:45:54	01.12.2016 10:04:26	409.14	x		Fall
F11	01.12.2016 10:04:30	08.12.2016 14:56:07	1405.37	–		Winter
F12	08.12.2016 14:56:15	15.12.2017 00:00:00	na	–		Winter
F13	15.12.2017 00:00:00	23.12.2016 16:21:07	2934.85	–		Winter
F14	23.12.2016 16:21:20	30.12.2106 16:21:08	1360.58	–		Winter
F15	30.12.2016 16:21:17		na	–		Winter
F16		12.01.2017 12:26:32	na	x		Winter
F17	12.01.2016 12:26:43	19.01.2017 12:26:31	1359.07	x		Winter
F18	19.01.2017 15:56:37	26.01.2017 12:47:08	1335.70	–	x	Winter
F19	26.01.2017 12:47:16	02.02.2017 13:18:40	1368.25	x		Winter
F20	02.02.2017 13:18:51	16.02.2017 13:44:07	2738.17	x	x	Winter
F21	16.02.2017 13:44:19	23.02.2017 13:25:35	1365.07	x	x	Spring
F22	23.02.2017 13:25:46	02.03.2017 13:01:41	1366.50	x	x	Spring
F23	02.03.2017 13:01:52	09.03.2017 13:11:38	1365.54	x		Spring
F24	09.03.2017 13:11:49	10.03.2017 09:36:00	124.64	x		Spring
F25	10.03.2017 09:36:50	16.03.2017 14:46:22	1203.29	x	x	Spring
F26	16.03.2017 14:46:33	23.03.2017 14:46:21	1369.13	–		Spring
F27	23.03.2017 18:10:27	30.03.2017 13:57:57	1203.29	–	x	Spring
F28	30.03.2017 13:58:10	06.04.2017 13:45:57	1367.94	–		Spring
F29	06.04.2017 13:49:15	13.04.2017 12:00:07	1354.70	–		Spring
F30	13.04.2017 12:00:19	20.04.2017 12:00:07	1339.07	x		Spring
F31	20.04.2017 14:49:47	27.04.2017 14:19:15	1356.74	x		Spring
F32	27.04.2017 14:19:26	04.05.2017 14:19:14	1363.52	x		Spring

protocol described in Dommergue et al. (2019) to remove DNA from quartz. Amplification, library prep (MiSeq Illumina sequencing, 2 × 250 bp, Nextera XT Library Preparation Kit) and sequencing was carried out at the Environmental Microbial Genomics group at the Laboratoire Ampère (ECL Lyon, University of Lyon, France). Community diversity was targeted: the V3-V4 region of the bacterial 16S rRNA SSU gene was amplified using 341F/785R primers (S-D-Bact-0341-b-S-17/S-D-Bact-0785-a-A-21, Klindworth et al., 2013) and the fungal internal transcribed spacer (ITS) regions were amplified with primer pair 5.8S_Fung/ITS4 targeting the ITS2 region (Taylor et al., 2016).

Bioinformatics and Statistics

For 16S sequences, the base quality of the reads 1 and 2 was controlled using the functions fastx_quality_stats and fastq_quality_boxplot_graph of the FASTX-Toolkit[1]. PANDAseq (Masella et al., 2012) was used to assemble read 1 and 2 using the RDP algorithm, the minimum and maximum length of the resulting sequences for 16S were 410 bp and 500 bp, and 390 bp and 500 bp for ITS, with a minimum and maximum overlap length of 20 bp and 100 bp, respectively.

The resulting sequences were stripped of their primers and annotated to the genus or family level by RDP Classifier (Wang et al., 2007) using the RDP 16srRNA and fungallsu databases. Singletons were removed. Negative control OTUs were subtracted for all samples (**Supplementary Figure S6** and **Supplementary Table S1** for rarefaction curves and sequence statistics). Raw sequences were stored at ftp://ftp-adn.ec-lyon.fr/Els_2020_amplicon_sequencing_air_snow/.

Statistical analyses were done in R (R Core Team, 2015) using the phyloseq (McMurdie and Holmes, 2013), vegan (Oksanen et al., 2018), and ggplot (Wickham, 2009) packages.

Mean raw bacterial and fungal read counts per sample were 20153 (+ −11280) and 20899 (+ −21582), respectively. The whole dataset comprised 1566 bacterial and 3127 fungal genera,

[1]http://hannonlab.cshl.edu/fastx_toolkit/

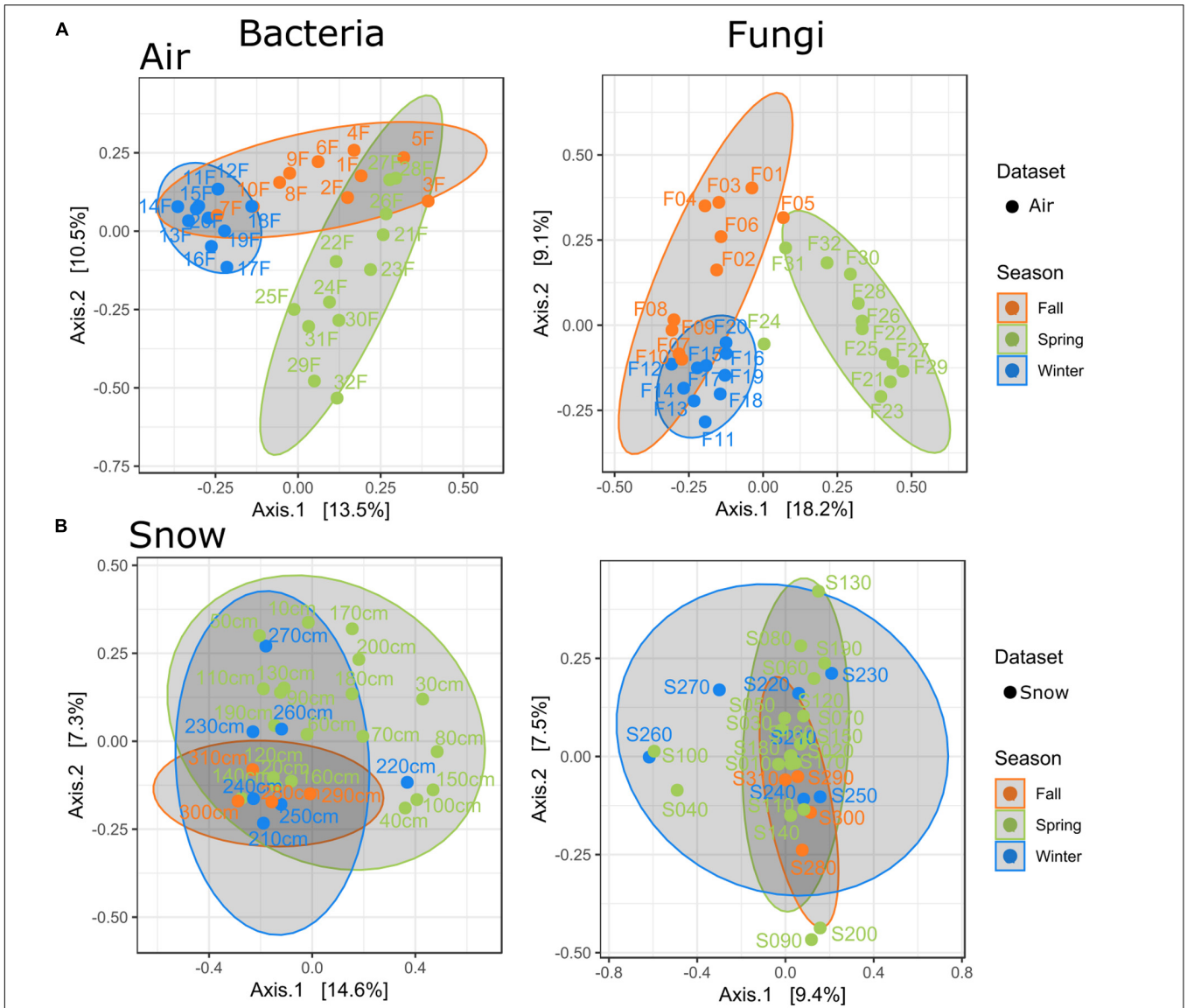

FIGURE 2 | PCoAs for air and snow by season **(A)** only air samples, **(B)** only snow samples, air filters are numbered in order of collection date, while numbers for the snow profile represent depth increments.

which accounted for 1058 bacterial and 1902 fungal genera after removal of blanks.

The statistical analyses were run both rarefied and untreated on the dataset, which did not show differences, but removed rare genera. To include otherwise removed genera and to present the data characteristics appropriately, relative abundance analysis was carried out on non-filtered data (Weiss et al., 2017). Bray-Curtis distances for bacteria and fungi were calculated on datasets normalized to relative abundance (Weiss et al., 2017) and ordinated with principal coordinate analysis (PCoA).

Pairwise PERMANOVA (permutational multivariate analysis of variance) was conducted using the package "pairwiseAdonis" (Martinez Arbizu, 2017), ANOSIM, ADONIS, Chao1, and Shannon indices were calculated using the package "phyloseq"(McMurdie and Holmes, 2013). Bonferroni *p*-value correction (i.e., p.adj) was applied as default for multiple corrections. Statistical parameters of ANOSIM (999 permutations), ADONIS (999 permutations), PERMANOVA and wilcoxon test statistics are reported in the **Supplementary Tables S2–S6**. The significance level was set to alpha = 0.05.

Microbial Quantification

To estimate the abundance of bacteria and fungi, both 16S rRNA genes [primer 338F/518R (Øvreås and Torsvik, 1998)] and 18S rRNA genes [primer set FR1/FF390 (Chemidlin Prévost-Bouré et al., 2011)] were quantified by qPCR using Quantifast 2X SYBR Green dye (QIAGEN). Non-template controls were subtracted.

Chemical Analysis

Snow Chemistry

Snow samples were kept frozen until analysis for which they have been carefully molten at 4°C. Conductivity and pH were measured with a conductivity cell and glass electrode. Anions (Cl^-, NO_3^-, and SO_4^{2-}) and cations (Na^+, K^+, NH_4^+, Ca^{2+}, Mg^{2+}) were measured by suppressed ion chromatography (Dionex ICS1100 resp. ICS-3000). Methods for the measurements, detection limits and quality control methods are applied according to Greilinger et al. (2016). All obtained chemical values were volumetrically weighted with the snow water equivalent of the respective layer as a function of snow density.

PM10 Quartz Fiber Filter Chemistry

Quartz fiber filters were analyzed for different compounds. The carbonaceous fraction of organic, elemental and total carbon (OC, EC, and TC, respectively), were thermal-optically measured. Therefore, a filter punch with 10 mm in diameter was used for analysis with the OC-EC analyzer (Sunset Lab), using the EUSAAR2 reference temperature program and automatic split point setting as performed by the evaluation software.

Anions (Cl^-, NO_3^-, and SO_4^{2-}) and cations (Na^+, K^+, NH_4^+, Ca^{2+}, Mg^{2+}) were determined using ion chromatography with the same setup as for the snow samples. Levoglucosan was also measured via ion chromatography (Dionex ICS-3000) but without using a suppressor. For the measurements of the cations a punch of 12 mm in diameter was placed in a polypropylene test tube and 3 mL of 38 mmol MSA (Methanesulfonic acid) were added. The sample was well mixed and placed in an ultrasonic bath (30°C and full power) for 20 min. Afterward the sample was centrifuged at 4000 rpm for 10 min and 1.1–1.5 mL of the eluate was used for analysis. For the measurement of the anions and levoglucosan the same punch size of 12 mm was used and the same extraction method was applied, just the eluent was changed to milli-Q water.

Mineral dust tracer such as Al and Fe were determined using a PANalytical AXIOS advanced wavelength dispersive X-ray fluorescence spectrometer with a rhodium target X-ray tube set at 50 kV with a current of 50 mA, a 20 mm aperture for exposure and an exposure time of 20 s per channel. A detailed methodological description can be found in Greilinger et al. (2019).

Canonical Analysis of Principal Components and Stepwise Regression

To evaluate the importance of environmental parameters on the variability of the microbial community a stepwise regression with backward elimination was conducted with "*ordistep*" in vegan (Oksanen et al., 2018) and visualized with a canonical analysis of principal components (CAP) based on Bray-Curtis distance on normalized community data. All biological, chemical and physical environmental parameters for CAP analysis and stepwise regression were z-standardized within the air and snow dataset, respectively to account for different scales of unit. See **Table 2** for an overview of all parameters used for the CAP analysis.

Snowpack Time Allocation Modeling

SNOWPACK (Lehning et al., 1999) is a 1D multi-layer snowpack model developed at SLF (Swiss Institute for Snow and Avalanche Research) for avalanche forecasting. It is driven by meteorological data that is filtered through a preprocessor for high alpine weather stations. It can simulate the development of the snowpack during the winter and show modeled snow profiles for a given location and time where meteorological data is available by solving mass and energy exchange equations between the snow cover, atmosphere, vegetation and soil, and treating mass and energy fluxes within these media. It takes into account snow metamorphism, settling, phase changes, wind erosion, water and vapor transport, heat conduction and more. The microscopic parameters of grain size, bond radius, sphericity and dendricity are derived from snow density, temperature and liquid water content for each layer. Based on these results, the macroscopic parameters of thermal conductivity and viscosity that are needed to compute the conservation equations are calculated.

In our simulation, the absolute snow height was used to calculate new snow sums. Neither the snow surface temperature nor the reflected short-wave radiation were measured, so for the upper boundary condition, we used the incoming long wave radiation and parameterized the albedo. This implies working with fluxes rather than temperatures, i.e., Neumann boundary conditions. Radiation data from Mt. Sonnblick used as input was obtained within the ARAD network (Olefs et al., 2016). Snow height was obtained from an automatic TAWES laser snow gauge

TABLE 2 | Overview over all measured chemical, biological, and physical parameters.

	Air	Snow
Bacterial resp. Fungal abundance	x	x
Shannon	x	x
Chao1	x	x
Season	x	x
NO3	x	x
NH4	x	x
SO4	x	x
Ca	x	x
Cl	x	x
Mg	x	x
Na	x	x
K	x	x
OC	x	
TC	x	
EC	x	
NO2	x	
Levoglucosan	x	
Al	x	
Fe	x	
Precipitation	x	
Snow-Water- Equivalent (SWE)		x
pH		x
Conductivity		x
Density		x

Analyzed samples for the respective environmental compartment indicated by "x".

next to the snow pit sampling site, data validation was carried out using data from daily manual snow height measurements and via quality control algorithms. Wind speed and direction, temperature, pressure and humidity were obtained from the meteorological measurements at the Sonnblick Observatory. Details on calculation and model settings and further references are available at https://gitlab.com/lwd.met/snowpack/sonnblick_2016/wikis/home.

The results of the simulated profile were compared with the measured grain type, grain size and snow density for the respective layers during field sampling (**Supplementary Figures S1, S2**). The end-result is the temporal evolution of the snow cover as a time series of modeled snow profiles at our experiment site (**Figure 3A**).

Boundary Layer Analyses

Periods with possible transfer of air from the ABL to the Sonnblick Observatory were determined based on time-series of mixing heights. The mixing height is defined as the height above the ground where air and suspended particles from near ground are transported up to by vertical mixing. Exchanges between the ABL and the FT in Alpine areas are caused by advective processes in connection with frontal systems and mountain venting as well as by mixing processes including deep convection, shallow convection, frontal convection and ABL turbulence (Zhang et al., 2018).

The heights of the lowest distinct aerosol layers within the ABL were obtained from backscatter profiles derived from a VAISALA CL51 ceilometer located at Kolm-Saigurn (the base of Mount Sonnblick at 1500 m asl.). Half hourly mixing layer heights were calculated from these aerosol layer heights in combination with wind speed data at 10 m above ground measured at Kolm-Saigurn using the approach described in Lotteraner and Piringer (2016). Cases with mixing heights larger than 1600 m were interpreted as conditions favorable for the transfer of ABL air to or above the top of Mount Sonnblick.

RESULTS

Seasonal Dynamics of Bacteria and Fungi in Air and Snow

Seasonal Allocation in Air and Snow

The bacterial and fungal communities from air filters and the snow profile differed significantly (ANOSIM bacteria $p = 0.001$, $R = 0.325$, fungi $p = 0.001$, $R = 0.287$). The bacterial community featured 45% of genera unique to the air filters and 45% common in the profile and the air filters, but only 9.8% unique to the snow profile, resp. 82.2% of the snow genera were also present in air. In the fungal community, 74.5% of the genera were unique to the air filters while only 3.4% were unique to the snow profile and 22.1% of genera occurred in air and snow, resp. 86.7% of the snow fungal genera also occurred in the air (see **Supplementary Figure S7**).

Among the ten most abundant bacterial phyla, the most prominent overall trend was the relative occurrence of more than twice as much Actinobacteria in the air-filters (air 28.09%, snow 10.50%), while Proteobacteria were more abundant in the snow profile (snow 39.15%, air 20.54%). Relative abundances of Bacteroidetes (air 10.11%, snow 12.69%), Chloroflexi (air 1.16%, snow 1.24%), Firmicutes (air 30.29%, snow 26.91%), Gemmatimonadetes (air 0.74%, snow 0.66%) and other less abundant phyla were similar in air and snow. Whereas Cyanobacteria appeared to be twice as common in snow (air 2.56%, snow 4.25%), Acidobacteria were more abundant in air (air 2.64%, snow 1.41%).

For the fungi, Dothideomycetes (air 19.17%, snow 27.16%), Microbotryomycetes (air 1.35%, snow 7.79%), Lecarnomycetes (air 0.93%, snow 10.45%), and Ustilaginomycetes (air 0.32%, snow 9.14%) were more abundant in snow, while Eurotiomycetes (air 27.34%, snow 9.75%) and Sordariomycetes (air 16.49%, snow 7.67%) were more abundant in air. Agaricomycetes (air 20.79%, snow 16.85%) and Leotiomycetes (air 5.97%, snow 4.19%) occurred at comparable relative abundances in air and snow (**Supplementary Table S7**).

Seasons were determined according to Greilinger et al. (2016) and validated with PCoA clustering of the samples (**Figure 2** and **Supplementary Figure S5**). Snow sample increments were allocated to their respective seasons by SNOWPACK modeling (**Figure 3** and **Table 3**).

Air microbial communities show a seasonal pattern (**Figure 2A**). Bacterial and fungal winter air samples were the most distinct and closely clustered, with some overlap in winter and fall air samples, but distinctly different to spring samples. The seasonal effect on snow samples was less apparent and showed highest variability in spring for bacteria and winter for fungi and the lowest variability in fall for both (**Figure 2B**).

In pairwise comparisons (PERMANOVA), the strongest similarity for snow bacteria and fungi was found between spring and winter (p.adj: 1.000), winter and fall (p.adj: 1.000), and fall and spring (p.adj.: bacteria: 0.090; fungi: 0.270). For bacteria, the air and snow autumn communities were the most similar (p.adj.: 0.075), followed by air in spring and the snow in fall and winter (p.adj.: 0.75, resp. 1.000). All other pairwise PERMANOVA comparisons were significantly different (**Supplementary Table S3**).

The 2016/17 winter accumulation of snow during September to February was 1 m (**Figure 3A**), during which a 5 week dry period (F10–F15) was observed. During spring, precipitation events led to the accumulation of 2 m of snow, but a 4 week dry period (F25–F29) was also observed, in addition to the formation of an ice lamella. When air filters are presented chronologically, Actinobacteria and Proteobacteria had a peak in spring, while Chloroflexi, Cyanobacteria, Deinococcus–Thermus and Gemmatimonadetes were present only in fall and winter and Firmicutes had a peak in fall. For fungi, Agaricomycetes were high in fall and early winter, while Eurotiomycetes were high in spring. Lecarnoromycetes and Microbotryomycetes occurred only in winter, Tremellomycetes occurred in fall and higher in winter (**Figure 3B** and see **Supplementary Figure S8A** for detailed temporal resolution per phyla resp. class). The snow profile showed a more patchy picture of the occurrence of certain phyla and classes of bacteria and fungi (**Figure 3C**). In winter and spring snow, Proteobacteria were more abundant than in fall, while Cyanobacteria were most abundant in fall

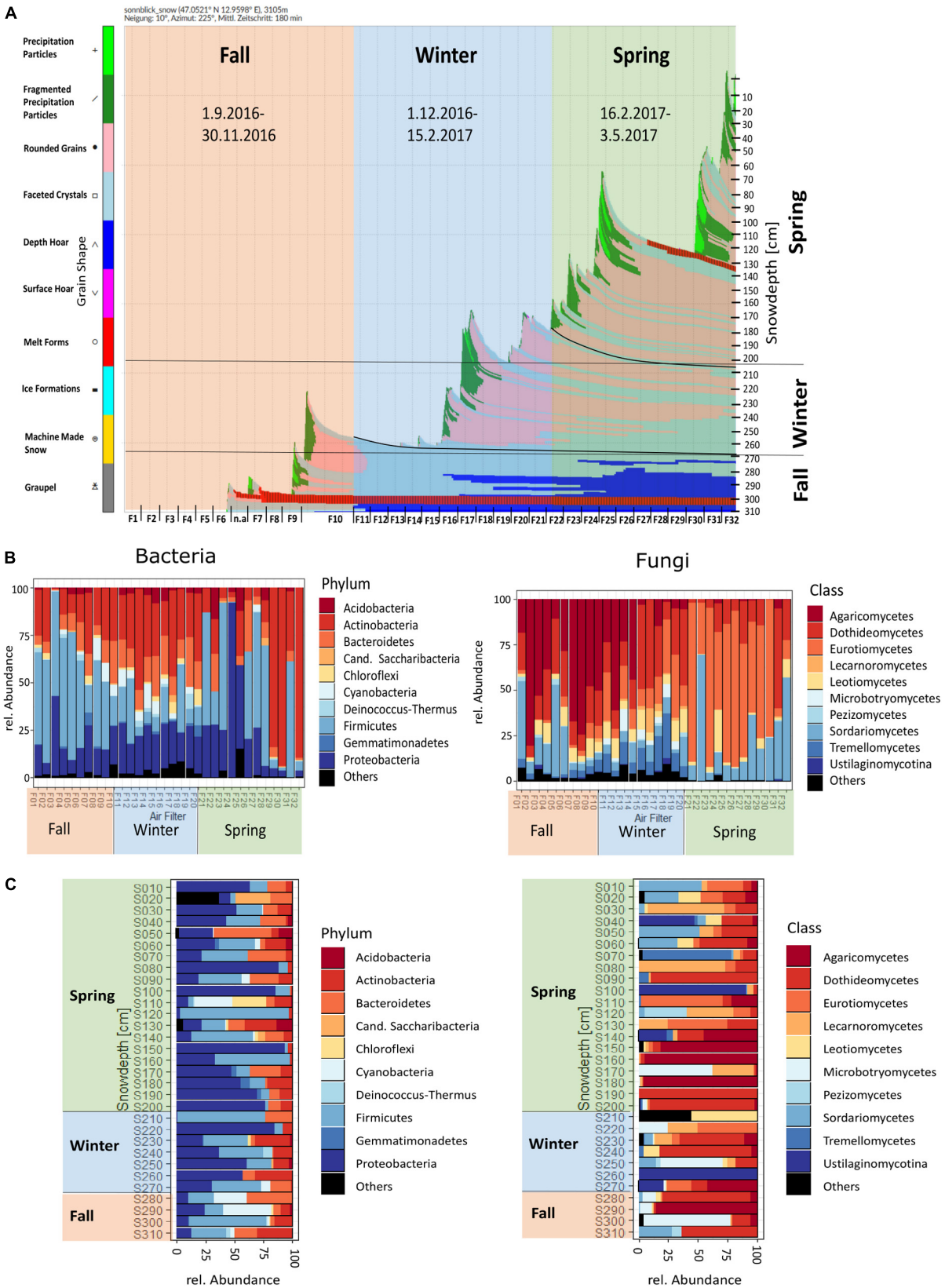

FIGURE 3 | (A) SNOWPACK temporal model output and derived seasonal grouping, **(B)** temporal order of air filters, **(C)** profile of snow samples for bacteria and fungi, depicted for the 10 most abundant bacterial phyla and fungal classes.

TABLE 3 | Overview of seasonal classification of air filters and snow samples.

	Time	Air Filter	Σ Air Filter	Snow depth	Σ Snow Increments
Fall	1.9-30.11.16	F1–F10	10	310-280	4
Winter	1.12.16-15.2.17	F11–F20	10	270-210	7
Spring	16.2.17-4.5.17	F21–F32	12	200-10	20

snow. The relative abundance of Microbotryomycetes is higher in fall snow and for Leotiomycetes higher in spring snow. In the spring snow Agaricomycetes and some other fungal classes that were not apparent in spring air could be detected (**Supplementary Figures S8A–D**).

Snow Air Comparison by Season and Core Community

Comparing bacterial and fungal genera shared between air and snow in the different seasons as a percentage of the snow dataset (**Figures 4A–C**), the highest overlap was in fall (75.7%) for bacteria, followed by winter (56.7%), and spring (49.8%) and in winter for fungi (83.9%), followed by fall (72.9%), and spring (66.3%). Spring made up the biggest dataset, with the most snow increments (i.e., 20) and air samples (i.e., 12), but had roughly half as many fungal genera in total in air and snow than winter (798 in spring, 1349 in winter, 1214 in fall). Bacteria had roughly the same number of genera in the dataset of each season (594 in fall, 592 in winter and 604 in spring).

Air bacterial diversity was significantly higher in winter (wilcoxon $p \leq 0.0002$) and no significant differences were observed in bacterial snow alpha diversity across seasons (**Figure 4D** and **Supplementary Tables S4–S6**). Fungal alpha diversity was highest in spring and fall air samples for all indicators and highest in fall snow in richness (Chao1, wilcox $p = 0.018$), but did not differ significantly in evenness (Shannon, wilcox $p = 1.000$).

Chemical Concentrations and Interaction With Microbial Community in Snow and Air

The temporal development of the chemical concentrations showed higher variability in fall and spring in the air filters (**Figure 5A**), especially for SO_4^{2-}, NO_3^-, Ca^{2+}, K^+, and Na^+. TC and OC were also more variable in the fall and spring (**Figure 5A**). In the snow profile (**Figure 5B**), NO_3^-, NH_4^+, SO_4^{2-}, and Ca^{2+} concentrations were highest in fall and spring, with NO_3^- concentrations varying the most throughout the snow profile.

The backward elimination analysis (**Table 4**) identified season, alpha-diversity indicators, SO_4^{2-} and Ca^{2+} as significant factors in explaining variability for the whole dataset. Sample type (i.e., air or snow) and Mg^{2+} were also shown to be significant when included in the analysis. When considering the air samples only, Mg^{2+}, Cl^-, TC/OC, Al/Fe, SO_4^{2-}, season, Chao1 and Shannon index were significant in explaining variability. For the snow only season, Chao1 and SO_4^{2-} were significant. For fungi the most important factor was season, NO_3^- was significant in the snow dataset, and Shannon diversity was significant in the air.

Canonical analysis of principal components analysis for the whole dataset (**Figure 6A**) shows that SO_4^{2-} was related to spring and fall air, while the Chao1-diversity was mostly linked to winter air samples and Shannon-diversity to winter and fall air samples. The whole dataset had 11.5% variability explained in the first two axes, but 14.9% when sample type was taken into account. OC/TC are related to fall and some spring filters, while Mg^{2+} and Cl^- are related to spring filters and Al/Fe to spring and fall. Air filters had the highest variability explained by the measured variables (i.e., 22.8% resp. 26.6% for the first two axes, **Figure 6B**).

The snow (**Figure 6C**) showed a slight grouping by season for the fall and winter samples, with only the S220 sample grouping with spring samples. Spring samples were most scattered and partially overlapped with winter snow samples. SO_4^{2-} in snow correlated with fall and winter samples, Chao1 correlated with winter and some spring samples.

SWE, density, conductivity and pH are not displayed, as they had the highest *p*-values (most insignificant *p* values) for snow. Snow had 15.2% resp. 11.8% explained variability for the first two axes.

Influence of Exchange Between Atmospheric Boundary Layer and Free Troposphere

Figure 7A illustrates the mean daily courses of the mixing height for the seasonal periods of investigation. Mixing heights on average were lowest during the winter period (up to 900 m AGL on average, i.e., 2400 m asl.). Due to seasonal position of the sun and the shading by the mountains, the mixing height started to rise up to 2 h later in the morning in winter-time and decreased with sunset up to 2 h earlier than in spring and fall. In spring, the mean mixing height during daytime rose to 1150 m AGL (i.e., 2650 m asl). The observatory is located at 1600 m AGL (i.e., 3100 m asl.), thus the average mixing heights during the investigated periods remained well below the sampling site.

All events with half hourly mixing heights of more than 1600 m are indicated by black vertical lines in **Figure 7B**, revealing when air might have been transported from the ABL up to the FT. These events occurred most frequently in early fall and in spring. The highest number of mixing layer half hour events reaching the observatory was recorded for fall Filter F02 followed by spring filters F27 and F28 (**Table 5**). These filters also showed the most prominent peaks in chemical concentrations and sum of ions (**Figures 5A,B**). The strongest correlation for both mixing height half hour sums between concentration values and the number of half hourly mixing heights above 1600 m was observed for EC > SO_4^{2-} > Fe > TC > Ca^{2+} > OC, linking the

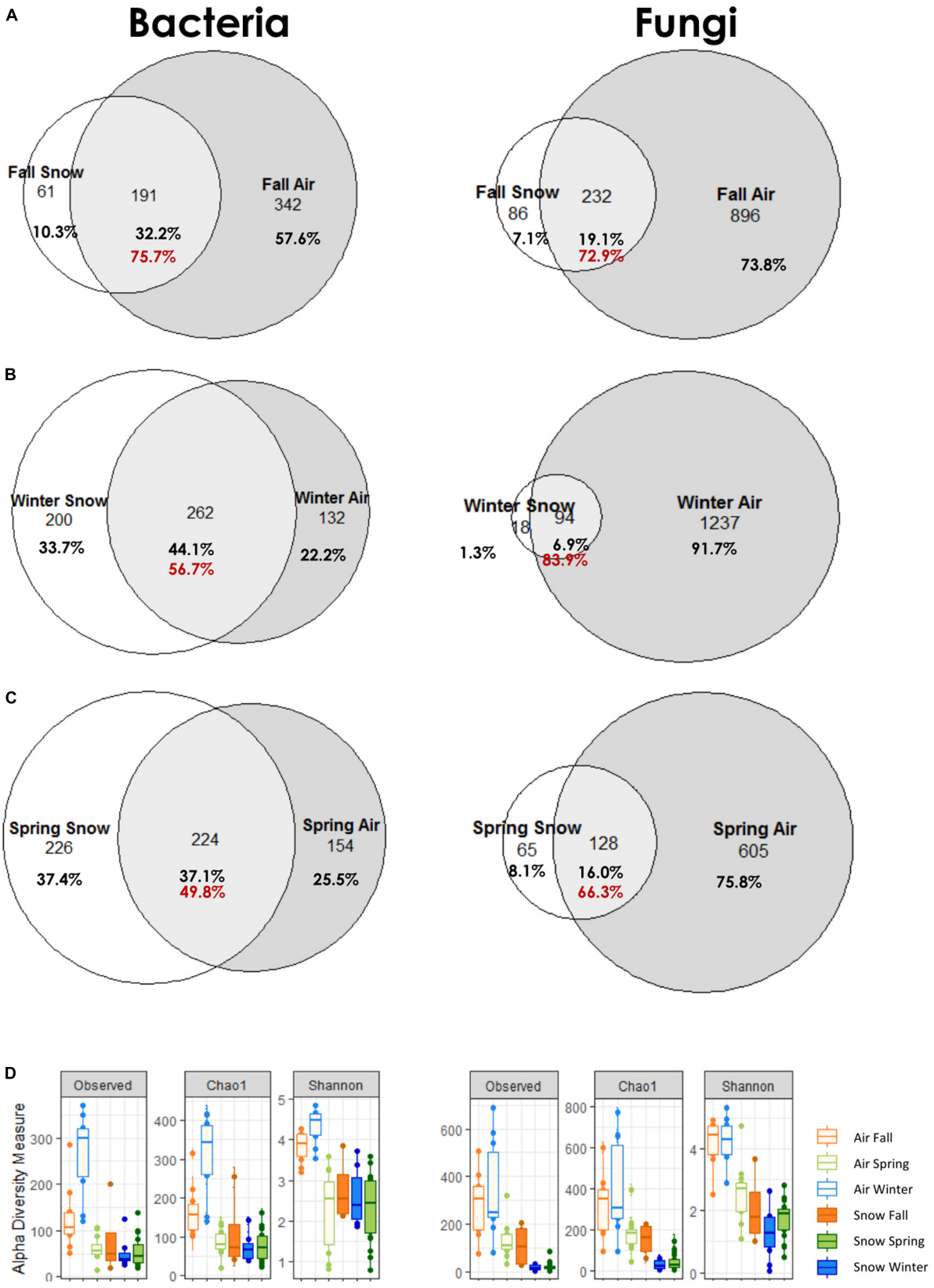

FIGURE 4 | Common genera of air and snow for each season **(A)** fall, **(B)** winter, **(C)** spring; red numbers indicate the percentage of atmosphere genera in the snow dataset; **(D)** alpha diversity measures Observed, Chao1, and Shannon by season for bacteria and fungi.

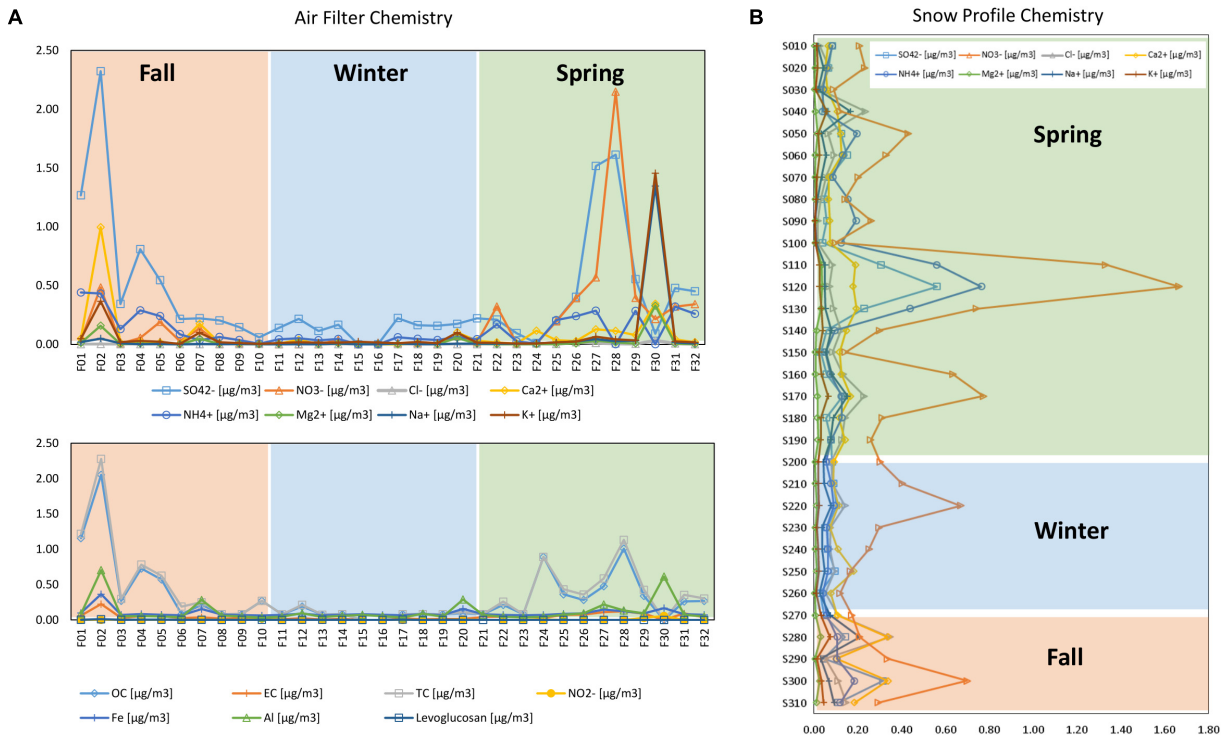

FIGURE 5 | Temporal trends in chemical concentrations in **(A)** air and **(B)** snow profile.

influence of ABL air transported upward to the concentration of chemicals measured at the mountain station.

DISCUSSION

Is Air a Bacterial and Fungal Seeding Source to Snowpacks?

The atmosphere has been suggested as a seeding source for snowpacks given that snowflakes form in the atmosphere and that the two ecosystems are connected (Maccario et al., 2019). Based on the venn diagram analysis, as the snowpack established in the fall, it shared almost 76% of the identified bacterial and 72.9% of fungal genera with the atmosphere (**Figure 4**), suggesting a strong interaction between the two compartments. As the snowpack evolved throughout the winter and spring, the overlap with the atmosphere diminished for bacteria (winter 56.7% and spring 49.8%), but increased during the winter for fungi (83.9%) and was lowest for fungi in spring (66.3%). Based on shared genera data, it appears that the snow is seeded by the atmosphere, however, when looking at community structure, the PCoA and statistics reveal a separation of air and snow bacterial and fungal genera. These differences suggest that a distinct air microbiome might exist that is not incorporated in clouds and thus not precipitated or scavenged in snow, or that post-depositional selection of low abundance airborne microorganisms occurs over time within the snowpack, as has previously been suggested (Segawa et al., 2005; Larose et al., 2010; Hell et al., 2013; Maccario et al., 2014). For example, Cyanobacteria were twice as common in snow than in air and have been suggested as being especially successful in establishing in the snow (Harding et al., 2011; Maccario et al., 2019).

In the few available datasets comparing air and snow microbial communities (Šantl-Temkiv et al., 2018; Els et al., 2019; Triadó-Margarit et al., 2019), a comparable or higher diversity in snow samples was generally observed. However, our results indicate a higher richness and evenness of bacterial and fungal organisms in the air, even though the capturing efficiency of the DIGITEL DHA80 (PM10High Volume sampler) for the size of free floating bacteria (approx. 0.2 µm) is likely not 100% due to losses at the inlets. We also expect losses from the removal of DNA from the quartzfiber-filter, due to the DNA binding characteristic of the quartz (Dommergue et al., 2019). Considering the expected losses of bacterial diversity by sampler size cut-off and DNA-extraction losses, the results of higher alpha diversity values in the air samples point toward an even higher expected air alpha diversity. It is possible that the sampling time of 1 week integrated different atmospheric weather processes, thus maximizing the potential for sampling diversity.

Do Deposition Pathways and Changes in Meteorology Affect Snow Community Structure?

Among all the seasons sampled, spring snow was the most diverse and also had the highest amount of unique bacterial genera. This might be related to the snow fall event that made up samples

TABLE 4 | Importance of environmental parameters on the variability of the microbial community determined by stepwise regression with backward elimination.

Bacteria					Fungi				
	Df	**AIC**	**F**	**Pr(>F)**		**Df**	**AIC**	**F**	**Pr(>F)**
Complete snow and air dataset including sampletype as a factor					**Complete snow and air dataset including sampletype as a factor**				
Ca	1	203.23	1.3309	0.060	Season	3	209.20	2.4461	0.005**
Mg	1	203.27	1.3621	0.060	Type	2	3.9110	3.9110	0.005**
Season	3	202.72	1.3238	0.040*					
SO4	1	203.68	1.7194	0.015*					
Shannon	1	203.81	1.8321	0.005**					
Chao1	1	203.89	1.9021	0.005**					
Type	2	206.52	4.2881	0.005**					
Complete snow and air dataset not including sampletype					**Complete snow and air dataset not including sampletype**				
Ca	1	205.54	1.3660	0.045*	Season	3	211.08	2.4034	0.005**
SO4	1	205.84	1.6450	0.020*					
Shannon	1	205.96	1.7517	0.010**					
Season	3	205.56	1.6155	0.005**					
Chao1	1	206.23	2.0023	0.005**					
Air dataset					**Air dataset**				
Mg	1	77.683	1.5469	0.015*	Shannon	1	77.292	1.7145	0.030*
Cl	1	77.772	1.6122	0.015*	Season	3	79.856	3.1350	0.005**
TC/OC	1	77.963	1.7540	0.015*					
SO4	1	78.421	2.0960	0.010*					
Season	3	77.773	1.5680	0.005**					
Chao1	1	77.996	1.7786	0.005**					
Fe/Al	1	78.006	1.7860	0.005**					
Shannon	1	78.334	2.0310	0.005**					
Snow dataset					**Snow dataset**				
Chao1	1	79.635	1.6228	0.040*	Season	3	83.486	1.2074	0.075.
SO4	1	79.395	1.4096	0.010**	NO_3	1	84.290	1.3024	0.030*
Season	3	79.603	1.7163	0.005**					

*Statistical significance level: *p ≤ 0.05, **p ≤ 0.01.*

S010-S130 of the total snow profile that fell in the last 3 weeks before sampling (F30–F32). Microorganisms in precipitation events are scavenged from the air (Franz and Eisenreich, 1998; Maria and Russell, 2005; Zhang et al., 2013), which might explain the higher diversity and variability observed in the spring samples. Snowflakes form in the atmosphere around particles, among them also ice nucleation active bacteria (Christner et al., 2008) and are then deposited. During precipitation, interstitial air, also containing microbes, is included in the snowpack, and can interact with the atmosphere over several meters depth (Domine and Shepson, 2002). During precipitation, snow crystals and supercooled liquid droplets can scavenge gas phase and aerosol species from the atmosphere, which are then introduced to the snowpack (Paramonov et al., 2011; Budhavant, 2014; Wang et al., 2014). In the snowpack, complex and not fully understood chemical conversions, enrichments and release of a range of chemical compounds take place. Snow is especially reactive to UV-radiation and photo-oxidation (Grannas et al., 2007; Domine et al., 2008). These factors may render the snowpack selective for certain types of microorganisms.

As shown in Els et al. (2019), there is a significant difference in the genera deposited with precipitation and present in air, which might also explain the higher amount of unique genera in the snow relative to the atmosphere. The unique snow genera might also be explained by DNA extraction and sequencing depth (Klindworth et al., 2013; Mizrahi-Man et al., 2013; Kennedy et al., 2014) or different seeding sources that were not sampled here.

In the winter, a long dry period was observed (F11–F15) and air masses were stable in terms of boundary layer dynamics. Winter air microbial communities were likely mainly characterized by long range transport, as little exchange or emission and boundary layer injections occurred. Winter air was most separate in bacterial diversity from snow and other groups (**Figure 2A**) and overlapped only with some fall samples (F07, F10). During the sampling of F07, a Sahara dust event occurred (see **Table 1**). These depositions are associated with long range transport of air and particles from northern Africa. Given the lack of precipitation events, dry deposition of microorganisms was probably the dominant colonization pathway to the snowpack. Fungi probably settle better in dry deposition, as they are bigger and have a higher density than bacteria (Smith et al., 2011). Their dispersal in the air is closely linked to the aerodynamic diameter of their spores (Yamamoto et al., 2012; Woo et al., 2018), but the most important factor is the seasonal availability of their

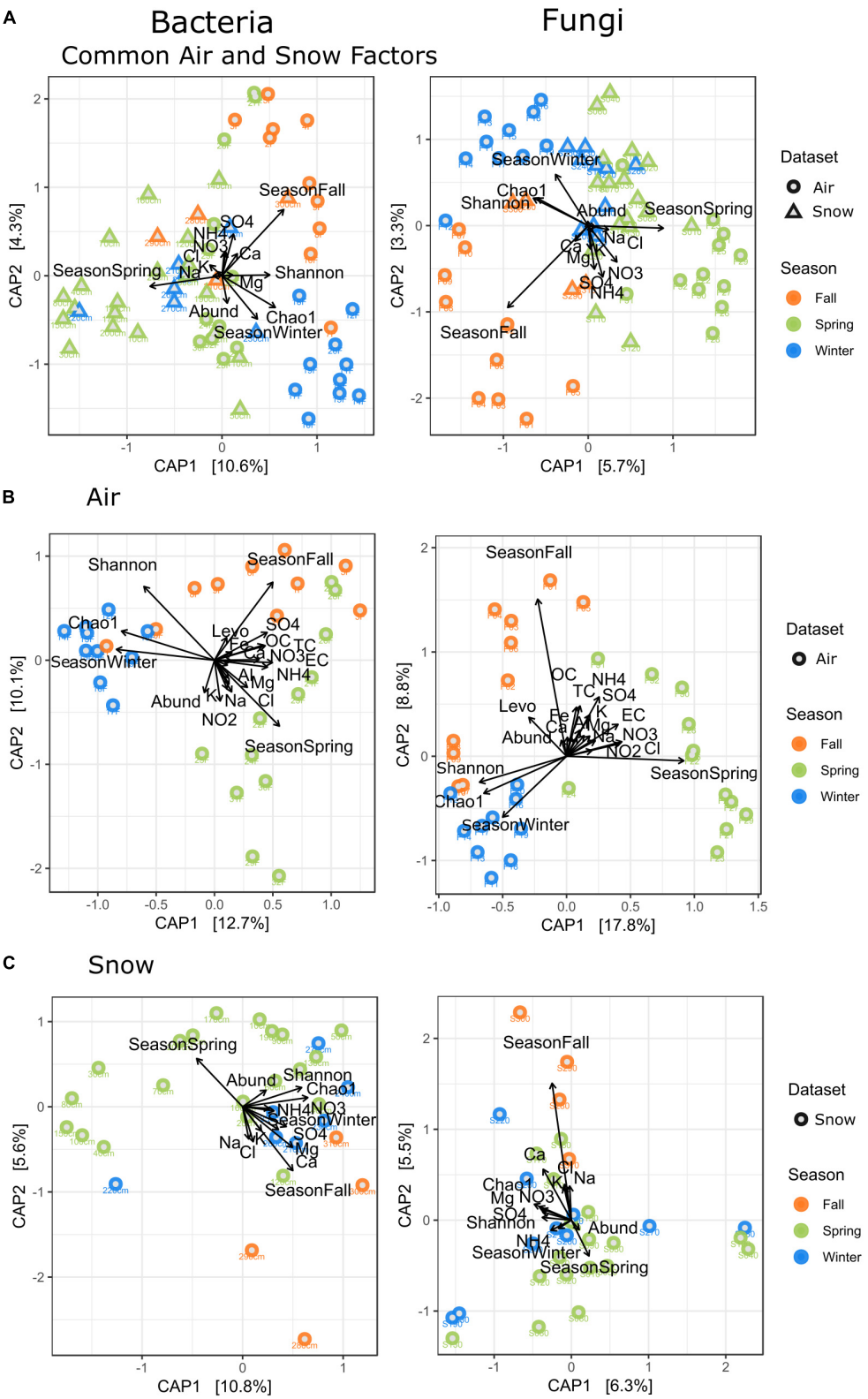

FIGURE 6 | Canonical analysis of principal components (CAP) of all factors measured for **(A)** all factors measured for air and snow, i.e., Season, NO_3, Cl, NH_4, SO_4, Ca, Mg, Na, K, Chao1, Shannon, Abundance, Sampletype, **(B)** for all factors measured for air, i.e., Seasons, NO_3, Cl, NH_4, SO_4, Ca, Mg, Na, K, Chao1, Shannon, Abundance, OC, TC, EC, NO_2, Levoglucosan, Al, Fe, Precipitation, **(C)** for all factors measured for snow, i.e., Season, NO_3, Cl, NH_4, Ca, Mg, Na, K Chao1, Shannon, Abundance.

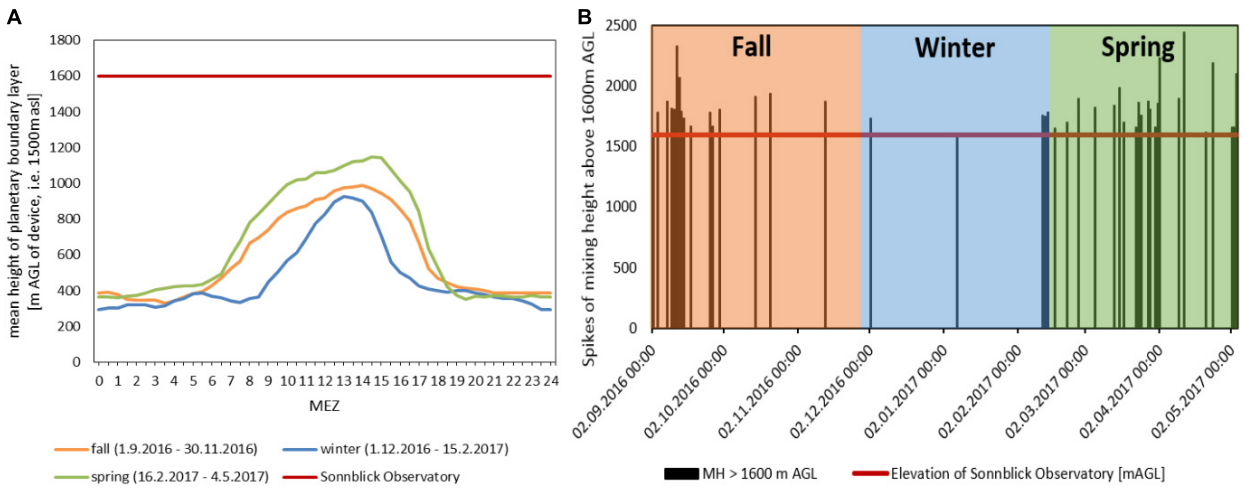

FIGURE 7 | (A) Mean height of planetary boundary layer above ground of measuring device (Kolm-Saigurn 1500 m asl), Sonnblick Observatory at 1600 m AGL, **(B)** half hour values of mixing heights [m AGL] reaching the Sonnblick Observatory.

spores due to their lifestyle (Pickersgill et al., 2017). The results from our study support this hypothesis with fungal communities exhibiting high dynamics in the fall that is not observed in winter or spring when the ground is snow-covered and higher boundary layer dynamics occur.

TABLE 5 | Sum of mixing heights reaching the Sonnblick Observatory, pearson correlation of sum with concentration of chemical species on the PM10 quartz air filters.

Season	Filter	Number of half hour spikes of mixing height above the observatory	Pearson correlation r^2	PM10 chemical conc. ~ Σhalf hour spikes
Fall	F01	8	**SO_4**	**0.7331**
	F02	65	**NO_3**	0.1811
	F03	11	**Cl**	0.0015
	F04	15	**Ca**	**0.5652**
	F05	13	**NH_4**	0.3858
	Fxx	6	**Mg**	0.0729
	F06	5	**Na**	0.0073
	F10	4	**K**	0.0081
Winter	F11	4	**OC**	**0.5573**
	F15	1	**EC**	**0.7889**
	F20	17	**TC**	**0.6019**
Spring	F21	7	**NO_2**	0.0086
	F22	3	**Fe**	**0.6448**
	F23	9	**Al**	0.3494
	F25	8	**Levoglucosan**	0.4624
	F26	13		
	F27	34		
	F28	21		
	F29	19		
	F31	10		
	F32	9		

In bold: values >0.5.

Are Microbes and Chemical Compounds Co-transported in Air Masses, and Thus Exhibit the Same Co-correlations in Air and Snow?

To connect air chemistry with air microbiology is challenging. In the case of the presented dataset, the chemistry was analyzed directly from the same filter as the microbiological analyses. The advantage of this is that all differences in sampling procedure, losses in pipes and inlets, cut-off sizes and the general filter sample handling and potential introduced biases are identical for the microbial and chemical sampling until the laboratory stage. The limitation of the method is that the filter samples represent a time integration over the duration of 1 week. This means that short peaks of chemical or microbial atmospheric events would likely not be detected in the samples, thus the data represents only major trends (Tignat-Perrier et al., 2019).

This can also be seen as an advantage in aerobiological sampling, as a range of studies stated high short-term variability of air microbial composition with little observable patterns (Fierer et al., 2008; Polymenakou and Mandalakis, 2013).

Our data shows that season and alpha diversity were the major drivers in microbial variability in snow and air, if regarded together or separately for each sample type, and only a few chemical markers could be identified as important in explaining the microbial variability. The variability explained by chemistry and season was generally low, the highest values were found for the air dataset alone (23.2% air bacteria, 26.8% for fungi), snow and air together reached the lowest explained values, indicating that different factors were driving microbiology in air and snow. Seasonal variability in airborne communities has been recurrently shown within the ABL and in the FT (Brodie et al., 2007; Fierer et al., 2008; Franzetti et al., 2011; Bowers et al., 2012, 2013; Bertolini et al., 2013). As a higher share of variability could be

explained by the measured parameters in air as compared to snow, this suggests that different processes are important for the microbial composition and variability in snow than the sampled parameters.

The strongest correlation between the chemical concentrations on the PM10 quartzfiber air filter and the mixing height half hour sums of elevation above the observatory was observed for EC > SO_4^{2} > Fe > TC > Ca^{2+} > OC implying that ABL air transfer to the mountain tops and to the FT is of high importance for the concentration and composition of inorganic aerosols in the free tropospheric atmosphere. Mountainous terrain exerts a profound influence on aerosol distribution in the atmosphere, with often enhanced mixing and transport processes compared to horizontally homogeneous terrain. Mechanisms like entrainment, advective venting, mountain venting or mountain cloud venting facilitate exchange of ABL air and the FT (De Wekker and Kossmann, 2015). The transport of gases and particles into a tropospheric cloud layer (Cotton et al., 1995) by mountain cloud venting is a particularly effective of these processes (Kalthoff et al., 2013). In air Cl^{-}, TC/OC, and SO_4^{2-} as well as Mg^{2+}, and Fe/Al and were identified as related to bacterial variability. At the investigated site the former components are related to anthropogenic activities whereas the latter ones are related to dust particles according to Pio et al. (2007) and Greilinger et al. (2016), implying that dust event related variation of microbes or human impact (SO_4^{2-}, TC/OC, Fe) are driving variability of the air microbial community in the FT.

Ca^{2+}, Mg^{2+}, and SO_4^{2-} were also identified driving the bacterial variability in the snow and air dataset. Ca^{2+} and Mg^{2+} are related to the occurrence of bigger crustal parts that might be easier deposited and thus important for air and snow microbial composition and are especially affected by Saharan dust inputs (Greilinger et al., 2018). Bacterial abundance is positively correlated to Ca^{2+} in snow (Margesin and Miteva, 2011). Atmospheric bacterial supply to the snowpack and mineral particle concentration in the snowpack are positively correlated (Segawa et al., 2005). SO_4^{2-} and Ca^{2+} in aerosols can have multiple sources (Li et al., 2006).

SO_4^{2-} was the only chemical factor being identified as significant to explain bacterial variability in air and snow and when both regarded together. Sulfate in the atmosphere originates from anthropogenic sources like fuel burning or smelting (Forbes and Garland, 2016). SO_4^{2-} can also originate from sea salt or biogenic emission of dimethylsulfide and other reduced gases from the ocean, but also volcanic eruptions (Harder et al., 2000), but these are unlikely sources for the atmosphere sampled in this study. The tropospheric residence time of SO_4^{2-} is 12 days (Harder et al., 2000). Gandolfi et al. (2015) found a significant correlation of SO_4^{2-}, Mg^{2+} and Ba with the microbial community structure of bioaerosols, but could not assess whether this was due to co-variation or taxa specific selection (Baumgartner et al., 2006; Dillon et al., 2007). SO_4^{2-} is a significant driver of high alpine soil bacterial community composition, particularly in fall (Lazzaro et al., 2015).

Fungi in air were only related to seasonal factors. NO_3^{-} was the only chemical parameter identified as important for fungal composition in snow. The NO_3^{-} radical is highly reactive with inorganic and organic compounds in cloud water (Herrmann et al., 1994). Thus, surface reactions of NO_3^{-} with certain fungal species in the cloud could be a possible explanation for this interaction, as fungal spores were recently identified as major input source of sodium salt in the amazon due to hygroscopic interactions at their surface (China et al., 2018). Fungi can oxidize NH_4^{+} to NO_3^{-} in grassland soils (Laughlin et al., 2008), thus also a co-emission of NO_3^{-} and fungal spores from the same sources within the ABL might be possible. Fungi in alpine soil are more determined by environmental factors (i.e., soil dry weight, altitude, plant species, soil temperature) than chemical composition (Lazzaro et al., 2015).

CONCLUSION

In this study we compared the bacterial and fungal communities in continuous PM10 air samples over the entire winter season with a snow profile of the entire winter season in terms of microbial and chemical patterns in the FT.

Most genera found in snow occur also in air, this is more pronounced for fungi than for bacteria (49.8–75.7% for bacteria, 66.3–83.9% for fungi), implying that snow is more similar to air, than air is to snow, thus air microbial composition likely effects snow community, but evolves differently over the seasons.

Fungi share less genera in air and snow than bacteria and generally feature a high unique share of air genera in total and seasonal air. The shared air-snow communities are most different for bacteria in spring and fungi in fall, implying different dispersal patterns. Fungi show a strong seasonal transition of abundant classes in air that is not depicted in snow.

The measured chemical tracers were more important for bacterial variability in air than in snow, either because chemicals in the snowpack are not important for post-depositional microbial selection or not the right compounds were measured. The differentiation between air and snow samples and seasonal (i.e., long-term) impact, and with it, changing alpha-diversity, are more important than chemical markers to explain variation in the bacterial and fungal microbial community in air and snow.

SO_4^{2-} was identified as an important chemical compound for bacterial composition in air and snow (next to Ca^{2+} and Mg^{2+} dust markers). Fungal composition is not explained by chemical variation, apart from NO_3^{-} in snow.

Peaks in transported chemicals in the air correlated with increased mixing layer heights rising above mountain top level. Not only inorganic, but also biological aerosols are transferred to the FT with ABL air mixed into the FT at the upper boundary of the convective mixing layer. This mechanism of convective mixing of boundary layer air into the FT seems to be an important factor for microbiological particles going into long-range transport.

The strong seasonal variation and transition of bacterial and fungal composition in air and snow highlight the need for long-term monitoring of bioaerosols to gain insights on their occurrence and reveal how little reliability can be drawn from ABL short-term sample campaigns.

DATA AVAILABILITY STATEMENT

Raw sequences analyzed in this study were stored under the link: ftp://ftp-adn.ec-lyon.fr/Els_2020_amplicon_sequencing_air_snow/. Details on SNOWPACK calculation and model settings and further references are available at: https://gitlab.com/lwd.met/snowpack/sonnblick_2016/wikis/home.

AUTHOR CONTRIBUTIONS

NE conceived the setup, did snow sample fieldwork, conducted the microbial lab work, analyzed the data, and wrote the manuscript. MG and AK-G did the snow profile sampling for chemical analyses, provided the quartz air filters, chemical analyses, a range of feedback on the analyses and the manuscript. MR did the SNOWPACK modeling. RT-P provided guidance with the microbial lab work and ran bioinformatical analyses. KB-S provided boundary layer data. AK-G and BS provided funding. CL supervised the microbial labwork and data analysis and contributed highly to the manuscript.

FUNDING

This work received funding from the European Union's Horizon 2020 Research and Innovation Program under the Marie Skłodowska-Curie Grant No. 675546 (MicroArctic). The snow chemistry sampling was supported by the Global Cryosphere Watch Project (GCW_glaciers) of the Federal Ministry of Agriculture, Regions and Tourism (BMLRT).

ACKNOWLEDGMENTS

We would like to thank the providers of radiation data for model input: Friedrich Obleitner (University of Innsbruck), Dietmar Baumgartner (University of Graz), Marc Olefs (ZAMG) and the Austrian radiation monitoring network ARAD, Christoph Lotteraner for boundary layer data, Hanna Gureczny and Peter Redl who did the chemistry analysis at TU Vienna, student participants of the "Gletscherpraktikum 2017" of Boku and TU Vienna who supported the snow profile digging, Elke Ludewig, Florian Geyer, Alexander Ohms and the ZAMG staff at the Sonnblick Observatory, the team of the Lyon lab for sequencing support and most important Klaus Unterberger.

SUPPLEMENTARY MATERIAL

The Supplementary Material for this article can be found online at: https://www.frontiersin.org/articles/10.3389/fmicb.2020.00980/full#supplementary-material

REFERENCES

Alsved, M., Holm, S., Christiansen, S., Smidt, M., Ling, M., Boesen, T., et al. (2018). Effect of aerosolization and drying on the viability of *Pseudomonas syringae* cells. *Front. Microbiol.* 9:3086. doi: 10.3389/fmicb.2018.03086

Amato, P., Parazols, M., Sancelme, M., Mailhot, G., Laj, P., and Delort, A.-M. (2007). An important oceanic source of micro-organisms for cloud water at the Puy de Dôme (France). *Atmos. Environ.* 41, 8253–8263. doi: 10.1016/j.atmosenv.2007.06.022

Baumgartner, L. K., Reid, R. P., Dupraz, C., Decho, A. W., Buckley, D. H., Spear, J. R., et al. (2006). Sulfate reducing bacteria in microbial mats: changing paradigms, new discoveries. *Sediment. Geol.* 185, 131–145. doi: 10.1016/j.sedgeo.2005.12.008

Bertolini, V., Gandolfi, I., Ambrosini, R., Bestetti, G., Innocente, E., Rampazzo, G., et al. (2013). Temporal variability and effect of environmental variables on airborne bacterial communities in an urban area of Northern Italy. *Appl. Microbiol. Biotechnol.* 97, 6561–6570. doi: 10.1007/s00253-012-4450-4450

Bianco, A., Voyard, G., Deguillaume, L., Mailhot, G., and Brigante, M. (2016). Improving the characterization of dissolved organic carbon in cloud water: amino acids and their impact on the oxidant capacity. *Sci. Rep.* 6:37420. doi: 10.1038/srep37420

Bowers, R. M., Clements, N., Emerson, J. B., Wiedinmyer, C., Hannigan, M. P., and Fierer, N. (2013). Seasonal variability in bacterial and fungal diversity of the near-surface atmosphere. *Environ. Sci. Technol.* 47, 12097–12106. doi: 10.1021/es402970s

Bowers, R. M., McCubbin, I. B., Hallar, A. G., and Fierer, N. (2012). Seasonal variability in airborne bacterial communities at a high-elevation site. *Atmos. Environ.* 50, 41–49. doi: 10.1016/j.atmosenv.2012.01.005

Bowers, R. M., Sullivan, A. P., Costello, E. K., Collett, J. L., Knight, R., and Fierer, N. (2011). Sources of bacteria in outdoor air across cities in the midwestern United States. *Appl. Environ. Microbiol.* 77, 6350–6356. doi: 10.1128/AEM.05498-5411

Brodie, E. L., DeSantis, T. Z., Parker, J. P. M., Zubietta, I. X., Piceno, Y. M., and Andersen, G. L. (2007). Urban aerosols harbor diverse and dynamic bacterial populations. *Proc. Natl. Acad. Sci. U.S.A.* 104, 299–304. doi: 10.1073/pnas.0608255104

Budhavant, K. B. (2014). Chemical composition of snow-water and scavenging ratios over Costal Antarctica. *Aerosol. Air Qual. Res.* 14, 666–676. doi: 10.4209/aaqr.2013.03.0104

Burrows, S. M., Butler, T., Jöckel, P., Tost, H., Kerkweg, A., Pöschl, U., et al. (2009). Bacteria in the global atmosphere–Part 2: modeling of emissions and transport between different ecosystems. *Atmos. Chem. Phys.* 9, 9281–9297.

Cáliz, J., Triadó-Margarit, X., Camarero, L., and Casamayor, E. O. (2018). A long-term survey unveils strong seasonal patterns in the airborne microbiome coupled to general and regional atmospheric circulations. *Proc. Natl. Acad. Sci. U.S.A* 115, 12229–12234. doi: 10.1073/pnas.1812826115

Carotenuto, F., Georgiadis, T., Gioli, B., Leyronas, C., Morris, C. E., Nardino, M., et al. (2017). Measurements and modeling of surface–atmosphere exchange of microorganisms in Mediterranean grassland. *Atmos. Chem. Phys.* 17, 14919–14936. doi: 10.5194/acp-17-14919-12017

Chemidlin Prévost-Bouré, N., Christen, R., Dequiedt, S., Mougel, C., Lelièvre, M., Jolivet, C., et al. (2011). Validation and application of a PCR primer set to quantify fungal communities in the soil environment by real-time quantitative PCR. *PLoS One* 6:e24166. doi: 10.1371/journal.pone.0024166

China, S., Burrows, S. M., Wang, B., Harder, T. H., Weis, J., Tanarhte, M., et al. (2018). Fungal spores as a source of sodium salt particles in the Amazon basin. *Nat. Commun.* 9:4793. doi: 10.1038/s41467-018-07066-7064

Christner, B. C., Morris, C. E., Foreman, C. M., Cai, R., and Sands, D. C. (2008). Ubiquity of biological ice nucleators in snowfall. *Science* 319, 1214–1214. doi: 10.1126/science.1149757

Chuvochina, M. S., Marie, D., Chevaillier, S., Petit, J.-R., Normand, P., Alekhina, I. A., et al. (2011). Community variability of bacteria in alpine snow (mont blanc) containing saharan dust deposition and their snow colonisation potential. *Microbes Environ.* 26, 237–247. doi: 10.1264/jsme2.ME11116

Cotton, W. R., Alexander, G. D., Hertenstein, R., Walko, R. L., McAnelly, R. L., and Nicholls, M. (1995). Cloud venting — A review and some new global annual estimates. *Earth Sci. Rev.* 39, 169–206. doi: 10.1016/0012-8252(95)00007-0

Cowan, D. A., Chown, S. L., Convey, P., Tuffin, M., Hughes, K., Pointing, S., et al. (2011). Non-indigenous microorganisms in the Antarctic: assessing the risks. *Trends Microbiol.* 19, 540–548. doi: 10.1016/j.tim.2011.07.008

De Wekker, S. F. J., and Kossmann, M. (2015). Convective boundary layer heights over mountainous terrain—a review of concepts. *Front. Earth Sci.* 3:77. doi: 10.3389/feart.2015.00077

Dillon, J. G., Fishbain, S., Miller, S. R., Bebout, B. M., Habicht, K. S., Webb, S. M., et al. (2007). High rates of sulfate reduction in a low-sulfate hot spring microbial mat are driven by a low level of diversity of sulfate-respiring microorganisms. *Appl. Environ. Microbiol.* 73, 5218–5226. doi: 10.1128/AEM.00357-357

Domine, F., Albert, M., Huthwelker, T., Jacobi, H.-W., Kokhanovsky, A. A., Lehning, M., et al. (2008). Snow physics as relevant to snow photochemistry. *Atmos. Chem. Phys.* 8, 171–208. doi: 10.5194/acp-8-171-2008

Domine, F., and Shepson, P. B. (2002). Air-snow interactions and atmospheric chemistry. *Science* 297, 1506–1510. doi: 10.1126/science.1074610

Dommergue, A., Amato, P., Tignat-Perrier, R., Magand, O., Thollot, A., Joly, M., et al. (2019). Methods to investigate the global atmospheric microbiome. *Front. Microbiol.* 10:243. doi: 10.3389/fmicb.2019.00243

Els, N., Larose, C., Baumann-Stanzer, K., Tignat-Perrier, R., Keuschnig, C., Vogel, T. M., et al. (2019). Microbial composition in seasonal time series of free tropospheric air and precipitation reveals community separation. *Aerobiologia* 35, 671–701. doi: 10.1007/s10453-019-09606-x

Evans, S. E., Dueker, M. E., Logan, J. R., and Weathers, K. C. (2019). The biology of fog: results from coastal Maine and Namib desert reveal common drivers of fog microbial composition. *Sci. Total Environ.* 647, 1547–1556. doi: 10.1016/j.scitotenv.2018.08.045

Fierer, N., Liu, Z., Rodríguez-Hernández, M., Knight, R., Henn, M., and Hernandez, M. T. (2008). Short-Term temporal variability in airborne bacterial and fungal populations. *Appl. Environ. Microbiol.* 74, 200–207. doi: 10.1128/AEM.01467-1467

Forbes, P. B. C., and Garland, R. M. (2016). "Chapter 4 - Outdoor Air Pollution," in *Comprehensive Analytical Chemistry The Quality of Air*, eds M. de la Guardia and S. Armenta (Amsterdam: Elsevier), 73–96. doi: 10.1016/bs.coac.2016.02.004

Franz, T. P., and Eisenreich, S. J. (1998). Snow scavenging of polychlorinated biphenyls and polycyclic aromatic hydrocarbons in minnesota. *Environ. Sci. Technol.* 32, 1771–1778. doi: 10.1021/es970601z

Franzetti, A., Gandolfi, I., Gaspari, E., Ambrosini, R., and Bestetti, G. (2011). Seasonal variability of bacteria in fine and coarse urban air particulate matter. *Appl. Microbiol. Biotechnol.* 90, 745–753. doi: 10.1007/s00253-010-3048-3047

Gallée, H., Guyomarc'h, G., and Brun, E. (2001). Impact of snow drift on the antarctic ice sheet surface mass balance: possible sensitivity to snow-surface properties. *Boundary Layer Meteorol.* 99, 1–19. doi: 10.1023/A:1018776422809

Gandolfi, I., Bertolini, V., Bestetti, G., Ambrosini, R., Innocente, E., Rampazzo, G., et al. (2015). Spatio-temporal variability of airborne bacterial communities and their correlation with particulate matter chemical composition across two urban areas. *Appl. Microbiol. Biotechnol.* 99, 4867–4877. doi: 10.1007/s00253-014-6348-6345

Grannas, A. M., Jones, A. E., Dibb, J., Ammann, M., Anastasio, C., Beine, H. J., et al. (2007). An overview of snow photochemistry: evidence, mechanisms and impacts. *Atmos. Chem. Phys.* 7, 4329–4373. doi: 10.5194/acp-7-4329-2007

Greilinger, M., Schauer, G., Baumann-Stanzer, K., Skomorowski, P., Schöner, W., and Kasper-Giebl, A. (2018). Contribution of saharan dust to ion deposition loads of high alpine snow packs in Austria (1987–2017). *Front. Earth Sci.* 6:126. doi: 10.3389/feart.2018.00126

Greilinger, M., Schöner, W., Winiwarter, W., and Kasper-Giebl, A. (2016). Temporal changes of inorganic ion deposition in the seasonal snow cover for the Austrian Alps (1983–2014). *Atmos. Environ.* 132, 141–152. doi: 10.1016/j.atmosenv.2016.02.040

Greilinger, M., Zbiral, J., and Kasper-Giebl, A. (2019). Desert dust contribution to PM10 loads in Styria (Southern Austria) and impact on exceedance of limit values from 2013–2018. *Appl. Sci.* 9:2265. doi: 10.3390/app9112265

Harder, S., Warren, S. G., and Charlson, R. J. (2000). Sulfate in air and snow at the South Pole: implications for transport and deposition at sites with low snow accumulation. *J. Geophys. Res. Atmos.* 105, 22825–22832. doi: 10.1029/2000JD900351

Harding, T., Jungblut, A. D., Lovejoy, C., and Vincent, W. F. (2011). Microbes in high arctic snow and implications for the cold biosphere. *Appl. Environ. Microbiol.* 77, 3234–3243. doi: 10.1128/AEM.02611-2610

Hauptmann, A. L., Stibal, M., Baelum, J., Sicheritz-Pontén, T., Brunak, S., Bowman, J. S., et al. (2014). Bacterial diversity in snow on North Pole ice floes. *Extremophiles* 18, 945–951. doi: 10.1007/s00792-014-0660-y

Hell, K., Edwards, A., Zarsky, J., Podmirseg, S. M., Girdwood, S., Pachebat, J. A., et al. (2013). The dynamic bacterial communities of a melting High Arctic glacier snowpack. *ISME J.* 7, 1814–1826. doi: 10.1038/ismej.2013.51

Herrmann, H., Exner, M., and Zellner, R. (1994). Reactivity trends in reactions of the nitrate radical (NO3) with inorganic and organic cloudwater constituents. *Geochim. Cosmochim. Acta* 58, 3239–3244. doi: 10.1016/0016-7037(94)90051-90055

Kalthoff, N., Träumner, K., Adler, B., Späth, S., Behrendt, A., Wieser, A., et al. (2013). Dry and moist convection in the boundary layer over the Black Forest - A combined analysis of in situ and remote sensing data. *Meteorol. Zeitschrift* 22, 445–461. doi: 10.1127/0941-2948/2013/0417

Kennedy, K., Hall, M. W., Lynch, M. D. J., Moreno-Hagelsieb, G., and Neufeld, J. D. (2014). Evaluating bias of Illumina-based bacterial 16S rRNA gene profiles. *Appl. Environ. Microbiol.* 80, 5717–5722. doi: 10.1128/AEM.01451-1414

Klindworth, A., Pruesse, E., Schweer, T., Peplies, J., Quast, C., Horn, M., et al. (2013). Evaluation of general 16S ribosomal RNA gene PCR primers for classical and next-generation sequencing-based diversity studies. *Nucleic Acids Res.* 41:e1. doi: 10.1093/nar/gks808

Larose, C., Berger, S., Ferrari, C., Navarro, E., Dommergue, A., Schneider, D., et al. (2010). Microbial sequences retrieved from environmental samples from seasonal Arctic snow and meltwater from Svalbard. *Norway. Extremophiles* 14, 205–212. doi: 10.1007/s00792-009-0299-2

Laughlin, R. J., Stevens, R. J., Müller, C., and Watson, C. J. (2008). Evidence that fungi can oxidize NH4+ to NO3- in a grassland soil. *Eur. J. Soil Sci.* 59, 285–291. doi: 10.1111/j.1365-2389.2007.00995.x

Lazzaro, A., Hilfiker, D., and Zeyer, J. (2015). Structures of microbial communities in alpine soils: seasonal and elevational effects. *Front. Microbiol.* 6:1330. doi: 10.3389/fmicb.2015.01330

Lehning, M., Bartelt, P., Brown, B., Russi, T., Stöckli, U., and Zimmerli, M. (1999). snowpack model calculations for avalanche warning based upon a new network of weather and snow stations. *Cold Reg. Sci. Technol.* 30, 145–157. doi: 10.1016/S0165-232X(99)00022-21

Li, Z., Edwards, R., Mosley-Thompson, E., Wang, F., Dong, Z., You, X., et al. (2006). Seasonal variability of ionic concentrations in surface snow and elution processes in snow–firn packs at the PGPI site on Ürümqi glacier No. 1, eastern Tien Shan, China. *Ann. Glaciol.* 43, 250–256. doi: 10.3189/172756406781812069

Lotteraner, C., and Piringer, M. (2016). Mixing-Height time series from operational ceilometer aerosol-layer heights. *Boundary Layer Meteorol.* 161, 265–287. doi: 10.1007/s10546-016-0169-162

Maccario, L., Carpenter, S. D., Deming, J. W., Vogel, T. M., and Larose, C. (2019). Sources and selection of snow-specific microbial communities in a Greenlandic sea ice snow cover. *Sci. Rep.* 9:2290. doi: 10.1038/s41598-019-38744-y

Maccario, L., Vogel, T. M., and Larose, C. (2014). Potential drivers of microbial community structure and function in Arctic spring snow. *Front. Microbiol.* 5:413. doi: 10.3389/fmicb.2014.00413

Margesin, R., and Miteva, V. (2011). Diversity and ecology of psychrophilic microorganisms. *Res. Microbiol.* 162, 346–361. doi: 10.1016/j.resmic.2010.12.004

Maria, S. F., and Russell, L. M. (2005). Organic and inorganic aerosol below-cloud scavenging by suburban New Jersey precipitation. *Environ. Sci. Technol.* 39, 4793–4800. doi: 10.1021/es0491679

Martinez Arbizu, P. (2017). *pairwiseAdonis: Pairwise Multilevel Comparison Using Adonis. R Package Version 0.0.1.*

Masella, A. P., Bartram, A. K., Truszkowski, J. M., Brown, D. G., and Neufeld, J. D. (2012). PANDAseq: paired-end assembler for illumina sequences. *BMC Bioinformatics* 13:31. doi: 10.1186/1471-2105-13-31

McMurdie, P. J., and Holmes, S. (2013). phyloseq: an R Package for reproducible interactive analysis and graphics of microbiome census data. *PLoS One* 8:e61217. doi: 10.1371/journal.pone.0061217

Meola, M., Lazzaro, A., and Zeyer, J. (2015). Bacterial composition and survival on sahara dust particles transported to the European Alps. *Front. Microbiol.* 6:1454. doi: 10.3389/fmicb.2015.01454

Mizrahi-Man, O., Davenport, E. R., and Gilad, Y. (2013). Taxonomic classification of bacterial 16S rRNA genes using short sequencing reads: evaluation of effective study designs. *PLoS One* 8:e53608. doi: 10.1371/journal.pone.0053608

Möhler, O., Demott, P. J., Vali, G., and Levin, Z. (2007). Microbiology and atmospheric processes: the role of biological particles in cloud physics. *Biogeosciences* 4, 1059–1071.

Monteil, C. L., Bardin, M., and Morris, C. E. (2014). Features of air masses associated with the deposition of *Pseudomonas syringae* and Botrytis cinerea by rain and snowfall. *ISME J.* 8, 2290–2304. doi: 10.1038/ismej.2014.55

Oksanen, J., Blanchet, F. G., Friendly, M., Kindt, R., Legendre, P., McGlinn, D., et al. (2018). *vegan: Community Ecology Package*. Available online at: https://CRAN.R-project.org/package=vegan (accessed May 4, 2018).

Olefs, M., Baumgartner, D. J., Obleitner, F., Bichler, C., Foelsche, U., Pietsch, H., et al. (2016). The Austrian radiation monitoring network ARAD – best practice and added value. *Atmos. Meas. Tech.* 9, 1513–1531. doi: 10.5194/amt-9-1513-2016

Øvreås, L., and Torsvik, V. (1998). Microbial diversity and community structure in two different agricultural soil communities. *Microb. Ecol.* 36, 303–315. doi: 10.1007/s002489900117

Paramonov, M., Grönholm, T., and Virkkula, A. (2011). Below-cloud scavenging of aerosol particles by snow at an urban site in Finland. *Boreal Environ. Res.* 16, 304–320.

Pedgley, D. E. (1991). "Aerobiology: the atmosphere as a source and sink for microbes," in *Microbial Ecology of Leaves Brock/Springer Series in Contemporary Bioscience*, eds J. H. Andrews and S. S. Hirano (New York, NY: Springer), 43–59.

Perrone, M. G., Gualtieri, M., Ferrero, L., Porto, C. L., Udisti, R., Bolzacchini, E., et al. (2010). Seasonal variations in chemical composition and in vitro biological effects of fine PM from Milan. *Chemosphere* 78, 1368–1377. doi: 10.1016/j.chemosphere.2009.12.071

Peter, H., Hörtnagl, P., Reche, I., and Sommaruga, R. (2014). Bacterial diversity and composition during rain events with and without Saharan dust influence reaching a high mountain lake in the Alps. *Environ. Microbiol. Rep.* 6, 618–624. doi: 10.1111/1758-2229.12175

Pickersgill, D. A., Wehking, J., Paulsen, H., Thines, E., Pöschl, U., Fröhlich-Nowoisky, J., et al. (2017). Lifestyle dependent occurrence of airborne fungi. *Biogeosci. Discuss.* 2017, 1–20. doi: 10.5194/bg-2017-2452

Pio, C. A., Legrand, M., Oliveira, T., Afonso, J., Santos, C., Caseiro, A., et al. (2007). Climatology of aerosol composition (organic versus inorganic) at nonurban sites on a west-east transect across Europe. *J. Geophys. Res.* 112:D23S02. doi: 10.1029/2006JD008038

Polymenakou, P. N. (2012). Atmosphere: a source of pathogenic or beneficial microbes? *Atmosphere* 3, 87–102. doi: 10.3390/atmos3010087

Polymenakou, P. N., and Mandalakis, M. (2013). Assessing the short-term variability of bacterial composition in background aerosols of the Eastern Mediterranean during a rapid change of meteorological conditions. *Aerobiologia* 29, 429–441. doi: 10.1007/s10453-013-9295-9291

R Core Team (2015). *R: A Language and Environment for Statistical Computing. R: A Language and Environment for Statistical Computing*. Available online at: https://www.R-project.org (accessed October 14, 2015).

Šantl-Temkiv, T., Gosewinkel, U., Starnawski, P., Lever, M., and Finster, K. (2018). Aeolian dispersal of bacteria in southwest Greenland: their sources, abundance, diversity and physiological states. *FEMS Microbiol. Ecol.* 94:fiy031. doi: 10.1093/femsec/fiy031

Segawa, T., Miyamoto, K., Ushida, K., Agata, K., Okada, N., and Kohshima, S. (2005). Seasonal change in bacterial flora and biomass in mountain snow from the Tateyama Mountains, Japan, analyzed by 16S rRNA gene sequencing and real-time PCR. *Appl. Environ. Microbiol.* 71, 123–130. doi: 10.1128/AEM.71.1.123-130.2005

Smith, D. J., Griffin Dale, W., and Jaffe Daniel, A. (2011). The high life: transport of microbes in the atmosphere. *Eos Trans. Am. Geophys. Union* 92, 249–250. doi: 10.1029/2011EO300001

Spear, J. R., Honeyman, A. S., and Day, M. L. (2018). Fresh snowfall microbiology and chemistry are driven by geography in storm-tracked events. *PeerJ* 6:e5961. doi: 10.1101/300772

Squizzato, S., Masiol, M., Brunelli, A., Pistollato, S., Tarabotti, E., Rampazzo, G., et al. (2013). Factors determining the formation of secondary inorganic aerosol: a case study in the Po Valley (Italy). *Atmos. Chem. Phys.* 13, 1927–1939. doi: 10.5194/acp-13-1927-2013

Taylor, D. L., Walters, W. A., Lennon, N. J., Bochicchio, J., Krohn, A., Caporaso, J. G., et al. (2016). Accurate estimation of fungal diversity and abundance through improved lineage-specific primers optimized for illumina amplicon sequencing. *Appl. Environ. Microbiol.* 82, 7217–7226. doi: 10.1128/AEM.02576-2516

Tignat-Perrier, R., Dommergue, A., Thollot, A., Keuschnig, C., Magand, O., Vogel, T. M., et al. (2019). Global airborne microbial communities controlled by surrounding landscapes and wind conditions. *Sci. Rep.* 9:14441. doi: 10.1038/s41598-019-51073-51074

Triadó-Margarit, X., Caliz, J., Reche, I., and Casamayor, E. O. (2019). High similarity in bacterial bioaerosol compositions between the free troposphere and atmospheric depositions collected at high-elevation mountains. *Atmos. Environ.* 203, 79–86. doi: 10.1016/j.atmosenv.2019.01.038

Wang, Q., Garrity, G. M., Tiedje, J. M., and Cole, J. R. (2007). Naive Bayesian classifier for rapid assignment of rRNA sequences into the new bacterial taxonomy. *Appl. Environ. Microbiol.* 73, 5261–5267. doi: 10.1128/AEM.00062-67

Wang, X., Zhang, L., and Moran, M. D. (2014). Development of a new semi-empirical parameterization for below-cloud scavenging of size-resolved aerosol particles by both rain and snow. *Geosci. Model Dev.* 7, 799–819. doi: 10.5194/gmd-7-799-2014

Weil, T., De Filippo, C., Albanese, D., Donati, C., Pindo, M., Pavarini, L., et al. (2017). Legal immigrants: invasion of alien microbial communities during winter occurring desert dust storms. *Microbiome* 5:32. doi: 10.1186/s40168-017-0249-247

Weiss, S., Xu, Z. Z., Peddada, S., Amir, A., Bittinger, K., Gonzalez, A., et al. (2017). Normalization and microbial differential abundance strategies depend upon data characteristics. *Microbiome* 5:27. doi: 10.1186/s40168-017-0237-y

Wickham, H. (2009). *ggplot2: Elegant Graphics for Data Analysis*. New-York, NY: Springer-Verlag.

Woo, C., An, C., Xu, S., Yi, S.-M., and Yamamoto, N. (2018). Taxonomic diversity of fungi deposited from the atmosphere. *ISME J.* 12:2051. doi: 10.1038/s41396-018-0160-167

Xia, Y., Conen, F., and Alewell, C. (2013). Total bacterial number concentration in free tropospheric air above the Alps. *Aerobiologia* 29, 153–159. doi: 10.1007/s10453-012-9259-x

Yamamoto, N., Bibby, K., Qian, J., Hospodsky, D., Rismani-Yazdi, H., Nazaroff, W. W., et al. (2012). Particle-size distributions and seasonal diversity of allergenic and pathogenic fungi in outdoor air. *ISME J.* 6, 1801–1811. doi: 10.1038/ismej.2012.30

Zhang, H., Zhou, X., Zou, J., Wang, W., Xue, L., Ding, Q., et al. (2018). A review on the methods for observing the substance and energy exchange between atmosphere boundary layer and free troposphere. *Atmosphere* 9:460. doi: 10.3390/atmos9120460

Zhang, L., Wang, X., Moran, M. D., and Feng, J. (2013). Review and uncertainty assessment of size-resolved scavenging coefficient formulations for below-cloud snow scavenging of atmospheric aerosols. *Atmos. Chem. Phys.* 13, 10005–10025. doi: 10.5194/acp-13-10005-12013

Conflict of Interest: The authors declare that the research was conducted in the absence of any commercial or financial relationships that could be construed as a potential conflict of interest.

frontiers in Microbiology

ORIGINAL RESEARCH
published: 25 May 2020
doi: 10.3389/fmicb.2020.00962

Low Turnover of Soil Bacterial rRNA at Low Temperatures

Morten Dencker Schostag[1,2,3], Christian Nyrop Albers[1,3], Carsten Suhr Jacobsen[1,4] and Anders Priemé[1,2]**

[1] Department of Geosciences and Natural Resource Management, Center for Permafrost (CENPERM), University of Copenhagen, Copenhagen, Denmark, [2] Department of Biology, University of Copenhagen, Copenhagen, Denmark, [3] Geological Survey of Denmark and Greenland, Copenhagen, Denmark, [4] Department of Environmental Science, Aarhus University, Roskilde, Denmark

Ribosomal RNA (rRNA) is used widely to investigate potentially active microorganisms in environmental samples, including soil microorganisms and other microbial communities that are subjected to pronounced seasonal variation in temperature. This raises a question about the turnover of intracellular microbial rRNA at environmentally relevant temperatures. We analyzed the turnover at four temperatures of RNA isolated from soil bacteria amended with ^{14}C-labeled uridine. We found that the half-life of recently produced RNA increased from 4.0 days at 20°C to 15.8 days at 4°C, and 215 days at −4°C, while no degradation was detected at −18°C during a 1-year period. We discuss the implications of the strong temperature dependency of rRNA turnover for interpretation of microbiome data based on rRNA isolated from environmental samples.

Keywords: ribosomal RNA, rRNA half-life, environmental RNA, uridine, temperature response

OPEN ACCESS

Edited by:
Alberto Robador, University of Southern California, United States

Reviewed by:
Purificacion Lopez-Garcia, Centre National de la Recherche Scientifique (CNRS), France
Alexander Tøsdal Tveit, UiT The Arctic University of Norway, Norway

****Correspondence:***
Morten Dencker Schostag
msn@geus.dk
Anders Priemé
aprieme@bio.ku.dk

Specialty section:
This article was submitted to Extreme Microbiology, a section of the journal Frontiers in Microbiology

Received: *18 February 2020*
Accepted: *22 April 2020*
Published: *25 May 2020*

Citation:
Schostag MD, Albers CN, Jacobsen CS and Priemé A (2020) Low Turnover of Soil Bacterial rRNA at Low Temperatures. Front. Microbiol. 11:962. doi: 10.3389/fmicb.2020.00962

INTRODUCTION

Microbial DNA isolated from environmental samples cannot differentiate between the live and dead fraction of the microbiome and is generally believed to persist for longer time spans compared to RNA, e.g., in soils where extracellular DNA from dead organisms may persist for years (Carini et al., 2016). The persistence of DNA in the environment obscures relationships between microbiomes and environmental parameters. Hence, analysis of the more dynamic RNA instead of DNA has over the last 10 years received increased attention in studies of e.g., the response of microbiomes to global change and environmental perturbation like thawing of frozen soil (Schostag et al., 2019), wetting of dry soil (Placella et al., 2012), and xenobiotics (Baelum et al., 2008). Ribosomal RNA (rRNA) is now widely used in microbiome studies to characterize the phylogenetic composition of potentially active members of microbial communities [see Blazewicz et al. (2013) for a discussion of the interpretation of rRNA in an ecological context]. The large interest in rRNA from environmental microbiomes contrasts the lack of knowledge on the turnover of microbial rRNA in the environment.

Bacterial rRNA is more stable than messenger RNA (mRNA) likely as a consequence of its incorporation into ribosomes and protection by ribosomal proteins (Deutscher, 2003), but rRNA is degraded by RNases intracellularly during stress, e.g., caused by starvation for organic carbon, amino acids or essential nutrients (Zundel et al., 2009), or when an RNA molecule is defective (Deutscher, 2006). Bacterial ribosomes may also be inactivated and maintained as such under no-growth conditions (Dai et al., 2016). Numerous studies and commercial laboratory suppliers have described the decay of RNA in bacterial strains or in environmental samples under different conditions (often in combination with substances that inhibit RNase activity), but these studies focus on the decay of mRNA or the total pool of RNA that also includes extracellular RNA.

Degradation of extracellular rRNA likely depends on environmental conditions as temperature, water availability, pH [RNA can undergo auto-hydrolysis at high pH when free hydroxide ions deprotonate the hydroxyl-group on the C2 of the ribose moiety (Elliot and Ladomery, 2011)], and soil mineralogy [RNA may sorb to soil minerals as known for DNA (Romanowski et al., 1991)]. To our knowledge, the present study is the first to estimate turnover of intracellular rRNA in an environmental microbiome at different temperatures.

MATERIALS AND METHODS

Studies of RNA turnover in bacterial cells often involve inhibition of RNA synthesis by actinomycin D (Levinthal et al., 1962) or rifampicin (Hambraeus et al., 2003). In contrast, we developed an experimental approach, which did not inhibit the general activity of the bacteria. In brief, we extracted bacterial cells from soil, enhanced their production of RNA by adding diluted tryptic soy broth (TSB) growth medium before adding ^{14}C-radiolabeled uridine (an RNA nucleoside), and finally returning the bacteria to the soil for incubation at −18, −4, 4, and 20°C, respectively. At different time points, RNA was isolated from the incubated soil samples and its content of ^{14}C was measured.

Soil

Soil was sampled in April 2016 at 0–10 cm depth from a permanent grassland at the University of Copenhagen experimental farm Højbakkegård, Tåstrup, Denmark. The mean annual air temperature is 8.2°C. The soil is a sandy loam with pH 6.4 and had a moisture content of 22.7% of dry weight at the time of sampling. The soil was gently homogenized by hand and sieved at 4 mm.

Extraction of Bacteria From Soil Matrix, Pre-incubation of Bacteria, and Amendment With ^{14}C-Uridine

Two batches of 100 g soil in 320 mL phosphate-buffered saline (PBS) were blended in a sterilized blender for 3 min. An additional 80 mL PBS was used to wash away remaining soil particles after transferring the blended soil slurry to eight 50-mL tubes, which were centrifuged at 1000*g* for 5 min at 4°C. Thirty mL of the supernatant and 60 mL 1-% TSB were transferred to eight incubation flasks for a final concentration of 1/150 TSB. The flasks were incubated at 4°C with shaking at 150 rpm. After 24 h, TSB was added to a final concentration of 1/75, and following an additional 24 h, TSB was added to a final concentration of 1/10 and the flasks were incubated for 24 h. A pilot experiment revealed that this gradual increase in TSB concentration was needed to achieve adequate incorporation of ^{14}C in RNA. The pilot experiment involved incubation of extracted bacteria at three separate concentrations of TSB (1/150, 1/75, and 1/10 TSB), and scintillation counting was conducted after 3 days of incubation to quantify the incorporation of ^{14}C into cells following amendment with ^{14}C-radiolabeled uridine (2-^{14}C-uridine, 53 mCi mmol^{-1}, purity 98.7%, Moravek, Brea, CA, United States). Twenty hours after addition of labeled uridine, the remaining radioactivity in the media was 11.2, 14.2, and 91.5% of the total added following incubation at 1/150, 1/75, and 1/10 TSB, respectively, and after centrifugation, 5.4% of the radioactivity was found in cells incubated with 1/150 TSB, 6.4% for 1/75 TSB, and 69.5% for 1/10 TSB. The low incorporation of radioactivity by cells incubated with 1/150 and 1/75 TSB was most likely caused by bacteria using the labeled uridine mainly as an energy source resulting in a loss of ^{14}C as $^{14}CO_2$.

The contents of the incubation flasks were combined and 60 mL were transferred to eight 250-mL flasks and amended with 60 μL of ^{14}C-uridine to a final concentration of 6.2×10^5 disintegrations per min (DPM) mL^{-1}. Uridine is specifically incorporated into RNA or used as an energy, carbon and/or nitrogen source by the soil microorganisms, but RNA can be selectively isolated from other cell substances that may contain some of the ^{14}C.

Following incubation of the eight flasks for 23 h at 4°C at 150 rpm, the content was transferred to fourteen 50-mL tubes and centrifuged at 6000*g* for 5 min at 10°C. The supernatant was decanted and cells were re-suspended in 30 mL PBS by vortexing. The cells were washed twice in 4 mL PBS by centrifuging as described above. 2.5 mL of re-suspended bacteria were mixed using a spatula into 25 g of soil that had been air-dried for 24 h at room temperature. Care was taken to distribute the suspension evenly in the soil. $1.4 \cdot 10^5$ bacterial cells mL^{-1} were transferred as estimated by counting the cells in a fluorescence microscope following acridine orange staining. Only bacterial cells were observed in the microscoped samples.

RNA Isolation and Calculation of rRNA Half-Life

The soil amended with ^{14}C-labeled bacteria was distributed in 2.0-g aliquots to 2-mL plastic tubes from the RNA isolation kit (RNeasy PowerSoil Total RNA Kit, MO BIO Laboratories, Qiagen, Carlsbad, CA, United States), and the soil samples were incubated in our laboratory in quadruplicates at −18°C, −4°C, 4°C, and 20°C, respectively. When sampling for RNA, the tubes were snap frozen in liquid nitrogen and stored at −80°C until RNA isolation using the RNeasy PowerSoil kit. From the final volume of 100 μL eluate, 40 μL was added to 10 mL scintillation liquid in a 20-mL scintillation vial, which was analyzed on a scintillation counter (Tri-Carb 2810 TR, PerkinElmer, Waltham, MA, United States).

A comparison of the radioactivity in the cell suspension ($n = 2$) and RNA isolated from the soil samples at initiation of the experiment ($n = 15$) indicated that the RNA isolation procedure was highly efficient, isolating 97.4% of the labeled RNA pool from the soil samples relative to the cell suspension. As a side note, our experimental setup may, thus, also be used to evaluate the efficiency of protocols for isolation of RNA from soil and other environmental samples.

We tested if ^{14}C in the eluate was incorporated in DNA and not as expected in RNA. We did this for the samples incubated at 4 and 20°C, respectively. Two μL DNase-free RNase (Roche Diagnostics, Mannheim, Germany) and 28 μL H_2O were added to 20 μL eluate from the RNA isolation

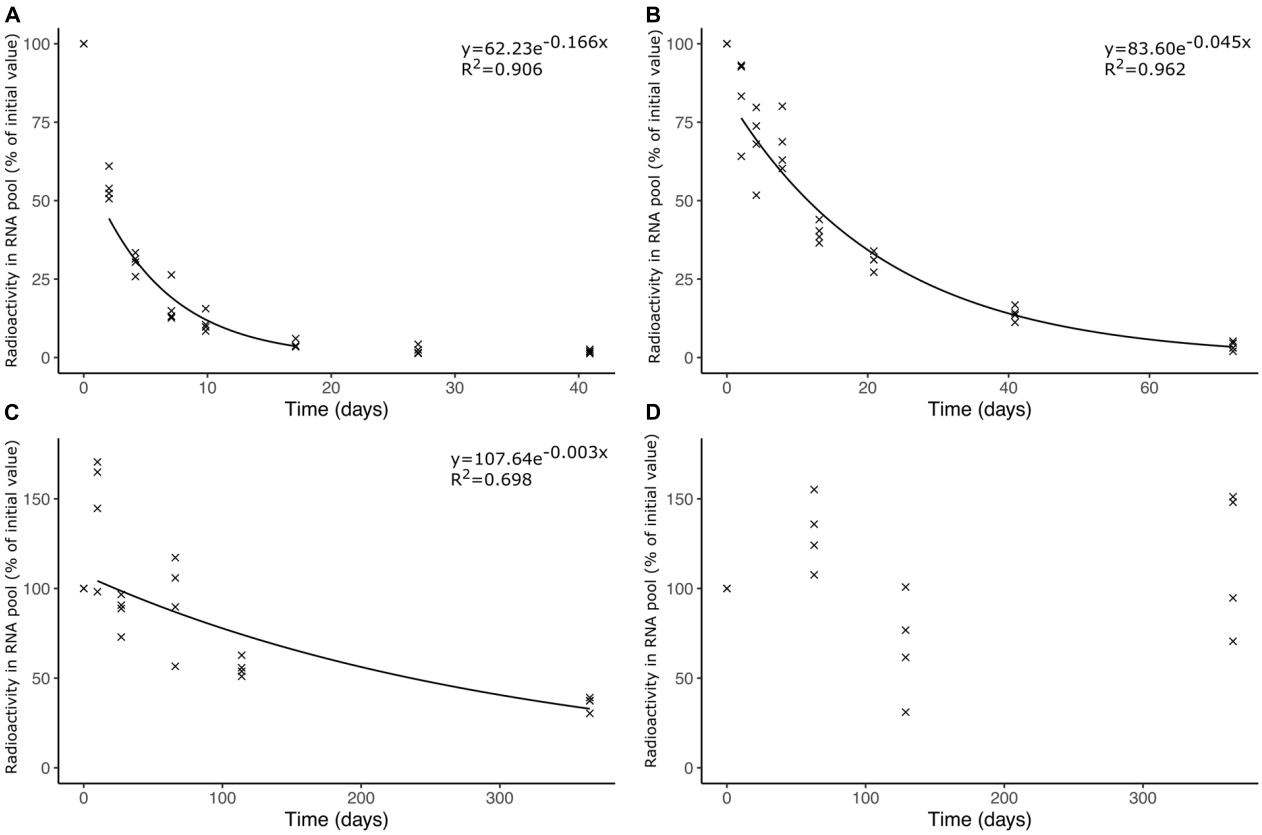

FIGURE 1 | Radioactivity in RNA isolated from soil samples incubated at different temperatures. The samples were amended with soil bacteria pre-incubated with ^{14}C-uridine normalized to the total amount of RNA isolated from individual samples. The soil samples were incubated at **(A)** 20°C, **(B)** 4°C, **(C)** –4°C, and **(D)** –18°C. Trend lines in **(A–C)** represent the average radioactivity of replicate samples and depict the time span with exponential decrease in radioactivity presumed to be related to rRNA turnover.

procedure, and the mix was incubated at 37°C for 1 h. DNA was isolated from the solution using the Genomic DNA Clean & Concentrator kit (Zymo Research, Irvine, CA, United States) according to the manufacturer's instructions. All flow-through liquid (presumed to contain nucleotides from degraded RNA) from the washing steps was combined and analyzed for radioactivity. The DNA concentration in the eluate (presumed to contain DNA) was quantified using a Qubit Fluorometer (Thermo Fisher Scientific, Hvidovre, Denmark) and the eluate was analyzed for radioactivity. This control experiment revealed that 99.55 ± 0.03% (n = 8) of the radioactivity in the eluate from the RNA isolation was found in the RNA fraction and only 0.45 ± 0.03% of the radioactivity was found in the DNA fraction.

As the total RNA pool in the soil may be affected by the experimental treatment we normalized the labeled RNA to the total RNA pool (estimated using Qubit 2.0 [Thermo Fisher Scientific]) at each sampling point (see **Supplementary Material**). Hereafter, the half-life of the labeled RNA was calculated from the relative normalized DPM assuming an exponential decrease in DPM with time (r^2 ranged from 0.435 to 0.765 for the four replicate samples incubated at −4°C, from 0.926 to 0.982 for the samples at 4°C, and from 0.924 to 0.944 for the samples at 20°C).

RESULTS

It has previously been shown that approximately 95% of total RNA isolated from soil microbiomes is rRNA and that the majority is bacterial (Tveit et al., 2013; Schostag et al., 2019). We assumed that the mRNA pool has a faster turnover compared to rRNA and that a large proportion of the initial RNA degradation would be due to degradation of mRNA. Because our focus was rRNA we excluded the first measurement of radioactivity, time 0, from the calculation of turnover rates. Also, the last two measurements at 20°C were excluded from the calculations because the radioactivity at these measurements did not follow the same exponential decrease as the previous measurements (at this point less than 10% of the initial radioactivity was found in the RNA pool). We expect that microRNA and small interfering RNA are too small to be collected by the RNA isolation kit. Thus, the reported turnover rates mainly represent turnover of bacterial 16S, 23S, and 5S rRNA, and to an unknown extent transfer RNA.

We found a strong temperature dependence of soil bacterial rRNA turnover (**Figure 1**) with undetectable degradation at −18°C, and a half-life for presumed rRNA of 215 ± 12 days (average ± standard error of the mean, n = 4) at −4°C, 15.8 ± 1.00 days at 4°C, and 4.04 ± 0.44 days at 20°C.

DISCUSSION

Little data exist on the turnover of intracellular rRNA in environmental microbiomes. Keith et al. (2005) found no change in the rRNA-based structure of the bacterial microbiome in activated sludge stored for 24 h at room temperature and only small changes when storing at 4°C, but the study does not report if changes in the amount of RNA occurred. Ostle et al. (2003) reported a turnover of bacterial and archaeal RNA of 20% day^{-1} corresponding to a half-life of 3.1 days in a grassland rhizosphere where plants were spiked with $^{13}CO_2$ (at air temperatures of ca. 15°C). This is faster than the turnover at 20°C in our study even though our experimental setup may overestimate the rRNA turnover. This possible overestimation may be due to the transferred bacteria being stimulated by the (albeit dilute) TSB growth medium before transfer to the soil where nutrient availability is expected to be lower, which may lead to starvation of the transferred bacteria and hence enhanced rRNA decay (Zundel et al., 2009). Also, extrinsic factors may increase the turnover of intracellular rRNA, e.g., protozoa may enhance the turnover of bacterial rRNA when grazing the labelled bacteria.

The slow RNA turnover we observed at −4°C is likely due to lack of liquid H_2O (Tilston et al., 2010) and is in accordance with Schostag et al. (2015) who found no differences in the number of 16S rRNA copies in an Arctic soil microbiome sampled monthly during winter, where the *in situ* temperature was below −4°C for five consecutive months. Thus, the rRNA isolated during winter probably did not reflect sustained microbial activity, but rather was produced by the microbiome during autumn and was conserved for several months due to the low soil temperature. Our lowest incubation temperature, −18°C, preserved bacterial rRNA within the time span of the experiment, which has also been observed by Sessitsch et al. (2002).

The large difference in half-life observed at −4 and 4°C is likely caused by not only temperature *per se*, but also by the different states of soil H_2O (ice and water, respectively) prevailing at the two temperatures. Ice lowers diffusion rates of nutrients and gases dramatically in the soil environment (Tilston et al., 2010) and, hence, strongly limits soil microbial activity. The 3.9-fold difference in half-life at 4 and 20°C indicates a Q_{10} of 2.3 for this temperature span. However, the Q_{10} value is based on only two temperatures and more detailed studies are needed to generate robust temperature response curves of the bacterial rRNA half-life in soil and other environments.

Pronounced seasonal variation in environmental temperature is part of life for microorganisms living in soil, shallow-water sediments, surface water, poikilothermic animals, or on plants. Our data indicate that half of the intracellular rRNA isolated from an environmental sample may have been produced by the microbiome more than 4 days before sampling if the environmental temperature is 20°C, or more than 15 days before if the temperature is 4°C. Thus, the time span during which one or more environmental parameters have affected microbial rRNA composition at the time of sampling varies with seasonal changes in temperature. It should be noted that our experimental set-up involved incubation at stable conditions. However, in most environments conditions are not stable and turnover rates *in situ* of microbial rRNA may be affected by daily or seasonal fluctuations in temperature, drought-induced lowering of soil water content, and other environmental fluctuations.

Our study involved a soil at low temperatures, but could be extended to unravel rRNA stability in other environments amenable to RNA preservation, e.g., environments with high osmolarity or low water activity. Precautions should be made when claims are made on the composition of the 'active' microbiome in these environments. Also, the stability of fungal and microeukaryotic rRNA awaits further studies.

In conclusion, the half-life of rRNA produced by a soil microbiome increased markedly with a decrease in environmentally relevant temperatures and was more than 7 months at −4°C. This means that rRNA may remain long after environmental conditions have changed and, thus, we should interpret with care correlations between rRNA-based microbiome structure and seasonal variation in ephemeral environmental parameters such as precipitation and concentration of soil water, redox potential, oxygen, inorganic nitrogen, and metabolomes.

DATA AVAILABILITY STATEMENT

All data generated during this study are included in this article and its **Supplementary Material Additional File 1**, which is a spreadsheet containing data from analyses of radioactivity and concentration of isolated RNA.

AUTHOR CONTRIBUTIONS

All authors designed the project, read, and approved the final manuscript. MS performed the experimental work. AP wrote the first draft of the manuscript with subsequent revisions performed by all authors.

FUNDING

The work was supported by the Danish National Research Foundation through Center for Permafrost (CENPERM, DNRF100).

ACKNOWLEDGMENTS

We thank P. B. Jacobsen, GEUS, for excellent technical support.

SUPPLEMENTARY MATERIAL

The Supplementary Material for this article can be found online at: https://www.frontiersin.org/articles/10.3389/fmicb.2020.00962/full#supplementary-material

REFERENCES

Baelum, J., Nicolaisen, M. H., Holben, W. E., Strobel, B. W., Sørensen, J., and Jacobsen, C. S. (2008). Direct analysis of tfdA gene expression by indigenous bacteria in phenoxy acid amended agricultural soil. *ISME J.* 2, 677–687. doi: 10.1038/ismej.2008.21

Blazewicz, S. J., Barnard, R. L., Daly, R. A., and Firestone, M. K. (2013). Evaluating rRNA as an indicator of microbial activity in environmental communities: limitations and uses. *ISME J.* 7, 2061–2068. doi: 10.1038/ismej.2013.102

Carini, P., Marsden, P. J., Leff, L. W., Morgan, E. E., Strickland, M. S., and Fierer, N. (2016). Relic DNA is abundant in soil and obscures estimates of soil microbial diversity. *Nat. Microbiol.* 2:16242. doi: 10.1038/nmicrobiol.2016.242

Dai, X., Zhu, M., Warren, M., Balakrishnan, R., Patsalo, V., Okano, H., et al. (2016). Reduction of translating ribosomes enables *Escherichia coli* to maintain elongation rates during slow growth. *Nat. Microbiol.* 2:16231. doi: 10.1038/nmicrobiol.2016.231

Deutscher, M. P. (2003). Degradation of stable RNA in bacteria. *J. Biol. Chem.* 278, 45041–45044.

Deutscher, M. P. (2006). Degradation of RNA in bacteria: comparison of mRNA and stable RNA. *Nucleic Acids Res.* 34, 659–666. doi: 10.1093/nar/gkj472

Elliot, D., and Ladomery, M. (2011). *Molecular Biology of RNA*. Oxford: Oxford University Press.

Hambraeus, G., von Wachenfeldt, C., and Hederstedt, L. (2003). Genome-wide survey of mRNA half-lives in *Bacillus subtilis* identifies extremely stable mRNAs. *Mol. Genet. Genomics* 269, 706–714. doi: 10.1007/s00438-003-0883-6

Keith, J. E., Boyer, J. G., and de los Reyes, F. L. (2005). Changes in the rRNA levels of specific microbial groups in activated sludge during sample handling and storage. *Lett. Appl. Microbiol.* 41, 208–215. doi: 10.1111/j.1472-765X.2005.01745.x

Levinthal, C., Keynan, A., and Higa, A. (1962). Messenger RNA turnover and protein synthesis in *B. subtilis* inhibited by actinomycin D. *Proc. Natl. Acad. Sci. U.S.A.* 48, 1631–1638. doi: 10.1073/pnas.48.9.1631

Ostle, N., Whiteley, A. S., Bailey, M. J., Sleep, D., Ineson, P., and Manefield, M. (2003). Active microbial RNA turnover in a grassland soil estimated using a 13CO2 spike. *Soil Biol. Biochem.* 35, 877–885.

Placella, S. A., Brodie, E. L., and Firestone, M. K. (2012). Rainfall-induced carbon dioxide pulses result from sequential resuscitation of phylogenetically clustered microbial groups. *Proc. Natl. Acad. Sci. U.S.A.* 109, 10931–10936. doi: 10.1073/pnas.1204306109

Romanowski, G., Lorenz, M. G., and Wackernagel, W. (1991). Adsorption of plasmid DNA to mineral surfaces and protection against DNase I. *Appl. Environ. Microbiol.* 57, 1057–1061.

Schostag, M., Priemé, A., Jacquiod, S., Russel, J., Ekelund, F., and Jacobsen, C. S. (2019). Bacterial and protozoan dynamics upon thawing and freezing of an active layer permafrost soil. *ISME J.* 13, 1345–1359. doi: 10.1038/s41396-019-0351-x

Schostag, M., Stibal, M., Jacobsen, C. S., Bælum, J., Taş, N., Elberling, B., et al. (2015). Distinct summer and winter bacterial communities in the active layer of Svalbard permafrost revealed by DNA-and RNA-based analyses. *Front. Microbiol.* 6:399. doi: 10.3389/fmicb.2015.00399

Sessitsch, A., Gyamfi, S., Stralis-Pavese, N., Weilharter, A., and Pfeifer, U. (2002). RNA isolation from soil for bacterial community and functional analysis: evaluation of different extraction and soil conservation protocols. *J. Microbiol. Meth.* 51, 171–179. doi: 10.1016/s0167-7012(02)00065-9

Tilston, E. L., Sparrman, T., and Öquist, M. G. (2010). Unfrozen water content moderates temperature dependence of sub-zero microbial respiration. *Soil Biol. Biochem.* 42, 1396–1407.

Tveit, A., Schwacke, R., Svenning, M. M., and Urich, T. (2013). Organic carbon transformations in high-Arctic peat soils: key functions and microorganisms. *ISME J.* 7, 299–311. doi: 10.1038/ismej.2012.99

Zundel, M. A., Basturea, G. N., and Deutscher, M. P. (2009). Initiation of ribosome degradation during starvation in *Escherichia coli*. *RNA* 15, 977–983. doi: 10.1261/rna.1381309

Conflict of Interest: The authors declare that the research was conducted in the absence of any commercial or financial relationships that could be construed as a potential conflict of interest.

frontiers in Microbiology

ORIGINAL RESEARCH
published: 29 May 2020
doi: 10.3389/fmicb.2020.01029

Over Winter Microbial Processes in a Svalbard Snow Pack: An Experimental Approach

Alexandra T. Holland[1], Benoît Bergk Pinto[2], Rose Layton[2,3], Christopher J. Williamson[1], Alexandre M. Anesio[4], Timothy M. Vogel[2], Catherine Larose[2] and Martyn Tranter[1]*

[1] Bristol Glaciology Centre, School of Geographical Sciences, University of Bristol, Bristol, United Kingdom, [2] Environmental Microbial Genomics, CNRS, École Centrale de Lyon, Université de Lyon, Lyon, France, [3] ENOVEO, Lyon, France, [4] Department of Environmental Science, Aarhus University, Copenhagen, Denmark

Snow packs cover large expanses of Earth's land surface, making them integral components of the cryosphere in terms of past climate and atmospheric proxies, surface albedo regulators, insulators for other Arctic environments and habitats for diverse microbial communities such as algae, bacteria and fungi. Yet, most of our current understanding of snow pack environments, specifically microbial activity and community interaction, is limited to the main microbial growing season during spring ablation. At present, little is known about microbial activity and its influence on nutrient cycling during the subfreezing temperatures and 24-h darkness of the polar winter. Here, we examined microbial dynamics in a simulated cold (−5°C), dark snow pack to determine polar winter season microbial activity and its dependence on critical nutrients. Snow collected from Ny-Ålesund, Svalbard was incubated in the dark over a 5-week period with four different nutrient additions, including glacial mineral particles, dissolved inorganic nitrogen (DIN), dissolved inorganic phosphorus (DIP) and a combined treatment of DIN plus DIP. Data indicate a consumption of dissolved inorganic nutrients, particularly DIN, by heterotrophic communities, suggesting a potential nitrogen limitation, contradictory to phosphorus limitations found in most aquatic environments. 16S amplicon sequencing also reveal a clear difference in microbial community composition in the particulate mineral treatment compared to dissolved nutrient treatments and controls, suggesting that certain species of heterotrophs living within the snow pack are more likely to associate with particulates. Particulate phosphorus analyses indicate a potential ability of heterotrophic communities to access particulate sources of phosphorous, possibly explaining the lack of phosphorus limitation. These findings have importance for understanding microbial activity during the polar winter season and its potential influences on the abundance and bioavailability of nutrients released to surface ice and downstream environments during the ablation season.

Keywords: snow pack, polar winter, particulate phosphorus, heterotrophic bacteria, nutrient addition

OPEN ACCESS

Edited by:
Axel Schippers, Federal Institute for Geosciences and Natural Resources, Germany

Reviewed by:
Matthias Labrenz, Leibniz Institute for Baltic Sea Research (LG), Germany
Emma Jane Rochelle-Newall, Institut de Recherche Pour le Développement (IRD), France

****Correspondence:***
Alexandra T. Holland
Alexandra.holland@bristol.ac.uk

Specialty section:
This article was submitted to Extreme Microbiology, a section of the journal Frontiers in Microbiology

Received: *10 January 2020*
Accepted: *27 April 2020*
Published: *29 May 2020*

Citation:
Holland AT, Bergk Pinto B, Layton R, Williamson CJ, Anesio AM, Vogel TM, Larose C and Tranter M (2020) Over Winter Microbial Processes in a Svalbard Snow Pack: An Experimental Approach. Front. Microbiol. 11:1029. doi: 10.3389/fmicb.2020.01029

INTRODUCTION

The cryosphere, at present, covers 10% of the Earth's surface (Anesio et al., 2009; Lutz et al., 2017) with seasonal snow packs comprising a large portion of the frozen water landscape that encompass the cryosphere, covering over one third ($\sim 47 \times 10^6$ km^2) of the Earth's land surface (Hinkler et al., 2008). Snow packs play many key roles as climate regulators, such as insulating soil, permafrost and

supraglacial environments from sub-freezing temperatures, as well as influencing global energy and moisture budgets (Hinkler et al., 2008). Snow packs also serve as geochemical reservoirs in Arctic environments. During winter they accumulate nutrients, then release them during the spring melt, fertilizing soils, supraglacial environments, and downstream ecosystems (Kuhn, 2001; Telling et al., 2012; Larose et al., 2013b; Williamson et al., 2018). For example, Telling et al. (2012) found that on the Greenland Ice Sheet (GrIS) the prevalence of microbial nitrogen fixation in supraglacial environments related to the time since snow line retreat, suggesting that the snow pack is a main source of nitrogen to these environments.

Snow is formed in the atmosphere, which leads to scavenging of nutrients and particulates, such as ammonium, nitrate aerosols, dust and bacteria, that are used in the initiation and formation of snow crystal (Jones, 2001; Kuhn, 2001; Christner et al., 2008). The content of the resulting snow pack is thus, heavily dependent on atmospheric conditions and concentrations. Snow cover undergoes physical metamorphism during the winter season, promoted by freeze-thaw cycles and temperature gradients, which further effects the distribution of solutes and nutrients within the snow pack and ice crystals themselves (Colbeck, 1991; Kuhn, 2001; Larose et al., 2010b). Recently, microbial activity has also been found to influence snow pack nutrient species, concentration, distribution and bioavailability, and even effect overlying atmospheric concentrations (Kuhn, 2001; Amoroso et al., 2010; Fujii et al., 2010; Larose et al., 2013a; Bergk Pinto et al., 2019). For example, one study has found that microbial nitrogen cycling, occurring predominantly at the base of the snow pack, leads to basal snow enriched in dissolved nitrogen compared to surface samples (Larose et al., 2013a). Yet, research on the influence of microbial activity on nutrient cycling in snow pack environments is still in its infancy.

Presently, most research on Arctic seasonal snow pack environments focuses on the polar summer, when there is 24-h sunlight, above freezing temperatures and snow melt. This is considered to be the main growth season for microbial life residing in these environments, and an important period for nutrient export to downstream ecosystems via snow melt (Kuhn, 2001; Telling et al., 2012; Larose et al., 2013b). In contrast, there are very few studies that investigate the polar winter, which features 24-h darkness, sub-freezing temperatures, and extremely limited quantities of liquid water in the snow cover (Amoroso et al., 2010). As such, it is assumed that microbial life becomes inert during this season. However, this may not be the case. Several studies of ice core, glacial and sea ice and snow environments have reported active microbial communities during sub-freezing temperatures and low liquid water content (Carpenter et al., 2000; Junge et al., 2004; Miteva et al., 2007; Miteva, 2008, 2011; Maccario et al., 2019). For example, ice core studies have found certain psychrophiles, cold adapted organisms, capable of living at temperatures as low as −30°C (Langdahl and Ingvorsen, 1997; Price and Sowers, 2004), while Antarctic snow environments were found to contain metabolizing bacteria at −17°C (Carpenter et al., 2000). To date though, only one biogeochemical study of a cold Arctic snow pack environment during the polar winter has been conducted, which found that microbial oxidation of ammonium lead to the production and emission of NO, NO_2 and gaseous nitrous acid (HONO) from the snow pack at levels high enough to alter the overlying atmospheric nitrogen concentration, even in the complete absence of light and at temperatures reaching −25°C (Amoroso et al., 2010). It is therefore highly possible that other macronutrient cycles in Arctic snow packs are also influenced by microbial communities during the polar winter.

Dissolved inorganic phosphorus (DIP) has long been considered the ultimate limiting nutrient in glacial environments, mainly because it is principally rock-derived (Stibal et al., 2008, 2009). Most of the phosphorus (hereafter, P) found in glacial environments is sediment bound (Säwström et al., 2002; Hodson et al., 2004, 2005). Sources of sediment and rock derived particles to snow pack and supraglacial environments are typically limited, comprised mostly of wind-blown debris from local terrestrial environments, atmospheric dust and melt-out of meteoric ice (Foreman et al., 2007; Wientjes et al., 2011; Bagshaw et al., 2013). Cryoconite, a material composed of nearby terrestrial rocks and dust deposited from the atmosphere that is later combined by 'glue-like' extracellular polymeric substances (EPS) secreted by cyanobacteria (Hodson et al., 2010b; Stibal et al., 2012; Yallop et al., 2012; Musilova et al., 2016), is readily found in supraglacial environments, covering up to 10% of glacier ablation zones in the Northern Hemisphere (Hodson et al., 2007, 2010a; Anesio et al., 2009). It exists both in cryoconite holes and as dispersed material on the ice surface following the melt or wash-out of the holes (Anesio et al., 2009; Hodson et al., 2010a; Telling et al., 2012, 2014; Yallop et al., 2012; Wadham et al., 2016). Cryoconite has the potential to act as a particulate inorganic phosphorus source to supraglacial environments, with potentially bioavailable phosphorus found in the particles in the order of 160 $\mu g\ P\ g^{-1}$, which is well in surplus of the maximum microbial demand of about 2 $\mu g\ P\ g^{-1}$ calculated for cryoconite microbial communities (Stibal et al., 2008). While cryoconite particles are not commonly found in snow pack environments, dust deposited from the atmosphere, that is later incorporated into cryoconite material, is commonly deposited to the snow pack via wet and dry deposition. Studies in other non-Arctic, P limited environments have found that rocks containing inclusions of P rich minerals, such as apatite and biotite, were highly colonized by local microbial communities and contained evidence of etching and bio-weathering (Rogers et al., 1998; Taunton et al., 2000a,b; Welch et al., 2002). To date, no study has investigated the ability or occurrence of Arctic microbial communities to access and utilize cryoconite particles as a source of P. We note that if microbial communities can access inorganic phosphorus from particles during the polar winter, then P may not be as limiting as previously considered and could indicate that other supraglacial microbial communities are capable of particulate inorganic phosphorus extraction too.

To this end, a laboratory experiment to examine the potential for microbial activity in a Svalbard snow pack during the polar winter was conducted. Dissolved nutrients and naturally occurring inorganic particulates were added to snow, which was then incubated in a cold (−5°C), dark environment. The aims of

this experiment were twofold, first, to determine the dynamics of heterotrophic bacteria in a cold, dark snow pack environment, and second, to determine if the addition of dissolved and particulate inorganic nutrients effected heterotrophic abundance and community composition. In particular, to determine if heterotrophs can access the bioavailable inorganic phosphorus in cryoconite material. We hypothesize the addition of dissolved inorganic nutrients will stimulate heterotrophic activity in a cold, dark snow pack environment, leading to measurable changes in abundance and/or community composition. Further, we hypothesize a specialization of the heterotrophic community within the particulate inorganic nutrient addition.

MATERIALS AND METHODS

Snow Collection

Snow samples were collected during a 2012 March field campaign in Ny-Ålesund (Svalbard, Norway, 78°56′ N, 11°52′ E). Freshly fallen snow samples were collected into 3 L sterile sampling bags using a sterilized Teflon shovel and stored at −20°C. Strict measures were taken to reduce human impact on sampling site and samples (Larose et al., 2009). Tyvex body suits and latex gloves were worn during sampling to avoid contamination, and gloves were worn during all subsequent handling of samples. Snow samples were maintained below 0°C during transport to Ecole Centrale de Lyon, where they were stored at −15°C until further utilization.

Microcosm Set Up

The snow was disaggregated in sterile Whirl-pak™ bags using a hammer in a −15°C cold room and transferred into two large polystyrene boxes lined with sterile Whirl-pak™ bags where it was homogenized using a sterilized Teflon shovel.

Four nutrient addition experiments plus two controls were conducted, as shown in **Figure 1**. Nutrient additions consisted of particulate inorganic phosphorus (PIP), in the form of cryoconite particles described below, dissolved inorganic phosphorus (DIP), dissolved inorganic nitrogen (DIN), and DIP plus DIN. 'Dry' controls consisted only of snow, whereas the 'wet' controls consisted of snow plus 1 mL of MiliQ water to mimic the dissolved nutrient addition (**Figure 1**). There were five time points in total for the 'dry' control and the particulate phosphorus microcosms, while the 'wet' control, DIP, DIN, and DIP plus DIN were only sampled at the first and last time points due to experimental constraints. Each time point had four replicates per treatment. The microcosms were held in 72, 2 L glass jars, which were rinsed with 10% HCl, washed in a dishwasher using bleach and MiliQ water at 72°C and furnaced at 220°C for 20 min with foil covering the top for sterilization. 300 g of snow was weighed and placed in each sterilized jar. The respective nutrient spikes (see below) were then added and homogenized. Snow and nutrients were homogenized by mixing with a sterilized spatula for roughly 10 s each. Controls were homogenized the same as the samples. The 'dry' control was 'homogenized' in order to prevent any discrepancy between sample and control. MiliQ water blanks were also included in three time points throughout the experiment by using MiliQ in place of snow to check for nutrient leaching from the incubation bottles. 300 mg of cryoconite particles, collected from the Greenland Ice Sheet in the summer of 2017 were added for the PIP addition. The particles were furnaced at 550°C for 4 h prior to addition in order to prevent any microbial or organic carbon contamination. A ratio of 2.2 mg Phosphorus/1 g Cryoconite was assumed to determine the concentration of inorganic phosphorus added to the microcosms by the cryoconite particles (Stibal et al., 2008). 1 ml of a concentrated solution was pipetted into the snow for the DIP, DIN, and DIP plus DIN addition. DIP concentrations were chosen in order to match the concentration of inorganic phosphorus added by the cryoconite particles. A 660 ppm solution comprised of PO_4^{3-}- P was used to obtain a final concentration of 2.2 ppm after a 300-time snow dilution. DIN was comprised of ammonium (NH_4^+) and nitrate (NO_3^-), as nitrite (NO_2^-) is typically below detection limits for Arctic environments (Telling et al., 2011, 2012; Wadham et al., 2016). DIN concentrations were determined from the PIP and DIP concentrations using a C:N:P ratio of 106:16:1 (Redfield et al., 1963). A 10,560 ppm solution comprised of 5,280 ppm dissolved NH_4^+ - N and 5,280 ppm dissolved NO_3^- - N was used to obtain a final concentration of 35.2 ppm after a 300-time snow dilution. 1 ml of crystal violet stain was added to an extra microcosm in order to test our method of homogenizing dissolved nutrients into the snow. The furnaced foil was replaced on top of the jars and a lid was added to keep the foil in place. The jars were stored in the dark at −5°C until sampling.

Sampling

The 'dry' control and cryoconite addition microcosms were destructively sampled every 5 days over a total of 3 weeks, by leaving the jars to melt overnight at room temperature. The 'wet' control and dissolved nutrient addition microcosms were destructively sampled in the same way, on the initial (T0, June 26) and final (T4, July 16) time points only. pH measurements were taken of the snow meltwater using a Consort C532 meter with an epoxy gel 1M BNC electrode (Fisher Scientific) and AVS TITRINORM® pH 7 (20°C) buffer solution (VWR Chemicals). Cryoconite treatments and 'dry' controls were filtered using a sterile plastic syringe and a 25 mm, 0.2 μm cellulose nitrate filter (Whatman™). The filtrate was collected into pre-cleaned high-density polyethylene plastic bottle (Nalgene™; 30 mL) and stored at −20°C, for DIP, dissolved organic phosphorus (DOP), DIN and dissolved organic nitrogen (DON) analysis. Filters retaining the cryoconite particles were stored in sterile polypropylene tubes at −20°C prior to particulate phosphate extractions. Roughly 250 ml of meltwater from the DIP, DIN, DIN plus DIP and 'wet' control treatments were filtered onto sterile 47 mm, 0.2 μm Isopore™ membrane Millex filters using a sterile filtration unit (Nalge Nunc International Corporation). The filters were collected into sterile polypropylene tubes and immediately stored at −20°C prior to qPCR analysis and 16S rRNA gene Illumina sequencing. The remaining meltwater was extracted using a sterile plastic syringe and filtered through a 25 mm, 0.22 μm cellulose nitrate inline syringe filter (Whatman™) for DIP, DOP, DIN, and DON analysis. The

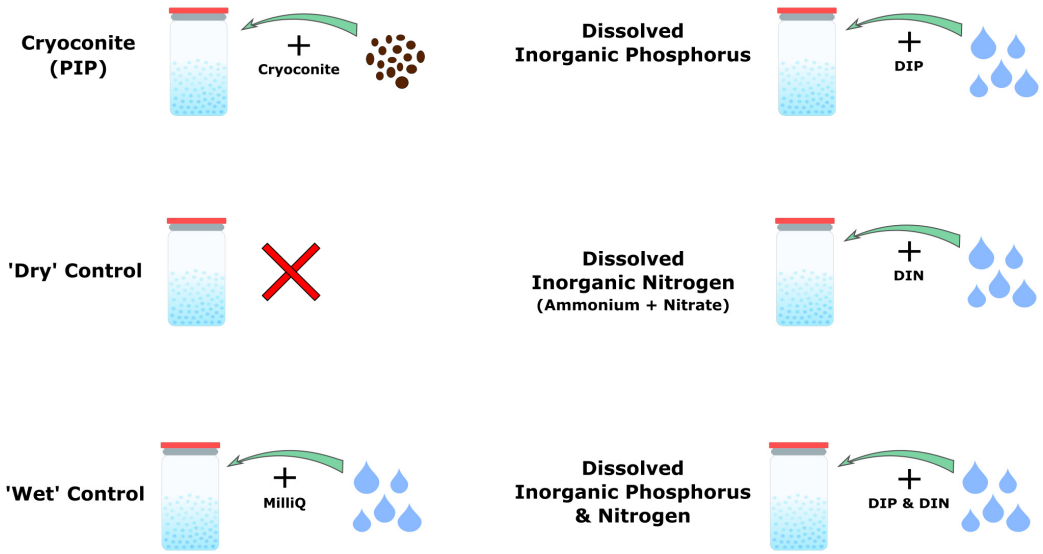

FIGURE 1 | Schematic depicting the four different nutrient addition treatments and two controls.

filtrate was stored in a pre-cleaned high-density polyethylene plastic bottle (Nalgene^{TM}; 30 mL) at −20°C. Samples were maintained at these temperatures during transport and storage at the LowTex Laboratory at the University of Bristol. Dissolved nutrient samples were thawed immediately prior to analysis using a hot water bath set at a temperature of ∼40°C. Procedural blanks were collected (n = 6) during the experiment, by processing deionized water in place of sample.

Analytical Methods

Dissolved Nutrients

DIP (principallyPO_4^{3-}) and total dissolved phosphorus (TDP) were determined on a Gallery Plus Automated Photometric Analyzer (Thermo Fisher Scientific, United Kingdom). TDP is the sum of DIP and DOP, and was determined by digesting the samples with a sulfuric acid persulfate digestion reagent and autoclaving at 121°C for 30 min (Jeffries et al., 1979). DOP was then calculated by subtracting DIP from TDP (i.e., DOP = TDP – DIP). The limit of detection (LoD) was 4.0 ppb (PO_4^{3-} and TDP/DOP). LoD was determined by the mean concentration plus three times the standard deviation of procedural blanks (n = 6). Precision was ± 0.43% (PO_4^{3-}) and ± 0.51% (TDP/DOP), and accuracy was + 0.12 (PO_4^{3-}) and −7.0% (TDP/DOP), as determined from comparison with gravimetrically diluted 1000 mg L^{-1} PO_4^{3-} - P certified stock standards to a concentration of 100 ppb (Sigma TraceCERT®). All DIP and DOP concentrations were field blank corrected, using values of 6.5 ppb, n = 5 and 10.9 ppb, n = 4 respectively.

Total dissolved inorganic nitrogen (TDIN) species include NO_2^-, NO_3^- and NH_4^+, which were quantified as follows. NO_2^-, total oxidized nitrogen (TON) (NO_2^- + NO_3^-) and NH_4^+ were quantified spectrophotometrically using a Gallery Plus Automated Photometric Analyzer (Thermo Fisher Scientific, United Kingdom). This combination of analyses allows the original NO_3^- concentration to be determined by subtracting NO_2^- from TON (i.e., NO_3^- = TON –NO_2^-). Total dissolved nitrogen (TDN) is the sum of TDIN and DON and was determined by digesting the samples with a potassium persulfate, sodium hydroxide and boric acid reagent and autoclaving at 121°C for 30 min (Grasshoff et al., 1999). This process causes the oxidation of organic nitrogen compounds, which can then be measured as TON as above. DON was then calculated by subtracting the sum of the TDIN from the TDN concentration of the digested samples (i.e., DON = TDN – TDIN). LoD was determined by the mean concentration plus three times the standard deviation of procedural blanks (n = 5). The LoDs were 1.5 ppb (NO_2^-), 5.5 ppb (TON), 14.0 ppb (NH_4^+) and 5.5 ppb (TDN/DON). Precision was ± 0.19% (NO_2^-), ± 1.1% (NO_3^-), ± 0.36% (NH_4^+) and ± 1.8% (TDN/DON), and accuracy was + 0.53% (NO_2^-), −7.6% (NO_3^-), −0.31% (NH_4^+) and −11.5% (TDN/DON), as determined from comparison with gravimetrically diluted 1000 mgL^{-1} NO_2^- - N, NO_3^- - N and NH_4^+ - N certified stock standards to a concentration of 30 ppb (NO_2^-) and 100 ppb (NO_3^-, NH_4^+, TDN/DON) (Sigma TraceCERT®). All TON, NH_4^+ and DON samples were field blank (n = 5) corrected by subtracting values of 8.1, 31.5, and 16.8 ppb respectively. NO_2^- field blanks fell below the LoD, 1.5 ppb, n = 6, so no blank correction was applied.

Particulate Phosphorus

Filters were removed from the −20°C storage prior to extraction and left to dry in a laminar flow hood. A five-step sequential extraction scheme, adapted from Stibal et al. (2008), was then used to operationally define phase association and bioavailability of particulate P in the cryoconite used in the incubations. The scheme used by Stibal et al. (2008) comprises of loosely bound P (Ext. 1), iron and aluminum bound P (Ext. 2), calcium and magnesium bound P (Ext. 3), organic P (Ext. 4) and residual

P (Ext. 5). Extraction 4, organic P, from Stibal et al. (2008) scheme was combined with Extraction 5, residual P, in our scheme as the cryoconite particles had been furnaced for organic contamination prior to addition, thus there was no need to formally quantify the organic phosphorus. Our scheme includes a step adapted from Hedley and Stewart (1982) instead, which quantifies the phosphorus incorporated into microbial biomass in the cryoconite treatment. This step most logically fits as Extraction 3 in our scheme as it uses NaOH as the solvent, the same solvent used in Extraction 2 to determine iron and aluminum bound P. A sediment: solute ratio of ∼150 mg: 3 mL used was similar to others (Hodson et al., 2004; Hawkings et al., 2016). The five-step extraction scheme used in this experiment is described in **Figure 2**. The content of P associated with different fractions of the cryoconite was quantified as DIP and DOP, as described above. Procedural blanks ($n = 3$) for all five extractions were conducted, using MiliQ water in place of sample to test for contamination. All DIP and DOP concentrations were blank corrected using a procedural blank. A conversion from dissolved phosphorus to particulate phosphorus concentration was applied to the cryoconite treatment and 'dry' control samples using the extract volume multiplied by the concentration divided by the sample weight.

DNA Extraction

DNA was extracted from filters of the DIP, DIN, DIN plus DIP and 'wet' control treatments using the DNeasy PowerWater Kit (Qiagen) following the manufacturer's instructions. DNA was quantified using the Qubit dsDNA HS Assay Kit (Thermo Fisher Scientific).

DNA was extracted from the particles in the cryoconite addition treatment using the protocol outlined in Nicol and Prosser (2011). Briefly, 0.5 mL CTAB phosphate buffer and 0.5 mL of phenol:chloroform:isoamyl alcohol (25:24:1) was added to each sample. Following cell lysis in a bead beater (30 s, 4 m s^{-1}), samples were centrifuged and the upper aqueous layer retained. Residual phenol was removed by the addition of 0.5 mL of chloroform:isoamyl alcohol, followed by centrifugation and retention of the upper aqueous layer. DNA was precipitated using 30% PEG/NaCl solution with an overnight incubation (5 degrees). The DNA pellet was collected by centrifugation, washed with 70% ethanol and resuspended in sterile molecular grade H_2O. DNA was also extracted from untreated, furnaced cryoconite, as described above, to act as a control and test for any remaining DNA after sterilization. Two separate DNA extraction methods were utilized due to the differing material from which the DNA was extracted. DNA extracted from filters utilized a method developed for low biomass filer extractions, while a method developed for sediment extraction was better suited for the cryoconite addition treatment.

16S rRNA qPCR

Real-time qPCR analyses on the 16S rRNA genes were carried out to approximate the concentration of bacterial cells per ml of melted snow or gram of cryoconite knowing that bacteria might have more than one copy of 16S rRNA per genome. The V3 region of the 16S rRNA gene was amplified using the GoTaq qPCR Master Mix (Promega, reference A6001) using primers sequences 341F and 534R (Muyzer, 1996; Watanabe et al., 2001) on a Rotorgene 3000 machine (Qiagen). The reaction mixture of 20 μL contained 10 μL of GoTaq qPCR Master Mix, 2 μL of DNA and RNAse-free water to complete the final 20 μL volume. The qPCR 2-steps program consisted of an initial step at 95°C for 2 min for enzyme activation, then 35 cycles of 5 s at 95°C and 20 s at 60°C hybridization and elongation. A final step was added to obtain a denaturation from 55 to 95°C with increments of 1°C s^{-1}. The amplicon length was around 200 bp. PCR products obtained from DNA from a pure culture of *Escherichia coli* were cloned in a plasmid (pCR2^{TM}.1-TOPO® vector, Invitrogen) and used as standard after quantification with the Broad-Range Qubit Fluorometric Quantification (Thermo Fisher Scientific).

16S rRNA Sequencing and Bioinformatics

Microbial community structure was determined by MiSeq Illumina amplicon sequencing of the bacterial V3–V4 region of the 16S rRNA gene using the Library Preparation Workflow recommended by Illumina (Illumina, Inc., San Diego, CA, United States). The V3–V4 region of the 16S rRNA gene was amplified using the Platinum Taq Polymerase (Thermo Fisher Scientific) using the primer set 783F – 1046R from Klindworth et al. (2013) resulting in the following sequences: 5′-TCGTCGGCAGCGTCAGATGTGTATAAGAGACAGCCTACGGGNGGCWGCAG-3′ as the forward primer sequence, and 5′-TCGTCGGCAGCGTCAGATGTGTATAAGAGACAGCCTACGGGNGGCWGCAG-3′ as the reverse primer sequence (Illumina, Inc., San Diego, CA, United States). The PCR program used was: 95°C for 3 min, 35 cycles of 95°C for 30 s, 55°C for 30 s and 72°C for 30 s, then a final step of 72°C for 5 min. Paired end sequencing was then carried out on a MiSeq sequencer (Illumina) at the laboratory in Lyon. Sequencing primers were removed using CutAdapt and filtered, trimmed and processed using Dada2. Taxonomy was assigned to the inferred sequence variants using the Dada2 formatted RDP dataset (RDP trainset 16).

Data Analysis

All geochemical measurements below the LoD were considered to be 0 for all statistical analyses. All DIN, DON, DIP, and DOP data were water blank-corrected using values from the respective procedural blanks. All PIP and POP data were water blank-corrected using values from the respective procedural blanks. Additionally, all blank corrected values that were negative were assumed to be 0 for all statistical analyses. Dada2 results and annotations were imported into R (R Development Core Team, 2011) and analyzed with the R package 'phyloseq' (McMurdie and Holmes, 2013). Amplicon sequence variants (ASVs) not taxonomically assigned to Bacteria were excluded from further analysis. Samples were rarefied to equal the sample with the lowest read counts using the 'rarefy even depth' phyloseq function prior to Alpha diversity calculations with the 'estimate richness' function. ASV count matrices were normalized by relative abundance prior to statistical analyses. Statistical analyses were performed in RStudio v.1.1.414 (RStudio Team, 2018).

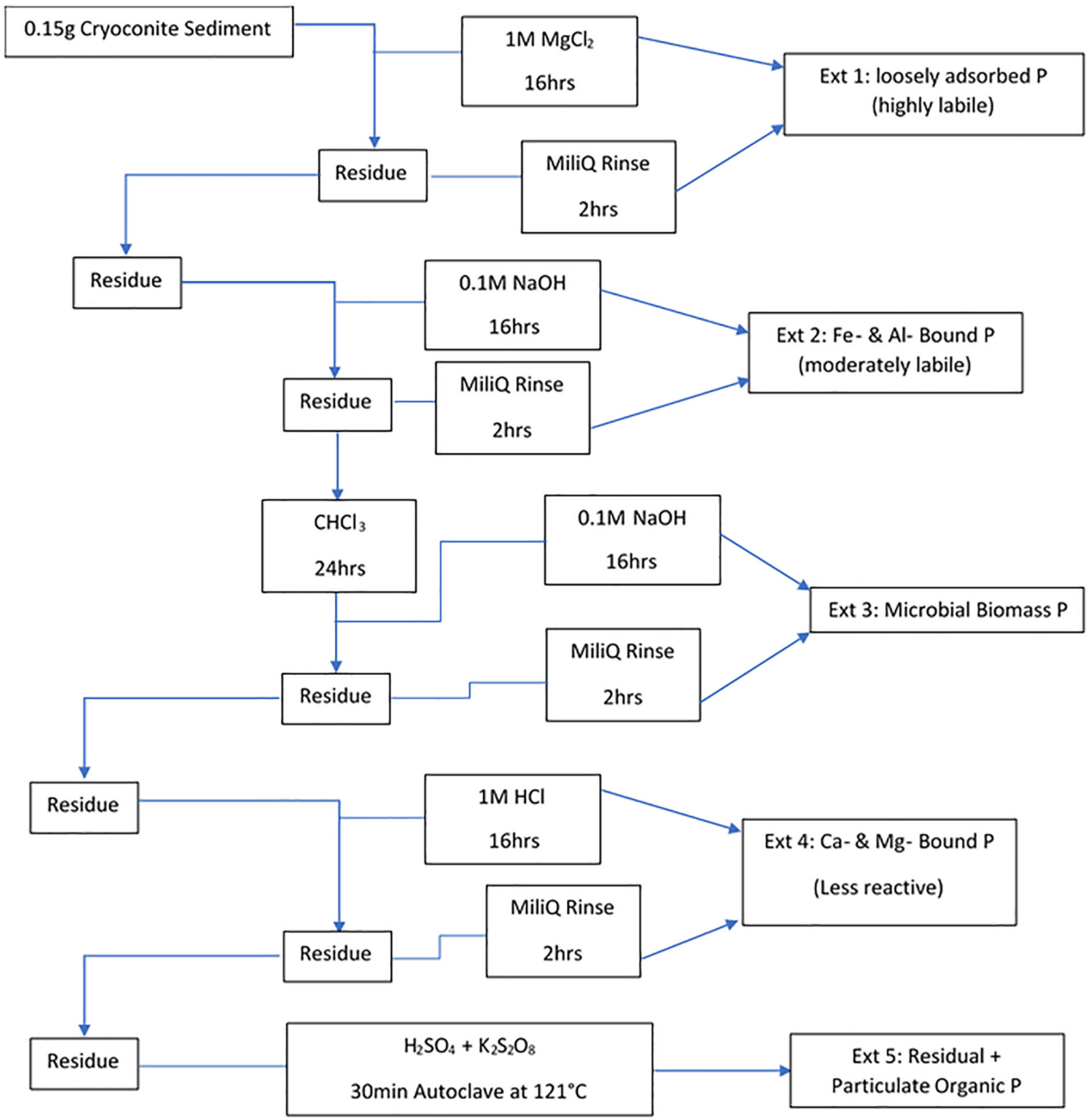

FIGURE 2 | Sequential extraction method for different forms of P in the cryoconite particles added to the cryoconite treatment. All steps were done under laboratory temperature and pressure unless stated otherwise.

Identification of statistical differences between nutrient concentrations, bacterial abundance of dissolved nutrient treatments, sample date and treatment type were achieved using two-way and one-way analysis of variance (ANOVA) comparisons, with *post hoc* Tukey HSD analysis applied to all significant ANOVA results. *t*-Tests were used to compare observed Alpha diversity measurements for each treatment between time points. Homogeneity of variance and normality of distribution were tested prior to all parametric analyses, and model assumptions were verified by examination of model criticism plots.

RESULTS

Dissolved Inorganic Nutrients

DIP and TDIN decreased significantly over the 5-week sampling period. The decrease in DIP and TDIN concentrations was not

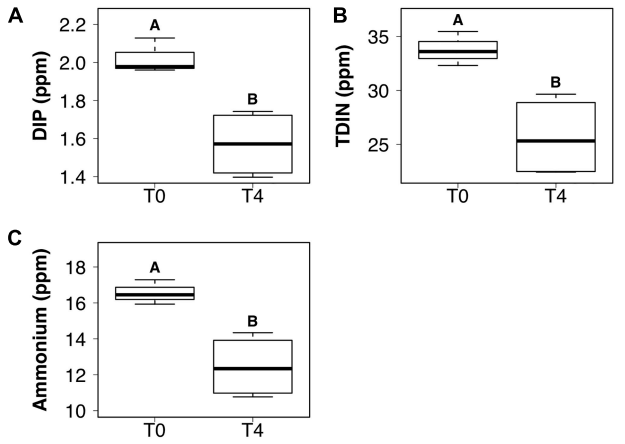

FIGURE 3 | Boxplots showing the median, upper and lower interquartile range of dissolved inorganic phosphorus (DIP) **(A)**, total dissolved inorganic nitrogen (TDIN) **(B)** and ammonium **(C)** concentrations for the combined DIP and dissolved inorganic nitrogen (DIN) treatment at the initial (T0) and final (T4) time points. *Uppercase letters* denote homogeneous subsets derived from *post hoc* Tukey HSD analysis on a significant two-way ANOVA in relation to the time point and treatment.

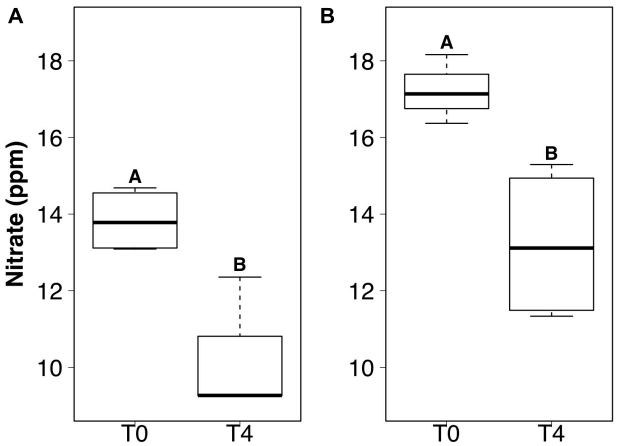

FIGURE 4 | Boxplots showing the median, upper, and lower interquartile range of nitrate concentrations for DIN treatment **(A)** and combined dissolved inorganic phosphorus (DIP) and DIN treatment **(B)** at the initial (T0) and final (T4) time points. *Uppercase letters* denote homogeneous subsets derived from *post hoc* Tukey HSD analysis on a significant two-way ANOVA in relation to the time point and treatment.

homogenous across all treatments, however. Both DIP and TDIN concentrations decreased significantly in the combined DIN plus DIP treatment only ($F_{1,10}$ = 17.5, $p < 0.01$ and $F_{1,10}$ = 1.0, $p < 0.01$, respectively) (**Figures 3A,B**). DIP concentrations in the combined treatment decreased from 2.02 ± 0.05 to 1.57 ± 0.09 ppm while TDIN concentrations decreased from 33.8 ± 0.92 to 25.7 ± 1.9 ppm. TDIN is composed of NH_4^+ and NO_3^-, as previously described, therefore, changes in each species of nitrogen were investigated in order to determine which N species was in higher demand. NH_4^+ decreased significantly from 16.6 ± 0.39 to 12.4 ± 0.87 ppm in the combined treatment only ($F_{1,10}$ = 1.6, $p < 0.05$) (**Figure 3C**). NO_3^- was the only added dissolved nutrient that significantly decreased in both the single and combined treatments ($F_{1,10}$ = 0.1, $p < 0.05$, for both) (**Figure 4**). NO_3^- concentrations decreased from 13.8 ± 0.42 to 10.3 ± 1 ppm in the DIN addition treatment and from 17.2 ± 0.52 to 13.2 ± 1 ppm in the combined treatment. No significant change occurred in any dissolved nutrient concentration in the 'wet' control, nor in DIP concentrations in the DIP treatment.

Bacterial Abundance and Taxonomy

The 'wet' control bacterial abundance was the only treatment that exhibited a significant decrease in abundance between the initial and final time points ($F_{3,20}$ = 6.27, $p < 0.05$) (**Figure 5A**). Bacterial abundance in all dissolved nutrient addition treatments were elevated in the final time point compared to the initial time point (**Figures 5D,G,J**). Bacterial abundance in the cryoconite treatment displayed an overall increasing trend across the timeseries, with all time points having at least a two order of magnitude increase compared to the untreated, furnaced cryoconite control and the final time point (T4) containing an order of magnitude higher bacterial abundance compared to all other time points (**Figure 5M**).

441 genera from 25 phyla were detected across the 4 treatments and the 'wet' control. Betaproteobacteria, more specifically *Massilia*, dominated the dissolved nutrient addition treatments and 'wet' control, whereas Alphaproteobacteria, more specifically *Methylobacterium*, had the highest abundance in the cryoconite treatment (**Figure 6**). There was also a clear diversification of the microbial community present in the cryoconite treatment compared to the untreated, furnaced control cryoconite particles, as only two common genera were detected, *Chryseobacterium* and *Propionibacterium* (**Figures 5O**, **6**). Alpha diversity measurements revealed an overall decrease in genera richness between T0 and T4 for the 'wet' control and DIN treatment, as seen in **Figures 5B,C,E,F**. Alpha diversity increased over the time series for both the combined treatment (**Figures 5K,L**) and DIP treatment, with a significant increase found in the DIP treatment (t = −2.82, $p < 0.05$) (**Figures 5H,I**). Alpha diversity also increased significantly after T0 in the cryoconite treatment (t = −3.23, $p < 0.05$) (**Figure 5N**).

Cryoconite Particulate Phosphorus

The mean total PIP content in the cryoconite particles added to the microcosms was 649.7 ± 46.8 μg g^{-1}, which falls within the range of P content within most rock types in the Earth's crust (230–670 μg P g^{-1}) (Hodson et al., 2004). Most PIP (82.8 ± 0.74%) was present in Extract 2 ('Fe- and Al-bound'), followed by Extract 4 ('Ca- and Mg-bound'; 8.8 ± 0.52%), Extract 5 ('Residual + Organic P'; 4.4 ± 0.11%), Extract 3 ('Microbial Biomass'; 4.3 ± 0.35%) and Extract 1 ('Loosely adsorbed P'; 0.51 ± 0.23%). One-way ANOVAs revealed significant changes in PIP content in Extracts 1–3 (Ext. 1: $F_{4,15}$ = 30.9, $p < 0.0001$,

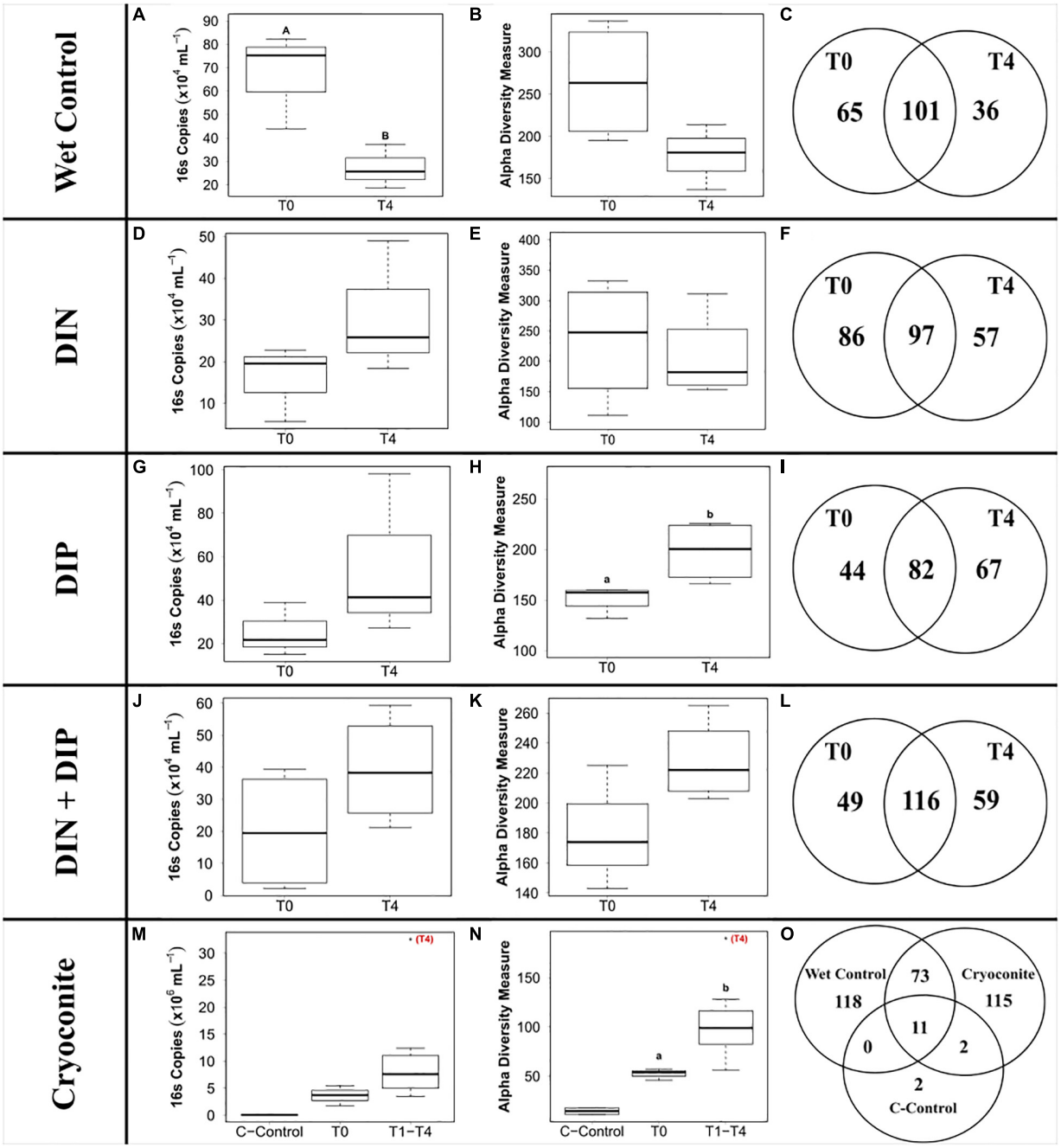

FIGURE 5 | Boxplots showing the median, upper and lower interquartile range of bacterial abundance **(A,D,G,J,M)** and observed Alpha diversity measurement **(B,E,H,K,N)** and Venn diagrams depicting genera richness **(C,F,I,L,O)** for all treatments. T0 and T4 represent initial and final time point, respectively. C-Control in the cryoconite treatment represents untreated, furnaced cryoconite control. DIN and DIP represent dissolved inorganic nitrogen and dissolved inorganic phosphorus, respectively. *Uppercase letters* denote homogeneous subsets derived from *post hoc* Tukey HSD analysis on a significant two-way ANOVA in relation to treatment and time point. *Lowercase letters* denote *t*-test comparisons in relation to time point.

Ext. 2: $F_{4,15} = 6.8$, $p < 0.001$, Ext. 3: $F_{4,15} = 3.5$, $p < 0.01$). A spike in PIP content found in Extracts 1–3 occurring on July 6th, time point 2 (T2), midway through the time series, drives this trend. DIP concentrations quantified from the filtrate of the cryoconite treatment revealed a significant decrease in concentration on the same date ($F_{4,15} = 84.3$, $p < 0.0001$). This relationship can be seen in **Figure 7**, which depicts the percent changes for Extracts 1–3 and DIP ($F_{4,15} = 27.2$, $p < 0.0001$, $F_{4,15} = 3.1$, $p < 0.01$, $F_{4,15} = 3.1$, $p < 0.01$, and $F_{4,15} = 58.6$, $p < 0.0001$, respectively). DOP and POP results from the filtrate and extracts displayed

FIGURE 6 | Relative abundances of taxa representing > 5% abundance and classified to genus level across all treatments and time points. CryoC* represents untreated, furnaced cryoconite control, with C2 and C3 representing the two replicates. T0–T4 represent time points 0–4, respectively. DIN and DIP represent dissolved inorganic nitrogen and dissolved inorganic phosphorus, respectively. P/DIN/DIP/DIPDIN/CH 1–4 represent the four replicates for each time point per treatment.

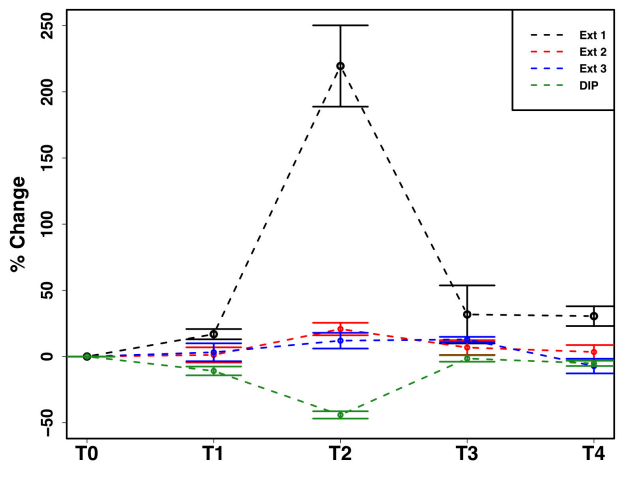

FIGURE 7 | Mean ± SE of the percent change in particulate phosphorus content of cryoconite particles (Ext. 1–3) and dissolved inorganic phosphorus (DIP) concentration of filtrate from cryoconite treatment throughout the time series, *n* = 4 for each time point of each extraction.

no change over time, apart from Extract 3. Extract 3, which quantified the organic phosphorus within the microbial biomass in the cryoconite treatment, demonstrated an initial decrease, followed by a sudden increase after T2 (**Figure 8**).

DISCUSSION

In this present study we show evidence of microbial community dynamics and their effect nutrient cycling within a simulated cold, dark snow pack environment. This has implications for how we view microbial activity during the polar winter, a season that has previously been considered inert. As the 24-h of darkness and subfreezing temperatures of the polar winter can comprise up to 6 months of the year, it is important to understand microbial influences on nutrient cycling as it could affect nutrients released during the ablation season.

Varied Heterotrophic Community Response to Dissolved Nutrient Additions

We demonstrate here the potential for active microbially-mediated nitrogen cycling in snow-packs, a dynamic already known to occur during spring and summer (Larose et al., 2013a), under simulated polar winter conditions. A clear community response was detected upon the addition of DIN, with an elevated final abundance and subsequent decline in genera richness suggesting potential specialization of heterotrophic communities, with genera better adapted to a nitrogen enriched environment potentially outcompeting other less suited bacteria (**Figures 5D–F**). This was supported by the presence throughout the time series of bacteria associated with the nitrogen cycle, e.g., *Bacillus* and *Caulobacter* genera known to perform N fixation (Różycki et al., 1999) and as efficient NH_4^+ scavengers (Poindexter, 1981), respectively, and the emergence of others, e.g., *Nitrospira* known for the oxidation of nitrite to nitrate (Spieck and Bock, 2015), by the final time point. As high, irregular inputs of nitrogen are common during the polar winter, via wet and dry deposition (Björkman et al., 2014), specialization in associated heterotrophic communities is likely to occur *in situ*, with consequences for the nitrogen cycle. For example, changes in bacterial assemblage composition associated with DIN addition during the present study likely underlaid

the observed preferential consumption of NO_3^- over NH_4^+, thus driving variability in the relative abundance of nitrogen species through time (**Figure 4A**), consistent with spring and summer *in situ* observations (Larose et al., 2013a).

In contrast to the assertion of DIP as the key limiting nutrient in glacial environments (Hodson et al., 2004; Stibal et al., 2008, 2009), DIP was only measurably consumed in the combined dissolved nutrient treatment during the present study; for which we propose two possible explanations. Firstly, it is likely that the abundance of DIN influenced the efficiency of DIP consumption, as evidenced by DIP being measurably consumed in the combined treatment only. With the absence of DIN in the DIP treatment, reduced DIP consumption would be required to maintain stoichiometric homeostasis (e.g., a C:N:P ratio of 20:4:1 for freshwater heterotrophic bacteria; Fagerbakke et al., 1996; Vrede, 1998), whereas in the combined treatment, both DIN and DIP were consumed effectively. Second, DIP may not be as limiting in supraglacial environments as previously believed (Hodson et al., 2004; Stibal et al., 2008, 2009), considering that DIN was consistently consumed during the present study when concentrations were artificially elevated. Such trends have also been reported in recent studies concerning both snow pack and surface ice environments, which suggested DIN to be in higher demand than DIP (Larose et al., 2013a; Holland et al., 2019). Overall, there is a clear response by the microbial community to all nutrient additions over the course of just 5-weeks in a cold, dark snow pack, indicating that the 24-h darkness and subfreezing temperatures of the polar winter may not be as limiting as previously thought.

Potential Extraction of Particulate Phosphorus

In addition to the utilization of dissolved nutrient resources, we further demonstrate the potential for microbial extraction of particulate phosphorus from cryoconite particles in snow pack environments in the present study. Inverse relationships observed between DIP and PIP pools suggested the capacity for phase changes between dissolved and loosely bound phosphorous fractions. For example, a simultaneous increase in PIP and decrease in DIP concentrations at T2 (**Figure 7**) indicated rebinding of DIP to available receptor sites on cryoconite particles (most likely as Extract 1), producing new, loosely bound PIP accessible to microbial communities via different methods such as carbonatation weathering, dissolution or acidification through the production of organic acids (Welch et al., 2002), as described below. DIP adsorbed onto particles, whether as loosely bound P or on poorly ordered Fe- and Al- oxyhydroxides, has been found to be readily bioavailable in cryospheric environments (Hodson et al., 2004; Stibal et al., 2008). Extract 1, the most labile and readily bioavailable form of PIP (Stibal et al., 2008), accounted for the smallest portion of total PIP extracted during the present study, suggesting consumption by microbial communities. Results from the present study are analogous to those in sediment rich, oligotrophic aquatic environments, whereby P adsorption to particulates has a significant impact on the fate and distribution of bioavailable P in the environment

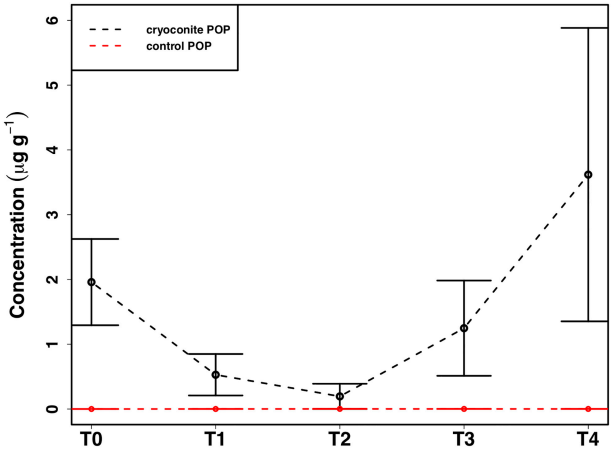

FIGURE 8 | Mean ± SE of the particulate organic phosphorus (POP) content of heterotrophic biomass associated with cryoconite particles in the cryoconite treatment throughout the time series and the 'dry' control, $n = 4$ for each time point of each treatment.

(Müller et al., 2006). An initial decrease in P within the microbial biomass, followed by an increase after T2, suggests a possible utilization of internal phosphorus stores, perhaps through storage in polyphosphates, before being able to access the newly adsorbed, bioavailable P (**Figure 8**). This storage and utilization of polyphosphate molecules as an energy source has been well-documented in many other heterotrophic communities (Kornberg, 1995; White et al., 2010; Achbergerová and Nahálka, 2011; Tocheva et al., 2013).

P liberation from particulate sources has previously been documented by microbes via etching, production of organic ligands, influencing the solution saturation state or most commonly lowering the pH either at the mineral surface or the bulk pH through the production of organic acids (Welch et al., 2002). The pH of the cryoconite treatment in the present study varied only slightly with an average pH of $\sim 6.02 \pm 0.13$. Even though our pH was slightly acidic, production of organic acids typically lower the bulk pH to between 3.5 and 5 (Welch et al., 2002), if microbial acidification was used to mine the loosely adsorbed P, then the pH may have only been altered at the particle surface, enough to access the labile P, but not enough to effect the bulk pH, or they utilized an alternate method such as the production of pyruvate, which has also been found to aid the dissolution of P containing minerals without altering pH (Welch et al., 2002).

Increased Abundance and Diversity Overtime in Particulate Associated Heterotrophic Community

We demonstrate a potential colonization of the cryoconite particles over time by genera found in the snow pack environment, as suggested by a combined increase in bacterial abundance and diversity over time in the cryoconite treatment and compared to the untreated, furnaced cryoconite control

(**Figures 5M,N**). A clear diversification in the main genera found in the cryoconite treatment compared to the 'wet' control and untreated, furnaced cryoconite is also present (**Figure 6**), indicating that certain genera from the snow pack environment might be better suited for colonizing the particles. Only 73 shared genera were detected between the treated cryoconite and 'wet' control, representing the genera that could act as early particulate colonizers (**Figure 5O**). For example, *Massilia* is found in both the treated cryoconite and 'wet' control. *Massilia* is not only a Betaproteobacteria, a class which has been previously identified as early colonizing bacteria with high abundance in snow pack environments that may play a key role in mineral weathering in debris covered glaciers (Pianka, 1970; Fierer et al., 2007, 2010; Larose et al., 2010a; Zumsteg et al., 2012; Franzetti et al., 2013; Hell et al., 2013), but also a genera that has species linked to solubilizing phosphate (Zheng et al., 2017). In fact, there is a clear increase in overall Betaproteobacteria abundance in the final time point of the cryoconite addition treatment compared to previous time points (**Figure 6**). Other non-betaproteobacteria such as *Arthrobacter*, that have been shown to assist in mineral dissolution by lowering pH, are also found among the 73 potential colonizers (Barker et al., 1998; Welch et al., 2002). Based on the notable increase in bacterial abundance and Alpha diversity after T0 (**Figures 5M,N**), it seems likely that given more time the colonization, and potential utilization, of the particles by microbes would have continued to increase. Any potential colonization or extraction of particulate inorganic substrates by heterotrophic communities in snow pack environments is likely to occur in other supraglacial or Arctic environments as snow packs have been considered to seed microbial communities in underlying environments during the ablation season (Musilova et al., 2015).

CONCLUSION

Our study indicates the presence of an active heterotrophic community in a cold (−5°C), dark snow pack environment. Snow collected from a seasonal snow pack in Ny-Ålesund, Svalbard was incubated with dissolved and particulate nutrient additions to determine whether the additions, in particular the naturally occurring inorganic substrate, affected heterotrophic abundance or community composition. Our results suggest a specialization within the heterotrophic community of genera known to influence N cycling in the presence of excess DIN, but diversification when abundant DIP is present. As high inputs of N are common to snow pack environments during the polar winter, this specialization may occur *in situ*, leading to efficient N cycling by heterotrophic bacteria. We also find strong evidence for the utilization of particulate phosphorus sources from an inorganic glacial sediment by the heterotrophic community, which also exhibits colonization by certain genera from the snow pack environment, e.g., *Betaproteobacteria*, known to be early colonizers of particulates. The ability of heterotrophic bacteria to access particulate phosphorus in snow pack and potentially other supraglacial environments may thus be a key factor influencing survival in oligotrophic glacial environments. Overall, we demonstrate that changes in heterotrophic community abundance and composition in snow pack environments influence nutrient cycling during the polar winter, which in turn impacts the speciation, abundance and bioavailability of nutrient resources relative to their depositional state, and thus their roles in supraglacial and downstream ecosystems during the ablation season.

DATA AVAILABILITY STATEMENT

Sequencing files can be accessed at ftp://ftp-adn.ec-lyon.fr/Holland_2020/. The full datasets generated for this study are available upon request to the corresponding author.

AUTHOR CONTRIBUTIONS

AH, BB, AA, TV, CL, and MT conceived and designed the study. CL collected the snow and analyzed the 16S qPCR samples with the assistance of RL. RL extracted the DNA, sequenced the rRNA and ran bioinformatics on the samples with the assistance of BB. AH wrote the manuscript with inputs from CW, CL, RL, AA, and MT. All authors reviewed the final manuscript.

FUNDING

This project received funding from the European Union's Horizon 2020 Research and Innovation Program under the Marie Skłodowska-Curie grant agreement No. 675546. This work received additional funding in part by the UK Natural Environment Research Council Consortium Grant 'Black and Bloom' (NE/M0212025).

ACKNOWLEDGMENTS

We would like to acknowledge and thank the technicians at both the LowTex laboratory in Bristol and the Laboratoire Ampere in Lyon for their help during the experiment and the later analysis of samples. We would also like to acknowledge IPEV MicroLife for their field support.

REFERENCES

Achbergerová, L., and Nahálka, J. (2011). Polyphosphate-an ancient energy source and active metabolic regulator. *Microb. Cell Fact.* 10:63. doi: 10.1186/1475-2859-10-63

Amoroso, A., Domine, F., Esposito, G., Morin, S., Savarino, J., Nardino, M., et al. (2010). Microorganisms in dry polar snow are involved in the exchanges of reactive nitrogen species with the atmosphere. *Environ. Sci. Technol.* 44, 714–719. doi: 10.1021/es902 7309

Anesio, A. M., Hodson, A. J., Fritz, A., Psenner, R., and Sattler, B. (2009). High microbial activity on glaciers: importance to the global carbon cycle. *Glob. Chang. Biol.* 15, 955–960. doi: 10.1111/j.1365-2486.2008.01758.x

Bagshaw, E. A., Tranter, M., Fountain, A. G., Welch, K., Basagic, H. J., and Lyons, W. B. (2013). Do cryoconite holes have the potential to be significant sources of C, N, and P to downstream depauperate ecosystems of Taylor Valley, Antarctica? *Arct. Antarct. Alp. Res.* 45, 440–454. doi: 10.1657/1938-4246-45.4.440

Barker, W., Welch, S., Chu, S., and Banfield, J. (1998). Experimental observations of the effects of bacteria on aluminosilicate weathering. *Am. Mineral.* 83, 1551–1563.

Bergk Pinto, B., Maccario, L., Dommergue, A., Vogel, T. M., and Larose, C. (2019). Do organic substrates drive microbial community interactions in Arctic Snow? *Front. Microbiol.* 10:2492. doi: 10.3389/fmicb.2019.02492

Björkman, M. P., Vega, C. P., Kühnel, R., Spataro, F., Ianniello, A., Esposito, G., et al. (2014). Nitrate postdeposition processes in Svalbard surface snow. *J. Geophys. Res. Atmos.* 119, 12953–12976. doi: 10.1002/2013JD021234

Carpenter, E. J., Lin, S., and Capone, D. G. (2000). Bacterial activity in South Pole snow. *Appl. Environ. Microbiol.* 66, 4514–4517. doi: 10.1128/aem.69.10.6340-6341.2003

Christner, B. C., Morris, C. E., Foreman, C. M., Cai, R., and Sands, D. C. (2008). Ubiquity of biological ice nucleators in snowfall. *Science* 319:1214. doi: 10.1126/science.1149757

Colbeck, S. (1991). The layered character of snow covers. *Rev. Geophys.* 29, 81–96.

Fagerbakke, K. M., Heldal, M., and Norland, S. (1996). Content of carbon, nitrogen, oxygen, sulfur and phosphorus in native aquatic and cultured bacteria. *Aquat. Microb. Ecol.* 10, 15–27.

Fierer, N., Bradford, M. A., and Jackson, R. B. (2007). Toward an ecological classification of soil bacteria. *Ecology* 88, 1354–1364. doi: 10.1890/05-1839

Fierer, N., Nemergut, D., Knight, R., and Craine, J. M. (2010). Changes through time: integrating microorganisms into the study of succession. *Res. Microbiol.* 161, 635–642. doi: 10.1016/j.resmic.2010.06.002

Foreman, C. M., Sattler, B., Mikucki, J. A., Porazinska, D. L., and Priscu, J. C. (2007). Metabolic activity and diversity of cryoconites in the Taylor Valley, Antarctica. *J. Geophys. Res. Biogeosci.* 112:G04S32. doi: 10.1029/2006JG000358

Franzetti, A., Tatangelo, V., Gandolfi, I., Bertolini, V., Bestetti, G., Diolaiuti, G., et al. (2013). Bacterial community structure on two alpine debris-covered glaciers and biogeography of Polaromonas phylotypes. *ISME J.* 7:1483. doi: 10.1038/ismej.2013.48

Fujii, M., Takano, Y., Kojima, H., Hoshino, T., Tanaka, R., and Fukui, M. (2010). Microbial community structure, pigment composition, and nitrogen source of red snow in Antarctica. *Microb. Ecol.* 59, 466–475. doi: 10.1007/s00248-009-9594-9

Grasshoff, K., Kremling, K., and Ehrhardt, M. (1999). *Methods of Seawater Analysis*. Hoboken, NJ: John Wiley & Sons.

Hawkings, J., Wadham, J., Tranter, M., Telling, J., Bagshaw, E., Beaton, A., et al. (2016). The Greenland Ice sheet as a hot spot of phosphorus weathering and export in the Arctic. *Glob. Biogeochem. Cycles* 30, 191–210. doi: 10.1002/2015gb005237

Hedley, M., and Stewart, J. (1982). Method to measure microbial phosphate in soils. *Soil Biol. Biochem.* 14, 377–385.

Hell, K., Edwards, A., Zarsky, J., Podmirseg, S. M., Girdwood, S., Pachebat, J. A., et al. (2013). The dynamic bacterial communities of a melting High Arctic glacier snowpack. *ISME J.* 7:1814. doi: 10.1038/ismej.2013.51

Hinkler, J., Hansen, B. U., Tamstorf, M. P., Sigsgaard, C., and Petersen, D. (2008). Snow and snow-cover in central Northeast Greenland. *Adv. Ecol. Res.* 40, 175–195. doi: 10.1016/S0065-2504(07)00008-6

Hodson, A., Anesio, A. M., Ng, F., Watson, R., Quirk, J., Irvine−Fynn, T., et al. (2007). A glacier respires: quantifying the distribution and respiration CO2 flux of cryoconite across an entire Arctic supraglacial ecosystem. *J. Geophys. Res. Biogeosci.* 112:G04S36. doi: 10.1029/2007JG000452

Hodson, A., Bøggild, C., Hanna, E., Huybrechts, P., Langford, H., Cameron, K., et al. (2010a). The cryoconite ecosystem on the Greenland ice sheet. *Ann. Glaciol.* 51, 123–129.

Hodson, A., Cameron, K., Bøggild, C., Irvine-Fynn, T., Langford, H., Pearce, D., et al. (2010b). The structure, biological activity and biogeochemistry of cryoconite aggregates upon an Arctic valley glacier, Longyearbreen, Svalbard. *J. Glaciol.* 56, 349–362.

Hodson, A., Mumford, P., and Lister, D. (2004). Suspended sediment and phosphorus in proglacial rivers: bioavailability and potential impacts upon the P status of ice−marginal receiving waters. *Hydrol. Process.* 18, 2409–2422. doi: 10.1002/hyp.1471

Hodson, A. J., Mumford, P. N., Kohler, J., and Wynn, P. M. (2005). The High Arctic glacial ecosystem: new insights from nutrient budgets. *Biogeochemistry* 72, 233–256. doi: 10.1007/s10533-004-0362-0

Holland, A. T., Williamson, C. J., Sgouridis, F., Tedstone, A. J., McCutcheon, J., Cook, J. M., et al. (2019). Dissolved organic nutrients dominate melting surface ice of the Dark Zone (Greenland Ice Sheet). *Biogeosciences* 16, 3283–3296. doi: 10.5194/bg-16-3283-2019

Jeffries, D. S., Dieken, F., and Jones, D. (1979). Performance of the autoclave digestion method for total phosphorus analysis. *Water Res.* 13, 275–279.

Jones, H. (2001). *Snow Ecology: An Interdisciplinary Examination of Snow-Covered Ecosystems*. Cambridge: Cambridge University Press.

Junge, K., Eicken, H., and Deming, J. W. (2004). Bacterial activity at- 2 to- 20 C in Arctic wintertime sea ice. *Appl. Environ. Microbiol.* 70, 550–557. doi: 10.1128/aem.70.1.550-557.2004

Klindworth, A., Pruesse, E., Schweer, T., Peplies, J., Quast, C., Horn, M., et al. (2013). Evaluation of general 16S ribosomal RNA gene PCR primers for classical and next-generation sequencing-based diversity studies. *Nucleic Acids Res.* 41:e1. doi: 10.1093/nar/gks808

Kornberg, A. (1995). Inorganic polyphosphate: toward making a forgotten polymer unforgettable. *J. Bacteriol.* 177, 491–496. doi: 10.1128/jb.177.3.491-496.1995

Kuhn, M. (2001). The nutrient cycle through snow and ice, a review. *Aquat. Sci.* 63, 150–167.

Langdahl, B. R., and Ingvorsen, K. (1997). Temperature characteristics of bacterial iron solubilisation and 14C assimilation in naturally exposed sulfide ore material at Citronen Fjord, North Greenland (83 N). *FEMS Microbiol. Ecol.* 23, 275–283.

Larose, C., Berger, S., Ferrari, C., Navarro, E., Dommergue, A., Schneider, D., et al. (2010a). Microbial sequences retrieved from environmental samples from seasonal Arctic snow and meltwater from Svalbard, Norway. *Extremophiles* 14, 205–212. doi: 10.1007/s00792-009-0299-2

Larose, C., Berger, S., Ferrari, C. P., Navarro, E., Dommergue, A., Marusczak, N., et al. (2009). "Assessing interactions between mercury and microbial populations in the snowpack: a metagenomic approach BAGECO 10," in *Proceedings of the 10th Symposium on Bacterial Genetics and Ecology – Coexisting on a Changing Planet 2009-06-15*, Uppsala.

Larose, C., Dommergue, A., De Angelis, M., Cossa, D., Averty, B., Marusczak, N., et al. (2010b). Springtime changes in snow chemistry lead to new insights into mercury methylation in the Arctic. *Geochim. Cosmochim. Acta* 74, 6263–6275. doi: 10.1016/j.gca.2010.08.043

Larose, C., Dommergue, A., and Vogel, T. M. (2013a). Microbial nitrogen cycling in Arctic snowpacks. *Environ. Res. Lett.* 8:035004. doi: 10.1088/1748-9326/8/3/035004

Larose, C., Dommergue, A., and Vogel, T. M. (2013b). The dynamic arctic snow pack: an unexplored environment for microbial diversity and activity. *Biology* 2, 317–330. doi: 10.3390/biology2010317

Lutz, S., Anesio, A. M., Edwards, A., and Benning, L. G. (2017). Linking microbial diversity and functionality of arctic glacial surface habitats. *Environ. Microbiol.* 19, 551–565. doi: 10.1111/1462-2920.13494

Maccario, L., Carpenter, S. D., Deming, J. W., Vogel, T. M., and Larose, C. (2019). Sources and selection of snow-specific microbial communities in a Greenlandic sea ice snow cover. *Sci. Rep.* 9, 1–14. doi: 10.1038/s41598-019-38744-y

McMurdie, P. J., and Holmes, S. (2013). phyloseq: an R package for reproducible interactive analysis and graphics of microbiome census data. *PLoS One* 8:e61217. doi: 10.1371/journal.pone.0061217

Miteva, V. (2008). "Bacteria in snow and Glacier Ice," in *Psychrophiles: From Biodiversity to Biotechnology*, eds R. Margesin, F. Schinner, J.-C. Marx, and C. Gerday (Berlin: Springer), 31–50.

Miteva, V. (2011). "Microorganisms associated with glaciers," in *Encyclopedia of Snow, Ice and Glaciers*, eds V. P. Singh, U. K. Haritashya, and P. Singh (Berlin: Springer), 741–744.

Miteva, V., Sowers, T., and Brenchley, J. (2007). Production of N2O by ammonia oxidizing bacteria at subfreezing temperatures as a model for assessing the N 2 O anomalies in the Vostok ice core. *Geomicrobiol. J.* 24, 451–459. doi: 10.1080/01490450701437693

Müller, B., Stierli, R., and Wüest, A. (2006). Phosphate adsorption by mineral weathering particles in oligotrophic waters of high particle content. *Water Resour. Res.* 42:W10414. doi: 10.1029/2005WR004778

Musilova, M., Tranter, M., Bamber, J. L., Takeuchi, N., and Anesio, A. (2016). Experimental evidence that microbial activity lowers the albedo of glaciers. *Geochem. Perspect. Lett.* 2, 106–116. doi: 10.7185/geochemlet.1611

Musilova, M., Tranter, M., Bennett, S. A., Wadham, J., and Anesio, A. M. (2015). Stable microbial community composition on the Greenland Ice Sheet. *Front. Microbiol.* 6:193. doi: 10.3389/fmicb.2015.00193

Muyzer, G. (1996). "Denaturing gradient gel electrophoresis of PCR-amplified 16S rDNA. A new molecular approach to analyze the genetic diversity of mixed microbial communities," in *Molecular Microbial Ecology Manual*, eds A. D. L. Akkermans, J. D. van Elsas, and F. J. de Bruijin (Dordrecht: Kluwer Academic Publishing), 3.4.4.1–3.4.4.22.

Nicol, G. W., and Prosser, J. I. (2011). Strategies to determine diversity, growth, and activity of ammonia-oxidizing archaea in soil. *Methods Enzymol.* 496, 3–34. doi: 10.1016/B978-0-12-386489-5.00001-4

Pianka, E. R. (1970). On r-and K-selection. *Am. Nat.* 104, 592–597.

Poindexter, J. S. (1981). The caulobacters: ubiquitous unusual bacteria. *Microbiol. Rev.* 45, 123–179.

Price, P. B., and Sowers, T. (2004). Temperature dependence of metabolic rates for microbial growth, maintenance, and survival. *Proc. Natl. Acad. Sci. U.S.A.* 101, 4631–4636. doi: 10.1073/pnas.0400522101

R Development Core Team (2011). *R: A Language and Environment for Statistical Computing*. Vienna: R Foundation for Statistical Computing. Available online at: http://www.R-project.org

Redfield, A., Ketchum, B., and Richards, F. (1963). "The influence of organisms on the composition of sea water," in *The sea*, Vol. 2, ed. M. H. Hill (New York, NY: Interscience), 26–77.

Rogers, J., Bennett, P., and Choi, W. (1998). Feldspars as a source of nutrients for microorganisms. *Am. Miner.* 83, 1532–1540.

Różycki, H., Dahm, H., Strzelczyk, E., and Li, C. (1999). Diazotrophic bacteria in root-free soil and in the root zone of pine (*Pinus sylvestris* L.) and oak (*Quercus robur* L.). *Appl. Soil Ecol.* 12, 239–250.

RStudio Team (2018). *RStudio: Integrated Development for R*. Boston, MA: RStudio, Inc. Available online at: http://www.rstudio.com/

Säwström, C., Mumford, P., Marshall, W., Hodson, A., and Laybourn-Parry, J. (2002). The microbial communities and primary productivity of cryoconite holes in an Arctic glacier (Svalbard 79 N). *Polar Biol.* 25, 591–596. doi: 10.1007/s00300-002-0388-5

Spieck, E., and Bock, E. (2015). "Nitrospira," in *Bergey's Manual of Systematics of Archaea and Bacteria*, eds W. Whitman, B. Rainey, F. Kämpfer, P. Trujillo, M. Chun, J. DeVos, et al. (Hoboken, NJ: Wiley), S1–S4.

Stibal, M., Anesio, A. M., Blues, C. J. D., and Tranter, M. (2009). Phosphatase activity and organic phosphorus turnover on a high Arctic glacier. *Biogeosciences* 6, 913–922.

Stibal, M., Šabacká, M., and Žárský, J. (2012). Biological processes on glacier and ice sheet surfaces. *Nat. Geosci.* 5, 771–774. doi: 10.1038/ngeo1611

Stibal, M., Tranter, M., Telling, J., and Benning, L. G. (2008). Speciation, phase association and potential bioavailability of phosphorus on a Svalbard glacier. *Biogeochemistry* 90, 1–13.

Taunton, A. E., Welch, S. A., and Banfield, J. F. (2000a). Geomicrobiological controls on light rare earth element, Y and Ba distributions during granite weathering and soil formation. *J. Alloys Compd.* 303, 30–36.

Taunton, A. E., Welch, S. A., and Banfield, J. F. (2000b). Microbial controls on phosphate and lanthanide distributions during granite weathering and soil formation. *Chem. Geol.* 169, 371–382.

Telling, J., Anesio, A. M., Tranter, M., Fountain, A. G., Nylen, T., Hawkings, J., et al. (2014). Spring thaw ionic pulses boost nutrient availability and microbial growth in entombed Antarctic Dry Valley cryoconite holes. *Front. Microbiol.* 5:694. doi: 10.3389/fmicb.2014.00694

Telling, J., Anesio, A. M., Tranter, M., Irvine-Fynn, T., Hodson, A., Butler, C., et al. (2011). Nitrogen fixation on Arctic glaciers, Svalbard. *J. Geophys. Res.* 116:G03039. doi: 10.1029/2010jg001632

Telling, J., Stibal, M., Anesio, A. M., Tranter, M., Nias, I., Cook, J., et al. (2012). Microbial nitrogen cycling on the Greenland Ice Sheet. *Biogeosciences* 9, 2431–2442. doi: 10.5194/bg-9-2431-2012

Tocheva, E. I., Dekas, A. E., McGlynn, S. E., Morris, D., Orphan, V. J., and Jensen, G. J. (2013). Polyphosphate storage during sporulation in the gram-negative bacterium *Acetonema longum*. *J. Bacteriol.* 195, 3940–3946. doi: 10.1128/JB.00712-13

Vrede, T. (1998). Elemental composition (C: N: P) and growth rates of bacteria and *Rhodomonas* grazed by *Daphnia*. *J. Plankton Res.* 20, 455–470.

Wadham, J. L., Hawkings, J., Telling, J., Chandler, D., Alcock, J., O'Donnell, E., et al. (2016). Sources, cycling and export of nitrogen on the Greenland Ice Sheet. *Biogeosciences* 13, 6339–6352. doi: 10.5194/bg-13-6339-2016

Watanabe, K., Kodama, Y., and Harayama, S. (2001). Design and evaluation of PCR primers to amplify bacterial 16S ribosomal DNA fragments used for community fingerprinting. *J. Microbiol. Methods* 44, 253–262. doi: 10.1016/s0167-7012(01)00220-2

Welch, S., Taunton, A., and Banfield, J. (2002). Effect of microorganisms and microbial metabolites on apatite dissolution. *Geomicrobiol. J.* 19, 343–367. doi: 10.1080/01490450290098414

White, A., Karl, D., Björkman, K., Beversdorf, L., and Letelier, R. (2010). Production of organic matter by Trichodesmium IMS101 as a function of phosphorus source. *Limnol. Oceanogr.* 55, 1755–1767. doi: 10.4319/lo.2010.55.4.1755

Wientjes, I. G. M., Van de Wal, R. S. W., Reichart, G. J., Sluijs, A., and Oerlemans, J. (2011). Dust from the dark region in the western ablation zone of the Greenland ice sheet. *Cryosphere* 5, 589–601. doi: 10.5194/tc-5-589-2011

Williamson, C. J., Anesio, A. M., Cook, J., Tedstone, A., Poniecka, E., Holland, A., et al. (2018). Ice algal bloom development on the surface of the Greenland Ice Sheet. *FEMS Microbiol. Ecol.* 94:fiy025. doi: 10.1093/femsec/fiy025

Yallop, M. L., Anesio, A. M., Perkins, R. G., Cook, J., Telling, J., Fagan, D., et al. (2012). Photophysiology and albedo-changing potential of the ice algal community on the surface of the Greenland ice sheet. *ISME J.* 6, 2302–2313. doi: 10.1038/ismej.2012.107

Zheng, B.-X., Bi, Q.-F., Hao, X.-L., Zhou, G.-W., and Yang, X.-R. (2017). *Massilia phosphatilytica* sp. nov., a phosphate solubilizing bacteria isolated from a long-term fertilized soil. *Int. J. Syst. Evol. Microbiol.* 67, 2514–2519. doi: 10.1099/ijsem.0.001916

Zumsteg, A., Luster, J., Göransson, H., Smittenberg, R. H., Brunner, I., Bernasconi, S. M., et al. (2012). Bacterial archaeal and fungal succession in the forefield of a receding glacier. *Microb. Ecol.* 63, 552–564. doi: 10.1007/s00248-011-9991-8

Conflict of Interest: RL was employed by ENOVEO.

The remaining authors declare that the research was conducted in the absence of any commercial or financial relationships that could be construed as a potential conflict of interest.

frontiers in Microbiology

ORIGINAL RESEARCH
published: 03 June 2020
doi: 10.3389/fmicb.2020.01165

Cryoconite Hole Location in East-Antarctic Untersee Oasis Shapes Physical and Biological Diversity

*Klemens Weisleitner[1,2], Alexandra Kristin Perras[3], Seraphin Hubert Unterberger[4], Christine Moissl-Eichinger[3], Dale T. Andersen[5] and Birgit Sattler[1,2]**

[1] Institute of Ecology, University of Innsbruck, Innsbruck, Austria, [2] Austrian Polar Research Institute, Vienna, Austria, [3] Center for Medical Research, Medical University of Graz, Graz, Austria, [4] Unit of Material Technology, University of Innsbruck, Innsbruck, Austria, [5] SETI Institute, Mountain View, CA, United States

Antarctic cryoconite holes (CHs) are mostly perennially ice-lidded and sediment-filled depressions that constitute important features on glaciers and ice sheets. Once being hydrologically connected, these microbially dominated mini-ecosystems provide nutrients and biota for downstream environments. For example, the East Antarctic Anuchin Glacier gradually melts into the adjacent perennially ice-covered Lake Untersee, and CH biota from this glacier contribute up to one third of the community composition in benthic microbial mats within the lake. However, biogeochemical features of these CHs and associated spatial patterns across the glacier are still unknown. Here we hypothesized about the CH minerogenic composition between the different sources such as the medial moraine and other zones. Further, we intended to investigate if the depth of the CH mirrors the CH community composition, organic matter (OM) content and would support productivity. In this study we show that both microbial communities and biogeochemical parameters in CHs were significantly different between the zones medial moraine and the glacier terminus. Variations in microbial community composition are the result of factors such as depth, diameter, organic matter, total carbon, particle size, and mineral diversity. More than 90% of all ribosomal sequence variants (RSV) reads were classified as Proteobacteria, Cyanobacteria, Bacteroidetes, Actinobacteria, and Acidobacteria. Archaea were detected in 85% of all samples and exclusively belonged to the classes Halobacteria, Methanomicrobia, and Thermoplasmata. The most abundant genus was *Halorubrum* (Halobacteria) and was identified in nine RSVs. The core microbiome for bacteria comprised 30 RSVs that were affiliated with Cyanobacteria, Bacteroidetes, Actinobacteria, and Proteobacteria. The archaeal fraction of the core microbiome consisted of three RSVs belonging to unknown genera of Methanomicrobiales and Thermoplasmatales and the genus *Rice_Cluster_I* (Methanocellales). Further, mean bacterial carbon production in cryoconite was exceptionally low and similar rates have not been reported elsewhere. However, bacterial carbon production insignificantly trended toward higher rates in shallow CHs and did not seem to be supported by accumulation of OM and nutrients, respectively, in deeper holes. OM fractions were significantly different between shallower CHs along

OPEN ACCESS

Edited by:
Jennifer F. Biddle, University of Delaware, United States

Reviewed by:
Anne D. Jungblut, Natural History Museum, United Kingdom
Nozomu Takeuchi, Chiba University, Japan

***Correspondence:**
Birgit Sattler
Birgit.Sattler@uibk.ac.at

Specialty section:
This article was submitted to Extreme Microbiology, a section of the journal Frontiers in Microbiology

Received: *02 March 2020*
Accepted: *07 May 2020*
Published: *03 June 2020*

Citation:
Weisleitner K, Perras AK, Unterberger SH, Moissl-Eichinger C, Andersen DT and Sattler B (2020) Cryoconite Hole Location in East-Antarctic Untersee Oasis Shapes Physical and Biological Diversity. Front. Microbiol. 11:1165. doi: 10.3389/fmicb.2020.01165

the medial moraine and deeper CHs at the glacier terminus. Overall, our findings suggest that wind-blown material originating south and southeast of the Anuchin Glacier and deposits from a nunatak are assumed to be local inoculation sources. High sequence similarities between samples from the Untersee Oasis and other Antarctic sites further indicate long-range atmospheric transport mechanisms that complement local inoculation sources.

Keywords: Anuchin Glacier, 16S rRNA, cryoconite holes, mineralogy, archaea, bacterial activity, biogeochemistry

INTRODUCTION

One typical characteristic of glaciers and ice sheets is the occurrence of cryoconite holes (CHs). These small water bodies form when dark organic and inorganic debris attach to ice surfaces and consequently decrease the albedo locally (Anesio et al., 2009). Solar irradiation promotes melting of the matter into deeper ice layers until the rates of downward movement and surface ice ablation enter a steady state equilibrium (Gribbon, 1979; Hodson et al., 2013). The basins are filled with sediments in the bottom and liquid water on the top (Takeuchi et al., 2001).

In the late 19th century, A. E. Nordenskiöld recognized the ecological importance of these miniature lakes on the Greenland ice sheet (Leslie, 2011). About one hundred years later, CH research was pioneered in Antarctica by Wharton et al. (1981) however, despite the gained knowledge and recent technological advances, they remain a "dark biological secret of the cryosphere" (Cook et al., 2016).

CHs are currently perceived as microbial hotspots (Edwards et al., 2013; Weisleitner et al., 2019a) because their biodiversity and productivity are much higher than in other supraglacial zones (Anesio et al., 2009; Cook et al., 2016). The presence of viruses, bacteria, micro-algae, fungi, protozoa, and sometimes metazoans indicate that CHs are simple trophic systems (Mueller et al., 2001; Mueller and Pollard, 2004; Porazinska et al., 2004; Hodson et al., 2008; Sommers et al., 2019). Primary producers such as cyanobacteria fix inorganic carbon via photosynthesis and provide nutrients for the heterotrophic fraction of the community (Mueller et al., 2001; Morgan-Kiss et al., 2006; Bagshaw et al., 2016). Production and respiration rates are mainly controlled by light availability and temperature regime and hence changes seasonally (Bagshaw et al., 2016). During austral summer, primary production can exceed respiration and liquid water may persist for up to 10 weeks in Antarctic CHs. This effect may be reversed during the dark season (Fountain et al., 2004; Bagshaw et al., 2007).

Biological processes within CHs play an important role in both local and downstream environments (Anesio et al., 2010). For example the build-up of dark organic matter (OM) within CHs enhances local supraglacial melt rates (Takeuchi et al., 2001) and hence increases the water availability within CHs. Further, in comparison to hydrologically connected CHs, isolated ones promote recycling and production of nutrients and hence support downstream ecosystems once being re-connected to a hydrological system (Bagshaw et al., 2007; Samui et al., 2018). Such a nutrient flush can be caused by a warming event as recorded in the McMurdo Dry Valleys (MDVs) that led to a temporarily increased primary production in Lake Fryxell (Bagshaw et al., 2013). Further, CH bacterial communities from the Anuchin Glacier damming the perennially ice-covered Lake Untersee (East-Antarctica) were identified as important microbial source inoculum for benthic microbial communities that occur in the lake (Weisleitner et al., 2019b). However, the question is still open how relevant those supraglacial communities are for the local carbon production. Antarctic productivity within CHs is generally extremely low and is hampered by harsh conditions (Foreman et al., 2007).

Compared to CHs from other regions such as the Alps or the High Arctic, where the limiting factor of a permanent ice cover of CHs is mostly missing, those in Antarctica often form perennial ice-lids and therefore attenuate most of the incoming photosynthetically active irradiation (PAR) before reaching the bottom of the CHs (Fountain et al., 2004). Also, Antarctic conditions such as low temperatures and strong katabatic winds reduce the occurrence of surface waters and therefore may increase the longevity of Antarctic CHs compared to their counterparts from other glaciated regions which may be flushed more frequently (Hodson et al., 2008) as a result of melt. Measurements of excess Cl^- in ice-lidded CHs from the Canada glacier suggest these habitats persist for up to 5 years (Bagshaw et al., 2007). In contrast, the first reported Antarctic radiocarbon data from CHs indicate that they may occur in isolation for even thousands of years (Lutz et al., 2019) and could provide long-term refugia for unfavorable conditions which were found during snowball earth (Vincent et al., 2000). Isolation also prevents further inoculation by bioaerosols once the lid is formed. Although being separated from the atmosphere, microbial communities in spatially close CHs are more similar to each other compared to those that are separated at a larger scale (Darcy et al., 2018), indicating that local sources lead to the formation of CHs and hence should be considered as an important aspect in the colonization of CHs (Webster-Brown et al., 2015).

In contrast to Alpine and Arctic regions the number of Antarctic CH studies is low and mostly limited to glaciers around the MDVs (e.g., Christner et al., 2003; Fountain et al., 2004, 2008; Porazinska et al., 2004; Fortner et al., 2005; Bagshaw et al., 2007, 2016; Foreman et al., 2007; Telling et al., 2014; Webster-Brown et al., 2015; MacDonell et al., 2016) with some geographical exceptions (e.g., Cameron et al., 2012; Hodson et al., 2013; Obbels et al., 2016; Zdanowski et al., 2017). Hence, compared to the "prime study sites" such as the MDVs, little is known about the

microbial ecology in CHs from e.g., Queen Maud Land (East-Antarctica). There, only a handful of studies were conducted (e.g., Obbels et al., 2016; Samui et al., 2018; Lutz et al., 2019; Weisleitner et al., 2019b) although this pristine area exceeds the size of Greenland and hence is under-represented on a geographical scale. One of the main study areas in Queen Maud Land is Lake Untersee with the adjacent Anuchin glacier from which microbial diversity and various inoculation vectors have been investigated, however, there is no information about activity within their ice-sealed environments.

For the past 10 years, the Anuchin Glacier in the Lake Untersee Oasis has been serving as a model habitat for these environments to shed light on microbial and biogeochemical processes outside the core location near McMurdo. CHs from glaciers have been identified as important source inoculum for the adjacent perennially ice-covered lakes as it has been shown for Anuchin Glacier and its role for Lake Untersee (Weisleitner et al., 2019b). Very little is known about the minerogenic composition and its role as nutrient source for microbial communities, or how active microbial communities can be under the peculiarity of permanently ice-covered CHs. Which role can we attribute bacteria in terms of carbon producers? In this study we further characterized these CHs by determining its archaeal and bacterial diversity and defined a core microbiome. Further, we explored local temperature variations within the ice matrix as proxy for cryoconite temperature conditions. We hypothesized (1) that the CH minerogenic composition differed between the medial moraine and those from other zones, and (2) that the CH community composition, OM content and productivity are mirrored by the depth of the CH due to possible accumulation.

STUDY SITE

The north-south orientated Anuchin Glacier is located in the Gruber Mountains (71.348°S, 13.517°E, **Figure 1**) and formed after the last glacial maximum (Schwab, 1998). It extends over an area of ∼34 km^2 (length ∼8 km, width 4.2 ± 1.2 km). A geodetic survey (Wand and Perlt, 1999) and interferometric synthetic-aperture measurements (Rignot et al., 2014) indicate that the glacier surface speed is ∼9 m a^{-1}. A similar flow speed (8.4 m a^{-1}) was recently reported by Faucher et al. (2019). The elevation difference between 8 km up-glacier and the glacier terminus is 218 m, corresponding to an average slope angle of 1.56° along the medial moraine (REMA dataset, Howat et al., 2018). The Anuchin Glacier dams the perennially ice-covered Lake Untersee at its northern end which is known for its modern, large conical stromatolites and its anoxic sub-basin with exceptional high methane production rates (Wand et al., 2006; Andersen et al., 2011). Supraglacial melt does not provide water for recharge but subaqueous glacier melt contributes 40–45% to the annual lake water budget which is likely complemented by subglacial inputs (Faucher et al., 2019). Lake Untersee has no outlet and hence water loss occurs by ablation of the ice cover (Hermichen et al., 1985). Here, the dominating ablation process is sublimation as a result of low summer temperatures and strong katabatic winds, reaching up to 40–75 cm a^{-1} (Andersen et al., 2015; Faucher et al., 2019). Similar ablation rates (50–60 cm a^{-1}) were measured at the lower part of the Anuchin Glacier (Wand et al., 2006). However, rates within the blue ice zone between the nearby Schirmacher and Untersee Oasis are significantly lower (5–15 cm a^{-1}, Scheinert et al., 2006), indicating that local meteorological conditions within the oasis promote ablation.

MATERIALS AND METHODS

Sampling

During November and December 2015 fourteen CHs were collected across the Anuchin Glacier. Four sites were grouped into two zones, namely "medial moraine" and "glacier terminus" (**Figure 2A**). The first zone "glacier terminus" (**Figure 2B**) included a site north of an ice ridge that separated the glacier ice from the lake ice (Anuchin North of Ridge, ANR) and the white ice patch that appears to be glacial ice embedded in the lake ice cover of Lake Untersee (White Ice Patch, WIP). The second zone was located further up-glacier along the medial moraine (Anuchin Moraine High, AMH) and at the lower part of the medial moraine (Anuchin Moraine Low, AML). At least 3 CHs were collected at each site. Representative medial moraine sites and a typical CH are shown in **Figures 2C,D**, respectively.

Depending on the depth of the CHs, samples were either collected with an ethanol-rinsed Kovacs ice corer (Mark III, 7.25 cm diameter) in combination with a Boschhammer GBH 36V-LI PLUS electrical drill or with a sterile spatula after removal of surface ice using a sterilized ice ax or chisel. For each hole, GPS location, diameter and depth were recorded. All samples were stored in sterile polyethylene bags and kept frozen until the end of the expedition and then shipped via Cape Town to the University of Innsbruck and subsequently stored at −20°C until further use.

Temperature Depth Profile Time Series

To study differences in the temperature regime of CHs, three sites that represented the medial moraine (AML/AMH), ANR and WIP were chosen. In contrast to ice at the medial moraine that was dark-colored and interspersed with particulates (**Figure 2C**), ice at the site ANR appeared white and macroscopically free of particles. Despite being embedded within the ice cover of Lake Untersee, the site WIP appeared like ice from the site ANR.

At each site, a 1 m deep hole was drilled and three Tidbit temperature loggers (accuracy ± 0.21°C from 0 to 50°C) were attached to a line and then placed into the hole at an initial depth of 1 m, 0.5 m and just below the surface (referred to as 0 m), respectively. The holes were re-filled with small pieces of ice once the loggers were put in place. Sensor readings were logged with an interval of 15 min and covered a period of 11 days (28.11.2015 – 08.12.2015. To ensure that the temperature loggers being used did not inadvertently skew the *in situ* cryoconite readings, the albedo was compared between the loggers and other CHs with a custom-built device utilizing an Ibsen OEM FHT-315 spectrometer. Milled samples were illuminated with a white LED and a tungsten filament and spectral reflectances of cryoconite and temperature loggers were recorded in a range of 470–1100 nm under identical light conditions. To allow a

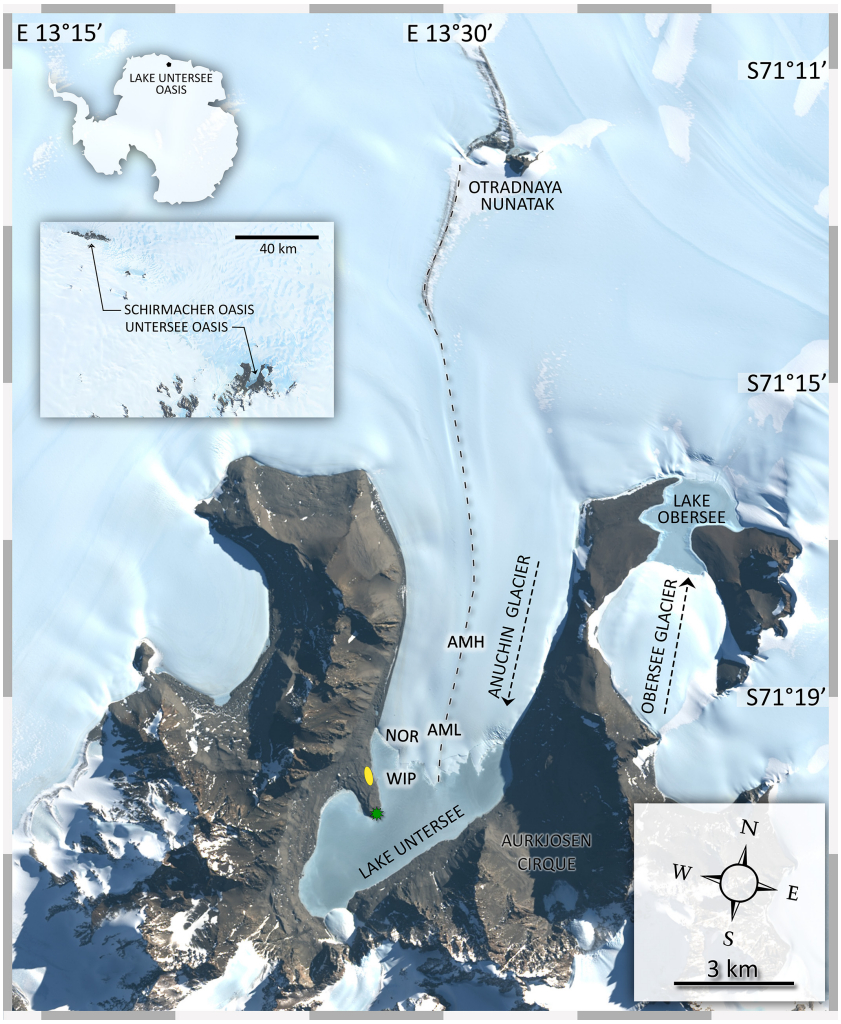

FIGURE 1 | Map of the study site. The insert map indicates the position of the study site in context with the Schirmacher Oasis. Lake Untersee (610 m a.s.l.) and Lake Obersee (805 m a.s.l.) are partly connected by the Anuchin Glacier. The position of the sampling sites for CHs (zone "medial moraine": AMH, AML, zone "glacier terminus": ANR, WIP) are indicated in the map. The green star shows the location of a meteorological station and the yellow ellipse depicts the position of the campsite during the expedition. The dashed line along the glacier indicates the position of the medial moraine. The flow directions of the Anuchin Glacier and the "Obersee Glacier" are indicated by dashed arrows. The image was captured by the Landsat 8 satellite on 09 MARCH 2019 (download via Earth Explorer by United States Geographical Survey). The true color image (4-3-2 RGB, 30 m px^{-1}) was combined with the high-resolution band 8 (grayscale, 15 m px^{-1}).

direct comparison, the integration time was adjusted to the brightest measured sample and then left unchanged for all other samples (**Supplementary Figure 1**). Further, solar radiation, soil temperatures (sensors buried at 0.01, 0.10, 0.22 m) and air temperature records from an automatic weather station operating at the shore of Lake Untersee (location shown in **Figure 1**) has been used (Andersen et al., 2015). Descriptive statistics were calculated with the R packages"Psych" (Revelle, 2019) and permutation distribution clustering was performed with the R package "PDC" (Brandmaier, 2015). Heatmaps were created with the R package ggplot2 (Wickham, 2011).

Particle Size

The following analyses including sub header 3.5 were done on sediments collected from CHs. Gravimetric particle size distribution was determined by sieving into five fractions (>400 μm, 100–400 μm, 40–100 μm, 10–40 μm, and <10 μm). Large fractions were dry sieved, and the two smallest fractions were wet sieved. Next, the samples were dried in pre-weighted containers at 40°C before determining the dry weight. The respective particle size distribution was expressed as the relative mass proportion per sample. The particle size distributions were visualized in a ternary plot using the R package "ggtern" (Hamilton and Ferry, 2018).

X-Ray Diffraction (XRD) and Thermogravimetric Analysis (TGA)

Samples for X-ray diffraction and thermogravimetric analysis were dried at 70°C for 48 h and subsequently milled with a

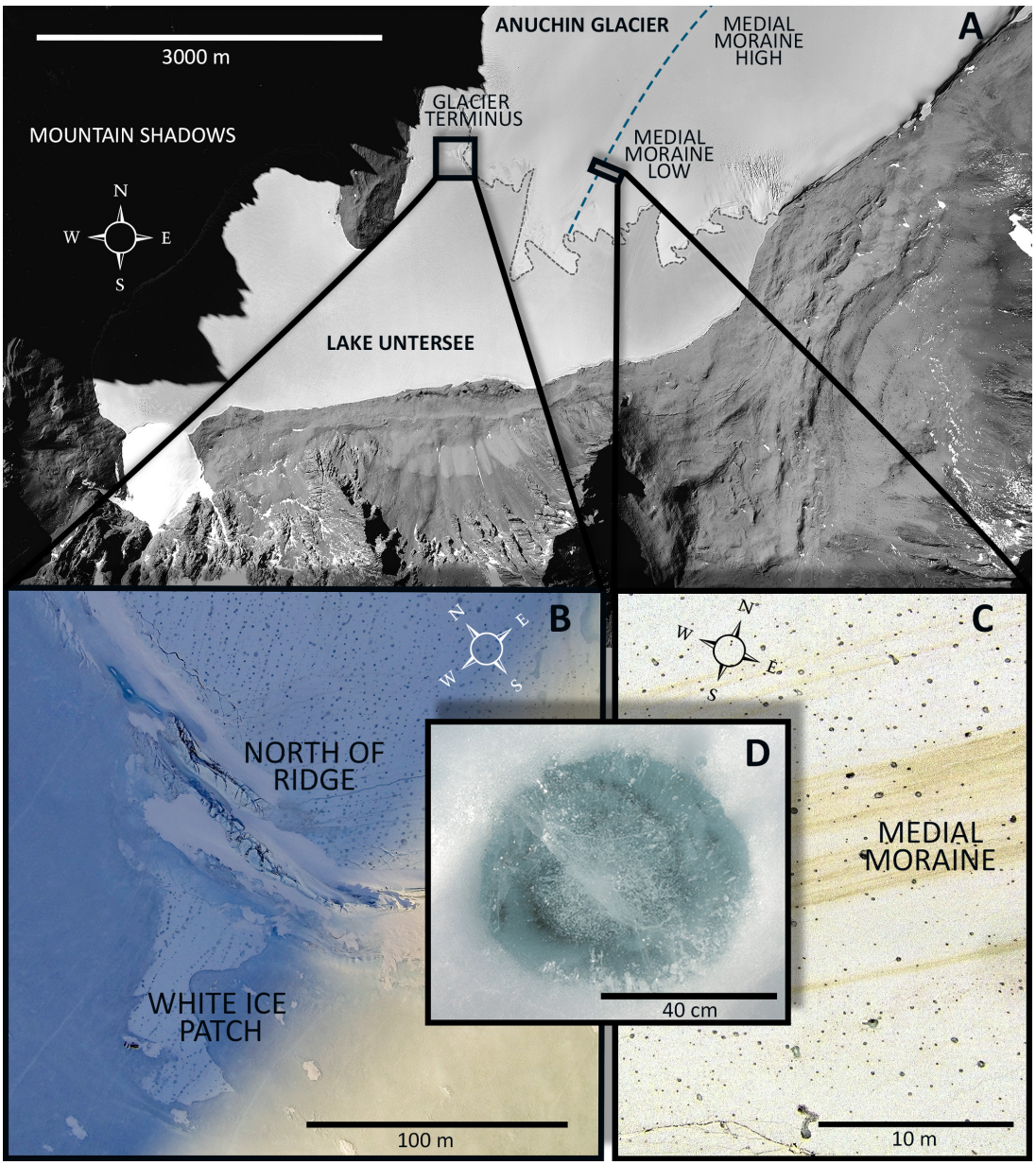

FIGURE 2 | (A) Aerial image of Lake Untersee and the lower part of the Anuchin Glacier (Bundesamt für Kartographie und Geodäsie, Frankfurt am Main, Germany). The medial moraine is indicated by a dashed blue line. The glacier-lake interface is indicated by a gray dashed line. **(B)** Aerial overview of the zone "glacier terminus." **(C)** Level and contrast enhanced aerial image showing a representative site along the medial moraine. **(D)** Typical morphology of an ice-lidded cryoconite hole from the Anuchin Glacier. Note that the orientations in **Figures 2A–C** differ from each other.

Retsch MS 1100 high-speed micromill equipped with an agate-beaker for 3 min.

Powder X-ray Diffraction (XRD)

The mineralogical composition in the homogenous powder was analyzed with a Panalytical Empyrean XRD diffractometer equipped with a monochromator and a 1D Pixel detector. XRD measurements were carried out with Cu Kα radiation operating at 40 kV and 40 mA. Spectra were collected over a 2θ range of 5–70° in 0.013 steps with a scan speed of 0.16° s^{-1} resulting in a total scan time of 7 min. All samples were measured using a standard sample holder except samples having insufficient mass (CRY1, CRY2) were measured using a silicon crystal sample holder. Spectra were analyzed using a Bruker DiffracEVA software by comparing with PDF2 patterns.

Thermogravimetric Analysis (TGA)

The total amount of OM was estimated by thermogravimetric analysis. Between 100 to 150 mg of dried and milled cryoconite sediment samples were loaded into a Netzsch STA 449. Weight

loss was recorded continuously while samples were heated at 10 K min^{-1} from 25°C up to 1000°C. Mass loss was calculated for the following temperature intervals: 38–105°C, 105–200°C, 200–350°C, 350–520°C, and 520–1000°C. STGA analysis enabled a differentiation between thermo-labile (200–350°C) and thermo-stable (350–520°C) OM. This classification was also used by Smith et al. (2016) for Antarctic CHs in the MDVs. The detection limit was set to Δ0.1% which corresponded to Δ10–15 μg OM – depending on the initial mass load in the thermal analyzer. This threshold was well above the measurement precision of the instrument (0.1 μg).

Total Carbon, Nitrogen, and Phosphorus

For total carbon and nitrogen analysis 50 mg of milled samples were transferred into tin capsules and combusted in a Nitrogen and Carbon Analyzer in the NC soils configuration (Flash EA 1112, Thermofisher Scientific). Acetanilide was used for the calibration line. The percentage of carbon and nitrogen was then referred to the sample mass as total C (mg g^{-1}) and total N (mg g^{-1}).

Total phosphorus was quantified with the molybdate method after Vogler (1966). Briefly, pre-weighed and pulverized sediments were suspended in deionized water, sulfuric acid and then heated to 160°C for 12 h. Next, the samples were oxidized with hydrogen peroxide, diluted with distilled water and cooled down to room temperature. Then, ascorbic acid (10%) and sodium hydroxide (20%) were added. After neutralizing the samples with Vogler solution, the absorbance features were measured against a H_3PO_4 standard (Tritisol, Merck, Darmstadt, Germany) at 885 nm with a U-2001 spectrophotometer (Hitachi, Tokyo, Japan).

Scanning Electron Microscopy (SEM)

For representative SEM images, 250 μL of dislodged cell-extract (Duhamel and Jacquet, 2006) and untreated samples were filtered onto 0.2 μm polycarbonate filters (Osmonics, DK) and dried overnight at 40°C. Samples were sputtered with tungsten and subsequent SEM images were recorded with a Quanta 3D 200 Double Beam SEM microscope (FEI, Eindhoven, Netherlands) using 20,000x magnification and 0.3 mbar at an acceleration voltage of 5.0 kV.

Microbial Abundance

Melted cryoconite was subsampled and weighed. Dry weights were calculated from aliquots after water removal at 70°C for 48 h. Next, cells were dislodged according to the protocol of Duhamel and Jacquet (2006) which is based on both; chemical (tween 80, pyrophosphate, formaline) and physical (sonic bath, pre-filtration and centrifugation) treatment. Then, 250 μl aliquots from the cell suspensions were diluted with 750 μl MilliQ water, stained with DAPI (4',6-Diamidine-2-phenylindol) at a final concentration of 0.2% v/v (Porter and Feig, 1980) and then filtered onto 0.2 μm polycarbonate filters (Osmonics, DK). Images were recorded with an Axiocam HRc attached to a Carl Zeiss Imager Z1 microscope using a 63x oil lens. For each sample aliquot, 40 randomly selected areas were photographed using a 365 nm excitation source and the filter set EX G 365, BS FT 395, EM BP 445/50. Cells were enumerated with the cell counter plugin within the imaging analysis software Fiji (Schindelin et al., 2012).

Bacterial Activity

Bacterial activity was estimated by the incorporation of ^{3}H-leucine by the micro-centrifuge method (Kirchman, 2001). Incubation for all samples took place under simulated *in situ* temperature conditions (0.1°C) in HAAKE water baths. ^{3}H-leucine was added with a final concentration of 40 nM to sample triplicates with ca. 1.5 mL of a mixture of sediment and water and two formalin-killed control samples. After 72 h, the incubation was terminated with 90 μL of 100% trichloroacetic acid (TCA). Next, the samples were centrifuged at 16,000 *g* for 10 min and then washed, centrifuged again and the supernatant was aspirated with 5% TCA and 80% EtOH. The final supernatant was aspirated and the remaining sediment weighted for the calculation of bacterial production. The samples were measured in a liquid scintillation counter (Beckman LSC 6000 IC) after adding 1 mL of scintillation cocktail (Beckman Ready Safe).

Microbial Community Composition and Statistics

Sample Processing and Next Generation Sequence Analysis

Cryoconite samples were carefully thawed and DNA was extracted with a PowerSoil DNA isolation kit. The 16S rRNA gene amplicons were generated with Illumina-tagged universal primers F515 and R806 as proposed by the Human Microbiome Project (Caporaso et al., 2012). For Archaea, primers 344f and 915r (Klindworth et al., 2013) in combination with a subsequent nested PCR approach with the primer pair S-D-Arch-0519-a-S-15/S-D-Bact-0785-b-A-18 were used (Koskinen et al., 2017). Next, library preparation and MiSeq sequencing were performed (Klymiuk et al., 2016). The R package DADA2 was used to process and filter the raw sequences according to the proposed pipeline (Callahan et al., 2016) and the taxonomy was assigned to the SILVA database (Quast et al., 2013). This procedure resulted in a Ribosomal Sequence Variants table (RSV). A more detailed workflow covering all steps from sample processing to NGS analysis and the use of negative controls is outlined in Weisleitner et al. (2019b) and references therein. Sequence accession numbers are listed in **Supplementary Table 1**.

Statistical Analysis

Based on the RSV table, alpha and beta diversity were calculated using the R package Phyloseq (ver 1.20.0) (McMurdie and Holmes, 2013). To compare the single sites (AML, AMH, ANR, WIP) and the zones (medial moraine, glacier terminus), Shannon, Observed and Inverse Simpson indices were compared. As previously discussed, counts were not rarefied (McMurdie and Holmes, 2014; Weisleitner et al., 2019b). The data distribution was tested with a Shapiro–Wilk test and depending on the outcome, significant differences were either tested with a Kruskal–Wallis test (for not normally distributed data) or with an Analysis of Variance (ANOVA, for normally distributed data). Dunn's test with Bonferroni correction was used as *post hoc* test.

We also tested for significantly different abundant taxa between samples from the medial moraine and outside the medial moraine following the R package DESEQ 2 (v.1.20.0) pipeline (Love et al., 2014). Differences in microbial communities between sites were visualized with a Principal Coordinates Analysis (PCoA, R package Phyloseq). Analysis of similarities (ANOSIM) based on a Bray–Curtis RSV dissimilarity matrix and PERMANOVA were calculated with the R package vegan (Oksanen et al., 2007).

The core microbiome was defined as RSVs that had a larger or equal average relative abundance of 0.1% across all sites (AMH, AML, ANR, WIP) - but not necessarily within all single samples. To put the core microbiome into context with other RSVs, the mean relative abundances across all sites of the core microbiome and RSVs that occurred at less sites with a mean relative abundance $\geq$0.1% were plotted in a sunburst diagram using the browser-based tool RawGraphs (Mauri et al., 2017).

For the metadata set, residual diagnostics were performed for all variables. Those that did not meet the criteria for analysis of variance (ANOVA) were log10 transformed and re-tested. ANOVA and Tukey's *post hoc* test were then used to test for significant differences between all four sites (AML, AMH, WIP, ANR). Differences between the zones medial moraine (AML, AMH) and the glacier terminus (ANR, WIP) were compared with Welch's *t*-test.

We used non-parametric statistical tests for log10 transformed variables that did not meet all criteria for the above-mentioned statistical approaches (TC, mineral diversity, Kruskal–Wallis test – instead of ANOVA or Mann–Whitney test – instead of Welch's *t*-test). Further, a principal component analysis (PCA) of all variables was computed to explain variations between sites.

RESULTS

Mineral Composition and Particle Size

In total 13 different minerals were identified (**Figure 3A**). The mineral diversity differed significantly between zones (Mann–Whitney *U* test, $W = 5.5$, p-value = 0.01696) and generally decreased with depth (Pearson correlation, adj. $r^2 = 0.36$, $p = 0.001$). The average mineral diversity was higher along the medial moraine (AMH: 7.25 $\pm$ 1.26, AML: 7.25 $\pm$ 2.75) than at the glacier terminus (ANR: 5 $\pm$ 0, WIP: 4.67 $\pm$ 0.58) and inferred that also the mineral composition differed between samples collected along the medial moraine (AMH, AML) and those from regions closer to Lake Untersee (ANR, WIP). Albite, Anorthite, Biotite, and Quartz were found in all samples except C8 and C9 which lacked Albite. Samples C1 and C2 harbored only four different minerals while C3 contained 10 different minerals. Sanidine, Grossular, Microcline, Sodium Aluminum Silicate, Rutile, Clinochlore, Chamosite, and Laumontite absent at the glacier terminus (**Figure 3A**).

Particle sizes were classified into five groups (>10 μm, 10–40 μm, 40–100 μm, 100–400 μm, >400 μm) and varied across the sites. CHs along the medial moraine had a slightly higher frequency of small particles compared to those from the glacier terminus (**Figure 3B**). The particle fraction 40–100 μm differed significantly between ANR-AMH, ANR-AML and WIP-AML [ANOVA, $F(3,10) = 7.047$, $p = 0.008$, Tukey's *post hoc* test] and the ratio of combined particle sizes < 100 μm and >100 μm increased with CH depth (Pearson correlation, adj. $r^2 = 0.37$, $p = 0.012$). The complete particle size distribution is shown in **Supplementary Figure 2** and representative SEM images of minerals are depicted in **Supplementary Figure 3**.

Proxy for Cryoconite Hole *in situ* Temperatures

The coldest overall mean CH proxy temperatures across all depths were recorded at the Anuchin Glacier (clean ice: −2.19 $\pm$ 4.73°C, medial moraine: −2.02 $\pm$ 3.12°C) while WIP was slightly warmer (−1.7 $\pm$ 3.14°C). Mean temperatures and temperature fluctuations across all sites decreased with depth (surface: 0.69 $\pm$ 5.24°C, middle: −2.51 $\pm$ 1.29°C, bottom: −4.09 $\pm$ 1.03°C). Further, the strongest temperature decrease with depth was at the clean ice (0.63°C 10 cm^{-1}) followed by the medial moraine (0.50°C 10 cm^{-1}) and the white ice patch (0.30°C 10 cm^{-1}). Further, Pearson correlation coefficients calculated from ambient air temperature (−1.9 $\pm$ 2.64°C) and the temperature loggers indicated that temperature dynamics at the medial moraine were more de-coupled from the air temperature ($r^2 = 0.64$) compared to the WIP ($r^2 = 0.68$) and clean ice site ($r^2 = 0.79$). This was confirmed by permutation distribution clustering (**Supplementary Figure 4**) which showed that air temperature and surface ice temperatures at the glacier were more similar than the surface temperature of the white ice patch despite being geographically closer to the automatic weather station that recorded ambient air temperatures 2 m above lake level and soil temperatures at various depths (Andersen et al., 2015).

The largest temperature difference between the surface and 1 m below the ice was recorded in clear ice (22.34°C). Average soil temperature differences between 0.01, 0.1, and 0.22 m depth were 9.51 and 9.91°C, respectively. Negative temperature differences (i.e., warmer ice at 1 m depth compared to the surface ice) were recorded at all sites except for the soils and the maximum was reached during the night at the WIP site (−3.55°C, **Figure 4** – top row). For sites at the glacier, negative differences between ice and air temperatures were observed more frequently at the ice surface while this was more common across all depths at the site WIP (**Figure 4** – bottom row).

Physical and Biogeochemical Characteristics

CH depths ranged from 0 to 62 cm and were on average 3.75 times deeper at the glacier terminus than those along the medial moraine [ANOVA, $F(3,10) = 130.9$, $p \leq 0.001$]. The sites within these zones differed by a factor 2.2 for the medial moraine (AML vs. AMH) and by 1.5 for the glacier terminus (ANR vs. WIP) and at least one sample was located every 10 cm across the full depth range (**Figure 5**). Deeper CH layers also trended toward larger CH diameter (Pearson correlation adj. $r^2 = 0.5$, $p = 0.029$) and were significantly different between the zones (Welch test: $t = -2.925$, df = 7.0437, p-value = 0.02203).

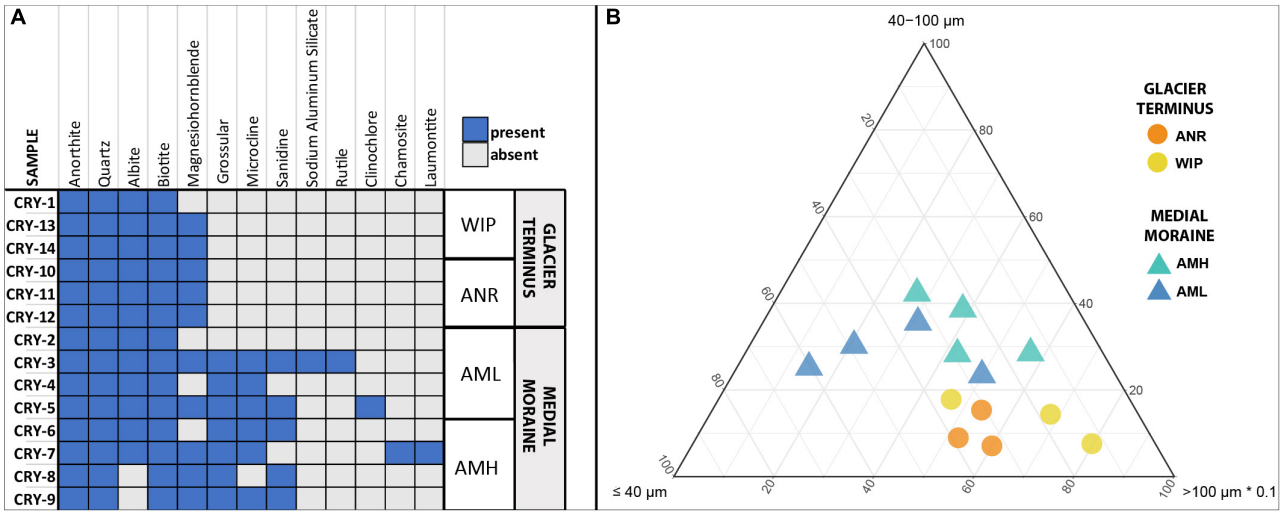

FIGURE 3 | (A) Site occurrences of minerals based on XRD measurements. **(B)** Ternary plot of particle sizes. Size classes were combined to capture all data within one plot (x ≤ 10 µm + 10 – 40 µm, *y* = 40 – 100 µm, *z* = 100 – 400 µm + >400 µm). Note that the *z*-axis is scaled with factor 0.1.

Total phosphorus contents in cryoconite were similar across all sites (0.51 – 0.53 mg g^{-1}) and C/N ratios were slightly higher at the glacier terminus than at the medial moraine (8.93 ± 4.39 and 6.37 ± 3.24, respectively). More pronounced differences [$F(3,10) = 10.12$, $p = 0.00225$] were observed for total nitrogen that ranged on average per site from 0.07 ± 0.03 mg g^{-1} at AML to 0.23 ± 0.05 mg g^{-1} at WIP. Also, total carbon contents were higher at the glacier terminus (Mann–Whitney *U* test, $W = 43$, *p*-value = 0.01265) and varied between 0.58 ± 0.30 mg g^{-1} at AML and 2.52 ± 1.77 mg g^{-1} at the site WIP (**Figure 6**).

Bacterial carbon production (BCP) was exceptionally low at all sites and ranged between $1.07*10^{-07}$ and $1.49*10^{-05}$ µg C g dw^{-1} h^{-1} (AMH: $1.28*10^{-06}$ ± $4.80*10^{-07}$ µg C g dw^{-1} h^{-1}, AML: $7.61*10^{-07}$ ± $9.12*10^{-07}$ µg C g dw^{-1} h^{-1}, ANR: $2.61*10^{-07}$ ± $1.77*10^{-07}$ µg C g dw^{-1} h^{-1}, WIP: $4.43*10^{-07}$ ± $0.94*10^{-07}$ µg C g dw^{-1} h^{-1}). CRY2 was not within the interquartile range as the BCP rate was two orders of magnitudes higher than most other samples. BCP generally decreased with depth (Pearson correlation, adj. $r^2 = 0.15$, $p = 0.1106$) and was not significantly different between sites (**Figure 6**).

Further, labile [ANOVA, $F(3,9) = 5.145$, $p = 0.0241$] and stable OM contents [ANOVA, $F(3,9) = 12.1$, $p = 0.00164$] were higher at the glacier terminus and correlated positively with depth (labile OM: adj. $r^2 = 0.6$, $p = 0.001$, stable OM: adj. $r^2 = 0.4$, $p = 0.012$). Consequently, total OM (sum of labile and stable OM fractions) showed the same trends (**Supplementary Figure 5**). In contrast, mean cell abundances were in the same order of magnitude at the medial moraine ($1.97*10^7$ ± $1.64*10^7$ cells g dw^{-1}) and the glacier terminus ($2.25*10^7$ ± $1.32*10^7$ cells g dw^{-1}) and did not follow any strong pattern along the depth gradient.

Descriptive statistics of all variables are listed in **Table 1** and selected variables plotted along a depth gradient are shown in **Figure 5**. Further, boxplots from most variables and corresponding statistical analyses are depicted in **Figure 6**.

Next, we performed a PCA to define dissimilarities between sites and variables that accounted for these differences (**Figure 7**). The first two PCA axes explained 62.2% of the data variability. CHs from the glacier terminus clustered separately and were more similar to each other than those from the medial moraine. The zone glacier terminus was positively correlated with depth, diameter, total nitrogen, and total carbon.

Microbial Community Composition

Bacteria

Amplicon sequencing for bacteria resulted in a total of 271,152 read counts ranging from 3,545 (CRY5) to 27,714 (CRY4) resulting in 559 taxonomic observations within 14 samples. CHs were dominated by Proteobacteria (26.54%, 197 RSVs), Cyanobacteria (25.45%, 25 RSVs), Bacteroidetes (23.49%, 118 RSVs), Actinobacteria (13.38%, 48 RSVs), and Acidobacteria (3.20%, 19 RSVs) which made up 92% of all counts. 12.05 and 1.98% of RSVs could not be assigned to a known genus or phylum, respectively. The two most abundant RSVs that were assigned on genus level belonged to the phylum Cyanobacteria (*Tychonema* 10.04%, *Chamaesiphon* 9.82%). The 100 most abundant bacteria related RSVs are depicted in **Figure 8A**.

Archaea

Archaea have been identified with the nested PCR approach in all CHs except in samples (CRY2, CRY10). Within the 12 remaining samples 88,149 read counts allocated to 24 RSVs and 14 of them were affiliated with the order Halobacteriales (89.1% of all counts). Members of Methanomicrobiales accounted for 10.01% of the reads and were affiliated to five RSVs. Combining counts from the remaining five sequences made up less than one percent and belonged to Methanocellales, Methanosarcinales, Thermoplasmatales. One RSV belonging to the genus *Halorubrum* accounted for 65.48% of all archaea

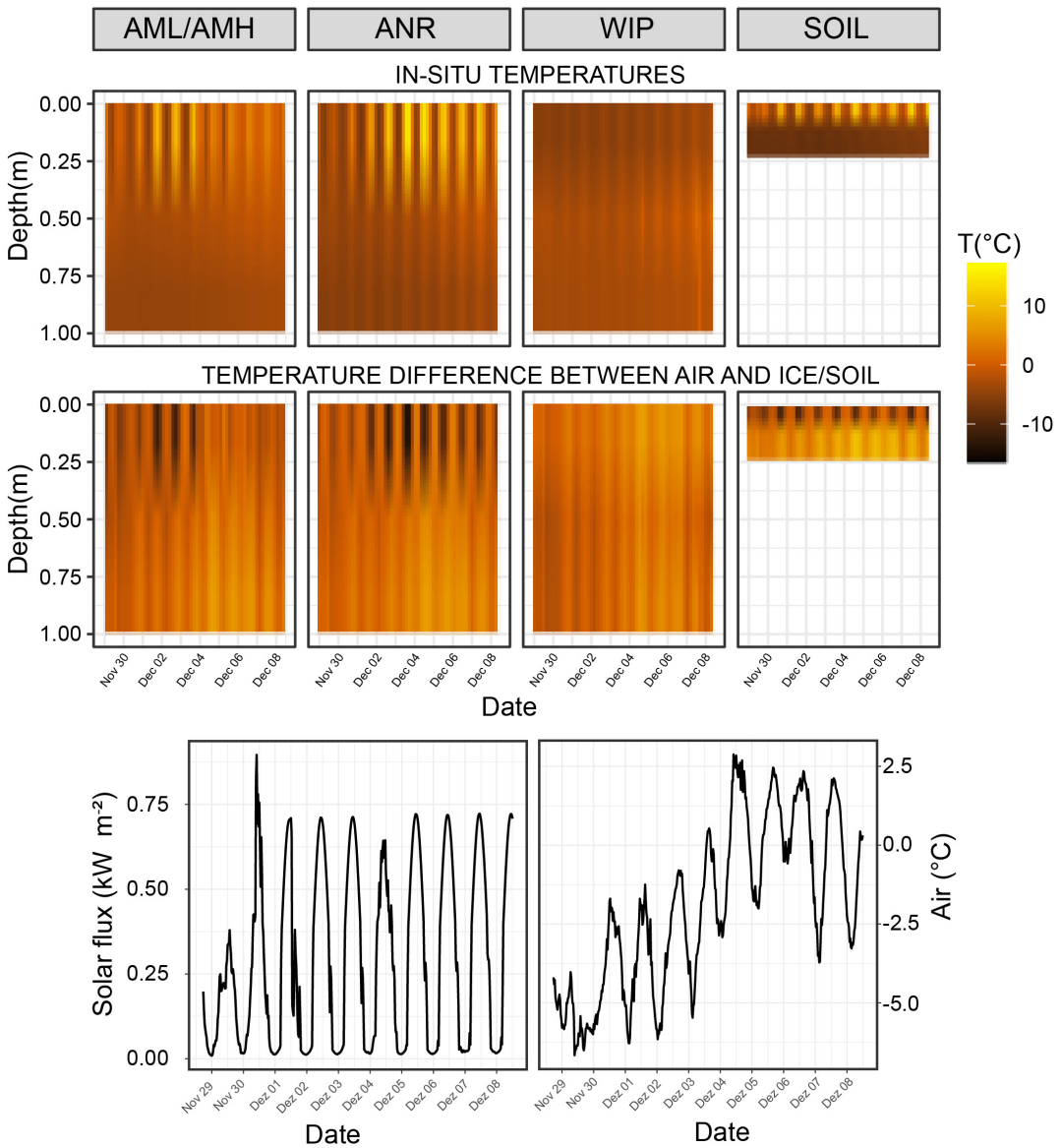

FIGURE 4 | Top row: Temperature time series of interpolated depth gradient. Temperature loggers were installed at 0, 0.5, and 1.0 m deep in the ice covers, respectively. Temperature probes for the soil time series were buried at 0.01, 0.1, and 0.22 m depth. **Bottom row:** Temperature differences between air temperature and CH/soil.

specific counts. The relative abundance of all archaeal RSVs at family level is depicted in **Figure 8B**.

Alpha Diversity

For alpha diversity, the indices "Observed," "InvSimpson" (both residuals normally distributed, Shapiro–Wilk test: "Observed" $p = 0.3994$, "InvSimpson" $p = 0.5301$) and "Shannon" (residuals not normally distributed, Shapiro–Wilk test: $p = 0.04203$) were calculated. An analysis of variance (ANOVA) was used for testing significant differences between sites for the indices "Observed" and "InvSimpson." For the Shannon index, the Kruskal–Wallis test was used. None of the indices indicated significant differences between the sites. This was also true for a comparison between the zones medial moraine (combining AMH and AML) and glacier terminus (combining ANR, WIP, *t*-test for normally distributed residuals of "Observed" and "InvSimpson" indices, Kruskal–Wallis test for "Shannon" index).

On average, 79.07 bacterial RSVs were detected in CHs and compared to samples from the medial moraine (mean 64.63 ± 29.26; AMH: 66.75 ± 33.84, AML: 62.5 ± 24.23) higher numbers were observed at the glacier terminus (mean 98.33 ± 45.63; ANR: 130.67 ± 36.26, WIP: 66 ± 27.58).

For archaea, the same diversity indices as for bacteria were calculated and distribution of residuals was tested for normality with the Shapiro–Wilk test ("Observed" $p = 0.007758$, "InvSimpson" $p = 0.02033$, "Shannon" $p = 0.07927$). Due to

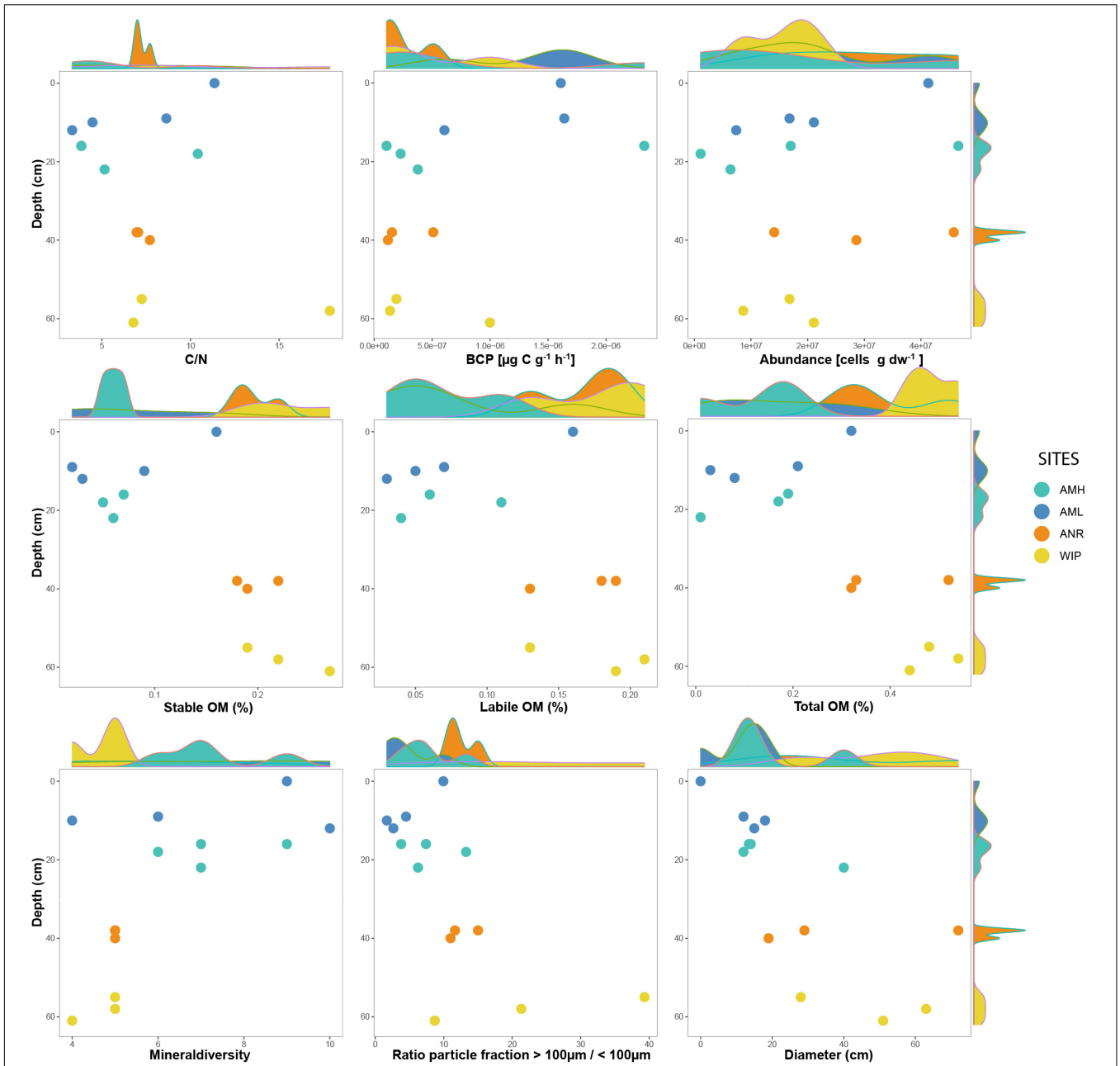

FIGURE 5 | Selected variables plotted along against depth. Marginal plots indicate the sample distribution for each variable.

the absence of archaea in two samples, statistical comparisons were not attempted between single sites but between all samples from the medial moraine and from the glacier terminus. Neither the Kruskal–Wallis tests for the indices "Observed" and "InvSimpson" nor a *t*-test for index "Shannon" indicated significant differences between the two sites. In comparison with the bacterial RSV counts, the number of observed archaeal RSVs was an order of magnitude lower (4.25 ± 3.44) and the distribution was in the same range for the medial moraine (4 ± 4.28) and samples from the glacier terminus (4.6 ± 1.62). Representative boxplots for bacterial and archaeal alpha diversity are depicted in **Supplementary Figure 6**.

Beta Diversity

To identify whether CH communities differed between sites, we performed an analysis of similarities (ANOSIM) based on a Bray–Curtis RSV dissimilarity matrix. CH communities between the zones medial moraine (combined AML and AMH) and glacier terminus (combined ANR and WIP) were significantly different (p = 0.04, 999 permutations) but dissimilarities between all four sites were not significant (p = 0.08, 999 permutations). This

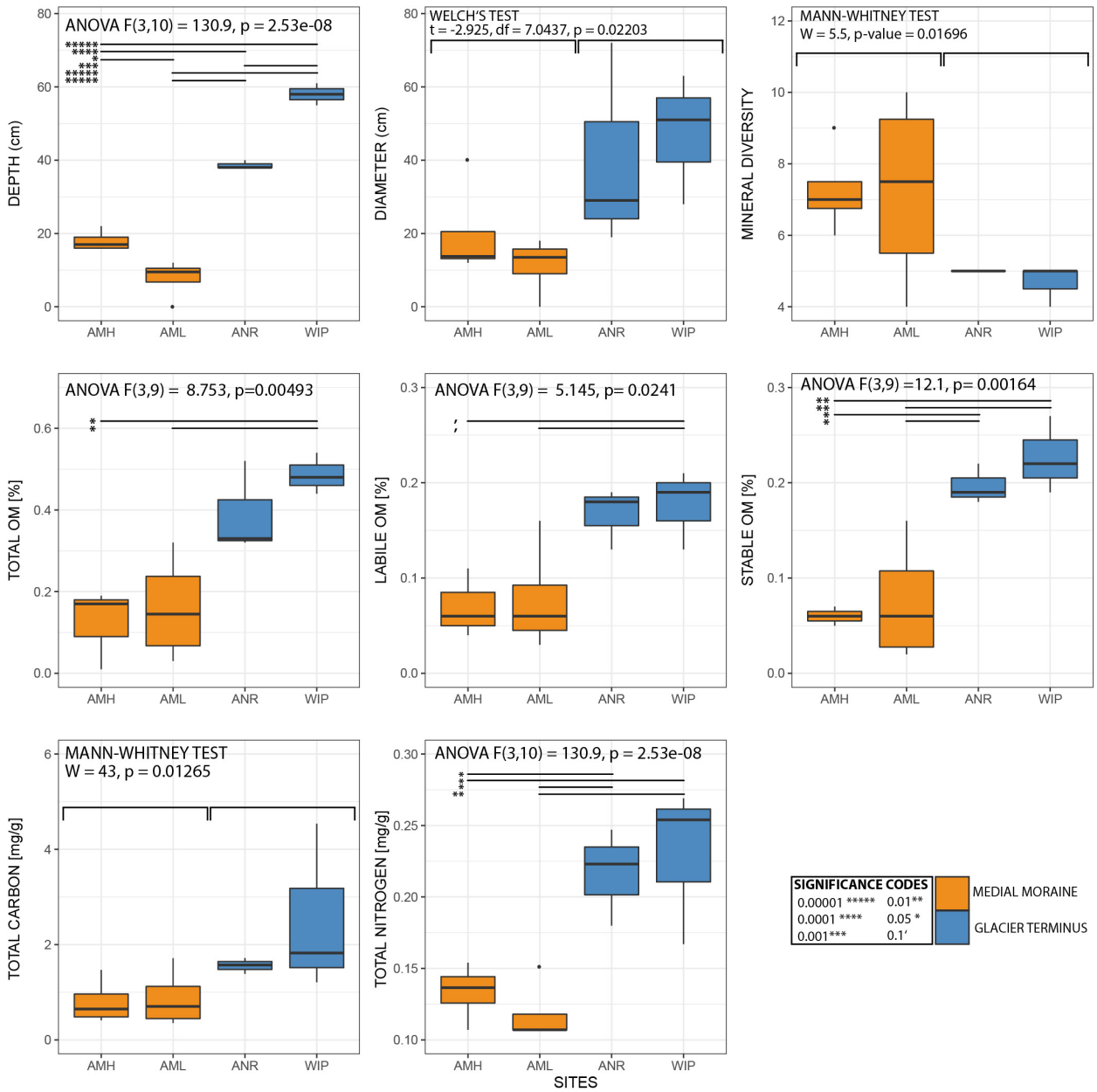

FIGURE 6 | Boxplots of selected variables. Note that sample CRY-7 was identified as outlier and hence was excluded from the boxplots and statistical analysis for organic matter.

is corroborated by a Principal Coordinates Analysis (PCoA) depicted in **Figure 9**. Samples from the glacier terminus were more similar to each other than those along the medial moraine. CHs from the medial moraine formed two clusters that were not attributed to their spatial position at the glacier.

To identify key parameters that explain community variances, we performed permutational analysis of variance (PERMANOVA). The variance was mostly explained by depth (20.52%), mineral diversity (12.04%), total OM (10.47%) and the particle distribution in the size range 40–100 μm (7.31%) (**Supplementary Table 2**).

Further we performed a differential abundance analysis to identify RSVs that accounted for compositional differences between the medial moraine and the glacier terminus. These differences were attributed to 26 RSVs belonging to the phyla Actinobacteria (n = 3), Armatimonadetes (n = 1), Bacteroidetes (n = 7), Cyanobacteria (n = 2), Planctomycetes (n = 2), Proteobacteria (n = 10), and Saccharibacteria (n = 1). The complete taxonomy of these differentially abundant RSVs are shown in **Supplementary Table 3**.

ANOSIM for archaeal-related RSVs were neither significant for all four sites (p = 0.544, 999 permutations) nor for between

TABLE 1 | Descriptive statistics of the metadata set (mean ± 1 sd).

	Medial moraine		Glacier terminus	
	AMH (*n* = 4)	**AML (*n* = 4)**	**ANR (*n* = 3)**	**WIP (*n* = 3)**
Depth (cm)	18 (± 2.83)	7.75 (± 5.32)	38.67 (± 1.15)	58 (± 3)
Diameter (cm)	19.88 (± 13.44)	15 (± 3)	40 (± 28.16)	47.34 (± 17.79)
TC (mg g^{-1})	0.8 (± 0.48)	0.58 (± 0.3)	1.56 (± 0.17)	2.52 (± 1.77)
TN (mg g^{-1})	0.12 (± 0.05)	0.07 (± 0.03)	0.22 (± 0.04)	0.23 (± 0.05)
TP (mg g^{-1})	0.052 (± 0.001)	0.053 (± 0.001)	0.051 (± 0)	0.052 (± 0.002)
C/N	6.97 (± 2.95)	8.32 (± 1.3)	7.25 (± 0.43)	10.67 (± 6.49)
Total OM (%)	0.78 (± 1.32)	0.1 (± 0.03)	0.38 (± 0.19)	0.45 (± 0.05)
Stable OM (%)	0.06 (± 0.01)	0.08 (± 0.06)	0.2 (± 0.02)	0.23 (± 0.04)
Labile OM (%)	0.07 (± 0.04)	0.08 (± 0.06)	0.17 (± 0.03)	0.18 (± 0.04)
Mineral diversity	7.25 (± 1.26)	6.67 (± 3.06)	5 (± 0)	4.67 (± 0.58)
Cell numbers (g dw^{-1})	$5.14*10^{07}$ ($\pm 6.39*10^{07}$)	$6.65*10^{07}$ ($\pm 6.90*10^{07}$)	$1.25*10^{08}$($\pm 1.10*10^{08}$)	$6.83*10^{07}$ ($\pm 4.28*10^{07}$)
BCP (μg C dw^{-1} h^{-1})	$4.43*10^{-07}$ ($\pm 3.94*10^{-07}$)	$4.68*10^{-06}$ ($\pm 5.89*10^{-06}$)	$7.61*10^{-07}$ ($\pm 9.12*10^{07}$)	$2.61*10^{-07}$ ($\pm 1.77*10^{-07}$)

*Sample CRY-7 (AMH) was excluded from the organic matter dataset because the mineral laumontite likely interfered with the TGA analysis (see full dataset in **Supplementary Figure 5**).*

the zones medial moraine and the glacier terminus ($p = 0.537$, 999 permutations). PERMANOVA and DESEQ2 were not applied to the archaeal dataset due to lower the amount of available data.

At phylum level, changes in relative abundance along a depth gradient indicated that members of Acidobacteria and Actinobacteria occurred more frequently in shallow CHs while Cyanobacteria, Proteobacteria and Bacteroidetes trended toward more similar frequencies with increasing depths (**Figure 10**).

Core Microbiome of Cryoconite Holes

The core microbiome of CHs from the Anuchin Glacier was defined as RSVs with an average abundance across all sites ≥ 0.1%. For bacteria, the core microbiome consisted of 30 RSVs that were mainly affiliated with Cyanobacteria (23.30%), Bacteroidetes (9.07%), Actinobacteria (8.61%), Proteobacteria (7.69%), and others (combined 4.32%). The most abundant genera within the bacterial core microbiome were *Tychonema* (9.36%), *Chamaesiphon* (9.09%), RSVs affiliated with a not assigned genus belonging to Microbacteriaceae (6.46%), *Leptolyngbya* (4.86%), and *Polaromonas* (2.55%). From all 24 archaea-related RSVs only four were present across all sites with a relative abundance of ≥0.1%. These sequences belonged to the classes Methanomicrobia (39.88%) and Thermoplasmata (2.43%) and the most abundant RSVs could not be assigned at genus level.

Supplementary Figure 7 depicts all RSVs for bacteria and archaea exceeding the ≥0.1% threshold according to their occurrence from 1 (i.e., occurrence at only one site) to 4 sites (i.e., core microbiome).

DISCUSSION

Mineral Composition Is Linked to Local Windblown Material

One aim of this study was to characterize the minerogenic composition of CHs across the Anuchin Glacier that is flanked by anorthite – norite alterations. We hypothesized that the CH minerogenic composition differed between the medial moraine and CH samples from other zones from the same glacier. Such dissimilarities may be considered as a proxy for differences in microbial community composition across the glacier. We found that particle size classes differed between sites and that minerals occurring at the glacier terminus (Albite, Anorthite, Biotite, Quartz, Magnesiohornblende) were also common in CHs along the medial moraine which were additionally enriched with other minerals (Sanidine, Grossular, Microcline, Sodium Aluminum Silicate, Rutile, Clinochlore, Chamosite, Laumontite). Some of these additional minerals were also identified approx. 15 km north of Lake Untersee at the Otradnaya Nunatak (Markl and Piazolo, 1998) which is considered as source material of the medial moraine. Similar geochemical compositions between the Nunatak and the medial moraine were also confirmed by Bormann and Fritzsche (1995). Therefore, CHs across the glacier can be classified according to a combination of their minerogenic contents and particle size distribution which is either linked to local and likely wind-blown material within the oasis (low mineral diversity) or to the further distant Otradnaya Nunatak (higher mineral diversity).

Physical Characteristics of CHs Depends on Location

We established a temperature depth gradient time series to identify differences between sites with clear ice, dark-colored ice from the medial moraine and ice from the white ice patch. The temperature loggers were considered as a proxy for cryoconite *in situ* temperatures as the reflectivity of the loggers and the sediments were in a similar range (**Supplementary Figure 1**). As expected, dark-colored medial moraine ice was warmer than clear glacier ice and the highest average *in-situ* temperatures were recorded at the WIP site which is likely thermally influenced by Lake Untersee and hence may promote additional melting. Further, the rate of temperature declined with depth but varied between sites. This decline was higher in clear

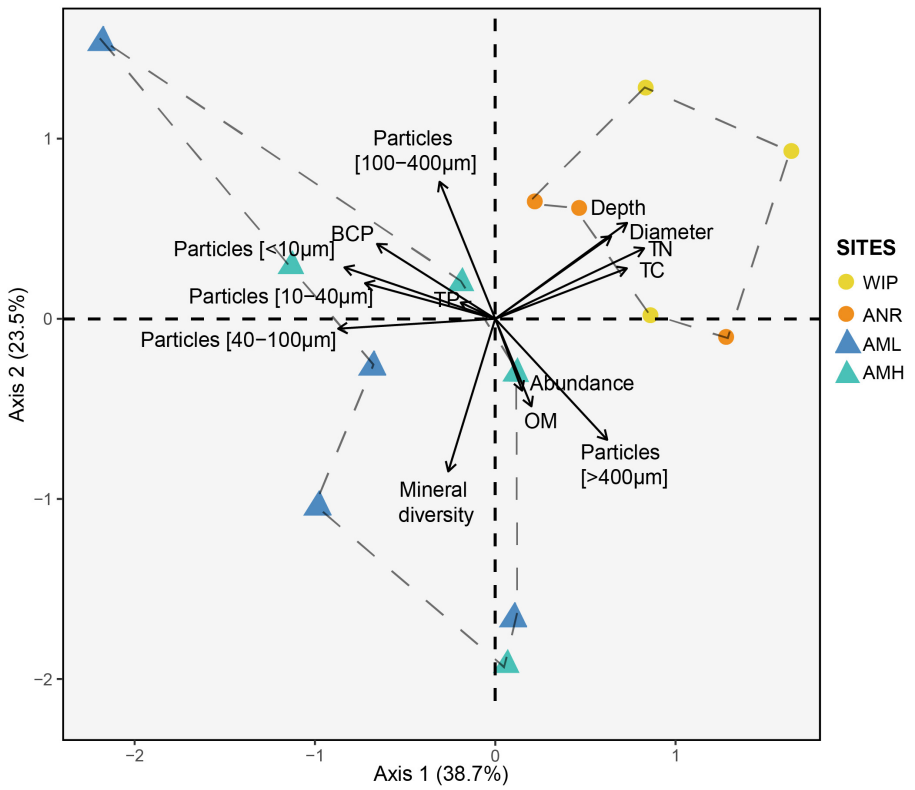

FIGURE 7 | Principal component analysis of the CH dataset (excluding 16S rRNA amplicon data). Circles and triangles represent samples from the glacier terminus and the medial moraine, respectively. Dashed lines serve as a visual guidance.

glacier ice than at the medial moraine and may be attributed to the absence of suppressing mineral material which enables the temperature wave unhindered penetration. The smallest differences over depth were found at WIP which therefore may not only enable deeper cryoconite layers but also less daily temperature fluctuations and hence more stable conditions. We found that CH proxy temperatures at least temporarily exceeded ambient air temperatures – especially between the surface and 0.5 depth. In comparison, CH temperatures at Canada Glacier were permanently higher than the local air temperature (Fountain et al., 2008; Bagshaw et al., 2011). However, the CH depths in these studies did not exceed 50 cm and a direct comparison with this study does not constitute meaningful information because different types of sensors were used and hence thermal inertia between the probes may not be comparable. However, even if considered as a relative measurement, differences between sites, depths and ambient temperature were evident and therefore provide valuable information for future temperature analyses.

Studies from the MDVs (Darcy et al., 2018) described CH size as "island size" implying that CHs are considered as islands across the supraglacial surface. Here they showed significant relations between size, depth and bacterial diversity. CHs were significantly shallower along the medial moraine (0 – 22 cm) compared to those at the glacier terminus (38 – 61 cm). Wharton et al. (1985) predicted that hole-deepening with respect to the ice surface slows down as the energy input required for melting decreases with depth until an equilibrium between surface ablation and hole-deepening rate is reached. Common equilibrium depths are reported between 30 and 50 cm (Gribbon, 1979). The hypothesis was supported by field experiments in the MDVs which further showed that CH equilibrium depths were reached by the end of the melt season (Fountain et al., 2008). The same study also concluded that the magnitude of subsurface melting depended on the optical properties of the overlaying ice. Such differences were also evident at the Anuchin Glacier. For example, the medial moraine contained micro-scale sized particles that visually darkened the ice and hence likely decreased the equilibrium depths by absorbing most solar irradiation before reaching the cryoconite layer. This would also explain the strongest de-coupling effect between *in-situ* proxy temperatures at the medial moraine and ambient air temperatures.

Further, the two sampling sites at the glacier terminus had distinctive depth characteristics. The deepest layers were found at the WIP site, possibly caused by heat transfer from Lake Untersee to the white ice matrix and its embedded CHs. Moreover, ablation rates north of Lake Untersee are lower than within the oasis (Scheinert et al., 2006) and hence may reduce the duration required to reach equilibrium depths. Additionally, satellite based observations showed that surface temperatures generally decrease with increasing distance from the oasis (**Supplementary Figure 8**), suggesting that equilibrium depths may also depend on the spatial location.

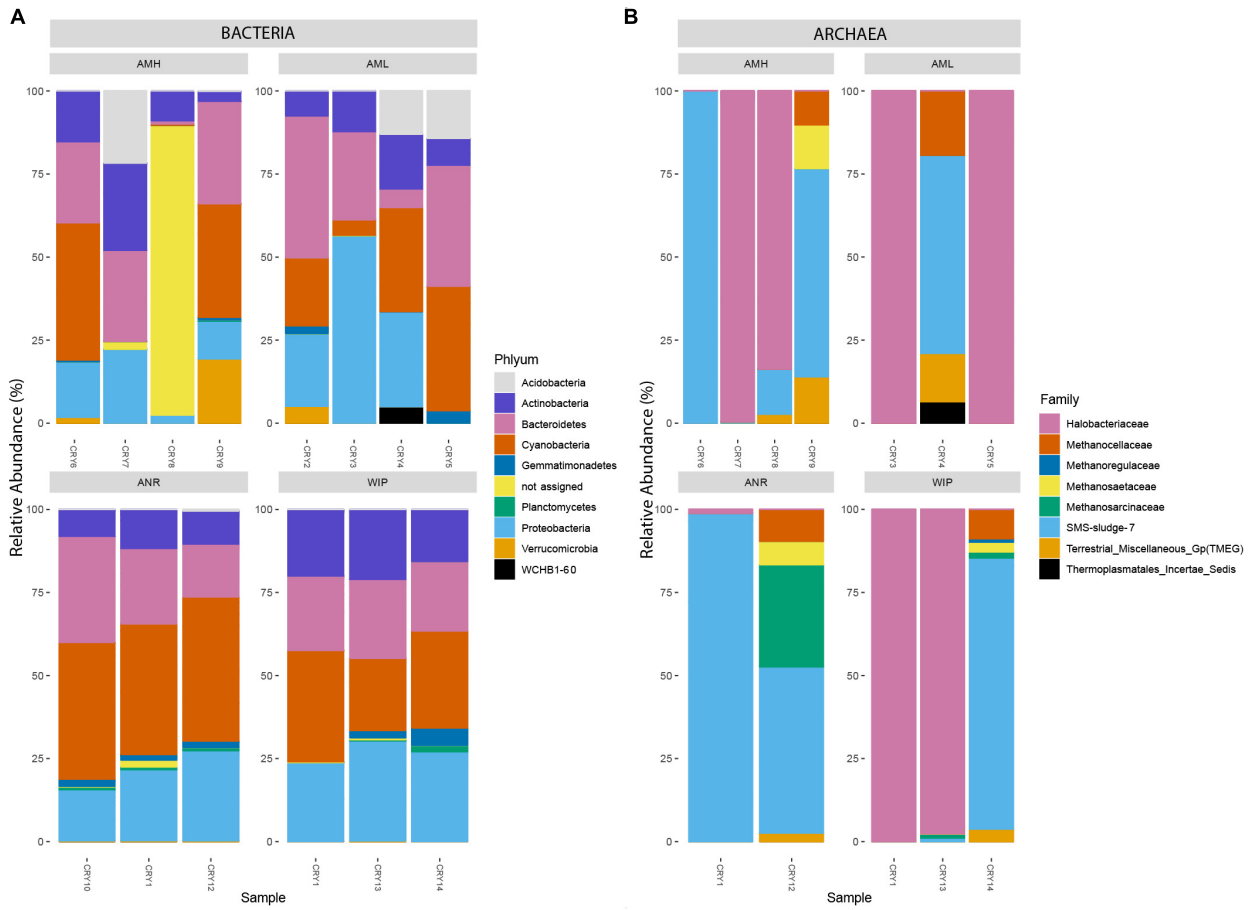

FIGURE 8 | (A) Relative abundance of the 100 most abundant RSVs categorized by their respective phyla. **(B)** Relative abundance of all archaea-related RSVs at family level. The upper two bar charts represent samples from the medial moraine and the lower bar charts depict samples from the glacier terminus.

In comparison, mean CH depths from five glaciers in Southern Victoria Land covering an altitudinal gradient from 30 to 950 m above sea level were 33–41 cm deep and did not differ significantly between glaciers. However, only CHs with diameter > 30 cm (and hence deeper CH) were targeted in their study (Webster-Brown et al., 2015).

Fountain et al. (2004) argued that CH diameters also depended on the initial sediment load that initialized the CH formation. This was observed at several glaciers across the MDVs (Porazinska et al., 2004). We found that CH diameters were different between sites and that diameters increased with the mineral diversity ($p = 0.056$, Adj. $r^2 = 0.21$) which was considered as an indicator whether the sediment load derived from vicinal windblown material or from the medial moraine and probably from adjacent steep slopes.

Extremely Low Nutrient Levels Do Not Support High Rates of Microbial Activity in Antarctic Cryoconite Holes

Landscape position impacts nutrient stoichiometry in the MDVs soils (Barrett et al., 2007) and such spatial patterns were also observed at the Anuchin Glacier. Total carbon contents were very low and significantly different between the zones and single sites, respectively. Average contents per site ranged from 0.58 to 2.52 mg g^{-1} and were in the same order of magnitude as reported from Canada Glacier in MDVs (Telling et al., 2014) but slightly higher than those near Princess Elisabeth station (Lutz et al., 2019). Also total nitrogen contents differed between sites and average values from each site ranged from 0.07 to 0.23 mg g^{-1} which is comparable with CHs from the nearby Sør Rondane mountains in Dronning Maud Land (Lutz et al., 2019). However, total nitrogen contents were 2 – 3 fold higher at the glacier terminus than further up-glacier. Total phosphorus was generally low and did not differ between the sites. Webster-Brown et al. (2015) reports about phosphorous levels in MDV entombed CHs close to detection limits. At Darwin Glacier (Victoria Land) they resulted the same low nutrient concentrations (Webster-Brown et al., 2010), however, these values derive from meltwater biogeochemistry.

Bacterial carbon production in CHs from the Anuchin Glacier did not significantly differ between sites or zones and was exceptionally low ($4.65*10^{-03} \pm 1.33*10^{-02}$ ng C g^{-1} h^{-1}). Thus far, these values represent the lowest BCP rates measured in

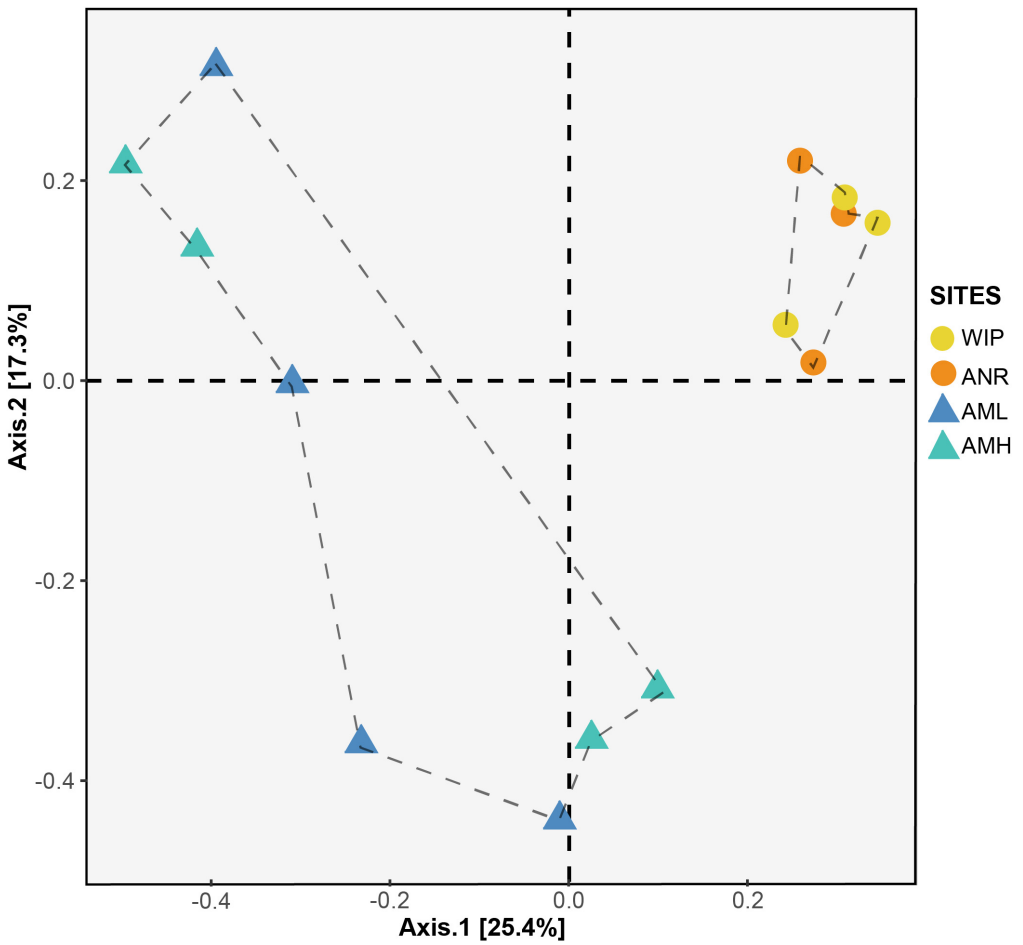

FIGURE 9 | PCoA plot based on Bray–Curtis distance matrix calculated from the RSV table. Circles and triangles represent samples from the glacier terminus and the medial moraine, respectively. Dashed lines serve as a visual guidance.

Antarctic CHs. In comparison, other studies reported BCP rates ranging from 23.4 ng C g^{-1} h^{-1} at Canada, Commonwealth and Taylor Glaciers (Anesio et al., 2010) to 11.2 ng C g^{-1} h^{-1} in the Patriot Hills. BCP in CH water from the Vestfold Hills was 1.58 ng C g^{-1} h^{-1} (Foreman et al., 2007). The reason for these low rates is the subject of ongoing studies.

Cell abundances did not show any pattern across the glacier and the depth gradient. Average numbers per site were in the order of 10^7 cells g dw^{-1}. These numbers are comparable with those from a blue ice CH system (Hodson et al., 2013) and cryoconite from the Patriot Hills (Anesio et al., 2010). Abundances reported from coastal Antarctica (Grzesiak et al., 2015) and the Taylor Valley (Foreman et al., 2007) were one and two orders of magnitude lower, respectively. Higher counts at the Anuchin Glacier may be explained by the application of an efficient cell-dislodgement protocol (Duhamel and Jacquet, 2006). To our knowledge, this protocol has not been used in other Antarctic CH studies yet and hence, the comparison of cell numbers is trustworthy.

Total OM contents in CHs were significantly higher at the glacier terminus (=deeper CHs). This suggests that OM may accumulate over time in deeper CHs, assuming that CHs across the glacier reach similar equilibrium depths. For statistical analysis we identified and consequently removed one outlier (CRY-7) that had a 5.8 times higher OM content as the overall observed mean value and exceeded the interquartile range for this parameter. We partly attribute this exceptional high mass loss to the presence of hydrogen-bonded (opposed to Ca-bonded) water in Laumontite ($Ca[Al_2Si_4O_{12}] \times 4–4.5\ H_20$) which was only detected in this sample. When heated, the mineral gradually releases structural water from 100 to 750°C (Földvári, 2011). As a consequence, loss on ignition (LOI) measurements in low biomass samples should be accompanied by mineral analyses to correctly interpret suspicious data.

Hodson et al. (2013) did not find significant correlations between BCP and OM contents in CHs and despite the low BCP rates at the Anuchin Glacier, OM fractions were in a comparable range with other studies. For example, CHs collected in the vicinity of Princess Elisabeth station had mean and maximum mass losses of 0.64 and 1.12% when heated up to 1000°C, respectively (Lutz et al., 2019). We re-calculated our TGA results (38 – 1000°C) for a direct comparison. The overall mean loss

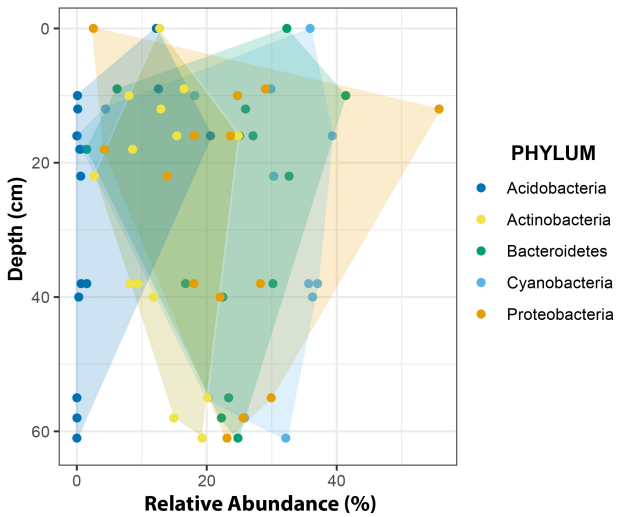

FIGURE 10 | Relative abundance of major phyla across a depth gradient. The borders of the colored areas indicate the outermost data points.

on ignition without outlier sample CRY-7 was in a similar range (mean: 0.48%, max: 1.07%). Therefore, CHs at the next closest study site (∼353 km west of Lake Untersee Oasis) are comparable with respect to their mass-loss properties. OM contents in CHs from a blue ice zone were slightly higher and ranged from 0.78 to 1.99% (Hodson et al., 2013).

By considering the higher cell number which is possibly due to the more efficient dislocation protocol and the low productivity we assume that the microbial activity of the respective CH communities must be extremely low. Moreover, the exceptional low content of OM would not provide the required sources therefore as well as the extremely restricted availability of liquid water.

Bacterial Phyla – "The Usual Suspects" Found in Antarctic Cryoconite Holes

In total, 92% of all RSV counts belonged to Proteobacteria, Cyanobacteria, Bacteroidetes, Actinobacteria, and Acidobacteria which are mirrored elsewhere in Antarctic environments (e.g., Christner et al., 2003; Webster-Brown et al., 2015). However, phyla with the most ribosomal sequence variants were Proteobacteria, Bacteroidetes, Actinobacteria, Planctomycetes, and Cyanobacteria. The presence of multiple sequence variants of the same genera may indicate a certain molecular plasticity in context with environmental conditions (Tikhonov et al., 2015).

Proteobacteria had the highest mean relative abundance in all samples (26.54%) and were mainly composed of Betaproteobacteria, Gammaproteobacteria, and Alphaproteobacteria. The most abundant RSV within this phylum was *Silanimonas* sp. which was also found in CHs of the Taylor Glacier in the MDVs (Christner et al., 2003; GenBank: AY124351.1: 99.62% similarity). The second most abundant RSV was the Alphaproteobacterium *Sphingomonas* sp. which was found in hypolithic microbial communities of quartz rocks from Miers Valley (Khan et al., 2011; GenBank: HQ197614.1, 99.63% similarity) and the ice cover of Lake Vida (Mosier et al., 2007; GenBank: DQ521492.1, 99.63% similarity). Another abundant RSV was *Polaromonas* sp. (Betaproteobacteria) that is also known from other polar regions and was identified in sediments of Lake Bonney (Tang et al., 2013, GenBank: JX948739.1, 99.26% similarity).

Cyanobacteria frequently occur in extreme environments and are known as important key members in supraglacial and other cold terrestrial zones (Vincent, 2000; Namsaraev et al., 2010; Chrismas et al., 2015). CHs from the Anuchin Glacier were also dominated by them (25,45%). The most abundant cyanobacterial RSVs were also found in soils of the Wright Valley (*Tychonema*: GenBank: KM052830.1; 100% similarity), Antarctic snow (Lopatina et al., 2013; GenBank: JX855325., 99.63% similarity). Filamentous Cyanobacteria play a key role in cryoconite granule formation (Jungblut and Vincent, 2017) and the granule size shapes the microbial community composition (Uetake et al., 2019). Here, typical cryoconite granule engineers (*Phormidium*, *Chamaesiphon*) were present but the granules were neither observed in other Antarctic regions. This might be due to a substantial lack of continuous flow of melt water along supraglacial surfaces which cause the original particles to roll in the flow where cells are attached on the outer side.

The main classes of Bacteroidetes in CHs were Cytophagia (dominated by *Algoriphagus* sp.) and Sphingobacteria (dominated *Ferruginibacter*). Similar *Algoriphagus* sequences were found in soils of the Antarctic Darwin Mountains (Aislabie et al., 2013; GenBank: KC442505.1, similarity: 98.90%) and *Ferruginibacter* is also known from other glacio-lacustrine Antarctic settings (GenBank: KP012224.1, similarity 99.63%).

Actinobacteria and Acidobacteria made up 16.58% of all counts. The most frequent sequences belonged to *Chryseoglobus* sp. and *Granulicella* sp., respectively. Similar *Chryseoglobus* signatures were found about 353 km west of Lake Untersee Oasis, nearby Utsteinen mountain (GenBank: FR682678.1; similarity: 98.90%). *Granulicella*-like sequences were reported from soils at South Georgia (Yergeau et al., 2007; GenBank: EF221026.1, similarity: 100%).

The overall phyla distribution changed with depth. Compared to shallow CHs the variability of relative abundances decreased in deeper CHs. This observation may be explained in two ways. First, environmental conditions in deeper CHs are more stable. For example, the temperature fluctuations are smaller than at the surface (e.g., **Figure 4**) because more light is attenuated by the overlaying ice cover (Bagshaw et al., 2016). This implies that approaching the CH equilibrium depth also reduces biotic inoculation by melting of surrounding ice and hence shapes more stable microbial communities. Secondly, CH depths are often linked with the isolation age, i.e., being disconnected from the atmosphere by the formation on an ice lid (Fountain et al., 2004; Bagshaw et al., 2007; Lutz et al., 2019). It is also likely that this isolation age may play a role in the formation of stable microbial communities in CHs.

Compositional differences in archaeal communities are linked with the selection of suitable primers and subsequent amplification steps (Pausan et al., 2019). In this study, the

universal primer approach resulted in 1,588 archaea- related counts and identified Archaea in 57% of the samples. These numbers were significantly improved by the use of archaea-targeting primers 344f and 915r (Klindworth et al., 2013) and subsequent nested PCR approach with the primer S-D-Arch-0519-a-S-15 (Koskinen et al., 2017). Overall, archaea were detected in 85% of the samples. Also, the number of detected RSVs increased from 18 to 24 ribosomal sequence variants.

All archaea-specific sequences in CHs belonged to the classes Halobacteria, Methanomicrobia and Thermoplasmata within the phylum Euryarchaeota. By far the most abundant genus was *Halorubrum* (Halobacteria) that was affiliated to nine ribosomal sequence variants but more than 97% of all counts were attributed to one RSV. The most similar blasted sequence derived from the hypersaline Deep Lake (Mou et al., 2012; GenBank:NR_117806.1, similarity: 89,14%). Blast search did not result in more similar sequences for the second and third-most abundant sequences.

To our surprise we found only two other Antarctic CH studies that reported Archaea in their samples. Cameron et al. (2012) compared CHs from polar regions and showed that archaea were only detectable in Antarctic CHs and that most reads were affiliated with Thaumarchaeota and the classes Methanobacteriaceae and Methanomicrobia within the phylum Euryarchaeota. Further, about 4% of all CH samples nearby the East-Antarctic Princess Elisabeth station harbored archaea and were classified as *Nitrososphaera* (Thaumarchaeota) (Lutz et al., 2019). Hence, this study provided the first evidence of the classes Halobacteria and Thermoplasmata in Antarctic CHs. This low detection rate might also be a result of the missing approach with nested PCR which improves the identification as shown in this study.

The Core Microbiome of Cryoconite Holes – A Matter of Definition

In this study, RSVs that were considered as part of the core microbiome had to fulfill two requirements: The mean relative abundance of all samples had to be $\geq$0.1% and the sequences had to occur at all sites. The first criterium was met by 67 sequences and after applying the second criterium only 30 RSVs remained in the dataset. Compared to the overall dominance of Proteobacteria in terms of relative abundance and RSV numbers, the core microbiome was dominated by Cyanobacteria, followed by Bacteroidetes, Actinobacteria, and Proteobacteria.

Sequence blasting showed that most RSVs of the CH core microbiome were similar to sequences that are already known from Antarctic environments. For example, cyanobacterial RSVs that were assigned to the genus *Chamaesiphon* were highly similar to those found in microbial mats of Lake Hoare (Hawes et al., 2016; GenBank: KU230337.1, 99.63% similarity), in CHs from the Lower Wright Glacier (Webster-Brown et al., 2015; GenBank: KT424939.1 99.26% similarity) and in dark soils of a glacier forefield at the Larsemann Hills (Bajerski and Wagner, 2013; GenBank: JX172501.1, 99.26% similarity). Further, RSVs affiliated with the cyanobacterial genus *Tychonema* were also found at the nearby Sør Rondane Mountains (GenBank: HM101190.1, 100% similarity) and in microbial mats of Lake Fryxell (GenBank: AY151751.1, similarity: 100%). Also RSVs assigned to the genus *Leptolyngbya* were highly similar to those retrieved from CH of the Diamond Glacier in Southern Victoria Land (Webster-Brown et al., 2015; GenBank: KT424929.1, similarity: 99.26%).

RSVs that belonged to Actinobacteria (genera Chryseoglobus, Cryobacterium, and Marisediminicola) were also found in the ice cover of Lake Vida (Mosier et al., 2007; GenBank: DQ521497.1, similarity: 99.63%), in soils at Robert Island (GenBank: MT072015.1, similarity: 99.63%) and in sediments of Lake Bonney (Tang et al., 2013; GenBank: JX948474.1, similarity: 99.63%), respectively.

The CH core microbiome was also composed of the genera *Thermomonas* (Gammaproteobacteria), *Polaromonas* (Betaproteobacteria) and *Rubellimicrobium* (Alphaproteobacteria) that were similar to those found in shallow groundwaters at Cape Hallett (Aislabie et al., 2009; GenBank: FJ164057.1, similarity: 97.07%), surface waters of Lake Limnopolar at Byers Peninsula (Papale et al., 2017; GenBank: KF928875.1, similarity: 99.63%) and sediments of Lake Bonney (Tang et al., 2013; GenBank: JX948518.1, similarity: 98.16%), respectively. Further, core RSVs assigned to the genus *Hymenobacter* (Bacteroidetes) were found in sediments of the Onyx River within the Wright Valley (Zeglin et al., 2011; GenBank: EU869634.1, similarity: 97.06%). These observations indicate that members of the CH core microbiome of the Anuchin Glacier also prevail in other habitats spread across Antarctica and that they cope with a wide range of environmental conditions.

Despite the lack of Archaea in 2 CHs, four RSVs passed our core microbiome criteria. These sequences belonged to unknown genera of the families Methanomicrobiales, Thermoplasmatales and to Methanocellales (*Rice_Cluster_I*). Blast results revealed only distant relatives within Antarctica which were present in Lake Fryxell (Karr et al., 2006; GenBank: AY299382.1, similarity: 95.09%), in endolithic communities from the Miers Valley (GenBank: KC476273.1, similarity: 84.50%) and in marine hydrothermal sediments (GenBank: FM868021.1, similarity: 87.4%).

A direct comparison of CH core microbiomes is hampered for two reasons. First, data availability of Antarctic CHs core microbiomes is scarce. Second, differences in methodological approaches limit such comparisons. For example, compared to the use of operational taxonomic units (OTUs, similarity threshold 97%; e.g., Lutz et al., 2019), the use of RSVs (e.g., this study) leads to an increased number of total sequences because RSVs are more exact than OTUs (Callahan et al., 2016). Consequently, read counts are allocated to more amplicon sequence variants and therefore the probability for a sequence being detected at all sites is reduced. As an example, the CH core microbiomes of the Anuchin Glacier and from a site in the Sør Rondane mountains (Lutz et al., 2019) broadly match at phylum level but differences at higher taxonomic resolution are evident. For instance, Lutz et al. (2019) found members of the family Sphingomonadaceae (Alphaproteobacteria) in their

core microbiome but in the present study none of the 17 Sphingomonadaceae assigned RSVs passed our core microbiome criteria. This example highlights that the core microbiome is a matter of definition (e.g., prevalence levels, site vs. sample occurrence) but it also depends on underlying methodological approaches (e.g., primer selection, bioinformatic pipelines).

Inoculation Sources and Their Role for Cryoconite Hole Establishment

Samples from the glacier terminus shared characteristics for most biogeochemical features and therefore clustered together in the PCA (**Figure 7**). The cluster formation was mainly attributed to the variables depth, diameter, total nitrogen, and total carbon. CHs from the medial moraine had a higher variability and cluster formation was not evident. Independent of this metadata analysis a principal coordinates analysis (**Figure 9**) revealed a striking similar pattern: Microbial communities from the glacier terminus were similar to each other while samples within the medial moraine showed greater differences between single samples.

Differential abundance analysis (DESEQ2) showed that the key differences in microbial community composition between the medial moraine and the glacier terminus samples were mainly caused by 26 RSVs belonging to the phyla Actinobacteria ($n = 3$), Armatimonadetes ($n = 1$), Bacteroidetes ($n = 7$), Cyanobacteria ($n = 2$), Planctomycetes ($n = 2$), Proteobacteria ($n = 10$), and Saccharibacteria ($n = 1$). Some of those sequences were also found elsewhere in Antarctica. For example, *Spirosoma* sp. was found along in ice-free soils near the Belgium Princess Elisabeth station which is only ∼350 km away from the study site (GenBank: MN031263.1, MN031264.1).

CHs form independently from each other and therefore may resemble discrete ecosystems. However, CH communities from the MDVs were similar to those from the surrounding soils (Christner et al., 2003). Contradictory, another study from the same region concluded that the CH composition did not mirror biota that was found in the surrounding (Porazinska et al., 2004). Also, CHs in close proximity tend to be more similar compared to further distant ones (Darcy et al., 2018) and hence clustered according to their location, suggesting local inoculum sources and environmental conditions (Lutz et al., 2019) which is also valid for other extreme Antarctic environments such as supraglacial ponds or soils (Webster-Brown et al., 2010; Lee et al., 2012).

Potential microbial source inocula at the Anuchin Glacier are numerous and varied, including those originating from surrounding ice and soils. Also, differences in mineral diversity between the medial moraine and the glacier terminus may be considered as an indicator for separate local inoculum sources. Further, re-surfacing wind-blown microbial mats from Lake Untersee may re-colonize CHs at the Anuchin glacier and consequently return to the lake by melt processes (Weisleitner et al., 2019b). Further, similarities between genera that were found at "nearby" Sør Rondane mountains (Obbels et al., 2016; Lutz et al., 2019) and more distant Antarctic sites (e.g., Aislabie et al., 2013; Lopatina et al., 2013) indicate long-range aeolian biotic sources that reach Lake Untersee Oasis.

The dynamics of bacterial and archaeal communities presented in this study are most likely controlled by a combination of environmental factors. One of these drivers for microbial evolution can be identified by viruses which play a key role in the microbial loop (Anesio and Bellas, 2011). As reported for Arctic CHs, they increase bacterial mortality by lysis and therefore promote nutrient re-utilization (Bellas et al., 2013). Also, transplantation experiments have shown that viruses from CHs also infect microbial communities of an adjacent proglacial lake (Anesio et al., 2007). This suggests that the impact of a potential CH viriome is not limited to the supraglacial zone of the Anuchin Glacier but likely controls microbial communities within adjacent Lake Untersee. However, despite the evidence of phage infections within the water column of Lake Untersee (Filippova et al., 2013), neither the genetic viral diversity nor their sources and interactions are presently known.

CONCLUSION

CHs at the Anuchin Glacier are considered as important biotic inoculum sources for adjacent Lake Untersee ecosystem (Weisleitner et al., 2019b). Here, we further identified differences in abiotic and biotic characteristics between CHs occurring along the medial moraine and the glacier terminus and defined the bacterial and archaeal core microbiome from this habitat.

Based on the mineral diversity distribution across sites, we accept the initial hypothesis that minerogenic composition differed between the medial moraine and the glacier terminus. These differences also indicate distinctive biotic inoculum sources (e.g., biota attached to windblown dust from within the oasis vs. sediments from Otradnaja Nunatak outside the oasis).

Our observations partially support the second hypothesis that community composition, OM contents and BCP rates are mirrored by the depth of the cryoconite layer. Depth was the most important variable that explained differences in the community composition. Also, both OM fractions (labile and stable) were significantly different between shallow CHs along the medial moraine and deeper ones that occurred at the glacier terminus. However, BCP insignificantly trended toward higher rates in shallow CHs and hence did not fully underpin our initial hypothesis. Further, the reported BCP rates represent the lowest records known from Antarctic CHs.

We used temperature loggers as proxies for *in situ* cryoconite temperatures. Despite similar reflectivity of cryoconite and the loggers, thermal inertia of the loggers likely underestimated the maximum temperatures within the ice. However, a relative comparison between the sites is valid. We demonstrated that temperature dynamics differed between dark colored ice that was interspersed with particulates, ice that appeared macroscopically free of particles and glacial ice that was embedded in the ice cover of Lake Untersee, respectively. Further, differences in CH depth distribution could be explained by a combination of optical properties of the overlaying ice and the temperature profiles which lead to distinct environmental conditions across the glacier.

We identified bacteria that are commonly found in CHs. However, this is the first study that identified members of the archaeal classes Halobacteria and Thermoplasmata in Antarctic CHs and to our knowledge the percentage of CHs that harbored archaea was higher than reported elsewhere. The role of archaea in CHs at the Anuchin Glacier are poorly studied and hence should be subject of future studies in context with Lake Untersee Oasis.

DATA AVAILABILITY STATEMENT

Sequence data presented in this manuscript is deposited in the NCBI database under the accession number SRP145579 and was published among other data in Weisleitner et al. (2019b). Accession numbers linking to single samples and their according primer sets are found in **Supplementary Table 1** of this manuscript.

AUTHOR CONTRIBUTIONS

KW designed the study, collected all the samples, and performed all the *in situ* measurements during an expedition that was led by DA. SU performed the TGA and XRD measurements and acquired the scanning electron microscopy images. KW and AP did the microbial community analysis. KW did the statistical analysis of microbial data and metadata. KW and BS wrote most of the manuscript (KW: main contributor) that was reviewed by all authors.

FUNDING

This study was supported by the Tawani Foundation of Chicago, the Trottier Family Foundation, NASA's Exobiology and Astrobiology Programs, and the Arctic and Antarctic Research Institute.

ACKNOWLEDGMENTS

Primary support for this research was provided by the Tawani Foundation and the Trottier Family Foundation. Logistics support was provided by Antarctic Logistics Centre International (ALCI), Cape Town, South Africa and the Von Braun Center for Science Innovation. We are especially thankful to Colonel (IL) J. N. Pritzker, IL ARNG (retired), of the Tawani Foundation, Lorne Trottier, and fellow field team members for their support during the expedition. We also thank Elias Dechent, Gry Larsen, and Salvador Morales-Gomez for help with chemical analyses. Willi Salvenmoser provided sample coating prior scanning electron microscopy. We are grateful for the improvement of the manuscript which was provided by the reviewers.

SUPPLEMENTARY MATERIAL

The Supplementary Material for this article can be found online at: https://www.frontiersin.org/articles/10.3389/fmicb.2020.01165/full#supplementary-material

REFERENCES

Aislabie, J. M., Lau, A., Dsouza, M., Shepherd, C., Rhodes, P., and Turner, S. J. (2013). Bacterial composition of soils of the Lake Wellman area, Darwin Mountains, Antarctica. *Extremophiles* 17, 775–786. doi: 10.1007/s00792-013-0560-6

Aislabie, J., Ryburn, J., and Sarmah, A. (2009). Culturable microbes in shallow groundwater underlying ornithogenic soil of Cape Hallett, Antarctica. *Can. J. Microbiol.* 55, 12–20. doi: 10.1139/W08-118

Andersen, D. T., McKay, C. P., and Lagun, V. (2015). Climate conditions at perennially ice-covered Lake Untersee, East Antarctica. *J. Appl. Meteorol. Climatol.* 54, 1393–1412. doi: 10.1175/jamc-d-14-0251.1

Andersen, D. T., Sumner, D. Y., Hawes, I., Webster-Brown, J., and Mckay, C. P. (2011). Discovery of large conical stromatolites in Lake Untersee, Antarctica. *Geobiology* 9, 280–293. doi: 10.1111/j.1472-4669.2011.00279.x

Anesio, A. M., and Bellas, C. M. (2011). Are low temperature habitats hot spots of microbial evolution driven by viruses? *Trends Microbiol.* 19, 52–57. doi: 10.1016/j.tim.2010.11.002

Anesio, A. M., Hodson, A. J., Fritz, A., Psenner, R., and Sattler, B. (2009). High microbial activity on glaciers: importance to the global carbon cycle. *Glob. Change Biol.* 15, 955–960. doi: 10.1111/j.1365-2486.2008.01758.x

Anesio, A. M., Mindl, B., Laybourn-Parry, J., Hodson, A. J., and Sattler, B. (2007). Viral dynamics in cryoconite holes on a high Arctic glacier (Svalbard). *J. Geophys. Res.* 112:G04S31. doi: 10.1029/2006JG000350

Anesio, A. M., Sattler, B., Foreman, C., Telling, J., Hodson, A., Tranter, M., et al. (2010). Carbon fluxes through bacterial communities on glacier surfaces. *Ann. Glaciol.* 51, 32–40. doi: 10.3189/172756411795932092

Bagshaw, E. A., Tranter, M., Fountain, A. G., Welch, K. A., Basagic, H., and Lyons, W. B. (2007). Biogeochemical evolution of cryoconite holes on Canada Glacier, Taylor Valley, Antarctica. *J. Geophys. Res.* 112:G04S35. doi: 10.1029/2007JG000442

Bagshaw, E. A., Tranter, M., Fountain, A. G., Welch, K.,Basagic, H. J., and Lyons, W. B. (2013). Do cryoconite holes have the potential to be significant sources of C, N, and P to downstream depauperate ecosystems of Taylor Valley, Antarctica? *Arct. Antarct. Alp. Res.* 45, 440–454. doi: 10.1657/1938-4246-45.4.440

Bagshaw, E. A., Tranter, M., Wadham, J. L., Fountain, A. G., Dubnick, A., and Fitzsimons, S. (2016). Processes controlling carbon cycling in Antarctic glacier surface ecosystems. *Geochem. Persp. Lett.* 2, 44–54. doi: 10.7185/geochemlet.1605

Bagshaw, E. A., Tranter, M., Wadham, J. L., Fountain, A. G., and Mowlem, M. (2011). High-resolution monitoring reveals dissolved oxygen dynamics in an Antarctic cryoconite hole. *Hydrol. Process.* 25, 2868–2877.

Bajerski, F., and Wagner, D. (2013). Bacterial succession in Antarctic soils of two glacier forefields on Larsemann Hills, East Antarctica. *FEMS Microbiol. Ecol.* 85, 128–142. doi: 10.1111/1574-6941.12105

Barrett, J. E., Virginia, R. A., Lyons, W. B., McKnight, D. M., Priscu, J. C., Doran, P. T., et al. (2007). Biogeochemical stoichiometry of Antarctic Dry Valley ecosystems. *J. Geophys. Res.* 112:G01010. doi: 10.1029/2005JG000141

Bellas, C., Anesio, A., Telling, J., Stibal, M., Tranter, M., and Davis, S. (2013). Viral impacts on bacterial communities in Arctic cryoconite. *Environ. Res. Lett.* 8:045021.

Bormann, P., and Fritzsche, D. (1995). *The Schirmacher Oasis, Queen Maud Land, East Antarctica, and Its Surroundings*. Gotha: Peterm. Geogr. Mitt. Erg, 448.

Brandmaier, A. M. (2015). pdc: an R package for complexity-based clustering of time series. *J. Stat. Softw.* 67, 1–23. doi: 10.18637/jss.v067.i05

Callahan, B. J., McMurdie, P. J., Rosen, M. J., Han, A. W., Johnson, A. J. A., and Holmes, S. P. (2016). DADA2: High-resolution sample inference from Illumina amplicon data. *Nat. Methods* 13, 581–583. doi: 10.1038/nmeth.3869

Cameron, K. A., Hodson, A. J., and Osborn, A. M. (2012). Structure and diversity of bacterial, eukaryotic and archaeal communities in glacial cryoconite holes

from the Arctic and the Antarctic. *FEMS Microbiol. Ecol.* 82, 254–267. doi: 10.1111/j.1574-6941.2011.01277.x

Caporaso, J. G., Lauber, C. L., Walters, W. A., Berg-Lyons, D., Huntley, J., Fierer, N., et al. (2012). Ultra-high-throughput microbial community analysis on the Illumina HiSeq and MiSeq platforms. *ISME J.* 6, 1621–1624. doi: 10.1038/ismej.2012.8

Chrismas, N. A. M., Anesio, A. M., and Sánchez-Baracaldo, P. (2015). Multiple adaptations to polar and alpine environments within cyanobacteria: a phylogenomic and Bayesian approach. *Front. Microbiol.* 6:1070. doi: 10.3389/fmicb.2015.01070

Christner, B. C., Kvitko, B. H., and Reeve, J. N. (2003). Molecular identification of bacteria and eukarya inhabiting an Antarctic cryoconite hole. *Extremophiles* 7, 177–183. doi: 10.1007/s00792-002-0309-0

Cook, J., Edwards, A., Takeuchi, N., and Irvine-Fynn, T. (2016). Cryoconite: the dark biological secret of cryosphere. *Prog. Phys. Geogr.* 40, 66–111. doi: 10.1177/0309133315616574

Darcy, J. L., Gendron, E., Sommers, P., Porazinska, D. L., and Schmidt, S. K. (2018). Island biogeography of cryoconite hole bacteria in Antarctica's Taylor Valley and around the world. *Front. Ecol. Evol.* 6:180. doi: 10.3389/fevo.2018.00180

Duhamel, S., and Jacquet, S. (2006). Flow cytometric analysis of bacteria-and virus-like particles in lake sediments. *J. Microbiol. Methods* 64, 316–332. doi: 10.1016/j.mimet.2005.05.008

Edwards, A., Pachebat, J. A., Swain, M., Hegarty, M., Hodson, A. J., Irvine-Fynn, T. D., et al. (2013). A metagenomic snapshot of taxonomic and functional diversity in an alpine glacier cryoconite ecosystem. *Environ. Res. Lett.* 8:035003. doi: 10.1088/1748-9326/8/3/035003

Faucher, B., Lacelle, D., Fisher, D., Andersen, D., and McKay, C. (2019). Energy and water mass balance of Lake Untersee and its perennial ice cover, East Antarctica. *Antarct. Sci.* 31, 271–285. doi: 10.1017/S0954102019000270

Filippova, S. N., Surgucheva, N. A., Kulikov, E. E., Sorokin, V. V., Akimov, V. N., Bej, A. K., et al. (2013). Detection of phage infection in the bacterial population of Lake Untersee (Antarctica). *Microbiology* 82, 383–386. doi: 10.1134/S0026261713030041

Földvári, M. (2011). *Handbook of Thermogravimetric System of Minerals and its Use in Geological Practice*, Vol. 213. Budapest: Geological Institute of Hungary, 1–180.

Foreman, C. M., Sattler, B., Mikucki, J. A., Porazinska, D. L., and Priscu, J. C. (2007). Metabolic activity and diversity of cryoconites in the Taylor Valley, Antarctica. *Aquat. Geochem.* 11, 391–412. doi: 10.1007/s10498-004-7373-2

Fortner, S. K., Tranter, M., Fountain, A., Lyons, W. B., and Welch, K. A. (2005). The geochemistry of supraglacial streams of Canada Glacier, Taylor Valley (Antarctica), and their evolution into proglacial waters. *Aquat. Geochem.* 11, 391–412.

Fountain, A. G., Nylen, T. H., Tranter, M., and Bagshaw, E. (2008). Temporal variations in physical and chemical features of cryoconite holes on Canada Glacier, McMurdo Dry Valleys, Antarctica. *J. Geophys. Res. Biogeosci.* 113:G01S92.

Fountain, A. G., Tranter, M., Nylen, T. H., Lewis, K. J., and Mueller, D. R. (2004). Evolution of cryoconite holes and their contribution to meltwater runoff from glaciers in the McMurdo Dry Valleys, Antarctica. *J. Glaciol.* 50, 35–45.

Gribbon, P. (1979). Cryoconite Holes on Sermikavsak, West Greenland. *J. Glaciol.* 22, 177–181. doi: 10.3189/S0022143000014167

Grzesiak, J., Zdanowski, M. K., Górniak, D., Świątecki, A., Aleksandrzak-Piekarczyk, T., Szatraj, K., et al. (2015). Microbial community changes along the ecology glacier ablation zone (King George Island, Antarctica). *Polar Biol.* 38, 2069–2083.

Hamilton, N. E., and Ferry, M. (2018). ggtern: ternary diagrams using ggplot2. *J. Stat. Softw.* 87, 1–17.

Hawes, I., Jungblut, A. D., Obryk, M. K., and Doran, P. T. (2016). Growth dynamics of a laminated microbial mat in response to variable irradiance in an Antarctic lake. *Freshw. Biol.* 61, 396–410. doi: 10.1111/fwb.12715

Hermichen, W. D., Kowski, P., and Wand, U. (1985). Lake Untersee, a first isotope study of the largest freshwater lake in the interior of East Antarctica. *Nature* 315, 131–133. doi: 10.1038/315131a0

Hodson, A., Anesio, A. M., Tranter, M., Fountain, A., Osborn, M., Priscu, J., et al. (2008). Glacial ecosystems. *Ecol. Monogr.* 78, 41–67. doi: 10.1890/07-0187.1

Hodson, A., Paterson, H., Westwood, K., Cameron, K., and Laybourn-Parry, J. (2013). A blue-ice ecosystem on the margins of the East Antarctic ice sheet. *J. Glaciol.* 59, 255–268. doi: 10.3189/2013JoG12J052

Howat, I., Morin, P., Porter, C., and Noh, M. J. (2018). *The Reference Elevation Model of Antarctica*. Washington, DC: Harvard Dataverse.

Jungblut, A. D., and Vincent, W. F. (2017). "Cyanobacteria in Polar and Alpine Ecosystems," in *Psychrophiles: From Biodiversity to Biotechnology*, ed. R. Margesin (Cham: Springer), 181–206.

Karr, E. A., Ng, J. M., Belchik, S. M., Sattley, W. M., Madigan, M. T., and Achenbach, L. A. (2006). Biodiversity of methanogenic and other Archaea in the permanently frozen Lake Fryxell, Antarctica. *Appl. Environ. Microbiol.* 72, 1663–1666.

Khan, N., Tuffin, M., Stafford, W., Cary, C., Lacap, D. C., Pointing, S. B., et al. (2011). Hypolithic microbial communities of quartz rocks from Miers Valley, McMurdo Dry Valleys, Antarctica. *Polar Biol.* 34, 1657–1668.

Kirchman, D. (2001). Measuring bacterial biomass production and growth rates from leucine incorporation in natural aquatic environments. *Methods Microbiol.* 30, 227–237.

Klindworth, A., Pruesse, E., Schweer, T., Peplies, J., Quast, C., Horn, M., et al. (2013). Evaluation of general 16S ribosomal RNA gene PCR primers for classical and next-generation sequencing-based diversity studies. *Nucleic Acids Res.* 41:e1. doi: 10.1093/nar/gks808

Klymiuk, I., Bambach, I., Patra, V., Trajanoski, S., and Wolf, P. (2016). 16S based microbiome analysis from healthy subjects' skin swabs stored for different storage periods reveal phylum to genus level changes. *Front. Microbiol.* 7:2012. doi: 10.3389/fmicb.2016.02012

Koskinen, K., Pausan, M. R., Perras, A. K., Beck, M., Bang, C., Mora, M., et al. (2017). First insights into the diverse human archaeome: specific detection of Archaea in the gastrointestinal tract, lung, and nose and on skin. *mBio* 8:e00824-17. doi: 10.1128/mBio.00824-17

Lee, C. K., Barbier, B. A., Bottos, E. M., McDonald, I. R., and Cary, S. C. (2012). The Inter-Valley Soil Comparative Survey: the ecology of Dry Valley edaphic microbial communities. *ISME J.* 6, 1046–1057. doi: 10.1038/ismej.2011.170

Leslie, A. (2011). *The Arctic Voyages of Adolf Erik Nordenskiöld*. Cambridge: Cambridge University Press, 1858–1879. doi: 10.1017/CBO9781139151597

Lopatina, A., Krylenkov, V., and Severinov, K. (2013). Activity and bacterial diversity of snow around Russian Antarctic stations. *Res. Microbiol.* 164, 949–958. doi: 10.1016/j.resmic.2013.08.005

Love, M. I., Huber, W., and Anders, S. (2014). Moderated estimation of fold change and dispersion for RNA-seq data with DESeq2. *Genome Biol.* 15:550. doi: 10.1186/s13059-014-0550-8

Lutz, S., Ziolkowski, L. A., and Benning, L. G. (2019). The biodiversity and geochemistry of Cryoconite Holes in Queen Maud Land, East Antarctica. *Microorganisms* 7:160. doi: 10.3390/microorganisms7060160

MacDonell, S., Sharp, M., and Fitzsimons, S. (2016). Cryoconite hole connectivity on the Wright Lower Glacier, McMurdo Dry Valleys, Antarctica. *J. Glaciol.* 62, 714–724. doi: 10.1017/jog.2016.62

Markl, G., and Piazolo, S. (1998). Halogen-bearing minerals in syenites and high-grade marbles of Dronning Maud Land, Antarctica: monitors of fluid compositional changes during late-magmatic fluid-rock interaction processes. *Contrib. Mineral. Petrol.* 132, 246–268.

Mauri, M., Elli, T., Caviglia, G., Uboldi, G., and Azzi, M. (2017). "RAWGraphs: a visualisation platform to create open outputs," in *Proceedings of the 12th Biannual Conference on Italian SIGCHI Chapter*, (New York, NY: ACM), 28.

McMurdie, P. J., and Holmes, S. (2013). Phyloseq: an R package for reproducible interactive analysis and graphics of microbiome census data. *PLoS ONE* 8:e61217. doi: 10.1371/journal.pone.0061217

McMurdie, P. J., and Holmes, S. (2014). Waste not, want not: why rarefying microbiome data is inadmissible. *PLoS Comput. Biol.* 10:e1003531. doi: 10.1371/journal.pcbi.1003531

Morgan-Kiss, R. M., Priscu, J. C., Pocock, T., Gudynaite-Savitch, L., and Huner, N. P. (2006). Adaptation and acclimation of photosynthetic microorganisms to permanently cold environments. *Microbiol. Mol. Biol. Rev.* 70, 222–252.

Mosier, A. C., Murray, A. E., and Fritsen, C. H. (2007). Microbiota within the perennial ice cover of Lake Vida, Antarctica. *FEMS Microbiol. Ecol.* 59, 274–288.

Mou, Y. Z., Qiu, X. X., Zhao, M. L., Cui, H. L., Oh, D., and Dyall-Smith, M. L. (2012). *Halohasta litorea* gen. nov. sp. nov., and *Halohasta litchfieldiae* sp. nov., isolated from the Daliang aquaculture farm, China and from Deep Lake, Antarctica, respectively. *Extremophiles* 16, 895–901. doi: 10.1007/s00792-012-0485-5

Mueller, D. R., and Pollard, W. H. (2004). Gradient analysis of cryoconite ecosystems from two polar glaciers. *Polar Biol.* 27, 66–74.

Mueller, D. R., Vincent, W. F., Pollard, W. H., and Fritsen, C. H. (2001). Glacial cryoconite ecosystems: a bipolar comparison of algal communities and habitats. *Nova Hedwigia Beiheft* 123, 173–198.

Namsaraev, Z., Mano, M., Fernandez, R., and Wilmotte, A. (2010). Biogeography of terrestrial cyanobacteria from Antarctic ice-free areas. *Ann. Glaciol.* 51, 171–177. doi: 10.3189/172756411795931930

Obbels, D., Verleyen, E., Mano, M. J., Namsaraev, Z., Sweetlove, M., Tytgat, B., et al. (2016). Bacterial and eukaryotic biodiversity patterns in terrestrial and aquatic habitats in the Sør Rondane Mountains, Dronning Maud Land, East Antarctica. *FEMS Microbiol. Ecol.* 92:fiw041. doi: 10.1093/femsec/fiw041

Oksanen, J., Kindt, R., Legendre, P., O'Hara, B., Stevens, M. H. H., Oksanen, M. J., et al. (2007). The vegan package. *Community Ecol. Package* 10, 631–637.

Papale, M., Rizzo, C., Villescusa, J. A., Rochera, C., Camacho, A., Michaud, L., et al. (2017). Prokaryotic assemblages in the maritime Antarctic Lake Limnopolar (Byers Peninsula, South Shetland Islands). *Extremophiles* 21, 947–961. doi: 10.1007/s00792-017-0955-x

Pausan, M. R., Csorba, C., Singer, G., Till, H., Schöpf, V., Santigli, E., et al. (2019). Exploring the archaeome: detection of archaeal signatures in the human body. *Front. Microbiol.* 10:2796. doi: 10.3389/fmicb.2019.02796

Porazinska, D. L., Fountain, A. G., Nylen, T. H., Tranter, M., Virginia, R. A., and Wall, D. H. (2004). The Biodiversity and biogeochemistry of cryoconite holes from McMurdo Dry Valley glaciers, Antarctica. *Arct. Antarct. Alp. Res.* 36, 84–91.

Porter, K. G., and Feig, Y. S. (1980). The use of DAPI for identifying and counting aquatic microflora 1. *Limnol. Oceanogr.* 25, 943–948.

Quast, C., Pruesse, E., Yilmaz, P., Gerken, J., Schweer, T., Yarza, P., et al. (2013). The SILVA ribosomal RNA gene database project: improved data processing and web-based tools. *Nucleic Acids Res.* 41, 590–596. doi: 10.1093/nar/gks1219

Revelle, W. (2019). psych: Procedures for Psychological, Psychometric, and Personality Research. Northwestern University, Evanston, Illinois. R package version 1.9.12. Available online at: https://CRAN.R-project.org/package=psych (accessed February 15, 2020).

Rignot, E., Mouginot, J., Morlighem, M., Seroussi, H., and Scheuchl, B. (2014). Widespread, rapid grounding line retreat of Pine Island, Thwaites, Smith, and Kohler glaciers, West Antarctica, from 1992 to 2011. *Geophys. Res. Lett.* 41, 3502–3509. doi: 10.1002/2014GL060140

Samui, G., Antony, R., and Thamban, M. (2018). Chemical characteristics of hydrologically distinct cryoconite holes in coastal Antarctica. *Ann. Glaciol.* 59, 69–76. doi: 10.1017/aog.2018.30

Scheinert, M., Ivins, E., Dietrich, R., and Rülke, A. (2006). "Vertical Crustal Deformation in Dronning Maud Land, Antarctica: Observation versus Model Prediction," in *Antarctica*, eds D. K. Fütterer, D. Damaske, G. Kleinschmidt, H. Miller, and F. Tessensohn (Berlin: Springer).

Schindelin, J., Arganda-Carreras, I., Frise, E., Kaynig, V., Longair, M., Pietzsch, T., et al. (2012). Fiji: an open-source platform for biological-image analysis. *Nat. Methods* 9, 676–682. doi: 10.1038/nmeth.2019

Schwab, M. (1998). Reconstruction of the late quaternary climatic and environmental history of the Schirmacher Oasis and the Wohlthat Massif (East Antarctica). *Rep. Polar Res.* 293, 1–128. doi: 10.1016/j.quaint.2010.11.025

Smith, H. J., Schmit, A., Foster, R., Littman, S., Kuypers, M. M., and Foreman, C. M. (2016). Biofilms on glacial surfaces: hotspots for biological activity. *NPJ Biofilms Microbiomes* 2:16008. doi: 10.1038/npjbiofilms.2016.8

Sommers, P., Fontenele, R. S., Kringen, T., Kraberger, S., Porazinska, D. L., Darcy, J. L., et al. (2019). Single-stranded DNA viruses in antarctic cryoconite holes. *Viruses* 11:1022.

Takeuchi, N., Kohshima, S., and Seko, K. (2001). Structure, Formation, and Darkening Process of Albedo-reducing Material (Cryoconite) on a Himalayan Glacier: a Granular Algal Mat Growing on the Glacier. *Arctic Antarct. Alp. Res.* 33, 115–122. doi: 10.1080/15230430.2001.12003413

Tang, C., Madigan, M. T., and Lanoil, B. (2013). Bacterial and archaeal diversity in sediments of west Lake Bonney, McMurdo Dry Valleys, Antarctica. *Appl. Environ. Microbiol.* 79, 1034–1038. doi: 10.1128/AEM.02336-12

Telling, J., Anesio, A. M., Tranter, M., Fountain, A. G., Nylen, T., Hawkings, J., et al. (2014). Spring thaw ionic pulses boost nutrient availability and microbial growth in entombed Antarctic Dry Valley cryoconite holes. *Front. Microbiol.* 5:694. doi: 10.3389/fmicb.2014.00694

Tikhonov, M., Leach, R. W., and Wingreen, N. S. (2015). Interpreting 16S metagenomic data without clustering to achieve sub-OTU resolution. *ISME J.* 9, 68–80. doi: 10.1038/ismej.2014.117

Uetake, J., Nagatsuka, N., Onuma, Y., Takeuchi, N., Motoyama, H., and Aoki, T. (2019). Bacterial community changes with granule size in cryoconite and their susceptibility to exogenous nutrients on NW Greenland glaciers. *FEMS Microbiol. Ecol.* 95:fiz075. doi: 10.1093/femsec/fiz075

Vincent, W. F. (2000). "Cyanobacterial dominance in the polar regions," in *The Ecology of Cyanobacteria*, eds B. A. Whitton, and M. Potts (Dordrecht: Springer), 321–340.

Vincent, W. F., Gibson, J. A. E., Pienitz, R., Villeneuve, V., Broady, P. A., Hamilton, P. B., et al. (2000). Ice shelf microbial ecosystems in the high Arctic and implications for life on Snowball Earth. *Naturwissenschaften* 87, 137–141.

Vogler, P. (1966). Zur Analytik kondensierter Phosphate und organischer Phosphate bei limnologischen Untersuchungen. *Int. Revue ges. Hydrobiol. Hydrogr.* 51, 775–785. doi: 10.1002/iroh.19660510507

Wand, U., and Perlt, J. (1999). Glacial boulders 'floating' on the ice cover of Lake Untersee, East Antarctica. *Antarct. Sci.* 11, 256–260. doi: 10.1017/S0954102099000310

Wand, U., Samarkin, V. A., Nitzsche, H. M., and Hubberten, H. W. (2006). Biogeochemistry of methane in the permanently ice-covered Lake Untersee, central Dronning Maud Land, East Antarctica. *Limnol. Oceanogr.* 51, 1180–1194.

Webster-Brown, J., Gall, M., Gibson, J., Wood, S., and Hawes, I. (2010). The biogeochemistry of meltwater habitats in the Darwin Glacier region (80oS), Victoria Land, Antarctica. *Antarct. Sci.* 22, 646–661. doi: 10.1017/S0954102010000787

Webster-Brown, J. G., Hawes, I., Jungblut, A. D., Wood, S. A., and Christenson, H. K. (2015). The effects of entombment on water chemistry and bacterial assemblages in closed cryoconite holes on Antarctic glaciers. *FEMS Microbiol. Ecol.* 91:fiv144. doi: 10.1093/femsec/fiv144

Weisleitner, K., Hunger, L., Kohstall, C., Frisch, A., Storrie-Lombardi, M. C., and Sattler, B. (2019a). Laser-Induced Fluorescence Emission (LIFE) as Novel Non-Invasive Tool for In-Situ Measurements of Biomarkers in Cryospheric Habitats. *J. Vis. Exp.* 152:e60447.

Weisleitner, K., Perras, A. K., Moissl-Eichinger, C., Andersen, D. T., and Sattler, B. (2019b). Source environments of the microbiome in perennially ice-covered Lake Untersee, Antarctica. *Front. Microbiol.* 10:1019. doi: 10.3389/fmicb.2019.01019

Wharton, R. A., McKay, C. P., Simmons, G. M., and Parker, B. C. (1985). Cryoconite holes on glaciers. *Bioscience* 35, 499–503. doi: 10.2307/1309818

Wharton, R. A., Vinyard, W. C., Parker, B. C., Simmons, G. M., and Seaburg, K. G. (1981). Algae in cryoconite holes on Canada Glacier in Southern Victoriland, Antarctica. *Phycologia* 20, 208–211. doi: 10.2216/i0031-8884-20-2-208.1

Wickham, H. (2011). ggplot2. *WIREs Comp. Stat.* 3, 180–185. doi: 10.1002/wics.147

Yergeau, E., Newsham, K. K., Pearce, D. A., and Kowalchuk, G. A. (2007). Patterns of bacterial diversity across a range of Antarctic terrestrial habitats. *Environ. Microbiol.* 9, 2670–2682.

Zdanowski, M. K., Bogdanowicz, A., Gawor, J., Gromadka, R., Wolicka, D., and Grzesiak, J. (2017). Enrichment of cryoconite hole anaerobes: implications for the subglacial microbiome. *Microb. Ecol.* 73, 532–538. doi: 10.1007/s00248-016-0886-6

Zeglin, L. H., Dahm, C. N., Barrett, J. E., Gooseff, M. N., Fitpatrick, S. K., and Takacs-Vesbach, C. D. (2011). Bacterial community structure along moisture gradients in the parafluvial sediments of two ephemeral desert streams. *Microb. Ecol.* 61, 543–556. doi: 10.1007/s00248-010-9782-7

Conflict of Interest: The authors declare that the research was conducted in the absence of any commercial or financial relationships that could be construed as a potential conflict of interest.

frontiers in Microbiology

ORIGINAL RESEARCH
published: 03 June 2020
doi: 10.3389/fmicb.2020.01036

Niche Differentiation in the Composition, Predicted Function, and Co-occurrence Networks in Bacterial Communities Associated With Antarctic Vascular Plants

Qian Zhang[1†], *Jacquelinne J. Acuña*[2,3], *Nitza G. Inostroza*[2,3], *Paola Duran*[3], *María L. Mora*[3], *Michael J. Sadowsky*[1,4†] *and Milko A. Jorquera*[2,3*†]

[1] *The BioTechnology Institute, University of Minnesota, St Paul, MN, United States,* [2] *Laboratorio de Ecología Microbiana Aplicada (EMALAB), Departamento de Ciencias Químicas y Recursos Naturales, Universidad de La Frontera, Temuco, Chile,* [3] *Network for Extreme Environment Research (NEXER), Scientific and Technological Bioresource Nucleus (BIOREN), Universidad de La Frontera, Temuco, Chile,* [4] *Department of Soil, Water, and Climate, and Department of Plant and Microbial Biology, University of Minnesota, St. Paul, MN, United States*

OPEN ACCESS

Edited by:
David Anthony Pearce, Northumbria University, United Kingdom

Reviewed by:
Mircea Podar, Oak Ridge National Laboratory (DOE), United States
Charles K. Lee, University of Waikato, New Zealand

***Correspondence:**
Milko A. Jorquera
milko.jorquera@ufrontera.cl

†ORCID:
Qian Zhang
orcid.org/0000-0001-8368-6260
Michael J. Sadowsky
orcid.org/0000-0001-8779-2781
Milko A. Jorquera
orcid.org/0000-0003-4760-6379

Specialty section:
This article was submitted to Extreme Microbiology, a section of the journal Frontiers in Microbiology

Received: *20 February 2020*
Accepted: *27 April 2020*
Published: *03 June 2020*

Citation:
Zhang Q, Acuña JJ, Inostroza NG, Duran P, Mora ML, Sadowsky MJ and Jorquera MA (2020) Niche Differentiation in the Composition, Predicted Function, and Co-occurrence Networks in Bacterial Communities Associated With Antarctic Vascular Plants. Front. Microbiol. 11:1036. doi: 10.3389/fmicb.2020.01036

Climate change directly affecting the Antarctic Peninsula has been reported to induce the successful colonization of ice-free lands by two Antarctic vascular plants (*Deschampsia antarctica* and *Colobanthus quitensis*). While studies have revealed the importance of microbiota for plant growth and stress tolerance in temperate climates, the role that plant-associated microbes play in the colonization of ice-free lands remains unknown. Consequently, we used high-throughput DNA sequence analyses to explore the composition, predicted functions, and interactive networks of plant-associated microbial communities among the rhizosphere, endosphere, and phyllosphere niches of *D. antarctica* and *C. quitensis*. Here we report a greater number of operational taxonomic units (OTUs), diversity, and richness in the microbial communities from the rhizosphere, relative to endosphere and phyllosphere. While taxonomic assignments showed greater relative abundances of *Proteobacteria*, *Bacteroidetes,* and *Actinobacteria* in plant niches, principal coordinate analysis revealed differences among the bacterial communities from the other compartments examined. More importantly, however, our results showed that most of OTUs were exclusively found in each plant niche. Major predicted functional groups of these microbiota were attributed to heterotrophy, aerobic heterotrophy, fermentation, and nitrate reduction, independent of plant niches or plant species. Co-occurrences network analyses identified 5 (e.g., *Microbacteriaceae*, *Pseudomonaceae*, *Lactobacillaceae,* and *Corynebacteriaceae*), 23 (e.g., *Chitinophagaceae* and *Sphingomonadaceae*) and 7 (e.g., *Rhodospirillaceae*) putative keystone taxa present in endosphere, phyllosphere, and rhizosphere, respectively. Our results revealed niche differentiation in Antarctic vascular plants, highlighting some putative microbial indicators and keystone taxa in each niche. However, more studies are required to determine the pivotal role that these microbes play in the successful colonization of ice-free lands by Antarctic plants.

Keywords: bacterial community, *Colobanthus quitensis*, *Deschampsia antarctica*, endosphere, phyllosphere, rhizosphere

INTRODUCTION

Climate change has become of global concern over the last several decades. This is of particular importance to the polar regions of the world, such as the Antarctic Peninsula. Studies have reported that the Antarctic Peninsula has been subjected to recent warming and cooling events, suggesting the uncovering of new ice-free lands (Lee et al., 2017). This may subsequently lead to the greater availability of potentially new habitats for colonization by numerous organisms and a higher connectivity between habitats (Lee et al., 2017). Recent Antarctic cooling events have resulted in deleterious effect on lichens, which are a dominant vegetation type in the Antarctic peninsula, creating new opportunities for expansion by other vegetation species (Sancho et al., 2017). In this context, the expansion of Antarctic vascular plants has been attributed to their efficient nitrogen acquisition capacity, competing with both soil microorganisms and lichens (Hill et al., 2011). More recently, Royles et al. (2013) proposed that the increase in terrestrial plant growth rates and soil microbial activity are consistent with recent warming events on the Antarctic peninsula. Moreover, studies have also shown that warming due to global climate events have significantly influenced the abundance, composition, and activity of soil microorganisms from Antarctic environments (Yergeau et al., 2012).

Previous molecular studies have revealed that the rhizosphere (the soil portion influenced by roots) of Antarctic vascular plants, including Antarctic hair grass (*Deschampsia antarctica*) and Antarctic pearlwort (*Colobanthus quitensis*), can harbor a wide diversity of bacteria (Teixeira et al., 2010; Jorquera et al., 2016). Differences in bacterial community composition in the rhizospheres of *D. antarctica* and *C. quitensis* were observed by Teixeira et al. (2010) and members of *Firmicutes* were more abundant in the rhizosphere of *D. antarctica* compared to that of *C. quitensis*.

Results from several studies have established that bacteria are relevant for growth and tolerance of plants to harsh conditions in extreme environments. For example, a plant growth-promoting bacteria (PGPB) was isolated from the rhizosphere of *D. antarctica* showing the ability to promote the plant root development *in vitro* inoculation assay (Berríos et al., 2013). Similarly, the salt tolerance and ecophysiological performance of *D. antarctica* and *C. quitensis* was improved when plants were inoculated with Antarctic bacteria isolated from their rhizosphere (Gallardo-Cerda et al., 2018). Despite these advances, the contribution of microbiota from the endosphere (inner tissues of plants) and phyllosphere (the aerial part of plant leaves) to plant fitness have scarcely been considered, especially since these compartments are thought to be essential for plant success (Cid et al., 2017). In addition, new studies have revealed that the plant microbiome is structured and complex and interconnected by microbial networks (Turner et al., 2013; Vandenkoornhuyse et al., 2015; Banerjee et al., 2018). Moreover, these microbial networks harbor keystone taxa that act as drivers of the structure and functioning of microbiome and are likely essential for plant health and ecosystem functioning (van der Heijden and Hartmann, 2016; Banerjee et al., 2018). Evidence for such a scenario also comes from a recent study showing that plant and microbiome interactions are also complicated by plant-plant-microbe interactions (Molina-Montenegro et al., 2018).

As global climate issues become of even more concern, there is a need to better understand the diversity, functionality, and response of plant-associated microbes under climate change, as well as their relevance for Antarctic vascular plants expansion onto ice-free lands. Under this scenario, the main goals of the present study were to: (1) determine if the composition, predicted function, and networks of bacterial communities significantly differ among niches (rhizosphere, endosphere and phyllosphere) of the Antarctic vascular plants (*D. antarctica* and *C. quitensis*); and (2) at the same time to identify putative microbial indicators and keystone taxa in each niche which may give cues on microbiota playing pivotal roles in the growth and/or colonization of ice-free lands by these plants.

MATERIALS AND METHODS

Sampling

Plant specimens and their respective rhizosphere soils were collected during Antarctic Scientific Expedition no. 53 (ECA53; February 2017) to the South Shetland Islands of Antarctica, organized by Chilean Antarctic Institute (INACH). The plant specimens were taken from mantles of *D. antarctica* and *C. quitensis* located at the following coordinates: 62°59′53″S, 60°35′17″W and 62°24′7″S, 58°18′29″W, respectively. The plant specimens were randomly taken in a 10 m transect by using a clean spade to remove intact roots from soil. Collected plants and soils were placed within plastic bags, stored at 4°C, and transported on ice to the Applied Microbial Ecology Laboratory (EMALAB) at La Frontera University for microbiological analyses.

Endosphere samples from four plants of each species were processed as described by Barra et al. (2016). Plant tissues (roots and leaves) were washed and surface sterilized by repeated immersion in 70% (v/v) ethanol for 3 min, followed by 2.5% (v/v) sodium hypochlorite (NaOCl) for 5 min, and exhaustive rinsing with sterile distilled water (SDW). Portions of tissues (1–2 g) were aseptically cut, frozen in liquid nitrogen, macerated and homogenized with a mortar and pestle, and stored at −80°C until DNA extraction. In parallel, quadruplicate phyllosphere leaf samples were processed as described by Cid et al. (2017). Briefly, 1 g portions of leaves were cut (aerial parts), gently washed, and vortexed for 10 min in 10 ml sterile saline solution (0.85% NaCl). Leaves were removed, and the recovered liquid was centrifuged at 15,700 × g for 10 min to collect detached bacterial cells. Bacterial cells were suspended in 50 μl of SDW, and this suspension was subsequently frozen in liquid nitrogen and thawed at room temperature three times. Samples were centrifuged at 15,700 × g for 40 min, and the supernatant (∼40 μl) was used as template DNA in PCR reactions. Rhizosphere soil samples from each plant specimen were processed, in quadruplicate, as described by Lagos et al. (2014). Briefly, soil aggregates were detached from roots by vigorous vortexing and collected in sterile polypropylene microtubes. Rhizosphere soils were gently mixed, and 1–2 g subsamples were stored at −80°C, and later subjected to DNA extraction.

The physicochemical properties of the rhizosphere soils were also determined as follow. The pH was measured in 1:2.5 soil/deionized water suspensions. Available phosphorus (P_{Olsen}) was extracted using 0.5 M Na-bicarbonate method and analyzed using the molybdate-blue method (Murphy and Riley, 1962). Organic matter contents were estimated by wet digestion (Walkley and Black, 1934). Exchangeable cations (K^+, Ca^{2+}, Mg^{2+}, and Na^+) were extracted with 1M CH_3COONH_4 at pH 7.0 and analyzed using flame atomic adsorption spectrophotometry (FAAS) (Warncke and Brown, 1998). Exchangeable aluminum (Al^{3+}) was extracted with 1M KCl and analyzed by FAAS (Bertsch and Bloom, 1996).

DNA Extraction

DNA from the endosphere and phyllosphere samples was extracted by using Quick–DNA™ Plant/seed Miniprep kits (Zymo Research, CA, USA). DNA from rhizosphere soil samples was extracted with PowerSoil® DNA isolation kit (Qiagen, MO BIO Laboratories, CA, USA), both kits were used according to manufacturer instructions.

High–Throughput DNA Sequencing

The distribution and relative abundances of endophytic bacteria in root endospheres, leaf phyllospheres, and rhizosphere soils, was assessed by high throughput DNA sequencing (HTS) analyses as follow. The V4 hypervariable region of the 16S rRNA was amplified, for bacteria and archaea, by using primer set 515F (5′- GTG CCA GCM GCC GCG GTA A−3′) and 806R (5′- GGA CTA CHV GGG TWT CTA AT−3′). Sequencing was done by the University of Minnesota Genomics Center (UMGC, Minneapolis, MN, USA) using barcoded primers and the dual indexing method (Gohl et al., 2016). Amplicons were gel purified, pooled, and paired–end sequenced at a read length of 300 nt on the Illumina MiSeq platform (Illumina, Inc., San Diego, CA, USA).

Bioinformatics and Statistical Analysis

Mothur ver. 1.34.0 was used for most sequence analyses (Schloss et al., 2009). In brief, after trimming low-quality regions at the ends of reads, the paried-end sequencing reads were merged by Fastq-join software (Aronesty, 2013), maintaining an average quality score >33. Primer sequences were removed from reads and high quality sequencing reads were aligned on the basis of the Greengenes ver.13.8 (McDonald et al., 2012). The UCHIME software package was used to identify and remove probable chimeric sequences (Edgar et al., 2011). Non-microbiota (e.g., chloroplast and mitochondria) sequence reads were removed via QIIME (Caporaso et al., 2010), and data was rarefied to 14,000 sequence reads per sample set prior to statistical analysis. Raw sequencing data were deposited in the Sequence Read Archive (SRA) of NCBI under Accession Number PRJNA509213. For statistical analysis, the mothur program was also used to calculate alpha diversity indices, including Good's coverage, the Shannon index, and the Abundance-based Coverage Estimate (ACE). Principal coordinate analysis (PCoA) was used to ordinate the samples. Differences in beta diversity among the community were evaluated by analysis of similarity (ANOSIM) using Bray-Curtis dissimilarity matrices (Bray and Curtis, 1957; Clarke, 1993). Molecular variance (AMOVA) was used to measure differences in sample clustering (Excoffier et al., 1992). The VennDiagram package in R (https://www.r-project.org/) was used to identify shared OTUs of bacterial communities between plant niches (Chen and Boutros, 2011). Putative indicator OTUs in Antarctic vascular plants that were in association with the differentiation of plant niches were identified on the basis of the *multipatt* function using the *indicspecies* package in R (de Caceres and Legendre, 2009). The associations were further considered to be significant by using a false discovery rate ($q < 0.1$) (Strimmer, 2008). Visualization of the putative association of indicators with plant niches in the Antarctic plants was produced by using *gplots* package in R package (heatmap) and by iTOL (tree) (Letunic and Bork, 2016). FAPROTAX was used to predict potential functions among members of the microbial community in the different niches (rhizosphere, endospheres, and phyllosphere). Potential functions were determined via the default settings on the basis of taxonomic information of microbiota in Antarctic vascular plant (Louca et al., 2016).

Network Analysis of Bacterial Community in Various Niches of Antarctic Vascular Plants

Rare microorganisms were defined as those that were not found above 0.01% relative abundance in the rhizosphere, endosphere and phyllosphere samples from *D. antarctica* and *C. quitensis*. The co-occurrence network was constructed as described by Ma et al. (2016). Briefly, a Spearman correlation matrix was used to generate the co-occurrence network via the WGCNA package. The nodes indicate the OTUs, while the edges, which are connecting the nodes, represent correlations between OTUs. Prior to network construction, random matrix theory (RMT) was

TABLE 1 | Physicochemical properties of rhizosphere soil samples from the Antarctic vascular plants used in this study.

	Deschampsia antarctica	*Colobanthus quitensis*
P_{Olsen} (mg kg^{-1})	85 ± 41.6†	25 ± 4.2
K (mg kg^{-1})	487.3 ± 85.9	277.7 ± 40.8
pH_{H2O}	6.1 ± 0.2	6.3 ± 0.2
Organic matter (g kg^{-1})	9.2 ± 4	1.9 ± 0.7
K ($cmol_{(+)}$ kg^{-1})	1.2 ± 0.2	0.7 ± 0.1
Na ($cmol_{(+)}$ kg^{-1})	5.3 ± 1.6	1.6 ± 0.2
Ca ($cmol_{(+)}$ kg^{-1})	10.3 ± 2.8	14.4 ± 2.8
Mg ($cmol_{(+)}$ kg^{-1})	6 ± 0.9	7.7 ± 0.9
Al ($cmol_{(+)}$ kg^{-1})	0.013 ± 0.03	0.057 ± 0.024
Al saturation (%)‡	0.063 ± 0.012	0.267 ± 0.136
CEC ($cmol_{(+)}$ kg^{-1})	22.8 ± 3.9	24.5 ± 3.3
Σ bases ($cmol_{(+)}$ kg^{-1})	22.8 ± 3.9	24.5 ± 3.4

† *The values represent means ± standard errors from n = 3.*
‡ *Calculated as (Al×100) / CEC, where CEC=cation exchange capacity = Σ (K, Ca, Mg, Na, and Al).*

performed to identify the appropriate similarity of 0.82 as the threshold (Luo et al., 2006), and the *P*-values of correlations were defined by using the Benjamini and Hochberg false discovery rate (FDR) of < 0.05 (Benjamini et al., 2006). The *igraph* package was used to measure the network properties (Csardi and Nepusz, 2006), while Gephi was further used to achieve the network image and calculations of closeness centrality and betweenness centrality for each node (Bastian et al., 2009). In addition, the occurrence of putative keystone taxa, which play pivotal roles in the structure and functioning of the microbial community (Banerjee et al., 2018), was determined in each niche as follows (Berry and Widder, 2014): For the endosphere network, OTUs with degree > 8, closeness centrality > 0.18, and betweenness centrality < 0.05 were used to identify putative keystone taxa. For the phyllosphere network, OTUs with > 5 degrees, closeness centrality > 0.15, and betweenness centrality < 0.05 were selected as putative keystone taxa. For the rhizosphere network, OTUs with > 7 degrees, closeness centrality > 0.17, and betweenness centrality < 11 were chosen as putative keystone taxa.

RESULTS

Physicochemical Properties of Rhizosphere Soils

The physicochemical properties of triplicate rhizosphere soils are summarized in **Table 1**. These analyses revealed differences between rhizosphere soils from both Antarctic plants. Rhizosphere soils from *D. antarctica* showed higher contents of available P, K, and organic matter compared with that from *C. quitensis*. In contrast, rhizosphere soils from *C. quitensis* had a greater higher cation exchange capacity (CEC) and Al saturation compared with those from *D. antarctica*. Despite these differences, both plant species had rhizosphere soils with similar pH_{H2O} values, 6.1 and 6.3 for *D. antarctica* and *C. quitensis*, respectively.

Coverage and Alpha Diversity of Bacterial Community

Sequencing resulted in an estimated 98 to 99% coverage of OTUs in the endosphere and phyllosphere samples from both Antarctic plants. Substantial, but significantly (Tukey's *post–hoc* test, $p < 0.05$) lower coverage (95 to 96%) was observed in the rhizosphere samples relative to those from the other plant niches (**Table 2**). Similarly, a significantly ($p < 0.05$) greater number of OTUs (define at a 97% similarity) was observed in rhizosphere samples (1,551 and 1,628 for *D. antarctica* and *C. quitensis*, respectively), compared with those found in other plant niches. In this sense, the numbers of OTUs observed in the endosphere and phyllospheres samples were lower in *D. antarctica* (434 and 522 OTUs, respectively) compared to those in *C. quitensis* (662 and 666 OTUs, respectively). Bacterial alpha diversity, revealed by the Shannon index, was significantly ($p < 0.05$) greater in rhizosphere samples (6.2 for both plant species) compared with endospheres (3.9 and 4.9 for *D. Antarctica* and *C. quitensis*, respectively) and phyllospheres (3.7 and 4.4 for *D. Antarctica* and *C. quitensis*, respectively). In addition, significantly lower ACE values ($p < 0.05$) were observed in the endosphere (525 and 884 for *D. Antarctica* and *C. quitensis*, respectively) and phyllosphere (865 and 1,312 for *D. Antarctica* and *C. quitensis*, respectively) samples compared with those in the rhizospheres (2,093 and 2,237 for *D. Antarctica* and *C. quitensis*, respectively).

Taxonomy Assignments of Bacterial Community

Assignment of taxonomic affiliation to members of bacterial communities indicated that members of the *phylum Proteobacteria* were relatively abundant in both Antarctic plants, with values of 48.8 to 58.9, 60.6 to 75.4, and 35.7 to 36.1% for endosphere, phyllosphere, and rhizosphere samples, respectively (**Figure 1**). While the endosphere communities in both plant species were also colonized by relatively large numbers of *Actinobacteria* (22.6 to 26.1%), *Bacteroidetes* (9.3 to 12%), and *Firmicutes* (5.3 to 7.9%) phyla, the phyllosphere was co-dominated by members of the phyla *Bacteroidetes* (14.3 to 30.9%) and *Actinobacteria* (4.8 to 7.5%). In contrast, the rhizosphere was also co-dominated by members of the phyla *Bacteroidetes* (14 to 19.7%), *Acidobacteria* (11.7 to 12.8%), *Actinobacteria* (9.2 to 13.7%), and *Verrucomicrobia* (8.7 to 9.9%). With respect to minor taxa, those present at < 10% of communities, a higher presence of bacterial groups was observed in rhizosphere samples compared with those in other niches, and were mainly attributed to members of the phyla *Armatimonadetes* (0.8 to 1%), *Chlorobi*

TABLE 2 | Coverage and alpha diversity (mean ± standard deviation) among bacterial communities by endosphere, phyllosphere, and rhizosphere in two Antarctic vascular plants, based on high–throughput DNA sequencing data in each plant species ($n = 4$).

Plant	Niche	Coverage (%)	$S^{\dagger}_{obs}$	Shannon index	ACE‡
Deschampsia antarctica	Endosphere	$99.25 \pm 0.34^{A*}$	434 ± 177^{A}	3.93 ± 1.06^{A}	525 ± 206^{A}
	Phyllosphere	98.58 ± 1.41^{A}	522 ± 576^{A}	3.74 ± 1.49^{A}	865 ± 754^{A}
	Rhizosphere	96.33 ± 0.46^{B}	1551 ± 66^{B}	6.23 ± 0.15^{B}	2093 ± 186^{B}
Colobanthus quitensis	Endosphere	98.59 ± 1.12^{A}	662 ± 458^{A}	4.34 ± 1.29^{A}	884 ± 615^{A}
	Phyllosphere	98.07 ± 0.86^{A}	666 ± 296^{A}	4.36 ± 0.66^{A}	1312 ± 544^{A}
	Rhizosphere	95.98 ± 0.51^{B}	1628 ± 188^{B}	6.25 ± 0.21^{B}	2237 ± 260^{B}

†S_{obs}: number of OTUs observed at 97% similarity.
‡ACE: abundance-based coverage estimate.
*Sample groups sharing the same letter in each niche did not vary significantly ($P \leq 0.05$) by ANOVA followed by Tukey's post-hoc test.

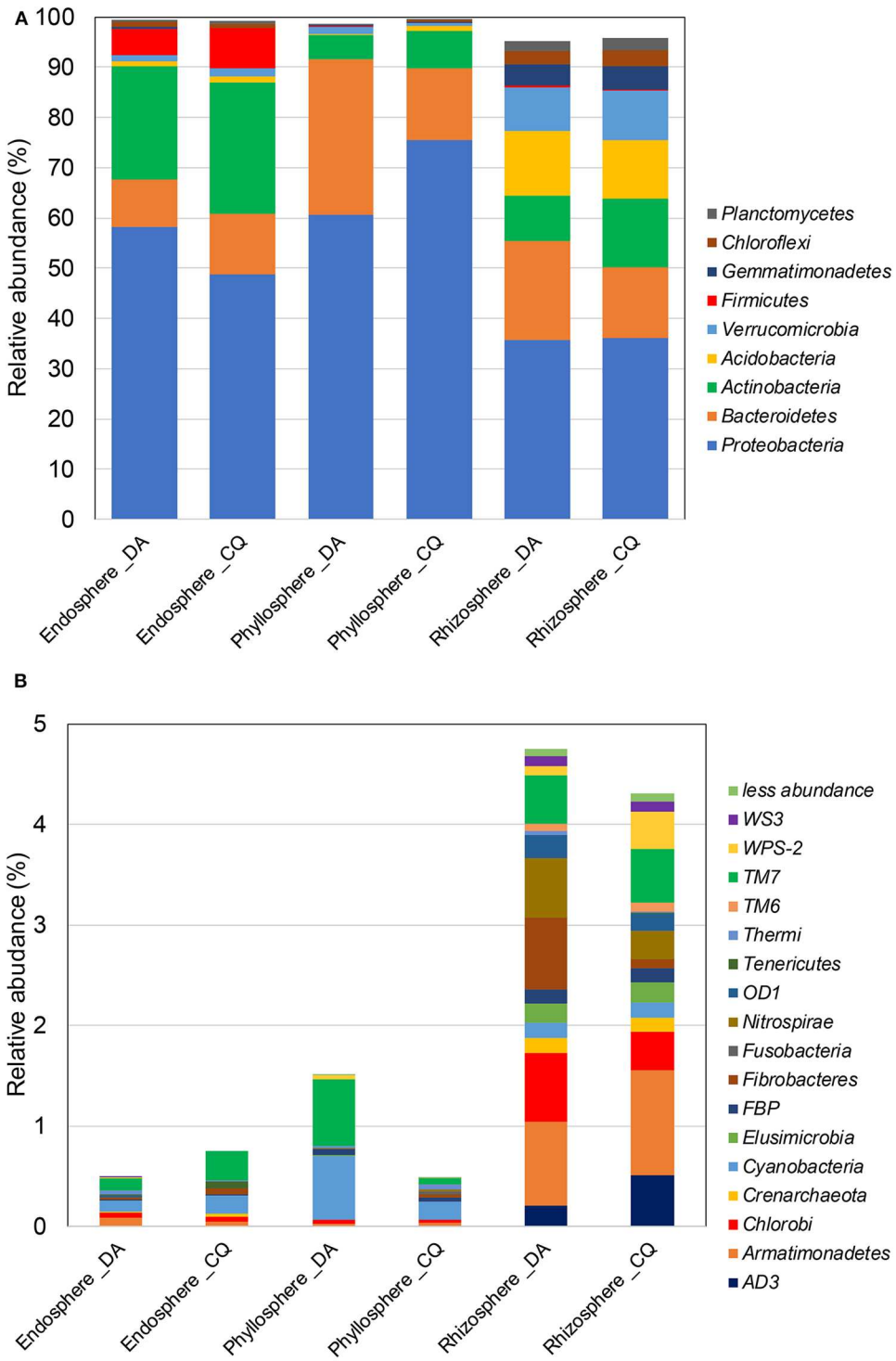

FIGURE 1 | Mean relative abundances of major **(A)** and minor **(B)** phylum-level taxa of bacterial communities in the endosphere, phyllosphere, and rhizosphere of the Antarctic vascular plants *Deschampsia antarctica* (DA) and *Colobanthus quitensis* (CQ).

(0.4 to 0.7%), *Saccharibacteria* (formerly TM7) (0.5%), and *Nitrospirae* (0.3 to 0.6%) in the rhizosphere of both plant species.

At the family level, a greater relative abundance of taxa in the endosphere were attributed to *Pseudomonadaceae* (18.7 to 26.2%), followed by *Enterobacteriaceae* (5.3 to 13.8%), and *Microbacteriaceae* (7.2 to 7.4%) (**Figure 2**). A greater diversity of families was observed in the phyllosphere samples, with higher relative abundances of *Pseudomonadaceae* (25.5

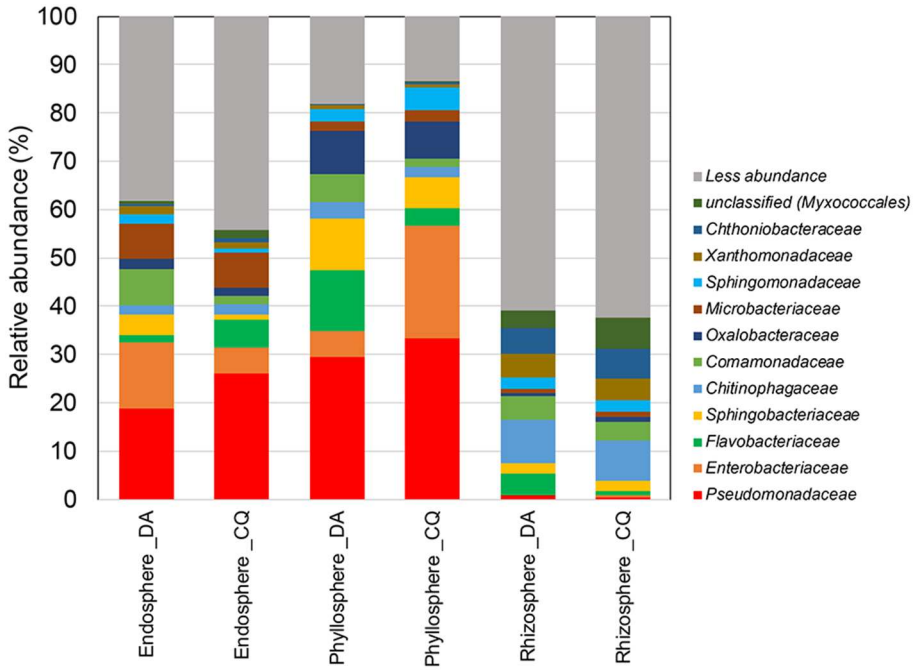

FIGURE 2 | Mean relative abundances of family-level taxa of bacterial communities in the endosphere, phyllosphere, and rhizosphere of the Antarctic vascular plants *Deschampsia antarctica* (DA) and *Colobanthus quitensis* (CQ).

to 33.3%) followed by *Enterobacteriaceae* (5.3 to 23.4%), *Sphingobacteriaceae* (6.5 to 10.7%), *Oxalobacteriacea* (7.7 to 9%), and *Flavobacteriaceae* (5.6 to 12.7%) families. Interestingly, *Pseudomonadaceae* were found as an abundant group in the endospheres and phyllospheres, but not in the rhizospheres. In contrast, the rhizosphere samples were dominated by members of the *Chitinophagaceae* (8.3 to 8.9%) followed by *Chthoniobacteraceae* (5.3 to 6.3%), *Xanthomonadaceae* (4.4 to 4.9%), and *Comamonadaceae* (3.8 to 4.8%) families.

Unique Microbial Communities Are Revealed by Beta Diversity Analyses

PCoA analyses showed a clear separation between microbiota in the rhizosphere and other plant niches in both Antarctic plants (**Figure 3**), but these differences were not seen between plant species. Our analysis also revealed that 24.2% (1,109 of 4,587) and 16.2% (678 of 4,181) of OTUs were shared between the three plant niches of *D. antarctica* and *C. quitensis*, respectively (**Figure 4**). In contrast, 75.8% (3,478 of 4,587) and 83.2% (3,503 of 4,181) of the OTUs were not shared and they were exclusively found in the individual plant niches of *D. antarctica* and *C. quitensis*, respectively. The greatest number of unique, not shared, sequences were found in rhizosphere samples, with 2,489 and 2,293 OTUs for *D. antarctica* and *C. quitensis*, respectively. The detailed distribution of shared and unique OTUs among bacterial communities in the plant niches are also shown in **Table S1**.

Predicted Functions of Bacterial Community Members

Presumptive microbial functional groups in each plant niches are shown in **Figure 5**. Independent of niches and species, the major functions were attributed to heterotrophy (30.5 to 44.3%) and aerobic heterotrophy (25.8 to 36.3%) (**Figure 5A**). Fermentation (3.4 to 9.7%) and nitrate reduction functions (1.8 to 5.2%) were also assigned in all niches. When minor functional groups were analyzed, a greater abundance of functional assignments were observed in rhizospheres, compared to those from the endosphere and phyllospheres (**Figure 5B**). A greater abundance of functions related to nitrogen cycling was observed in the rhizosphere of *D. antarctica* and *C. quitensis*. In contrast, in the phyllosphere samples the functions were mainly attributed to degradation of aliphatic and aromatic hydrocarbons. Lastly, samples from the endosphere also showed functions related to nitrogen cycling and hydrocarbon degradation, and dark oxidation of sulfur compounds.

Microbial Indicators of Niches in Antarctic Plants

Indicator analyses, based on taxonomic assignments from the genus to phylum levels, was used to investigate the association between taxon abundance and plant niches. Detailed information on the average abundance of each bacterium in each niche, their maximum association, the significance of associations (p-value), and the false discovery rate correction value (q) can be found in **Figure 6** and **Figure S1** and **Table S2**. Overall, our analyses identified 256 OTUs that were significantly associated

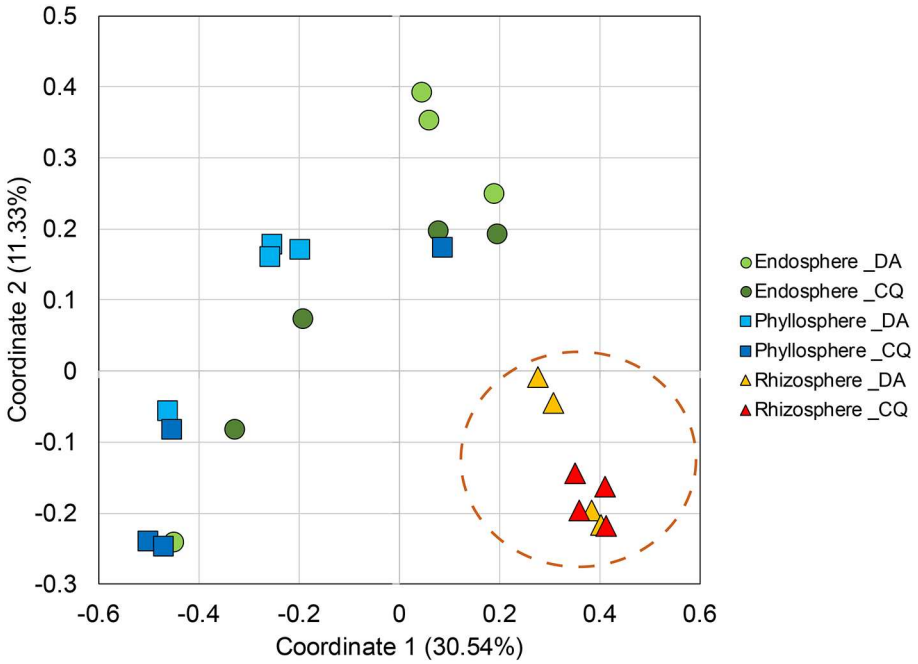

FIGURE 3 | Principal coordinate analysis (PCoA) of Bray-Curtis dissimilarity matrices of bacterial communities in the endosphere, phyllosphere, and rhizosphere of the Antarctic vascular plants *Deschampsia antarctica* (DA) and *Colobanthus quitensis* (CQ) ($r^2 = 0.57$). Pairwise comparison (Bonferroni) of bacterial communities between three plant compartments were performed by ANOSIM.

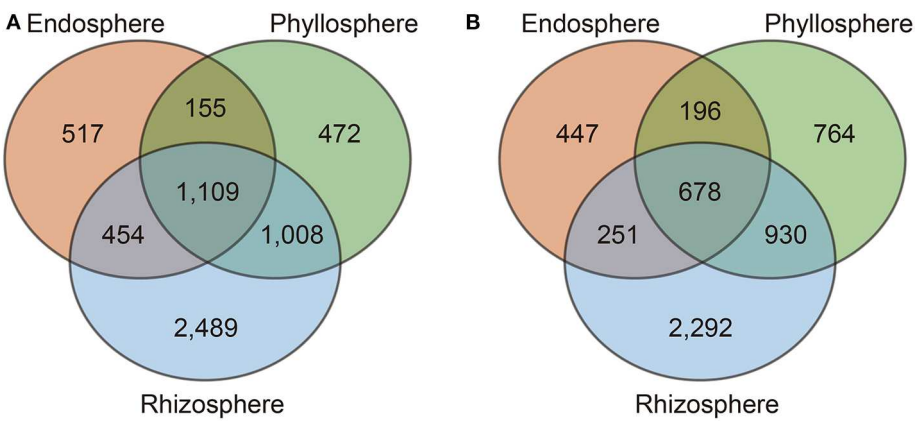

FIGURE 4 | Shared operational taxonomic units (OTUs) among bacterial communities present in the endosphere, phyllosphere, and rhizosphere of the Antarctic vascular plants *Deschampsia antarctica* **(A)** and *Colobanthus quitensis* **(B)**.

with various plant niches. Of these, however, only 84 taxa could be classified to the genus-level. While these 84 taxa were distributed among 12 phyla, most belonged to the *Proteobacteria*, *Actinobacteria*, and *Firmicutes*. Notably, *Pseudomonas*, which had the greatest abundance among the three plant niches, could be used as putative indicator taxa in the endosphere, where it was significantly associated with this niche. Moreover, *Clavibacter* was also greatly associated (R=0.91) with the endosphere. In contrast, *Novosphingobium* was the best putative indicator bacterium representing the phyllospheres, although it had the highest association (R=0.86) among the three niches. In contrast, *Dactylosporangium* (R=0.95) and *Bradyrhizobium* (R=0.65) were the best putative indicators of the rhizosphere niche in Antarctic plants (R=0.95), and.

Niche-Specific Co-occurrence Networks in Antarctic Plants

Due to the differences in microbial community structure and microbiota composition across the three plant niches, we further

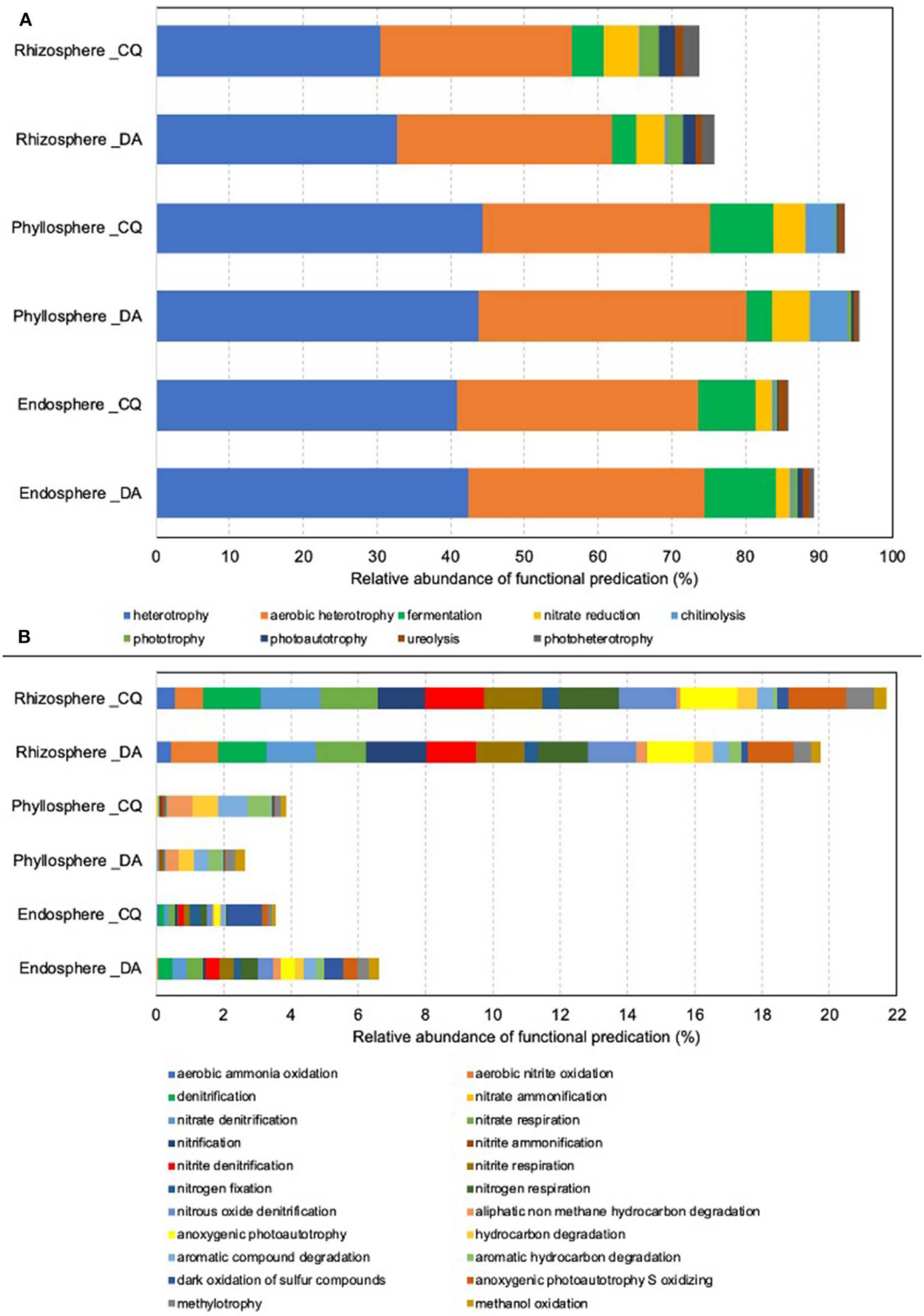

FIGURE 5 | Mean relative abundances of microbial functional groups in the rhizosphere, endosphere, and phyllosphere of *Deschampsia Antarctica and Colobanthus quitensis.* **(A)** Major functional groups and **(B)** minor functional groups.

investigated the bacterial network and putative keystone taxa for each niche separately (**Figure 7** and **Tables S3–S5**). Network analysis of the endosphere included 842 nodes (e.g., OTUs) and 1,062 edges, indicative of the association between OTUs. Results in **Figure 7A** show five putative keystone taxa in the endosphere network: *Microbacteriaceae* (0.05%), *Pseudomonadaceae* (0.6%),

two *Lactobacillaceae* (0.14% and 0.06%), and *Corynebacteriaceae* (0.02%). Most notably, the family *Microbacteriaceae* was the most critical keystone taxon, bridging the maximum number of nodes and associations in the endosphere network. The family *Pseudomonadaceae*, which had greater relative abundance among these five putative keystone taxa identified, was coordinated with *Pseudomonas* as an putative indicator bacterium at the genus-level in the endosphere (**Figures 6**, **7A** and **Figure S1**). In contrast, network analysis of the phyllosphere identified only 567 nodes and 386 edges. Impressively, although the phyllosphere network had fewer nodes and edges, 23 putative keystone taxa were identified (**Figure 7B**). The majority of the associations in the phyllosphere were from the families *Chitinophagaceae* (4 out of 23) and *Sphigomonadaceae* (3 out of 23). In the case of the phyllosphere, *Sphigomonadaceae*, in association with *Novosphingobium*, at the genus-level, was the best putative indicator in the phyllosphere samples ($R = 0.86$). In contrast, and perhaps expected due to its high diversity, the rhizosphere network consisted of 1,392 nodes and 2,682 edges, by far the largest of the three compartmental niches. Despite its large size, however, this highly complex rhizosphere network only had 7 putative keystone taxa (**Figure 7C**). Moreover, among these seven putative keystone taxa, only *Rhodospirillaceae* was identified at the family-level.

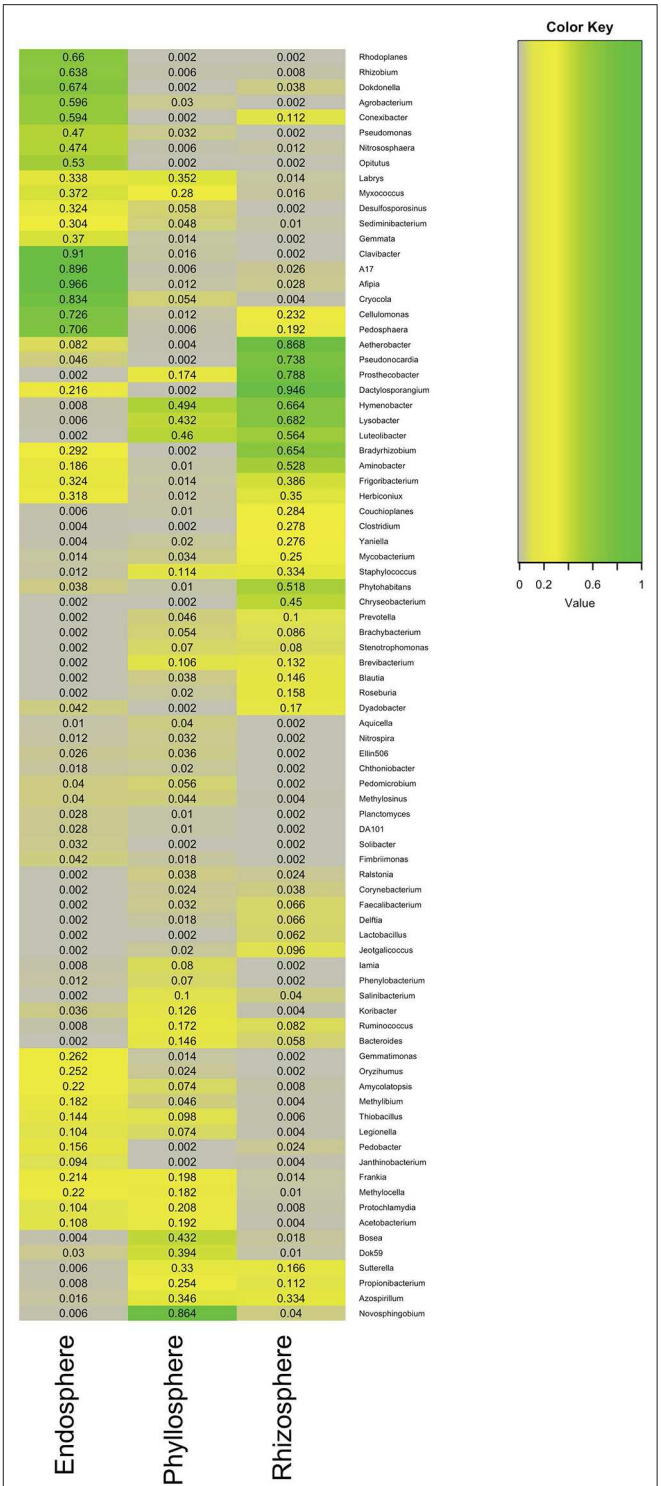

FIGURE 6 | Indicator heatmap showing the taxonomy and taxon-treatment-association strength of 84 microbial genera significantly ($q < 0.1$) associated with different compartments within Antarctic plants. The values represent the association strength.

DISCUSSION

During the last 30 years, climate change has influenced the distribution and abundance of species worldwide and is attributed to be a major cause of the acceleration of world-wide species extinction (Urban, 2015). The polar regions are not an exception, and climate change has also affected the ecology of plants and animals in Arctic and Antarctic ecosystems. In this sense, the successful expansion of vascular plants on the Antarctic peninsula has been attributed to the impact of climate change (Lee et al., 2017). Similarly, it has been reported that invasion of generalist microbes from warmer latitudes will replace many local specialist microbes, and this along with the retraction and losses of ice, will further reduce opportunities for niche specialization (Vincent, 2010). Thus, given the importance of microbes on the growth, fitness and productivity of plants (Turner et al., 2013; Vandenkoornhuyse et al., 2015), additional studies are needed to better understand the impacts of climate change on the colonization of ice-free lands by Antarctic vascular plants and the extinction risks to species in polar regions.

In this study, we examined the diversity and richness of plant-associated microbiota in three plant compartments (niches) of Antarctic vascular plants. Differences in microbial community structure were found in the rhizosphere compared with the endosphere and phyllosphere. The rhizosphere is considered as the main hotspot for microbial colonization and activity in soils, harboring a great abundance and diversity of bacteria compared with other plant and soil niches (Prashar et al., 2014). In contrast, the endosphere is considered as a restricted niche where colonization by endophytes depends of diverse variables associated with the degree of intimacy between endophytic bacteria (e.g., opportunistic or facultative) and the host plant. Another recent study also pointed out that penetration route

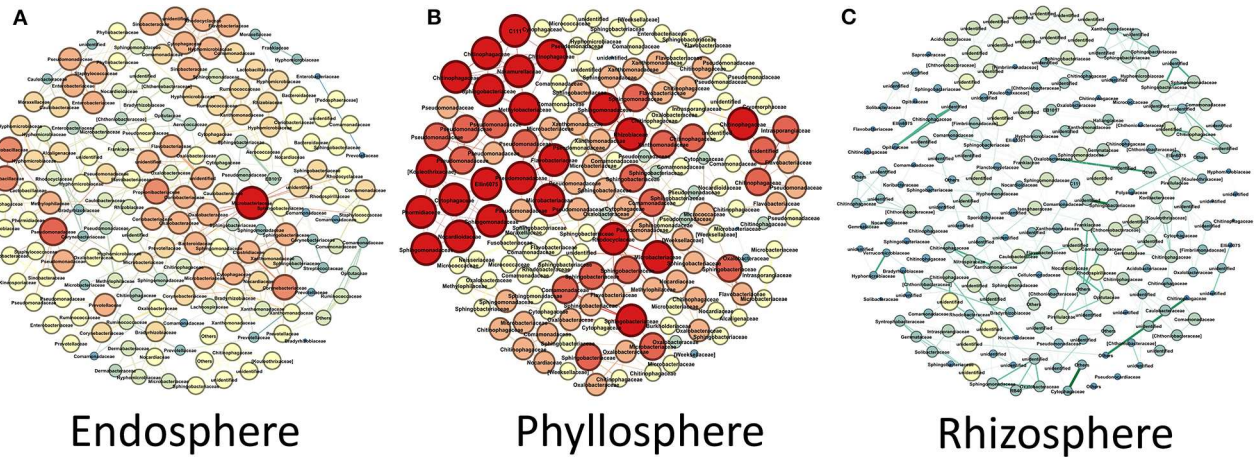

FIGURE 7 | Antarctic plant niche-specific co-occurrence networks among microorganisms in the **(A)** endosphere, **(B)** phyllosphere, and **(C)** rhizosphere. The size of each node (OTU) is the proportional to the number of connections.

(e.g., root hairs, stomata, flower, etc.), plant genotype, and strain type, also have a large impact on colonization (Hardoim et al., 2015). Similarly, the phyllosphere has been categorized as a hostile environment to bacteria and is governed by diverse abiotic factors (such as ultraviolet radiation, temperature, desiccation, etc.) that can change within few minutes, hours, days, or even seasons (Yang et al., 2001; Lindow and Brandl, 2003). Therefore, only adapted, non-fastidious bacterial populations can survive and/or proliferate in the endospheres and phyllospheres of Antarctic vascular plants.

Independent of plant species or niche studied, our Illumina-based sequence analyses revealed the dominance of members of the phyla *Proteobacteria* in all studied bacterial communities. Members of the *Proteobacteria* have been found to be dominant in plant niches, including the endosphere (Hardoim et al., 2015; Proença et al., 2017; Yang et al., 2017), phyllosphere (Whipps et al., 2008; Tian et al., 2017) and rhizosphere (Wang et al., 2018; Lei et al., 2019). Coincidently, our study also showed that members of phyla *Actinobacteria* and *Bacteroidetes* were dominant in both Antarctic plants. Several other studies have shown that the *Actinobacteria* and *Bacteroidetes* are the dominant bacterial groups in the plant microbiome (Turner et al., 2013; Vandenkoornhuyse et al., 2015; Venkatachalam et al., 2016). This association has also been noted in relation to the rhizosphere and phyllosphere of Antarctic vascular plants (Teixeira et al., 2010; Jorquera et al., 2016; Cid et al., 2017; Molina-Montenegro et al., 2018).

Interestingly, our study also revealed that the majority of OTUs observed were not shared, particularly those found in the rhizosphere samples. These findings are consistent with studies showing niche differentiation in plants (Coleman-Derr et al., 2016; Beckers et al., 2017; Cheng et al., 2018; Rilling et al., 2018). Similarly, one of our recent studies revealed that most of OTUs were not shared between endospheres (leaves and roots) of indigenous plants, suggesting the effect of the plant genotype (species) on the bacterial endophyte communities in Chilean extreme environments (Zhang et al., 2019). This niche differentiation might be influenced by a combination of different factors, including the chemical properties of rhizosphere soil as observed in our analysis (**Table 1**), and as suggested by Rilling et al. (2018).

With respect to the predicted functions of bacterial communities, our study showed major assignments to heterotrophy, aerobic heterotrophy, fermentation, and nitrate reduction. In a minor degree, functions were also found to be related to nitrogen cycling and hydrocarbon degradation were found. Functional studies in bacterial communities associated with Antarctic vascular plants are very limited. A recent metagenomic study observed revealed a higher diversity of functional genes and abundance of stress tolerance genes in the rhizosphere of *D. antarctica* plus *C. quitensis* than *C. quitensis* (Molina-Montenegro et al., 2018). In addition, the sequencing of genome from culturable bacteria isolated from *D. antarctica* phyllosphere, showed genes associated with nutrient uptake, bioactive metabolites, and antimicrobial compounds (Cid et al., 2018). Similar to our study, *Pseudomonas* are commonly found in the rhizospheres and phyllospheres of Antarctic vascular plants (Teixeira et al., 2010; Peixoto et al., 2016; Cid et al., 2017). *Pseudomonas* is recognized as a metabolically versatile bacterial group that exhibits a wide battery of activities such as nutrient cycling, degradation of organic compounds, among others (Timmis, 2002; Loeschcke and Thies, 2015). However, it is necessary to mention that our results are predictive, based on 16S rRNA gene sequences, and the functionality of microbiota in each plant species must be determined by experimental setting *in vitro* and *in situ*.

Microbial indicator analyses allowed identification of taxa mainly clustered into the phyla *Proteobacteria*, *Actinobacteria,* and *Firmicutes*, independent of niche and plant species. Members of *Proteobacteria*, *Actinobacteria,* and *Firmicutes* phyla are frequently reported as the dominant bacterial taxa in soil and plant microbiome in Arctic and Antarctic environments (Teixeira et al., 2010; Jorquera et al., 2016; Peixoto et al., 2016; Poosakkannu et al., 2017; Molina-Montenegro et al.,

2018). In relation to three niche co-occurrence networks, our results showed significant difference among the plant niches investigated, where 5 (*Microbacteriaceae*, *Pseudomonaceae*, *Lactobacillaceae*, and *Corynebacteriaceae*), 23 (*Chitinophagaceae* and *Sphingomonadaceae*), and 7 (*Rhodospirillaceae*) major putative keystone taxa at family-level were observed in endosphere, phyllosphere and rhizosphere, respectively. *Rhizobium* spp. have been proposed as keystone taxa *in planta*, whereas *Gemmatimonas* and *Acidobacteria* have been proposed in soil (Banerjee et al., 2018). In Chilean extreme ecosystems, we recently reported to *Bacillaceae* and *Enterobacteriacea* as keystone taxa in endophytic bacterial communities associated with plants (Zhang et al., 2019).

To our knowledge, the occurrence of keystone taxa in Antarctic plants has not been reported thus far, so comparison to other studies are difficult. Moreover, because there are scarce studies simultaneously analyzing different niches in plants, comparisons of the putative microbial indicators or keystone taxa proposed here with those in related plant species grown in other continents is difficult. That said, however, the diversity of microbiomes across plant niches (leaves, stems, roots and soils) for *Populus* trees has been reported (Cregger et al., 2018). Even without network analyses, some studies have shown plant host-induced microbial populations changes. For example, studies on rhizobacterial communities associated with *Deschampsia caespitosa*, a metal-tolerant plants in European heavy metal polluted soils, revealed that the *Cytophagaceae* family is a specie-specific dominant group, and that there are distinctive profiles of microbial traits that are influence by soil properties and plant genotype (Cavalca et al., 2015; Borymski et al., 2018).

This study represents our first directed approach to examine the influence of environmental and biological factors (e.g., season, weather, and plant development) on niche differentiation of microbial communities in Antarctic vascular plants. This analysis suggests the presence of putative niche-specific microbial indicators and major keystone taxa. However, further investigations, including longitudinal gradient samplings, are required to demonstrate if specific bacterial communities (or specific group) are pivotal to the successful colonization (or expansion) of ice-free lands by plants in the Antarctic.

DATA AVAILABILITY STATEMENT

The datasets generated for this study can be found in the Raw sequencing data were deposited in the Sequence Read Archive (SRA) of NCBI under Accession Number PRJNA509213.

AUTHOR CONTRIBUTIONS

QZ, JA, NI, MS, and MJ designed the research and performed laboratory work and data analysis. QZ, MS, and MJ wrote the manuscript and designed tables and figures. JA, PD, MS, and MM made critical revisions of the main manuscript. All authors revised the manuscript and approved the final version.

FUNDING

This study was funded by Chilean Antarctic Institute (INACH) project code RT_02_16. The authors also thanks to financial support by The National Fund for Scientific and Technological Development (FONDECYT) projects no. 1160302 (to MJ), 11160112 (to JA), and 1181050 (to MM), by INACH project RT_06_17 (to MJ and PD), by SATREPS-MACH JPMJSA1705 by JST/JICA Japan (to MJ and JA), by the Minnesota Corn Research & Promotion Council (to QZ), and by the Minnesota Agricultural Experiment Station (to MS).

SUPPLEMENTARY MATERIAL

The Supplementary Material for this article can be found online at: https://www.frontiersin.org/articles/10.3389/fmicb.2020.01036/full#supplementary-material

REFERENCES

Aronesty, E. (2013). Comparison of sequencing utility programs. *Open Bioinforma. J.* 7, 1–8. doi: 10.2174/1875036201307010001

Banerjee, S., Schlaeppi, K., and van der Heijden, M. G. A. (2018). Keystone taxa as drivers of microbiome structure and functioning. *Nat. Rev. Microbiol.* 16, 567–576. doi: 10.1038/s41579-018-0024-1

Barra, P. J., Inostroza, N. G., Acuña, J. J., Mora, M. L., Crowley, D. E., and Jorquera, M. A. (2016). Formulation of bacterial consortia from avocado (*Persea americana* mill.) and their effect on growth, biomass and superoxide dismutase activity of wheat seedlings under salt stress. *Appl. Soil Ecol.* 102, 80–91. doi: 10.1016/j.apsoil.2016.02.014

Bastian, M., Heymann, S., Jacomy, M. (2009). "Gephi: an open source software for exploring and manipulating networks" in *Third International AAAI Conference on Weblogs and Social Media* (San Jose, CA).

Beckers, B., De Beeck, M. O., Weyens, N., Boerjan, W., and Vangronsveld, J. (2017). Structural variability and niche differentiation in the rhizosphere and endosphere bacterial microbiome of field-grown poplar trees. *Microbiome* 5:25. doi: 10.1186/s40168-017-0241-2

Benjamini, Y., Krieger, A. M., and Yekutieli, D. (2006). Adaptive linear step-up procedures that control the false discovery rate. *Biometrika* 93, 491–507. doi: 10.1093/biomet/93.3.491

Berríos, G., Cabrera, G., Gidekel, M., and Gutiérrez-Moraga, A. (2013). Characterization of a novel antarctic plant growth-promoting bacterial strain and its interaction with antarctic hair grass (*Deschampsia antarctica* desv). *Polar Biol.* 36, 349–362. doi: 10.1007/s00300-012-1264-6

Berry, D., and Widder, S. (2014). Deciphering microbial interactions and detecting keystone species with co-occurrence networks. *Front. Microbiol.* 5:219. doi: 10.3389/fmicb.2014.00219

Bertsch, P., Bloom, P. (1996). "Aluminum," in *Methods of Soil Analysis, Part 3—Chemical Methods*, eds J. M. Bigham (Madison,WI: Soil Science Society of America), 526–527.

Borymski, S., Cycon, M., Beckmann, M., Mur, L. A. J., and Piotrowska-Seget, Z. (2018). Plant species and heavy metals affect biodiversity of microbial communities associated with metal-tolerant plants in metalliferous soils. *Front. Microbiol.* 9:1425. doi: 10.3389/fmicb.2018.01425

Bray, J. R., and Curtis, J. T. (1957). An ordination of the upland forest communities of southern wisconsin. *Ecol. Monogr.* 27, 326–349. doi: 10.2307/1942268

Caporaso, J. G., Kuczynski, J., Stombaugh, J., Bittinger, K., Bushman, F. D., Costello, E. K., et al. (2010). Qiime allows analysis of high-throughput community sequencing data. *Nat. Methods*. 7, 335–336. doi: 10.1038/nmeth.f.303

Cavalca, L., Corsini, A., Canzi, E., Zanchi, R. (2015). Rhizobacterial communities associated with spontaneous plant species in long-term arsenic contaminated soils. *World J. Microbiol. Biotechnol*. 31, 735–746. doi: 10.1007/s11274-015-1826-1

Chen, H., and Boutros, P. C. (2011). Venndiagram: a package for the generation of highly-customizable Venn and Euler diagrams in r. *BMC Bioinform*. 12:35. doi: 10.1186/1471-2105-12-35

Cheng, D., Tian, Z., Feng, L., Xu, L., and Wang, H. (2018). Diversity analysis and function prediction of rhizo-and endophytic bacterial communities of *Senecio vulgaris* L. (Asteraceae) in an invasive range. *PeerJ. Prepr*. 6:e26701v1. doi: 10.7287/peerj.preprints.26701

Cid, F. P., Inostroza, N. G., Graether, S. P., Bravo, L. A., and Jorquera, M. A. (2017). Bacterial community structures and ice recrystallization inhibition activity of bacteria isolated from the phyllosphere of the antarctic vascular plant deschampsia antarctica. *Polar Biol*. 40, 1319–1331. doi: 10.1007/s00300-016-2036-5

Cid, F. P., Maruyama, F., Murase, K., Graether, S. P., Larama, G., Bravo, L. A., et al. (2018). Draft genome sequences of bacteria isolated from the deschampsia antarctica phyllosphere. *Extremophiles*. 22, 537–552. doi: 10.1007/s00792-018-1015-x

Clarke, K. R. (1993). Non-parametric multivariate analyses of changes in community structure. *Aust. J. Ecol*. 18, 117–143. doi: 10.1111/j.1442-9993.1993.tb00438.x

Coleman-Derr, D., Desgarennes, D., Fonseca-Garcia, C., Gross, S., Clingenpeel, S., Woyke, T., et al. (2016). Plant compartment and biogeography affect microbiome composition in cultivated and native agave species. *New Phytol*. 209, 798–811. doi: 10.1111/nph.13697

Cregger, M. A., Veach, A. M., Yang, Z. K., Crouch, M. J., Vilgalys, R., Tuskan, G. A., et al. (2018). The Populus holobiont: dissecting the effects of plant niches and genotype on the microbiome. *Microbiome* 6:31. doi: 10.1186/s40168-018-0413-8

Csardi, G., and Nepusz, T. (2006). The igraph software package for complex network research. *Inter. J. Complex Syst*. 1695, 1–9. Available online at: https://pdfs.semanticscholar.org/1d27/44b83519657f5f2610698a8ddd177ced4f5c.pdf?_ga=2.102773952.1172527413.1589302647-216860011.1586286922

de Caceres, M., and Legendre, P. (2009). Associations between species and groups of sites: indices and statistical inference. *Ecology*. 90, 3566–3574. doi: 10.1890/08-1823.1

Edgar, R. C., Haas, B. J., Clemente, J. C., Quince, C., and Knight, R. (2011). Uchime improves sensitivity and speed of chimera detection. *Bioinformatics* 27, 2194–2200. doi: 10.1093/bioinformatics/btr381

Excoffier, L., Smouse, P. E., and Quattro, J. M. (1992). Analysis of molecular variance inferred from metric distances among DNA haplotypes - application to human mitochondrial-DNA restriction data. *Genetics* 131, 479–491.

Gallardo-Cerda, J., Levihuan, J., Lavín, P., Oses, R., Atala, C., Torres-Díaz, C., et al. (2018). Antarctic rhizobacteria improve salt tolerance and physiological performance of the antarctic vascular plants. *Polar Biol*. 41, 1973–1982. doi: 10.1007/s00300-018-2336-z

Gohl, D. M., Vangay, P., Garbe, J., MacLean, A., Hauge, A., Becker, A., et al. (2016). Systematic improvement of amplicon marker gene methods for increased accuracy in microbiome studies. *Nat. Biotechnol*. 34, 942–949. doi: 10.1038/nbt.3601

Hardoim, P. R., Van Overbeek, L. S., Berg, G., Pirttil,ä A. M., Compant, S., Campisano, A., et al. (2015). The hidden world within plants: Ecological and evolutionary considerations for defining functioning of microbial endophytes. *Microbiol. Mol. Biol. Rev*. 79, 293–320. doi: 10.1128/MMBR.00050-14

Hill, P. W., Farrar, J., Roberts, P., Farrell, M., Grant, H., Newsham, K. K., et al. (2011). Vascular plant success in a warming antarctic may be due to efficient nitrogen acquisition. *Nat. Clim. Chang*. 1:50. doi: 10.1038/nclimate1060

Jorquera, M. A., Maruyama, F., Ogram, A. V., Navarrete, O. U., Lagos, L. M., Inostroza, N. G., et al. (2016). Rhizobacterial community structures associated with native plants grown in chilean extreme environments. *Microb. Ecol*. 72, 633–646. doi: 10.1007/s00248-016-0813-x

Lagos, L. M., Navarrete, O. U., Maruyama, F., Crowley, D. E., Cid, F. P., Mora, M. L., et al. (2014). Bacterial community structures in rhizosphere microsites of ryegrass (lolium perenne var. Nui) as revealed by pyrosequencing. *Biol. Fert. Soils*. 50, 1253–1266. doi: 10.1007/s00374-014-0939-2

Lee, J. R., Raymond, B., Bracegirdle, T. J., Chades, I., Fuller, R. A., Shaw, J. D., et al. (2017). Climate change drives expansion of antarctic ice-free habitat. *Nature* 547, 49–54. doi: 10.1038/nature22996

Lei, S., Xu, X., Cheng, Z., Xiong, J., Ma, R., Zhang, L., et al. (2019). Analysis of the community composition and bacterial diversity of the rhizosphere microbiome across different plant taxa. *Microbiologyopen* 8:e00762. doi: 10.1002/mbo3.762

Letunic, I., and Bork, P. (2016). Interactive tree of life (itol) v3: An online tool for the display and annotation of phylogenetic and other trees. *Nucleic Acids Res*. 44, W242–W245. doi: 10.1093/nar/gkw290

Lindow, S. E., and Brandl, M. T. (2003). Microbiology of the phyllosphere. *Appl. Environ. Microbiol*. 69, 1875–1883. doi: 10.1128/AEM.69.4.1875-1883.2003

Loeschcke, A., and Thies, S. (2015). Pseudomonas putida—a versatile host for the production of natural products. *Appl. Microbiol. Biotechnol*. 99, 6197–6214. doi: 10.1007/s00253-015-6745-4

Louca, S., Parfrey, L. W., and Doebeli, M. (2016). Decoupling function and taxonomy in the global ocean microbiome. *Science* 353, 1272–1277. doi: 10.1126/science.aaf4507

Luo, F., Zhong, J., Yang, Y., Scheuermann, R. H., and Zhou, J. (2006). Application of random matrix theory to biological networks. *Phys. Lett. A*. 357, 420–423. doi: 10.1016/j.physleta.2006.04.076

Ma, B., Wang, H. Z., Dsouza, M., Lou, J., He, Y., Dai, Z. M., et al. (2016). Geographic patterns of co-occurrence network topological features for soil microbiota at continental scale in eastern China. *ISME J*. 10, 1891–1901. doi: 10.1038/ismej.2015.261

McDonald, D., Price, M. N., Goodrich, J., Nawrocki, E. P., DeSantis, T. Z., Probst, A., et al. (2012). An improved greengenes taxonomy with explicit ranks for ecological and evolutionary analyses of bacteria and archaea. *ISME J*. 6, 610–618. doi: 10.1038/ismej.2011.139

Molina-Montenegro, M. A., Ballesteros, G. I., Castro-Nallar, E., Meneses, C., Torres-Díaz, C., and Gallardo-Cerda, J. (2018). Metagenomic exploration of soils microbial communities associated to antarctic vascular plants. *PeerJ Prepr*. 6:e26508v26501. doi: 10.7287/peerj.preprints.26508

Murphy, J., and Riley, J. P. (1962). A modified single solution method for the determination of phosphate in natural waters. *Anal. Chim. Acta* 27, 31–36. doi: 10.1016/S0003-2670(00)88444-5

Peixoto, R. J. M., Miranda, K. R., Lobo, L. A., Granato, A., de Carvalho Maalouf, P., de Jesus, H. E., et al. (2016). Antarctic strict anaerobic microbiota from deschampsia antarctica vascular plants rhizosphere reveals high ecology and biotechnology relevance. *Extremophiles* 20, 875–884. doi: 10.1007/s00792-016-0878-y

Poosakkannu, A., Nissinen, R., Männist,ö M., and Kytöviita, M. M. (2017). Microbial community composition but not diversity changes along succession in arctic sand dunes. *Environ. Microbiol*. 19, 698–709. doi: 10.1111/1462-2920.13599

Prashar, P., Kapoor, N., and Sachdeva, S. (2014). Rhizosphere: its structure, bacterial diversity and significance. *Rev. Environ. Sci. Bio*. 13, 63–77. doi: 10.1007/s11157-013-9317-z

Proença, D. N., Francisco, R., Kublik, S., Schöler, A., Vestergaard, G., Schloter, M., et al. (2017). The microbiome of endophytic, wood colonizing bacteria from pine trees as affected by pine wilt disease. *Sci. Rep*. 7:4205. doi: 10.1038/s41598-017-04141-6

Rilling, J. I., Acuña, J. J., Sadowsky, M. J., and Jorquera, M. A. (2018). Putative nitrogen-fixing bacteria associated with the rhizosphere and root endosphere of wheat plants grown in an andisol from southern chile. *Front. Microbiol*. 9:2710. doi: 10.3389/fmicb.2018.02710

Royles, J., Amesbury, M. J., Convey, P., Griffiths, H., Hodgson, D. A., Leng, M. J., et al. (2013). Plants and soil microbes respond to recent warming on the antarctic peninsula. *Curr. Biol*. 23, 1702–1706. doi: 10.1016/j.cub.2013.07.011

Sancho, L. G., Pintado, A., Navarro, F., Ramos, M., De Pablo, M. A., Blanquer, J. M., et al. (2017). Recent warming and cooling in the antarctic peninsula region has rapid and large effects on lichen vegetation. *Sci. Rep*. 7:5689. doi: 10.1038/s41598-017-05989-4

Schloss, P. D., Westcott, S. L., Ryabin, T., Hall, J. R., Hartmann, M., Hollister, E. B., et al. (2009). Introducing mothur: open-source, platform-independent, community-supported software for describing and comparing microbial communities. *Appl. Environ. Microbiol.* 75, 7537–7541. doi: 10.1128/AEM.01541-09

Strimmer, K. (2008). A unified approach to false discovery rate estimation. *BMC Bioinform*. 9:303. doi: 10.1186/1471-2105-9-303

Teixeira, L. C., Peixoto, R. S., Cury, J. C., Sul, W. J., Pellizari, V. H., Tiedje, J., et al. (2010). Bacterial diversity in rhizosphere soil from Antarctic vascular plants of Admiralty Bay, maritime Antarctica. *ISME J*. 4:989. doi: 10.1038/ismej.2010.35

Tian, X., Shi, Y., Geng, L., Chu, H., Zhang, J., Song, F., et al. (2017). Template preparation affects 16s rrna high-throughput sequencing analysis of phyllosphere microbial communities. *Front. Plant Sci*. 8:1623. doi: 10.3389/fpls.2017.01623

Timmis, K. (2002). Pseudomonas putida: a cosmopolitan opportunist par excellence. *Environ. Microbiol.* 4, 779–781. doi: 10.1046/j.1462-2920.2002.00365.x

Turner, T. R., James, E. K., and Poole, P. S. (2013). The plant microbiome. *Genome Biol*. 14:209. doi: 10.1186/gb-2013-14-6-209

Urban, M. C. (2015). Accelerating extinction risk from climate change. *Science* 348, 571–573. doi: 10.1126/science.aaa4984

van der Heijden, M. G., and Hartmann, M. (2016). Networking in the plant microbiome. *PLoS Biol*. 14:e1002378. doi: 10.1371/journal.pbio.1002378

Vandenkoornhuyse, P., Quaiser, A., Duhamel, M., and Le Van A, Dufresne, A. (2015). The importance of the microbiome of the plant holobiont. *New Phytol*. 206, 1196–1206. doi: 10.1111/nph.13312

Venkatachalam, S., Ranjan, K., Prasanna, R., Ramakrishnan, B., Thapa, S., and Kanchan, A. (2016). Diversity and functional traits of culturable microbiome members, including cyanobacteria in the rice phyllosphere. *Plant Biol*. 18, 627–637. doi: 10.1111/plb.12441

Vincent, W. F. (2010). Microbial ecosystem responses to rapid climate change in the arctic. *ISME J*. 4:1087. doi: 10.1038/ismej.2010.108

Walkley, A., and Black, I. A. (1934). An examination of the degtjareff method for determining soil organic matter, and a proposed modification of the chromic acid titration method. *Soil Sci*. 37, 29–38. doi: 10.1097/00010694-193401000-00003

Wang, X., Wang, Z., Jiang, P., He, Y., Mu, Y., Lv, X., et al. (2018). Bacterial diversity and community structure in the rhizosphere of four ferula species. *Sci. Rep*. 8:5345. doi: 10.1038/s41598-018-22802-y

Warncke, D., and Brown, J. (1998). *Potassium and Other Basic Cations. Recommended Chemical Soil Test Procedures for the North Central Region*. North Central Regional Research.

Whipps, J., Hand, P., Pink, D., and Bending, G. D. (2008). Phyllosphere microbiology with special reference to diversity and plant genotype. *J. Appl. Microbiol.* 105, 1744–1755. doi: 10.1111/j.1365-2672.2008.03906.x

Yang, C.-H., Crowley, D. E., Borneman, J., and Keen, N. T. (2001). Microbial phyllosphere populations are more complex than previously realized. *Proc. Natl. Acad. Sci. U.S.A.* 98, 3889–3894. doi: 10.1073/pnas.051633898

Yang, R., Liu, P., and Ye, W. (2017). Illumina-based analysis of endophytic bacterial diversity of tree peony (paeonia sect. Moutan) roots and leaves. *Braz. J. Microbiol*. 48, 695–705. doi: 10.1016/j.bjm.2017.02.009

Yergeau, E., Bokhorst, S., Kang, S., Zhou, J., Greer, C. W., Aerts, R., et al. (2012). Shifts in soil microorganisms in response to warming are consistent across a range of antarctic environments. *ISME J*. 6:692. doi: 10.1038/ismej.2011.124

Zhang, Q., Acuna, J. J., Inostroza, N. G., Mora, M. L., Radic, S., Sadowsky, M. J., et al. (2019). Endophytic bacterial communities associated with roots and leaves of plants growing in chilean extreme environments. *Sci. Rep*. 9:4950. doi: 10.1038/s41598-019-41160-x

Conflict of Interest: The authors declare that the research was conducted in the absence of any commercial or financial relationships that could be construed as a potential conflict of interest.

frontiers in Microbiology

ORIGINAL RESEARCH
published: 14 July 2020
doi: 10.3389/fmicb.2020.01530

Genomic Insights of *Cryobacterium* Isolated From Ice Core Reveal Genome Dynamics for Adaptation in Glacier

Yongqin Liu[1,2,3], Liang Shen[1,4], Yonghui Zeng[5], Tingting Xing[1,3], Baiqing Xu[1,2] and Ninglian Wang[2,6]*

[1] Key Laboratory of Tibetan Environment Changes and Land Surface Processes, Institute of Tibetan Plateau Research, Chinese Academy of Sciences, Beijing, China, [2] CAS Center for Excellence in Tibetan Plateau Earth Sciences, Beijing, China, [3] University of Chinese Academy of Sciences, Beijing, China, [4] College of Life Sciences, Anhui Normal University, Wuhu, China, [5] Department of Environmental Science, Aarhus University, Roskilde, Denmark, [6] College of Urban and Environmental Science, Northwest University, Xi'an, China

Glacier is the dominant cold habitat in terrestrial environments, providing a model ecosystem to explore extremophilic strategies and study early lives on Earth. The dominant form of life in glaciers is bacteria. However, little is known about past evolutionary processes that bacteria underwent during adaptation to the cryosphere and the connection of their genomic traits to environmental stressors. Aiming to test the hypothesis that bacterial genomic content and dynamics are driven by glacial environmental stressors, we compared genomes of 21 psychrophilic *Cryobacterium* strains, including 14 that we isolated from three Tibetan ice cores, to their mesophilic counterparts from the same family Microbacteriaceae of Actinobacteria. The results show that psychrophilic *Cryobacterium* underwent more dynamic changes in genome content, and their genomes have a significantly higher number of genes involved in stress response, motility, and chemotaxis than their mesophilic counterparts ($P < 0.05$). The phylogenetic birth-and-death model imposed on the phylogenomic tree indicates a vast surge in recent common ancestor of psychrophilic *Cryobacterium* (gained the greatest number of genes by 1,168) after the division of the mesophilic strain *Cryobacterium mesophilum*. The expansion in genome content brought in key genes primarily of the categories "cofactors, vitamins, prosthetic groups, pigments," "monosaccharides metabolism," and "membrane transport." The amino acid substitution rates of psychrophilic *Cryobacterium* strains are two orders of magnitude lower than those in mesophilic strains. However, no significantly higher number of cold shock genes was found in psychrophilic *Cryobacterium* strains, indicating that multi-copy is not a key factor for cold adaptation in the family Microbacteriaceae, although cold shock genes are indispensable for psychrophiles. Extensive gene acquisition and low amino acid substitution rate might be the strategies of psychrophilic *Cryobacterium* to resist low temperature, oligotrophy, and high UV radiation on glaciers. The exploration of genome evolution and survival strategies of psychrophilic *Cryobacterium* deepens our understanding of bacterial cold adaptation.

Keywords: glacier, *Cryobacterium*, genomic, evolutionary processes, cold adaptation

OPEN ACCESS

Edited by:
David Anthony Pearce, Northumbria University, United Kingdom

Reviewed by:
Isao Yumoto, National Institute of Advanced Industrial Science and Technology (AIST), Japan
Stefano Raimondi, University of Modena and Reggio Emilia, Italy

****Correspondence:***
Yongqin Liu
yqliu@itpcas.ac.cn;
tibetsunsnow@gmail.com

Specialty section:
This article was submitted to Extreme Microbiology, a section of the journal Frontiers in Microbiology

Received: *20 December 2019*
Accepted: *12 June 2020*
Published: *14 July 2020*

Citation:
Liu Y, Shen L, Zeng Y, Xing T, Xu B and Wang N (2020) Genomic Insights of Cryobacterium Isolated From Ice Core Reveal Genome Dynamics for Adaptation in Glacier. Front. Microbiol. 11:1530. doi: 10.3389/fmicb.2020.01530

INTRODUCTION

Glaciers and ice sheets have been recognized as biomes, uniquely dominated by microorganisms (Hodson et al., 2008; Anesio and Laybourn-Parry, 2012; Grinsted, 2013). Microbial metabolism occurs on glaciers and many community members not only perform basal metabolic functions but also grow and divide (Price, 2000). Microorganisms living in these environments have evolved unique features in their proteins, enzyme, membranes, and genetic responses to low temperature and nutrient concentrations and excessive UV radiation (Siddiqui et al., 2013; De Maayer et al., 2014).

Genomic survival strategies have been investigated in a few glacial model organisms. Genes encoding proteins with known or predicted roles in cold adaptation, i.e., cold-shock protein, proteorhodopsin, osmoprotection, and membrane-related proteins, were found in genomes of psychrophilic species *Flavobacterium bomense* sp. nov. isolated from glaciers (Liu et al., 2019a). Genome of an ice core strain *Dyadobacter tibetensis* Y620-1 contained high percentage of new novel genes and genes required for the serine-glyoxylate cycle in one-carbon metabolism, which may contribute to its survival in glacier (Shen et al., 2019). Although glacier bacteria and psychrophiles from arctic soil are both cold acclimated, glacier bacteria show different genomic adaptation characteristics mainly connected to the genes devoted to CRISPR (Clustered Regularly Interspaced Short Palindromic Repeats) defense system, osmotic adaptation, and metabolism of monosaccharides, nitrogen, and aromatic compounds, due to the different environmental pressures experienced by glacier bacteria and psychrophiles from arctic soils (Shen et al., 2017). The survival strategies of psychrophiles at the genome level have been well investigated during past decades (Saunders et al., 2003; Methé et al., 2005; De Maayer et al., 2014; Raymond-Bouchard et al., 2018). However, the role of microevolution, genomic adaptive strategies, and environmental factors in shaping the genomes of bacteria colonizing glaciers are largely unknown. Glaciers not only are the dominant cold habitat to explore the extremophilic strategies in the terrestrial land but also are the representative habitats of early lives on the Earth and perhaps on other planets as well (Priscu et al., 2004).

Species of *Cryobacterium* are widely distributed in cold environments and well adapted to cold conditions (Liu et al., 2018). The genus *Cryobacterium*, proposed by Suzuki et al. (1997), is consisting of Gram-positive aerobes that have a pleomorphic rod-shaped morphology. The type species of *Cryobacterium psychrophilum* is an obligate psychrophilic actinomycete. At the time of writing, the genus *Cryobacterium* comprises 11 recognized species, *C. psychrophilum* (Suzuki et al., 1997; Inoue and Komagata, 2006), *Cryobacterium psychrotolerans* (Zhang et al., 2007), *Cryobacterium mesophilum* (Dastager et al., 2008), *Cryobacterium roopkundense* (Reddy et al., 2010), *Cryobacterium arcticum* (Bajerski et al., 2011), *Cryobacterium flavum* and *Cryobacterium luteum* (Liu et al., 2012), *Cryobacterium levicorallinum* (Liu et al., 2013), *Cryobacterium zongtaii* (Liu et al., 2018), *Cryobacterium soli* (Gong et al., 2019), and *Cryobacterium melibiosiphilum* (Liu et al., 2019b). All type strains of *Cryobacterium* except *C. mesophilum* described by Dastager et al. (2008) were isolated from cold environments and recognized as psychrophiles with optional growth temperature ranging from 15 to 20°C and growth occurs between 0 and 25°C. The strain *C. mesophilum* grew between 20 and 28°C, with optimum growth occurring at 25–28°C (Dastager et al., 2008). Phenotypic analysis showed that the genus *Cryobacterium* differed from its Microbacteriaceae counterparts in the presence of a significant amount of 12-methyl pentadecenoic acid (i.e., a-15:l). The presence of a-15:l is unusual but reasonable for psychrophilic Gram-positive bacteria in order to maintain membrane fluidity at low temperatures (Suzuki et al., 1997).

Most of the reported novel *Cryobacterium* species were isolated from glacial environments (Liu et al., 2018). The culturable bacteria in two ice cores from the Tibetan Plateau were dominated by *Cryobacterium* (Liu et al., 2019c). *Cryobacterium* exhibited high diversity in more than 10 glaciers around world (Segawa et al., 2005; Liu et al., 2016, 2018), indicating that *Cryobacterium* species have developed strategies to endure the harsh glacier habitats. Previous studies were most focused on adaptation features of *Cryobacterium* isolates to cold environments using polyphasic and multilocus sequence analysis (Sathyanarayana Reddy et al., 2014; Singh et al., 2015; Lee et al., 2016; Liu et al., 2018). However, a detailed comparative genomic study of multiple *Cryobacterium* genomes is lacking, which could contribute markedly to and validate our understanding of molecular strategies underlying this genus' cold adaptation. In the present study, we analyzed the genomes of 21 psychrophilic *Cryobacterium* isolates of ice core origin in comparison to their mesophilic counterparts with the aim to deepen our understanding of how bacteria adapt to glacial environments. Our data suggest that the combination of comparative genomics approach and biogeography can be a powerful tool to decipher the bacterial cold adaptation mechanisms in psychrophiles.

MATERIALS AND METHODS

Fourteen psychrophilic *Cryobacterium* strains were selected from our culture collection including five strains isolated from the Muztag Ata glacier (named M series, mean annual air temperature −4°C, 36.4° N, 87.3° E, 6,973 m a.s.l.), three isolates from the Noijin Kangsang glacier (N, mean annual air temperature −8°C, 90.2° E, 29.0° N, 5,950 m a.s.l.), and six isolates from the Yuzhufeng glacier (Y, mean annual air temperature −5°C, 35.5° N, 94.2° E, 6,178 m a.s.l.), respectively (**Table 1**) (Liu et al., 2019c). Growth at various temperatures (0–40°C, with an interval of 5°C) was measured (0°C was maintained with an ice–water mixture and the remaining settings were achieved using a constant-temperature incubator). OD_{600} was measured with a micro plate reader (MD Spectra Max M5) to assess the growth. Growth of these strains occurred between 0 and 25°C with optimum growth at 18–20°C.

For genome sequencing, high-quality genomic DNA was extracted from cells grown on R2A for 3 days at 20°C using TIANamp Bacteria DNA Kit (TIANGEN, Beijing)

TABLE 1 | Information of the genomes of 21 psychrophilic and one mesophilic *Cryobacterium*.

Strain ID	Size (Mbp)	*CDSs	RNAs	**Location	G + C% mol	CRISPRs	Cold Shock	Completeness (%)	Specific gene families
M15	3.67	3497	49	Muztag Ata	63.4	0	2	98.99	1070
M23	3.55	3347	52	Muztag Ata	66.8	1	2	99.49	1029
M25	3.35	3177	53	Muztag Ata	67.0	0	2	99.49	949
M91	3.99	3822	48	Muztag Ata	64.2	0	2	98.99	1338
M96	3.30	3096	51	Muztag Ata	67.0	1	2	99.49	858
N19	4.29	4070	50	Noijin Kangsang	64.5	0	2	98.99	1420
N21	4.14	3944	53	Noijin Kangsang	64.4	1	2	98.99	1429
N22	4.06	3751	53	Noijin Kangsang	68.3	0	2	99.37	803
Y11	4.03	3891	51	Yuzhufeng	63.3	3	2	99.24	1114
Y29	3.66	3484	49	Yuzhufeng	63.5	0	2	98.99	1059
Y50	4.40	4344	49	Yuzhufeng	63.2	0	2	98.65	1567
Y57	4.01	3884	50	Yuzhufeng	63.2	0	2	98.99	1196
Y62	4.23	4179	48	Yuzhufeng	63.2	0	2	99.49	1559
Y82	3.69	3556	50	Yuzhufeng	63.6	0	2	98.74	1008
CGMCC 1.11215	4.04	3906	51	No.1 Glacier	64.7	0	2	98.99	928
CGMCC 1.11211	3.75	3531	51	No.1 Glacier	64.5	0	2	98.74	805
CGMCC 1.11210	3.83	3600	52	No.1 Glacier	65.1	0	2	98.99	719
CGMCC 1.5382	3.25	3016	51	No.1 Glacier	68.3	0	2	96.49	350
RuG17	4.36	4048	50	Himalaya	65.3	3	2	98.74	776
PAMC 27867	4.17	3826	61	Antarctic	68.6	1	2	99.49	692
MLB-32	4.27	3214	72	Arctic	64.9	0	2	96.49	804
§ CGMCC 1.10440	2.41	2342	48	Korea	66.5	0	2	96.04	143

**CDSs, coding sequences; **all the strains isolated from Tibetan Plateau except where noted; §mesophilic Cryobacterium strain.*

following the manufacturer's instructions. The purity of genomic DNA was assessed with NanoDrop (2000c, Thermo Scientific, United States) and all had an OD 260:280 ratio of 1.8–2.0. DNA was stored in TE buffer (pH 8.0) for genome sequencing.

Sequencing was performed on an Illumina Hiseq 2000 instrument. Reads were assembled using SPAdes v3.11.1 with default options (Bankevich et al., 2012). As the algorithm is sensitive to sequencing errors, low-quality reads were filtered prior to *de novo* assembly using Fastp with default options (Chen et al., 2018). The genome sequences were deposited at DDBJ/ENA/GenBank under accession numbers PJJJ00000000-PJJX00000000. The version described in this paper is PJJJ01000000-PJJX01000000.

In addition to the 14 *Cryobacterium* genomes sequenced in this study, 18 genomes were downloaded from the NCBI genome database (last access in April 2017, **Supplementary Table S1**). These include seven psychrophilic *Cryobacterium* strains isolated from the No. 1 Glacier in China and soils from Himalaya, Arctic, and Antarctic (Liu et al., 2013, 2018); one mesophilic *Cryobacterium* strain from a Korean soil (Dastager et al., 2008); and 10 genomes in the family *Microbacteriaceae* and 2 *Rubrobacter* genomes. At the time of writing, there was only one mesophilic strain's genome available in the genus *Cryobacterium*, and thus we included 10 type strains in the family Microbacteriaceae that were phylogenetically close to *Cryobacterium* in order to perform a statistically sound comparative analysis. These 34 genomes were divided into two groups: the psychrophilic *Cryobacterium* genomes (referencing to strains from poles and Tibetan Plateau), and the reference genomes (mesophiles, referencing to *C. mesophilum* CGMCC 1.10440^{T}and the 10 genomes in the family *Microbacteriaceae*). Two strains (*Rubrobacter radiotolerans* RSPS-4 and *Rubrobacter xylanophilus* DSM9941) were used as out-group in the phylogenetic analysis; the out-group strains were not included in the comparative genomics analysis.

The completeness of genomes was calculated using CheckM (Parks et al., 2015). 16S rRNA genes for phylogenetic analysis were generated from the genomes using RNAmmer (v.1.2) (Lagesen et al., 2007). To remove potential differences introduced through different annotation methods, all genomes were re-annotated in the present study with RAST (Rapid Annotation using Subsystem Technology) (Overbeek et al., 2014). An all-versus-all search was performed with BLAST + 2.2.28, with an *E*-value cutoff of 1e−5. Genes without orthologs (pv_cutoff 1-e5 –pi_cutoff 70 –pmatch_cutoff 70) were considered as specific genes. CRISPRs were identified with CRISPR-finder (Grissa et al., 2007a). Codon usage, amino acid composition and protein comparisons between genomes were carried out with the PERL scripts "CodonAaUsage.pl," "aminoacidUsage.pl," and the programs "matrix_createConfig" and "matrix" (Vesth et al., 2013). Heatmaps were produced with R (Ihaka and Gentleman, 1996). Multiple alignments were performed using ClustalW, and topology trees of the 16S rRNA genes and functional genes were constructed using MEGA v10.0.5 with bootstrap method (1,000 iterations) (Kumar et al., 2018).

The same set of 32 genomes was used for gene family clustering analysis (*R. radiotolerans* RSPS-4 and *R. xylanophilus* DSM9941 served as out-groups). An all-versus-all BLAST search was performed, and the FastOrtho software (–pv_cutoff 1-e5 –pi_cutoff 70 –pmatch_cutoff 70)[1] was used to identify gene families. The output of FastOrtho analysis was parsed using custom-made PERL scripts. Gene families that were not present in any other genomes were considered as strain-specific gene families. One hundred and nine shared orthologs were identified at the amino acid level using an *E*-value threshold of $10^{-5}$and 74 of them were single-copy orthologs. Then, the 74 single-copy orthologs were concatenated using custom-made PERL scripts to perform phylogeny construction. The concatenated sequences and the detailed description of the genes are available in the **Supplementary Table S2**. These genes include RNA polymerase sigma factor *rpoD*, enolase, translation elongation factor G (EF-G) and DNA gyrase subunit A (*gyrA*), which are core genes of bacteria (Gil et al., 2004).

As the first step for genome tree construction, the concatenated orthologous genes were aligned at the amino acid sequence level using the Muscle software v3.8.31 (Edgar, 2004). Then non-conserved segments in the alignments were trimmed using the Gblock (Castresana, 2000) software with all gap-containing columns discarded using the parameter values (-b1 = 50 -b4 = 5, and other parameters as default values) as suggested by Luo et al. (2013). Secondly, two probabilistic phylogenetic approaches were used to analyze the concatenation data (19,306 sites) of the 74 homologs. One is a maximum-likelihood (ML) method (Felsenstein, 1981) using the MPI version of RAxML v8.2.4 software (Stamatakis, 2014) and the other is Bayesian method using the MPI version of MrBayes v3.2.6 (Ronquist and Huelsenbeck, 2003). As the evolutionary models for different sites in multi-gene concatenated alignments may differ, the PartitionFinder software v2.1.0 (Lanfear et al., 2012) was used to identify the best scheme for RAxML and MrBayes. Amino acid substitution rate was extracted from the ML tree.

The 34 genomes were further used for ancestral reconstruction. The out-group species Rhodothermaceae bacterium and *Pseudoclavibacter soli* DSM 23366 were not included because the reconstruction of ancestral genome content using COUNT does not require out-group species (Csuroes, 2010). Maximum-likelihood birth-and-death models and the Dollo parsimony method implemented in the COUNT software were used to reconstruct the size of ancestral gene families. Ancestral history reconstruction was performed using posterior probabilities: 100 rounds of rate optimization were computed with a convergence threshold of 10^{-3} prior to ancestral reconstruction; other parameters were set as default as suggested by Oliveira et al. (2017). The genomes were split into subcategories, and calculations and text processing, such as extracting sequences from genome files and parsing BLAST outputs, were performed using custom-made PERL scripts, which are available from the authors on request.

[1]http://enews.patricbrc.org/fastortho/

RESULTS

Overview of *Cryobacterium* Genomes From Tibetan Plateau Glaciers

The genome size of 14 *Cryobacterium* stains from Tibetan Plateau glaciers range from 3.30 Mbp (3,096 protein coding sequences) to 4.40 Mbp (4,344 protein coding sequences) with an average of 3.88 Mbp (3,614 protein coding sequences) (**Table 1**). The genomic GC content ranged from 63.2 to 68.3%, with an average of 64.7%. The number of strain-specific gene families ranged from 803 to 1,567, and the number of rRNA genes differed from 48 to 53. All 14 strains have 2 predicted cold shock genes and 14 heat shock genes. CRISPRs were identified in four strains, one in each of strains M23, M96, and N21 and three in strain Y11, lower than the average occurrence frequency (∼39%) of CRISPR loci in the sequenced bacterial genomes (Grissa et al., 2007b).

Phylogeny Reconstruction

The maximum-likelihood tree based on 74 concatenated single-copy orthologous genes shows that the *Cryobacterium* species are well separated from the mesophilic Microbacteriaceae species (**Figure 1** and **Supplementary Figure S1**). The 14 strains from the Tibetan Plateau glacier are placed in five different branches, clustered into lineage 1 (N19 and N21), lineage 2 (Y29, M15, Y57, and Y82), lineage 3 (M91, Y62, and Y50), lineage 4 (M96, M23, M25, and N22), and strain Y11 forms a branch with a single lineage. Each lineage includes a type strain except one lineage composed by Y29, M15, Y57, and Y82. All lineages have strains isolated from different sources, and the most diverse branch contained strains isolated from four sources, i.e., Muztag Ata (M96, M23, and M25), NJKS (N21), No. 1 Glacier (*C. psychrotolerans* CGMCC 1.5832^{T}), and Antarctic (*C. arcticum* PAMC 27867^{T}, PAMC represents Polar and Alpine Microbial Collection).

Features in Main Functional Categories and Amino Acid Composition

The percentages of gene functional categories were calculated based on RAST annotation system. Genes related to stress response, photosynthesis, motility and chemotaxis, metabolism of aromatic compounds, dormancy and sporulation, and carbohydrates increased significantly in proportion ($P < 0.05$, **Figure 2**) in *Cryobacterium* compared to reference strains.

Genes involved in "RNA metabolism," "protein metabolism," "nucleosides and nucleotides," "DNA metabolism," "cofactors, vitamins, prosthetic groups, pigments," "cell wall and capsule," and "amino acids and derivatives" decreased significantly ($P < 0.05$, **Figure 2**) in proportion in *Cryobacterium* compared to the reference strains. Genes involved in "virulence disease and defense," "sulfur metabolism," "regulation and cell signaling," "potassium metabolism," "phosphorus metabolism," "membrane transport," "iron acquisition and metabolism," "fatty acids lipids and isoprenoids," and "cell division and cell cycle" did not show significant differences ($P > 0.05$, **Figure 2**).

The pattern of amino acid distribution in *Cryobacterium* spp. displays an overall similar trend in their genomes, with Arg being

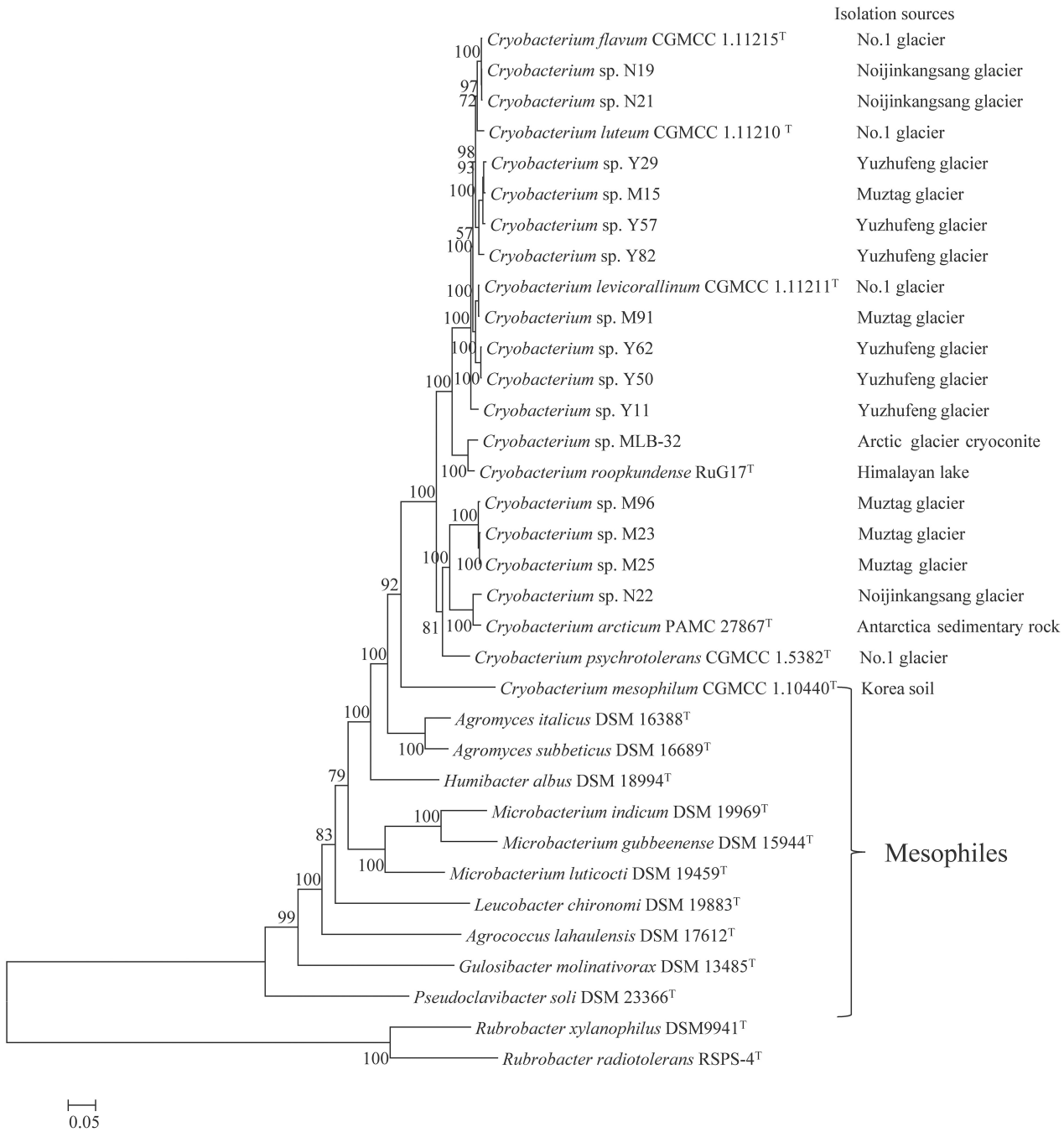

FIGURE 1 | Phylogenetic clustering of 32 Microbacteriaceae strains. Phylogeny is based on concatenated alignment of 74 orthologous proteins with 1,000 bootstraps using RAxML. *Rubrobacter xylanophilus* DSM9941 and *R. radiotolerans* RSPS-4 were used as out-groups. Bar represents accumulated changes per amino acid.

the most abundant, followed by Ala, Gly, and Pro, while Met, Lys, and Tyr were infrequent. Composition of Ala, Asp, Glu, Arg, and Ser decreased significantly in proportion in psychrophilic *Cryobacterium* strains compared to reference strains (one-way ANOVA, $P < 0.005$, **Figure 3**). However, composition of Cys, Phe, Gln, Lys, Leu, Asn, Trp, and Tyr increased significantly ($P < 0.005$, **Figure 3**).

Heatmap Analysis of the Subsystem Categories

To explore the division between the species in terms of their metabolic capabilities and to highlight cold adaptations between the strains, heatmap analysis was employed to compare the subsystem groupings based on functional categories.

FIGURE 2 | Proportional differences of functional category between psychrophilic *Cryobacterium* strains and those of reference mesophilic strains, *P*-values were obtained using one-way ANOVA. *Cryobacterium* genomes from poles and Tibetan Plateau represent the psychrophilic group, and the mesophiles' genomes include *C. mesophilum* CGMCC 1.10440^T and the 10 genomes in the family Microbacteriaceae as described in Section "Materials and Methods."

Genes Associated With Carbohydrates

Genes affiliated with the functional category "carbohydrates" of the Tibetan Plateau glacier isolates ranged from 559 (in strain Y50) to 377 (in strain Y29). The heatmap of RAST subsystem carbohydrates (genes involved in carbohydrate transport and metabolism) across all the *Cryobacterium* genomes resulted in a gene presence/absence matrix displaying three groups separated by the reference genomes (**Supplementary Table S3** and **Figure 4A**). The cold adapted *Cryobacterium* strains in Group 1 and Group 3 form a single cluster separated from their mesophilic counterparts (**Figure 4A**). The difference in the proportion of carbohydrate utilization and metabolism between psychrophiles and mesophiles was demonstrated both inter genus and intra genus, as the only mesophilic strain *C. mesophilum*

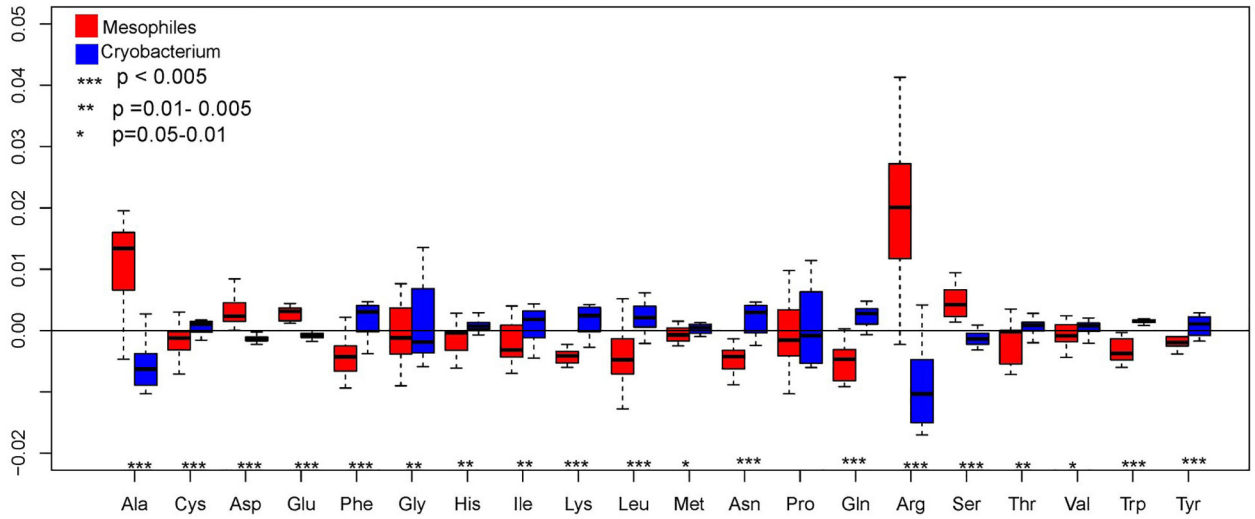

FIGURE 3 | Box plot showing the comparison of genome-wide amino acid composition between *Cryobacterium* strains and reference strains, *P*-values were obtained using one-way ANOVA. *Cryobacterium* genomes from poles and Tibetan Plateau represent the psychrophilic group and the mesophiles' genomes include *C. mesophilum* CGMCC 1.10440^T and the 10 genomes in the family Microbacteriaceae as described in Section "Materials and Methods."

and the reference strains form a single separate cluster (Group 2 in **Figure 4A**). A similar clustering was also identified in the category "cofactors/vitamin/prosthetic groups/pigment" (**Supplementary Figure S3**).

Genes Associated With Respiration

Genes affiliated with the respiration category of the Tibetan Plateau glacier-derived genomes ranged from 45 (in strain N22) to 76 (in strains M19, Y50, and Y62). All the cold adapted *Cryobacterium* strains form a single cluster separate from both their inter and intra genus counterparts (**Figure 4B**). The mesophilic strain *C. mesophilum* and the reference strains also form a single separate cluster (Group 2) same as that in **Figure 4A**. This implies that the respiration profile of cold adapted *Cryobacterium* relatives has a strong consistency.

Genes Associated With Motility and Chemotaxis

Genes of the Tibetan Plateau glacier isolates that are involved in the category "motility and chemotaxis" ranged from 39 (in strain M91) to 49 (in strain Y82). Genes assigned to "motility and chemotaxis" are present in the cold adapted *Cryobacterium* strains but absent from reference strains (**Figure 4C**).

Specific Gene Families

Gene families specific to each strain (no paralogs in the FastOrtho analysis) within the genus *Cryobacterium* with respect to their mesophilic counterparts in family Microbacteriaceae ranged from 543 (in strain *C. psychrotolerans* CGMCC1.5382^T) to 1567 (in strain Y50) (**Supplementary Table S4**). The proportion of function assignable genes to unknown function is approximately 1:2 (**Figure 5A**). This is not abnormal, since genes that have no hit in the RAST database are mostly classified as specific ones. The psychrophilic *Cryobacterium* species shared a similar affiliation of specific gene families to functional categories, which were mainly assigned to "cofactors, vitamins, prosthetic groups, pigments," "carbohydrates," and ABC transporters in "membrane transport." Specific genes in the category "cofactors, vitamins, prosthetic groups, pigments" were predominated by the subcategory "folate, pterines, and biotin synthesis" (**Figure 5B**). While that in the category "carbohydrates" was most represented by the subcategory "monosaccharides metabolism" and "central carbohydrate metabolism" (**Figure 5C**).

Cold Shock Genes

All the 14 genomes obtained from the present study and the references genomes have two predicted cold shock genes (**Table 1**). Neither numeric differences nor gene family differences (50% amino acid sequence similarity and 50% coverage) were observed between the psychrophilic *Cryobacterium* and the mesophilic *C. mesophilum*. We further compared the *Cryobacterium* species to reference strains at the family level. Surprisingly, no numeral advantage of cold adapted genes was detected in *Cryobacterium* genomes over the reference strains (**Supplementary Table S3**).

Gene Gain and Loss

The phylogenetic birth-and-death model imposed on the phylogenomic tree indicates a complicated evolutionary path of the *Cryobacterium* species with their relatives in the family Microbacteriaceae. The most recent common ancestor (∼1,541 genes) experienced early expansion in gene content, leading to the nodes N29, N28, N27, N24, N23, N23, N21, N20, N14, and N12 in **Figure 6**. After the early expansion, the extant lineages all experienced light gene loss (**Figure 6**). In comparison with the genomes of mesophilic Microbacteriaceae and *C. mesophilum*, the extant psychrophilic *Cryobacterium* species increased significantly in genome size ($P < 0.01$).

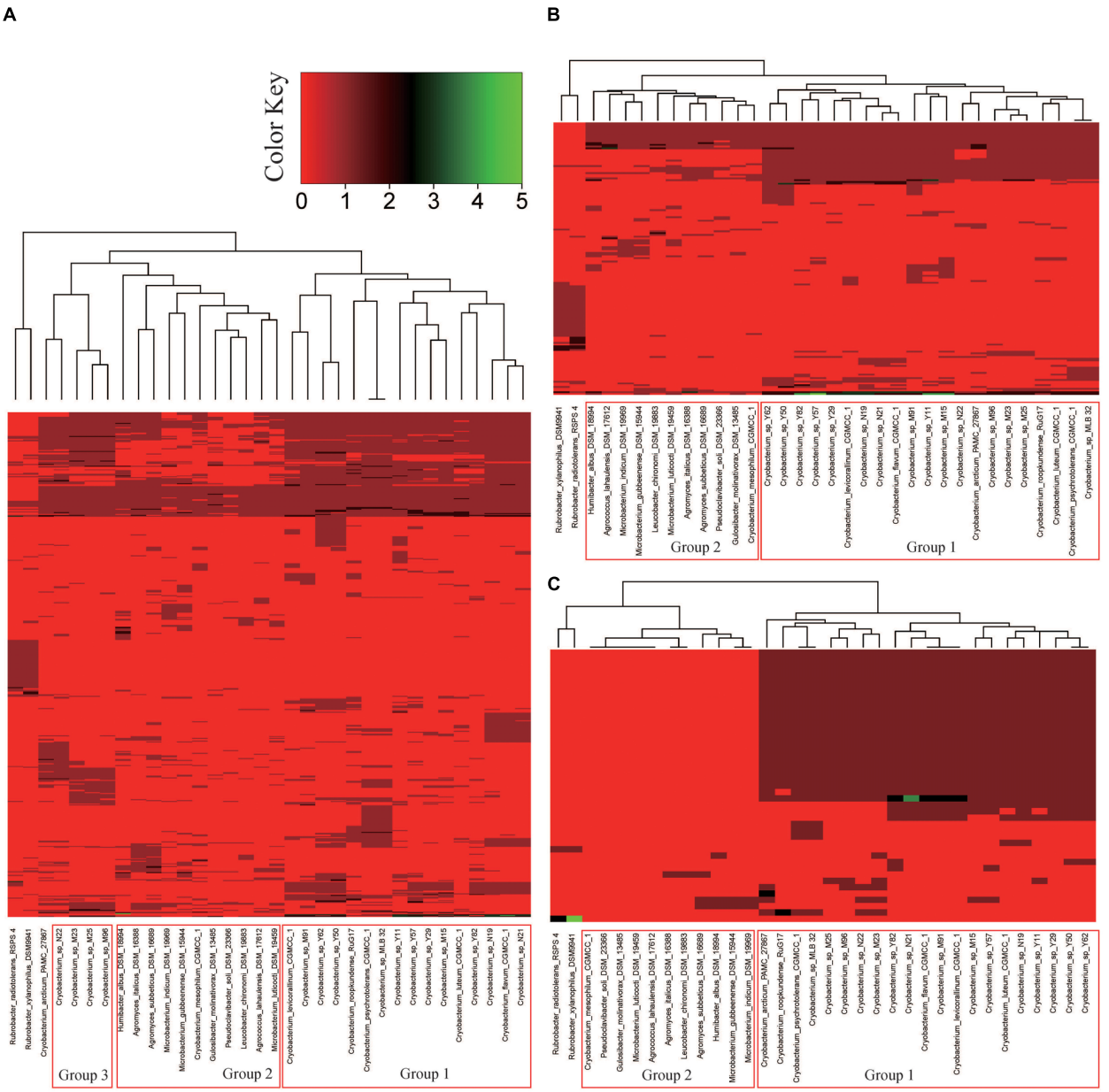

FIGURE 4 | Hierarchical clustering analysis representing the presence/absence of gene families based on the RAST annotations. Genes in each panel: **(A)** "carbohydrates," **(B)** "respiration," and **(C)** "motility and chemotaxis." The categories "carbohydrates," "respiration," and "motility and chemotaxis" contain 575, 154, and 43 genes, respectively. Details of the genes employed in each functional category are presented in **Supplementary Table S6**. Group 1 includes psychrophilic strains from poles and Tibetan Plateau, Group 2 includes *C. mesophilum* CGMCC 1.10440^T and the 10 genomes in the family Microbacteriaceae as described in Section "Materials and Methods," and Group 3 includes five psychrophilic *Cryobacterium* strains.

The remarkable surge in genome content was in the node N20, which gained 1,168 genes and lead to the psychrophilic *Cryobacterium* cluster. Genes gained at the node N20 with known function are involved in the categories of "cofactors, vitamins, prosthetic groups, pigments" (17%), "carbohydrates" (15%), "membrane transport" (8%), "motility and chemotaxis" (7%), and "amino acids and derivatives" (7%) (**Figure 6**).

Mesophilic strain *C. mesophilum* was located at the base of the *Cryobacterium* cluster with a streamlined genome (lost 2,190 genes, **Supplementary Table S5**). Despite a continuous increase in genome content of the nearest ancestor, *C. mesophilum* escaped the surge that occurred to its psychrophilic relatives, evolving directly toward genomes of 1,742 genes (**Figure 6**). The psychrophilic *Cryobacterium* ancestors (e.g., N14, N12, N11, and N7) show either genome surge or slightly expansion. The basal lineages diverged at node N22 show monotonically an increase in genome content since *Cryobacterium* ancestor.

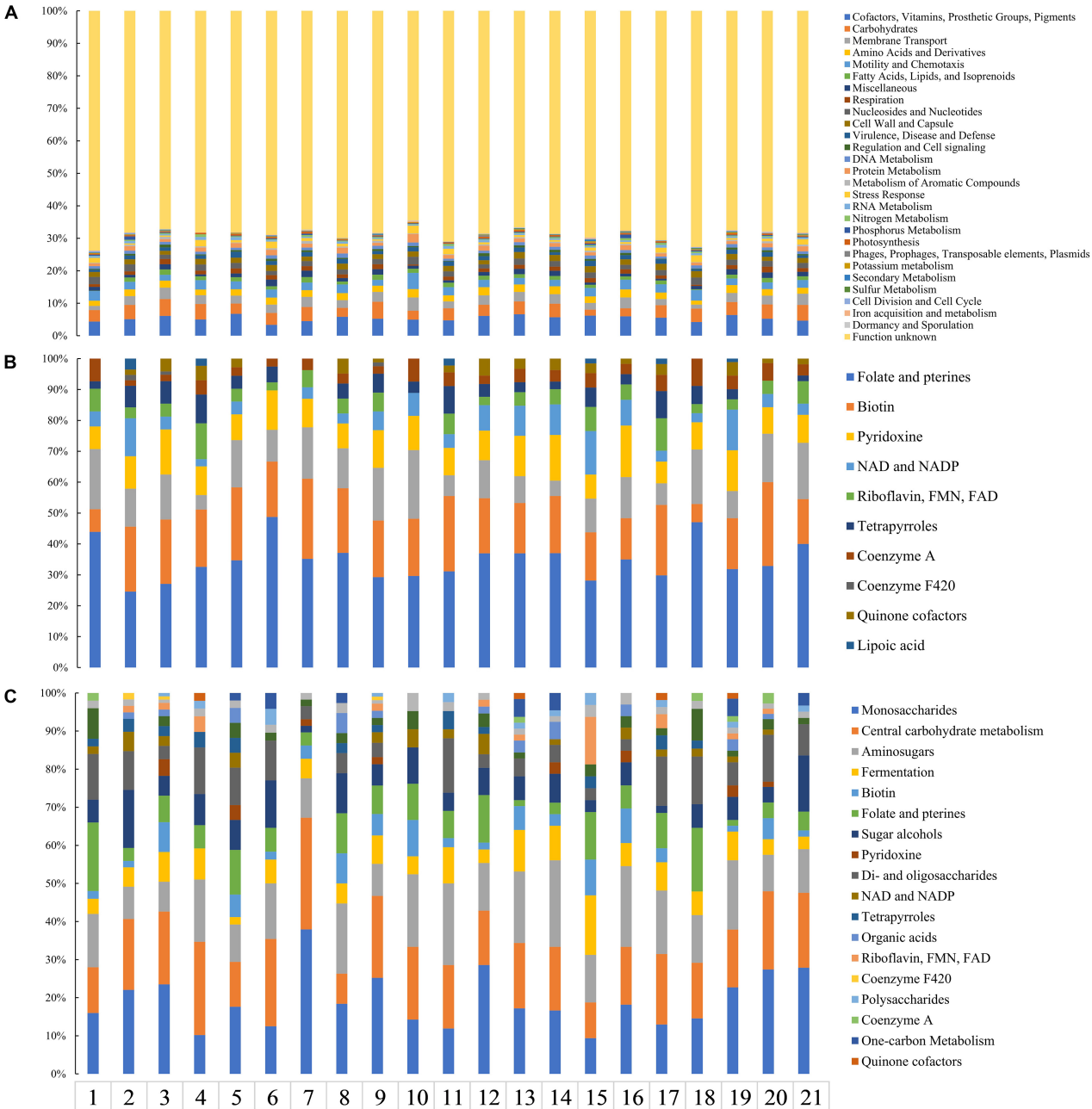

FIGURE 5 | Distribution of specific genes harbored by psychrophilic strains 1, *C. arcticum*; 2, *Cryobacterium* sp. Y11; 3, *Cryobacterium* sp. Y50; 4, *Cryobacterium* sp. M96; 5, *Cryobacterium* sp. M15; 6, *Cryobacterium* sp. MLB-32; 7, *C. levicorallinum*; 8, *Cryobacterium* sp. Y29; 9, *Cryobacterium* sp. Y62; 10, *C. psychrotolerans*; 11, *Cryobacterium* sp. M25; 12, *Cryobacterium* sp. Y57; 13, *C. flavum*; 14, *Cryobacterium* sp. N19; 15, *C. luteum*; 16, *Cryobacterium* sp. Y82; 17, *Cryobacterium* sp. M23; 18, *Cryobacterium* sp. N22; 19, *Cryobacterium* sp. N21; 20, *Cryobacterium* sp. M91; 21, *C. roopkundense*. **(A)** Overall pattern of all genomes at the category level. Gene affiliation to subcategory level involved in **(B)** the category "cofactors, vitamins, prosthetic groups, pigments" and **(C)** the category "carbohydrates."

Analysis of gene gain and gene loss rates versus amino acid substitution rates shows that gene gain and loss rates are at the same order of magnitude (**Figures 7A,B**). However, the amino acid substitution rates of *Cryobacterium* differed significantly (two orders of magnitude lower, P = 6.28E-8) from reference strains.

DISCUSSION

Study of microbial diversity in polar and high alpine regions has revealed a higher diversity of viruses, bacteria, and eukaryotic microbes than expected, and these extreme cold habitants are hot spots of microbial diversity and evolution

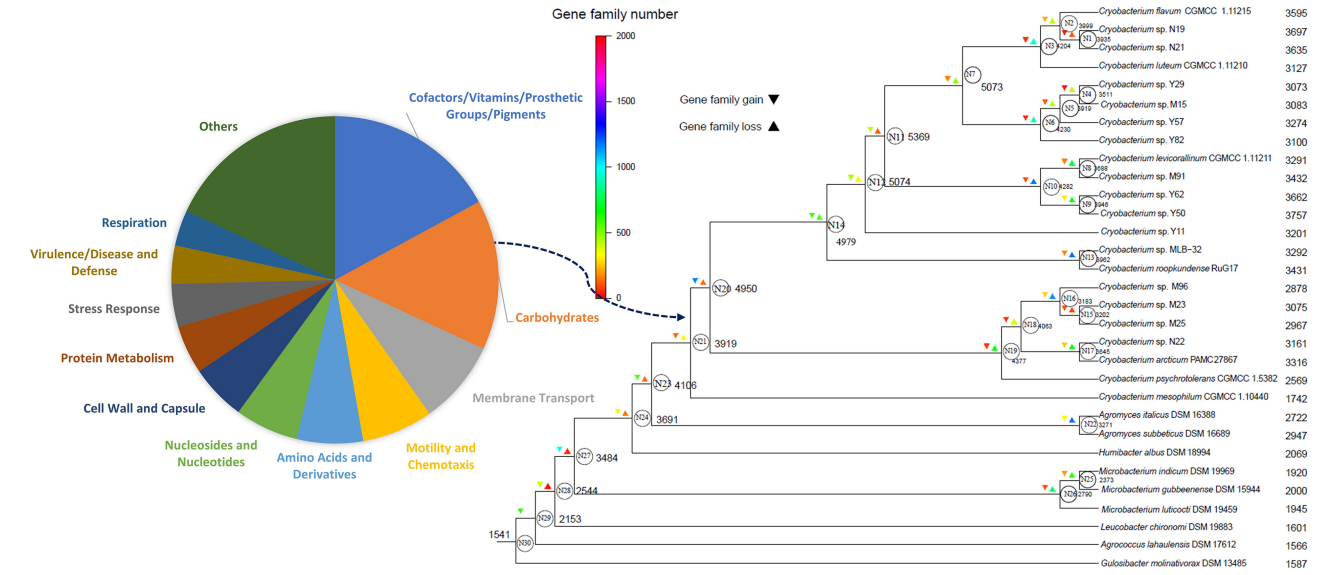

FIGURE 6 | Gene gain and loss events during the evolution of *Cryobacterium* strains and the reference strains in the family Microbacteriaceae reconstructed using the COUNT software. The numbers next to each node and tip represent the genome size, and *N* represents node number. The log-scale color coding represents numbers of reconstructed gain and loss events of each lineage. Function distribution of the genes gained at node N20 is highlighted in the left panel.

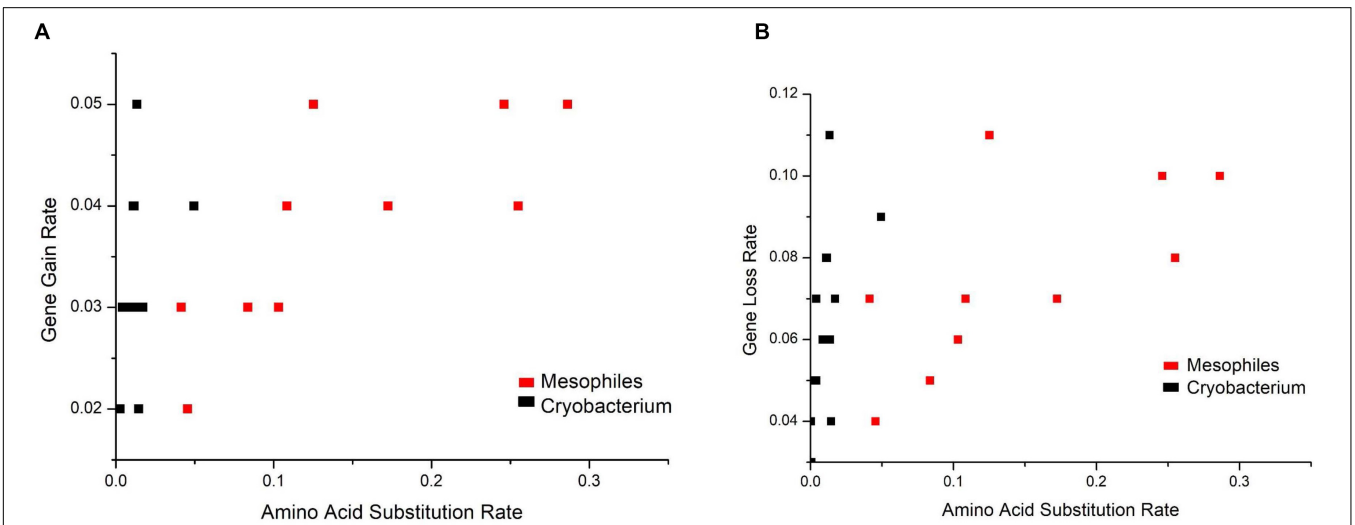

FIGURE 7 | Analysis of gene gain rate **(A)** and gene loss rate **(B)** versus amino acid substitution rate. The phylogeny was constructed using RAxML. The amino acid substitution rate was extracted from the ML tree, and gene gain and loss rates were calculated in the ancestor reconstruction analysis.

(Anesio and Bellas, 2011; Margesin and Collins, 2019). In the present study, we compared 21 genomes of psychrophilic *Cryobacterium* to their mesophilic counterparts from the same family Microbacteriaceae with the aim to identify unique genomic features of the psychrophilic *Cryobacterium* strains isolated from polar and alpine environments. Psychrophilic *Cryobacterium* were revealed to have undergone more dynamic changes in genome content than their mesophilic counterparts, which likely led to the enhanced capabilities of resisting low temperatures, oligotrophy, and high UV radiation on glaciers.

Universal Adaptation Strategies in Psychrophiles Are Selectively Adopted by *Cryobacterium*

Significant changes in amino acid composition were found in the genomes of psychrophilic *Cryobacterium*. Enzymes evolved specific compositional biases (i.e., changes in amino acid composition) to achieve structural flexibility that is required to afford enzyme activity at low temperatures (De Maayer et al., 2014). We identified a reduced use of acidic amino acids (aspartic acid and glutamic acid) and arginine, and an

increased use of lysine in psychrophilic *Cryobacterium*, which is consistent with increased protein flexibility of psychrophiles at low temperatures (Ayala-del-Río et al., 2010; Siddiqui et al., 2013; De Maayer et al., 2014). However, we did not detect the reduced use of proline, the content of which generally decreased in other psychrophiles; this may be attributed to genus-specific adaptation (Rabus et al., 2004; Murray and Grzymski, 2007; De Maayer et al., 2014). Our results suggest that a combination of multi-taxa in comparative genomics is required to understand the universal adaptation strategy that can be identified on a large scale across psychrophiles (Raymond-Bouchard et al., 2018).

No apparent differences in the number and feature of cold shock genes were detected in psychrophilic *Cryobacterium*. Cold shock proteins (CSPs) are induced upon cold shock and are thought to bind a single-stranded RNA motif, resulting in reduced secondary structure formation in the RNA and thus increased translation efficiency (Rabus et al., 2004; De Maayer et al., 2014). It is important for bacteria to be able to synthesize proteins at low temperatures (Thomas and Cavicchioli, 2002; Rabus et al., 2004). Thus, cold shock genes are necessary for cold adaptation (Siddiqui et al., 2013). However, the number of CSP genes varied widely in the genomes of 22 bacterial and archaeal psychrophiles, and no quantitative superiority was observed in CSP genes harbored by psychrophiles (Siddiqui et al., 2013). Furthermore, proteomic profiles of psychrophile *Pseudoalteromonas haloplanktis* TAC 125 was reported to have no cold-induced proteins in response to a temperature shift from 18 to 4°C (Piette et al., 2012). The additional copies of CSP coding gene CspA in *Agromyces italicus* DSM 16388, *Gulosibacter molinativorax* DSM 13485, and *Humibacter albus* DSM 18994, in contrast to the psychrophilic *Cryobacterium* species, did not enable them to become psychrophiles (Manaia et al., 2004; Jurado et al., 2005; Vaz-Moreira et al., 2008). We also detected a decrease in the proportion of genes related to the category "respiration." Low oxygen level was suggested as a trigger for enhancement of respiratory metabolism (Rintala et al., 2009). High altitude of Tibetan glacier connects with low oxygen content, but bacteria inhabiting there did not show an increase in the number of respiration genes. This might be because low temperature in snow and ice could increase the solubility of oxygen and result in less respiratory stress (Allen et al., 2009), which causes the decreasing of the proportion of genes in the category "respiratory' in psychrophilic *Cryobacterium*. This speculation was supported by the fact that the gene proportion of the category "respiration" in Tibetan glacial strains (∼2.63%) are higher than that in polar regions (∼2.35%, $P < 0.05$). Our results, together with the evidence from these previous studies, indicate that gene multicopy may not be a key strategy used for cold adaptation.

Niche Adaptation Governs the Genomic Contents in *Cryobacterium*

The enrichment of stressor response associated genes has been detected in glacier ice metagenome (Simon et al., 2009). Since the solubility of gasses increases rapidly at low temperatures, the ability to respond to reactive oxygen species is an essential function for organisms living at low temperatures (Simon et al., 2009). Not unexpectedly, one of the most striking differences in genome content between psychrophilic *Cryobacterium* strains and references is in the stress response genes. Genes related to "osmotic stress," "oxidative stress," and "periplasmic stress" are all involved in the category "stress response" (Overbeek et al., 2014).

The comparison of the subsystem groupings is based on functions, and differences can be detected from gene presence and absence matrixes, such as genes involved in "carbohydrates," "respiration," and "motility and chemotaxis." However, the psychrophilic *Cryobacterium* genomes are very divergent, with more than 39 genes involved in "motility and chemotaxis" while the mesophilic counterparts have less than 10 genes of the same category. Literature has rarely reported the correlation between the presence of genes involved in "motility and chemotaxis" and the ability of cold adaptation (De Maayer et al., 2014). For the psychrophilic *Cryobacterium* strains, the presence of genes involved in motility and chemotaxis may be one of the key genomic advantages for coping with cold environments. This may be especially true for the isolates from ice cores (M/N/Y series of strains in this study), as genes involved in "motility and chemotaxis" can help them to move toward interstitial veins that exist at the grain boundaries of ice crystals and thus acquire metabolites (Price, 2000; Amato and Christner, 2009; Mackelprang et al., 2017).

Niche adaptation appears to play a significant role in governing the genetic content of the *Cryobacterium* strains isolated from Tibetan Plateau, Antarctic, and Arctic as indicated by the distribution pattern of specific gene families. Studies performed on *Lactococcus* and *Novosphingobium* genomes also suggest that there are habitat-specific genes (Kelleher et al., 2017; Kumar et al., 2017), for example, strengthening in ultraviolet radiation resistance and preferential utilization of simpler forms of carbohydrates (Singh et al., 2014; Shen et al., 2019). Niche adaptation relies heavily on the acquisition of new metabolic capabilities as well as the loss of unnecessary functions (Feng et al., 2014). Comparison of whole genomes of psychrophilic *Cryobacterium* strains with respect to the reference strains in this study revealed the presence of between 543 and 1,422 specific gene families for *Cryobacterium* strains. Of these specific gene families, all the genomes have similar dominating functional groups ("cofactors, vitamins, prosthetic groups, pigments," "carbohydrates," "membrane transport," "motility and chemotaxis," and "amino acids and derivatives"), reflecting the resultant adaptive changes in the genomes of *Cryobacterium* strains in response to harsh glacial environments. The distribution of specific genes also differed between psychrophilic *Cryobacterium* strains and the reference strains. For example, the most dominant functional group of *C. mesophilum* is "amino acids and derivatives" (**Supplementary Figure S2**). Our results revealed a different distribution of functional genes between psychrophilic *Cryobacterium* strains and the reference strains, and the biased distribution of functional genes may be due to the

high genome plasticity of the cold adapted microorganisms (Allen et al., 2009).

Psychrophilic *Cryobacterium* Evolved by Gene Gains and Losses

We used amino acid substitution rate as a proxy of genome evolution at the basal level, i.e., accumulation of natural neutral mutations that occur across all *Cryobacterium* genomes at an equal rate. This is a passive process leading to genome variations without affecting fitness. In contrast, gene gain and loss are more proactive processes leading to rapid niche differentiation. The large difference in the rates of these two different evolutionary processes highlights the importance of gene gain/loss events during the evolution of psychrophilic *Cryobacterium*.

Based on the genome dynamics analysis, we identified a genomic expansion event in psychrophilic *Cryobacterium* genomes during the initial period, which may have facilitated the species in adapting to cold environments, like Tibetan Plateau glaciers, Himalayan lake, and Antarctica sedimentary rock, which were further divided into subgroups. The early surge in gene content, leading to the N20 node, may eventually lead to the origin of psychrophilic *Cryobacterium* species. This was supported by the fact that the only mesophilic strain *C. mesophilum* CGMCC1.10440^T was not involved in this surge.

Genes gained at the nod N20 are predominated by the functional category "cofactors, vitamins, prosthetic groups, pigments." Genes involved in this category process a series of key compounds (e.g., folate, pterines, biotin, pyridoxine, riboflavin, and carotenoids) in bacteria coping with environmental stressors. The vast surge in the genome content of the common ancestor of psychrophilic *Cryobacterium* may be induced by the environmental pressure. Adaptation to environmental stressor is dependent on the time necessary to accumulate mutations or new genes and the degree of perturbation (Jansson and Hofmockel, 2020). Our study revealed that microorganisms in low-temperature environments with long generation times (Mackelprang et al., 2017) gaining genes via horizontal transfer may be the most effective way. The added genome content can help psychrophilic *Cryobacterium* to cope with low temperatures, high ultraviolet radiation, and oligotrophic glacial environments (Domingues and Nielsen, 2017). This is consistent with phenotypic characteristics commonly observed in microbes from cold habitats, for example, the pigmentation of microorganisms isolated from the Northern Schneeferner, Tibetan Plateau, and Greenland (Miteva et al., 2004; Simon et al., 2009; Shen et al., 2014). The classification of specific genes and genes gained at the nod N20 is similar, which may suggest that *Cryobacterium*-specific genes are likely the genes that provided *Cryobacterium* with psychrophilic functionality.

Genes gained by psychrophilic *Cryobacterium* spp. are mostly involved in "cofactors, vitamins, prosthetic groups, pigments," while genes gained by the psychrophilic bacterium *Psychroflexus torquis* ATCC 700755 from sea ice are mostly referred to exopolysaccharide (EPS) and polyunsaturated fatty acid (PUFA) biosynthesis when compared to its closely related mesophilic sister species (Feng et al., 2014). This inconsistency of functional genes gained by cold adapted species indicates different key environmental factors existing for shaping the genome content of bacteria from alpine glacier and sea ice. The intensive ultraviolet radiation may be an underestimated environmental factor in addition to low temperatures, high osmotic pressures, and low nutrient availability in glaciers on the Tibetan Plateau, which together exert a constant and strong evolutionary pressure on the genomes of glacial bacteria. The traits of anti-ultraviolet radiation were also illustrated in mammals living on Tibetan Plateau (Huerta-Sanchez et al., 2014; Yang et al., 2017). For example, the folate-increasing allele of rs1801133 has an increased frequency in Tibetans, which is probably a consequence of adaptation to high UV radiation (Yang et al., 2017). The folate genes are also involved in the category "cofactors, vitamins, prosthetic groups, pigments" in bacterial genomes (Overbeek et al., 2014), the main category gained by psychrophilic *Cryobacterium* genomes. Our results support the view that low-temperature habitats are hot spots of microbial evolution (Anesio and Bellas, 2011).

CONCLUSION

Our study suggests that cold adaptation appears to play a significant part in governing the genome content of glacial bacteria. This is supported by the findings that the vast surge and biased gene gains by the common ancestor of *Cryobacterium* occurred after the divergence of the mesophilic *C. mesophilum*. Considering the surge in genome content and the low amino acid substitution rate, the transfer of genes between glacial bacteria (e.g., mediated by viruses, plasmids, and other mobile elements) may be higher than previously thought despite their long generation time. Further studies on the gene expression patterns in both psychrophilic and mesophilic *Cryobacterium* are required to establish the direct link between genome differences and cold adaptation.

DATA AVAILABILITY STATEMENT

The datasets generated for this study can be found in the DDBJ/ENA/GenBank PJJJ00000000–PJJX00000000.

AUTHOR CONTRIBUTIONS

YL designed the study. LS performed the bioinformatics analysis. TX performed the lab experiments. BX and NW collected the samples. YL, LS, and YZ together wrote the manuscript. All authors approved the final version.

FUNDING

This study was financially supported by the National Natural Science Foundation of China (Grant Nos. 91851207, 41701085, and 41425004), the Strategic Priority Research Program of

Chinese Academy of Sciences (Grant No. XDA20050101), and Second Tibetan Plateau Scientific Expedition and Research (STEP) program (Grant No. 2019QZKK0503). This work was also partially supported by a Villum Experiment grant (No. 17601) awarded to YZ.

SUPPLEMENTARY MATERIAL

The Supplementary Material for this article can be found online at: https://www.frontiersin.org/articles/10.3389/fmicb.2020.01530/full#supplementary-material

REFERENCES

Allen, M. A., Lauro, F. M., Williams, T. J., Burg, D., Siddiqui, K. S., De Francisci, D., et al. (2009). The genome sequence of the Psychrophilic archaeon, *Methanococcoides burtonii*: the role of genome evolution in cold adaptation. *ISME J.* 3, 1012–1035. doi: 10.1038/ismej.2009.45

Amato, P., and Christner, B. C. (2009). Energy metabolism response to low-temperature and frozen conditions in *Psychrobacter cryohalolentis*. *Appl. Environ. Microbiol.* 75, 711–718. doi: 10.1128/aem.02193-08

Anesio, A. M., and Bellas, C. M. (2011). Are low temperature habitats hot spots of microbial evolution driven by viruses? *Trends. Microbiol.* 19, 52–57. doi: 10.1016/j.tim.2010.11.002

Anesio, A. M., and Laybourn-Parry, J. (2012). Glaciers and ice sheets as a biome. *Trends. Ecol. Evol.* 27, 219–225. doi: 10.1016/j.tree.2011.09.012

Ayala-del-Río, H. L., Chain, P. S., Grzymski, J. J., Ponder, M. A., Ivanova, N., Bergholz, P. W., et al. (2010). The genome sequence of *Psychrobacter arcticus* 273-4, a psychroactive Siberian permafrost bacterium, reveals mechanisms for adaptation to low-temperature growth. *Appl. Environ. Microbiol.* 76, 2304–2312. doi: 10.1128/AEM.02101-09

Bajerski, F., Ganzert, L., Mangelsdorf, K., Lipski, A., and Wagner, D. (2011). *Cryobacterium arcticum* sp. nova, a psychrotolerant bacterium from an Arctic soil. *Int. J. Syst. Evol. Micr.* 61, 1849–1853. doi: 10.1099/ijs.0.027128-0

Bankevich, A., Nurk, S., Antipov, D., Gurevich, A. A., Dvorkin, M., Kulikov, A. S., et al. (2012). Spades: a new genome assembly algorithm and its applications to single-cell sequencing. *J. Comput. Biol.* 19, 455–477. doi: 10.1089/cmb.2012.0021

Castresana, J. (2000). Selection of conserved blocks from multiple alignments for their use in phylogenetic analysis. *Mol. Biol. Evol.* 17, 540–552. doi: 10.1093/oxfordjournals.molbev.a026334

Chen, S., Zhou, Y., Chen, Y., and Gu, J. (2018). fastp: an ultra-fast all-in-one FASTQ preprocessor. *Bioinformatics* 34, i884–i890. doi: 10.1093/bioinformatics/bty560

Csuroes, M. (2010). Count: evolutionary analysis of phylogenetic profiles with parsimony and likelihood. *Bioinformatics* 26, 1910–1912. doi: 10.1093/bioinformatics/btq315

Dastager, S. G., Lee, J. C., Ju, Y. J., Park, D. J., and Kim, C. J. (2008). *Cryobacterium mesophilum* sp. nov., a novel mesophilic bacterium. *Int. J. Syst. Evol. Micr.* 58, 1241–1244. doi: 10.1099/ijs.0.65650-0

De Maayer, P., Anderson, D., Cary, C., and Cowan, D. A. (2014). Some like it cold: understanding the survival strategies of psychrophiles. *Embo Rep.* 15, 508–517. doi: 10.1002/embr.201338170

Domingues, S., and Nielsen, K. M. (2017). Membrane vesicles and horizontal gene transfer in prokaryotes. *Curr. Opin. Microbiol.* 38, 16–21. doi: 10.1016/j.mib.2017.03.012

Edgar, R. C. (2004). MUSCLE: a multiple sequence alignment method with reduced time and space complexity. *BMC Bioinformatics* 5:113. doi: 10.1186/1471-2105-5-113

Felsenstein, J. (1981). Evolutionary trees from DNA sequences: a maximum likelihood approach. *J. Mol. Evol.* 17, 368–376. doi: 10.1007/BF01734359

Feng, S., Powell, S. M., Wilson, R., and Bowman, J. P. (2014). Extensive gene acquisition in the extremely psychrophilic bacterial species *Psychroflexus torquis* and the link to sea-ice ecosystem specialism. *Genome Biol. Evol.* 6, 133–148. doi: 10.1093/gbe/evt209

Gil, R., Silva, F. J., Pereto, J., and Moya, A. (2004). Determination of the core of a minimal bacterial gene set. *Microbiol. Mol. Biol. Rev.* 68, 518–537. doi: 10.1128/MMBR.68.3.518-537.2004

Gong, C., Lai, Q., Cai, H., Jiang, Y., Liao, H., Liu, Y., et al. (2019). *Cryobacterium soli* sp. nov., isolated from forest soil. *Int. J. Syst. Evol. Micr.* 70, 675–679. doi: 10.1099/ijsem.0.003820

Grinsted, A. (2013). An estimate of global glacier volume. *Cryosphere* 7, 141–151. doi: 10.5194/tc-7-141-2013

Grissa, I., Vergnaud, G., and Pourcel, C. (2007a). CRISPRFinder: a web tool to identify clustered regularly interspaced short palindromic repeats. *Nucleic Acids Res.* 35, W52–W57. doi: 10.1093/nar/gkm360

Grissa, I., Vergnaud, G., and Pourcel, C. (2007b). The CRISPRdb database and tools to display CRISPRs and to generate dictionaries of spacers and repeats. *BMC Bioinformatics* 8:172. doi: 10.1186/1471-2105-8-172

Hodson, A., Anesio, A. M., Tranter, M., Fountain, A., Osborn, M., Priscu, J., et al. (2008). Glacial ecosystems. *Ecol. Monogr.* 78, 41–67. doi: 10.1890/07-0187.1

Huerta-Sanchez, E., Jin, X., Asan, Bianba, Z., Peter, B. M., and Vinckenbosch, N. (2014). Altitude adaptation in Tibetans caused by introgression of Denisovan-like DNA. *Nature* 512, 194–197. doi: 10.1038/nature13408

Ihaka, R., and Gentleman, R. (1996). R: a language for data analysis and graphics. *J. Comput. Graph. Statist.* 5, 299–314. doi: 10.1080/10618600.1996.10474713

Inoue, K., and Komagata, K. (2006). Taxonomic study on obligately psychrophilic bacteria isolated from antarctica. *J. Gen. Appl. Microbiol.* 22, 165–176. doi: 10.2323/jgam.22.165

Jansson, J. K., and Hofmockel, K. S. (2020). Soil microbiomes and climate change. *Nat. Rev. Microbiol.* 18, 35–46. doi: 10.1038/s41579-019-0265-7

Jurado, V., Groth, I., Gonzalez, J. M., Laiz, L., Schuetze, B., and Saiz-Jimenez, C. (2005). *Agromyces italicus* sp. nov., *Agromyces humatus* sp. nov., and *Agromyces lapidis* sp. nov., isolated from Roman catacombs. *Int. J. Syst. Evol. Micr.* 55, 871–875. doi: 10.1099/ijs.0.63414-0

Kelleher, P., Bottacini, F., Mahony, J., Kilcawley, K. N., and van Sinderen, D. (2017). Comparative and functional genomics of the *Lactococcus lactis* taxon; insights into evolution and niche adaptation. *BMC Genomics* 18:267. doi: 10.1186/s12864-017-3650-5

Kumar, S., Stecher, G., Li, M., Knyaz, C., and Tamura, K. (2018). MEGA X: molecular evolutionary genetics analysis across computing platforms. *Mol. Biol. Evol.* 35, 1547–1549. doi: 10.1093/molbev/msy096

Kumar, R., Verma, H., Haider, S., Bajaj, A., Sood, U., Ponnusamy, K., et al. (2017). Comparative genomic analysis reveals habitat-specific genes and regulatory hubs within the genus *Novosphingobium*. *mSystems* 2:e00020-17. doi: 10.1128/mSystems.00020-17

Lagesen, K., Hallin, P., Rodland, E. A., Staerfeldt, H.-H., Rognes, T., and Ussery, D. W. (2007). RNAmmer: consistent and rapid annotation of ribosomal RNA genes. *Nucleic Acids Res.* 35, 3100–3108. doi: 10.1093/nar/gkm160

Lanfear, R., Calcott, B., Ho, S. Y. W., and Guindon, S. (2012). PartitionFinder: combined selection of partitioning schemes and substitution models for phylogenetic analyses. *Mol. Biol. Evol.* 29, 1695–1701. doi: 10.1093/molbev/mss020

Lee, J., Cho, A., Yang, J. Y., Woo, J., Lee, H. K., Hong, S. G., et al. (2016). Complete genome sequence of *Cryobacterium arcticum* strain PAMC 27867, isolated from a sedimentary rock sample in northern Victoria land, Antarctica. *Genome Announc* 4:e00885-16. doi: 10.1128/genomeA.00885-16

Liu, Q., Liu, H. C., Wen, Y., Zhou, Y. G., and Xin, Y. H. (2012). *Cryobacterium flavum* sp. nov. and *Cryobacterium luteum* sp. nov., isolated from glacier ice. *Int. J. Syst. Evol. Micr.* 62, 1296–1299. doi: 10.1099/ijs.0.033738-0

Liu, Q., Liu, H. C., Zhang, J. L., Zhou, Y. G., and Xin, Y. H. (2013). *Cryobacterium levicorallinum* sp. nov., a psychrophilic bacterium isolated from glacier ice. Int. J. Syst. Evol. Micr. 63, 2819–2822. doi: 10.1099/ijs.0.046896-0

Liu, Q., Liu, H.-C., Zhou, Y.-G., and Xin, Y.-H. (2018). Genetic diversity of glacier-inhabiting Cryobacterium bacteria in China and description of *Cryobacterium zongtaii* sp. nov. and *Arthrobacter glacialis* sp. nov. *Syst. Appl. Microbiol.* 42, 168–177. doi: 10.1016/j.syapm.2018.10.005

Liu, Q., Liu, H. C., Zhou, Y. G., and Xin, Y. H. (2019a). Microevolution and adaptive strategy of psychrophilic species *Flavobacterium bomense* sp. nov. isolated from glaciers. *Front. Microbiol.* 10:1069. doi: 10.3389/fmicb.2019.01069

Liu, Q., Tian, J.-H., Liu, H.-C., Zhou, Y.-G., and Xin, Y.-H. (2019b). *Cryobacterium melibiosiphilum* sp. nov., a psychrophilic bacterium isolated from glacier ice. *Int. J. Syst. Evol. Micr.* 69, 3276–3280. doi: 10.1099/ijsem.0.003620

Liu, Y. Q., Priscu, J. C., Yao, T. D., Vick-Majors, T. J., Michaud, A. B., and Sheng, L. (2019c). Culturable bacteria isolated from seven high-altitude ice cores on the Tibetan Plateau. *J. Glaciol.* 65, 29–38. doi: 10.1017/jog.2018.86

Liu, Y., Priscu, J. C., Yao, T., Vick-Majors, T. J., Xu, B., Jiao, N., et al. (2016). Bacterial responses to environmental change on the Tibetan Plateau over the past half century. *Environ. Microbiol.* 18, 1930–1941. doi: 10.1111/1462-2920.13115

Luo, H., Cusros, M., Hughes, A. L., and Moran, M. A. (2013). Evolution of divergent life history strategies in marine alphaproteobacteria. *mBio* 4:e00373-13. doi: 10.1128/mBio.00373-13

Mackelprang, R., Burkert, A., Haw, M., Mahendrarajah, T., Conaway, C. H., Douglas, T. A., et al. (2017). Microbial survival strategies in ancient permafrost: insights from metagenomics. *ISME J.* 11, 2305–2318. doi: 10.1038/ismej.2017.93

Manaia, C. M., Nogales, B., Weiss, N., and Nunes, O. C. (2004). *Gulosibacter molinativorax* gen. nov., sp. nov., a molinate-degrading bacterium, and classification of 'Brevibacterium helvolum' DSM 20419 as *Pseudoclavibacter helvolus* gen. nov., sp. nov. *Int. J. Syst. Evol. Micr.* 54, 783–789. doi: 10.1099/ijs.0.02851-0

Margesin, R., and Collins, T. (2019). Microbial ecology of the cryosphere (glacial and permafrost habitats): current knowledge. *Appl. Microbiol. Biotechnol.* 103, 2537–2549. doi: 10.1007/s00253-019-09631-3

Methé, B. A., Nelson, K. E., Deming, J. W., Momen, B., Melamud, E., Zhang, X. J., et al. (2005). The psychrophilic lifestyle as revealed by the genome sequence of *Colwellia psychrerythraea* 34H through genomic and proteomic analyses. *Proc. Natl. Acad. Sci. U.S.A.* 102, 10913–10918. doi: 10.1073/pnas.0504766102

Miteva, V. I., Sheridan, P. P., and Brenchley, J. E. (2004). Phylogenetic and physiological diversity of microorganisms isolated from a deep Greenland glacier ice core. *Appl. Environ. Microbiol.* 70, 202–213. doi: 10.1128/aem.70.1.202-213.2004

Murray, A. E., and Grzymski, J. J. (2007). Diversity and genomics of Antarctic marine micro-organisms. *Philos. Trans. R. Soc. B* 362, 2259–2271. doi: 10.1098/rstb.2006.1944

Oliveira, P. H., Touchon, M., Cury, J., and Rocha, E. P. C. (2017). The chromosomal organization of horizontal gene transfer in bacteria. *Nat. Commun.* 8:841. doi: 10.1038/s41467-017-00808-w

Overbeek, R., Olson, R., Pusch, G. D., Olsen, G. J., Davis, J. J., Disz, T., et al. (2014). The SEED and the rapid annotation of microbial genomes using subsystems technology (RAST). *Nucleic Acids Res.* 42, D206–D214. doi: 10.1093/nar/gkt1226

Parks, D. H., Imelfort, M., Skennerton, C. T., Hugenholtz, P., and Tyson, G. W. (2015). CheckM: assessing the quality of microbial genomes recovered from isolates, single cells, and metagenomes. *Genome Res.* 25:1043. doi: 10.1101/gr.186072.114

Piette, F., Leprince, P., and Feller, G. (2012). Is there a cold shock response in the antarctic psychrophile pseudoalteromonas haloplanktis? *Extremophiles* 16, 681–683. doi: 10.1007/s00792-012-0456-x

Price, P. B. (2000). A habitat for psychrophiles in deep Antarctic ice. *Proc. Natl. Acad. Sci. U.S.A.* 97, 1247–1251. doi: 10.1073/pnas.97.3.1247

Priscu, J. C., Johnson, L., and Christner, B. C. (2004). *Earth's icy Biosphere*. Washington, D.C: American Society for Microbiology.

Rabus, R., Ruepp, A., Frickey, T., Rattei, T., Fartmann, B., Stark, M., et al. (2004). The genome of *Desulfotalea psychrophila*, a sulfate-reducing bacterium from permanently cold Arctic sediments. *Environ. Microbiol.* 6, 887–902. doi: 10.1111/j.1462-2920.2004.00665.x

Raymond-Bouchard, I., Goordial, J., Zolotarov, Y., Ronholm, J., Stromvik, M., Bakermans, C., et al. (2018). Conserved genomic and amino acid traits of cold adaptation in subzero-growing Arctic permafrost bacteria. *FEMS Microbiol. Ecol.* 94:fiy023. doi: 10.1093/femsec/fiy023

Reddy, G. S. N., Pradhan, S., Manorama, R., and Shivaji, S. (2010). *Cryobacterium roopkundense* sp nov., a psychrophilic bacterium isolated from glacial soil. *Int. J. Syst. Evol. Micr.* 60, 866–870. doi: 10.1099/ijs.0.011775-0

Rintala, E., Toivari, M., Pitkanen, J. P., Wiebe, M. G., Ruohonen, L., and Penttila, M. (2009). Low oxygen levels as a trigger for enhancement of respiratory metabolism in *Saccharomyces cerevisiae*. *BMC Genomics* 10:461. doi: 10.1186/1471-2164-10-461

Ronquist, F., and Huelsenbeck, J. P. (2003). MrBayes 3: bayesian phylogenetic inference under mixed models. *Bioinformatics* 19, 1572–1574. doi: 10.1093/bioinformatics/btg180

Sathyanarayana Reddy, G., Sreenivas, A., and Shivaji, S. (2014). Draft genome sequence of Cryobacterium roopkundensis strain RuGl7, Isolated from a soil sample in the vicinity of roopkund Lake, Himalayas, India. *Genome Announc* 2:e01206-14. doi: 10.1128/genomeA.01206-14

Saunders, N. F., Thomas, T., Curmi, P. M., Mattick, J. S., Kuczek, E., Slade, R., et al. (2003). Mechanisms of thermal adaptation revealed from the genomes of the Antarctic Archaea *Methanogenium frigidum* and *Methanococcoides burtonii*. *Genome Res.* 13, 1580–1588. doi: 10.1101/gr.1180903

Segawa, T., Miyamoto, K., Ushida, K., Agata, K., Okada, N., and Kohshima, S. (2005). Seasonal change in bacterial flora and biomass in mountain snow from the Tateyama Mountains, Japan, analyzed by 16S rRNA gene sequencing and real-time PCR. *Appl. Environ. Microbiol.* 71, 123–130. doi: 10.1128/aem.71.1.123-130.2005

Shen, L., Liu, Y. Q., Wang, N. L., and Adhikari, N. P. (2019). Genomic insights of *Dyadobacter tibetensis* Y620-1 isolated from ice core reveal genomic features for succession in glacier environment. *Microorganisms* 7:211. doi: 10.3390/microorganisms7070211

Shen, L., Liu, Y. Q., Xu, B. Q., Wang, N. L., Zhao, H. B., Liu, X. B., et al. (2017). Comparative genomic analysis reveals the environmental impacts on two *Arcticibacter* strains including sixteen Sphingobacteriaceae species. *Sci. Rep.* 7:2055. doi: 10.1038/s41598-017-02191-4

Shen, L., Yao, T. D., Liu, Y. Q., Jiao, N. Z., Kang, S. C., Xu, B. Q., et al. (2014). Downward-shifting temperature range for the growth of snow-bacteria on glaciers of the Tibetan Plateau. *Geomicrobiol. J.* 31, 779–787. doi: 10.1080/01490451.2014.891418

Siddiqui, K. S., Williams, T. J., Wilkins, D., Yau, S., Allen, M. A., Brown, M. V., et al. (2013). Psychrophiles. *Annu. Rev. Earth. Planet. Sci.* 41, 87–115. doi: 10.1146/annurev-earth-040610-133514

Simon, C., Wiezer, A., Strittmatter, A. W., and Daniel, R. (2009). Phylogenetic diversity and metabolic potential revealed in a glacier ice metagenome. *Appl. Environ. Microbiol.* 75, 7519–7526. doi: 10.1128/aem.00946-09

Singh, P., Kapse, N., Arora, P., Singh, S. M., and Dhakephalkar, P. K. (2015). Draft genome of *Cryobacterium* sp. *MLB*-32, an obligate psychrophile from glacier cryoconite holes of high Arctic. *Mar. Genom.* 21, 25–26. doi: 10.1016/j.margen.2015.01.006

Singh, P., Singh, S. M., and Dhakephalkar, P. (2014). Diversity, cold active enzymes and adaptation strategies of bacteria inhabiting glacier cryoconite holes of High Arctic. *Extremophiles* 18, 229–242. doi: 10.1007/s00792-013-0609-6

Stamatakis, A. (2014). RAxML version 8: a tool for phylogenetic analysis and post-analysis of large phylogenies. *Bioinformatics* 30, 1312–1313. doi: 10.1093/bioinformatics/btu033

Suzuki, K. I., Sasaki, J., Uramoto, M., Nakase, T., and Komagata, K. (1997). *Cryobacterium psychrophilium* gen. nov., sp. nov., nom. rev., comb. nov., an obligately psychrophilic actinomycete to accommodate *"Curtobacterium psychrophilum"* Inoue and Komagata 1976. *Int. J. Syst. Evol. Micr.* 47, 474–478. doi: 10.1099/00207713-47-2-474

Thomas, T., and Cavicchioli, R. (2002). Cold adaptation of archaeal elongation factor 2 (EF-2) proteins. *Curr. Protein Pept. Sci.* 3, 223–230. doi: 10.2174/1389203024605359

Vaz-Moreira, I., Nobre, M. F., Ferreira, A. C. S., Schumann, P., Nunes, O. C., and Manaia, C. M. (2008). *Humibacter albus* gen. nov., sp nov., isolated from sewage sludge compost. Int. J. Syst. Evol. Micr. 58, 1014–1018. doi: 10.1099/ijs.0.65266-0

Vesth, T., Lagesen, K., Acar, O., and Ussery, D. (2013). CMG-Biotools, a free workbench for basic comparative microbial genomics. *PLoS One* 8:e60120. doi: 10.1371/journal.pone.0060120

Yang, J., Jin, Z. B., Chen, J., Huang, X. F., Li, X. M., Liang, Y. B., et al. (2017). Genetic signatures of high-altitude adaptation in Tibetans. *Proc. Natl. Acad. Sci. U.S.A.* 114, 4189–4194. doi: 10.1073/pnas.1617042114

Zhang, D. C., Wang, H. X., Cui, H. L., Yang, Y., Liu, H. C., Dong, X. Z., et al. (2007). *Cryobacterium psychrotolerans* sp. nov., a novel psychrotolerant bacterium isolated from the China No. 1 glacier. *Int. J. Syst. Evol. Micr.* 57, 866–869. doi: 10.1099/ijs.0.64750-0

Conflict of Interest: The authors declare that the research was conducted in the absence of any commercial or financial relationships that could be construed as a potential conflict of interest.

frontiers in Microbiology

ORIGINAL RESEARCH
published: 28 July 2020
doi: 10.3389/fmicb.2020.01721

Alpine Snow Algae Microbiome Diversity in the Coast Range of British Columbia

*Kurt M. Yakimovich, Casey B. Engstrom and Lynne M. Quarmby**

Department of Molecular Biology and Biochemistry, Simon Fraser University, Burnaby, BC, Canada

Snow algae blooms contain bacteria, fungi, and other microscopic organisms. We surveyed 55 alpine snow algae blooms, collecting a total of 68 samples, from 12 mountains in the Coast Range of British Columbia, Canada. We used microscopy and rDNA metabarcoding to document biodiversity and query species and taxonomic associations. Across all samples, we found 173 algal, 2,739 bacterial, 380 fungal, and 540 protist/animalia operational taxonomic units (OTUs). In a previous study, we reported that most algal species were distributed along an elevational gradient. In the current study, we were surprised to find no corresponding distribution in any other taxa. We also tested the hypothesis that certain bacterial and fungal taxa co-occur with specific algal taxa. However, despite previous evidence that particular genera co-occur, we found no significant correlations between taxa across our 68 samples. Notably, seven bacterial, one fungal, and two cercozoan OTUs were widely distributed across our study regions. Taken together, these data suggest that any mutualisms with algae may not be taxon specific. We also report evidence of snow algae predation by rotifers, tardigrades, springtails, chytrid fungi, and ciliates, establishing the framework for a complex food web.

Keywords: algae, microbiomes, bacteria, fungi, protists, snow

OPEN ACCESS

Edited by:
David Anthony Pearce, Northumbria University, United Kingdom

Reviewed by:
Mohammad Moniruzzaman, Virginia Tech, United States
Anne D. Jungblut, Natural History Museum, United Kingdom

***Correspondence:**
Lynne M. Quarmby
quarmby@sfu.ca

Specialty section:
This article was submitted to Extreme Microbiology, a section of the journal Frontiers in Microbiology

Received: *20 March 2020*
Accepted: *30 June 2020*
Published: *28 July 2020*

Citation:
Yakimovich KM, Engstrom CB and Quarmby LM (2020) Alpine Snow Algae Microbiome Diversity in the Coast Range of British Columbia. Front. Microbiol. 11:1721. doi: 10.3389/fmicb.2020.01721

INTRODUCTION

Alpine snow algae microbiomes are threatened by global warming as glaciers and permanent snowfields disappear. Annual snow coverage in the northern hemisphere has decreased by 5–6 days over the last 50 years (Bormann et al., 2018). At the same time, snow algae blooms amplify the rate of snow loss by decreasing snow surface albedo (Thomas and Duval, 1995; Lutz et al., 2016; Ganey et al., 2017), and microbial growth on snow contributes to accelerated snow melt on a global scale (Ganey et al., 2017; Williamson et al., 2020). We seek to understand the microbial diversity that supports these at-risk alpine microbiomes. It is likely that mutualist interactions are essential for algae growth in this extreme and ephemeral habitat, as is the case in aquatic environments (Seymour et al., 2017). Therefore, a key step toward understanding bloom development is to identify the non-algal components of the blooms.

Snow algae blooms can form a patchwork of red, green, or orange snow that covers large areas (Remias et al., 2013b; Lutz et al., 2016; Ganey et al., 2017; Segawa et al., 2018; Davey et al., 2019; Hoham and Remias, 2020). The blooms support rich communities, including viruses, bacteria, fungi, ciliates, and small metazoans (Thomas and Duval, 1995; Duval et al., 1999; Takeuchi et al., 2006; Brown et al., 2015; Hisakawa et al., 2015; Lutz et al., 2016;

Segawa et al., 2018; Davey et al., 2019). Snow algae blooms are typically dominated by algae of the phylum *Chlorophyta*, although blooms dominated by phylum *Ochrophyta* have also been reported (Leya, 2013; Remias et al., 2013a, 2020; Hamilton and Havig, 2017; Hoham and Remias, 2020). These bloom-forming algae are widely distributed at low densities in white snow around the globe (Brown and Jumpponen, 2019; Maccario et al., 2019).

Bacteria can promote algal growth through the exchange of metabolites (e.g., vitamins, amino acids, or plant hormones) for fixed carbon (Ramanan et al., 2016; Seymour et al., 2017). These relationships have not been documented in snow algae microbiomes, but there is some evidence for their existence. In a metabolomic study of green snow in Antarctica, Davey et al. (2019) found calystegine, an alkaloid noted for plant-bacterial communication. In a laboratory experiment, Terashima et al. (2017) showed that a *Chloromonas* spp. isolated from snow grew better in the presence of bacteria from a field sample than when plated with an antibiotic. Another study, co-culturing snow bacteria and *Chloromonas brevispina*, showed increased iron containing mineral dissolution, which stimulated algae growth, suggesting bacteria could help snow algae obtain bioavailable iron from mineral dust (Harrold et al., 2018). Although little data exist for algae-fungal mutualisms outside of lichens, metabolite exchange can occur between yeast (*Saccharomyces cerevisiae*) and microalgae (*Chlamydomonas reinhardtii*; Hom and Murray, 2014).

A few studies document snow algae microbiome diversity and geographic variation, but all are limited to a few samples from a limited number of sites (Brown et al., 2016; Lutz et al., 2016; Hamilton and Havig, 2017; Terashima et al., 2017). Lutz et al. (2016) compared the variation in bacterial and algae communities in Arctic environments. They found that sites in Northern Sweden (n = 24) had similar bacterial community composition as sites in Svalbard (n = 12), but the two locations varied in their relative abundance profiles. In contrast, on Mount Asahi, Japan, patches of red and green snow within a few hundred meters had distinct bacterial profiles (Terashima et al., 2017). Because the algal communities were different (three of the blooms were red and one was green), the authors suggest that different algal species might recruit different bacterial assemblages. Another alpine study, this one in the Austrian Alps by Krug et al. (2020), reports that specific algal genera from red (n = 3), green (n = 1), and orange (n = 1) patches of snow positively correlate with specific bacterial genera.

In the current study, we set out to robustly document the microbial diversity in the mountains of Southwestern British Columbia. Previously, we reported that *Sanguina* and *Chloromonas* dominated distinct blooms and that they were found at different elevations (Engstrom et al., 2020). Based on the work of Terashima et al. (2017) and Krug et al. (2020), we predicted that specific microbial taxa would be associated with the distinct algal blooms.

Over the 2018 melt season, we collected 68 samples from 55 snow algae blooms on 12 different mountains near Vancouver, Canada. Sample sites ranged in elevation from 880 to 2,150 m above sea level, ranging from below and above tree line. We surveyed the algal, protist, metazoan, fungal, and bacterial communities using both microscopy and 16S/18S rDNA metabarcoding. Across all samples, we found 173 algal, 2,739 bacterial, 380 fungal, and 540 protist/animalia operational taxonomic units (OTUs). We did not find any significant co-occurrence patterns, even when examining the specific genera highlighted by Krug et al. (2020). We found only seven bacterial, one fungal, and two glissomonad OTUs that were present in more than 90% of snow algae samples. Also ubiquitous were *Chytridiomycota*, which we observed physically attached to algae cells. We also report photomicrographs of rotifers, tardigrades, and various ciliates with snow algae in their guts.

MATERIALS AND METHODS

Sample Collection

Samples were collected during the 2018 melt season between May and September from 12 mountains near Vancouver, Canada (**Supplementary Table 1**). Our sampling efforts focused on collecting a wide range of colored snow, including green (n = 20), red (n = 31), and orange (n = 17) from 880 to 2,150 m above sea level. Samples were collected in either a Whirl-Pak® sample bag or a 50 ml centrifuge tube, and the brightest colored snow from a patch was collected until the container was full. In total, 68 samples were analyzed from 55 snow algae bloom sites.

Upon collection, samples were packed together, with extra white snow to ensure they were kept cool until they were returned to the lab. We thawed samples on a lab bench at room temperature, and 1 ml aliquots were fixed in 2% glutaraldehyde for microscopy. Samples were examined at 100x, 630x, and 1,000x magnification on an Axioskop 2 (Zeiss) using differential interference contrast (DIC), and photographed using a Canon EOS T6 camera (Canon, Tokyo, Japan). Samples were then stored at −20°C until processing for DNA extractions.

DNA Extractions

Samples were thawed at room temperature, and DNA extracted and purified using a chloroform method (Cubero et al., 1999), with a CTAB buffer for the cell lysis steps (3% w/v CTAB, 100 mM Tris pH 8.0, 20 mM EDTA, 2.8 M NaCl, and 1% w/v PVP). We used two different cell lysis methods because after completing the first sequencing run with lysis method 1, we developed lysis method 2, which has fewer steps, thereby reducing points for possible contamination. We also opted for manually grinding cells for cell lysis in method 2 to improve the efficiency of lysing fungi and algae. For 42 samples, we used cell lysis method 1: cells were collected on a 0.2 µm nitrocellulose filter (Sartorius AG) and then the filters were cut into strips and placed in a 2 ml tube filled with 0.1 mm glass beads (Qiagen). Seven hundred microlitres of CTAB extraction buffer was added, and the tubes were sonicated at 40% amplitude for 30 s (Bronson Digital Sonifier 450). After sonication, the samples were shaken for 4.5 min at 5000 rpm in a Precellys 24 tissue homogenizer (Bertin Instruments). Finally, the tubes were incubated at 60°C for 1 h. For 26 samples, we used cell lysis method 2: cells were freeze-dried in the 50 ml collection

tubes. The dried pellet was transferred to a 1.5 ml microcentrifuge tube and ground for 1 min by hand using a mini-pestle. Seven hundred microlitres of CTAB extraction buffer was added, and samples incubated for 1 h at 60°C. DNA was quantified using a Qubit (Invitrogen). The lysate from both methods was then carried forward into a chloroform extraction step, and a subsequent EtOH precipitation step after Cubero et al. (1999).

Amplicon Library Preparation and Sequencing for Metabarcoding

From each sample, we generated amplicons for two targets, the 16S rDNA gene of prokaryotes using the primer set Pro341F (5'-CCT ACG GGN BGC ASC AG-3') and Pro805R (5'-GAC TAC NVG GGT ATC TAA TCC-3'; Takahashi et al., 2014) and the 18S rDNA gene of eukaryotes using the primer pair Euk1181 (5'-TTA ATT TGA CTC AAC RCG GG-3') and Euk1624 (5'-CGG GCG GTG TGT ACA AAG G-3'; Wang et al., 2014). We used a two-step PCR library construction: initial primers of the target gene had a universal adapter attached, generating targeted fragments with the universal 5' and 3' adapter sequence appended to their respective ends. Five microlitres of the original amplicon PCR was placed into a second reaction using primers with the universal adaptor sequence and a unique 6 bp index, resulting in the addition of the 6 bp index sequence to the 3' end of each amplicon (one barcode per sample for all gene targets), and a universal barcode on the 5' end. The cycling conditions were the same for both the 16S and 18S primer pairs. For the first PCR, the reactions were done with a total volume of 25 µl, consisting of 12.5 µl of the Q5 high fidelity 2X MM (New England BioLabs, Inc.), 1.25 µl of each respective forward and reverse primer (10 µM), and 9 µl of ddH_2O. For the second PCR the ddH_2O was reduced to 5 µl to compensate for the increased template volume input. For the first PCR, we did an initial denaturation at 98°C for 30 s, followed by 30 cycles of 98°C for 5 s, 58°C for 10 s, and 72°C for 25 s, and then a final extension at 72°C for 2 min. The indexing PCR started with an initial denaturation at 98°C for 30 s, then 10 cycles of 98°C for 10 s, 65°C for 30 s, and 72°C for 30 s with a final denaturation of 72 s for 5 min. After each PCR, the product was purified with the Agencourt AMPure XP kit (Beckman Coulter, Inc.) according to manufacturer specifications. After indexing, they were quantified using a Qubit and standardized for pooling. The pooled library was then loaded and run on a MiSeq (Illumina). Samples used from this study came from two sequencing runs. Amplicons from samples lysed by method 1 were sequenced with a MiSeq V2 kit (Illumina). Amplicons from samples lysed by method 2 were sequenced using a MiSeq V3 kit (Illumina). All raw fastq files were uploaded to the European Nucleotide Archive under the project accession PRJEB34539.

Sequence Data Processing

Reads for both 16S and 18S rDNA were first demultiplexed using CUTADAPT v2.3 (Martin, 2011), and primer sequences were removed. The reads were quality filtered and merged through the *dada2* default pipeline in R v3.6.1 (Callahan et al., 2016; R Core Team, 2019). For the 16S and 18S rDNA sequences, taxonomy assignments were done by using the Silva small subunit database v132 (Quast et al., 2013), formatted for *dada2*[1]. Taxonomy was assigned using the naïve Bayesian classifier RDP (Wang et al., 2007), implemented by *dada2*. The newly defined genus *Sanguina* (Procházková et al., 2019) is absent from the Silva V132 database; therefore, we aligned all *Chlamydomonas* 18S sequences to the NCBI GenBank database (Clark et al., 2016) using BLAST (Altschul et al., 1990). Sequences were reassigned to *Sanguina* if it was the unambiguous top match (no other matches with identity >92%). Taxonomic assignments were used to define fungal, algal, and other 18S rDNA reads. All analyses were done using relative abundance values unless otherwise stated.

The amplicon sequencing variants (ASVs) output from *dada2* were used to assess the distribution of bacteria and eukaryotes sharing identical 16S or 18S sequences. To further assess the distribution of putative bacterial and fungal species, we grouped 16S and fungal 18S rDNA into OTUs. OTUs were clustered using SWARM v2.0 with the default settings (Mahé et al., 2014), which include a strict sequence clustering threshold of 1 base pair difference during the initial alignment phase. Richness was calculated for each sample by counting the total number of ASVs or OTUs. All subsequent analyses for bacteria and fungi were done on both ASVs and OTUs to assess potential population and species level variation, whereas protist/metazoan communities were assessed with OTUs.

Community data was analyzed in R to ascertain co-occurrences [using Kendall's tau rank correlations (τ)] between algae and the fungal, bacterial, and protist communities, using relative abundances. Community trends across elevational gradients were assessed for all microbial groups separately by using a distance-based redundancy analysis (dbRDA) with a Bray-Curtis distance matrix in *vegan* (Oksanen et al., 2017) and with elevation, snow color, and dominant algae genus separately as constraints. The adjusted R^2 values were also calculated to assess the amount of variation explained by each variable. Community structure was also assessed using nonmetric multidimensional scaling (NMDS) and using 95% confidence ellipses to assess community structure by snow color and dominant algae genera. We used the dominant algae genera detected in each sample as a constraint in a dbRDA of the bacterial 16S rDNA data to ask whether dominant algae sequences contributed to structuring the bacterial community. Correlation matrices were computed between all algal-bacterial and algal-fungal ASVs and OTUs to assess co-occurrence patterns. Heatmaps were also constructed in R using the *ggplot2* (Wickham, 2016) and *heatmaply* (Galili et al., 2017) packages, and hierarchical clustering was done in base R to order the samples by similarity along the both axis.

[1]https://benjjneb.github.io/dada2/training.html

RESULTS

Microscopic Documentation of Microbiome Diversity

Examination of snow melt samples with light microscopy revealed a diverse set of organisms. Samples often had a visual abundance of prokaryotes in proximity to algae cells (**Figure 1A**) and in biofilms. Larger fungal cells were often present with various morphologies (**Figure 1B**). Additionally, small flagellated and larger mature chytrid cells were frequently seen attached to algae cells (**Figure 1C**). The morphological species called *Selenotila nivalis* were commonly seen (**Figure 1D**; Light and Belcher, 1968), as was an unidentified micro-eukaryote with a thick outer shell, harboring green spheroids (**Figure 1E**). We frequently observed presumptive algal predators with their guts full of red-pigmented algae cells. These included diverse ciliates (**Figure 1F**) and multicellular organisms, tardigrades (**Figure 1H**), rotifers (**Figure 1I**), and springtails (Collembola; **Figure 1J**).

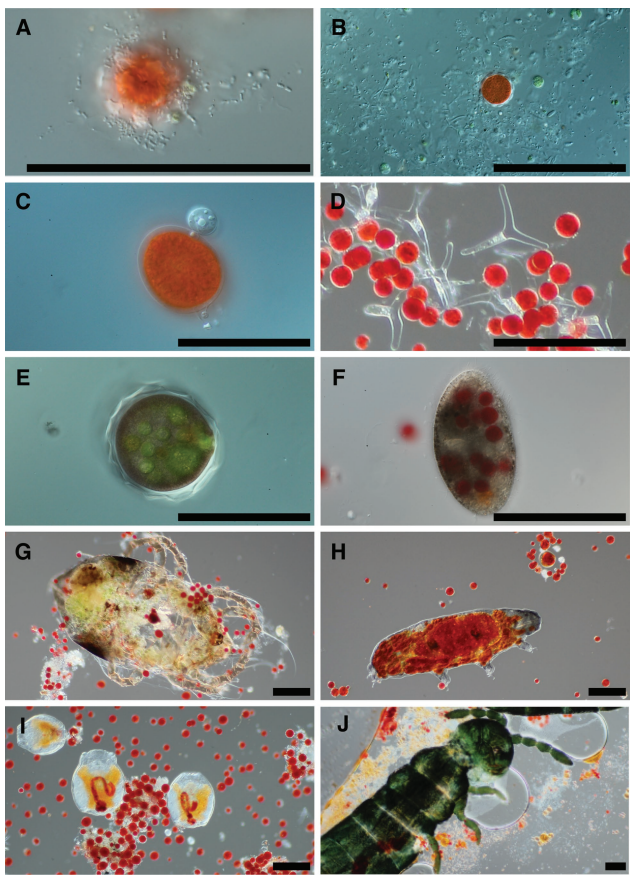

FIGURE 1 | Representative photomicrographs of snow algae bloom samples. Bacteria are seen in the foreground of panel **(A)** with a red pigmented algae cell in the background, and various cells putatively designated as fungi due to size are in panel **(B)**. Panel **(C)** is of two chytrid cells attached to the outside of an algae cell. Panel **(D)** shows a fungal morphological species called *Selenotila nivalis*. Panel **(E)** shows an unidentified micro-eukaryote and panel **(F)** shows a ciliate. Panels **(G–J)** are representative of animals seen in samples, and in order are a mite, tardigrade, rotifers, and a springtail (*Collembola*). All scale bars are 100 μm.

Metabarcoding Results

To identify the organisms observed by microscopy and to assess the species richness of the microbial groups, we examined the metabarcoding data. Our analysis pipeline outputs a total of 3,742,232 16S rDNA reads with an average of 53,446 (*SD* ± 15,315) reads per sample and 2,392,864 18S rDNA reads with an average of 34,184 (*SD* ± 12,400) reads per sample. Because our data set includes two different sequencing runs, we chose two samples (GAR18.01 and SEY18.74) to compare sequencing run one (MiSeq V2 kit and lysis method 1) with sequencing run two (MiSeq V3 kit and lysis method 2). There were no significant differences in the 16S or 18S rDNA ASV profiles between the batch control samples (Chi-square test $p = 1$; visualized *via* heatmap **Supplementary Figure 1**). To test for systematic bias, we examined the overall community compositions as a function of sequencing run and found no significant effects (dbRDA: 16S rDNA $R^2 = 0.02$, 18S rDNA $R^2 = 0.04$, analyzed *via* NMDS as **Supplementary Figure 2**). The lack of run bias is further documented in **Figure 2**, which shows high level taxa for all samples, so we chose to analyze the data from the two sequencing runs together.

Samples were generally dominated by three bacterial phyla: *Proteobacteria*, *Bacteroidetes*, and *Actinobacteria* (**Figure 2**). The 18S sequencing reads from each sample were assigned primarily to *Cercozoa*, *Chlorophyta*, *Ciliophora*, and Fungi (**Figure 2**). Sequences belonging to methanogens were the only archaea detected and were excluded from analysis due to low read number and infrequent occurrence (<0.04% relative abundance in only four samples). In total, we detected 3,309 bacterial, 380 fungal, 656 protist/animalia, and 173 algal ASVs. When ASVs were grouped into OTUs to estimate species richness, there were 2,739 bacterial, 315 fungal, 540 protist/animalia, and 131 algal OTUs, with on average more ASVs per sample than OTUs (**Figure 3**).

Algal Community Composition

Our sampling scheme encompassed a variety of snow conditions across a wide range of elevations on several mountains. We detected 145 ASVs from *Chlorophyta* (*Archaeplastida*), and 28 from *Ochrophyta* (Stramenopiles). In addition to greater sequence diversity, the *Chlorophyta* were more abundant with 114x more total sequencing reads than *Ochrophyta*. The *Chlorophyta* were comprised mostly of *Chlorophyceae*, with some *Trebouxiophyceae* and *Mamiellophyceae*. All snow samples were dominated by either *Chloromonas* spp. or *Sanguina* spp.; *Chloromonas*-dominated sites were the most common (**Figure 4**). The families of *Ochorophyta* detected included *Chrysophyceae*, *Chrysocapsales*, *Mallomonadaceae*, and *Xanthophyceae*. For a higher resolution analysis of the algal communities within our study region see Engstrom et al. (2020).

Bacterial Communities

Although we found similar phlyum-level bacterial diversity at all sites (see **Figure 2**), we wanted to examine the community structure at ASV and OTU level to test for specific co-occurrence, particularly of bacteria and fungi with algae. We used both

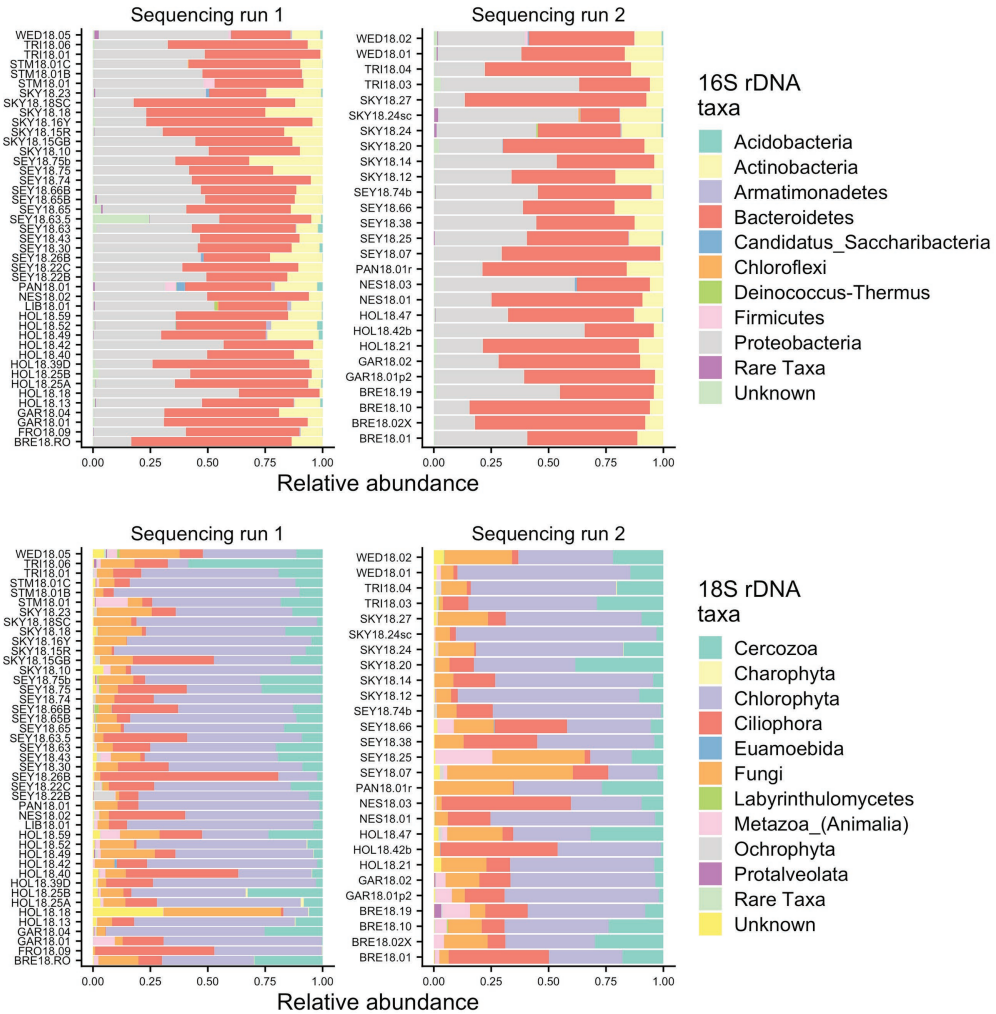

FIGURE 2 | Relative abundance bar plots of all samples from the 16S and 18S rDNA metabarcoding analyses from both sequencing runs. The plots are made based on the taxonomic assignments of the ASVs, and include all ASVs that were above 1% relative abundance in at least one sample. The group "Rare Taxa" includes all ASVs that were below 1% relative abundance and "Unknown" are all ASVs that were unassigned.

unconstrained (NMDS) and constrained (dbRDA) ordinations to test variation in the community structure. Both NMDS and dbRDA found that the bacterial community structure did not correspond to that of the algae community (dbRDA constrained by dominant algal genus; ASVs R^2 = 0.07: OTUs R^2 = 0.07; NMDS **Supplementary Figure 3**). We constructed correlation matrices of bacterial 16S rDNA ASVs/OTUs against algae 18S rDNA ASVs/OTUs and did not find any significant correlates (all Kendall's tau rank correlations; $\tau < 0.5$). We then looked for correlations between bacterial genera, and the two dominant algal genera, *Chloromonas* and *Sanguina*, and again found no correlations (<0.5 for all). Next, we examined the bacterial-algal genera reported by Krug et al. (2020) to be positively correlated in snow algal blooms found in the Austrian Alps and found no significant relationships (**Figure 5A**). The strongest correlations for *Sanguina* and *Chloromonas* were with *Hymenobacter* (τ = 0.45) and *Aquaspirillum* (τ = 0.43), respectively, but visualized as scatterplots, these correlations were largely driven by a handful of sites and were not representative of all samples (**Figures 5B,C**). The bacterial community showed little variation between samples with different snow colors, as revealed by a dbRDA constrained by snow color (ASVs R^2 = 0.05; NMDS **Supplementary Figure 4**), and bacterial OTUs showed similarly low variation (OTUs R^2 = 0.07; NMDS **Supplementary Figure 4**). Therefore, according to the dbRDAs, large amounts of the variation in the community composition of ASVs or OTUs could be explained neither by dominant algae taxa nor by snow color. Nor did we find any large shifts in bacterial communities based on changes in elevation using either an NMDS analysis or a dbRDA analysis with elevation as a constraining variable (R^2 = 0.11 for ASVs, and R^2 = 0.11 for OTUs, **Supplementary Figure 5**). There were no regional patterns based on mountain when analyzed by NMDS (**Supplementary Figure 6**).

Across all samples, 10 bacterial families (out of 120 total families) were prevalent, occurring in at least 75% of samples

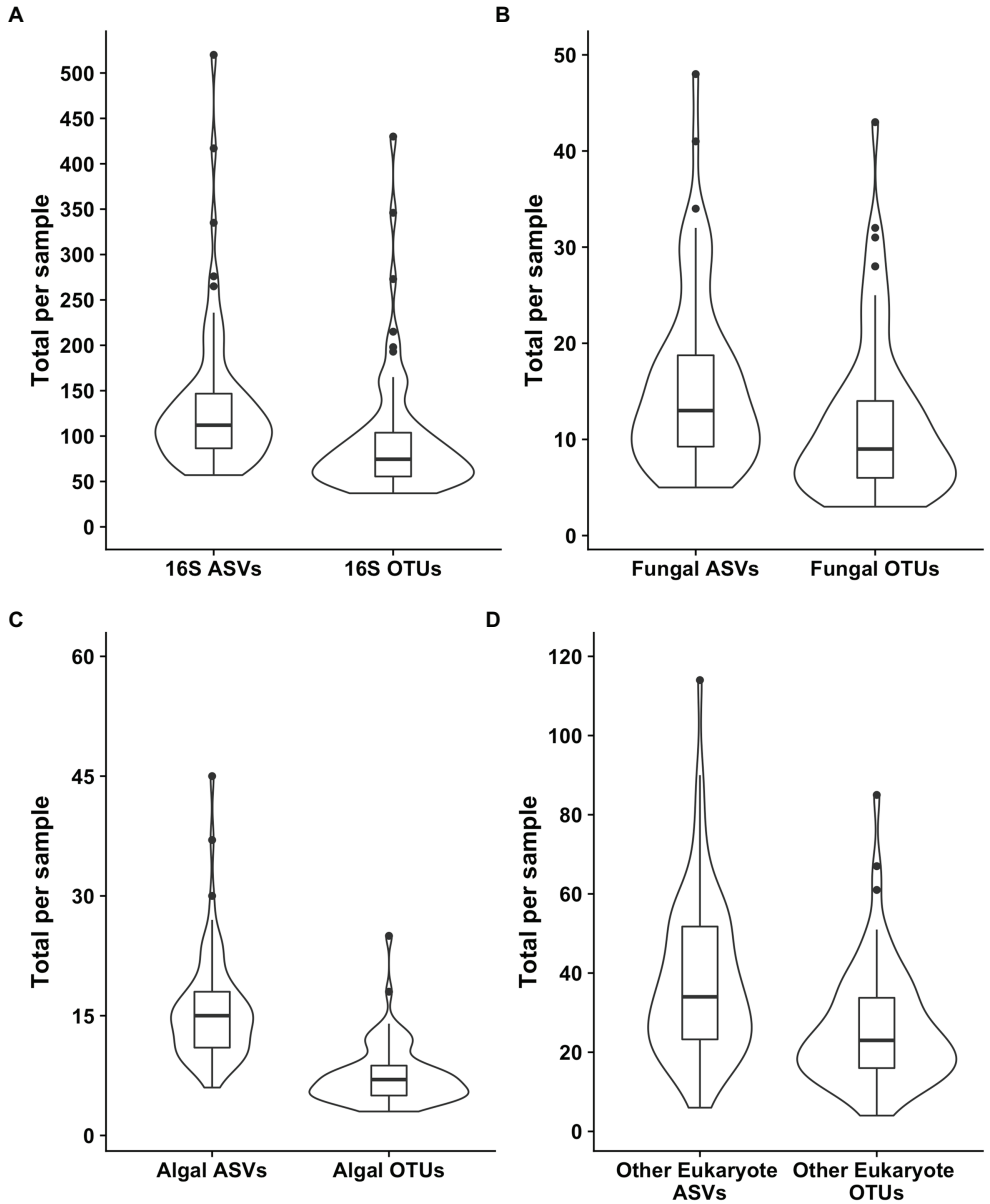

FIGURE 3 | Violin plots of the richness values for both ASVS and those ASVs clustered into operational taxonomic units (OTUs). Plot **(A)** shows the bacterial 16S values, **(B)** the fungal 18S, **(C)** the algal 18S, and **(D)** the "other eukaryotes", which encompass protists and metazoans.

with six being found in all samples (**Figure 6** and **Table 1**). While most OTUs were only found in a few samples, seven OTUs were widespread, occurring in at least 61 out of our 68 samples (≥90%; **Figure 7**; **Supplementary Figure 7**). The seven widespread OTUs did not comprise the top seven most abundant OTUs on average (**Figure 7A**) and, therefore, were not necessarily representative of the dominant community in any one sample. Several predominant families were not represented by any of the widespread OTUs. These include *Chitonphagacea*, *Comamonadaceae*, *Cytophagaceae*, *Neisseriaceae*, and *Pseudomonadaceae* (**Figures 6, 7** and **Table 1**).

Fungi and Protists

Out of 74 detected fungal families, the most common in our samples included *Camptobasidiaceae*, *Cordycipitaceae*, *Gromochytriaceae*, *Kriegeriaceae*, and *Rhizophydiaceae* (**Figure 8**). Fungal OTU 1 (assigned to *Camptobasidium*) was found in all samples but one (NES18.03). Fungal OTU 1 comprises an average of 29% (*SE* ± 1.9%) of detected fungal sequences. We commonly saw *Chytridiomycota*, which were morphologically identified as translucent spheroids attached to algal cells (**Figure 1C**). In total, there were 22 *Chytridiomycota* OTUs belonging to the groups *Gromochytriaceae* (found in 87% of samples) and *Rhizophydiales*

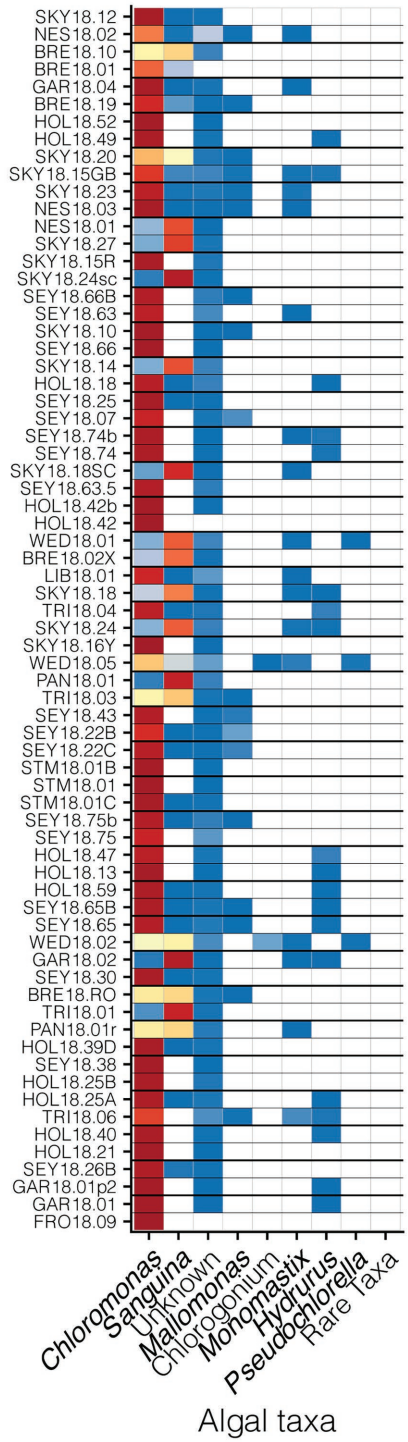

FIGURE 4 | Relative abundances of algal genera across sites presented in a heat map organized by hierarchical clustering analysis. The group "Rare Taxa" includes all ASVs that were below 1% relative abundance and "Unknown" are all ASVs that were unassigned.

(found in 69% of samples). Although no single *Chytridiomycota* OTU was widespread, as a group they were detected in most samples (**Table 2**).

To examine fungal co-occurrence with algae, we created a correlation matrix of the relative abundances of the fungal families against *Chloromonas* and *Sanguina*. We found no significant correlations (τ < 0.5). The fungal community composition showed little variation that corresponded to changes in elevation (OTU R^2 = 0.04, ASV R^2 = 0.04; NMDS **Supplementary Figure 8**), dominant algae genus (OTU R^2 = 0.03, ASV R^2 = 0.03; NMDS **Supplementary Figure 9**), or snow color (OTU R^2 = 0.03, ASV R^2 = 0.03; NMDS **Supplementary Figure 10**).

Other taxa detected by 18S sequencing included cercozoans, ciliates, and metazoans (**Figure 9**). Two cercozoan OTUs were widespread (**Table 2**). The remaining ASVs were primarily attributed to *Cercozoa* (290 additional OTUs) and *Ciliophora* (115 OTUs), with each group represented in every sample. Common taxa of Animalia included Rotifers (of the classes *Bdelloidea* and *Monogononta*), *Collembola* (springtails), and *Acari* spp. (mites), which taken together were detected in 72% of our samples (**Table 2**). Interestingly, *Cercozoa* and *Ciliophora* tended to be dominant at different sites (**Figure 9**). When we examined the genera driving this pattern, we found a negative correlation between the cercozoan *Heteromita* and the ciliate *Stokesia* (τ = −0.48). The protist/metazoan community showed little variation across elevation (dbRDA for OTU R^2 = 0.02, OTU R^2 = 0.03; NMDS **Supplementary Figure 11**), dominant algal genus (dbRDA for OTU R^2 = 0.03, OTU R^2 = 0.03; NMDS **Supplementary Figure 12**), or sample snow color (dbRDA for OTU R^2 = 0.01, OTU R^2 = 0.02; NMDS **Supplementary Figure 13**).

DISCUSSION

We found an abundance of bacteria, fungi, protists, and metazoans thriving alongside algae in the mountains of southwestern British Columbia. Key bacterial families and a few specific OTUs were predominant across all samples. This was a robust pattern observed across a total of 68 samples from 55 unique blooms that encompassed red, green, and orange snow. We failed to observe the co-occurrence of any specific bacteria-alga combinations. Our sequencing data provide insight into the taxa involved at each node of a hypothetical snow algae food web (**Supplementary Figure 14**) and create a framework for future work exploring trophic connections.

Bacteria are often noted as vital components near the base of food webs (Fenchel, 2008), turning nutrients and various carbon sources into biomass and making them bioavailable for higher trophic levels. Even though algae are likely the dominant source of fixed carbon in their microbiome, there may be other sources of bioavailable carbon that may enter the food web *via* bacteria (and possibly fungal decomposers). Black carbon particulate deposited from the atmosphere onto snow surfaces can spur microbial growth (Malits et al., 2015; Weinbauer et al., 2017). In addition, decomposition of detritus has been noted as an important carbon source in aquatic food webs (Matveev and Robson, 2014) and likely plays a role in the

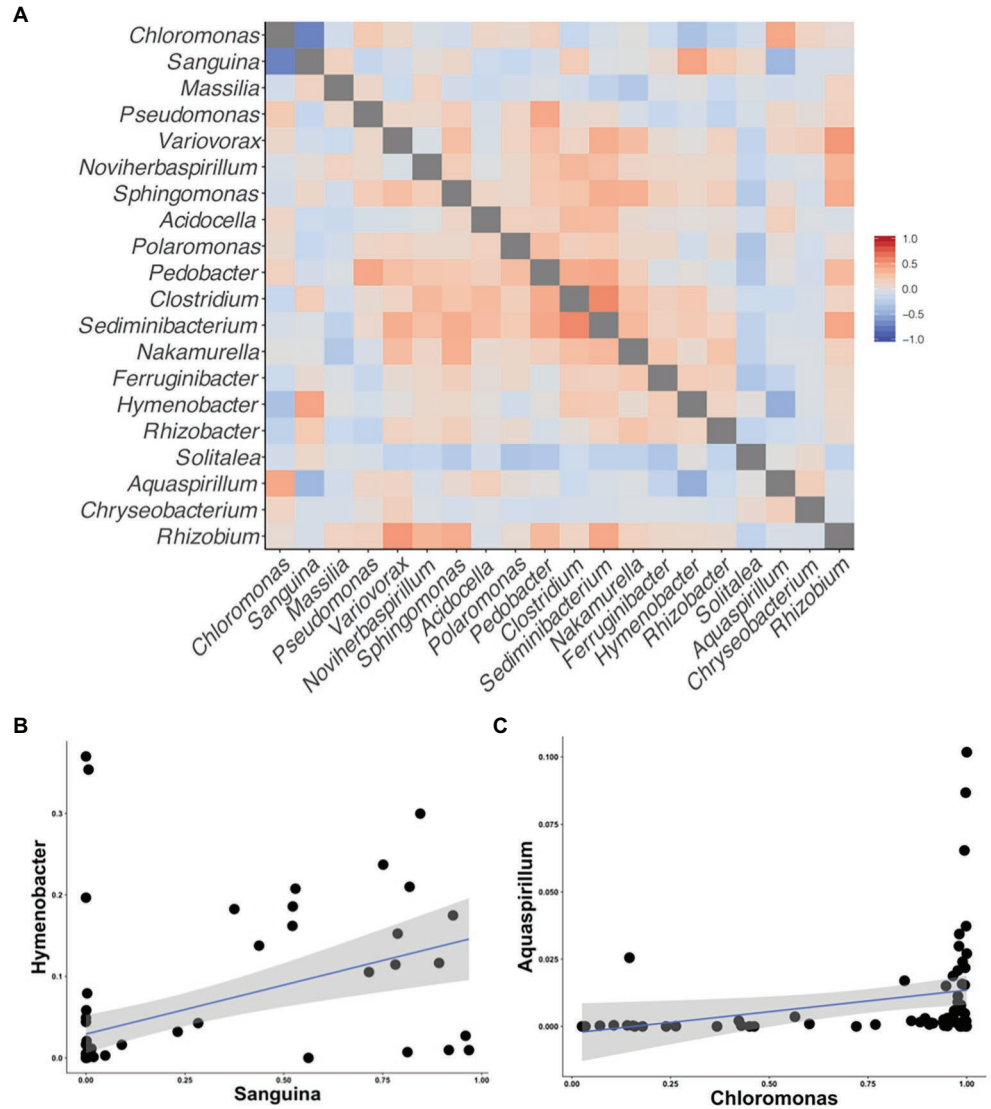

FIGURE 5 | Correlation matrices of the taxa reported by Krug et al. (2020) to be correlated with snow algal taxa in the Alps. All correlations were calculated using Kendall's tau rank correlations (τ). **(A)** A heatmap of the correlations between taxa on the axis. **(B)** A scatterplot between *Sanguina* and the highest correlated bacterial genus ($\tau = 0.45$) from the heatmap in **(A)**. **(C)** A scatterplot between *Chloromonas* and highest correlated bacterial genus ($\tau = 0.43$) from the heatmap in **(A)**.

cycling of carbon within the snow algae microbiome. At present, the relative contribution of each carbon source to the snow algae microbiome is unknown.

Seymour et al. (2017) argue that algal-bacterial mutualistic relationships may be more prevalent than antagonistic ones, as these organisms work together to survive in a wide range of environments. The bacteria that were widespread in our study, all of which had populations larger than the vast majority of detected bacteria, may include mutualist partners of snow algae. Previous work reported many of the same bacterial taxa (**Figures 6, 7B** and **Table 1**) and widely distributed OTUs (**Figure 7B**) from both polar and alpine snow algae blooms, including *Sphingobacteriaceae*, *Chitonphagaceae*, and *Cytophagia* (Brown et al., 2015; Lutz et al., 2016; Hamilton and Havig, 2017; Terashima et al., 2017; Davey et al., 2019). Various *Proteobacteria* are also often reported, including *Oxalobacteraceae* (e.g., *Glaciimonas*), *Comamonadaceae* (e.g., *Polaromonas*), and *Pseudomonas* (Lutz et al., 2016; Hamilton and Havig, 2017; Terashima et al., 2017; Davey et al., 2019). The most abundant OTU in our study was assigned to the genus *Solitalea* (**Figure 7**). Previously, a comparative analysis of 18 *Sphingobacteriaceae* strains revealed diversity in genes related to cold adaptations, osmotic regulation, and secondary metabolisms (N and C species processing; Shen et al., 2017). As *Sphingobacteriaceae* are a prolific group in terms of abundance and distribution, they likely play an important role in biogeochemical cycling within the snow algae microbiome. Genomic analysis of these

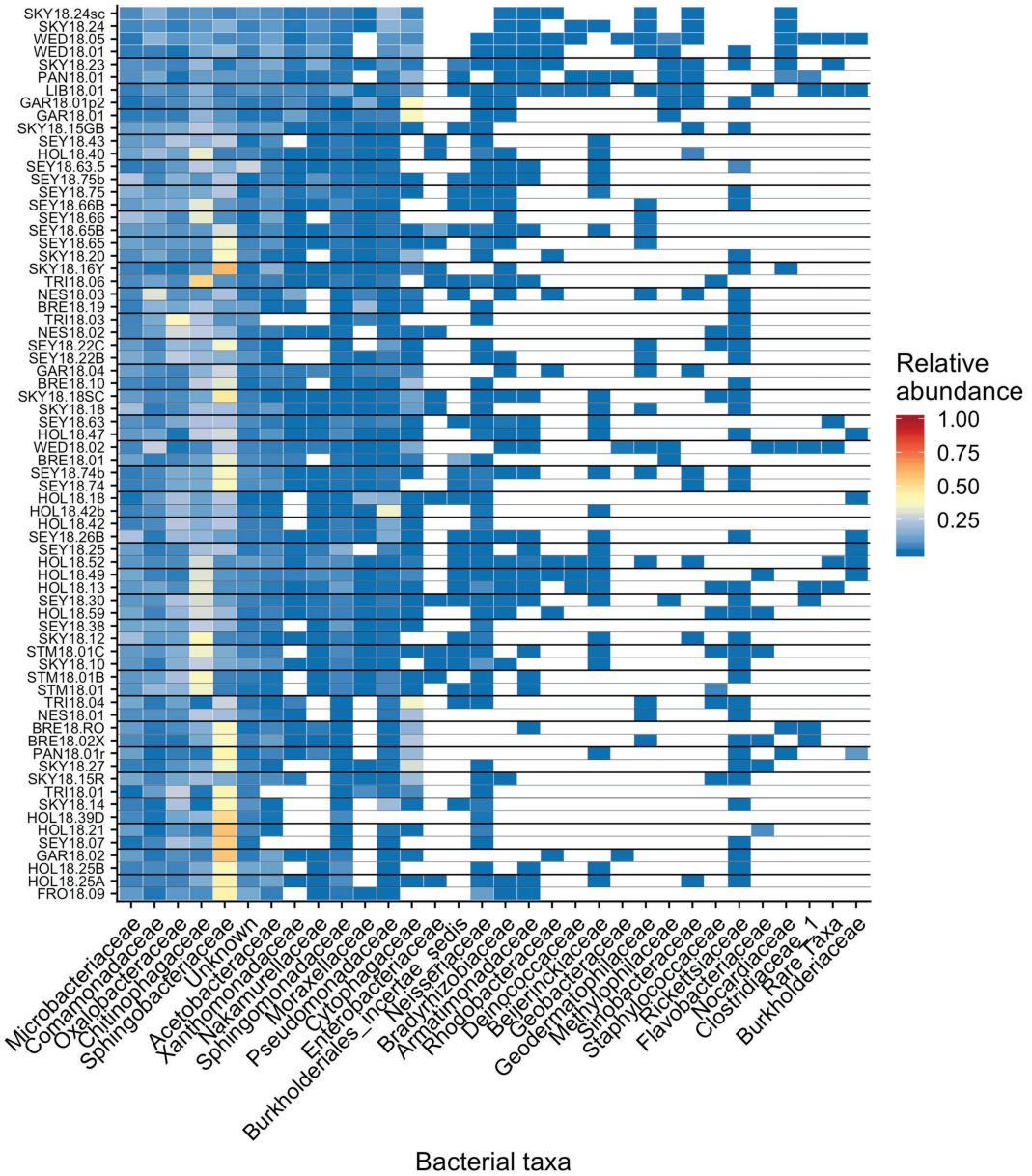

FIGURE 6 | Relative abundance of the most prevalent bacterial families across sites, presented as a heat map organized by hierarchical clustering analysis. The group "Rare Taxa" includes all ASVs that were below 1% relative abundance and "Unknown" are all ASVs that were unassigned.

TABLE 1 | Bacterial families found in >75% of samples.

Family	% occurrence
Acetobacteraceae	96
Chitinophagaceae	100
Comamonadaceae	100
Cytophagaceae	79
Microbacteriaceae	100
Neisseriaceae	79
Oxalobacteraceae	100
Pseudomonadaceae	99
Sphingobacteriaceae	100
Sphingomonadaceae	100

snow-borne bacteria will be necessary to differentiate their metabolic niches within the microbiome.

The only bacterial OTU found in all samples belonged to the genus *Novosphingobium*, which contains species capable of degrading various aromatic compounds (Wang et al., 2018). Interestingly, while the family *Sphingomonadaceae* (although not *Novosphingobium* specifically) has been reported in the Alps by Krug et al. (2020), it was not reported by Terashima et al. (2017) on Mount Asahi in Japan or by Hamilton and Havig (2017) on Mountains in the Pacific Northwest of the USA. Neither *Novosphingobium* nor *Sphingomonadaceae* were reported in studies from the Arctic (Lutz et al., 2016) or Antarctic

A

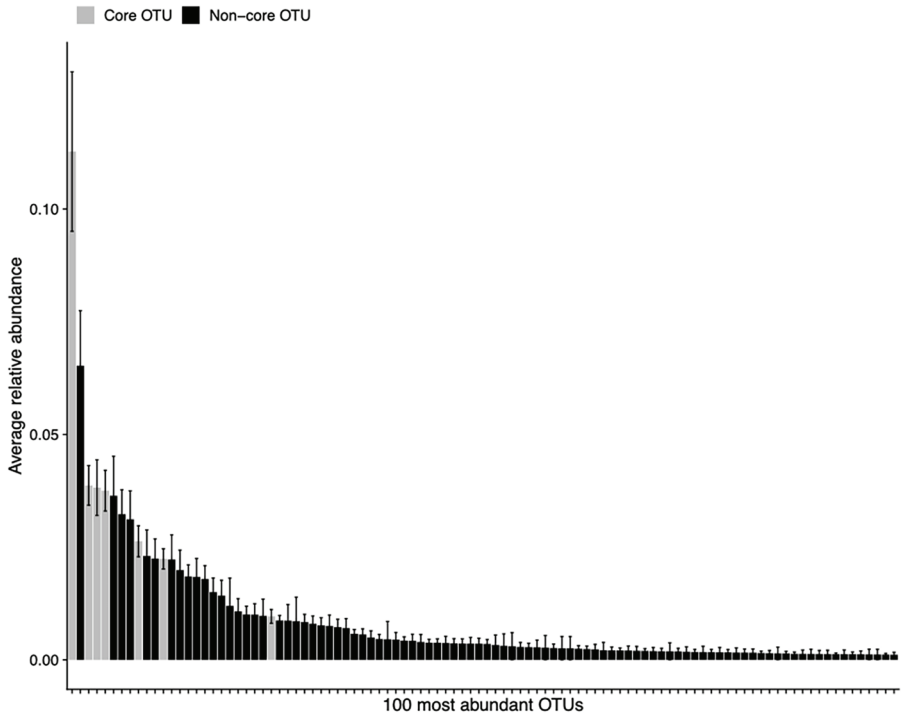

B

OTU	Family	Genus	% occurrence	# of ASVs	Average relative abundance (%)	Range of relative abundance (%)
1	Sphingobacteriaceae	*Solitalea*	93	3	11	0 - 55
3	Acetobacteraceae	Unknown	94	4	3.9	0 - 16
4	Oxalobacteraceae	*Herminiimonas*	93	6	3.8	0 - 31
8	Microbacteriaceae	Unknown	91	8	3.7	0 - 20
13	Sphingomonadaceae	*Novosphingobium*	100	5	2.6	0.2 - 16
10	Microbacteriaceae	Unknown	91	3	2.2	0 - 8
30	Oxalobacteraceae	Unknown	93	9	1	0 - 7

FIGURE 7 | The top abundant bacterial OTUs in our study including seven that are widespread. Panel **(A)** shows the average relative abundance across all 68 samples for the top 100 most abundant OTUs, error bars are standard error. Panel **(B)** shows the taxonomic assignments for each widespread OTU (in >90% of samples). These are shown as gray bars in panel **(A)**. Percentage of sites indicates the occurrence of each OTU; # of ASVs refers to the total number of ASVs constituting each OTU. The OTUs in **(B)** are ordered as they appear left to right in **(A)**.

(Davey et al., 2019) regions. But using transects across Fennoscandia and Colorado, USA, Brown and Jumpponen (2019) found that *Novosphingobium* was widely distributed in white snow on both continents. While regional variation could account for the absence of *Novosphingobium* at some sites, we propose it may be widely distributed, but because it is low abundance (**Figure 7**), it may go unreported in studies focused on between-site differences.

In a study at two sites in the Austrian Alps, Krug et al. (2020) reported correlations between *Chloromonas* and the bacterial genera *Ferruginibacter* and *Hymenobacter* and *Chlamydomonas* (*Sanguina* in our study) with *Aquaspirillum*, *Chryseobacterium*, and *Rhizobium*. We did not find these associations in our 68 samples snow algae samples, from 55 sites (**Figure 5A**). These results suggest that the co-occurrence patterns reported by Krug et al. (2020) are unlikely to be indicative of taxa or species-specific mutualisms. The general lack of specific algal-bacteria associations in our study suggests a paucity of obligate mutualisms. However, based on the importance of bacterial-algal mutualisms in other aquatic systems (Seymour et al., 2017), it is possible that non-specific mutualisms are at work in snow algae microbiomes.

It has been hypothesized that fungi play an important role in algae blooms because they are enriched relative to adjacent white snow (Brown et al., 2015). Many snow-borne fungi found in blooms are presumptive yeasts (Brown et al., 2015; Davey et al., 2019). A widespread OTU in our study belongs to the genus *Camptobasidium*, which is a member of *Kriegeriales*, an order with known yeast forms. The type

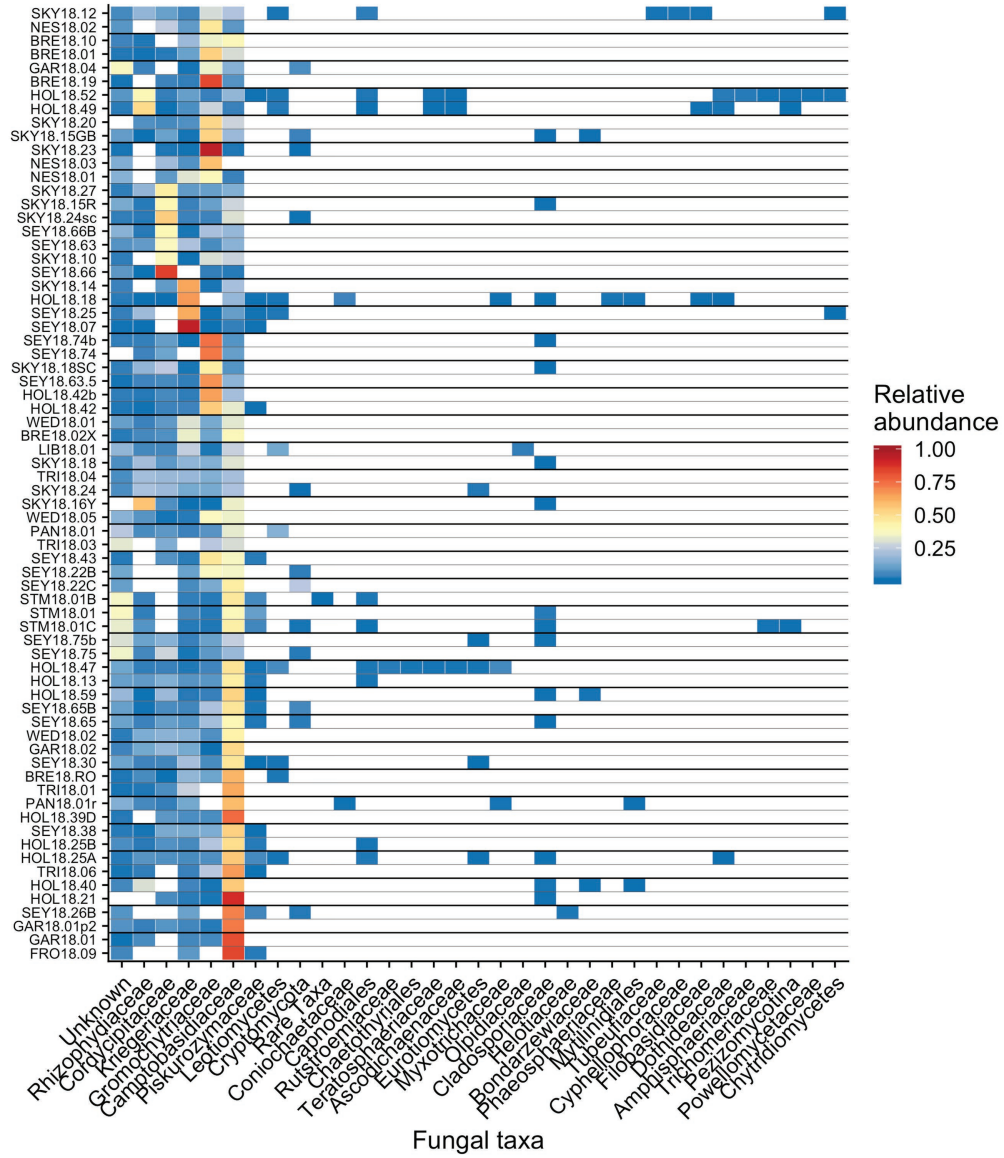

FIGURE 8 | Relative abundance of the most prevalent bacterial families across sites shown as a heatmap organized by hierarchical clustering analysis. The group "Rare Taxa" includes all ASVs that were below 1% relative abundance and "Unknown" are all ASVs that were unassigned.

TABLE 2 | Eukaryotic taxa found in snow algae blooms *via* 18S rDNA sequencing.

OTU#	Phyla or Family	Genus	% of sites	# of ASVs
1	Camptobasidiaceae	*Camptobasidium*	97	5
-	Chytridiomycota	-	94	78
3	Glissomonadida	*Heteromita*	97	15
7	Glissomonadida	Unknown	91	7
-	Rotifera	-	63	23
-	Acari	-	25	21
-	Collembola	-	26	16

Shown are the widespread fungi, protists, and multicellular eukaryotes (Animalia). Taxonomic assignments were based on the most abundant ASVs within an operational taxonomic unit (OTU).

of symbiotic relationships, if any, these fungi have within the microbiome is unknown, but they likely metabolize carbon fixed by algae. Similar fungal taxa can also be found in other cryosphere environments, such as on ice sheets in Greenland, where Perini et al. (2019) found the family *Microbotryomycetes* in super glacial water, sediment, and water from cryoconite

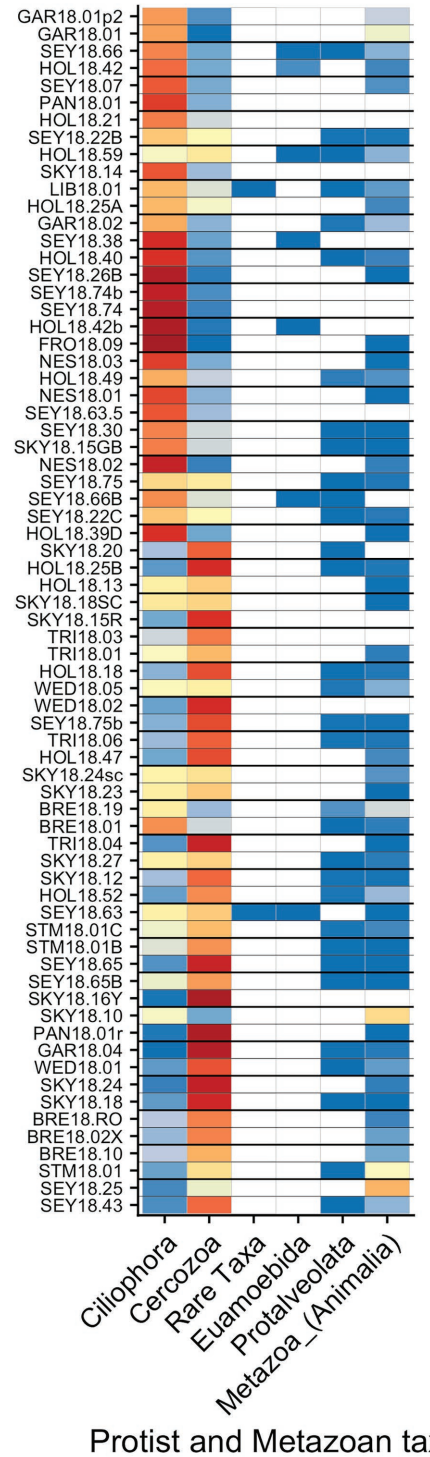

FIGURE 9 | Relative abundance of the remaining eukaryotic groups across sites presented a heatmap organized by hierarchical clustering analysis. The group "Rare Taxa" includes all ASVs that were below 1% relative abundance and "Unknown" are all ASVs that were unassigned.

holes. *Microbotryomycetes* was widespread and abundant in our study, primarily represented by *Camptobasidiaceae* and *Kriegeriaceae* (**Figure 8**).

We observed chytrid fungi attached to snow algae (**Figure 1**), reminiscent of the chytrid *Gromochytrium mamkaevae*, a known parasite of freshwater algae (**Figure 1**; Karpov et al., 2014). Gromochytriaceae was prevalent in our 18S metabarcoding data (**Figure 8**) and is known to have over 225 aquatic species that are primarily algae parasites within the genus *Rhizophydium* alone (Karpov et al., 2014). Our observations are consistent with those made in alpine snows in Colorado, where chytrids have been noted to attach to algal cells (Stein and Amundsen, 1967). Therefore, it is likely that *Chytridiomycota* play a role in the carbon cycling within a bloom by parasitizing algae and are part of the snow food web (Naff et al., 2013).

Many of the fungal and bacterial taxa found in our snow algae samples have also been detected in white snow (Brown and Jumpponen, 2019), as well as in other alpine and polar snow algae blooms (Lutz et al., 2016; Hamilton and Havig, 2017; Terashima et al., 2017). Particularly, OTUs from the families *Sphingobacteriaceae*, *Pseudomonadaceae*, *Chitinophagaceae*, and *Oxalobacteraceae* were dominant in white snow samples from Colorado and Fennoscandia, and found in polar snow packs within snow algae blooms (Lutz et al., 2016; Brown and Jumpponen, 2019; Davey et al., 2019). The overlap in bacterial taxa between these diverse and globally distributed studies indicates the global distribution of these taxa in both white snow and red snow. Brown and Jumpponen (2019) found several fungal genera to be widespread (i.e., *Cryptococcus*, *Kabatiella*, and *Sydowia*) that were not in our study, indicating possible larger scale geographical variation not captured by our study.

Predation plays an important role in the structure of food webs (Fox, 2007), but predator-prey relationships have not yet been explored in snow algae microbiomes. Taxa of protists that could act as algae predators have been noted in blooms before, such as euglenids, nematodes, and ciliates (Bidigare et al., 1993; Ling and Seppelt, 1993; Duval et al., 1999; Davey et al., 2019), but until now, there has been no photographic documentation of protists preying on snow algae cells (**Figure 1**).

As anticipated based on our microscopy, sequencing revealed an abundance of protist sequences present in all samples. Several OTUs were assigned as *Heteromita* spp. with one found in all but one sample: *Heteromita globosa* is closely related to our widely distributed protist OTU 3, which is a bacterivorous testate amoeba that has been isolated from both temperate and cold environments. A second protist OTU that was widely distributed in our samples was a glissomonad, of undetermined genus. Because our collection protocol was not optimized for the collection of mobile metazoans, which are larger than algae and therefore occur at lower densities, our data set may underestimate their true distributions.

CONCLUSION

Over the course of a single season and across 12 mountains near Vancouver, B.C. We documented the diversity of microbial communities within snow algae microbiomes. We found that

variation in the bacterial and fungal communities did not reflect variation in the algal communities, nor did they change with elevation. We found similar bacterial taxa (phyla and families) as previously found in other alpine and in polar snow algae blooms. Importantly, we found that certain families and some OTUs were prevalent across an entire region. Unicellular predators, predominantly a testate amoeba and another unidentified cercozoan were found in all samples. Other widespread taxa included *Chytidiomycota*, *Rotifera*, *Acari* (mites), and *Collembola* (springtails). We found no evidence to support specific associations between algae and bacteria.

DATA AVAILABILITY STATEMENT

The raw sequence data presented in this study are publicly accessible in the European Nucleotide Archive under accession number PRJEB34539.

AUTHOR CONTRIBUTIONS

KY, CE, and LQ all contributed to the design of this project and collection of field samples. KY and CE did the lab work, and KY analyzed the data and wrote the manuscript with input from all authors. All authors contributed to the article and approved the submitted version.

FUNDING

This project was funded with a Sector Innovation Grant from Genome BC (SIP016) and a NSERC Discovery Grant, both awarded to LQ.

ACKNOWLEDGMENTS

We acknowledge Tyler T. Kelly for assistance in using Adobe Illustrator to design figures. We also thank Lea Tooman and Kevin Bushell from the Morin Lab at Simon Fraser University for assistance with running the Illumina MiSeq. Undergraduate student, Sadie Pater, supported protocol development for this study.

SUPPLEMENTARY MATERIAL

The Supplementary Material for this article can be found online at: https://www.frontiersin.org/articles/10.3389/fmicb.2020.01721/full#supplementary-material.

REFERENCES

Altschul, S. F., Gish, W., Miller, W., Myers, E. W., and Lipman, D. J. (1990). Basic local alignment search tool. *J. Mol. Biol.* 215, 403–410. doi: 10.1016/S0022-2836(05)80360-2

Bidigare, R. R., Onderusek, M. E., Kennicutt, M. C. II., Iturriaga, R., Harvey, H. R., Hoham, R. W., et al. (1993). Evidence for a photoproptective function for secondary carotenoids of snow algae. *J. Phycol.* 34, 427–434.

Bormann, K. J., Brown, R. D., Derksen, C., and Painter, T. H. (2018). Estimating snow-cover trends from space. *Nat. Clim. Chang.* 8, 924–928. doi: 10.1038/s41558-018-0318-3

Brown, S. P., and Jumpponen, A. (2019). Microbial ecology of snow reveals taxa-specific biogeographical structure. *Microb. Ecol.* 77, 946–958. doi: 10.1007/s00248-019-01357-z

Brown, S. P., Olson, B. J. S. C., and Jumpponen, A. (2015). Fungi and algae co-occur in snow: an issue of shared habitat or algal facilitation of heterotrophs? *Arct. Antarct. Alp. Res.* 47, 729–749. doi: 10.1657/aaar0014-071

Brown, S. P., Ungerer, M. C., and Jumpponen, A. (2016). A community of clones: snow algae are diverse communities of spatially structured clones. *Int. J. Plant Sci.* 177, 432–439. doi: 10.1086/686019

Callahan, B. J., McMurdie, P. J., Rosen, M. J., Han, A. W., Johnson, A. J. A., and Holmes, S. P. (2016). DADA2: high-resolution sample inference from illumina amplicon data. *Nat. Methods* 13, 581–583. doi: 10.1038/nmeth.3869

Clark, K., Karsch-Mizrachi, I., Lipman, D. J., Ostell, J., and Sayers, E. W. (2016). GenBank. *Nucleic Acids Res.* 44, D67–D72. doi: 10.1093/nar/gkv1276

Cubero, O. F., Crespo, A., Fatehi, J., and Bridge, P. D. (1999). Plant systematics and evolution DNA extraction and PCR amplification method suitable for fresh, herbarium-stored, lichenized, and other fungi. *Plant Syst. Evol.* 216, 243–249. doi: 10.1007/BF01084401

Davey, M. P., Norman, L., Sterk, P., Huete-Ortega, M., Bunbury, F., Loh, B. K. W., et al. (2019). Snow algae communities in Antarctica: metabolic and taxonomic composition. *New Phytol.* 222, 1242–1255. doi: 10.1111/nph.15701

Duval, B., Duval, E., and Hoham, R. W. (1999). Snow algae of the sierra Nevada, Spain, and high atlas mountains of Morocco. *Int. Microbiol.* 2, 39–42.

Engstrom, C. B., Yakimovich, K. M., and Quarmby, L. M. (2020). Variation in snow algae blooms in the coast mountains of British Columbia. *Front. Microbiol.* 11:569. doi: 10.3389/fmicb.2020.00569

Fenchel, T. (2008). The microbial loop—25 years later. *J. Exp. Mar. Biol. Ecol.* 366, 99–103. doi: 10.1016/j.jembe.2008.07.013

Fox, J. W. (2007). The dynamics of top-down and bottom-up effects in food webs of varying prey diversity, composition, and productivity. *Oikos* 116, 189–200. doi: 10.1111/j.0030-1299.2007.15280.x

Galili, T., O'Callaghan, A., Sidi, J., and Sievert, C. (2017). Heatmaply: an R package for creating interactive cluster heatmaps for online publishing. *Bioinformatics* 34, 1600–1602. doi: 10.1093/bioinformatics/btx657

Ganey, G. Q., Loso, M. G., Burgess, A. B., and Dial, R. J. (2017). The role of microbes in snowmelt and radiative forcing on an Alaskan icefield. *Nat. Geosci.* 10, 754–759. doi: 10.1038/ngeo3027

Hamilton, T. L., and Havig, J. (2017). Primary productivity of snow algae communities on stratovolcanoes of the Pacific Northwest. *Geobiology* 15, 280–295. doi: 10.1111/gbi.12219

Harrold, Z. R., Hausrath, E. M., Garcia, A. H., Murray, A. E., Tschauner, O., Raymond, J., et al. (2018). Bioavailability of mineral-bound iron to a snow algae-bacteria co-culture and implications for albedo-altering snow algae blooms. *Appl. Environ. Microbiol.* 84, e02322–e023217. doi: 10.1128/AEM.02322-17

Hisakawa, N., Quistad, S. D., Hester, E. R., Martynova, D., Maughan, H., Sala, E., et al. (2015). Metagenomic and satellite analyses of red snow in the Russian Arctic. *PeerJ.* 3:e1491. doi: 10.7717/peerj.1491

Hoham, R. W., and Remias, D. (2020). Snow and glacial algae: a review. *J. Phycol.* 56, 264–282. doi: 10.1111/jpy.12952

Hom, E. F. Y., and Murray, A. W. (2014). Niche engineering demonstrates a latent capacity for fungal-algal mutualism. *Science* 345, 94–98. doi: 10.1126/science.1253320

Karpov, S. A., Kobseva, A. A., Mamkaeva, M. A., Mamkaeva, K. A., Mikhailov, K. V., Mirzaeva, G. S., et al. (2014). Gromochytrium mamkaevae gen. & sp. nov. and two new orders: Gromochytriales and Mesochytriales (*Chytridiomycetes*). *Persoonia Mol. Phylogeny Evol. Fungi* 32, 115–126. doi: 10.3767/003158514X680234

Krug, L., Erlacher, A., Markut, K., Berg, G., and Cernava, T. (2020). The microbiome of alpine snow algae shows a specific inter-kingdom connectivity

and algae-bacteria interactions with supportive capacities. *ISME J.* doi: 10.1038/s41396-020-0677-4 [Epub ahead of print]

Leya, T. (2013). "Snow algae: adaptation strategies to survive on snow and ice" in *Polyextremophiles: Life under multiple forms of stress*. eds. J. Seckbach, A. Oren and H. Stan-lotter (New York, USA: Springer), 401–425.

Light, J. J., and Belcher, J. H. (1968). A snow microflora in the Cairngorm Mountains, Scotland. *Br. Phycol. Bull.* 3, 471–473. doi: 10.1080/00071616800650061

Ling, H. U., and Seppelt, R. D. (1993). Snow algae of the windmill islands continental Antarctica chloromonas rubroleosa volvocales chlorophyta an alga of red snow. *Eur. J. Phycol.* 28, 77–84. doi: 10.1080/09670269300650131

Lutz, S., Anesio, A. M., Raiswell, R., Edwards, A., Newton, R. J., Gill, F., et al. (2016). The biogeography of red snow microbiomes and their role in melting arctic glaciers. *Nat. Commun.* 7, 1–9. doi: 10.1038/ncomms11968

Maccario, L., Carpenter, S. D., Deming, J. W., Vogel, T. M., and Larose, C. (2019). Sources and selection of snow-specific microbial communities in a Greenlandic Sea ice snow cover. *Sci. Rep.* 9, 1–4. doi: 10.1038/s41598-019-38744-y

Mahé, F., Rognes, T., Quince, C., de Vargas, C., and Dunthorn, M. (2014). Swarm: robust and fast clustering method for amplicon-based studies. *PeerJ.* 2014:e593. doi: 10.7717/peerj.593

Malits, A., Cattaneo, R., Sintes, E., Gasol, J., Herndl, G., and Weinbauer, M. (2015). Potential impacts of black carbon on the marine microbial community. *Aquat. Microb. Ecol.* 75, 27–42. doi: 10.3354/ame01742

Martin, M. (2011). Cutadapt removes adapter sequences from high-throughput sequencing reads. *EMBnet. j.* 17, 10–12. doi: 10.14806/ej.17.1.200

Matveev, V., and Robson, B. J. (2014). Aquatic food web structure and the flow of carbon. *Fr. Rev.* 7, 1–24. doi: 10.1608/FRJ-7.1.720

Naff, C. S., Darcy, J. L., and Schmidt, S. K. (2013). Phylogeny and biogeography of an uncultured clade of snow chytrids. *Environ. Microbiol.* 15, 2672–2680. doi: 10.1111/1462-2920.12116

Oksanen, J., Blanchet, F. G., Friendly, M., Kindt, R., Legendre, P., McGlinn, D., et al. (2017). Vegan: Community Ecology Package. Available at: https://cran.r-project.org/package=vegan

Perini, L., Gostinčar, C., Anesio, A. M., Williamson, C., Tranter, M., and Gunde-Cimerman, N. (2019). Darkening of the Greenland ice sheet: fungal abundance and diversity are associated with algal bloom. *Front. Microbiol.* 10:557. doi: 10.3389/fmicb.2019.00557

Procházková, L., Leya, T., Křížková, H., and Nedbalová, L. (2019). Sanguina nivaloides and Sanguina aurantia gen. Et spp. nov. (*Chlorophyta*): The taxonomy, phylogeny, biogeography and ecology of two newly recognised algae causing red and orange snow. *FEMS Microbiol. Ecol.* 95:fiz064. doi: 10.1093/femsec/fiz064

Quast, C., Pruesse, E., Yilmaz, P., Gerken, J., Schweer, T., Yarza, P., et al. (2013). The SILVA ribosomal RNA gene database project: improved data processing and web-based tools. *Nucleic Acids Res.* 41, D590–D596. doi: 10.1093/nar/gks1219

R Core Team (2019). *R: A language and environment for statistical computing*. Vienna, Austria: R Foundation for Statistical Computing. Available at: https://www.r-project.org/

Ramanan, R., Kim, B. -H., Cho, D. -H., Oh, H. -M., and Kim, H. (2016). Algae–bacteria interactions: evolution, ecology and emerging applications. *Biotechnol. Adv.* 34, 14–29. doi: 10.1016/j.biotechadv.2015.12.003

Remias, D., Jost, S., Boenigk, J., Wastian, J., and Lütz, C. (2013a). Hydrurus-related golden algae (*Chrysophyceae*) cause yellow snow in polar summer snowfields. *Phycol. Res.* 61, 277–285. doi: 10.1111/pre.12025

Remias, D., Procházková, L., Nedbalová, L., Andersen, R. A., and Valentin, K. (2020). Two new Kremastochrysopsis species, K. austriaca sp. nov. and *K. americana* sp. nov. (*Chrysophyceae*)[1]. *J. Phycol.* 56, 135–145. doi: 10.1111/jpy.12937

Remias, D., Wastian, H., Lütz, C., and Leya, T. (2013b). Insights into the biology and phylogeny of Chloromonas polyptera (*Chlorophyta*), an alga causing orange snow in maritime Antarctica. *Antarct. Sci.* 25, 648–656. doi: 10.1017/S0954102013000060

Segawa, T., Matsuzaki, R., Takeuchi, N., Akiyoshi, A., Navarro, F., Sugiyama, S., et al. (2018). Bipolar dispersal of red-snow algae. *Nat. Commun.* 9:3094. doi: 10.1038/s41467-018-05521-w

Seymour, J. R., Amin, S. A., Raina, J. B., and Stocker, R. (2017). Zooming in on the phycosphere: the ecological interface for phytoplankton-bacteria relationships. *Nat. Microbiol.* 2:17065. doi: 10.1038/nmicrobiol.2017.65

Shen, L., Liu, Y., Xu, B., Wang, N., Zhao, H., Liu, X., et al. (2017). Comparative genomic analysis reveals the environmental impacts on two Arcticibacter strains including sixteen *Sphingobacteriaceae* species. *Sci. Rep.* 7:2055. doi: 10.1038/s41598-017-02191-4

Stein, J. R., and Amundsen, C. C. (1967). Studies on snow algae and fungi from the front range of Colorado. *Can. J. Bot.* 45, 2033–2045. doi: 10.1139/b67-221

Takahashi, S., Tomita, J., Nishioka, K., Hisada, T., and Nishijima, M. (2014). Development of a prokaryotic universal primer for simultaneous analysis of bacteria and archaea using next-generation sequencing. *PLoS One* 9:e105592. doi: 10.1371/journal.pone.0105592

Takeuchi, N., Dial, R., Kohshima, S., Segawa, T., and Uetake, J. (2006). Spatial distribution and abundance of red snow algae on the Harding Icefield, Alaska derived from a satellite image. *Geophys. Res. Lett.* 33:L21502. doi: 10.1029/2006GL027819

Terashima, M., Umezawa, K., Mori, S., Kojima, H., and Fukui, M. (2017). Microbial community analysis of colored snow from an Alpine snowfield in Northern Japan reveals the prevalence of *Betaproteobacteria* with snow algae. *Front. Microbiol.* 8:1481. doi: 10.3389/fmicb.2017.01481

Thomas, W. H., and Duval, B. (1995). Sierra Nevada, California, U.S.A., snow algae: snow albedo changes, algal-bacterial interrelationships, and ultraviolet radiation effects. *Arct. Alp. Res.* 27, 389–399. doi: 10.2307/1552032

Wang, Q., Garrity, G. M., Tiedje, J. M., and Cole, J. R. (2007). Naive Bayesian classifier for rapid assignment of rRNA sequences into the new bacterial taxonomy. *Appl. Environ. Microbiol.* 73, 5261–5267. doi: 10.1128/AEM.00062-07

Wang, Y., Tian, R. M., Gao, Z. M., Bougouffa, S., and Qian, P. Y. (2014). Optimal eukaryotic 18S and universal 16S/18S ribosomal RNA primers and their application in a study of symbiosis. *PLoS One* 9:e90053. doi: 10.1371/journal.pone.0090053

Wang, J., Wang, C., Li, J., Bai, P., Li, Q., Shen, M., et al. (2018). Comparative genomics of degradative *Novosphingobium* strains with special reference to microcystin-degrading *Novosphingobium* sp. THN1. *Front. Microbiol.* 9:2238. doi: 10.3389/fmicb.2018.02238

Weinbauer, M. G., Guinot, B., Migon, C., Malfatti, F., and Mari, X. (2017). Horizons skyfall-neglected roles of volcano ash and black carbon rich aerosols for microbial plankton in the ocean. *J. Plankton Res.* 39, 187–198. doi: 10.1093/plankt/fbw100

Wickham, H. (2016). *ggplot2: Elegant graphics for data analysis*. New York: Springer-Verlag.

Williamson, C. J., Cook, J., Tedstone, A., Yallop, M., McCutcheon, J., Poniecka, E., et al. (2020). Algal photophysiology drives darkening and melt of the Greenland ice sheet. *Proc. Natl. Acad. Sci. U. S. A.* 117, 5694–5705. doi: 10.1073/pnas.1918412117

Conflict of Interest: The authors declare that the research was conducted in the absence of any commercial or financial relationships that could be construed as a potential conflict of interest.

frontiers in Microbiology

ORIGINAL RESEARCH
published: 31 July 2020
doi: 10.3389/fmicb.2020.01783

Physiological Capabilities of Cryoconite Hole Microorganisms

Ewa A. Poniecka[1], Elizabeth A. Bagshaw[1], Henrik Sass[1], Amelia Segar[1], Gordon Webster[2], Christopher Williamson[3], Alexandre M. Anesio[4] and Martyn Tranter[3]*

[1] School of Earth and Ocean Sciences, Cardiff University, Cardiff, United Kingdom, [2] School of Biosciences, Cardiff University, Cardiff, United Kingdom, [3] Bristol Glaciology Centre, School of Geographical Sciences, University of Bristol, Bristol, United Kingdom, [4] Department of Environmental Science, Aarhus University, Roskilde, Denmark

Cryoconite holes are miniature freshwater aquatic ecosystems that harbor a relatively diverse microbial community. This microbial community can withstand the extreme conditions of the supraglacial environment, including fluctuating temperatures, extreme and varying geochemical conditions and limited nutrients. We analyzed the physiological capabilities of microbial isolates from cryoconite holes from Antarctica, Greenland, and Svalbard in selected environmental conditions: extreme pH, salinity, freeze-thaw and limited carbon sources, to identify their physiological limits. The results suggest that heterotrophic microorganisms in cryoconite holes are well adapted to fast-changing environmental conditions, by surviving multiple freeze-thaw cycles, a wide range of salinity and pH conditions and scavenging a variety of organic substrates. Under oxic and anoxic conditions, the communities grew well in temperatures up to 30°C, although in anoxic conditions the community was more successful at colder temperatures (0.2°C). The most abundant cultivable microorganisms were facultative anaerobic bacteria and yeasts. They grew in salinities up to 10% and in pH ranging from 4 to 10.5 (Antarctica), 2.5 to 10 (Svalbard), and 3 to 10 (Greenland). Their growth was sustained on at least 58 single carbon sources and there was no decrease in viability for some isolates after up to 100 consecutive freeze-thaw cycles. The elevated viability of the anaerobic community in the lowest temperatures indicates they might be key players in winter conditions or in early melt seasons, when the oxygen is potentially depleted due to limited flow of meltwater. Consequently, facultative anaerobic heterotrophs are likely important players in the reactivation of the community after the polar night. This detailed physiological investigation shows that despite inhabiting a freshwater environment, cryoconite microorganisms are able to withstand conditions not typically encountered in freshwater environments (namely high salinities or extreme pH), making them physiologically more similar to arid soil communities. The results also point to a possible resilience of the most abundant microorganisms of cryoconite holes in the face of rapid change regardless of the location.

Keywords: cryoconite, microbial physiology, cultivation, freeze-thaw, extreme conditions

OPEN ACCESS

Edited by:
Samuel Cirés, Autonomous University of Madrid, Spain

Reviewed by:
Ian Hawes, University of Waikato, New Zealand
Felipe Gómez, Centro de Astrobiología (CSIC-INTA), Spain

****Correspondence:***
Ewa A. Poniecka
ponieckaEA@cardiff.ac.uk

Specialty section:
This article was submitted to Extreme Microbiology, a section of the journal Frontiers in Microbiology

Received: *12 March 2020*
Accepted: *07 July 2020*
Published: *31 July 2020*

Citation:
Poniecka EA, Bagshaw EA, Sass H, Segar A, Webster G, Williamson C, Anesio AM and Tranter M (2020) Physiological Capabilities of Cryoconite Hole Microorganisms. Front. Microbiol. 11:1783. doi: 10.3389/fmicb.2020.01783

INTRODUCTION

Ice sheets and glaciers are the biggest freshwater ecosystem on the planet (Edwards et al., 2013), which is undergoing rapid changes (Stocker et al., 2013). It is therefore crucial to understand the biogeochemical processes occurring to predict future changes, their impacts on surrounding environments, and potential losses of functional biodiversity. Complex microbial communities on the surface of glaciers and ice sheets are concentrated in small melt pools called cryoconite holes (Wharton et al., 1985). Cryoconite is a matrix of mineral particles and biological material deposited on glaciers by wind and meltwater, most likely of local origin (Porazinska et al., 2004). Having lower albedo than surrounding ice, it absorbs heat and melts downwards, creating a suitable habitat for microbial life in the supraglacial environment (McIntyre, 1984; Tranter et al., 2004; Cook et al., 2016). The structure of cryoconite holes ensures that the organisms that inhabit them have access to liquid water throughout the ablation season (Fountain et al., 2004; Hodson et al., 2008) and ensures relative high density of different life forms when compared to other supraglacial habitats (Edwards et al., 2011). This also provides protection from extreme fluctuations in air temperature and partial UV screening, either by ice lidding or by the formation of granules (Hodson et al., 2010; Bagshaw et al., 2016): those that form in "cold" ice tend to remain isolated by a refrozen ice lid (Fountain et al., 2004), whereas those formed in regions with more extensive surface meltwater flows experience frequent redistribution (Cook et al., 2010), which promotes the formation of cryoconite granules (Langford et al., 2010). Large granules and thick accumulations of cryoconite material enable formation of anoxic zones (Poniecka et al., 2018), creating a niche for anaerobic microorganisms (Zdanowski et al., 2016).

Rates of microbial activity in cryoconite sediment are similar to those found in temperate freshwater sediments (Anesio and Laybourn-Parry, 2012). Yet microorganisms in cryoconite holes are subjected to multiple stresses resulting from low temperatures and fluctuations of environmental conditions. These include, but are not limited to, freeze-thaw cycles, geochemical extremes including high pH and low nutrient availability, decrease in diffusion rates, increased viscosity of fluids, osmotic stress, and UV exposure. For microorganisms to adapt to this environment, they need to respond to numerous interacting stresses that are usually unspecific (Anesio and Laybourn-Parry, 2012; Collins and Margesin, 2019), and we need to understand how they interact. Cold-environment constraints often induce cross-protection against other stressors. For example, adaption to freeze-thaw stress will also provide protection against heat and cold shock, oxidative stress, metabolic stress (starvation on C or N sources), and/or osmotic stress (Park et al., 1997; Fonseca et al., 2001; Wilson et al., 2012). Identified mechanisms which allow survival of freezing and accompanying stresses include the increased fluidity of the cell membrane (Fonseca et al., 2001; Meneghel et al., 2017), excretion of antifreeze proteins (Park et al., 1997; Raymond, 2016) or other cryoprotectants (Pegg, 2007; Wilson et al., 2012), as well as the production of stress proteins following exposure (Park et al., 1997; Fonseca et al., 2001).

Metagenomic and molecular studies of Alpine cryoconite hole communities have attempted to characterize the mechanisms of adaptation to these extreme stressors. At Rotmoosferner, Austria, it was demonstrated that microbial community members not only have a large array of stress response genes, but that they also have significant genetic potential for effective nutrient and organic carbon scavenging/recycling (Edwards et al., 2013). Utilization of various carbon substrates was also determined in the Austrian Alps (Margesin et al., 2002) and the Himalaya, and also in Antarctica (Foreman et al., 2007; Sanyal et al., 2018). At Forni, Italy, and Baltoro, Pakistani Karakoram, a metagenomic study confirmed the presence of versatile and diverse metabolisms in the cryoconite communities (Franzetti et al., 2016). Genes encoding metabolic pathways of heterotrophic anoxygenic phototrophs and anaerobes were found, as well as enzymes for multiple organic carbon sources such as cellulose, chitin and other polysaccharides [e.g., Extracellular Polymeric Substances (EPS)]. Yet it still remains mostly unknown which groups of microorganisms are capable of effective recycling, if they complement each other or else if they are all efficient scavengers.

Much of the research on polar cryoconite holes has been focused on geochemistry, net ecosystem productivity and carbon cycling (Stibal et al., 2008; Cook et al., 2012; Bagshaw et al., 2013), whilst the actual functionality of these microbial communities remains largely unidentified and physiological limits are untested. Metagenomes of microbial communities on the Greenland Ice Sheet (GrIS) show the potential for resistance to and degradation of anthropogenic contaminants (Hauptmann et al., 2017), but the genetic potential of Antarctic communities has not been investigated. The phenotypic diversity of organisms will affect the robustness of ecosystem and its response to change (Petchey and Gaston, 2006; Srivastava et al., 2019). Ice sheet surfaces are an extreme low temperature environment, but also a very changeable habitat. Cryoconite holes can be saturated with oxygen (Bagshaw et al., 2011) or anoxic (Poniecka et al., 2018); too dark or too light (Perkins et al., 2017); change from hypersaline to low ionic strength (Telling et al., 2014); become acidic or alkaline (Tranter et al., 2004); be frozen and thawed multiple times (Bagshaw et al., 2011); and can be spiked with nutrients or become nutrient limited (Telling et al., 2014; Holland et al., 2019). We therefore hypothesize that the microorganisms that inhabit polar cryoconite holes can tolerate and grow over a wide range of extreme conditions. We further expect them to have a significant potential for scavenging multiple carbon sources. Finally, we predict that Antarctic microorganisms should be able to withstand harsher conditions than their Arctic counterparts. This study presents the microbial ecophysiology of a collection of isolates from cryoconite sediments from sampling locations in Antarctica, Greenland, and Svalbard. The microbial isolates were characterized using cultivation-based techniques in a range of extreme conditions, and the response assessed for each sample location.

MATERIALS AND METHODS

Sampling

Cryoconite material was collected from three polar locations (Antarctica, Greenland, and Svalbard), with three samples from each location analyzed. Antarctic samples (n = 3) were collected from ice-lidded cryoconite holes on Canada Glacier in McMurdo Dry Valleys [−77.6175, 162.9734] in the Austral summer of 2005/2006. Svalbard samples (n = 3) were collected from Midtre Lovénbreen glacier, approximately 4 km from the United Kingdom Arctic Research Station in Ny-Ålesund [78.8800, 12.0700] in the melt season of 2016. The Greenland study site (n = 3), "Black and Bloom" (Williamson et al., 2020), was located 60 km [67.0748, −49.3586] east of Kangerlussuaq, and approximately 2 km east of weather station S6 (Smeets et al., 2018) in the summer melt season of 2016. Antarctic and Svalbard samples were scooped from cryoconite holes using clean, disposable nitrile gloves and transferred into Ziploc plastic bags or tubes pre-washed with deionized water. Ice lids were removed from Antarctic cryoconite holes using a Sipre corer prior to sampling (see Bagshaw et al., 2007). Greenland samples were collected with a pre-washed turkey baster and transferred into sterile Whirlpack® bags. All samples were frozen prior to temperature-controlled transport to Cardiff University, where they were stored in a −20°C freezer until laboratory experiments commenced.

Total Cell Counts

The total cell count of each of the sediment sample was performed using the epifluorescence microscopy following method of Cragg and Kemp (1995). Briefly, cryoconite sediment from each location (n = 9) was diluted 1 to 10 in substrate free medium, then fixed in 1.6% formaldehyde and stained with acridine orange. Total cell counts were determined in three technical replicates with a Zeiss Axioskop microscope after staining.

MPNs and Cultivability

The Most Probable Number (MPN) technique was used to enumerate viable cell counts in the cryoconite sediment (n = 3 for Greenland and Svalbard, n = 2 for Antarctica). Following initial dilution of ∼1 g of the sediment in the 9 ml of water, a series of eight 10-fold dilutions in three replicates was prepared on a 96-well plate (Köpke et al., 2005). Samples were grown at temperatures 0.2, 4, 10, 15, 20, and 30°C under oxic or anoxic conditions. For aerobic microorganisms, a freshwater medium was used (Sass et al., 1997), containing the following components: NaCl (0.1 g l^{-1}), $MgCl_2 \cdot 6H_2O$ (0.25 g l^{-1}), $CaCl_2 \cdot 2H_2O$ (0.1 g l^{-1}), KCl (0.1 g l^{-1}), NH_4Cl (0.1 g l^{-1}), KH_2PO_4 (0.1 g l^{-1}), casamino acids (0.25 g l^{-1}), and yeast extract (0.05 g l^{-1}). The medium was supplemented with 1 ml l^{-1} of the trace element solution SL 10, 0.2 ml l^{-1} of a selenite and tungstate solution (Sass et al., 1997). It was buffered with HEPES (2.38 g l^{-1}) and the pH was adjusted to 7.2 with 1 M NaOH prior to autoclaving. After autoclaving, the medium was supplemented with 2 ml l^{-1} of vitamin solution (Wolin et al., 1963) and glucose (4 mM l^{-1}). For anaerobic microorganisms, a bicarbonate-buffered fermenter medium was used, containing: $MgCl_2 \cdot 6H_2O$ (0.1 g l^{-1}), $CaCl_2 \cdot 2H_2O$ (0.35 g l^{-1}), KCl (0.1 g l^{-1}), NH_4Cl (0.1 g l^{-1}), KH_2PO_4 (0.1 g l^{-1}), casamino acids (0.25 g l^{-1}), vitamin solution (2 ml l^{-1}), glycine betaine (0.5 mM), sodium acetate (0.5 mM), TCA mixture [0.5 mM (Köpke et al., 2005)], choline (0.5 mM), methylamine (0.5 mM), trace element solution SL 10 (1 ml l^{-1}), selenite and tungstate solution (0.2 ml l^{-1}). The medium was reduced with Na_2S (1.25 mM) and $FeCl_2$ (0.25 mM) solutions. Plates were incubated in air-tight bags with AnaeroGen sachet (Oxoid). MPN values were recorded after 71 days of incubation. Oxic growth was scored after visual inspection of the MPN plates. In anoxic incubations, growth was analyzed after staining with SYBR green I dye (Martens-Habbena and Sass, 2006) and fluorescence analysis on a plate reader. MPN values with standard error and 95% confidence intervals were calculated according to de Man (1983). Viable cell counts obtained with the MPN technique were related to the total counts to estimate culturability.

Microbial Isolates

The cultivable microorganisms were isolated from the highest positive MPN dilution, therefore representing the most abundant members of community. A sample of 20 μl from the MPN dilution was streaked on to a 1.5% (w/v) agar plate with freshwater medium or anaerobic medium. Anaerobic cultures were prepared in an anoxic chamber and cultured in air-tight bags with AnaeroGen sachet (Oxoid). At least three subsequent subcultures were streaked to obtain a pure culture. Anaerobic cultures were tested for growth in oxic conditions and for alternative electron acceptor utilization (nitrate, thiosulphate, iron, manganese, TMO, DMSO) (Süß et al., 2008).

16S rRNA Gene Sequencing

Genomic DNA of each microbial isolate was extracted by bead beating at speed 5.5 m s^{-1} for 30 s (FastPrep 24 Instrument, MP biomedicals) in Guanidine Isothiocyanate lysis buffer (Invitrogen), and then purified with the use of an automated Maxwell 16 Instrument and tissue DNA purification kits (Promega), following the manufacturer's instructions. Briefly, DNA cleaning steps were performed with the use of magnetic beads binding to the DNA. Genomic DNA concentrations were then quantified using a Qubit 2.0 fluorometer (Invitrogen), following the manufacturer's instructions.

Extracted DNA was amplified using primers targeting 16S rRNA genes, 27F (5′-AGA GTT TGA TCM TGG CTC AG -3′) and 907R (5′-GGT TAC CTT GTT ACG ACT T -3′) (Webster et al., 2006). Fungal ITS fragment was amplified using primers ITS1f (5′-CTTGGTCATTTAGAGGAAGTAA-3′) (Ihrmark et al., 2012) and ITS4 (5′-TCCTCCGCTTATTGATATGC-3′) (White et al., 1990) in the following PCR conditions: initial denaturation at 95°C for 5 min, followed by 35 cycles of 95°C for 30 s, 56°C for 30 s and 72°C for 30 s; with final extension of 72°C for 7 min. The yield of PCR reaction was visualized on 1.2% agarose gel. Amplicons were then sequenced by Sanger sequencing with 27F or ITS1f at Eurofins Genomics (Germany) or DNA Sequencing and Services (University of Dundee).

The nucleotide BLAST online tool[1] was used to determine the closest relative for each isolate. The 16S rRNA gene sequences determined in this study have been deposited in GenBank under the accession numbers MT430950, MT432272- MT432304, MT473233, and MT473713-MT473721.

Salinity, Temperature and pH Tolerance

The tolerance of the cryoconite isolates to environmental (temperature) and geochemical (pH and salinity) stresses was tested. Selected isolates were grown in duplicate in liquid freshwater medium at a range of temperatures (1–40°C), salinities (0.1–10%) and pH (2.5–10.5). Salinities from 0.1 to 10% were achieved by adding saturated MgCl (18.75 g l^{-1}) and NaCl (290 g l^{-1}) solution to the freshwater medium. The pH was adjusted with 1M HCl, with different buffering solutions for pH 5.5–10.5 adopted from Kaksonen et al. (2006). For pH 2.5–5, 100 mM K_2HPO_4 was used. Growth was deemed positive or negative by presence of visible cell pellets when compared to negative control (uninoculated freshwater medium) after 30 days of incubation. Differences between microbial isolates' maximum salinity tolerance according to location, oxic/anoxic isolation or bacterial/yeasts were compared using the Kruskal–Wallis test. Differences in the range of pH tolerated by the isolates were established by comparing the inoculated pH media with positive growth after 30 days. The number of tubes with positive growth at each pH was then compared between locations, oxic vs. anoxic conditions and presence or absence of yeasts using ANOVA, followed by Tukey HSD.

Freeze-Thaw Survival

To identify whether cells from the isolated polar microorganisms were susceptible to freezing damage, microbial cultures were subject to alternating freeze-thaw cycles in Weiss VT low-temperature environmental cabinets. All of the bacterial isolates from oxic conditions (16) and representative yeast isolates (7 out of 9) were tested. The isolates were washed with mineral medium (NaCl (0.025 g l^{-1}), $MgCl_2 \cdot 6H_2O$ (0.09 g l^{-1}), $CaCl_2 \cdot 2H_2O$ (0.025 g l^{-1}), KCl (0.025 g l^{-1}), counted and diluted to equal cell numbers in the mineral medium to exclude the potentially protective effect of substrate-rich medium and to minimize growth in between the cycles (Carvalho et al., 2004).

Each cycle consisted of 6 h at -18°C and 3 h at 0.9°C. Subsamples were taken after 1, 5, 25, and 100 cycles and cell viability was determined using the MPN technique after 30 days of incubation.

Substrate Test

Substrate tests were set up in 96-well plates as described by Süß et al. (2008) to assess the physiological capabilities of microbial isolates. A total of 58 substrates were tested, including carbohydrates, carboxylic acids, amino acids, alcohols and others. The substrates were chosen to cover a wide range of possible substrates typically produced and utilized by microbes, as well as to cover a range of enzymes needed for different substrates (**Supplementary Table 1**). Bacterial isolate inocula were washed three times in substrate free medium (freshwater medium with no casamino acids, yeast extract, glucose or vitamins added) prior to the experiment to avoid substrate carry-over. Washed cells were resuspended in substrate-free media and 50 µl added to each well containing 200 µl of medium containing a single substrate. Each substrate was tested at least in duplicate. The wells with positive growth were recorded when compared visually to negative controls (substrate-free medium).

Pearson correlation analysis of the response to the experimental conditions was performed in the "Performance analytics" package in R for each pairwise combination: minimum and maximum pH tolerated, maximum salinity, maximum temperature, average substrate utilization, and freeze-thaw survival for each isolate.

[1]blast.ncbi.nlm.nih.gov

RESULTS

Total Cell Counts

Total cells were counted in the sediment samples, which were subsequently used for MPNs. The cell numbers are uniform across the samples, with no significant differences between Antarctica, Svalbard and Greenland (**Table 1**). Mean total cell counts in Antarctic cryoconite holes were 5.85×10^8 cells g^{-1}, compared with 9.22×10^8 cells g^{-1} in Svalbard and 5.83×10^8 cells g^{-1} in Greenland.

MPN Counts and Cultivability

Freshwater medium and fermenter medium inoculated with cryoconite sediment yielded viable cells under oxic and anoxic conditions, and all temperatures tested. Oxic conditions yielded higher numbers of cultivable microorganisms: mean counts of 4.60×10^8 g^{-1}, 1.30×10^7 g^{-1}, 1.69×10^7 g^{-1} for Svalbard, Greenland, and Antarctic cryoconite respectively (**Figure 1**), compared with 3.98×10^5 g^{-1}, 9.61×10^3 g^{-1}, 8.04×10^5 g^{-1} for Svalbard, Greenland, and Antarctic cryoconite in anoxic conditions (**Figure 2**). The number of cultivable cells in oxic conditions was in the same order of magnitude at each location after 71 days of incubation between 0.2 and 20°C (**Figure 1**). At 30°C, viable counts were on average 100 times lower than those at 20°C, but these samples unfortunately dried out after 1 month (marked on **Figure 1** with stripes). When incubated in an anoxic

TABLE 1 | Abundance of microorganisms in cryoconite sediments.

Location	Sample	Total cell counts per g of wet sediment	95% Confidence Interval
Svalbard	01	4.85×10^8	0.04
	02	1.82×10^9	0.36
	03	4.61×10^8	0.18
Greenland	04	4.33×10^8	0.20
	05	8.86×10^8	0.22
	06	4.30×10^8	0.02
Antarctica	07	5.27×10^8	0.21
	08	4.62×10^8	0.04
	09	7.68×10^8	0.26

atmosphere, viability peaked at the coldest temperatures tested (0.2°C) and the number of cultivable cells was comparable between the temperatures from 4 to 30°C (**Figure 2**).

The cultivability of cryoconite microorganisms was estimated based on total cell counts and MPN counts after 71 days of cultivation. Cryoconite microorganisms yielded very high viable counts under the conditions tested (**Table 2**). Under oxic conditions, the culturable bacterial count of Svalbard microorganisms was an order of magnitude higher than for Greenland and Antarctic (p = 0.00). There were no statistically significant differences between the locations under anoxic conditions. However, it is notable that Antarctic and Svalbard samples have especially high culturability in the lowest temperature tested (0.2°C).

At all temperatures, the cultivability in anoxic conditions was several orders of magnitude lower than in oxic conditions, with values up to 15200, 3400, and 400 times lower for Svalbard, Greenland, and Antarctica, respectively. However, at 0.2°C, the differences between oxic and anoxic incubations were less pronounced (**Table 2**).

None of the anoxic samples had statistically significant differences in cultivability. ANOVA, followed by Tukey HSD, revealed that oxic samples from Svalbard and Greenland were statistically different at 0.2, 10, 15, and 20 degrees (p = 0.00, p = 0.02, p = 0.04 and p = 0.00, respectively), whereas Svalbard and Antarctic samples were different at 0.2 and 20 degrees (p = 0.00 and p = 0.00, respectively). There were no statistically significant differences between Greenland and Antarctic samples' cultivability.

Microbial Isolates

The highest positive dilution of MPNs was used to inoculate solid agar plates with freshwater medium and isolate the most abundant culturable microbes of cryoconite holes. A total of 44 isolates were isolated and identified by 16S rRNA gene sequencing (**Table 3**). Svalbard cryoconite samples yielded 13 bacterial isolates and 4 fungi (yeast) isolates, Greenland 12 bacteria and 5 fungi, and Antarctica 10 bacteria, respectively. No yeasts were isolated from Antarctic cryoconite. Most bacterial isolates affiliated with the Actinobacteria (79%), followed by Bacteroidetes (18%) and Proteobacteria (3%). All isolates were capable of fermentation, but did not utilize alternative electron acceptors.

pH Tolerance

Antarctic isolates grew in medium with pH ranging from 4 to 10.5, whereas those from Svalbard grew in 2.5 to 10, and those from Greenland, 3 to 10 (**Table 3**). Comparison of the differences in these pH ranges was analyzed by ANOVA followed by Tukey HSD and showed that the pH range tolerated by Antarctic isolates was significantly different from Svalbard and from Greenland (p = 0.00 and p = 0.00, respectively) (**Figure 3**). The mean pH of the successful growth media was highest in the Antarctic samples; the mean pH of media with detectable growth was 8.2, compared to 6.2 for Greenland and 6.5 for Svalbard. There was no statistical difference between oxic and anoxic conditions, or between yeasts and bacteria. Most yeasts grew at pH $\geq$ 3; Svalbard yeasts were able to grow from pH 3 to 10, although interestingly yeasts from Greenland samples that were assigned to the same OTUs could only grow at pH 3 to 8.5 (**Table 3**). One bacterial isolate grew at pH 2.5, but the remainder did not tolerate pH $\leq$ 4.

Salinity Tolerance

The microbial isolates from cryoconite holes were able to grow in a surprisingly wide salinity range (**Table 3**). Most (34 out of 39) were able to grow in up to 5% salinity (∼42000 μS cm^{-1}). The highest tested salinity of growth medium was 10% (∼77000 μS cm^{-1}), where 16 isolates tested positive for growth (**Supplementary Figure 1**). Interestingly, there was no significant difference of maximum salinity tolerance between yeasts and bacteria from Svalbard and Greenland, nor between isolates from the different sites of origin, or those isolated under anoxic or oxic conditions.

Temperature Range

Twelve isolates were tested to determine the temperature range in which they were able to grow (**Table 3**). All tested isolates grew at the lowest tested temp (1°C). All of the bacterial isolates were able to grow above 22°C, with Antarctic isolate AN4A7 having a maximum growth temperature of 36°C, whereas yeasts were limited to 22°C.

Freeze-Thaw Survival

Isolates from all sample locations had a mixed response to freezing: some isolates survived multiple freeze-thaw cycles without losing viability (e.g., Antarctic isolate An15O7), whereas others did not (e.g., Antarctic isolate An02O7) (**Figure 4**). All the yeast strains survived numerous (>100×) freeze and thaw cycles without a significant decrease in viability, when assessed by MPN. In some yeast strains cell counts increased after 100 cycles, whereas others showed a slight decrease, but none were completely inviable (**Figure 4A**). Two of the yeast isolates (Gr4O5 and Gr4O4) increased in viable cell counts after a single cycle, which might indicate an adaptation to freeze-thaw stress and cells transitioning from non-culturable to culturable state.

Bacterial isolates showed greater variability in response to freeze-thaw stress. The majority (10 out of 15) of the cultures tested belong taxonomically to Gram-positive bacteria (Actinobacteria). Of these, 8 out of 10 remained viable after 25 cycles, and three (all from Antarctica) were viable after 100 cycles. In contrast, none of the Gram-negative strains survived 100 cycles, and they generally lost culturability more rapidly after freeze-thaw stress. The viability of cultures following treatment was variable, regardless of the sampling site. However, the bacteria isolated from Antarctic cryoconite differed from the Arctic (Svalbard, Greenland): the only three bacterial isolates (An15O7, An4O8, An15O8) able to survive 100 cycles of freezing and thawing came from Antarctic samples, although it should also be noted that some Antarctic isolates survived only 1–5 cycles (**Figure 4B**). Svalbard bacteria viability decayed rapidly, with only one able to survive 25 freeze-thaw cycles (**Figure 4C**). Greenland bacteria ceased to be viable between 25 and 100 cycles (**Figure 4D**). Freeze-thaw survival appears to follow phylogeny and hence cellular structure, as isolates belonging to the same

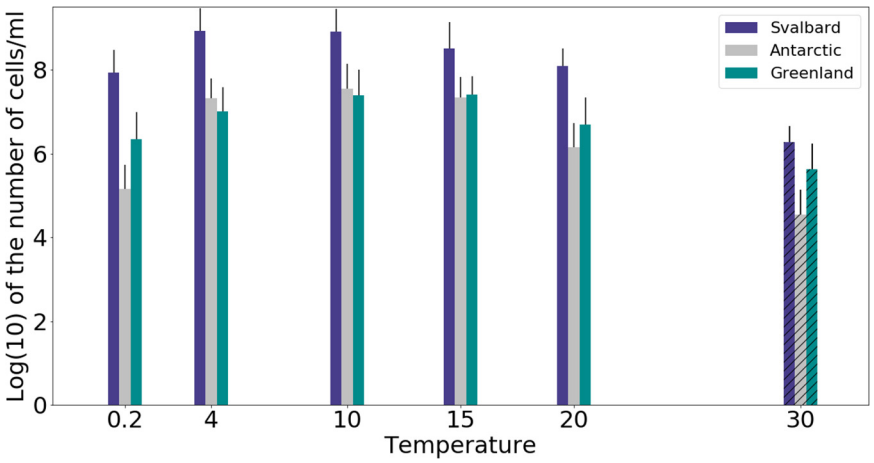

FIGURE 1 | MPN counts of aerobic (oxic) microbial community of cryoconite holes in freshwater medium. Microbial growth was measured by MPN counts as the (average of 3 different cryoconite holes sediments for each location after 71 days of incubation. Samples incubated at 30°C dried out after 30 days, but they are included on the graph for comparison (marked with stripes).

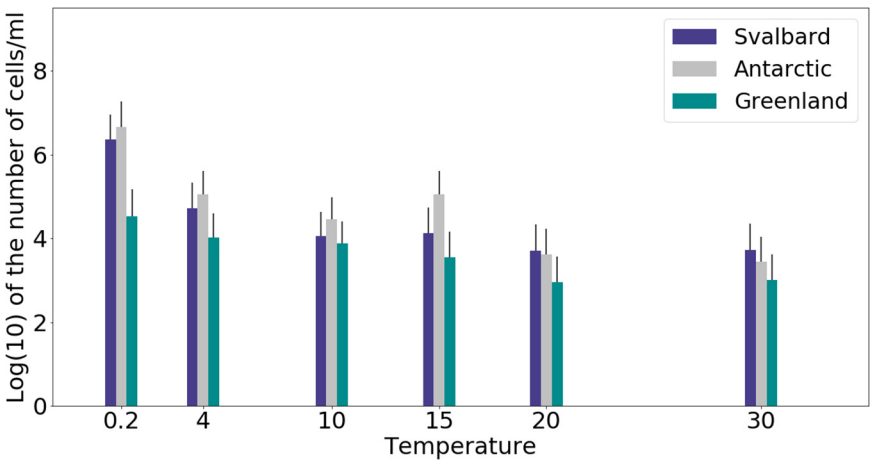

FIGURE 2 | MPN counts of anaerobic (anoxic) microbial community of cryoconite holes in fermenter medium. Microbial growth was measured by MPN counts as the average of 3 different cryoconite holes sediments for each location after 71 days of incubation.

TABLE 2 | Cultivability of microorganisms from cryoconite holes expressed as% of total cell counts which can be cultured by MPN technique in the aerobic and anaerobic conditions.

	Anoxic conditions			Oxic conditions		
Temp (°C)	**Svalbard**	**Greenland**	**Antarctica**	**Svalbard**	**Greenland**	**Antarctica**
0.2	0.28 ± 0.19	0.01 ± 0.01	0.96 ± 0.79	7.28 ± 0.47	0.48 ± 0.35	0.03 ± 0.01
4	0.01 ± 0.01	0.00 ± 0.00	0.02 ± 0.03	48.38 ± 46.97	1.79 ± 1.25	4.37 ± 3.81
10	0.00 ± 0.00	0.00 ± 0.00	0.01 ± 0.01	53.62 ± 8.79	3.70 ± 2.12	7.65 ± 5.16
15	0.00 ± 0.00	0.00 ± 0.00	0.02 ± 0.03	27.05 ± 2.86	5.98 ± 9.69	5.13 ± 0.07
20	0.00 ± 0.00	0.00 ± 0.00	0.00 ± 0.00	13.16 ± 0.15	1.06 ± 1.46	0.31 ± 0.13
30	0.00 ± 0.00	0.00 ± 0.00	0.00 ± 0.00	0.17* ± 0.11	0.10* ± 0.15	0.01* ± 0.00

**In the oxic conditions at 30°C samples were measured after 23 days.*

TABLE 3 | Physiology of microbial isolates of cryoconite holes.

Isolate	Closest relative	%	Phylum	Site	Isolation	Salinity (%)	pH range	Substr (%)	Freeze-thaw	Colony colour	T_{max} (°C)
Bacteria											
An02O7	Flavobacterium sp. R-36976	99	Bacte	Ant	ox	10	6.5–10	69	1	orange	
An4O7	Flavobacterium sp. R-36976	99	Bacte	Ant	ox	7	6.5–10	66	1	orange	
An15O7	Arthrobacter agilis strain LV7	99	Actino	Ant	ox	6	7–10.5	44	100	yellow	32
An15A7	Tessaracoccus sp. strain AU I5	99	Actino	Ant	anox		7–10.5			yellow	
An15A8	Tessaracoccus sp. strain AU I5	99	Actino	Ant	anox		7–10.5			orange-yellow	
An4A7	Bacterium CS117	99	Actino	Ant	anox	10	4.0–10	74		yellow	36
An4A8	Bacterium CS117	99	Actino	Ant	anox	8	6.5–10.5	38		orange	
An4O8	Marisediminicola sp. N26	99	Actino	Ant	ox	10	6.5–10.5	63	100	orange	
An15O8	Marisediminicola sp. N26	99	Actino	Ant	ox	6.5	6.5–10.5	28	100	orange	
An02O8	Cryobacterium sp. 1021	99	Actino	Ant	ox	8	5–10.5	43	25	red	24
Gr15O6	Frigoribacterium sp. MP117	99	Actino	Gr	ox	8	4–8.5	38	25	orange	
Gr15O5	Frigoribacterium sp. MP117	99	Actino	Gr	ox	2.5	4–8.5	17	25	orange	
Gr02A4	Antarctic bacterium 2CA	99	Actino	Gr	anox	10	4–8.5	28		pale yellow	
Gr15O4	Glaciihabitans tibetensis strain TGC-6	99	Actino	Gr	ox	2	4–8.5	16	25	orange-yellow	
Gr4O4P	Uncultured Bacteroidetes clone IC4058	99	Bacte	Gr	ox				5	pink	
Gr4O6	Rugamonas rubra strain HCR18a	99	Proteo	Gr	ox	0.75	4.5–8	50	25	white	31
Gr4A5	Cryobacterium sp. MDB2-A-1	99	Actino	Gr	anox	10	4–8.5	72		pale yellow	24
Gr02O4	Cryobacterium psychrotolerans MLB-34	99	Actino	Gr	ox	8	4.0–10	59	5	yellow	
Gr02A6	Cryobacterium psychrotolerans ZS14-85	99	Actino	Gr	anox	10	4.0–10	41		pale yellow	
Gr02A5	Cryobacterium sp. MDB1-44	99	Actino	Gr	anox	10	4–9.5	50		pale yellow	
Gr4A4	Cryobacterium sp. MDB1-44	99	Actino	Gr	anox	10	4–8.5	42		pale yellow	
Gr4A6	Cryobacterium sp. MDB1-44	99	Actino	Gr	anox	10	4–8.5	70		pale yellow	
Sv4A3	Cryobacterium sp. MDB1-44	99	Actino	Sv	anox	10	4–8.5	67		pale yellow	
Sv4A2	Cryobacterium sp. MDB2-A-1	99	Actino	Sv	anox	8	4–8.5	48		pale yellow	25
Sv15A2	Cryobacterium sp. MDB2-A-1	99	Actino	Sv	anox	5.5	4–8.5	23		yellow	
Sv02A1	Antarctic bacterium 2CA	99	Actino	Sv	anox	5.5	4–8.5	23		yellow	
Sv4A1	Antarctic bacterium 2CA	99	Actino	Sv	anox	8	4–8.5	66		pale yellow	34
Sv02A3	Antarctic bacterium 2CA	99	Actino	Sv	anox	8	4–8.5	21		yellow	
Sv4O2	Uncultured bacterium clone LE201D02	99	Bacte	Sv	ox	10	6.0–10	7	25	orange	
Sv02O2	Flavobacterium sp. KJF4-15	99	Bacte	Sv	ox	8	6.0–10	47	5	orange	25
Sv02A2	Flavobacterium sp. TMS1-10 16S	99	Bacte	Sv	anox	8	4–9.5	34		yellow	
Sv15A1	Cellulomonas cellasea strain WB102	99	Actino	Sv	anox		2.5–8			pale yellow	
Sv15O1	Frigoribacterium sp. Ha8	99	Actino	Sv	ox	2	5.0–10	54	5	yellow	31
Sv15A3	Actinobacterium Muzt-D93	99	Actino	Sv	anox		4–8.5			pale yellow	
Sv15O3	Glaciihabitans tibetensis strain SD-70	99	Actino	Sv	ox	2	4–8.5	41	25	orange	
Fungi											
Gr02O5	Basidiomycota sp. TP-Snow-Y1	91	Basidio	Gr	ox	10	3–8.5	41	100	pale pink	
Gr4O5	Basidiomycota sp. TP-Snow-Y1	91	Basidio	Gr	ox	8	5.5–8.5	27	100	pale pink	19
Gr4O4	Basidiomycota sp. TP-Snow-Y1	91	Basidio	Gr	ox	10	3–8.5	24	100	pale pink	
Gr02O4w	Basidiomycota sp. TP-Snow-Y1	91	Basidio	Gr	ox	10	3–8.5	33		white	18
Gr02O6	Basidiomycota sp. TP-Snow-Y1	91	Basidio	Gr	ox	7	3–8.5	34	100	pale pink	
Sv02O1	Basidiomycota sp. TP-Snow-Y1	92	Basidio	Sv	ox	5	3.0–10	48	100	pale pink	
Sv4O1	Basidiomycota sp. TP-Snow-Y1	92	Basidio	Sv	ox	8	3–8.5	23		pale pink	
Sv02O3	Mrakia sp. isolate J-36	99	Basidio	Sv	ox	10	3.0–10	52	100	white	22
Sv4O3	Mrakia robertii isolate J-127	100	Basidio	Sv	ox	10	3.0–10	66	100	orange	

Closest relative of isolates is based on rRNA gene sequencing and similarity is expressed in percent (%). Isolation was done in oxic (ox) or anoxic (anox) conditions. Carbon substrates utilization (substr) is expressed as the percent used of tested. "Salinity" is the maximum salinity and "pH range" is the range of media pH in which positive growth was recorded. All the isolates were able to grow at lowest tested salinity of 0.1%. Freeze-thaw survival is the number of cycles after which a culture was viable. Tmax is the maximum temperature that growth could be detected. All tested isolates grew at the lowest tested temp (1°C). Phyla detected include Actinobacteria (Actino), Bacteroidetes (Bacte), and Proteobacteria (Proteo). Sampling sites are Antarctica (Ant), Greenland (Gr), and Svalbard (Sv).

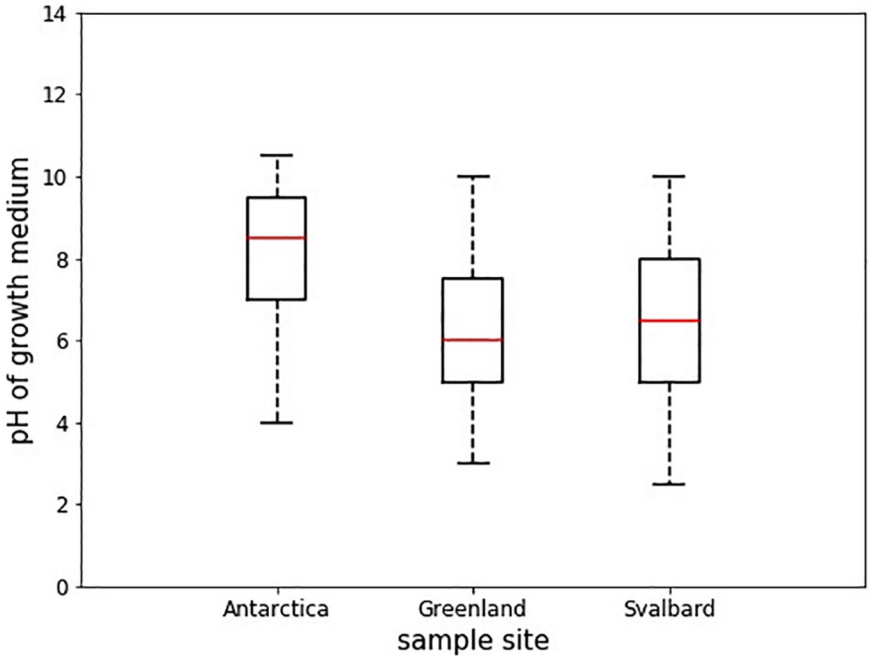

FIGURE 3 | Boxplots showing the median pH tolerance of all microbial isolates from cryoconite holes from Greenland, Svalbard, and Antarctica. The pH of all incubations with positive growth after 30 days (n = 43) was noted, and compared between the locations. The red line depicts the median pH, the box envelops an interquartile range and the whiskers mark the 97th centile. There were no outliers.

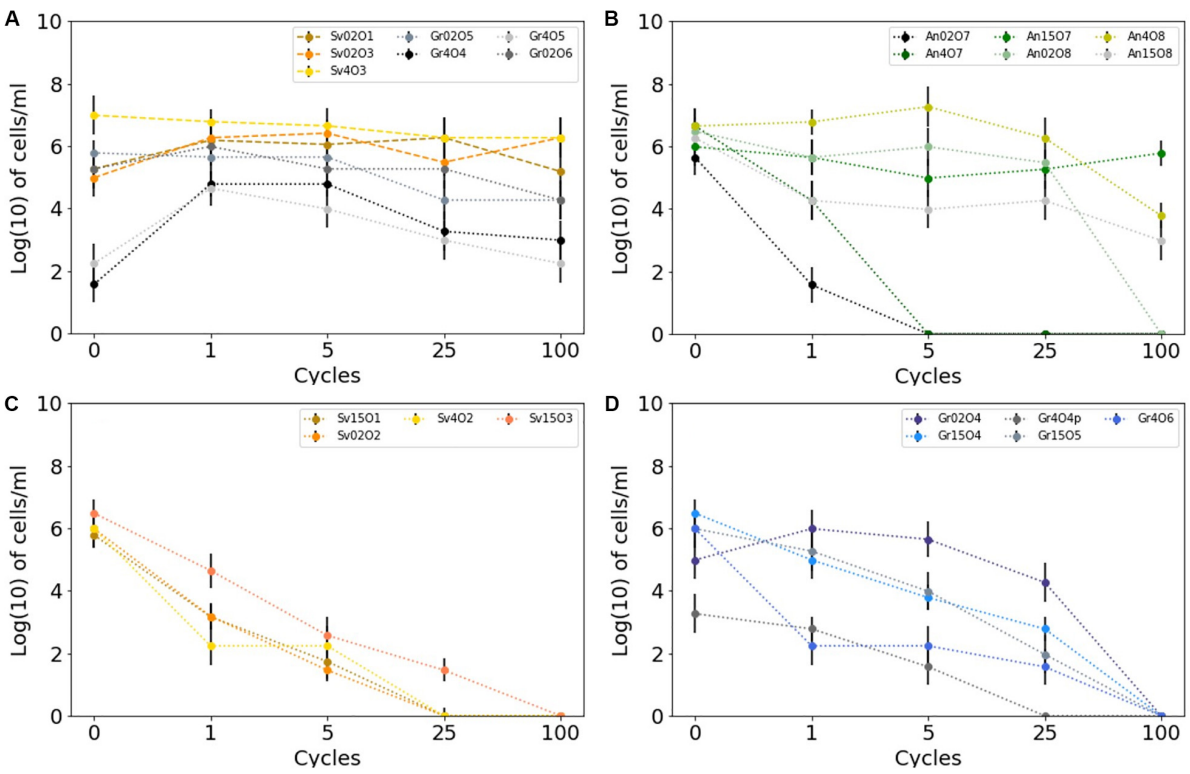

FIGURE 4 | Survival of cryoconite isolates subjected to multiple freeze-thaw cycles as measured by MPN technique. Error bars depicts 95% confidence levels calculated for MPNs. **(A)** Greenland and Svalbard yeasts, **(B)** Antarctic bacteria, **(C)** Svalbard bacteria, **(D)** Greenland bacteria.

TABLE 4 | Mean utilization of carbon substrates by cryoconite microorganisms expressed as proportion of all carbon substrates tested in percent.

Mean substrate utilization (%)	Carboxylic Acids	Carbohydrates	Amino Acids	Polyhydric Alcohols	Alcohols	Other
Isolates						
Anaerobic bacteria	44	68	53	44	14	4
Aerobic bacteria	47	46	56	34	19	12
Yeasts	46	45	29	37	41	0
Locations						
Antarctica	57	65	62	42	15	31
Greenland	40	50	48	38	22	0
Svalbard	45	53	42	39	26	0

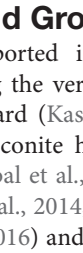

All the isolates are divided into groups based on isolation or location. Colors indicate a heatmap of substrates' utilization, with red hues representing a higher proportion of substrates being utilized by selected isolates and blue hues representing low proportion to none substrates being utilized.

genus but obtained from different sites showed a similar response. For example, *Cryobacterium* sp. from Antarctica and from Greenland survived well during the initial cycles and collapsed after 25 cycles. *Flavobacterium* sp. from Svalbard and Antarctica did not cope well and survived 1 to 5 cycles.

There was no significant correlation between the pigmentation of the strains, resistance to salinity and/or extreme pH and freeze-thaw survival (**Table 3**). Among the isolates with the highest freeze-thaw resistance (25−100 cycles), there were cultures which survived only salinities up to 0.75% (isolate Gr4O6), but also up to 10% (An4O8); dark pigmented isolates (orange) which survived one cycle (A02O7) and 25 cycles (Gr15O6); and strains able to survive extreme pH 10 with both minimal (1 cycle only, An02O7) and good freeze-thaw tolerance (25 cycles, Sv4O2). The three isolates most resistant to freezing (Antarctic isolates An15O8, An4O8, An15O7) were pigmented, resistant to pH 10.5 and able to cope with high salinities (6.5, 10 and 6%, respectively).

Substrate Test

The cultures tested utilized a wide range of carbon sources from different groups (carboxylic acids, simple and complex carbohydrates, amino acids, alcohols and polyalcohol and other complex substances). There was no strong preference for one single type of carbon source such as carboxylic acids, carbohydrates or amino acids (**Table 4**), and some isolates were able to live on almost all substrates tested (e.g., genera *Flavobacterium* sp. or *Cryobacterium* sp.). There are some exceptions, for example most isolates belonging to *Antarctic bacterium* species only utilized a small selection of carboxylic acids.

Antarctic isolates used a bigger pool of substrates (45% of those tested) when compared to Svalbard (34%) and Greenland isolates (32%), however, the differences were not statistically significant. Interestingly, Antarctic isolates were the only ones able to utilize the "other" substrates (**Supplementary Table 1**) which include "non-competitive" choline, betaine and methylamine. Yeasts had a greater capability to use alcohols and were less likely to use amino acids when compared to bacteria. Microbes isolated in anoxic conditions decomposed more types of carbohydrates than those obtained under oxic conditions.

DISCUSSION

Microbial Abundance and Growth

The spread of cell numbers reported in the literature is astonishingly wide. After excluding the very extreme values of $0.5-7.5 \times 10^{14}$ cells g^{-1} in Svalbard (Kastovská et al., 2005), the cell numbers reported in cryoconite holes worldwide are between 10^6 and 10^9 cells g^{-1} (Stibal et al., 2006; Anesio et al., 2010; Hodson et al., 2010; Singh et al., 2014; Telling et al., 2014; Musilova et al., 2015; Cook et al., 2016) and our data are within this range. Svalbard, Greenland, and Antarctic samples showed no significant differences in the cell counts (mean counts of 9.2, 5.8, and 5.8×10^8 cells g^{-1}, respectively).

The microbial diversity and community structure of cryoconite holes is often based on only "snapshots" of the community measured at a given place and time (Edwards et al., 2013), so there is clearly variability in reported results. However, many of the microorganisms isolated in this study have been identified elsewhere (**Supplementary Table 2**), for example, Flavobacteria class is often dominant in freshwater polar environments (Michaud et al., 2012) and the Cytophaga-Flavobacteria group, to which 18% of isolates in this study belong, was found to be dominant (87.2%) in Canada Glacier cryoconite holes from Antarctica (Foreman et al., 2007). *Flavobacterium, Cryobacterium*, and *Arthrobacter* spp. were also isolated in Antarctic cryoconite holes from Canada Glacier (Christner et al., 2003). *Cryobacterium* spp. was also common in Svalbard soils (Hansen et al., 2007) and basidiomycetous yeasts were predominant in Svalbard sea and glacial ice (Gunde-Cimerman et al., 2003). Lutz et al. (2019) found Cyanobacteria, Proteobacteria, and Actinobacteria phyla to be the most abundant in Antarctic cryoconite holes from Queen Maud Land. The dominance of Actinobacteria, in this study, followed by Bacteroidetes and Proteobacteria, is therefore consistent with these previous findings.

Our experiments showed that oxic conditions yielded higher numbers of viable, cultivable microorganisms than anoxic. Cryoconite holes are largely oxygen rich environments, with aerobic metabolisms and consequent dominance of aerobic microorganisms, but there are anoxic niches (Poniecka et al., 2018) where a thriving anaerobic community can be found. Oxic microorganisms have quite uniform viable counts across the temperatures of 0.2 to 20°C, with visible decline at 30°C, whereas the highest cultivability in anoxic conditions was observed at 0.2°C and the majority of the anaerobic community was still growing at 30°C. It is interesting to speculate the cause of the maximal cultivability at lower temperatures. The anaerobic part of the community could be specifically adapted and active at the times of lower melt. During initial spring melt, there is a lack

of mixing by meltwater that can lead to anoxic zones and an ionic pulse (Telling et al., 2014) likely supports higher metabolic activity. Facultative anaerobic heterotrophs may therefore be important in the reactivation of the community after the polar night (Vick-Majors et al., 2014).

Limits of Cryoconite Microorganisms

Cryoconite microorganisms were able to grow in a wide range of pH values. Reported pH of cryoconite holes in Antarctica was pH ∼6–11 (Porazinska et al., 2004; Tranter et al., 2004; Bagshaw et al., 2007; Stanish et al., 2013), in Svalbard ∼4.7–8.6 (Kastovská et al., 2005; Singh and Singh, 2012), in Greenland ∼4.35 to 6.7 (Chandler, 2012, unpublished; Stibal, unpublished; Black and Bloom Team, 2016, unpublished), and in the Alps ∼5 (Margesin et al., 2002). To some extent, this growth range reflects the physical differences between Arctic and Antarctic holes, with Antarctic microorganisms growing in the highest pH in the laboratory and values up to pH 11 being measured in the field (Tranter et al., 2004). Most of Antarctic cryoconite isolates (7 out of 10) were able to grow in pH 10.5, suggesting that some of them could perhaps withstand even more alkaline conditions. At the other end of the spectrum are the yeast isolates, which seem to be more acidophilic than bacteria, tolerating pH of 3. The individual strains had specific tolerances that were similar to those previously published; for example, *Arthrobacter agilis* strain L77 from a lake in Himalayas (water pH 8.7 to 9.1) had a pH range of 6–9 and tolerated 5% salinity (Singh et al., 2014), whereas *Arthrobacter agilis* strain LV7 in this study from Antarctic cryoconite hole had a pH range of 7–10.5 and tolerated 6% salinity.

Tolerance of high salinity was a universal trait regardless of the sampling site, with all the isolated microorganisms able to grow outside the salinities typically found in cryoconite holes and on the glacier surfaces. Electrical conductivity (EC) of cryoconite holes in southwest Greenland was 2.2–3 $\mu S\ cm^{-1}$ (Chandler, 2012, unpublished) and in Antarctica 5–20 $\mu S\ cm^{-1}$ on Canada Glacier (Bagshaw et al., 2011) and ∼60–110 $\mu S\ cm^{-1}$ on Taylor Glacier (Porazinska et al., 2004). This compares with adjacent habitats which frequently have extreme EC: Lake Hoare and Lake Bonney (Taylor Valley) were 65–7798 $\mu S\ cm^{-1}$ (Courtright et al., 2001); Fresh, Orange, and Salt Ponds on the McMurdo Ice Shelf were 158, 937, and 52900 $\mu S\ cm^{-1}$ respectively (Jungblut et al., 2005) and soils in Wright Valley > 1500 $\mu S\ cm^{-1}$ (Courtright et al., 2001). In Svalbard, in the forefield of Midtre Lovenbreen, a 2347-year-old permafrost soil was ∼8200 $\mu S\ cm^{-1}$ (Hansen et al., 2007). These habitats are likely important inoculum for cryoconite holes (Porazinska et al., 2004; Bagshaw et al., 2013). Salinity tolerance may also assist in freeze-thaw protection: cryoconite holes undergo multiple freeze-thaw events in their lifetime, so microorganisms must either survive freezing, or avoid it by persisting in high salinity brine veins within the ice crystal structure (Mader et al., 2006; Telling et al., 2014). Fungi isolated from Svalbard sea ice and glacial ice grew better on halotolerant media than on the traditional media, with fungal growth up to 24% salinity, indicating that a high number of halophilic species can be found on glaciers and sea ice (Gunde-Cimerman et al., 2003). Another possibility is that resistance to salinity is the by-product of resilience to other environmental conditions such as high UV, dehydration or freezing (Poli et al., 2010). Cyanobacteria from hypersaline ponds on McMurdo Ice Shelf use organic osmolytes as a protection from osmotic stress (Jungblut et al., 2005) and large quantities of EPS were found in the brine channels in sea ice (Nichols et al., 2005). Mechanical damage to cell walls during freezing results either from intracellular ice crystals formation or recrystallization of extracellular small ice crystals into large grains, or by osmotic stress caused by dehydration following extracellular freezing and electrolyte concentration in the remaining liquid phase (Fonseca et al., 2001; Pegg, 2007; Raymond, 2016). The similar mechanisms of cell damage by dehydration, freezing and hypersaline solution often results in cross-protection, however, there was no correlation between high salinity resistance and other variables such as freeze-thaw survival in this study.

Physical damage sustained to the cell during freezing depends on its shape, structure and membrane rigidity (Jordan et al., 2008; Mai-Prochnow et al., 2016), hence it might explain some of the differences between the isolates. Yeasts have a thick cell wall composed of polysaccharides. Gram-positive bacteria have a thick (20–80 nm), rigid cell wall built of peptidoglycan, and Gram-negative bacteria have a thin wall. Gram-positive bacteria were classically considered to be typical for soil ecosystem and consequently adapted to dry conditions (Barka et al., 2016). In this study, all the yeasts survived well, and typically Gram-positive bacteria generally survived better (almost all survived 25 cycles and some survived 100) than Gram-negative (none survived 100 cycles). The structure of cell envelope has a major impact, but additional protection against concomitant damaging factors such as reactive oxygen species generated during thawing can be achieved by carotenoids – pigments which protect from photosensitization and from reactive oxygen species (Dahl et al., 1989; Park et al., 1997; Dieser et al., 2010; Mai-Prochnow et al., 2016). Most of the isolated cryoconite hole microorganisms are pigmented (**Table 3**). Another protective strategy is excreting protective antifreeze proteins and/or EPS (Poli et al., 2010; Sathiyanarayanan et al., 2015; Raymond, 2016; Perkins et al., 2017). Many cryophilic genera found also in cryoconite holes were shown to produce EPS, such as *Flavobacterium* sp. (Nichols et al., 2005; Sathiyanarayanan et al., 2015) or *Arthrobacter* sp. (Singh et al., 2014). The *Arthrobacter* genus was reported to survive multiple freeze thaw cycles (Muñoz et al., 2017). Moreover, numerous cryosphere bacteria show antifreeze proteins activity, including Actinobacteria and Bacteroidetes from Antarctic moss (Raymond, 2016), *Sphingomonas, Plantibacter, Pseudomonas*, and *Arthrobacter* sp. from Antarctic ice and sediments (Muñoz et al., 2017), or *Cryobacterium, Pseudomonas*, and *Subtercola* sp. among Arctic cryoconite bacteria (Singh et al., 2014). Most of the isolated bacteria in this study belong to Actinobacteria, and there are also several isolates of *Cryobacterium* from all locations.

Several isolates were tested to estimate the temperature range in which they were able to grow. Bacterial isolates were psychrotolerant, all being able to grow above the arbitrary

threshold for psychrophilic growth of 22°C (Cavicchioli, 2016). Yeasts, which only grew in the lower incubation temperatures and were able to better withstand freezing-thawing cycles, were psychrophiles. Although the sample size is small, it is interesting to debate the difference between bacteria and yeasts isolated form these cold environments. The results suggest that yeasts are better adapted to lower temperatures and stresses encountered in glacial environments such as freeze-thaw. Conversely, bacteria present a greater variability in their physiology, with some species adapted as well as yeasts to freeze-thaw and with similarly good salinity tolerance and broad pH range.

Survival of bacteria is therefore determined by multiple factors, including the structure of the cell envelope, internal pigments, excreted antifreeze proteins and compatible solutes. As the detailed mechanisms by which each species survives freeze-thawing were not the aim of this study, we can only speculate the cause of the differences. It was notable that yeasts are very resistant to freezing, yet they are not found as the dominant group in other studies of cryoconite community. The most abundant retrievable microorganisms of cryoconite holes are resistant to a wide range of fluctuating environmental conditions and stressors. Such conditions, including freeze-thaw cycles, high salinities, temporary anaerobic conditions and pH variability are typically encountered in arid polar soil habitats (Courtright et al., 2001; Paul, 2006; White, 2006; Poage et al., 2008; Bagshaw et al., 2013), which are likely to be seeding grounds for cryoconite holes.

Organic Carbon Utilization and Metabolic Capabilities

It is well known that organic matter is plentiful in cryoconite holes (Tranter et al., 2004; Musilova et al., 2016) and that there are genes present for biodegradation (Edwards et al., 2013) that are able to decompose organic matter (Sanyal et al., 2018). Thus, unsurprisingly, we detected strains which are known to decompose organic matter [e.g., *Flavobacterium* sp. (Williams et al., 2013), *Cryobacterium* sp. (Sanyal et al., 2018)]. Overall, cryoconite holes microorganisms produce a variety of enzymes for different groups of carbon substrates, suggesting they are effective in scavenging carbon substrates when and if they become available. Isolates obtained under anoxic conditions tend to utilize a higher proportion of carbohydrates when compared to those obtained aerobically. Facultatively anaerobic microorganisms have a different type of metabolism, depending on the availability of oxygen, and will commonly use monomeric sugars as their electron acceptor, hence it is unsurprising that they specialize in carbohydrates. Antarctic bacteria have the capacity to use a bigger pool of substrates, including "non-competitive" organic matter such as choline and betaine, when compared to the Arctic microorganisms. This can be explained by a smaller input of carbon sources due to entombment of Antarctic cryoconite holes (Telling et al., 2014; Webster-Brown et al., 2015), whereas the Arctic holes are frequently flushed with melt water during the melt season. Whilst the differences are not statistically significant, due to a very high variability among isolates, none of the Arctic isolates utilize "non-competitive" carbon substrates.

Some closely related isolates assigned to the same OTU showed striking differences in their metabolic capabilities. Without further studies it is impossible to pinpoint the source of the differences, but possible reasons include the initial incubation temperature, fitness of the culture and the metabolic impact of genome rearrangement in stressed and starving microorganisms. Such differences are quite common, for example *Cellulomonas* strains can have differences in their physiology (Hatayama et al., 2013), even when they are closely related (∼98% sequence similarity, which is enough to assign them to the same OTU). Another example is *Flavobacterium* genus, which is also widespread in cryoconite holes, where two distinct species had 98.9% 16S rRNA gene sequence similarity (Peeters and Willems, 2011). The resolution of 16S rRNA gene at species level is often limited, as it is a highly conserved gene (Peeters and Willems, 2011). Isolates which share the same OTU are not necessarily the same bacterium, it only means that they have a high degree of similarity in one gene. Even if they have highly similar 16S rRNA genes, their entire genome is not likely to be the same (Woese, 1987; Rosselló-Mora and Amann, 2001). Finally, culturing is a selective process, so it is possible that a single bacterium which gave a pure isolate was devoid of an enzymatic pathway. Therefore, while it is useful to investigate the capabilities of the organisms, we cannot exclude that in the environment their metabolic capabilities could differ, depending on overall fitness and competition. Regardless of these differences, microorganisms of cryoconite holes clearly complement each other and partly specialize in the types of substrates used. We might only speculate that it depends on the microniches within the cryoconite holes and the relationships with other microorganisms, as well as the availability of particular substrates, but there is not enough data in the literature on the composition of cryoconite organic matter to draw clearer conclusions. What can be concluded from this experiment is that isolates in pure culture were able to utilize a broad range of carbon substrates and as a community, they can scavenge almost all substrates tested. They seem well adapted to the extremely low organic matter content, which is typically encountered in glacial environments (Anesio and Laybourn-Parry, 2012) and barren Antarctic soils (Poage et al., 2008).

CONCLUSION

Microorganisms inhabiting cryoconite holes are exposed to a wide range of extreme conditions, and this study demonstrates their broad tolerance. The generally oxygen-rich cryoconite holes harbor an active, culturable anaerobic community. Anaerobic cultivability is better in the coldest conditions tested, which suggests their adaptation to and dominance of the beginning or end of the melt season, when anoxic conditions are likely to occur. Apart from anoxia, cultured microorganisms can withstand a wide range of other physical stresses, including extreme pH and salinity. As pH tolerance broadly reflected the values found in the samples locations, this may indicate that

extreme salinities could also be found in cryoconite holes in certain conditions, for example, during freeze-thaw cycles, or that the microbial community is seeded from nearby saline habitats, such as arid soils or melt ponds. Cryoconite microorganisms use a wide range of substrates and as a community are effective in scavenging limited carbon sources in cryoconite holes. Their metabolic capabilities seem to depend not only on the genetic affiliation, but also, perhaps, fitness of the culture and phenotypic differences between closely related species. Such phenotypic differences are especially likely, as the bacteria with a high 16S rRNA gene similarity show differences in their physiology. Antarctic isolates showed greater resistance to freezing and thawing cycles and greater use of variable carbon sources when compared to Arctic ones, suggesting they might be adapted to harsher conditions of Antarctic cryoconite holes. However, we found some of the same genera in both Arctic and Antarctic cryoconite holes, similar total cell numbers and the same range of salinities withstood, demonstrating that cryoconite hole microorganisms from both poles also share some physiological traits.

DATA AVAILABILITY STATEMENT

The datasets generated for this study can be found in the Genbank MT430950, MT432272–MT432304, MT473233, and MT473713–MT473721.

AUTHOR CONTRIBUTIONS

EP, EB, HS, MT, and AA contributed to the conception and design of the study. EP, HS, GW, CW, and AS performed the research. EP, EB, and HS analyzed the data. All authors contributed to the manuscript.

FUNDING

All authors acknowledge United Kingdom-funded Natural Environment Research Council (NERC) Consortium Grant "Black and Bloom" (NE/M021025/1). EP acknowledges NERC studentship (NE/L002434/1).

ACKNOWLEDGMENTS

We would like to thank Black and Bloom Team for field assistance. Details of the Black and Bloom Team can be found at: http://blackandbloom.org.

SUPPLEMENTARY MATERIAL

The Supplementary Material for this article can be found online at: https://www.frontiersin.org/articles/10.3389/fmicb.2020.01783/full#supplementary-material

REFERENCES

Anesio, A. M., and Laybourn-Parry, J. (2012). Glaciers and ice sheets as a biome. *Trends Ecol. Evol.* 27, 219–225. doi: 10.1016/j.tree.2011.09.012

Anesio, A. M., Sattler, B., Foreman, C., Telling, J., Hodson, A., Tranter, M., et al. (2010). Carbon fluxes through bacterial communities on glacier surfaces. *Ann. Glaciol.* 51, 32–40. doi: 10.3189/172756411795932092

Bagshaw, E. A., Tranter, M., Fountain, A. G., Welch, K., Basagic, H. J., and Lyons, W. B. (2013). Do cryoconite holes have the potential to be significant sources of C, N, and P to downstream depauperate ecosystems of Taylor Valley, Antarctica? Arctic, Antarct. *Alp. Res.* 45, 440–454. doi: 10.1657/1938-4246-45.4.440

Bagshaw, E. A., Tranter, M., Fountain, A. G., Welch, K. A., Basagic, H., and Lyons, W. B. (2007). Biogeochemical evolution of cryoconite holes on Canada Glacier, Taylor Valley, Antarctica. *J. Geophys. Res. Biogeosci.* 112, 4–35. doi: 10.1029/2007JG000442

Bagshaw, E. A., Tranter, M., Wadham, J. L., Fountain, A. G., Dubnick, A., and Fitzsimons, S. (2016). Processes controlling carbon cycling in Antarctic glacier surface ecosystems. *Geochem. Perspect. Lett.* 2, 44–54. doi: 10.7185/geochemlet.1605

Bagshaw, E. A., Tranter, M., Wadham, J. L., Fountain, A. G., and Mowlem, M. (2011). High-resolution monitoring reveals dissolved oxygen dynamics in an Antarctic cryoconite hole. *Hydrol. Process.* 25, 2868–2877. doi: 10.1002/hyp.8049

Barka, E. A., Vatsa, P., Sanchez, L., Gaveau-Vaillant, N., Jacquard, C., Klenk, H.-P., et al. (2016). Taxonomy, Physiology, and Natural Products of Actinobacteria. *Microbiol. Mol. Biol. Rev.* 80, 1–43. doi: 10.1128/mmbr.00019-15

Carvalho, A. S., Silva, J., Ho, P., Teixeira, P., Malcata, F. X., and Gibbs, P. (2004). Relevant factors for the preparation of freeze-dried lactic acid bacteria. *Int. Dairy J.* 14, 835–847. doi: 10.1016/j.idairyj.2004.02.001

Cavicchioli, R. (2016). On the concept of a psychrophile. *ISME J.* 10, 793–795. doi: 10.1038/ismej.2015.160

Christner, B. C., Kvitko, B. H., and Reeve, J. N. (2003). Molecular identification of Bacteria and Eukarya inhabiting an Antarctic cryoconite hole. *Extremophiles* 7, 177–183. doi: 10.1007/s00792-002-0309-300

Collins, T., and Margesin, R. (2019). Psychrophilic lifestyles: mechanisms of adaptation and biotechnological tools. *Appl. Microbiol. Biotechnol.* 103, 2857–2871. doi: 10.1007/s00253-019-09659-9655

Cook, J., Edwards, A., Takeuchi, N., and Irvine-Fynn, T. (2016). Cryoconite: the dark biological secret of the cryosphere. *Prog. Phys. Geogr.* 40, 66–111. doi: 10.1177/0309133315616574

Cook, J., Hodson, A., Telling, J., Anesio, A., Irvine-Fynn, T., and Bellas, C. (2010). The mass-area relationship within cryoconite holes and its implications for primary production. *Ann. Glaciol.* 51, 106–110. doi: 10.3189/172756411795932038

Cook, J. M., Hodson, A. J., Anesio, A. M., Hanna, E., Yallop, M., Stibal, M., et al. (2012). An improved estimate of microbially mediated carbon fluxes from the Greenland ice sheet. *J. Glaciol.* 58, 1098–1108. doi: 10.3189/2012JoG12J001

Courtright, E. M., Wall, D. H., and Virginia, R. A. (2001). Determining habitat suitability for soil invertebrates in an extreme environment: the McMurdo Dry Valleys, Antarctica. *Antarct. Sci.* 13, 9–17. doi: 10.1017/S0954102001000037

Cragg, B. A., and Kemp, A. E. S. (1995). "Bacterial Profiles in Deep Sediment Layers from the Eastern Equatorial Pacific Ocean, Site 851," in *Proceedings of the Ocean Drilling Program, 138 Scientific Results*, Texas, doi: 10.2973/odp.proc.sr.138.130.1995

Dahl, T. A., Midden, W. R., and Hartman, P. E. (1989). Comparison of killing of gram-negative and gram-positive bacteria by pure singlet oxygen. *J. Bacteriol.* 171, 2188–2194. doi: 10.1128/jb.171.4.2188-2194.1989

de Man, J. C. (1983). MPN tables, corrected. *Eur. J. Appl. Microbiol. Biotechnol.* 17, 301–305. doi: 10.1007/BF00508025

Dieser, M., Greenwood, M., and Foreman, C. M. (2010). Carotenoid pigmentation in Antarctic heterotrophic bacteria as a strategy to withstand environmental stresses. *Arctic, Antarct. Alp. Res.* 42, 396–405. doi: 10.1657/1938-4246-42.4.396

Edwards, A., Anesio, A. M., Rassner, S. M., Sattler, B., Hubbard, B., Perkins, W. T., et al. (2011). Possible interactions between bacterial diversity, microbial activity and supraglacial hydrology of cryoconite holes in Svalbard. *ISME J.* 5, 150–160. doi: 10.1038/ismej.2010.100

Edwards, A., Pachebat, J. A., Swain, M., Hegarty, M., Hodson, A. J., Irvine-Fynn, T. D. L., et al. (2013). A metagenomic snapshot of taxonomic and functional diversity in an alpine glacier cryoconite ecosystem. *Environ. Res. Lett.* 8:035003. doi: 10.1088/1748-9326/8/3/035003

Fonseca, F., Béal, C., and Corrieu, G. (2001). Operating conditions that affect the resistance of lactic acid bacteria to freezing and frozen storage. *Cryobiology* 43, 189–198. doi: 10.1006/cryo.2001.2343

Foreman, C. M., Sattler, B., Mikucki, J. A., Porazinska, D. L., and Priscu, J. C. (2007). Metabolic activity and diversity of cryoconites in the Taylor Valley, Antarctica. *J. Geophys. Res. Biogeosci.* 112:G04S32. doi: 10.1029/2006JG000358

Fountain, A. G., Tranter, M., Nylen, T. H., Lewis, K. J., and Mueller, D. R. (2004). Evolution of cryoconite holes and their contribution to meltwater runoff from glaciers in the McMurdo Dry Valleys, Antarctica. *J. Glaciol.* 50, 35–45. doi: 10.3189/172756504781830312

Franzetti, A., Tagliaferri, I., Gandolfi, I., Bestetti, G., Minora, U., Mayer, C., et al. (2016). Light-dependent microbial metabolisms drive carbon fluxes on glacier surfaces. *ISME J.* 10, 2984–2988. doi: 10.1038/ismej.2016.72

Gunde-Cimerman, N., Sonjak, S., Zalar, P., Frisvad, J. C., Diderichsen, B., and Plemenitaš, A. (2003). Extremophilic fungi in arctic ice: a relationship between adaptation to low temperature and water activity. *Phys. Chem. Earth* 28, 1273–1278. doi: 10.1016/j.pce.2003.08.056

Hansen, A. A., Herbert, R. A., Mikkelsen, K., Jensen, L. L., Kristoffersen, T., Tiedje, J. M., et al. (2007). Viability, diversity and composition of the bacterial community in a high Arctic permafrost soil from Spitsbergen, Northern Norway. *Environ. Microbiol.* 9, 2870–2884. doi: 10.1111/j.1462-2920.2007.01403.x

Hatayama, K., Esaki, K., and Ide, T. (2013). *Cellulomonas soli* sp. nov. and *Cellulomonas oligotrophica* sp. nov., isolated from soil. *Int. J. Syst. Evol. Microbiol.* 63(Pt 1), 60–65. doi: 10.1099/ijs.0.038364-38360

Hauptmann, A. L., Sicheritz-Pontén, T., Cameron, K. A., Baelum, J., Plichta, D. R., Dalgaard, M., et al. (2017). Contamination of the Arctic reflected in microbial metagenomes from the Greenland ice sheet. *Environ. Res. Lett.* 12:aa7445. doi: 10.1088/1748-9326/aa7445

Hodson, A., Anesio, A. M., Tranter, M., Fountain, A., Osborn, M., Priscu, J., et al. (2008). Glacial ecosystems. *Ecol. Monogr.* 78, 41–67. doi: 10.1890/07-0187.1

Hodson, A., Cameron, K., Bøggild, C., Irvine-Fynn, T., Langford, H., Pearce, D., et al. (2010). The structure, biological activity and biogeochemistry of cryoconite aggregates upon an arctic valley glacier: Longyearbreen. *Svalbard. J. Glaciol.* 56, 349–362. doi: 10.3189/002214310791968403

Holland, A. T., Williamson, C. J., Sgouridis, F., Tedstone, A. J., McCutcheon, J., Cook, J. M., et al. (2019). Dissolved organic nutrients dominate melting surface ice of the Dark Zone (Greenland Ice Sheet). *Biogeosciences* 16, 3283–3296. doi: 10.5194/bg-16-3283-2019

Ihrmark, K., Bödeker, I. T. M., Cruz-Martinez, K., Friberg, H., Kubartova, A., Schenck, J., et al. (2012). New primers to amplify the fungal ITS2 region - evaluation by 454-sequencing of artificial and natural communities. *FEMS Microbiol. Ecol.* 82, 666–677. doi: 10.1111/j.1574-6941.2012.01437.x

Jordan, S., Hutchings, M. I., and Mascher, T. (2008). Cell envelope stress response in Gram-positive bacteria. *FEMS Microbiol. Rev.* 32, 107–146. doi: 10.1111/j.1574-6976.2007.00091.x

Jungblut, A. D., Hawes, I., Mountfort, D., Hitzfeld, B., Dietrich, D. R., Burns, B. P., et al. (2005). Diversity within cyanobacterial mat communities in variable salinity meltwater ponds of McMurdo Ice Shelf, Antarctica. *Environ. Microbiol.* 7, 519–529. doi: 10.1111/j.1462-2920.2005.00717.x

Kaksonen, A. H., Plumb, J. J., Robertson, W. J., Spring, S., Schumann, P., Franzmann, P. D., et al. (2006). Novel thermophilic sulfate-reducing bacteria from a geothermally active underground mine in Japan. *Appl. Environ. Microbiol.* 72, 3759–3762. doi: 10.1128/AEM.72.5.3759-3762.2006

Kastovská, K., Elster, J., Stibal, M., and Santrùcková, H. (2005). Microbial assemblages in soil microbial succession after glacial retreat in Svalbard (high arctic). *Microb. Ecol.* 50, 396–407. doi: 10.1007/s00248-005-0246-244

Köpke, B., Wilms, R., Engelen, B., Cypionka, H., and Sass, H. (2005). Microbial diversity in coastal subsurface sediments: a cultivation approach using various electron acceptors and substrate gradients. *Appl. Environ. Microbiol.* 71, 7819–7830. doi: 10.1128/AEM.71.12.7819-7830.2005

Langford, H., Hodson, A., Banwart, S., and Bøggild, C. (2010). The microstructure and biogeochemistry of Arctic cryoconite granules. *Ann. Glaciol.* 51, 87–94. doi: 10.3189/172756411795932083

Lutz, S., Ziolkowski, L. A., and Benning, L. G. (2019). The biodiversity and geochemistry of cryoconite holes in queen maud land, East Antarctica. *Microorganisms* 7:160. doi: 10.3390/microorganisms7060160

Mader, H. M., Pettitt, M. E., Wadham, J. L., Wolff, E. W., and Parkes, R. J. (2006). Subsurface ice as a microbial habitat. *Geology* 34, 169–172. doi: 10.1130/G22096.1

Mai-Prochnow, A., Clauson, M., Hong, J., and Murphy, A. B. (2016). Gram positive and Gram negative bacteria differ in their sensitivity to cold plasma. *Sci. Rep.* 6:38610. doi: 10.1038/srep38610

Margesin, R., Zacke, G., and Schinner, F. (2002). Characterization of heterotrophic microorganisms in alpine glacier cryoconite. *Arctic Antarct. Alp. Res.* 34, 88–93. doi: 10.2307/1552512

Martens-Habbena, W., and Sass, H. (2006). Sensitive determination of microbial growth by nucleic acid staining in aqueous suspension. *Appl. Environ. Microbiol.* 72, 87–95. doi: 10.1128/AEM.72.1.87-95.2006

McIntyre, N. F. (1984). Cryoconite hole thermodynamics. *Can. J. Earth Sci.* 21, 152–156. doi: 10.1139/e84-016

Meneghel, J., Passot, S., Dupont, S., and Fonseca, F. (2017). Biophysical characterization of the *Lactobacillus delbrueckii* subsp. bulgaricus membrane during cold and osmotic stress and its relevance for cryopreservation. *Appl. Microbiol. Biotechnol.* 101, 1427–1441. doi: 10.1007/s00253-016-7935-7934

Michaud, L., Caruso, C., Mangano, S., Interdonato, F., Bruni, V., and Lo Giudice, A. (2012). Predominance of *Flavobacterium*, *Pseudomonas*, and *Polaromonas* within the prokaryotic community of freshwater shallow lakes in the northern Victoria Land, East Antarctica. *FEMS Microbiol. Ecol.* 82, 391–404. doi: 10.1111/j.1574-6941.2012.01394.x

Muñoz, P. A., Márquez, S. L., González-Nilo, F. D., Márquez-Miranda, V., and Blamey, J. M. (2017). Structure and application of antifreeze proteins from Antarctic bacteria. *Microb. Cell Fact.* 16:138. doi: 10.1186/s12934-017-0737-732

Musilova, M., Tranter, M., Bamber, J. L., Takeuchi, N., and Anesio, A. (2016). Experimental evidence that microbial activity lowers the albedo of glaciers. *Geochemical Perspect. Lett.* 2, 106–116. doi: 10.7185/geochemlet.1611

Musilova, M., Tranter, M., Bennett, S. A., Wadham, J., and Anesio, A. M. (2015). Stable microbial community composition on the Greenland Ice Sheet. *Front. Microbiol.* 6:193. doi: 10.3389/fmicb.2015.00193

Nichols, C. M., Lardière, S. G., Bowman, J. P., Nichols, P. D., Gibson, J. A. E., and Guézennec, J. (2005). Chemical characterization of exopolysaccharides from Antarctic marine bacteria. *Microb. Ecol.* 49, 578–589. doi: 10.1007/s00248-004-0093-98

Park, J. I., Grant, C. M., Attfield, P. V., and Dawes, I. W. (1997). The freeze-thaw stress response of the yeast *Saccharomyces cerevisiae* is growth phase specific and is controlled by nutritional state via the RAS- Cyclic AMP signal transduction pathway. *Appl. Environ. Microbiol.* 63, 3818–3824. doi: 10.1128/aem.63.10.3818-3824.1997

Paul, E. A. (2006). *Soil Microbiology, Ecology and Biochemistry*, 3rd Edn. Amsterdam: Elsevier, doi: 10.1016/C2009-0-02816-2815

Peeters, K., and Willems, A. (2011). The gyrB gene is a useful phylogenetic marker for exploring the diversity of *Flavobacterium* strains isolated from terrestrial and aquatic habitats in Antarctica. *FEMS Microbiol. Lett.* 321, 130–140. doi: 10.1111/j.1574-6968.2011.02326.x

Pegg, D. E. (2007). Principles of cryopreservation. *Methods Mol. Biol.* 368, 39–57. doi: 10.1007/978-1-59745-362-2_3

Perkins, R. G., Bagshaw, E., Mol, L., Williamson, C. J., Fagan, D., Gamble, M., et al. (2017). Photoacclimation by arctic cryoconite phototrophs. *FEMS Microbiol. Ecol.* 93:fix018. doi: 10.1093/femsec/fix018

Petchey, O. L., and Gaston, K. J. (2006). Functional diversity: back to basics and looking forward. *Ecol. Lett.* 9, 741–758. doi: 10.1111/j.1461-0248.2006.00924.x

Poage, M. A., Barrett, J. E., Virginia, R. A., and Wall, D. H. (2008). The influence of soil geochemistry on nematode distribution, Mcmurdo Dry Valleys, Antarctica. *Arctic, Antarct. Alp. Res.* 40, 119–128. doi: 10.1657/1523-0430(06-0

Poli, A., Anzelmo, G., and Nicolaus, B. (2010). Bacterial exopolysaccharides from extreme marine habitats: production, characterization and biological activities. *Mar. Drugs* 8, 1779–1802. doi: 10.3390/md8061779

Poniecka, E. A., Bagshaw, E. A., Tranter, M., Sass, H., Williamson, C. J., and Anesio, A. M. (2018). Rapid development of anoxic niches in supraglacial ecosystems. *Arctic, Antarct. Alp. Res.* 50:S100015. doi: 10.1080/15230430.2017.1420859

Porazinska, D. L., Fountain, A. G., Nylen, T. H., Tranter, M., Virginia, R. A., and Wall, D. H. (2004). The biodiversity and biogeochemistry of cryoconite holes from McMurdo Dry Valley glaciers, Antarctica. *Arctic, Antarct. Alp. Res.* 36, 84–91. doi: 10.1657/1523-0430(2004)036[0084:tbaboc]2.0.co;2

Raymond, J. A. (2016). Dependence on epiphytic bacteria for freezing protection in an Antarctic moss, *Bryum argenteum*. *Environ. Microbiol. Rep.* 8, 14–19. doi: 10.1111/1758-2229.12337

Rosselló-Mora, R., and Amann, R. (2001). The species concept for prokaryotes. *FEMS Microbiol. Rev.* 25, 39–67. doi: 10.1016/S0168-6445(00

Sanyal, A., Antony, R., Samui, G., and Thamban, M. (2018). Microbial communities and their potential for degradation of dissolved organic carbon in cryoconite hole environments of Himalaya and Antarctica. *Microbiol. Res.* 208, 32–42. doi: 10.1016/j.micres.2018.01.004

Sass, H., Cypionka, H., and Babenzien, H. D. (1997). Vertical distribution of sulfate-reducing bacteria at the oxic-anoxic interface in sediments of the oligotrophic Lake Stechlin. *FEMS Microbiol. Ecol.* 22, 245–255. doi: 10.1016/S0168-6496(96)00096-97

Sathiyanarayanan, G., Yi, D. H., Bhatia, S. K., Kim, J. H., Seo, H. M., Kim, Y. G., et al. (2015). Exopolysaccharide from psychrotrophic Arctic glacier soil bacterium *Flavobacterium* sp. ASB 3-3 and its potential applications. *RSC Adv.* 5, 84492–84502. doi: 10.1039/c5ra14978a

Singh, P., Hanada, Y., Singh, S. M., and Tsuda, S. (2014). Antifreeze protein activity in Arctic cryoconite bacteria. *FEMS Microbiol. Lett.* 351, 14–22. doi: 10.1111/1574-6968.12345

Singh, P., and Singh, S. M. (2012). Characterization of yeast and filamentous fungi isolated from cryoconite holes of Svalbard, Arctic. *Polar Biol.* 35, 575–583. doi: 10.1007/s00300-011-1103-1101

Smeets, P. C. J. P., Kuipers Munneke, P., van As, D., van den Broeke, M. R., Boot, W., Oerlemans, H., et al. (2018). The K-transect in west Greenland: automatic weather station data (1993–2016). *Arctic Antarct. Alp. Res.* 50:S100002. doi: 10.1080/15230430.2017.1420954

Srivastava, N., Gupta, B., Gupta, S., Danquah, M. K., and Sarethy, I. P. (2019). Analyzing functional microbial diversity: an overview of techniques. *Microb. Divers. Genomic Era* 2019, 79–102. doi: 10.1016/B978-0-12-814849-5.00006-X

Stanish, L. F., Bagshaw, E. A., McKnight, D. M., Fountain, A. G., and Tranter, M. (2013). Environmental factors influencing diatom communities in Antarctic cryoconite holes. *Environ. Res. Lett.* 8:45006.

Stibal, M., Šabacká, M., and Kaštovská, K. (2006). Microbial communities on glacier surfaces in Svalbard: impact of physical and chemical properties on abundance and structure of cyanobacteria and algae. *Microb. Ecol.* 52, 644–654. doi: 10.1007/s00248-006-9083-9083

Stibal, M., Tranter, M., Benning, L. G., and Rìhák, J. (2008). Microbial primary production on an Arctic glacier is insignificant in comparison with allochthonous organic carbon input. *Environ. Microbiol.* 10, 2172–2178. doi: 10.1111/j.1462-2920.2008.01620.x

Stocker, T. F., Qin, D., Plattner, G. K., Tignor, M. M. B., Allen, S. K., Boschung, J., et al. (2013). *Climate Change 2013 the Physical Science Basis: Working Group I Contribution to the Fifth Assessment Report of the Intergovernmental Panel on Climate Change*. Cambridge: Cambridge University Press, doi: 10.1017/CBO9781107415324

Süß, J., Herrmann, K., Seidel, M., Cypionka, H., Engelen, B., and Sass, H. (2008). Two distinct Photobacterium populations thrive in ancient *Mediterranean sapropels*. *Microb. Ecol.* 55, 371–383. doi: 10.1007/s00248-007

Telling, J., Anesio, A. M., Tranter, M., Fountain, A. G., Nylen, T., Hawkings, J., et al. (2014). Spring thaw ionic pulses boost nutrient availability and microbial growth in entombed Antarctic Dry Valley cryoconite holes. *Front. Microbiol.* 5:694. doi: 10.3389/fmicb.2014.00694

Tranter, M., Fountain, A. G., Fritsen, C. H., Lyons, W. B., Priscu, J. C., Statham, P. J., et al. (2004). Extreme hydrochemical conditions in natural microcosms entombed within Antarctic ice. *Hydrol. Process.* 18, 379–387. doi: 10.1002/hyp.5217

Vick-Majors, T. J., Priscu, J. C., and Amaral-Zettler, L. A. (2014). Modular community structure suggests metabolic plasticity during the transition to polar night in ice-covered Antarctic lakes. *ISME J.* 8, 778–789. doi: 10.1038/ismej.2013.190

Webster, G., John Parkes, R., Cragg, B. A., Newberry, C. J., Weightman, A. J., and Fry, J. C. (2006). Prokaryotic community composition and biogeochemical processes in deep subseafloor sediments from the Peru Margin. *FEMS Microbiol. Ecol.* 58, 65–85. doi: 10.1111/j.1574-6941.2006.00147.x

Webster-Brown, J. G., Hawes, I., Jungblut, A. D., Wood, S. A., and Christenson, H. K. (2015). The effects of entombment on water chemistry and bacterial assemblages in closed cryoconite holes on Antarctic glaciers. *FEMS Microbiol. Ecol.* 91:fiv144. doi: 10.1093/femsec/fiv144

Wharton, R. A., McKay, C. P., Simmons, G. M., and Parker, B. C. (1985). Cryoconite holes on glaciers. *Bioscience* 35, 499–503. doi: 10.2307/1309818

White, R. E. (2006). *Principles and Practice of Soil Science: The Soil as a Natural Resource*. Bengaluru: Wiley India Pvt. Limited, doi: 10.1002/msj.20251

White, T. J., Bruns, T., Lee, S., and Taylor, J. (1990). "Amplification and direct sequencing of fungal ribosomal RNA genes for phylogenetics," in *PCR Protocols: A Guide to Methods and Applications*, eds J. J. Sninsky, D. H. Gelfand, T. J. White, and M. A. Innis, (Amsterdam: Elsevier), 315–322. doi: 10.1016/b978-0-12-372180-8.50042-50041

Williams, T. J., Wilkins, D., Long, E., Evans, F., Demaere, M. Z., Raftery, M. J., et al. (2013). The role of planktonic Flavobacteria in processing algal organic matter in coastal East Antarctica revealed using metagenomics and metaproteomics. *Environ. Microbiol.* 15, 1302–1317. doi: 10.1111/1462-2920.12017

Williamson, C. J., Cook, J., Tedstone, A., Yallop, M., McCutcheon, J., Poniecka, E., et al. (2020). Algal photophysiology drives darkening and melt of the Greenland Ice Sheet. *Proc. Natl. Acad. Sci.* 2020:201918412. doi: 10.1073/pnas.1918412117

Wilson, S. L., Grogan, P., and Walker, V. K. (2012). Prospecting for ice association: characterization of freeze-thaw selected enrichment cultures from latitudinally distant soils. *Can. J. Microbiol.* 58, 402–412. doi: 10.1139/W2012-010

Woese, C. R. (1987). Bacterial evolution. *Microbiol. Rev.* 10, 283–291. doi: 10.1128/mmbr.51.2.221-271.1987

Wolin, E. A., Wolin, M. J., and Wolfe, R. S. (1963). Formation of methane by bacterial extracts. *J. Biol. Chem.* 238, 2882–2886.

Zdanowski, M. K., Bogdanowicz, A., Gawor, J., Gromadka, R., Wolicka, D., and Grzesiak, J. (2016). Enrichment of Cryoconite Hole Anaerobes: implications for the Subglacial Microbiome. *Microb. Ecol.* 2016, 1–7.

Conflict of Interest: The authors declare that the research was conducted in the absence of any commercial or financial relationships that could be construed as a potential conflict of interest.

frontiers in Microbiology

ORIGINAL RESEARCH
published: 18 December 2020
doi: 10.3389/fmicb.2020.540404

The Total and Active Bacterial Community of the Chlorolichen *Cetraria islandica* and Its Response to Long-Term Warming in Sub-Arctic Tundra

Ingeborg J. Klarenberg[1,2], Christoph Keuschnig[3], Denis Warshan[2], Ingibjörg Svala Jónsdóttir[2] and Oddur Vilhelmsson[1,4,5]*

[1] Natural Resource Sciences, University of Akureyri, Akureyri, Iceland, [2] Faculty of Life and Environmental Sciences, University of Iceland, Reykjavík, Iceland, [3] Environmental Microbial Genomics, Laboratoire Ampère, CNRS, École Centrale de Lyon, Écully, France, [4] BioMedical Center, University of Iceland, Reykjavík, Iceland, [5] School of Biological Sciences, University of Reading, Reading, United Kingdom

OPEN ACCESS

Edited by:
David Anthony Pearce, Northumbria University, United Kingdom

Reviewed by:
Soon Gyu Hong, Korea Polar Research Institute, South Korea
Claudia Colesie, University of Edinburgh, United Kingdom

***Correspondence:**
Ingeborg J. Klarenberg
ingeborg.klarenberg@gmail.com

Specialty section:
This article was submitted to Extreme Microbiology, a section of the journal Frontiers in Microbiology

Received: *04 March 2020*
Accepted: *30 November 2020*
Published: *18 December 2020*

Citation:
Klarenberg IJ, Keuschnig C, Warshan D, Jónsdóttir IS and Vilhelmsson O (2020) The Total and Active Bacterial Community of the Chlorolichen Cetraria islandica and Its Response to Long-Term Warming in Sub-Arctic Tundra. Front. Microbiol. 11:540404. doi: 10.3389/fmicb.2020.540404

Lichens are traditionally defined as a symbiosis between a fungus and a green alga and or a cyanobacterium. This idea has been challenged by the discovery of bacterial communities inhabiting the lichen thalli. These bacteria are thought to contribute to the survival of lichens under extreme and changing environmental conditions. How these changing environmental conditions affect the lichen-associated bacterial community composition remains unclear. We describe the total (rDNA-based) and potentially metabolically active (rRNA-based) bacterial community of the lichen *Cetaria islandica* and its response to long-term warming using a 20-year warming experiment in an Icelandic sub-Arctic tundra. 16S rRNA and rDNA amplicon sequencing showed that the orders Acetobacterales (of the class Alphaproteobacteria) and Acidobacteriales (of the phylum Acidobacteria) dominated the bacterial community. Numerous amplicon sequence variants (ASVs) could only be detected in the potentially active community but not in the total community. Long-term warming led to increases in relative abundance of bacterial taxa on class, order and ASV level. Warming altered the relative abundance of ASVs of the most common bacterial genera, such as *Granulicella* and *Endobacter*. The potentially metabolically active bacterial community was also more responsive to warming than the total community. Our results suggest that the bacterial community of the lichen *C. islandica* is dominated by acidophilic taxa and harbors disproportionally active rare taxa. We also show for the first time that climate warming can lead to shifts in lichen-associated bacterial community composition.

Keywords: lichen, lichen microbiome, tundra, climate change, host–microbiome, lichen-associated bacteria, long-term warming

INTRODUCTION

The notion that lichens harbor diverse bacterial and fungal communities has challenged the traditional view of the lichen as a symbiosis between a fungus (mycobiont) and an alga and/or a cyanobacterium (photobiont) (González et al., 2005; Spribille et al., 2016). Nonetheless, the first lichen-associated bacteria were already discovered in the 1920s (Uphof, 1925). To date, bacterial communities of a wide-range of lichen species have been revealed by molecular approaches (Cardinale et al., 2006, 2008; Grube et al., 2009; Hodkinson and Lutzoni, 2009; Bjelland et al., 2011; Mushegian et al., 2011; Weiss et al., 2011; Sigurbjörnsdóttir et al., 2015; Park et al., 2016). Alphaproteobacteria usually dominate the lichen microbiome, but other taxa such as Actinobacteria, Firmicutes, Acidobacteria, Betaproteobacteria, Deltaproteobacteria, and Gammaproteobacteria are also found. These bacteria can form highly structured, biofilm-like assemblages on fungal surfaces and within the lichen thallus (Grube et al., 2009). The bacterial communities inhabiting the lichen thalli play important roles in the lichen holobiont (the lichen and its microbiome), by contributing to nutrient supply, resistance against biotic and abiotic stresses, production of vitamins and support of fungal and algal growth by the production of hormones, detoxification of metabolites and degradation of senescing parts of the lichen thallus (Grube et al., 2015; Sigurbjörnsdóttir et al., 2015). Thereby, the bacterial part of the lichen holobiont is suggested to contribute to the survival of lichens under extreme and changing environmental conditions.

The composition of associated bacterial communities of lichens may be shaped by intrinsic and extrinsic factors. Among intrinsic factors affecting the lichen microbiome are thallus age (Cardinale et al., 2012b), mycobiont species, and photobiont species (Grube et al., 2009; Weiss et al., 2011; Hodkinson et al., 2012; Wedin et al., 2016; Coleine et al., 2019). The composition of lichen bacterial communities can also be influenced by extrinsic factors such as sunlight exposure and substrate type (Cardinale et al., 2012b; Park et al., 2016), geography and local habitat (Cardinale et al., 2012a; Hodkinson et al., 2012; Printzen et al., 2012; West et al., 2018), altitude (Coleine et al., 2019), drought (Cernava et al., 2019), and arsenic contamination (Cernava et al., 2018). Some lichens can adapt to changing environmental factors by switching photobionts depending on the ecological niche of the photobiont (Domaschke et al., 2013; Rolshausen et al., 2018). Some lichens have also been shown to be able to acclimate to higher temperature by increasing their respiration (Lange and Green, 2005) or net photosynthesis (Colesie et al., 2018). However, not all lichens are able to adapt to changing environments in these ways. Lichens might also be able to acclimate through changes in their associated bacterial communities. This strategy has been demonstrated for several environmental factors, such as drought (Cernava et al., 2019) and arsenic contamination (Cernava et al., 2018). Substrate type is another extrinsic factor that can influence the composition of bacterial communities (Cardinale et al., 2012b). Therefore, changes in C (carbon) or N (nitrogen) availability in the environment, for instance as a result of changes in plant litter quality due to shrubification (McLaren et al., 2017), might be factors altering the structure of the lichen microbiome. However, little is known about the effect of long-term environmental changes on the bacterial communities associated with lichens.

High-latitudes are especially rich in lichen species and biomass (Cornelissen et al., 2007; Nash, 2008), where they make significant contributions to ecosystem functioning (Asplund and Wardle, 2017). Mat-forming lichens such as Cetraroid species contribute to primary production and nutrient cycling, control soil chemistry and water retention (Cornelissen et al., 2007). Currently, climate in high-latitudes warms twice as fast as elsewhere (IPCC, 2019) resulting in increased abundance of shrubs, particularly in the low and sub-Arctic (Elmendorf et al., 2012; Myers-Smith et al., 2019). Direct effects of warming on lichens include changes in C-based secondary compounds (Asplund et al., 2017) and increased biomass (Biasi et al., 2008). Warming also has indirect effects on lichens. In many low and sub-Arctic tundra ecosystems shrubification results in increased shading and greater amounts of litter, which can lead to decreased lichen photosynthesis rates causing a decline in lichen biomass (Nash and Olafsen, 1995; Cornelissen et al., 2001; Elmendorf et al., 2012; Fraser et al., 2014; Alatalo et al., 2017). Yet, the effect of long-term warming on the bacterial communities of lichens in high-latitudes needs to be investigated.

In this study we investigate the total and potentially metabolically active bacterial community of the lichen *Cetraria islandica* (L.) Ach. (English "Iceland moss") and its response to two decades of warming in open top chambers (OTCs) in an Icelandic sub-Arctic alpine dwarf-shrub heath. *C. islandica* is a mat-forming chlorolichen with foliose thalli and forms a major component of the vegetation in Arctic, sub-Arctic and alpine environments throughout the northern hemisphere (Kärnefelt et al., 1993). 16S rRNA and rDNA sequencing was used to characterize the potentially active and total bacterial community in control plots and OTCs. We also quantified 16S rRNA gene abundance by quantitative PCR to compare the absolute abundance of bacteria in the controls and OTCs. Finally, it was recently demonstrated that N_2-fixing bacteria could associate with chlorolichens (Almendras et al., 2018). Thus, we also quantified the number of *nifH* genes by quantitative PCR in order to test if the *C. islandica* microbiome could potentially perform N_2-fixation and how warming influences the abundance of associated N_2-fixers.

We predicted that long-term warming and the associated increase in tundra shrubs and litter will lead to an increase in heterotrophic, biopolymer-degrading bacterial taxa and a higher incidence of potentially lichenivorous or lichenopathogenic bacteria, such as shown for the plant phyllosphere (Aydogan et al., 2018). Thus, in terms of taxonomic composition, we expected an increase in detritivorous taxa, endosymbionts and pathogens of fungi such as chitinolytic bacteria (Kobayashi and Crouch, 2009), whereas the relative abundance of cold-adapted and facultatively lithotrophic bacteria may decrease.

We also hypothesized that the potentially metabolically active (16S rRNA based) community shows a larger change in richness, diversity and community structure to the warming treatment

than the total bacterial community, as has been shown for the effect of drought (Bastida et al., 2017).

MATERIALS AND METHODS

Study Site and Experimental Design

The study site is located in a *Betula nana* heath in the Icelandic central highlands at an altitude of 450 m. According to Köppen's climate definitions, the sampling site, called Auðkúluheiði (65°16′N, 20°15′W, 480 m above sea level) is situated in the lower Arctic. The vegetation is characterized as a relatively species-rich dwarf shrub heath, with *B. nana* being the most dominant vascular species and the moss *Racomitrium lanuginosum* and the lichen *C. islandica* as the dominating cryptogam species (Jonsdottir et al., 2005).

Ten OTCs were set up to simulate a warmer summer climate in August 1996 in a fenced area to exclude sheep grazing (Hollister and Webber, 2000; Jonsdottir et al., 2005). The OTCs raise the mean daily temperature by 1–2°C during summer and minimize secondary experimental effects such as differences in atmospheric gas concentration and reduction in ambient precipitation. Control plots were established adjacent to the OTCs, but without any treatment, thus exposing the environment to ambient temperatures. Air temperatures measured in the growing season from 1999 to 2002 at the surface of the cryptogam layer indicated an average increase of 0.7–1.0°C in the OTCs (Jonsdottir et al., 2005). Air temperature measured 10 cm above the moss layer in summer 2016 was on average 1.4°C higher in the OTC than in the control plot of one of the plot pairs ($t = -8.2$, $P < 0.001$) (**Supplementary Table 1**). Relative humidity measured in the same plot pair and period was 3% lower in the OTC than in the control plot ($t = 26.9$, $P < 0.001$) (**Supplementary Table 1**). Temperatures on the moss surface measured in all OTCs and control plots from mid-August 2018 to mid-June 2019 were on average 0.22°C higher in the OTCs compared to the control plots ($t = -16.4$, $P < 0.001$) (**Supplementary Table 1**).

The response of the vegetation was monitored by a detailed vegetation analysis after peak biomass at a few year intervals using the point intercept method following standard protocols of the International Tundra Experiment (ITEX: 100 points per plot, all hits (intercepts) per species recorded in each point through the canopy; relates to biomass) (Jonsdottir et al., 2005). In 2014, the abundance of *B. nana* was on average 2.5 times larger in the OTCs than in the control plots and litter was 2.7 times more abundant in the OTCs than in the control plots (Jónsdóttir, unpublished data). In this study we use these data on abundance (total number of hits per plot) of *B. nana* and litter to test the effect of vegetation change on the richness, diversity, community structure of the lichen associated bacterial community as well 16S rRNA and *nifH* gene abundance.

Per warmed (OTC) and control plot, the upper parts (2 × 2 cm) of five lichen thalli were randomly selected and collected with sterile tweezers. The samples were immediately soaked in RNAlater (Ambion) to prevent RNA degradation and kept cool until storage at −80°C. The lichen samples were collected in June 2017.

RNA and DNA Extraction and Sequencing

Prior to RNA and DNA extraction, the samples were washed with RNase free water to get rid of soil particles and RNAlater and ground for six minutes using a Mini-Beadbeater and two sterile steel beads. RNA and DNA were extracted simultaneously using the RNeasy PowerSoil Total RNA Kit (Qiagen) and the RNeasy PowerSoil DNA Elution Kit (Qiagen), following the manufacturer's instructions. DNA and RNA concentrations were measured with a Qubit Fluorometer (Life Technologies) and purity was assessed with a NanoDrop (NanoDrop Technologies) and integrity by Bioanalyzer (Agilent Technologies). cDNA was synthesized using the High-Capacity cDNA Reverse Transcription Kit (Thermofisher) following the manufacturer's instructions and quantified on a Qubit Fluorometer (Life Technologies). From the 100 DNA and 100 cDNA samples, we selected 48 DNA samples (24 from each treatment) and 48 cDNA samples (24 from each treatment) for sequencing based on the RNA and DNA quantity and quality. Library preparation and sequencing of the V3–V4 region of the 16S rRNA gene on an Illumina MiSeq platform was performed by Macrogen (Seoul), using the standard Illumina protocol. The primer pair 337F/805R and the same PCR condition described in Klindworth et al. (2013) were used.

Sequence Processing

In order to obtain high-resolution data, we processed the raw sequences using the DADA2 pipeline (Callahan et al., 2016, 2017). Hereby, sequences are not clustered into operational taxonomic units (OTUs), but exact sequences or amplicon sequence variants (ASVs). Forward reads were truncated at 260 bp and reverse reads at 250 bp. Assembled ASVs were assigned taxonomy against the SILVA_132 database (Quast et al., 2013) using the Ribosomal Database Project (RDP) naïve Bayesian classifier (Wang et al., 2007) in DADA2. We discarded samples with less than 10,000 non-chimeric sequences and/or less than 50 ASVs. We removed ASVs assigned to chloroplasts and mitochondria, singletons, doubletons and ASVs occurring in only one sample. In total, for 82 samples, 1,954 ASVs remained. The data were normalized using cumulative-sum scaling (CSS) (Paulson et al., 2013) to account for uneven sequencing depths.

The 16S rDNA based community is hereafter sometimes referred to as the DNA based community and the 16S rRNA (cDNA) based community is hereafter referred to as the cDNA based community. We interpret the cDNA based community as the "potentially metabolically active bacterial community," acknowledging that 16S rRNA is not a direct indicator of activity but rather protein synthesis potential (Blazewicz et al., 2013).

Quantitative Real-Time PCR of nifH and 16S rRNA Genes

We used all 100 DNA extractions (50 replicates per treatment) for quantification of *nifH* and 16S rRNA genes, which was

performed by quantitative PCR (Corbett Rotor-Gene) using the primer set PolF/PolR and 341F/534R, respectively (Poly et al., 2001). The specificity of the *nifH* primers for our samples was confirmed by SANGER sequencing of 10 clone fragments. Standards for *nifH* reactions were obtained by amplifying one cloned *nifH* sequence with flanking regions of the plasmid vector (TOPO TA cloning Kit, Invitrogen). Standard curves were obtained by serial dilutions (E = 0.9–1.1, R^2 = > 0.99 for all reactions). Each reaction had a volume of 20 μL, containing 1× QuantiFast SYBR Green PCR Master Mix (Qiagen), 0.2 μL of each primer (10 μM), 0.8 μL BSA (5 μg/μL), 6.8 μL RNase free water, and 2 μL template. The cycling program was 5 min at 95°C, 30 cycles of 10 s at 95°C and 30 s at 60°C.

Statistical Analysis

Statistical analyses were conducted in R version 3.6.1. Richness (number of ASVs) and Shannon diversity were calculated with the R packages "vegan" (Oksanen et al., 2013) and "phyloseq" (McMurdie and Holmes, 2013).

Differences in 16S rRNA and *nifH* gene abundance, ASV richness and Shannon diversity between the treatments and the DNA and cDNA were assessed with Bayesian (Markov chain Monte Carlo) generalized linear models using the R package "MCMCglmm" (Hadfield, 2010) with treatment as a fixed and plot as a random factor to take into account the variation caused by pseudoreplication. We considered differences significant if the modeled 95% confidence intervals did not overlap. In addition to the effect of treatment, we included *B. nana* and litter abundance in these generalized linear models. The effect of *B. nana* and/or litter abundance was considered significant if 95% High Posterior Density Credible Interval (95% CrI) were not overlapping zero.

Distances between the community composition of the control and OTC samples were based on Bray-Curtis distances. The effect of the treatment, *B. nana* abundance and litter abundance on the bacterial community composition was tested by permutational-MANOVA (PERMANOVA) (Anderson, 2001) analysis of the Bray-Curtis distance matrices using the *adonis* function in the R package "vegan" with plot as strata. Principal coordinate analysis was used to ordinate the Bray-Curtis distance matrices and to visualize the relationships between samples from OTC and control plots.

For the comparisons of relative abundances of taxa on phylum, class and order level between the warmed and the control samples, pseudoreplicates were averaged by the OTC or control plot they originated from. These average relative abundances were then compared using Wilcoxon rank-sum tests.

We used two methods to determine taxa sensitive to warming. For both methods, we used the average abundances of ASVs in each plot. First, differential abundance of bacterial ASVs between warmed and control samples was assessed using DESeq2 (Love et al., 2014) on the non-CSS normalized datasets with the R package "DESeq2" (Love et al., 2014). The adjusted *P*-value cut-off was 0.1 (Love et al., 2014). Differential abundance analysis only uses ASVs present in both the OTC and control samples. The second method we used to find taxa sensitive to warming, was indicator species analysis. To find bacterial taxa indicative for the warming or the control treatment, correlation-based indicator species analysis was done with all possible site combinations using the function *multipatt* of the R package "indicSpecies" (De Caceres and Legendre, 2009) based on 10^3 permutations. The indicator species analysis takes into account ASVs present in both OTC and control samples, but also ASVs present in only one of the treatments. We combined results of the DESeq2 and indicator species analysis for a final list of ASVs sensitive to warming.

For visualizations of the data, we showed all samples when we could account for pseudoreplication (Bayesian generalized linear models and Permanovas) and we showed plot averages when we compared between the control and warmed treatment (Wilcoxon rank-sum tests).

RESULTS

Effect of OTC Treatment on ASV Richness, Diversity and Community Structure

The ASV richness and Shannon diversity of the bacterial communities associated with *C. islandica* were not significantly affected by the warming treatment (**Figure 1** and **Supplementary Figures 1–4**). However, we found that *B. nana* abundance tended to positively influence the cDNA-based bacterial richness and Shannon diversity (**Supplementary Figures 3, 4**). A significant difference was found for the richness, which was higher for the cDNA-based bacterial community than the DNA-based community in the warmed treatment (**Supplementary Figure 7**). The cDNA-based Shannon index tended to be higher than the DNA-based Shannon index (**Figure 1** and **Supplementary Figure 5**).

Some level of clustering between the control and warmed samples could be observed in the principal coordinate analysis (**Figure 2**). Based on the results of a PERMANOVA, the warmed lichen associated bacterial communities were significantly different from the communities in the control samples (DNA: R^2 = 0.07 and P = 0.001; RNA: R^2 = 0.07 and P = 0.005) (**Supplementary Tables 2, 3**). In addition, litter abundance was associated with variation in the cDNA-based bacterial community (Permanova: R^2 = 0.04 and P = 0.05).

Effect of OTC Treatment on the Taxonomic Composition and Abundance of the *C. islandica* Bacteriota

The bacterial community found associated with the lichen *C. islandica* is described at the phylum level (**Figure 3A**) and at the class and order level (**Figure 4**). No clear differences were found for the relative abundance at the phylum level between the control and warmed treatment for the total bacteria community (**Figure 3A**). Similarly, we did not detect differences between the control and warmed

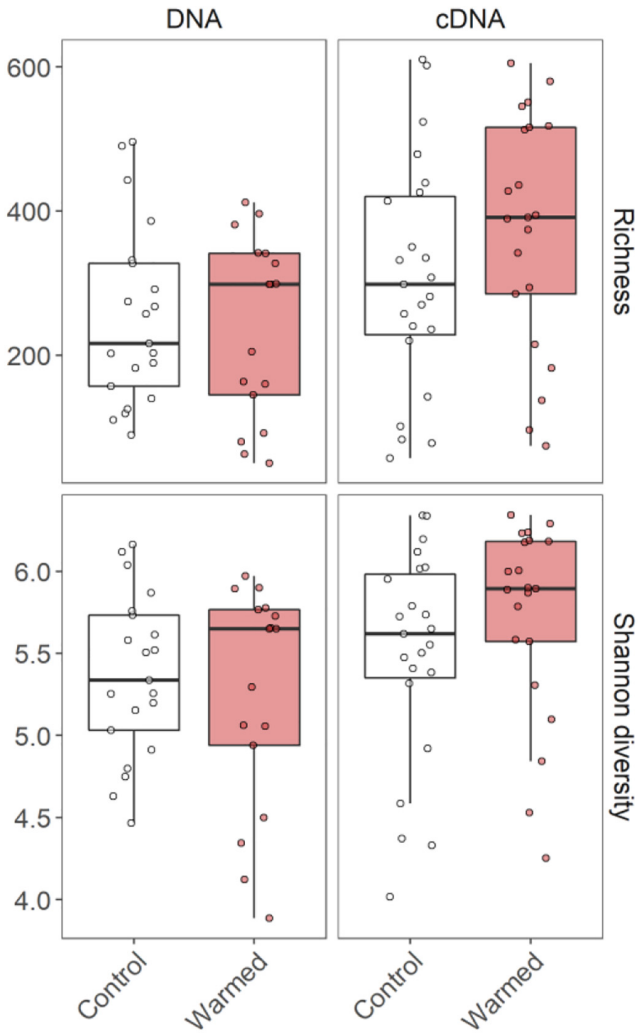

FIGURE 1 | ASV richness and Shannon diversity of the DNA and cDNA-based bacterial communities associated with the lichen *C. islandica* in control and warmed samples. *N* = 82, *n* = 21 for DNA control, *n* = 17 for DNA warmed, *n* = 23 for cDNA control and *n* = 21 for cDNA warmed.

treatment in the cDNA-based bacterial community at the phylum level (**Figure 3A**). The total bacterial community was dominated by Proteobacteria and Acidobacteria (DNA: 58 and 34% average relative abundance across all control and warmed samples, for Proteobacteria and Acidobacteria, respectively). Proteobacteria and Acidobacteria were also the main phyla in the cDNA-based bacterial community (cDNA: 63 and 29%, respectively) (**Figure 3A**). At lower taxonomic level, the orders Acetobacterales and Acidobacteriales were the dominant taxa (DNA: 44%; cDNA: 51%, DNA: 34%; cDNA 29%, **Figure 4A**). Within the acidobacterial family Acetobacteraceae, about 14% could not be assigned to a genus (**Supplementary Figure 7**). The most abundant genera in the cDNA and DNA-based bacterial communities were the proteobacterial genera *Acidiphilium* (DNA: 8%, cDNA: 11%) and *Endobacter* (DNA: 19%, cDNA: 20%) and the acidobacterial genera *Bryocella* (DNA: 10%, cDNA: 9%) and *Granulicella* (DNA: 15%, cDNA: 11%) (**Supplementary Figure 7**).

A total of 295 ASVs were only detected in the cDNA-based samples and not in the DNA-based samples. These taxa belonged to abundant genera such as *Endobacter* and *Acidiphilium* (**Supplementary Tables 4, 5**). Genera that were exclusively found in the cDNA-based community were *Lactococcus*, *Lachnospiraceae NK4A136* group, *Ktedonobacter*, *Methylovirgula*, *Frigoribacterium*, *Amnibacterium*, *Rhizobacter*, *Telmatobacter*, *Kineosporia*, and *Acidiphilium* (**Supplementary Tables 4, 5**).

The bacterial load was on average 671 and 1944 16S rRNA copies per ng DNA for control and warmed plots, respectively (**Figure 3B**). However, no differences could be found between the overall 16S rRNA gene copy numbers, or *nifH* gene copy numbers in the control and warmed plots (**Figure 3B** and **Supplementary Figures 8, 9**). Nevertheless, *B. nana* abundance positively affected both *nifH* and 16S rRNA gene copy numbers, whereas litter abundance negatively affected *nifH* gene copy numbers (**Supplementary Figures 8, 9**).

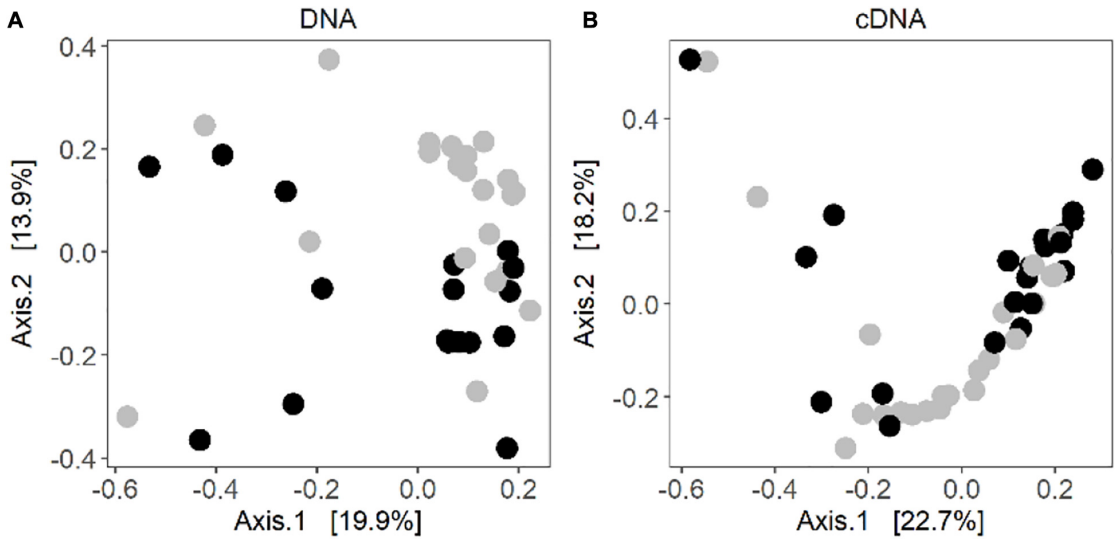

FIGURE 2 | Principal coordinate analysis of Bray-Curtis distances of the **(A)** DNA-based community composition and **(B)** cDNA-based community composition of the lichen *C. islandica*. Warmed samples are represented as black circles and control samples as gray circles. $N = 28$, $n = 21$ for DNA control, $n = 17$ for DNA warmed, $n = 23$ for cDNA control and $n = 21$ for cDNA warmed.

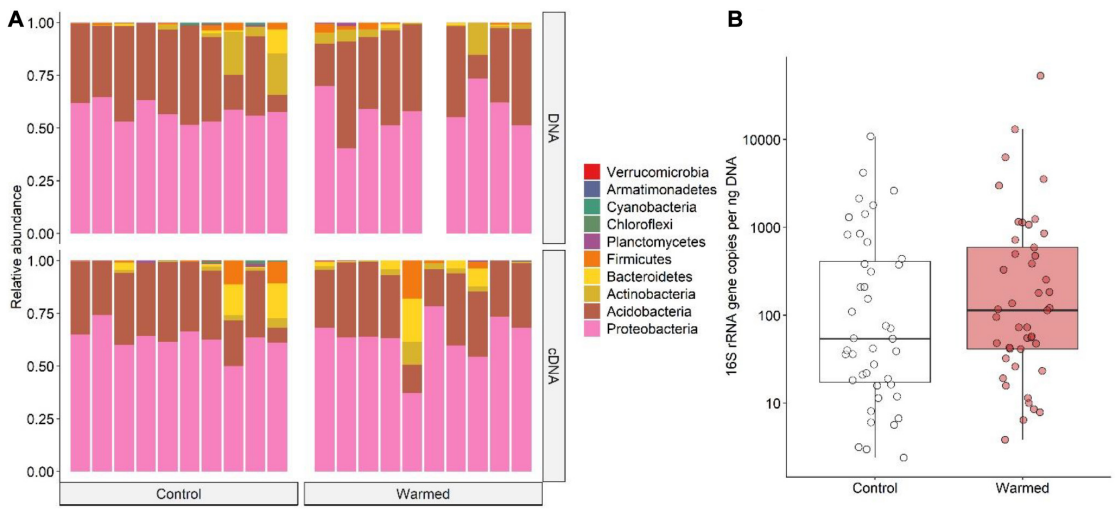

FIGURE 3 | (A) Barplots of the bacterial community composition associated with the lichen *C. islandica* in the control and warmed plots. Data are presented at the phylum level for DNA and cDNA. Bars represent pooled samples from each separate plot. **(B)** 16S rRNA gene abundance per ng extracted DNA in control (white) and warmed (red) samples. $N = 88$, $n_{warmed} = 45$, $n_{control} = 43$.

In the DNA-based samples, the only proteobacterial class found significantly affected by warming were the Gammaproteobacteria with an increase of 50% in the warmed samples (Wilcoxon rank-sum test, $P = 0.033$; **Figure 4A**). Most of this increase was due to an increase in relative abundance of the order Betaproteobacteriales ($P = 0.046$) (**Figure 4B**). The order Sphingomonadales (Alphaproteobacteria) increased by a factor of 2.5 in relative abundance ($P = 0.009$) (**Figure 4B**). In the cDNA-based bacterial community, we did not detect differences in relative abundance on Proteobacterial class level between the control and warmed treatment (**Figure 4A**). Changes were found on order level with the alphaproteobacterial order Caulobacterales being twice as abundant in the cDNA-based bacterial community in the warmed plots ($P = 0.038$) than in the control plots. Similarly, the order Sphingomonadales was 2.7 times more active in the warmed treatment ($P = 0.007$) (**Figure 4B**). The order Diplorickettsiales (Gammaproteobacteria) was four times as abundant in the cDNA-based bacterial community in the warmed plots ($P = 0.040$) (**Figure 4B**).

While the phylum Actinobacteria was not among the most common phyla (DNA: 4%, cDNA: 2%), its order

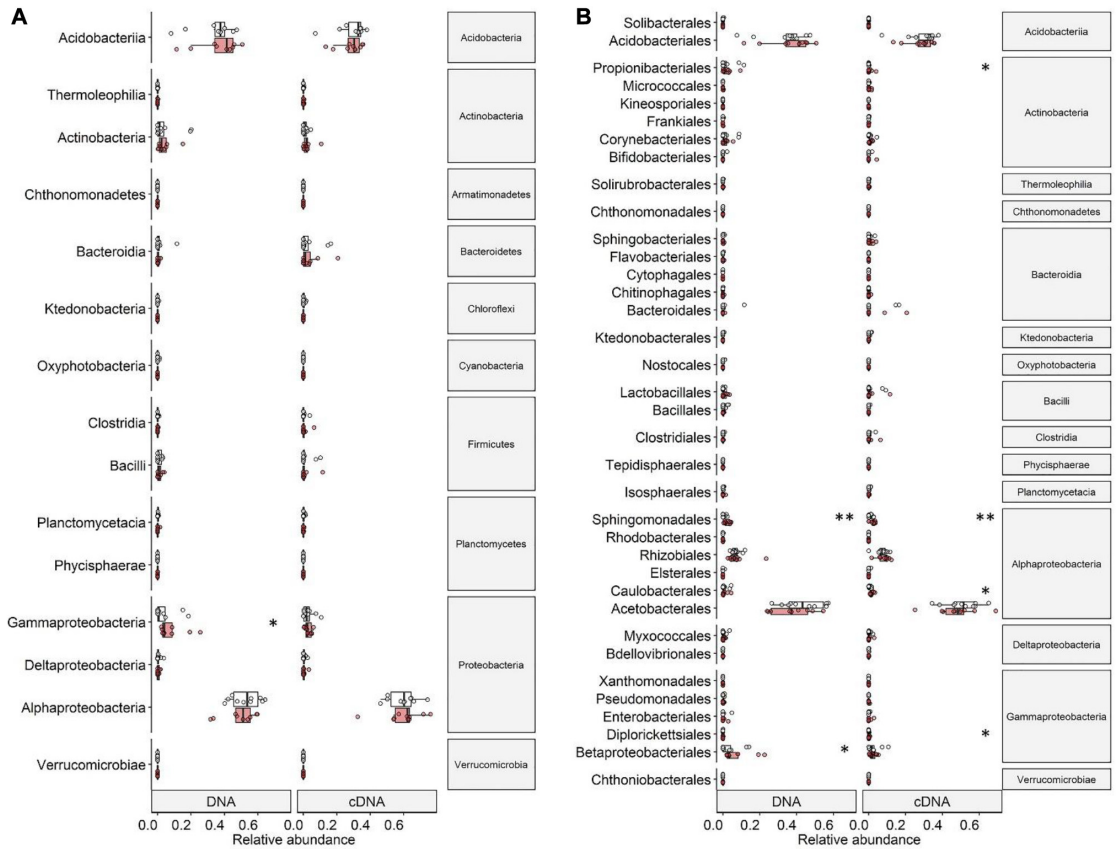

FIGURE 4 | Relative abundances of **(A)** classes and **(B)** orders of DNA- and cDNA-based bacterial communities associated with the lichen *C. islandica* in control (white) and warmed (red) samples. Points indicate average relative abundance values per control or warmed plot. Boxplots represent minimum values, first quartiles, medians, third quartiles, and maximum values. Significance levels (*$p < 0.05$ and **$p < 0.01$) are based on Wilcoxon rank-sum tests.

Propionibacteriales was 20 times as abundant in the cDNA-based bacterial community in the warmed plots compared to the control plots ($P = 0.040$) (**Figure 4B**).

Effect of OTC Treatment on the Relative Abundance of Bacterial ASVs

For the DNA-based communities, we detected 61 ASVs with a higher relative abundance in the warmed samples with a total relative abundance of 1% (**Supplementary Table 4**). We detected 96 ASVs with a lower relative abundance in the warmed samples compared to the control samples making up 1.7% of the total abundance (**Supplementary Table 4**). For the cDNA-based bacterial communities, we detected 190 ASVs with a higher relative abundance in the warmed samples (2.12%) and 77 ASVs with a lower relative abundance in the warmed samples compared to the control samples (0.9%) (**Supplementary Table 5**).

Of the ASVs only detected in cDNA-based bacterial community, 14 ASVs had a higher relative abundance in the warmed plots. All these rare ASVs belonged to the Proteobacteria, except one ASV that was classified as Bacteroidetes.

Amplicon sequence variants within the Proteobacteria showed mainly increased relative abundance in the warmed samples (**Figure 5** and **Supplementary Tables 4, 5**). Only ASVs classified under the genus *Acidiphilium* had more often a lower relative abundance in the warmed samples as well as a few ASVs of the genera *Acidisphaera* and *Endobacter*. In the cDNA-based samples, more proteobacterial ASVs with increased relative abundances under warming were detected than in the DNA-based samples.

Acidobacterial ASVs showed mixed differences between the control and warmed samples (**Figure 5** and **Supplementary Tables 4, 5**). ASVs of the genus *Bryocella* were less abundant under warming in both the DNA- and cDNA-based samples. ASVs of the genus *Granulicella* were equally more and less abundant in the warmed DNA-based samples, but had more often higher relative abundances in the warmed cDNA-based samples (**Figure 5** and **Supplementary Tables 4, 5**).

DISCUSSION

We assessed the effect of long-term (20 years) warming by OTCs on the bacterial community composition associated with the lichen *C. islandica* in an Icelandic sub-Arctic alpine dwarf-shrub heath. The community was dominated by Acidobacteria

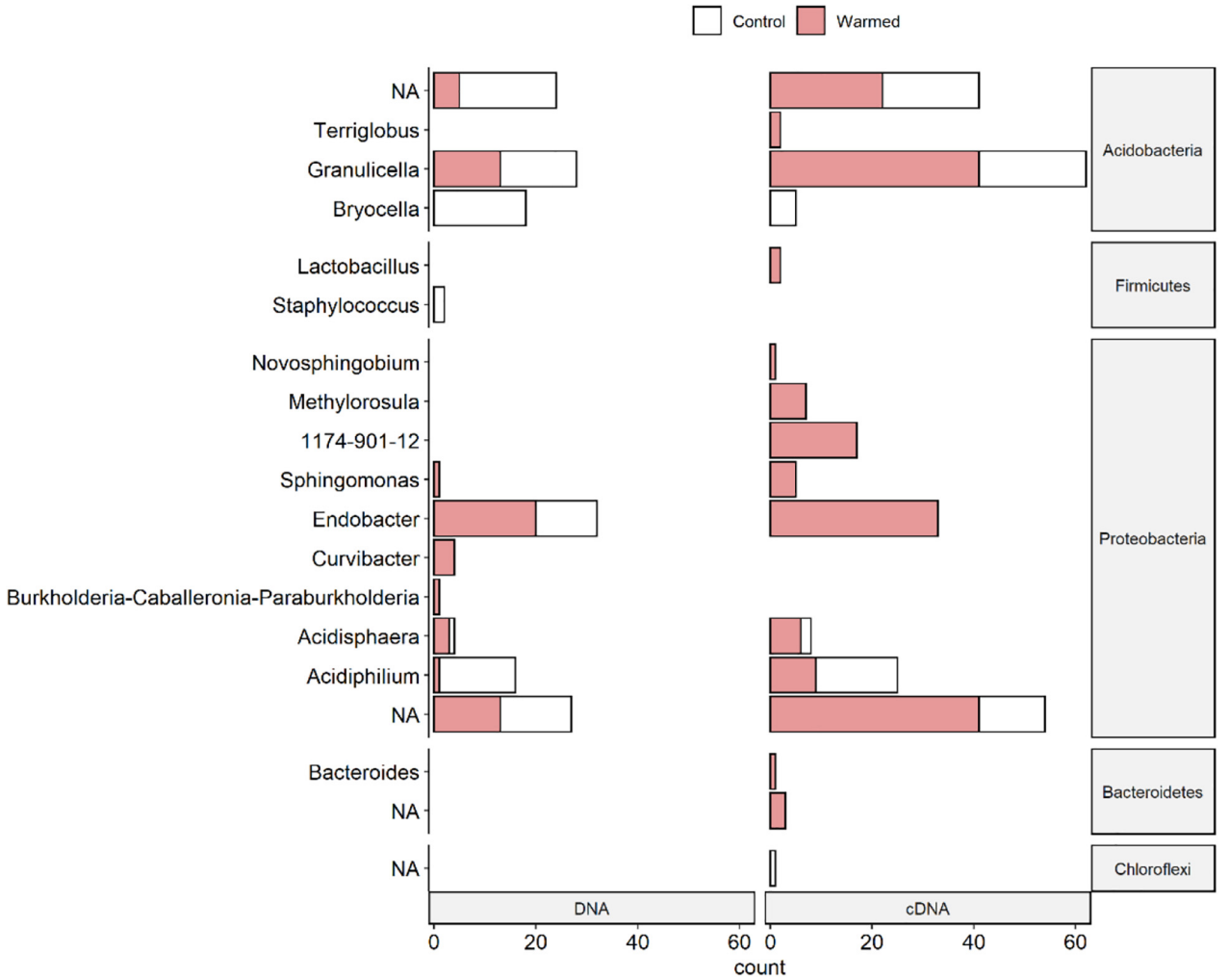

FIGURE 5 | Number of ASVs (amplicon sequence variants) per genus sensitive to warming for DNA and cDNA-based bacterial communities associated with the lichen *C. islandica*. Sensitivity to warming was determined by differential abundance analysis (DESeq2) and indicator species analysis. ASVs not assigned to genus level are called "NA." The number of ASVs indicative for the OTC (warmed) treatment is indicated in red and the number of ASVs indicative for the control treatment is indicated in white.

and Proteobacteria in both total and potentially active bacterial communities in both control and warmed plots. Warming did not induce compositional or structural changes at higher taxonomical levels. Nevertheless, we found indications of multiple warming-induced shifts in the community composition at the class, order and ASV levels. The most prominent increases in relative abundance were found in several genera belonging to the Proteobacteria. Our results illustrate that the long-term warming treatment affects the bacterial community composition of the lichen symbiosis at fine taxonomical levels.

The Bacterial Community of *Cetraria islandica*

While the dominance of the class Alphaproteobacteria has been described as a general characteristic of lichen bacterial communities (Cardinale et al., 2008; Weiss et al., 2011; Printzen et al., 2012), a striking feature of the *C. islandica* microbiome is the strong dominance of the family Acetobacteriaceae (Alphaproteobacteria). While the presence of Acetobacteriaceae in lichens has been observed before, notably in the reindeer lichen *Cladonia arbuscula* (Cardinale et al., 2008), this strong dominance does seem unusual. Indeed, the Rhizobiaceae, often held to be the dominant Alphaproteobacteria in lichens (Weiss et al., 2011; Hodkinson et al., 2012), only make up a minor part of the *C. islandica* bacteriome. The second dominant group in the *C. islandica* bacteriome are members of the family Acidobacteriaceae (Acidobacteria). Even at the genus level, the *C. islandica* bacteriome is surprisingly homogeneous, with approximately half of the reads being assigned to only four genera, the acetobacterial genera *Endobacter* and *Acidiphilium*, and the acidobacterial genera *Granulicella* and *Bryocella*. This pronounced dominance of presumptively acidophilic taxa is noteworthy. Acidobacteria were also reported earlier in

living parts of bog and tundra (Pankratov, 2012) and lichens in Alpine soil crusts (Muggia et al., 2013). The presence of acidophilic taxa may be explained by organic acid secondary metabolites produced by *C. islandica*, such as protolichesterinic and fumaroprotocetraric acids (Xu et al., 2018).

Another feature of the *C. islandica* microbiota is the difference between the potentially metabolically active and total community. The richness of the potentially active bacterial communities was higher compared the to total bacterial communities. One possible explanation for this is that the detection of taxa in 16S rRNA sequences, but not in 16S rDNA sequences, can occur when rare taxa have a high metabolic potential. The occurrence of these "phantom taxa" could be a result of cDNA synthesis errors that do not occur in the rDNA samples, but are introduced in the rRNA sequences. Another explanation could be variation in metabolic activity among taxa (Campbell et al., 2011; Baldrian et al., 2012; Klein et al., 2016; Jia et al., 2019). Rare taxa have been observed to be disproportionally active compared to abundant members (Jones and Lennon, 2010) and thereby might contribute more to ecosystem functioning than one would expect based on their abundance (Jousset et al., 2017). The rare bacterial taxa of *C. islandica* were mostly composed of not assigned genera and members of the genera *Endobacter*, *Acidiphilium*, *Lactococcus*, *Mucilaginibacter*, and *Bacteroides*. The fermenting bacteria from the genus *Lactococcus* have been described before in a bioreactor as being rare while having high potential activity levels (Lawson et al., 2015).

N_2-fixation is an important process in N-limited tundra ecosystems and previous work has shown that biocrust chlorolichens can show significant nitrogenase activity (Torres-Cruz et al., 2018). As *C. islandica* is a chlorolichen and does not have N_2-fixing Cyanobacteria as a photobiont, this raises the question if other taxa could be N_2-fixers. The N_2-fixing capability of *C. islandica* is unknown, but the presence of *nifH* genes indicates that potential N_2-fixers are present in the *C. islandica* bacterial community. Indeed, we detected putative N_2-fixers such as *Curvibacter* (Ding, 2004) and members of the Burkholderiaceae. On the other hand, lichens might also obtain nutrients dissolved in precipitation or through runoff from taller vegetation, or via a moisture gradient resulting in upward movement of soil moisture and dissolved nutrients (Longton, 1992). Nevertheless, our data indicate that the indirect effect of warming through changes in litter and *B. nana* abundance can influence the abundance of N_2-fixing bacteria. More studies on the N_2-fixation capabilities of chlorolichens in tundra ecosystems are necessary to elucidate their role as N_2-fixers.

The *C. islandica*-associated microbiota was found to be markedly different to that of the moss *Racomitrium lanuginosum* which was studied in the same warming experiment (Klarenberg et al., 2019), further supporting the host-specific selection of bacteria from the environment and symbiotic nature of both bryophyte and lichen holobionts proposed in the recent literature (Aschenbrenner et al., 2016; Holland-Moritz et al., 2018). Specifically, we found that *C. islandica* harbored a less rich and diverse bacterial community than *R. lanuginosum*, and the microbiota composition was profoundly different. Whereas the moss was dominated by the genera *Haliangium*, *Acidiphilium*, *Nostoc*, *Conexibacter*, *Granulicella*, *Solibacter*, and *Bryobacter*, the lichen was dominated by a few genera (*Bryocella*, *Granulicella*, *Acidiphilium*, and *Endobacter*) as reported herein. The same difference between the bacterial diversity of a lichen and a moss was shown by Aschenbrenner et al. (2017).

The Effect of OTC Warming on Bacterial Richness, Diversity and Community Structure

While we did not see any significant changes in richness or diversity of the bacterial community with warming, the warmed bacterial community structure significantly differed from the control community, both for the total as well as the potentially active communities. Overall, the potentially active community tended to be more affected by warming than the total bacterial community. For instance, more indicator taxa were found in the potentially active community and many more of these indicators were found in the warmed treatment. In addition, indirect effects of warming via shrubification and litter modification were found to affect the bacterial community. A positive effect of *B. nana* abundance was found on the richness and diversity of the potentially active community as well as on 16S rRNA and *nifH* gene abundance. Litter abundance was positively associated with *nifH* gene abundance and with the structure of the potentially active bacterial community.

At a coarse taxonomic level, the bacterial community structure was quite similar between the control and warmed treatment. One possible explanation for the similarity between the richness, diversity and composition of the warmed and control lichen bacterial communities could be that over long periods of warming bacterial communities acclimatize (Bradford et al., 2008; Crowther and Bradford, 2013; Romero-Olivares et al., 2017). Nonetheless, at lower taxonomic levels (class, order, and ASV) we detected differences in relative abundances. Shifts in individual taxa can affect microbe–microbe and microbe–host interactions and potentially change functionality or stability of the lichen-associated bacterial communities and thereby influence host health and ecosystem functioning, as proposed for plant–microbiomes (Agler et al., 2016; van der Heijden and Hartmann, 2016; Aydogan et al., 2018).

Long-term warming decreased the relative abundance of ASVs belonging to the Acidobacterial genera *Granulicella* and *Bryocella* and the alphaproteobacterial genus *Acidiphilium* in the total bacterial communities. *Acidiphilium* and *Granulicella* have been observed in other lichen microbiomes (Bates et al., 2011; Pankratov, 2012; Park et al., 2016; Aschenbrenner et al., 2017). These genera are chemoorganotrophic or chemolithotrophic and might thus survive on C sources present in the lichen thallus. *Granulicella* encompasses several acidophilic, cold-adapted species described from tundra soil isolates (Männistö et al., 2012). It has hydrolytic properties such as the ability to degrade chitin (Pankratov and Dedysh, 2010; Pankratov, 2012; Park et al., 2016; Belova et al., 2018), which suggest a role for these bacteria in the degradation of senescing lichen thalli. While some ASVs of the genus *Granulicella* decreased

in relative abundance, the increased potential activity might result in increased degradation of dead lichen material. In contrast, the decreased relative abundance and potential activity of *Bryocella* and *Acidiphilium* might result in slower degradation of dead lichen material. The genus *Acidiphilium* showed an increase in relative abundance in a moss microbiome in the same warming experiment (Klarenberg et al., 2019). This suggests that the responses of microbiome components to environmental change are at least in part dependent upon host vegetation identity rather than constituting a direct response of the bacteria themselves to extrinsic environmental factors. Thus leading to different outcomes for the various microbiomes within the same environment.

The alphaproteobacterial genera *Acidisphaera*, *Sphingomonas*, and *Endobacter* showed an increased relative abundance and potential activity with warming. *Sphingomonas* and *Acidisphaera* have been identified in other lichen bacterial communities (Cardinale et al., 2008). *Endobacter* is a poorly characterized genus of which only one species has been described (Ramirez-Bahena et al., 2013). *Acidisphaera* is chemoorganotrophic and contains bacteriochlorophyll (Hiraishi et al., 2000). *Sphingomonas* is known for its ability to degrade plant biomass, the utilization of recalcitrant matter in oligotrophic environments, and the use of sulfonated compounds as sources of C and sulfur (Aylward et al., 2013), which may be linked to the increase in litter abundance. The increase in relative abundance and potential activity of these genera in the warmed conditions might enhance C and nutrient availability in the lichen thalli.

Overall, all genera that dominated the bacterial community of *C. islandica* contained ASVs that were affected by the warming treatment in their relative abundances and potential metabolic activity. The genera that were affected in relative abundance are likely to play roles in nutrient recycling and supply in the lichen symbiosis. As most of these ASVs increased in relative abundance with warming, nutrient turnover in the lichen might be accelerated.

OTCs have been deployed to study warming effects in a wide range of ecosystems and plant responses correspond well to responses to natural climate warming (Hollister and Webber, 2000). We have shown that the OTC treatment leads to changes in the composition of the bacterial community associated with the lichen *C. islandica*, and that part of this change could be attributed to the increase in *B. nana* and litter abundance in the OTCs. This secondary effect of the OTC treatment may shield radiation from reaching the lichen layer or soil and thereby reduce the warming effect of the OTCs (Bokhorst et al., 2013), reducing the amount of PAR reaching the lichen and potentially affecting the bacterial communities. The increase in *B. nana* leaf litter may also increase C turnover as it is easily decomposable (McLaren et al., 2017) and thereby influence the lichen bacterial community. It should be noted that multiple caveats can be associated with the use of OTCs. Snow trapped in OTCs can increase temperatures at the soil surface, but at the same time decrease photosynthetically active radiation (Bokhorst et al., 2013). The walls of the OTCs may act as a barrier for new species to arrive (Richardson et al., 2000), even though it is unknown how important this side effect of the OTCs is on microbial communities. In addition, temperature-induced changes in lichen traits such as thallus nutrient content, as well as soil organic matter content, and soil moisture are environmental factors that could potentially influence the lichen bacterial community composition. Warming could also affect the secondary metabolites of the lichen (Asplund et al., 2017) and thereby alter the composition of the lichen microbiota.

In conclusion, we found that the bacterial community of *C. islandica* was dominated by acidophilic taxa and harbored rare, but potentially active taxa. Our results also showed that twenty years of warming and an increase dwarf-shrub and litter abundance can lead to changes in lichen bacterial communities at a fine taxonomic level as well as richness and diversity. The lichen microbiome plays an important role in the growth of lichens and climate-driven changes in the lichen microbiota, irrespective of whether they are due to direct or indirect effects of climate change, might affect decomposition of lichens and thereby nutrient cycling in sub-Arctic ecosystems.

DATA AVAILABILITY STATEMENT

The original contributions presented in the study are publicly available. This data can be found in NCBI, under accession PRJEB37116.

AUTHOR CONTRIBUTIONS

IJ, IK, and OV designed the study. IK conducted the sampling, the laboratory work, the bioinformatics processing, and the statistical analysis. CK performed the qPCR measurements. IK wrote the manuscript with contributions from OV, IJ, CK, and DW. All authors contributed to the article and approved the submitted version.

FUNDING

This work was funded by the MicroArctic Innovative Training Network grant supported by the European Commissions's Horizon 2020 Marie Sklodowska-Curie Actions program under project number 675546.

ACKNOWLEDGMENTS

We kindly thank Margrét Auður Sigurbjörnsdóttir for providing insightful comments on the manuscript.

SUPPLEMENTARY MATERIAL

The Supplementary Material for this article can be found online at: https://www.frontiersin.org/articles/10.3389/fmicb.2020.540404/full#supplementary-material

REFERENCES

Agler, M. T., Ruhe, J., Kroll, S., Morhenn, C., Kim, S.-T., Weigel, D., et al. (2016). Microbial hub taxa link host and abiotic factors to plant microbiome variation. *PLoS Biol.* 14:e1002352. doi: 10.1371/journal.pbio.1002352

Alatalo, J. M., Jägerbrand, A. K., Chen, S., and Molau, U. (2017). Responses of lichen communities to 18 years of natural and experimental warming. *Ann. Bot.* 120, 159–170. doi: 10.1093/aob/mcx053

Almendras, K., García, J., Carú, M., and Orlando, J. (2018). Nitrogen-fixing bacteria associated with peltigera cyanolichens and cladonia chlorolichens. *Molecules* 23:3077. doi: 10.3390/molecules23123077

Anderson, M. J. (2001). A new method for non-parametric multivariate analysis of variance. *Austral. Ecol.* 26, 32–46. doi: 10.1111/j.1442-9993.2001.01070.pp.x

Aschenbrenner, I. A., Cernava, T., Berg, G., and Grube, M. (2016). Understanding microbial multi-species symbioses. *Front. Microbiol.* 7:180. doi: 10.3389/fmicb.2016.00180

Aschenbrenner, I. A., Cernava, T., Erlacher, A., Berg, G., and Grube, M. (2017). Differential sharing and distinct co-occurrence networks among spatially close bacterial microbiota of bark, mosses and lichens. *Mol. Ecol.* 26, 2826–2838. doi: 10.1111/mec.14070

Asplund, J., Siegenthaler, A., and Gauslaa, Y. (2017). Simulated global warming increases usnic acid but reduces perlatolic acid in the mat-forming terricolous lichen *Cladonia stellaris*. *Lichenologist* 49, 269–274. doi: 10.1017/S0024282917000159

Asplund, J., and Wardle, D. A. (2017). How lichens impact on terrestrial community and ecosystem properties. *Biol. Rev.* 92, 1720–1738. doi: 10.1111/brv.12305

Aydogan, E. L., Moser, G., Müller, C., Kämpfer, P., and Glaeser, S. P. (2018). Long-term warming shifts the composition of bacterial communities in the phyllosphere of galium album in a permanent grassland field-experiment. *Front. Microbiol.* 9:144. doi: 10.3389/fmicb.2018.00144

Aylward, F. O., McDonald, B. R., Adams, S. M., Valenzuela, A., Schmidt, R. A., Goodwin, L. A., et al. (2013). Comparison of 26 sphingomonad genomes reveals diverse environmental adaptations and biodegradative capabilities. *Appl. Environ. Microbiol.* 79, 3724–3733. doi: 10.1128/AEM.00518-13

Baldrian, P., Kolařík, M., Štursová, M., Kopecký, J., Valášková, V., Větrovský, T., et al. (2012). Active and total microbial communities in forest soil are largely different and highly stratified during decomposition. *ISME J.* 6, 248–258. doi: 10.1038/ismej.2011.95

Bastida, F., Torres, I. F., Andrés-Abellán, M., Baldrian, P., López-Mondéjar, R., Větrovský, T., et al. (2017). Differential sensitivity of total and active soil microbial communities to drought and forest management. *Glob. Change Biol.* 23, 4185–4203. doi: 10.1111/gcb.13790

Bates, S. T., Cropsey, G. W. G., Caporaso, J. G., Knight, R., and Fierer, N. (2011). Bacterial communities associated with the lichen symbiosis. *Appl. Environ. Microbiol.* 77, 1309–1314. doi: 10.1128/AEM.02257-10

Belova, S. E., Ravin, N. V., Pankratov, T. A., Rakitin, A. L., Ivanova, A. A., Beletsky, A. V., et al. (2018). Hydrolytic capabilities as a key to environmental success: chitinolytic and cellulolytic acidobacteria from acidic sub-arctic soils and boreal peatlands. *Front. Microbiol.* 9:2775. doi: 10.3389/fmicb.2018.02775

Biasi, C., Meyer, H., Rusalimova, O., Hämmerle, R., Kaiser, C., Baranyi, C., et al. (2008). Initial effects of experimental warming on carbon exchange rates, plant growth and microbial dynamics of a lichen-rich dwarf shrub tundra in Siberia. *Plant Soil* 307, 191–205. doi: 10.1007/s11104-008-9596-2

Bjelland, T., Grube, M., Hoem, S., Jorgensen, S. L., Daae, F. L., Thorseth, I. H., et al. (2011). Microbial metacommunities in the lichen-rock habitat: microbial metacommunities in the lichen-rock habitat. *Environ. Microbiol. Rep.* 3, 434–442. doi: 10.1111/j.1758-2229.2010.00206.x

Blazewicz, S. J., Barnard, R. L., Daly, R. A., and Firestone, M. K. (2013). Evaluating rRNA as an indicator of microbial activity in environmental communities: limitations and uses. *ISME J.* 7, 2061–2068. doi: 10.1038/ismej.2013.102

Bokhorst, S., Huiskes, A., Aerts, R., Convey, P., Cooper, E. J., Dalen, L., et al. (2013). Variable temperature effects of open top chambers at polar and alpine sites explained by irradiance and snow depth. *Glob. Change Biol.* 19, 64–74. doi: 10.1111/gcb.12028

Bradford, M. A., Davies, C. A., Frey, S. D., Maddox, T. R., Melillo, J. M., Mohan, J. E., et al. (2008). Thermal adaptation of soil microbial respiration to elevated temperature. *Ecol. Lett.* 11, 1316–1327. doi: 10.1111/j.1461-0248.2008.01251.x

Callahan, B. J., McMurdie, P. J., and Holmes, S. P. (2017). Exact sequence variants should replace operational taxonomic units in marker-gene data analysis. *ISME J.* 11, 2639–2643. doi: 10.1038/ismej.2017.119

Callahan, B. J., McMurdie, P. J., Rosen, M. J., Han, A. W., Johnson, A. J. A., and Holmes, S. P. (2016). DADA2: high-resolution sample inference from Illumina amplicon data. *Nat. Methods* 13, 581–583. doi: 10.1038/nmeth.3869

Campbell, B. J., Yu, L., Heidelberg, J. F., and Kirchman, D. L. (2011). Activity of abundant and rare bacteria in a coastal ocean. *PNAS* 108, 12776–12781. doi: 10.1073/pnas.1101405108

Cardinale, M., Grube, M., Castro, J. V., Müller, H., and Berg, G. (2012a). Bacterial taxa associated with the lung lichen Lobaria pulmonaria are differentially shaped by geography and habitat. *FEMS Microbiol. Lett.* 329, 111–115. doi: 10.1111/j.1574-6968.2012.02508.x

Cardinale, M., Puglia, A. M., and Grube, M. (2006). Molecular analysis of lichen-associated bacterial communities: lichen-associated bacterial communities. *FEMS Microbiol. Ecol.* 57, 484–495. doi: 10.1111/j.1574-6941.2006.00133.x

Cardinale, M., Steinová, J., Rabensteiner, J., Berg, G., and Grube, M. (2012b). Age, sun and substrate: triggers of bacterial communities in lichens: ecology of lichen-associated bacterial communities. *Environ. Microbiol. Rep.* 4, 23–28. doi: 10.1111/j.1758-2229.2011.00272.x

Cardinale, M., Vieira de Castro, J., Müller, H., Berg, G., and Grube, M. (2008). In situ analysis of the bacterial community associated with the reindeer lichen Cladonia arbuscula reveals predominance of Alphaproteobacteria: lichen-associated bacterial community. *FEMS Microbiol. Ecol.* 66, 63–71. doi: 10.1111/j.1574-6941.2008.00546.x

Cernava, T., Aschenbrenner, I. A., Soh, J., Sensen, C. W., Grube, M., and Berg, G. (2019). Plasticity of a holobiont: desiccation induces fasting-like metabolism within the lichen microbiota. *ISME J.* 13:547. doi: 10.1038/s41396-018-0286-7

Cernava, T., Vasfiu, Q., Erlacher, A., Aschenbrenner, I. A., Francesconi, K., Grube, M., et al. (2018). Adaptions of lichen microbiota functioning under persistent exposure to arsenic contamination. *Front. Microbiol.* 9:2959. doi: 10.3389/fmicb.2018.02959

Coleine, C., Stajich, J. E., Pombubpa, N., Zucconi, L., Onofri, S., Canini, F., et al. (2019). Altitude and fungal diversity influence the structure of Antarctic cryptoendolithic Bacteria communities. *Environ. Microbiol. Rep.* 11, 718–726. doi: 10.1111/1758-2229.12788

Colesie, C., Büdel, B., Hurry, V., and Green, T. G. A. (2018). Can Antarctic lichens acclimatize to changes in temperature? *Glob. Change Biol.* 24, 1123–1135. doi: 10.1111/gcb.13984

Cornelissen, J. H. C., Callaghan, T. V., Alatalo, J. M., Michelsen, A., Graglia, E., Hartley, A. E., et al. (2001). Global change and arctic ecosystems: is lichen decline a function of increases in vascular plant biomass? *J. Ecol.* 89, 984–994. doi: 10.1111/j.1365-2745.2001.00625.x

Cornelissen, J. H. C., Lang, S. I., Soudzilovskaia, N. A., and During, H. J. (2007). Comparative cryptogam ecology: a review of bryophyte and lichen traits that drive biogeochemistry. *Ann. Bot.* 99, 987–1001. doi: 10.1093/aob/mcm030

Crowther, T. W., and Bradford, M. A. (2013). Thermal acclimation in widespread heterotrophic soil microbes. *Ecol. Lett.* 16, 469–477. doi: 10.1111/ele.12069

De Caceres, M., and Legendre, P. (2009). Associations between species and groups of sites: indices and statistical inference. *Ecology* 90, 3566–3574. doi: 10.1890/08-1823.1

Ding, L. (2004). Proposals of *Curvibacter gracilis* gen. nov., sp. nov. and *Herbaspirillum putei* sp. nov. for bacterial strains isolated from well water and reclassification of [Pseudomonas] huttiensis, [Pseudomonas] lanceolata, [Aquaspirillum] delicatum and [Aquaspirillum] autotrophicum as *Herbaspirillum huttiense* comb. nov., *Curvibacter lanceolatus* comb. nov., *Curvibacter delicatus* comb. nov. and *Herbaspirillum autotrophicum* comb. nov. *Int. J. Syst. Evol. Microbiol.* 54, 2223–2230. doi: 10.1099/ijs.0.02975-0

Domaschke, S., Vivas, M., Sancho, L. G., and Printzen, C. (2013). Ecophysiology and genetic structure of polar versus temperate populations of the lichen *Cetraria aculeata*. *Oecologia* 173, 699–709. doi: 10.1007/s00442-013-2670-3

Elmendorf, S. C., Henry, G. H. R., Hollister, R. D., Björk, R. G., Bjorkman, A. D., Callaghan, T. V., et al. (2012). Global assessment of experimental climate warming on tundra vegetation: heterogeneity over space and time: warming

effects on tundra vegetation. *Ecol. Lett.* 15, 164–175. doi: 10.1111/j.1461-0248.2011.01716.x

Fraser, R. H., Lantz, T. C., Olthof, I., Kokelj, S. V., and Sims, R. A. (2014). Warming-induced shrub expansion and lichen decline in the Western Canadian Arctic. *Ecosystems* 17, 1151–1168. doi: 10.1007/s10021-014-9783-3

González, I., Ayuso-Sacido, A., Anderson, A., and Genilloud, O. (2005). Actinomycetes isolated from lichens: evaluation of their diversity and detection of biosynthetic gene sequences. *FEMS Microbiol. Ecol.* 54, 401–415. doi: 10.1016/j.femsec.2005.05.004

Grube, M., Cardinale, M., de Castro, J. V., Müller, H., and Berg, G. (2009). Species-specific structural and functional diversity of bacterial communities in lichen symbioses. *ISME J.* 3, 1105–1115. doi: 10.1038/ismej.2009.63

Grube, M., Cernava, T., Soh, J., Fuchs, S., Aschenbrenner, I. A., Lassek, C., et al. (2015). Exploring functional contexts of symbiotic sustain within lichen-associated bacteria by comparative omics. *ISME J.* 9, 412–424. doi: 10.1038/ismej.2014.138

Hadfield, J. D. (2010). MCMC methods for multi-response generalized linear mixed models: the MCMCglmm R package. *J. Stat. Softw.* 33, 1–22. doi: 10.18637/jss.v033.i02

Hiraishi, A., Matsuzawa, Y., Kanbe, T., and Wakao, N. (2000). *Acidisphaera rubrifaciens* gen. nov., sp. nov., an aerobic bacteriochlorophyll-containing bacterium isolated from acidic environments. *Int. J. Syst. Evol. Microbiol.* 50, 1539–1546. doi: 10.1099/00207713-50-4-1539

Hodkinson, B. P., Gottel, N. R., Schadt, C. W., and Lutzoni, F. (2012). Photoautotrophic symbiont and geography are major factors affecting highly structured and diverse bacterial communities in the lichen microbiome: prokaryotic communities of the lichen microbiome. *Environ. Microbiol.* 14, 147–161. doi: 10.1111/j.1462-2920.2011.02560.x

Hodkinson, B. P., and Lutzoni, F. (2009). A microbiotic survey of lichen-associated bacteria reveals a new lineage from the Rhizobiales. *Symbiosis* 49, 163–180. doi: 10.1007/s13199-009-0049-3

Holland-Moritz, H., Stuart, J., Lewis, L. R., Miller, S., Mack, M. C., McDaniel, S. F., et al. (2018). Novel bacterial lineages associated with boreal moss species. *Environ. Microbiol.* 20, 2625–2638. doi: 10.1111/1462-2920.14288

Hollister, R. D., and Webber, P. J. (2000). Biotic validation of small open-top chambers in a tundra ecosystem. *Glob. Change Biol.* 6, 835–842. doi: 10.1046/j.1365-2486.2000.00363.x

IPCC (2019). *Special Report on the Ocean and Cryosphere in a Changing Climate (SROCC)*. Geneva: IPCC.

Jia, Y., Leung, M. H. Y., Tong, X., Wilkins, D., and Lee, P. K. H. (2019). Rare taxa exhibit disproportionate cell-level metabolic activity in enriched anaerobic digestion microbial communities. *mSystems* 4, e208–e218. doi: 10.1128/mSystems.00208-18

Jones, S. E., and Lennon, J. T. (2010). Dormancy contributes to the maintenance of microbial diversity. *PNAS* 107, 5881–5886. doi: 10.1073/pnas.0912765107

Jonsdottir, I. S., Magnusson, B., Gudmundsson, J., Elmarsdottir, A., and Hjartarson, H. (2005). Variable sensitivity of plant communities in Iceland to experimental warming. *Glob. Change Biol.* 11, 553–563. doi: 10.1111/j.1365-2486.2005.00928.x

Jousset, A., Bienhold, C., Chatzinotas, A., Gallien, L., Gobet, A., Kurm, V., et al. (2017). Where less may be more: how the rare biosphere pulls ecosystems strings. *ISME J.* 11, 853–862. doi: 10.1038/ismej.2016.174

Kärnefelt, I., Mattsson, J.-E., and Thell, A. (1993). The lichen genera arctocetraria, cetraria, and cetrariella (parmeliaceae) and their presumed evolutionary affinities. *Bryologist* 96, 394–404. doi: 10.2307/3243869

Klarenberg, I. J., Keuschnig, C., Colmenares, A. J. R., Jungblut, A. D., Jónsdóttir, I. S., and Vilhelmsson, O. (2019). Long-term warming effects on the microbiome and nitrogen fixation associated with the moss *Racomitrium lanuginosum* in a subarctic alpine heathland. *bioRxiv* [Preprint]. doi: 10.1101/838581

Klein, A. M., Bohannan, B. J. M., Jaffe, D. A., Levin, D. A., and Green, J. L. (2016). Molecular evidence for metabolically active bacteria in the atmosphere. *Front. Microbiol.* 7:772. doi: 10.3389/fmicb.2016.00772

Klindworth, A., Pruesse, E., Schweer, T., Peplies, J., Quast, C., Horn, M., et al. (2013). Evaluation of general 16S ribosomal RNA gene PCR primers for classical and next-generation sequencing-based diversity studies. *Nucleic Acids Res.* 41:e1. doi: 10.1093/nar/gks808

Kobayashi, D. Y., and Crouch, J. A. (2009). Bacterial/fungal interactions: from pathogens to mutualistic endosymbionts. *Annu. Rev. Phytopathol.* 47, 63–82. doi: 10.1146/annurev-phyto-080508-081729

Lange, O. L., and Green, T. G. A. (2005). Lichens show that fungi can acclimate their respiration to seasonal changes in temperature. *Oecologia* 142, 11–19. doi: 10.1007/s00442-004-1697-x

Lawson, C. E., Strachan, B. J., Hanson, N. W., Hahn, A. S., Hall, E. R., Rabinowitz, B., et al. (2015). Rare taxa have potential to make metabolic contributions in enhanced biological phosphorus removal ecosystems. *Environ. Microbiol.* 17, 4979–4993. doi: 10.1111/1462-2920.12875

Longton, R. (1992). "The role of bryophytes and lichens in terrestrial ecosystems," in *Bryophytes and Lichens in a Changing Environment*, eds J. Bates and A. M. Farmer (Oxford: Oxford University Press), 32–76. doi: 10.1017/cbo9780511565212.003

Love, M. I., Huber, W., and Anders, S. (2014). Moderated estimation of fold change and dispersion for RNA-seq data with DESeq2. *Genome Biol.* 15:550. doi: 10.1186/s13059-014-0550-8

Männistö, M. K., Rawat, S., Starovoytov, V., and Häggblom, M. M. (2012). *Granulicella arctica* sp. nov., *Granulicella mallensis* sp. nov., *Granulicella tundricola* sp. nov. and *Granulicella sapmiensis* sp. nov., novel acidobacteria from tundra soil. *Int. J. Syst. Evol. Microbiol.* 62, 2097–2106. doi: 10.1099/ijs.0.031864-0

McLaren, J. R., Buckeridge, K. M., van de Weg, M. J., Shaver, G. R., Schimel, J. P., and Gough, L. (2017). Shrub encroachment in *Arctic tundra*: *Betula nana* effects on above- and belowground litter decomposition. *Ecology* 98, 1361–1376. doi: 10.1002/ecy.1790

McMurdie, P. J., and Holmes, S. (2013). phyloseq: an R package for reproducible interactive analysis and graphics of microbiome census data. *PLoS One* 8:e61217. doi: 10.1371/journal.pone.0061217

Muggia, L., Klug, B., Berg, G., and Grube, M. (2013). Localization of bacteria in lichens from Alpine soil crusts by fluorescence in situ hybridization. *Appl. Soil Ecol.* 68, 20–25. doi: 10.1016/j.apsoil.2013.03.008

Mushegian, A. A., Peterson, C. N., Baker, C. C. M., and Pringle, A. (2011). Bacterial diversity across individual lichens. *Appl. Environ. Microbiol.* 77, 4249–4252. doi: 10.1128/AEM.02850-10

Myers-Smith, I. H., Grabowski, M. M., Thomas, H. J. D., Angers-Blondin, S., Daskalova, G. N., Bjorkman, A. D., et al. (2019). Eighteen years of ecological monitoring reveals multiple lines of evidence for tundra vegetation change. *Ecol. Monogr.* 89:e01351. doi: 10.1002/ecm.1351

Nash, T. H. (2008). *Lichen Biology*, 2nd Edn. Cambridge, MA: Cambridge University Press.

Nash, T. H., and Olafsen, A. G. (1995). Climate change and the ecophysiological response of Arctic lichens. *Lichenologist* 27, 559–565. doi: 10.1016/s0024-2829(05)80014-3

Oksanen, J., Blanchet, F. G., Kindt, R., Legendre, P., Minchin, P. R., O'hara, R. B., et al. (2013). *Package 'vegan.' Community ecology package, version 2, 296*.

Pankratov, T. A. (2012). Acidobacteria in microbial communities of the bog and tundra lichens. *Microbiology* 81, 51–58. doi: 10.1134/S0026261711060166

Pankratov, T. A., and Dedysh, S. N. (2010). *Granulicella paludicola* gen. nov., sp. nov., *Granulicella pectinivorans* sp. nov., *Granulicella aggregans* sp. nov. and *Granulicella rosea* sp. nov., acidophilic, polymer-degrading acidobacteria from Sphagnum peat bogs. *Int. J. Syst. Evol. Microbiol.* 60, 2951–2959. doi: 10.1099/ijs.0.021824-0

Park, C. H., Kim, K. M., Kim, O.-S., Jeong, G., and Hong, S. G. (2016). Bacterial communities in Antarctic lichens. *Antarctic Sci.* 28, 455–461. doi: 10.1017/S0954102016000286

Paulson, J. N., Stine, O. C., Bravo, H. C., and Pop, M. (2013). Differential abundance analysis for microbial marker-gene surveys. *Nat. Methods* 10, 1200–1202. doi: 10.1038/nmeth.2658

Poly, F., Monrozier, L. J., and Bally, R. (2001). Improvement in the RFLP procedure for studying the diversity of nifH genes in communities of nitrogen fixers in soil. *Res. Microbiol.* 152, 95–103. doi: 10.1016/S0923-2508(00)01172-4

Printzen, C., Fernández-Mendoza, F., Muggia, L., Berg, G., and Grube, M. (2012). Alphaproteobacterial communities in geographically distant populations of the lichen *Cetraria aculeata*. *FEMS Microbiol. Ecol.* 82, 316–325. doi: 10.1111/j.1574-6941.2012.01358.x

Quast, C., Pruesse, E., Yilmaz, P., Gerken, J., Schweer, T., Yarza, P., et al. (2013). The SILVA ribosomal RNA gene database project: improved data processing and web-based tools. *Nucleic Acids Res.* 41, D590–D596. doi: 10.1093/nar/gks 1219

Ramirez-Bahena, M. H., Tejedor, C., Martin, I., Velazquez, E., and Peix, A. (2013). *Endobacter medicaginis* gen. nov., sp. nov., isolated from alfalfa nodules in an acidic soil. *Int. J. Syst. Evol. Microbiol.* 63, 1760–1765. doi: 10.1099/ijs.0.0 41368-0

Richardson, S. J., Hartley, S. E., and Press, M. C. (2000). Climate warming experiments: are tents a potential barrier to interpretation? *Ecol. Entomol.* 25, 367–370. doi: 10.1046/j.1365-2311.2000.00263.x

Rolshausen, G., Grande, F. D., Sadowska-Deś, A. D., Otte, J., and Schmitt, I. (2018). Quantifying the climatic niche of symbiont partners in a lichen symbiosis indicates mutualist-mediated niche expansions. *Ecography* 41, 1380–1392. doi: 10.1111/ecog.03457

Romero-Olivares, A. L., Allison, S. D., and Treseder, K. K. (2017). Soil microbes and their response to experimental warming over time: a meta-analysis of field studies. *Soil Biol. Biochem.* 107, 32–40. doi: 10.1016/j.soilbio.2016.12.026

Sigurbjörnsdóttir, M. A., Andrésson, ÓS., and Vilhelmsson, O. (2015). Analysis of the Peltigera membranacea metagenome indicates that lichen-associated bacteria are involved in phosphate solubilization. *Microbiology* 161, 989–996. doi: 10.1099/mic.0.000069

Spribille, T., Tuovinen, V., Resl, P., Vanderpool, D., Wolinski, H., Aime, M. C., et al. (2016). Basidiomycete yeasts in the cortex of ascomycete macrolichens. *Science* 353, 488–492. doi: 10.1126/science.aaf8287

Torres-Cruz, T. J., Howell, A. J., Reibold, R. H., McHugh, T. A., Eickhoff, M. A., and Reed, S. C. (2018). Species-specific nitrogenase activity in lichen-dominated biological soil crusts from the Colorado Plateau, USA. *Plant Soil* 429, 113–125. doi: 10.1007/s11104-018-3580-2

Uphof, J. C. T. (1925). Purple bacteria as symbionts of a lichen. *Science* 61:67. doi: 10.1126/science.61.1568.67

van der Heijden, M. G. A., and Hartmann, M. (2016). Networking in the plant microbiome. *PLoS Biol.* 14:e1002378. doi: 10.1371/journal.pbio.1002378

Wang, Q., Garrity, G. M., Tiedje, J. M., and Cole, J. R. (2007). Naive Bayesian classifier for rapid assignment of rRNA sequences into the new bacterial taxonomy. *Appl. Environ. Microbiol.* 73, 5261–5267. doi: 10.1128/AEM.0 0062-07

Wedin, M., Maier, S., Fernandez-Brime, S., Cronholm, B., Westberg, M., and Grube, M. (2016). Microbiome change by symbiotic invasion in lichens: microbiome change by symbiotic invasion in lichens. *Environ. Microbiol.* 18, 1428–1439. doi: 10.1111/1462-2920.13032

Weiss, S. T., Cropsey, G. W. G., Caporaso, J. G., Knight, R., and Fierer, N. (2011). Bacterial communities associated with the lichen symbiosis. *Appl. Environ. Microbiol.* 77, 1309–1314. doi: 10.1128/AEM. 02257-10

West, N. J., Parrot, D., Fayet, C., Grube, M., Tomasi, S., and Suzuki, M. T. (2018). Marine cyanolichens from different littoral zones are associated with distinct bacterial communities. *PeerJ* 6:e5208. doi: 10.7717/peerj. 5208

Xu, M., Heidmarsson, S., Thorsteinsdottir, M., Kreuzer, M., Hawkins, J., Omarsdottir, S., et al. (2018). Authentication of Iceland Moss (Cetraria islandica) by UPLC-QToF-MS chemical profiling and DNA barcoding. *Food Chem.* 245, 989–996. doi: 10.1016/j.foodchem.2017. 11.073

Conflict of Interest: The authors declare that the research was conducted in the absence of any commercial or financial relationships that could be construed as a potential conflict of interest.

Advantages of publishing in Frontiers

OPEN ACCESS
Articles are free to read for greatest visibility and readership

FAST PUBLICATION
Around 90 days from submission to decision

HIGH QUALITY PEER-REVIEW
Rigorous, collaborative, and constructive peer-review

TRANSPARENT PEER-REVIEW
Editors and reviewers acknowledged by name on published articles

Frontiers
Avenue du Tribunal-Fédéral 34
1005 Lausanne | Switzerland

Visit us: www.frontiersin.org
Contact us: frontiersin.org/about/contact

REPRODUCIBILITY OF RESEARCH
Support open data and methods to enhance research reproducibility

DIGITAL PUBLISHING
Articles designed for optimal readership across devices

FOLLOW US
@frontiersin

IMPACT METRICS
Advanced article metrics track visibility across digital media

EXTENSIVE PROMOTION
Marketing and promotion of impactful research

LOOP RESEARCH NETWORK
Our network increases your article's readership